2018:00170- Unrestricted

Report

EERA DeepWind'2018 Conference
17 – 19 January 2018

Radisson Blu Royal Garden Hotel, Trondheim

John Olav Tande (editor)

SINTEF Energy Research AS
Power Conversion and Transmission
2018-02-08

SINTEF

SINTEF Energi AS
SINTEF Energy Research AS
Address:
Postboks 4761 Torgarden
NO-7465 Trondheim
NORWAY
Switchboard: +47 73592000

Enterprise /VAT No:
NO 939 350 675 MVA

KEYWORDS:

Report

EERA DeepWind'2018 Conference
17 – 19 January 2018

Radisson Blu Royal Garden Hotel, Trondheim

VERSION
1.0

DATE
2018-02-08

AUTHOR(S)
John Olav Tande (editor)

CLIENT(S)

CLIENT'S REF.

PROJECT NO.
2018:00170

NUMBER OF PAGES/APPENDICES:
323

ABSTRACT

This report includes the presentations from the 15th Deep Sea Offshore Wind R&D Conference, EERA DeepWind'2018, 17 – 19 January 2018 in Trondheim, Norway.

Presentations include plenary sessions with broad appeal and parallel sessions on specific technical themes:
a) New turbine and generator technology
b) Grid connection and power system integration
c) Met-ocean conditions
d) Operations & maintenance
e) Installation & sub-structures
f) Wind farm optimization
g) Experimental Testing and Validation
h) Wind farm control systems

Plenary presentations include frontiers of science and technologies and strategic outlook. The presentations and further conference details are also available at the conference web page: https://www.sintef.no/projectweb/eera-deepwind

PREPARED BY
John Olav Tande

SIGNATURE

CHECKED BY
Hans Christian Bolstad

SIGNATURE

APPROVED BY
Knut Samdal

SIGNATURE

REPORT NO.	ISBN	CLASSIFICATION	CLASSIFICATION THIS PAGE
2018:00170	978-82-14-06671-5	Unrestricted	Unrestricted

Document history

VERSION	DATE	VERSION DESCRIPTION
1.0	2018-02-06	

Table of contents

Closing session - Strategic Outlook

Wednesday 17 January		
09.00	Registration & coffee	
	Opening session – Frontiers of Science and Technology Chairs: John Olav Tande, SINTEF and Trond Kvamsdal, NTNU	
09.30	Opening note by chair	
09.35	Alexandra Bech Gjørv, CEO, SINTEF	
09.50	Jørn Scharling Holm, Technology Partnerships Manager, Ørsted	
10.05	Hanne Wigum, Manager Renewable Technology, Statoil	
10.20	Matthijs Soede, Research Programme Officer, EC	
10.35	Aiden Cronin, ETIPwind	
10.50	Nils Røkke, Chair, European Energy Research Alliance (EERA)	
11.05	Panel debate, moderated by Prof Johan Hustad: *the role of R&I to maximize the economic attractiveness of offshore wind.*	
11.55	Closing by chair	
12.00	Lunch	
	Parallel sessions	
	A1) New turbine and generator technology Chairs: Harald G. Svendsen, SINTEF Energi	**C1) Met-ocean conditions** Chairs: Joachim Reuder, Uni of Bergen, Birgitte Rugaard Furevik, met.no
13.00	Introduction by Chair	Introduction by Chair
13.05	*Lightweight design of the INNWIND.EU and AVATAR rotors through multi-disciplinary optimization algorithms,* A.Croce, Politecnico di Milano	*Assessing Smoothing Effects of Wind Power around Trondheim via Koopman Mode Decomposition,* Y. Susuki, Osaka Prefecture University
13:30	*Initial Design of a 12 MW Floating Offshore Wind Turbine,* P.T.Dam, University of Ulsan, Korea	*An interactive global database of potential floating wind park sites,* L. Frøyd, 4Subsea AS
13:50	*Performance Assessment of a High Definition Modular Multilevel Converter for Offshore Wind Turbines,* R.E.Torres-Olguin, SINTEF Energi	*Offshore Wind: How an Industry Revolutionised Itself,* M. Smith, Zephir Ltd
14:10	*Mitigation of Loads on Floating Offshore Wind Turbines through Advanced Control Strategies*, D. Ward, Cranfield University	
14:30	Closing by Chair	Closing by Chair
14.35	Refreshments	
	A2) New turbine and generator technology (cont.)	**C2) Met-ocean conditions (cont.)**
15.05	Introduction by Chair	Introduction by Chair
15.10	*Integrated design of a semi-submersible floating vertical axis wind turbine (VAWT) with active blade pitch control,* F.Huijs, GustoMSC	*Wind conditions in a Norwegian fjord derived from tall meteorological masts and synchronized doppler lidars,* H. Agustsson, Kjeller Vindteknikk
15.30	*Evaluation of control methods for floating offshore wind turbines,* W.Yu, University of Stuttgart	*Complementary use of wind lidars and land-based met-masts for wind characterization in a wide fjord,* E. Cheynet, University of Stavanger
15.50	*Impact of the aerodynamic model on the modelling of the behaviour of a Floating Vertical Axis Wind Turbine,* V.Leroy, LHEEA and INNOSEA	*Simulation and observations of wave conditions in Norwegian fjords*, B.R. Furevik, Meteorologisk institutt
16.10	Closing by Chair	Closing by Chair
18.00	We welcome you to an informal reception at Dokkhuset. A jazz club and concert venue in an old industrial building by the old dock. There will be a musical performance by Kristoffer Lo and some light refreshments.	

Thursday 18 January		
	Parallel sessions	
	D1) Operation & maintenance Chairs: Thomas Welte, SINTEF Energi Marcel Wiggert, Fraunhofer IWES	**E1) Installation and sub-structures** Chairs: Michael Muskulus, NTNU, Arno van Wingerde, Fraunhofer IWES
09.00	Introduction by Chair	Introduction by Chair
09.05	*Wind Turbine Gearbox Planet Bearing Failure Prediction Using Vibration Data,* S. Koukoura, University of Strathclyde	*Floating offshore wind turbine design stage summary in LIFES50+ project*, G. Pérez, TECNALIA
09.30	*Data Insights from an Offshore Wind Turbine Gearbox Replacement*, A.K. Papatzimos, University of Edinburgh	*A comprehensive method for the structural design and verification of the INNWIND 10MW tri-spar floater*, D. Manolas, NTUA
09.50	*Further investigation of the relationship between main-bearing loads and wind field characteristics*, A. Turnbull, University of Strathclyde	*Reducing cost of offshore wind by integrated structural and geotechnical design*, K. Skau, NGI and NTNU
10.10	Damage Localization using Model Updating on a Wind Turbine Blade, K. Schröder, University of Hannover	*Catenary mooring chain eigen modes and the effects on fatigue life*, T.A.Nygaard, IFE
10.30	Refreshments	
	D2) Operation & maintenance (cont.)	**E2) Installation and sub-structures (cont.)**
11.00	*Using a Langevin model for the simulation of environmental conditions in an offshore wind farm,* H.Seyr, NTNU	*A numerical study of a catamaran installation vessel for installing offshore wind turbines,* Z. Jiang, NTNU
11.20	*The LEANWIND suite of logistics optimisation and full life-cycle simulation models for offshore wind farms*, F.D. McAuliffe, Univeristy College Cork	*FSFound – Development of an Instrumentation System for novel Float / Submerge Gravity Base Foundations,* P. McKeever, ORE Catapult
11.40	*Analysis, comparison and optimization of the logistic concept for wind turbine commissioning*, M. Wiggert, Fraunhofer IWES	*Integrated conceptual optimal design of jackets and foundations*, M. Stolpe, Technical University of Denmark
12.00	Closing by Chair	Closing by Chair
12.05	Lunch	
	B1) Grid connection and power system integration Chairs: Prof Kjetil Uhlen, NTNU Prof Olimpo Anaya-Lara, Strathclyde University	**G1) Experimental Testing and Validation** Chairs: Tor Anders Nygaard, IFE Ole David Økland, SINTEF Ocean, Amy Robertson, NREL
13.05	Introduction by Chair	Introduction by Chair
13.10	*Ancillary services from wind farms,* Prof William Leithead	*Wind tunnel experiments on wind turbine wakes in yaw: Redefining the wake width,* J.Schottler, ForWind, University of Oldenburg
13.35	*North Seas Offshore Network: Challenges and its way forward,* P.Härtel, Fraunhofer IWES	*A Detached - Eddy - Simulation study: Proper - Orthogonal - Decomposition of the wake flow behind a model wind turbine,* J.Göeing, Technische Universität Berlin
13.55	*Towards a fully integrated North Sea Offshore Grid: An engineering-economic assessment of a Power Link Island,* M. Korpås, NTNU	*BOHEM (Blade Optical HEalth Monitoring)*, P. McKeever, ORE Catapult
14.15	*Generic Future Grid Code regarding Wind Power in Europe,* T.K.Vrana, SINTEF Energi	*Scaled Wind Turbine Setup in Turbulent Wind Tunnel,* F. Berger, CvO University of Oldenburg
14.35	Refreshments	
	B2) Grid connection and power system integration (cont.)	**G2) Experimental Testing and Validation (cont.)**
15.05	*Statistical Analysis of Offshore Wind and other VRE Generation to Estimate the Variability in Future Residual Load*, M.Koivisto, DTU Wind Energy	*Documentation, Verification and Validation of Real-Time Hybrid Model tests for the 10MW OO-Star Wind Floater semi FOWT,* M.Thys, SINTEF Ocean
15.25	*A demonstrator for experimental testing integration of offshore wind farms with HVDC connection,* S.D'Arco, SINTEF Energi	*Validation of the real-time-response ProCap measurement system for full field flow measurements in a model-scale wind turbine wake, J.Bartl, NTNU*
15.45	*Optimal Operation of Large Scale Flexible Hydrogen Production in Constrained Transmission Grids with Stochastic Wind Power,* E.F.Bødal, NTNU	*Experimental Study on Slamming Load by Simplified Substructure,* Byoungcheon Seo, University of Ulsan, Korea
16.05	*Small signal modelling and eigenvalue analysis of multiterminal HVDC grids*, Salvatore D'Arco, SINTEF Energi AS	*Physical model testing of the TetraSpar floater in two configurations,* M.Borg, DTU Wind Energy
16.25	Closing by Chair	Closing by Chair
16.30	Refreshments	
17.00	Poster session	
19.00	Conference dinner	

Side event 1645-1845: Presentation of French research centres and companies involved in offshore wind energy
http://www.france.no/no/norge-oslo/fransk-delegasjon-pa-erra-deepwind-2018/

Thursday 18 January

17.00: Poster Session with refreshments

Session A

1. *Load estimation and O&M costs of Multi Rotor Array turbine for the south Baltic Sea*, M. Karczewski, Lodz University of Technology
2. *Dynamic Responses Analysis for Initial Design of a 12 MW Floating Offshore Wind Turbine with a Semi-Submersible Platform*, J.Kim, University of Ulsan, Korea

Session B

3. *Experimental Validation of a Novel Inertia-less VSM Algorithm*, Luis Reguera Castillo, University of Strathclyde
4. *Reducing Rapid Wind Farm Power Fluctuations Using the Modular Multilevel Converter,* A.A.Taffese, NTNU
5. *SiC MOSFETs for Offshore Wind Applications,* S. Tiwari, NTNU/SINTEF Ocean

Session C

6. *Extreme met-ocean conditions in a Norwegian fjord,* Z. Midjiyawa, Meteorologisk instiutt
7. *Modelling of non-neutral wind profiles - current recommendations vs. coastal wind climate measurements*, P. Domagalski, Lodz University of Technology
8. *Uncertainty estimations for offshore wind resource assessment and power verification,* D. Foussekis, Centre for Renewable Energy Sources

Session D

9. *Using a Langevin model for the simulation of environmental conditions in an offshore wind farm,* H.Seyr, M.Muskulus, NTNU
10. *On the effects of environmental conditions on wind turbine performance – an offshore case study,* E. González, CIRCE – Universidd de Zaragoza

Session E

11. *Design optimization with genetic algorithms: How does steel mass increase if offshore wind monopiles are designed for a longer service life?* L. Ziegler, Rambøll Wind
12. *Coupled Hybrid Mooring Systems for Floating Offshore Wind Farms for Increased System Stability*, M. Goldschmidt, Offshore Wind Consultants Ltd.
13. *Experimental Study on Slamming Load by Simplified Substructure*, A. Krogstad, NTNU
14. *Effect of hydrodynamic load modelling on the response of floating wind turbines and its mooring system in small water depths*, Kun Xu, NTNU
15. *A GPS/accelerometer integrated hub position monitoring algorithm for offshore wind turbine with monopile foundation*, Z. Ren, NTNU
16. *Supply chains for floating offshore wind substructures - a TLP example,* H.Hartmann, University Rostock
17. *Critical Review of Floating Support Structures for Offshore Wind Farm Deployment*, M Leimeister, REMS, Cranfield University
18. *Asessment of the state-of-the-art ULS design procedure for offshore wind turbine sub-structures*, C. Hübler, Leibniz Univ Hannover
19. *Offshore Floating Platforms: Analysis of a Solution for Motion Mitigation*, A.Rodriguez Marijuan, Saitec Offshore Technologies
20. *State-of-the-art model for the LIFES50+ OO-Star Wind Floater Semi 10MW floating wind turbine*, A. Pegalajar-Jurado, DTU
21. *Validation of a CFD model for the LIFES50+ OO-Star Wind Floater Semi 10MW and investigation of viscous flow effects,* H. Sarlak, DTU
22. *Nonlinear Wave Load Effects on Structure of Monopile Wind Turbines*, M. Mobasheramini, Queens University, Bryden Center
23. *Designing FOWT mooring system in shallow water depth*, V. Arnal, LHEEA, Centrale Nantes
24. *Construction Possibilities for Serial Production of Monolithic Concrete Spar Buoy Platforms,* C. Molins, UPC-Barcelona Tech
25. *Extreme response estimation of offshore wind turbines with an extended contour-line method, J-T.Horn, NTNU*
26. *Fabrication and Installation of OO-Star Wind Floater, T.Landbø, Dr.techn.Olav Olsen*

Session F

27. *Experimental validation of analytical wake and downstream turbine performance modelling*, F. Polster, Technical University of Berlin
28. *Reduce Order Model for the prediction of the aerodynamic lift around the NACA0015 airfoil, M.S. Siddiqui, NTNU*
29. *Fast divergence-conforming reduced orders models for flow, E. Fonn, SINTEF Digital*

Session G

30. *Sensitivity analysis of the dynamic response of a floating wind turbine*, R. Siavashi, University of Bergen
31. *Offshore Wind: How an Industry Revolutionised Itself*, M. Smith, Zephir Ltd
32. *Parameter Estimation of Breaking Wave Load Model using Monte Carlo Simulation*, S. Wang, DTU Wind Energy
33. *Emulation of ReaTHM testing*, L. Eliassen, SINTEF Ocean
34. *Multiple degrees of freedom real-time actuation of aerodynamic loads in model testing of floating wind turbines using cable-driven parallel robots*, V. Chabaud, NTNU/SINTEF Ocean
35. *A 6DoF hydrodynamic model for real time implementation in hybrid testing*, I. Bayati, Politecnico di Milano
36. *Kalman Estimation of Position and Velocity for ReaTHM Testing Applications,* E.Bachmann Mehammer, Imperial College London/SINTEF Energi
37. *Numerical modelling and validation of a semisubmersible floating offshore wind turbine under wind and wave misalignment*, S.OH, ClassNK

Session H

38. *Impact on wind turbine loads from different down regulation control strategies,* C. Galinos, DTU

Side event 1645-1845: Presentation of French research centres and companies involved in offshore wind energy
http://www.france.no/no/norge-oslo/fransk-delegasjon-pa-erra-deepwind-2018/

19.00: Dinner

Friday 19 January		
	Parallel sessions	
	H) Wind farm control systems Chairs: Karl Merz, SINTEF Energi Prof Olimpo Anaya-Lara, Strathclyde University	**F) Wind farm optimization** Chairs: Yngve Heggelund, CMR Henrik Bredmose, DTU Wind Energy
09.00	Introduction by Chair	Introduction by Chair
09.05	*Real-time wind field estimation & model calibration using SCADA data in pursuit of closed-loop wind farm control,* B.Doekemeijer, Delft University of Technology	*The DIMSELO Project (Dimensioning Sea Loads for Offshore Wind Turbines),* F. Pierella, IFE
09.25	*Mitigating Turbine Mechanical Loads Using Engineering Model Predictive Wind Farm Controller,* J.Kazda, DTU Wind Energy	*A savings procedure based construction heuristic for the offshore wind inter-array cable layout optimization problem*, S. Fotedar, University of Bergen
09.45	*Local stability and linear dynamics of a wind power plant*, K.Merz, SINTEF Energi	*Calibration and Initial Validation of FAST.Farm Against SOWFA,* J.Jonkman, National Renewable Energy Laboratory
10.05	*Wind farm control,* Prof William Leithead, Strathclyde University	*An Experimental Study on the Far Wake Development behind a Yawed Wind turbine,* F. Mühle, NMBU
10.25	Closing by Chair	Closing by Chair
10.30	Refreshments	
	Closing session – Strategic Outlook Chairs: John Olav Tande, SINTEF and Michael Muskulus, NTNU	
11.00	Introduction by Chair	
11.05	*WindBarge: floating wind production at intermediate water depths, J. Krokstad, NTNU*	
11.25	*OO-Star Wind Floater – The cost effective solution for future offshore wind developments*,Trond Landbø, Dr.techn.Olav Olsen	
11.55	*The first floating wind turbine in France: Status, Feedbacks & Perspectives*, I. Le Crom, Cenrale Nantes	
12.25	*Progress of EERA JPwind towards stronger collaboration and impact;* Peter Hauge Madsen, DTU Wind Energy	
12.40	Poster award and closing	
13.00	Lunch	

Side event (0800-1700): IEA OC5 meeting

Last Name	First name	Institution
Ágústsson	Hálfdán	Kjeller Vindteknikk
Anaya-Lara	Olimpo	Strathclyde University
Armada	Sergio	SINTEF
Arnal	Vincent	LHEEA-ECN
Aubrun	Sandrine	Ecole Centrale Nantes
Bachynski	Erin	NTNU
Bartl	Jan	NTNU
Bayati	Ilmas	Politecnico di Milano
Berg	Arve	Fugro Norway
Berger	Frederik	ForWind - University of Oldenburg
Berthelsen	Petter Andreas	SINTEF Ocean
Bolstad	Hans Christian	SINTEF Energi AS
Borg	Michael	DTU Wind Energy
Bozonnet	Pauline	IFPEN
Bredmose	Henrik	DTU Wind Energy
Bødal	Espen Flo	NTNU
Cai	Zhisong	China General Certification
Chabaud	Valentin	NTNU
Cheynet	Etienne	University of Stavanger
Croce	Alessandro	Politecnico di Milano
Cronin	Aiden	ETIPWind
Curien	Jean-Baptiste	VALIDE AS
D'Arco	Salvatore	SINTEF Energi AS
De Vaal	Jabus	IFE
Depina	Ivan	SINTEF Building and Infrastructure
Devoy McAuliffe	Fiona	University College Cork
Doekemeijer	Bart	Delft University of Technology
Domagalski	Piotr	Generative Urban Small Turbine/Lodz University of Technology
Dragsten	Gunder	Lloyd's Register
Eliassen	Lene	SINTEF Ocean
Fonn	Eivind	SINTEF
Forbord	Børge	Lloyds Register
Fotedar	Sunney	University of Bergen
Foussekis	Dimitri	Centre for Renewable Energy Sources (CRES)
Fredheim	Arne	SINTEF Ocean
Frøyd	Lars	4Subsea
Furevik	Birgitte	Meteorologisk Institutt
Galinos	Christos	Technical University of Denmark-DTU
Gao	Zhen	NTNU
Garpestad	Eimund	ConocoPhillips Scandinavia
Gebhardt	Cristian	Leibniz Universität Hannover
Germain	Nicolas	FRANCE ENERGIES MARINES

Gilloteaux	Jean-Christophe	Centrale Innovation
Gjørv	Alexandra Bech	SINTEF
Groussard	Mathieu	Statkraft
Göing	Jan	TU Berlin
Hartmann	Hauke	University Rostock
Heggelund	Yngve	Christian Michelsen Research
Hetland	Steinar	Kvaerner
Holm	Jørn Scharling	Dong Energy
Horn	Harald	Ferrx as
Horn	Jan-Tore	NTNU
Huijs	Fons	GustoMSC
Hübler	Clemens	Leibniz Universität Hannover
Härtel	Philipp	Fraunhofer IEE (formerly IWES)
Jakobsen	Jasna Bogunovic	University of Stavanger
Jiang	Zhiyu	NTNU
Jonkman	Jason	National Renewable Energy Laboratory (NREL)
Kaarstad	Vemund	Siemens AS
Karczewski	Maciej	Generative Urban Small Turbine/Lodz University of Technology
Karl	Christian	Leibniz Universität Hannover
Kazda	Jonas	DTU Wind Energy
Kerkeni	Sofien	D-ICE ENGINEERING
Kim	Junbae	University of Ulsan, Korea
Koivisto	Matti	Technical University of Denmark
Koltsidopoulos Papatzimos	Alexios	EDF Energy/ University of Edinburgh
Korpås	Magnus	NTNU
Koukoura	Sofia	University of Strathclyde
Krogstad	Ask S.	NTNU
Krokstad	Jørgen Ranum	NTNU/Norconsult
Kvamsdal	Trond	NTNU
Lacas	Pierre Paul	STX France Solutions
Landbø	Trond	Dr.techn. Olav Olsen AS
Le Crom	Izan	Ecole Centrale de Nantes
Le Dreff	Jean-Baptiste	EDF R&D France
Leimeister	Mareike	Fraunhofer IEE
Leithead	William	University of Strathclyde
Leroy	Vincent	Centrale Nantes - Centrale Innovation
Lynch	Mattias	INNOSEA
Madsen	Peter Hauge	DTU Wind Energy
Malmo	Oddbjørn	Kongsberg Maritime AS
Manolas	Dimitrios	National Technical University of Athens
Marinin	Anatolij	Technical University of Berlin
Martí	Ignacio	DTU Wind Energy
McKeever	Paul	ORE Catapult

Mehammer	Eirill Bachmann	SINTEF Energi AS
Merz	Karl	SINTEF Energi AS
Molins	Climent	Universitat Politècnica de Catalunya
Muskulus	Michael	NTNU
Mutoh	Kazuo	Hitachi, Ltd.
Mühle	Franz	NMBU
Nielsen	Finn Gunnar	Universitetet i Bergen
Nybø	Astrid	Universitetet i Bergen
Nygaard	Tor Anders	IFE
Oh	Sho	ClassNK
Olguin	Raymundo Torres	SINTEF Energi
Olsen	Pål Keim	NTNU
Ottesen	David	Norwegian Energy Partners
Page	Ana	NTNU
Park	Heon-Joon	KAIST
Pegalajar-Jurado	Antonio	DTU Wind Energy
Pereyra	Brandon	NTNU
Perez	German	TECNALIA
Perignon	Yves	LHEEA-ECN
Pham	Thanh Dam	University of Ulsan, Korea
Picotti	Giovanni Battista	Statoil ASA
Pierella	Fabio	IFE
Polster	Felix	NTNU
Popko	Wojciech	Fraunhofer IEE
Portefaix	Jean-Michel	French Embassy in Norway
Qvist	Jacob	4Subsea
Rasmussen	Simen Kleven	Dr.techn. Olav Olsen
Reuder	Joachim	Univ of Bergen
Robertson	Amy	NREL
Rodriguez	Alberto	SAITEC OFFSHORE TECHNOLOGIES, S.L.U
Røkke	Nils	EERA
Sarlak	Hamid	DTU Wind Energy
Schaumann	Peter	Leibniz Universität Hannover
Schottler	Jannik	ForWind, University of Oldenburg
Schröder	Karsten	Leibniz Universität Hannover
Seo	Byoungcheon	University of Ulsan, Korea
Seyr	Helene	NTNU
Siavashi	Rouzbeh	UiB
Skau	Kristoffer Skjolden	NGI
Smilden	Emil	NTNU
Smith	Matt	Zephir Ltd
Soede	Matthijs	EC
Stenbro	Roy	IFE
Stobbe	Ole	Ideol

Stolpe	Mathias	DTU Wind Energy
Susuki	Yoshihiko	Osaka Prefecture University
Svendsen	Harald G	SINTEF Energi AS
Sørum	Stian Høegh	NTNU
Tande	John Olav	SINTEF Energi AS
Thomassen	Paul	Simis AS
Throo	Alexandre	TechnipFMC
Thys	Maxime	SINTEF Ocean
Tiwari	Subhadra	NTNU
Tsakalomatis	Dimitrios	FloatMast LTD
Turnbull	Alan	University of Strathclyde
Uhlen	Kjetil	NTNU
Van Wingerde	Arno	Fraunhofer IEE
Vatne	Sigrid	SINTEF Ocean
Vince	Florent	ECOLE CENTRALE DE NANTES
Vrana	Til Kristian	SINTEF Energi AS
Wang	Shaofeng	DTU Wind Energy
Ward	Dawn	Cranfield University
Welte	Thomas	SINTEF Energi AS
Wiggert	Marcel	Fraunhofer IEE
Wigum	Hanne	Statoil ASA
Xu	Kun	NTNU
Yu	Wei	University of Stuttgart
Zakari	Midjiyawa	Meteorologisk Institutt
Ziegler	Lisa	Ramboll
Økland	Ole David	SINTEF Ocean

Scientific Committee and Conference Chairs

An international Scientific Committee is established with participants from leading institutes and universities. These include:

Anaya-Lara, Olimpo, Strathclyde University
Bredmose, Henrik, DTU
Busmann, Hans-Gerd, Fraunhofer IWES
Eecen, Peter, ECN
Faulstich, Stefan, Fraunhofer IWES
Furevik, Birgitte, R., Meteorologisk Institutt
Heggelund, Yngve, CMR
Jørgensen, Hans Ejsing, DTU
Kvamsdal, Trond, NTNU
Leithead, William, Strathclyde University
Madsen, Peter Hauge, DTU
Merz, Karl, SINTEF Energi
Muskulus, Michael, NTNU
Nielsen, Finn Gunnar, UiB
Nygaard, Tor Anders, IFE
Reuder, Joachim, UiB
Robertson, Amy, NREL
Rohrig, Kurt, Fraunhofer IWES
Sempreviva, Anna Maria, CNR
Tande, John Olav, SINTEF Energi
Uhlen Kjetil, NTNU
Van Wingerde, Arno, Fraunhofer IWES
Van Bussel, Gerard, TU Delft
Welte, Thomas, SINTEF Energi
Wiggert, Marcel, Fraunhofer IWES
Økland, Ole David, SINTEF Ocean

The Scientific Committee will review submissions and prepare the programme. Selection criteria are relevance, quality and originality.

The conference chairs were:

- John Olav Giæver Tande, Chief scientist, SINTEF Energi AS
- Trond Kvamsdal, Professor NTNU
- Michael Muskulus, Professor NTNU

Opening session – Frontiers of Science and Technology

Opening note by chair

Alexandra Bech Gjørv, CEO, SINTEF

Jørn Scharling Holm, Technology Partnerships Manager, Ørsted

Hanne Wigum, Manager Renewable Technology, Statoil

Matthijs Soede, Research Programme Officer, EC

Aiden Cronin, ETIPwind

Nils Røkke, Chair, European Energy Research Alliance (EERA)

A world-leading research institute

Our main goal: A world-leading research institute.

We develop solutions to some of society's grand challenges by being at the forefront of our strategic focus areas.

SINTEF

One of Europe's largest independent research organisations

2000 Employees

75 Nationalities

4000 Customers

NOK 3.1 billion Revenues

NOK 450 MILL International sales

SINTEF

Major participant in EU research programs

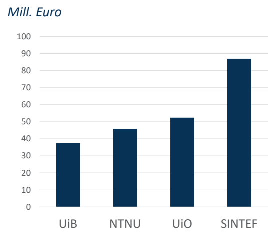

- Participate in 133 projects, with a project volume of € 1371 mill.
- Coordinate 37 projects with a project volume of € 201 mill.
- SINTEF research funding from EU: € 87 mill.

Participation in Horizon 2020, as of October 2017.
Source: RCN, EU's contract data base.

SINTEF

Applied research, technology and innovation

Expertise from ocean space to outer space:

Renewable energy | Ocean space | Industry | Buildings and infrastructure | Materials | Micro-, nano- and biotechnology

Climate and environment | Oil and gas | Health and welfare | Society | Digitalization | Transport

SINTEF

Partnership with NTNU

- Strategic and operational cooperation since 1950
- Joint use of laboratories and equipment
- Cooperation covers research projects, research centers and teaching

SINTEF

Close working relationships generate innovation and high quality

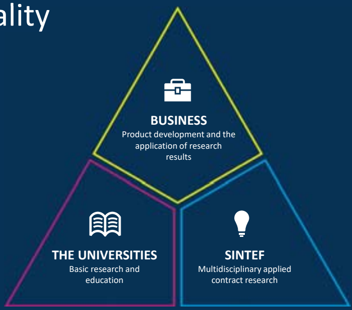

Hywind model test (2005)

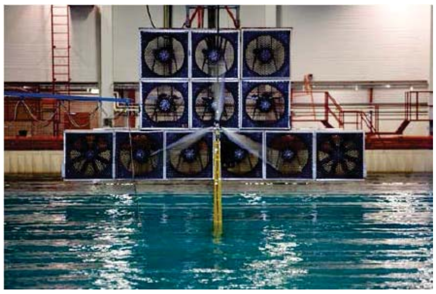

Laboratories and test facilities

- World-leading within a range of technology areas
- From nano and micro electronics to high voltage and ocean laboratories

Bold visions – in 2006

Bringing digital strength into SINTEF's industrial domains

Offshore wind research priorities

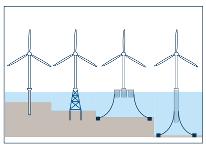

- Support structures
- Marine operations
- Materials

- Grid connection
- System integration
- Energy storage

- Asset management
- Wind farm control
- Digitalization

NOWITECH has 40 innovations in progress

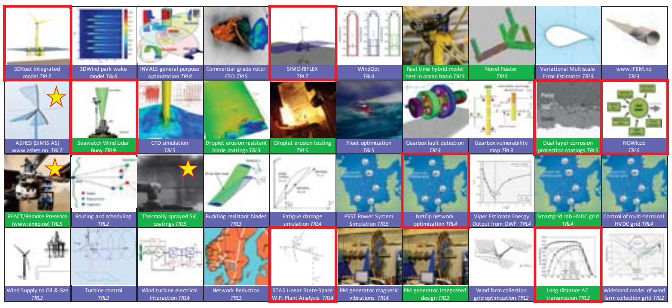

NOWITECH Norwegian Research Centre for Offshore Wind Technology

Numerical model | Technology / process | Quantified potential | New business entity (spin-off)

SINTEF

Technology for a better society

Potential value of innovations

NPV: > 5000 MEUR*

IMPELLO

* Result from analysis carried out by Impello Management AS for a subset of innovations by NOWITECH. NPV is calculated as socio-economic value of applying the innovations to a share of new offshore wind farms expected in Europe until 2030.

NOWITECH Norwegian Research Centre for Offshore Wind Technology

Wind goes digital

Mind-map made by ETIPwind

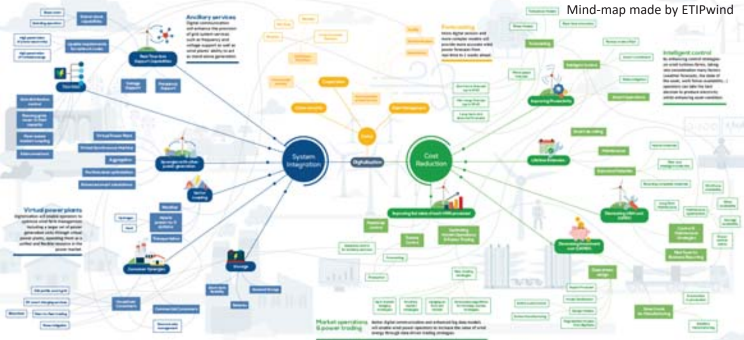

ØRSTED WIND POWER WAY OF WORKING WITH RD&D

Trondheim,
17th January 2018

Jørn Scharling Holm,
Technology Partnership Manager

Ørsted

Ørsted R&D strategy and types of collaboration

1 R&D strategy review

Foundation concept
Wake models
Geoscience models

2

- Project outcome, scope and impact
- Project management efficiency and administration
- Confidentiality and IPR
- Competence match
- Internal / external funding

3

Internal R&D projects
Small collaborative R&D projects
R&D Programmes
Joint Industry Projects
Large R&D consortiums

Ørsted

Ørsted's overview of levers for CoE reduction

Multiple levers to drive down cost in offshore wind power

1 Scale	2 Innovation	3 Industrialisation
▪ Turbines size ▪ Sites size ▪ Vessel size	▪ Foundation ▪ Electrical infrastructure	▪ Transition from single supply to multiple global suppliers
✓	✓	✓

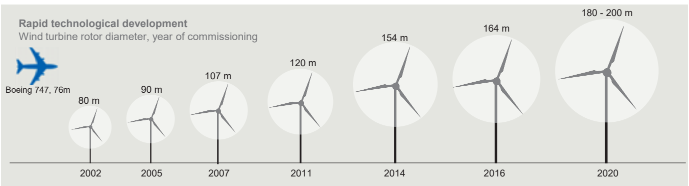

Ørsted

Ørsted's R&D Programme

R&D Strategy
- organised in 5 Roadmaps

Roadmap 1 Wind & Waves	Roadmap 2 Foundations, Geoscience and Marine	Roadmap 3 Electrical Infrastructure	Roadmap 4 WTG O&M	Roadmap 5 Logistics
Measurements: Lidar, radar, buoys Modelling: Lay-out, AEP, Loads, etc. Power curve validation	Geotechnical survey methods Monopile/ jacket design methods Soil-structure interaction Underwater noise damping Corrosion protection	Substation design Array and export cables layout and installation Grid simulations Grid connection Ancillary services	Component reliability New components New O&M inspection and replacement methods	Logistics modelling and optimisation Accomodation set-up development

Objectives
Enable the pipeline, CoE reduction, Risk reduction, HSE performance, Design standard improvements and competence development

Ørsted

Ørsted R&D strategy and types of collaboration

1 R&D strategy review

Foundation concept
Wake models
Geoscience models

2

- Project outcome, scope and impact
- Project management efficiency and administration
- Confidentiality and IPR
- Competence match
- Internal / external funding

3

Internal R&D projects
Small collaborative R&D projects
R&D Programmes
Joint Industry Projects
Large R&D consortium projects

Ørsted

Collaboration with universities and research institutions
- building competences leading to improved R&D

Input on research topics
Student Projects Programme
Guest lectures/ cases
University
PhDs
Data packages
Research projects

List not exhaustive.

Ørsted

Example on joint demonstration and commercialisation
- Carbon Trust OWA

CARBON TRUST

Six research areas - Focusing on everything but the turbine, representing roughly **70% of offshore wind energy costs**

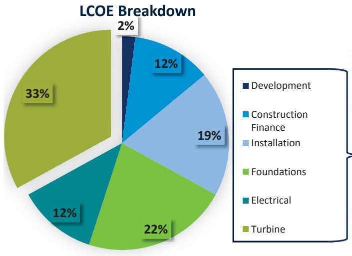

Source: Navigant

Ørsted

From basic research to commercial deployment
- how, who, what…

6: Innovation

IEA-RETD

Innovation is critical to delivering cost reduction and building supply chain capability

- Balance of support required across technology readiness levels (TRL)
- Forging links between industry and academia can maximise market penetration of new technologies
- Greater information and data sharing can accelerate technology innovation

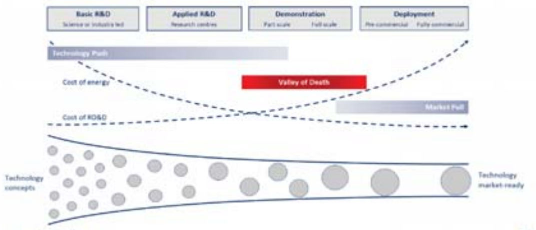

www.iea-retd.org 18

Ørsted

IEA - Renewable Energy Technology Deployment, published in March 2017

Thank you for your attention

Ørsted


Statoil
Statoil's journey in offshore wind
Hanne Wigum-Manager R&D Renewable Technology- Statoil
EERA DeepWind'18


Statoil
Shaping the future of energy
Competitive at all times
Transforming the oil and gas industry
Providing energy for a low carbon future

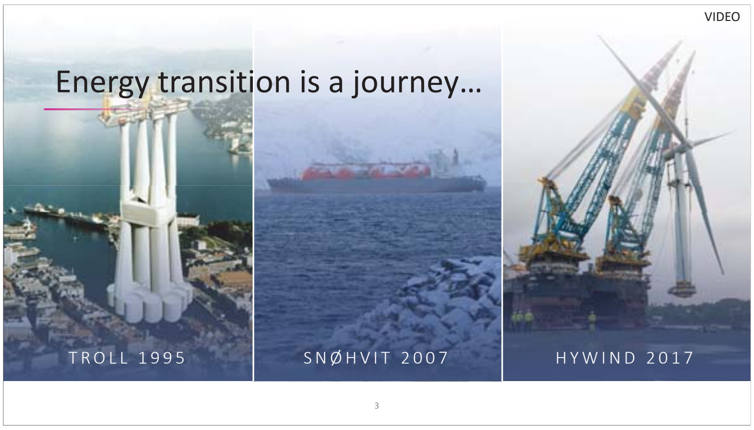
VIDEO
Energy transition is a journey…
TROLL 1995
SNØHVIT 2007
HYWIND 2017
3

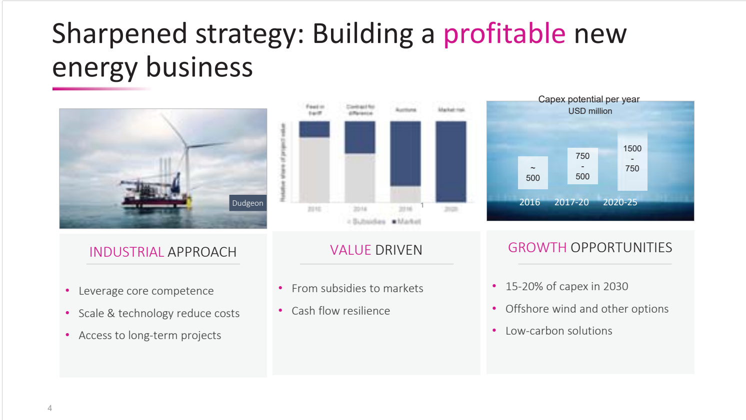
Sharpened strategy: Building a profitable new energy business
Dudgeon
Capex potential per year
USD million
~ 500
750 - 500
1500 - 750
2016
2017-20
2020-25
INDUSTRIAL APPROACH
Leverage core competence
Scale & technology reduce costs
Access to long-term projects
VALUE DRIVEN
From subsidies to markets
Cash flow resilience
GROWTH OPPORTUNITIES
15-20% of capex in 2030
Offshore wind and other options
Low-carbon solutions
4

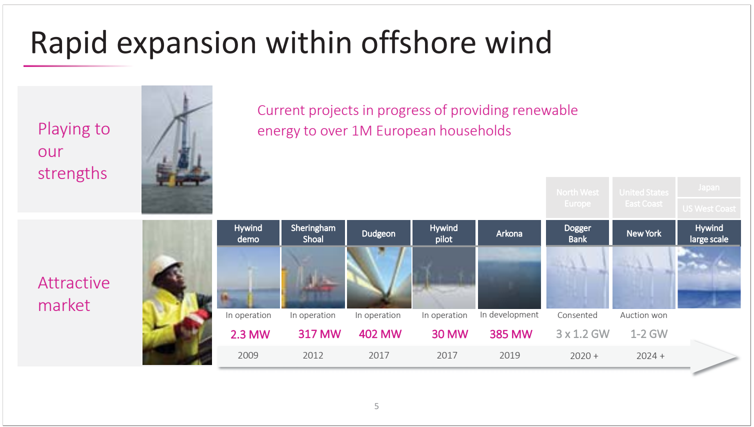
Rapid expansion within offshore wind
Playing to our strengths
Attractive market
Current projects in progress of providing renewable energy to over 1M European households
Hywind demo
Sheringham Shoal
Dudgeon
Hywind pilot
Arkona
Dogger Bank
New York
Hywind large scale
In operation
In development
Consented
Auction won
2.3 MW
317 MW
402 MW
30 MW
385 MW
3 x 1.2 GW
1-2 GW
2009
2012
2017
2017
2019
2020 +
2024 +
5

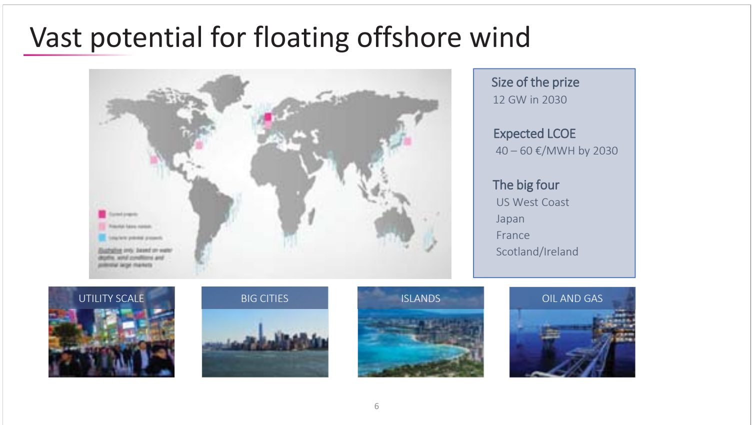
Vast potential for floating offshore wind
Size of the prize
12 GW in 2030
Expected LCOE
40 – 60 €/MWH by 2030
The big four
US West Coast
Japan
France
Scotland/Ireland
UTILITY SCALE
BIG CITIES
ISLANDS
OIL AND GAS
6

Next step for Hywind - lead floating wind to industrial scale

Cost

Hywind cost roadmap

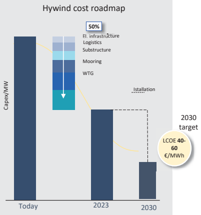

Deployment

Scalability critical for market success

Concept development

Technology development focused on:

- Site selection and park layout
- Design for scale and weight
- Proprietary motion controller
- Installation and maintenance

What colour do you dream in?

Hywind Factory
- a systematic approach to Hywind industrialisation

1 Extract and systemise learnings from projects

2 Leverage three pillars for Hywind cost reduction

Build on bottom fixed industry	Establish industry standards for floating wind	Optimise Hywind technology
1) Larger turbines	1) Mooring and anchoring	1) Low cost substructure
2) Standardised vessels	2) Cables and substations	2) Site-independent installation method
3) Operations and maintenance	3) Marine operations	3) Robust logistics

Statoil

Targeted technology development to support a growing business

Wind resource

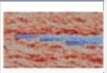

- Global wind resource models
- Measurement technologies
- Wind conditions, turbulence and wake

Energy harvesting

- Large WTG models
- Wind turbine controller
- Power and thrust curves
- Optimised park design and control

Structural design and production

- Methods and software for optimised design

WTG O&M

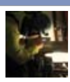

- Full scale measurements
- O&M data analysis
- Condition based maintenance

Marine operations and Logistics

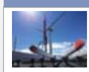

- New concepts for assembly and heavy lift operation
- Grid systems, infrastructure and transmission

Statoil

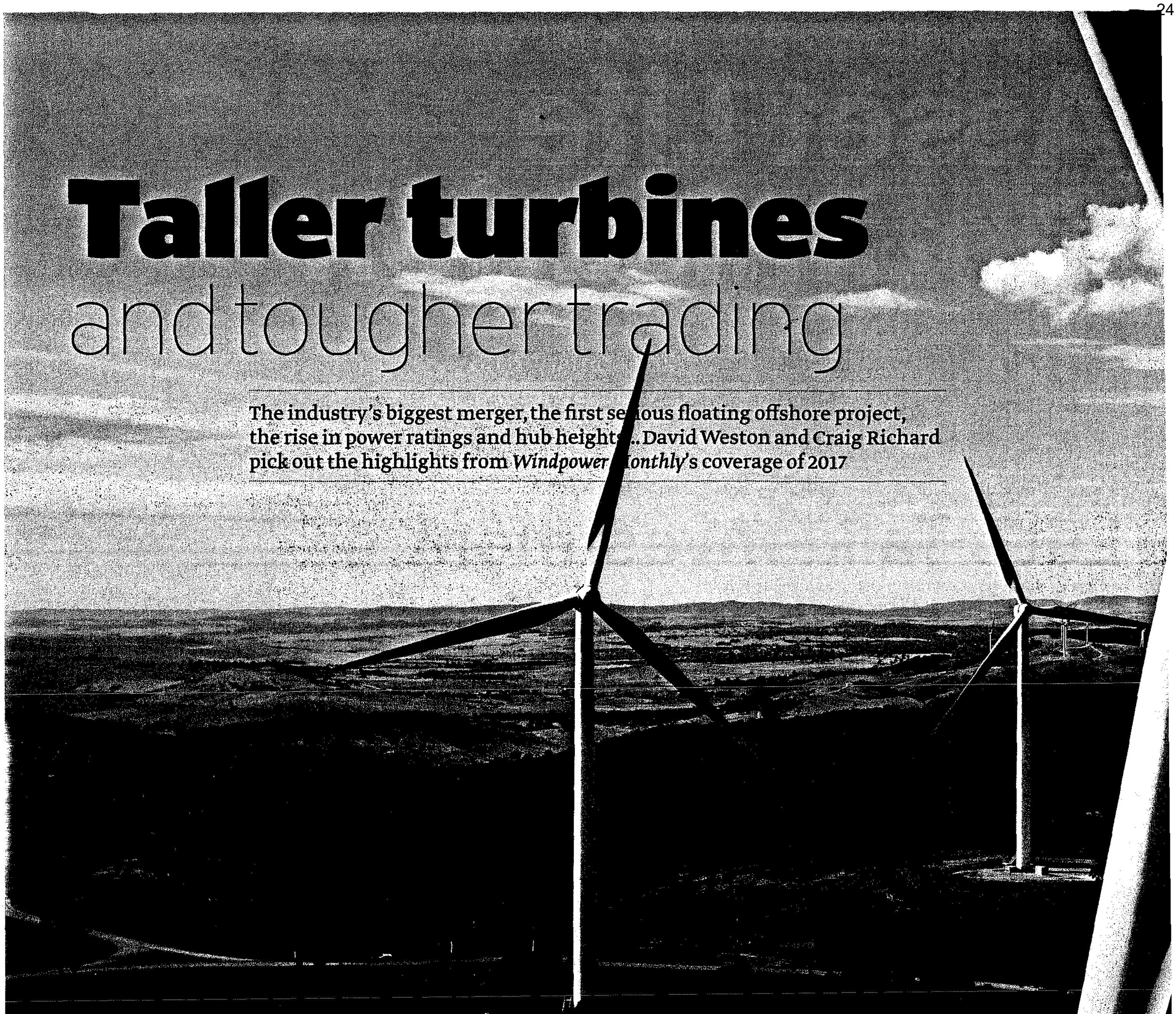

Taller turbines and tougher trading

The industry's biggest merger, the first serious floating offshore project, the rise in power ratings and hub heights... David Weston and Craig Richard pick out the highlights from *Windpower Monthly*'s coverage of 2017

January

● **Investment in offshore wind** reaches a new high, according to Bloomberg New Energy Finance (BNEF), at $29.9 billion in 2016, 40% up on the previous year. But total investment in clean energy falls 18% year-on-year to $287.5 billion. ● **MHI Vestas unveils a 9MW** evolution of its V164 offshore turbine. It would grow again within a few months. ● The UK Court of Appeal **dismisses Wobben Properties' claim** that Siemens infringed a storm-control technology patent developed for Enercon.

February

● Nordex takes control of Danish blade designer and manufacturer **SSP Technology**, putting the acquisition to good use with the announcement of a 4.0-4.5MW turbine with a 149-metre rotor diameter later in the year. ● Saudi Arabia announces a tender for 400MW of wind and 300MW of solar PV. ● FTI Consulting releases preliminary findings of its *Global Wind Market Upgrade 2016*, showing **Vestas as the world's top OEM**. Previous leader, Goldwind drops to third behind GE as a result of the slowing Chinese market. ● Siemens Wind Power confirms it will **close its blade factory** in Engesvang, west Denmark, due to "significant changes in the global wind-power market". The 430 jobs lost are on top of the 150 to be cut from another of its blade plants in Aalborg in the north of the country. ● GE Renewable Energy appoints Anne McEntee to **lead its servicing business**, while Peter McCabe takes on her old role as onshore wind chief executive.

March

● Vestas installs a new **tower design using support cables** to spread the increased load of taller turbines. The concept enables turbines to be installed on narrower towers, cutting manufacturing and transport

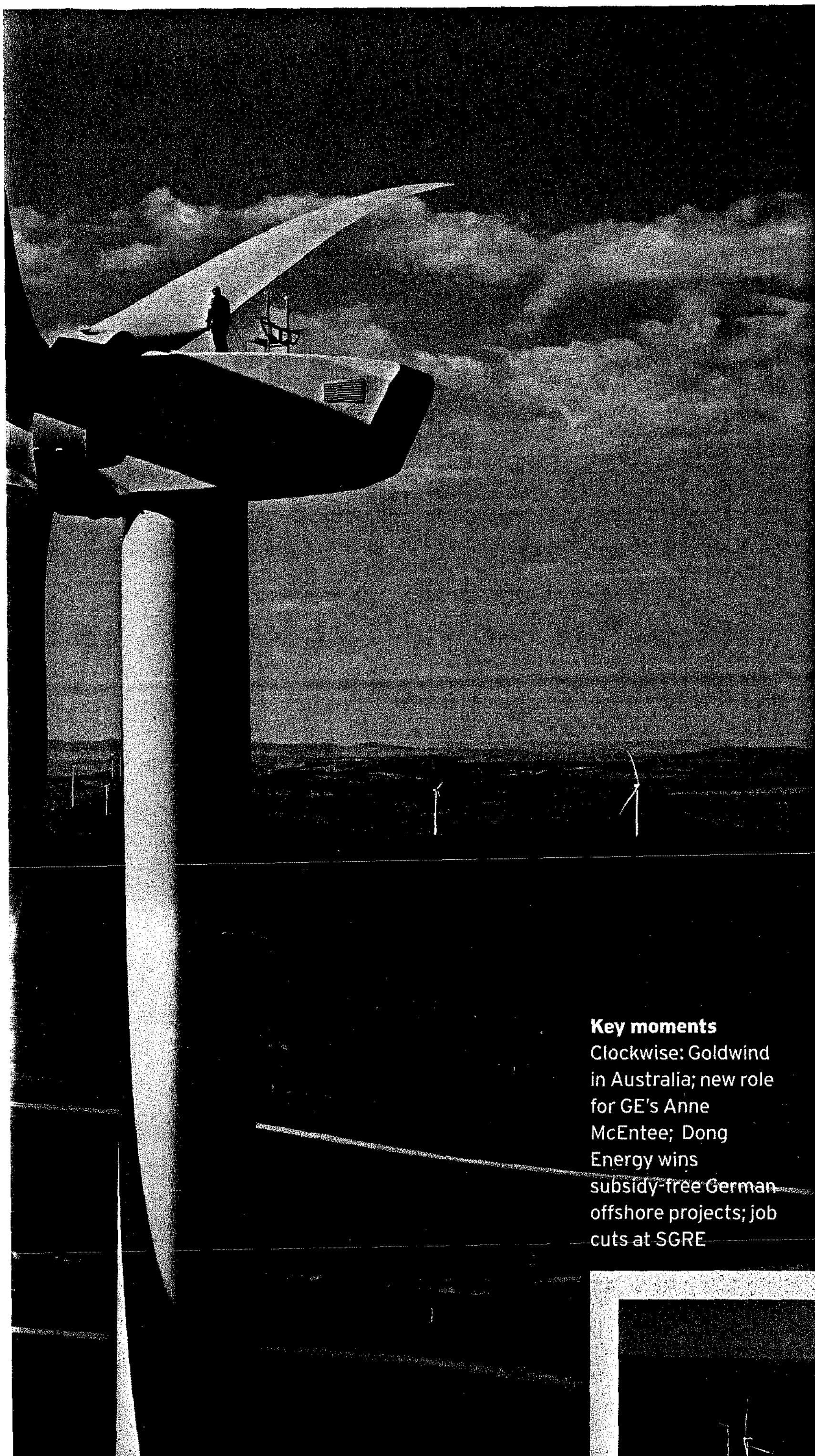

costs. ● Siemens installs a prototype of its new **low-wind SWT-3.15-142** turbine at Drantum, central Denmark. It will be available with hub heights of up to 165 metres for a tip height of around 234 metres. ● Nordex CEO **Lars Bondo Krogsgaard resigns** after the company reduced its forecast for the 2017 and 2018 financial years. Former Acciona Wind Power chief Jose Luis Blanco steps in. ● **Senvion cuts 780 jobs** with production sites at Trampe and Husum in Germany taking most of the losses. The company predicts the global move to competitive tendering will create short-term pricing pressures as it announces a two-year "transition" to adjust to market demands.

April

● The long-anticipated **merger of Siemens and Gamesa** comes into effect, creating a company with 75GW of installed wind capacity across 90 countries, and 27,000 employees. Combined annual revenue stands at €11 billion, and the company has an order backlog worth €21 billion. ● *Windpower Monthly* gets exclusive access to two new product series. **Enercon's 4.2MW EP4 platform**, the first of several 4MW-plus onshore turbines now on the market, offers an industry-first 30-year design life. **Vestas upgrades** its best-selling **V110-2MW** turbine with rotor diameters of 116 and 120 metres to boost annual energy production. ● Developers Dong Energy and EnBW are awarded licences for four projects in Germany's first competitive auction, with three sites to be built **without subsidy**. Both companies have operating offshore sites in the country already.

Key moments
Clockwise: Goldwind in Australia; new role for GE's Anne McEntee; Dong Energy wins subsidy-free German offshore projects; job cuts at SGRE

May

● Senvion lets slip at the AWEA Windpower 2017 event in California that it is working towards a **10MW-plus offshore wind turbine.** No specifics were forthcoming in London, but the Senvion-led Realcoe collaboration

would apply for EU funding to speed up development in November. ● Wind projects are allocated 2,979MW of the 3GW available in **Spain's second renewables auction**, underlining renewed interest in the country's wind market. All winning bids are made with "full discount" — meaning operators accept zero subsidy and will receive only the wholesale price for electricity generated. ● **Goldwind acquires** the up-to-530MW Stockyard Hill project in Victoria, Australia, from Origin Energy, and agrees to sell the power back to the utility. The PPA is believed to be the largest wind deal to date in Australia.

June

● Vestas shifts its 3MW platform into the **rapidly growing 4MW class**, unveiling three models with a power rating of up to 4.2MW. The low-wind V150 boasts the largest rotor diameter yet seen onshore, while the high-wind V117 takes the turbine into typhoon territory for the first time. ● MHI Vestas unveils an upgrade to its V164 offshore turbine, taking **rated capacity up to 9.5MW**. It is later specified for the UK's 950MW Moray East and 860MW Triton Knoll projects in the North Sea. ● In a first step to **align Adwen with its new parent** company, Siemens Gamesa Renewable Energy (SGRE), two separate legal entities are to be created: Adwen Operations, which will focus on four German projects equipped with its 5MW (formerly Areva) turbines, and French Pipeline, to develop 1.5GW of French offshore sites up to the start of construction. Three months later SGRE stops production plan for Adwen's 8MW offshore turbine. ● Vestas is announced as preferred turbine **supplier for 1GW** of projects won by developer Fortum in the Russian tender. Fortum will develop its capacity alongside Russian energy company Rusnano, spread across 26 projects between 2018 and 2022.

July

● Enercon is set to **refurbish up to 1,200 turbines** in India, following the conclusion of a decade-long legal dispute with former joint venture Wind World India. The firm says some 860MW of its turbines could be re-activated and updated after its ten-year absence from the world's fourth largest market, where Enercon has roughly 6,700 turbines installed. ● Elsewhere in India, the country's 1GW power auction receives 2.8GW of bids, following the success of its first auction earlier in the year. The results, announced later in October, will see prices fall to a **new low of INR 2.64/kWh** ($0.04/kWh). ● In Europe, developer **Vattenfall reshuffles its wind unit**, splitting it in three —onshore, offshore, and solar PV with storage. Vattenfall Wind CEO Gunnar Groeblar says the move "creates a lean business model ... that can respond to different markets". ● Nordex's record-breaking 230-metre high turbine in south-west Germany **produces more than 9GWh** of electricity in its first year of operation.

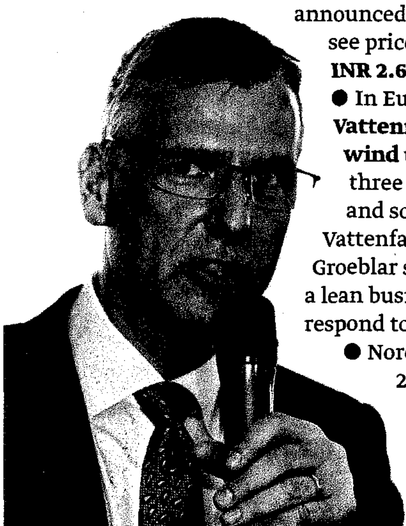

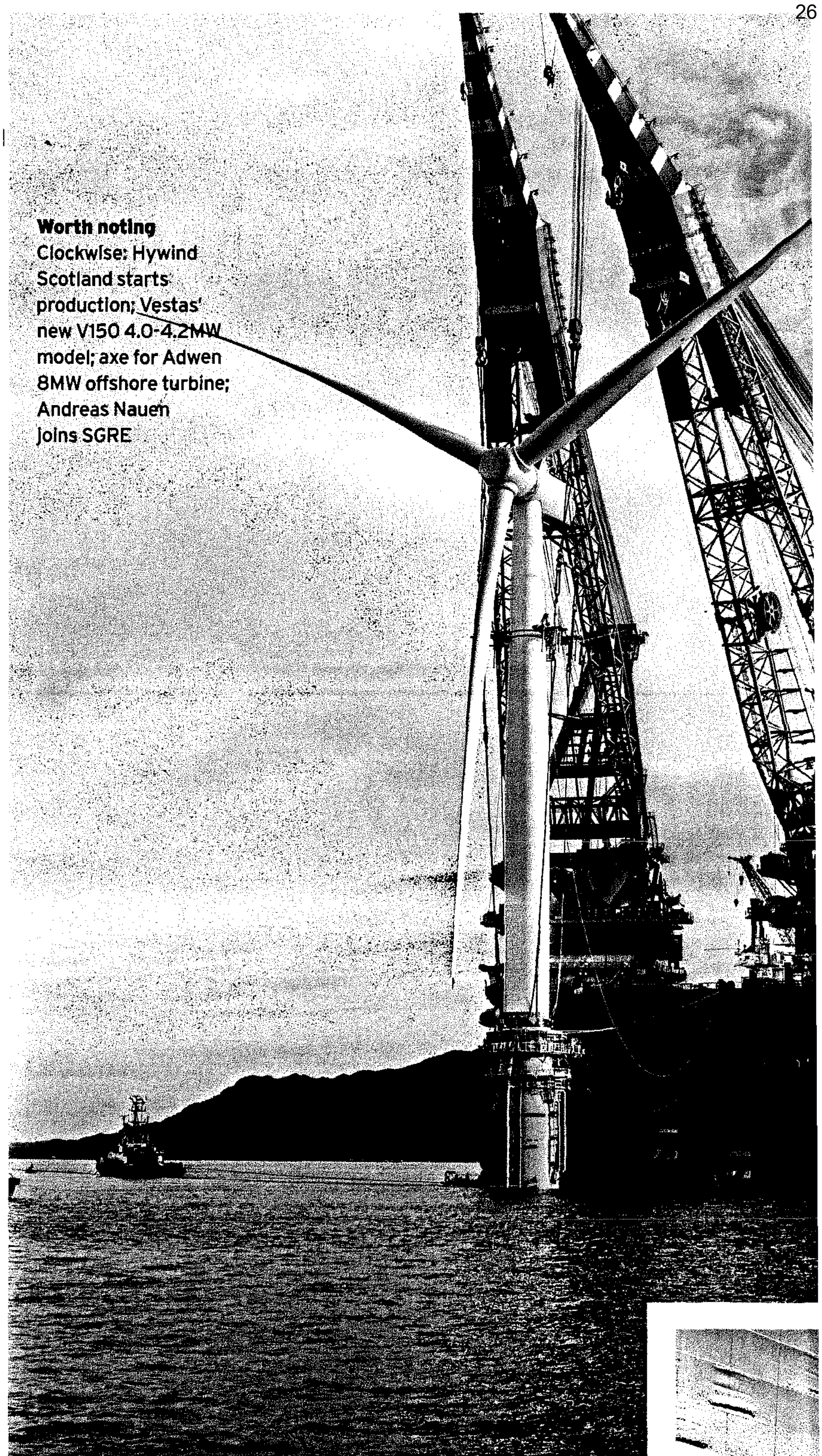

Worth noting
Clockwise: Hywind Scotland starts production; Vestas' new V150 4.0-4.2MW model; axe for Adwen 8MW offshore turbine; Andreas Nauen joins SGRE

August

In a *Windpower Monthly* exclusive, Enercon unveils a **new modular approach** it is taking with its 3MW platform. The move is in response to the shift to auction-based systems around the world forcing margins to be compressed, meaning Enercon was losing out to cheaper rivals. All future Enercon turbines will be based on the new design approach and will meet IEC wind class demands exactly, rather than exceed them, the manufacturer says. ● Rival manufacturer SGRE announces it is making up to **600 further job cuts** at its

blade plant in Aalborg. The move comes just eight months after an initial 580 jobs were cut, prior to the merger. ● GE Renewable Energy files a dispute in California claiming market leader Vestas was in breach of its **zero-voltage ride-through (ZVRT) technology patent.** ● MHI Vestas launches an investigation after its 9.5MW prototype in Osterild, Denmark, **catches fire.** The subsequent examination finds a component "damaged during installation" was the cause. MHI Vestas says the part is "unique to a prototype environment" and that the rollout of the turbine will not be affected. ● Gamesa also suffers a fire at a 13-year-old turbine in Japan. Several local news outlets show a **burned-out nacelle.**

September

● GE Renewable Energy continues the year's big technological trend, with the launch of a new 4.8MW onshore turbine for low- to medium-wind markets like Germany, the Netherlands, Turkey, Chile and Australia.

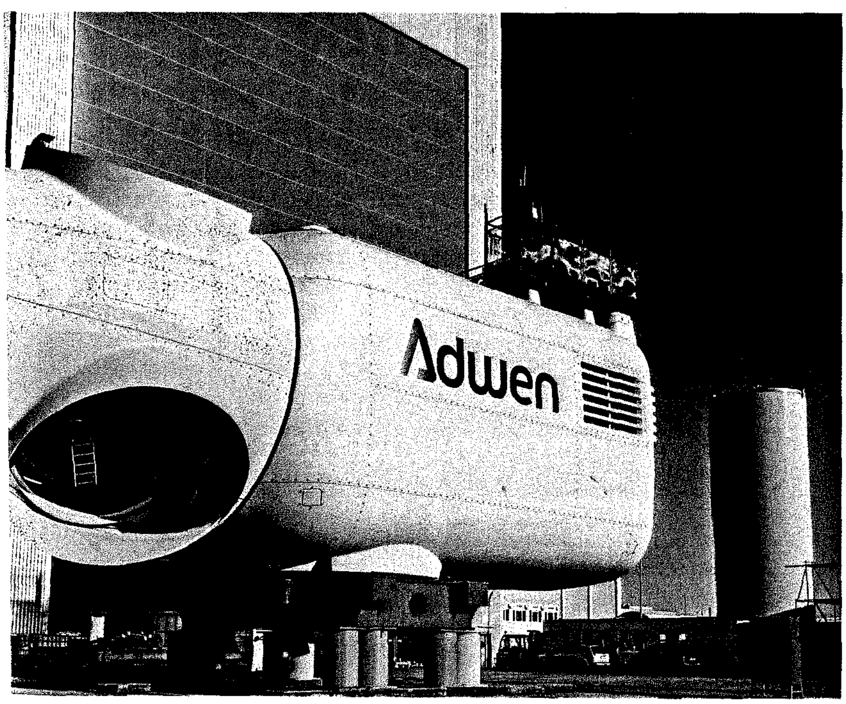

The new model features a 158-metre rotor and will offer the industry's **largest annual energy production,** GE claims. ● Vestas confirms it is **working with Elon Musk's Tesla** on energy storage solutions. Vestas is looking to increase its involvement in integrating wind and storage solutions and has been working on a number of small-scale projects over recent years.
● The year is shaping up to be a **difficult one for the leading manufacturers.** Nordex announces a €45 million cost- cutting programme, which would also see up to 500 jobs lost, mostly in Germany. ● Vestas, meanwhile, signs a deal to set up a **manufacturing hub in Russia,** on the back of potentially winning a 1GW deal with Finnish developer Fortum and its joint venture partner Rusnano, which won the majority of capacity up for grabs in June's 1.65GW tender.

October

● Andreas Nauen is back as a leading light at a major manufacturer. The former Senvion CEO is appointed to lead SGRE's offshore division, following the **departure of Michael Hannibal.** In a small reshuffle at SGRE, driven by poor financial forecasts, Miguel Angel Lopez is appointed as chief financial officer, replacing Andrew Hall, and Jürgen Bartl replaces Jose Antonio Cortajarena as general secretary. ● Max Bögl breaks its own record for the **tallest onshore turbine** in the world, reaching a tip height of 246.5 metres. The 3.4MW GE turbine, installed near Stuttgart, south-west Germany, incorporates a 40-metre high water reservoir at the base of the tower as part of a pumped-hydro storage solutions. ● October marks the **birth of floating offshore** wind. Statoil's 30MW Hywind Scotland project begins production, while Ideol inaugurates its ring-shaped pool-dampening floater, topped with a Vestas 2MW turbine, in the port of St-Nazaire, France. Ideol CEO Paul de la Guérivière describes the moment as a "turning point" in the floating wind sector.

November

● **Turbine launches at WindEurope**'s conference and exhibition in Amsterdam include SGRE's 8MW direct-drive offshore model, equipped with a 167-metre rotor and a power-mode option to increase output to 9MW. SGRE also launches a new 4MW geared platform with one model per wind-speed class. Envision reveals three new onshore models including a 4.5MW machine.
● Leading Indian manufacturer Suzlon showcases a textbook **reversal of fortune** for many turbine makers by recording a 56% year-on-year fall in income in Q3, due to the market uncertainty in the subcontinent. The firm reported a profit of INR 681 million ($10 million) in the third quarter — a 72.07% reduction year-on-year.

December

● Germany's energy regulator devises a plan to avoid some of the unintended consequences of its new onshore auction system, setting a **maximum bid price of €63/MWh** in 2018, after 2017's tenders pushed prices below current generation costs. ● Argentina's wind power gathers pace with **eight wind farms totalling almost 666MW** awarded PPAs in the second renewables tender at an average price of $41.23/MWh. **W**

ETIP Wind
EUROPEAN TECHNOLOGY & INNOVATION PLATFORM ON WIND ENERGY

ETIPWind a meeting of minds

EERA DeepWind'18, Trondheim, 17 - 19 January 2018

etipwind.eu

Turbine Manufacturers

Vestas, GE, MHI Vestas Offshore Wind, Siemens Gamesa Renewable Energy, Senvion, Enercon, Nordex

Universities, research institutes and consultants

DTU Wind Energy Department of Wind Energy, ECN, DNV·GL, Fraunhofer, SINTEF

Utilities and developers

Iberdrola Renewables, edp renewables, EDF energies nouvelles, DONG energy, e.on, res, enel, Statoil, Vattenfall

Others

ABB, LM Wind Power

ETIP Wind

etipwind.eu

What are ETIPs?

European Technology and Innovation Platforms are industry-led stakeholder fora recognised by the European Commission

Goals

- Drive innovation, knowledge transfer and European competitiveness
- Develop research and innovation agendas and roadmaps for action at EU and national levels

Many companies are in Norway because of its R&D support schemes – EU needs to emulate this success

ETIP Wind

etipwind.eu

ETIPWind publications

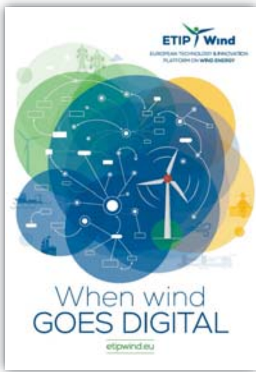

ETIP Wind

etipwind.eu

Why is ETIP needed ?

- Give EU direction in what R&I areas should be supported
- A forum where industry, research bodies and academia can meet and forge a common vision of the future
- Advisory group of CTO´s now have a forum to discuss what should be done together
- Steering Committee is the workhorse that gets stuff done.
- The key raw material for the continued success of the EU Wind industry is well trained scientists and engineers – ETIPWind can help ensure this !

ETIP Wind

etipwind.eu

Objectives of the SRIA – update in 2018

Reduce costs

Facilitate system integration

Reinforce European technological leadership

Ensure first-class human resources

ETIP Wind

etipwind.eu

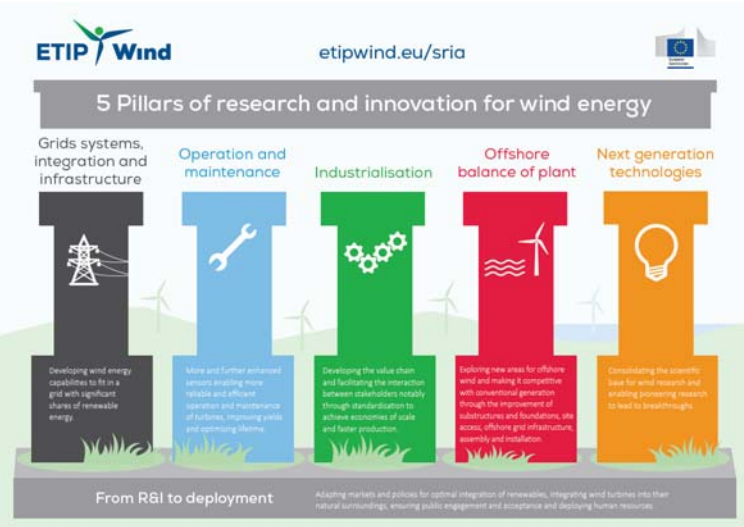

Some of what has happened
When industry meets well trained creative brains

- Vinderby 11x 450 kw erected in 11 days 1991
- Middelgrunden 20 x 2MW in 2000 - iconic
- Horns Rev 1 with 80 x 2MW first big offshore park
- BTM UK offshore report.
- A2SEA installer – Coaster with legs
- Hywind – 2.3MW floater – Statoil a first floater off Norway called "crazy" now Hywind 2 in Scotland
- London Array Phase 1 630MW - huge
- Ørsted q European world champion in wind

ETIP Wind etipwind.eu

Scope of the discussion

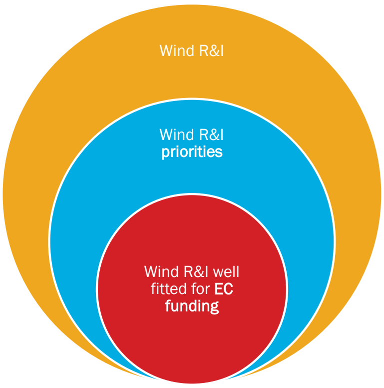

ETIP Wind etipwind.eu

Technology

ETIP Wind etipwind.eu

ETIP Wind
EUROPEAN TECHNOLOGY & INNOVATION PLATFORM ON WIND ENERGY

What has and is happening in offshore wind ?

etipwind.eu

What needs to happen

- Costs needs to continue to drop
  - Structures need industrialization
  - Cables
  - Installation and maintenence
  - Robotics
- Offshore wind is bulk electricity – challenges
  - Large scale storage
  - Watershed – Grid has to become renewable friendly not the opposite

ETIP Wind etipwind.eu

All wind actors need to

- Drive digitalization
- Drive storage
- Drive cyber security
- Drive and enable the electrification of society
- Provide a credible back bone to climate change challenged electricity system

If you do cannot drive you are left behind

In weather terms offshore is coming onshore with increased flooding and marinisation of land

ETIP Wind

etipwind.eu

ETIP Wind

EUROPEAN TECHNOLOGY & INNOVATION PLATFORM ON WIND ENERGY

Thank you
www.etipwind.eu

etipwind.eu


EERA
European Energy Research Alliance
The European Energy Research Alliance &Wind
Dr. Nils A. Røkke – Chair EERA
EERA – DeepWind 2018 – 17-19 January 2018

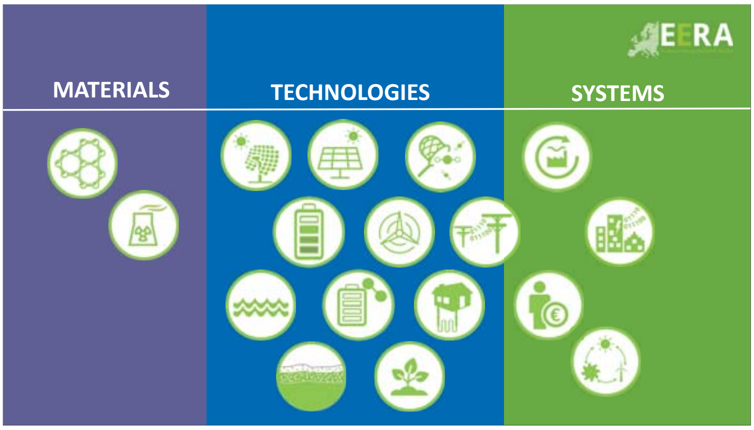
EERA
MATERIALS
TECHNOLOGIES
SYSTEMS

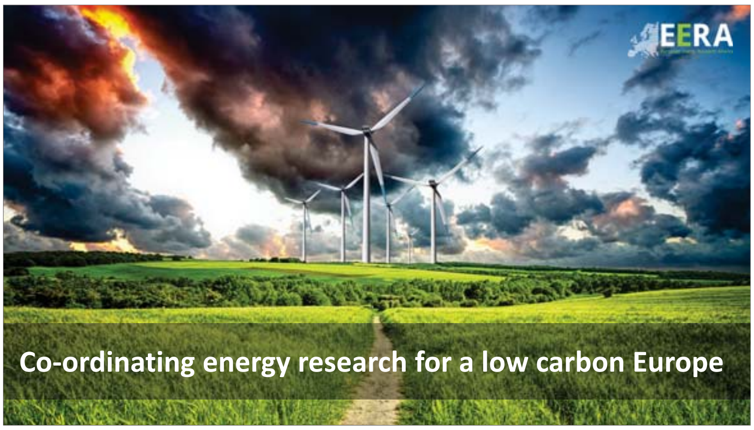
EERA
Co-ordinating energy research for a low carbon Europe

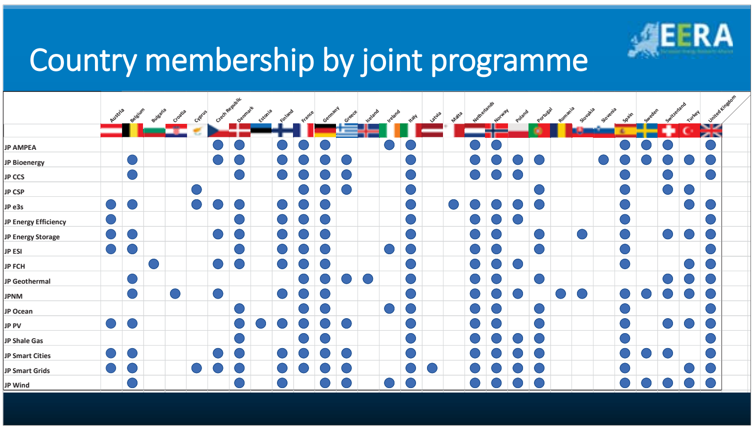
Country membership by joint programme
EERA
JP AMPEA
JP Bioenergy
JP CCS
JP CSP
JP e3s
JP Energy Efficiency
JP Energy Storage
JP ESI
JP FCH
JP Geothermal
JPNM
JP Ocean
JP PV
JP Shale Gas
JP Smart Cities
JP Smart Grids
JP Wind


Most influential energy research community in EU & globally
EERA
50 000 +
Experts
250 +
Organisations
29
Countries
All 10
SET Key Actions
17
Joint Research Programs
All 9
ETIPS and other platforms
35%
Cross-cutting & societal challenges
4 out of 7
Mission Innovation Challenges … so far

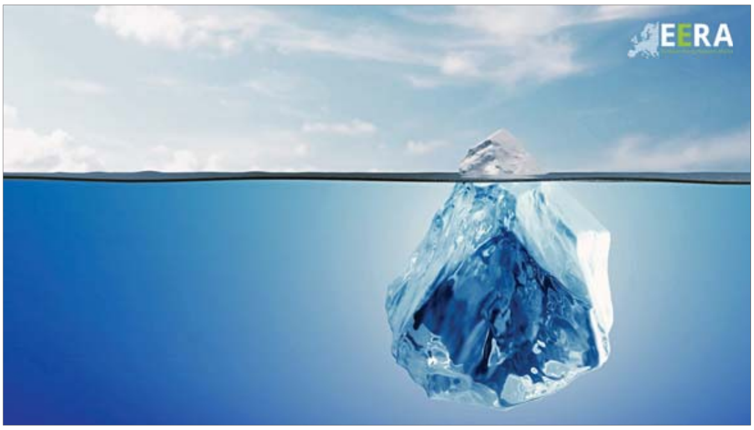
EERA

IRPWIND

IRPWind

Total budget: €9.8 million

- €6 million for 3 Core Projects (each linked to national projects)
  - Offshore
  - Structural Reliability
  - Integration
- 4 M EUR for CSA
  - Mobility
  - Research Infrastructure
  - Secretariat, management
  - Access to data

Nationally funded collaborative projects

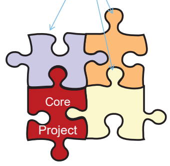

Not all EERA Wind members directly involved (but CSA-part benefits all)
Ends in April 2018

Supported by

EERA JP WIND structure and sub-programmes

- **Joint Programme Coordinator:** DTU Wind Energy
- **Wind Conditions.** Coordinated by DTU, Denmark.
- **Aerodynamics.** Coordinated by ECN, the Netherlands.
- **Offshore Wind Energy.** Coordinated by SINTEF, Norway.
- **Grid Integration.** Coordinated by Fraunhofer IWES, Germany.
- **Research Facilities.** Coordinated by CENER, Spain.
- **Structures and Materials.** Coordinated by CRES, Greece
- **Wind Integration – economic and social aspects.** Coordinated by DTU, Denmark

- **14 Full Participants and 36 Associate Participants**
- **Election of new Management Board in March 2018**

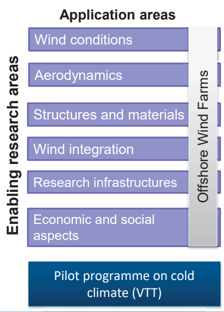

EERA

EERA JP WIND port folio

IRPWind

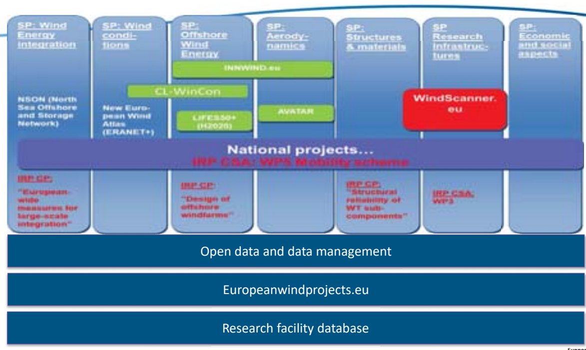

Supported by

Funding for EERA activities

National projects (competitive)	**In-kind** (institutional)
EU calls (H2020) e.g. CSA, IRP, ECRIAs	Other types of **Joint Programming** e.g. ERANET+, Berlin Model

- **Coordination** of research activities
- Collaboration for **common R&I agendas**
- Co-creation of new **joint R&I projects and programmes**

EERA 9


EERA
European Energy Research Alliance
Co-ordinating Energy Research for a Low Carbon Europe

A1) New turbine and generator technology

Lightweight design of the INNWIND.EU and AVATAR rotors through multi-disciplinary optimization algorithms, A.Croce, Politecnico di Milano

Initial Design of a 12 MW Floating Offshore Wind Turbine, P.T.Dam, University of Ulsan

Performance Assessment of a High Definition Modular Multilevel Converter for Offshore Wind Turbines, R.E.Torres-Olguin, SINTEF Energi

Mitigation of Loads on Floating Offshore Wind Turbines through Advanced Control Strategies, D. Ward, Cranfield University

POLItecnico di Milano

POLITECNICO MILANO 1863

Lightweight design of the INNWIND.EU and AVATAR rotors through multi-disciplinary optimization algorithms

A. Croce[1], L. Sartori [1], P. Bortolotti[2], C.L. Bottasso[2,1]

[1] Department of Aerospace Science and Technology,Politecnico di Milano, Italy
[2] Technische Universität München, Germany

EERA DeepWind 2018, 17 January 2018, Trondheim

EERA DeepWind 2018

Holistic Design of Wind Turbines

Classical approach to design: (weak) loops between specialist groups

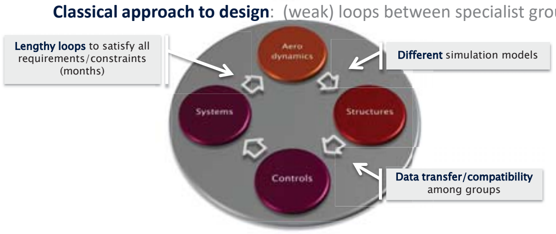

There is a need **for multi-disciplinary optimization tools**, which must:

- Be **fast** (hours/days) (on standard hardware!)
- Provide solutions **in all areas** (aerodynamics, structures, controls, sub-systems)
- **Account** ab-initio for all complex **couplings** (no fixes a posteriori)
- Use **fully-integrated** tools (manual intervention very limited)

These tools will never replace the experienced designer! … but would greatly speed-up design, improve exploration/knowledge of design space

POLITECNICO MILANO 1863 POLI-Wind Research Lab

EERA DeepWind 2018

Outline

- Background
- Multi-disciplinary design algorithms for wind turbines
  - **Cp-Max:** a modular design framework
- Passive load-alleviation techniques
- Applications
  - Lightweight redesign of the INNWIND.EU rotor
  - Lightweight redesign of the AVATAR rotor
- Conclusions

POLITECNICO MILANO 1863 POLI-Wind Research Lab

EERA DeepWind 2018

Cp-Max: a modular design framework

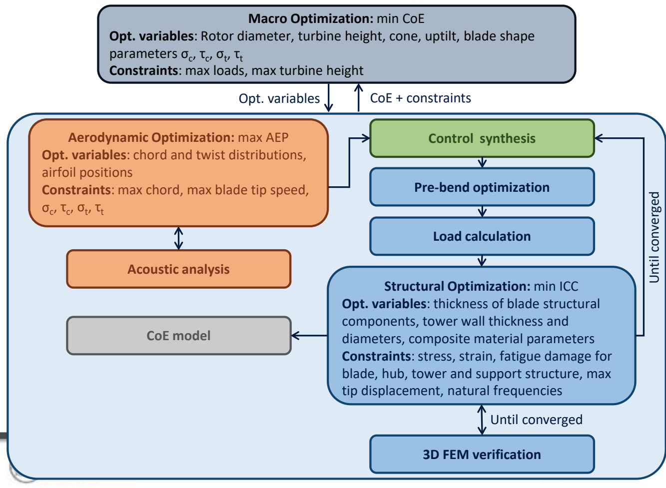

EERA DeepWind 2018

Background

- Large rotors for 10+ MW wind turbines:
  - Strong aero-servo-elastic couplings
  - High mass and loads due to slender and flexible components
- Load-mitigation:
  - Passive and active techniques
  - Reduced loads on blades and fixed infrastructure
  - Impact on the AEP
- **MDAOs** help the design process:
  - High-fidelity models *plus* dedicated optimization methods
  - Automatic management of preliminary/detailed design of WTs
  - Trade-offs and cost-oriented studies

POLITECNICO MILANO 1863 POLI-Wind Research Lab

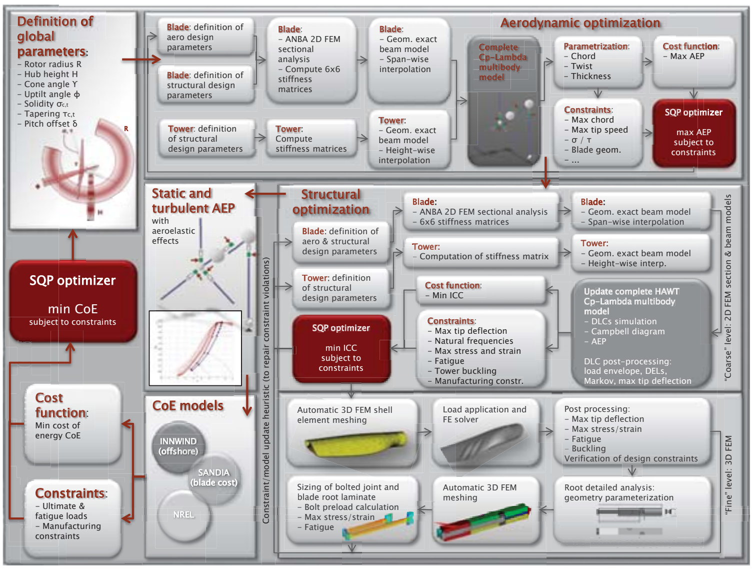

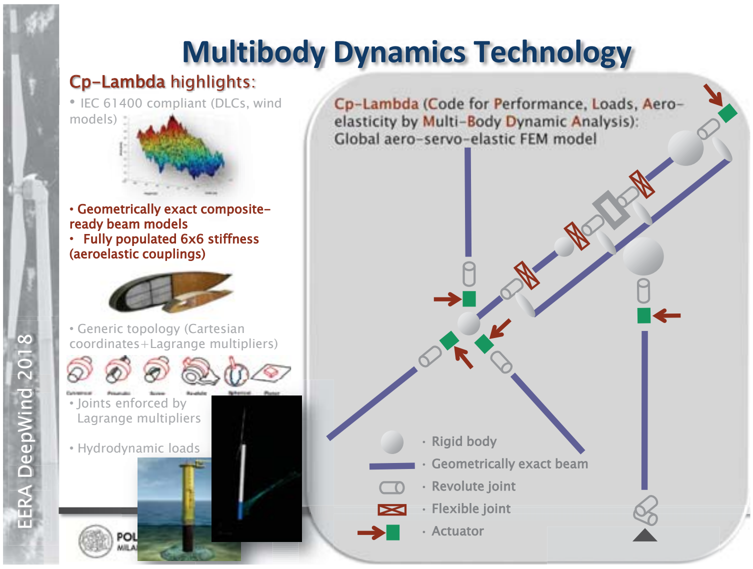
Multibody Dynamics Technology
Cp-Lambda highlights:
• IEC 61400 compliant (DLCs, wind models)
• Geometrically exact composite-ready beam models
• Fully populated 6x6 stiffness (aeroelastic couplings)
• Generic topology (Cartesian coordinates+Lagrange multipliers)
• Joints enforced by Lagrange multipliers
• Hydrodynamic loads
Cp-Lambda (Code for Performance, Loads, Aero-elasticity by Multi-Body Dynamic Analysis):
Global aero-servo-elastic FEM model
· Rigid body
· Geometrically exact beam
· Revolute joint
· Flexible joint
· Actuator
EERA DeepWind 2018


Manufactured Blades
2MW – 45m (MAIT-Gurit) ▼
300kW – 16m (Italtech-Gurit-Euros) ▼
700kW – 24m (ETA-Gurit-ECN) ▼
100kW – 10m (ETA) ▼
EERA DeepWind 2018
POLITECNICO MILANO 1863
POLI-Wind Research Lab

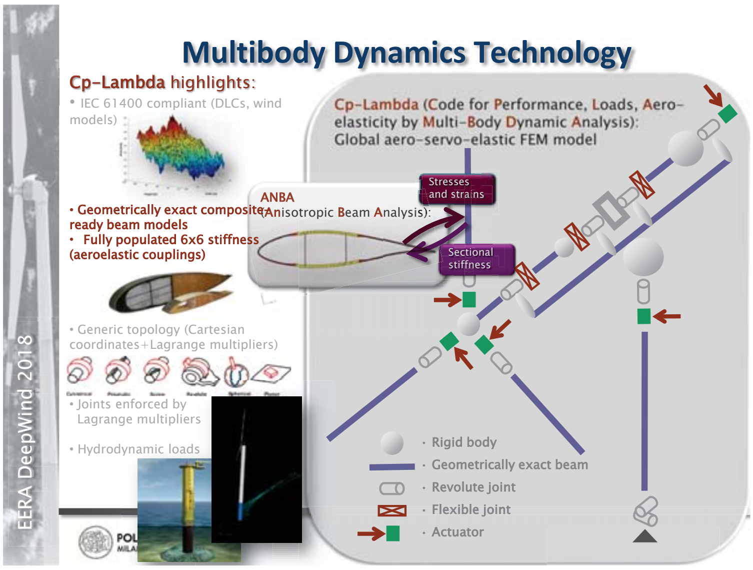
Multibody Dynamics Technology
Cp-Lambda highlights:
• IEC 61400 compliant (DLCs, wind models)
• Geometrically exact composite-ready beam models
• Fully populated 6x6 stiffness (aeroelastic couplings)
• Generic topology (Cartesian coordinates+Lagrange multipliers)
• Joints enforced by Lagrange multipliers
• Hydrodynamic loads
Cp-Lambda (Code for Performance, Loads, Aero-elasticity by Multi-Body Dynamic Analysis):
Global aero-servo-elastic FEM model
ANBA (Anisotropic Beam Analysis):
Stresses and strains
Sectional stiffness
· Rigid body
· Geometrically exact beam
· Revolute joint
· Flexible joint
· Actuator
EERA DeepWind 2018

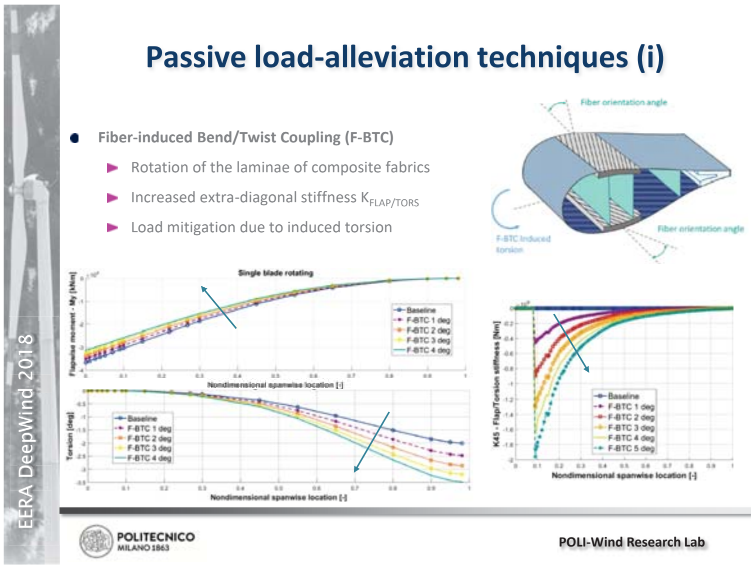
Passive load-alleviation techniques (i)
• Fiber-induced Bend/Twist Coupling (F-BTC)
▶ Rotation of the laminae of composite fabrics
▶ Increased extra-diagonal stiffness $K_{FLAP/TORS}$
▶ Load mitigation due to induced torsion
Fiber orientation angle
F-BTC induced torsion
Single blade rotating
Baseline
F-BTC 1 deg
F-BTC 2 deg
F-BTC 3 deg
F-BTC 4 deg
F-BTC 5 deg
Nondimensional spanwise location [-]
EERA DeepWind 2018
POLITECNICO MILANO 1863
POLI-Wind Research Lab

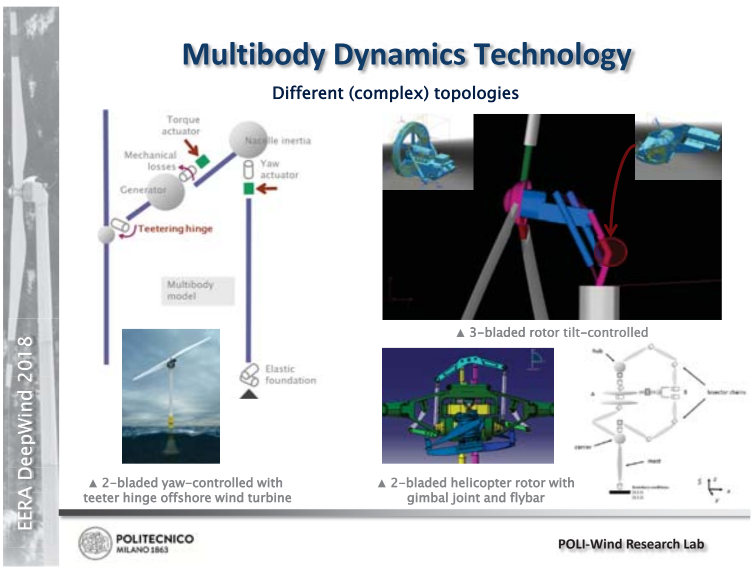
Multibody Dynamics Technology
Different (complex) topologies
Torque actuator
Nacelle inertia
Mechanical losses
Yaw actuator
Generator
Teetering hinge
Multibody model
Elastic foundation
▲ 3-bladed rotor tilt-controlled
▲ 2-bladed yaw-controlled with teeter hinge offshore wind turbine
▲ 2-bladed helicopter rotor with gimbal joint and flybar
EERA DeepWind 2018
POLITECNICO MILANO 1863
POLI-Wind Research Lab

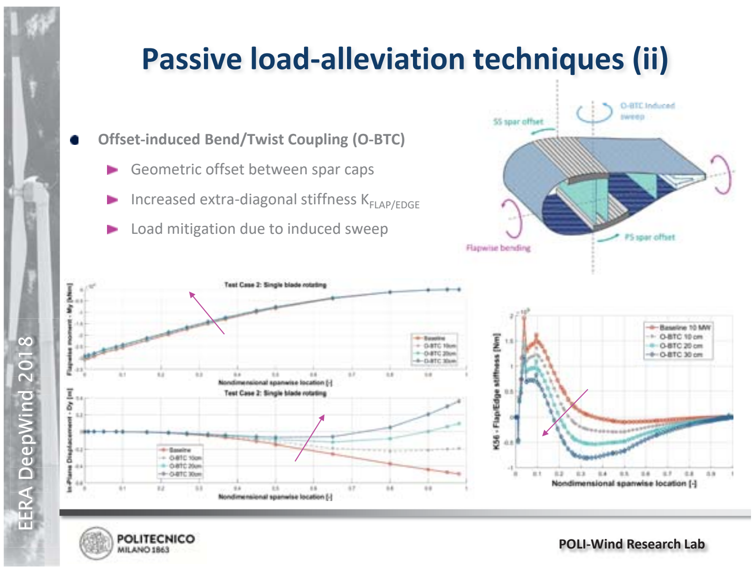
Passive load-alleviation techniques (ii)
• Offset-induced Bend/Twist Coupling (O-BTC)
▶ Geometric offset between spar caps
▶ Increased extra-diagonal stiffness $K_{FLAP/EDGE}$
▶ Load mitigation due to induced sweep
O-BTC induced sweep
SS spar offset
PS spar offset
Flapwise bending
Test Case 2: Single blade rotating
Baseline 10 MW
O-BTC 10 cm
O-BTC 20 cm
O-BTC 30 cm
Nondimensional spanwise location [-]
EERA DeepWind 2018
POLITECNICO MILANO 1863
POLI-Wind Research Lab

EERA DeepWind 2018

Reference wind turbines

	INNWIND.EU	AVATAR
Design philosophy	Classic, max(Cp)	Low Induction
Rated power [MW]	10	10
IEC Class [–]	1A	1A
Blade length [m]	86.35	100.08
Rotor diameter [m]	178.3	205.76
Hub height [m]	119	132.5
Nacelle up-tilt [deg]	5	5
Rotor pre-cone [deg]	2.5	2.5
Rotor speed [RPM]	9.6	9.6
Blade mass [kg]	42481	50126
Tower mass [kg]	628441	628441

EERA DeepWind 2018

Lightweight redesign of the AVATAR rotor

Parametric lightweight redesign

- Parametric F-BTC (carbon spar caps) + pitch re-scheduling

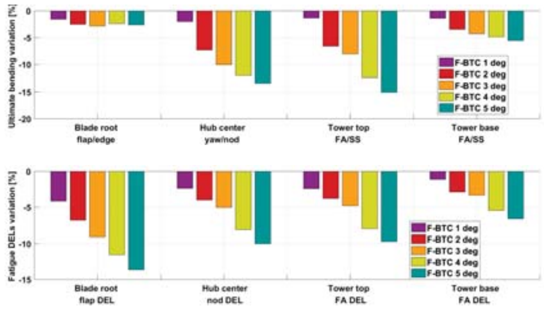

Comparisons against the Baseline 10 MW – 206m

EERA DeepWind 2018

Lightweight redesign of the AVATAR rotor

Low-Induction Rotors

- Classic WTs operate at Optimal C_P ($a \approx 1/3$)
- By operating at Lower Induction, one could trade some efficiency to achieve lower loads[1]
- Impact on COE and support structure is still not very well studied

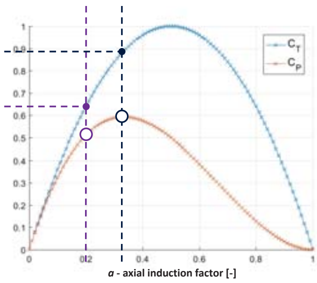

Reference:

[1] Chaviaropoulos, P. K., Beurskens, H. J. M. and Voutsinas, S. G., " Moving towards large(r) rotors - is that a good idea?" Proceedings of EWEA 2013, Vienna, Austria.

EERA DeepWind 2018

Lightweight redesign of the AVATAR rotor

Parametric lightweight redesign

- Parametric F-BTC (carbon spar caps) + pitch re-scheduling

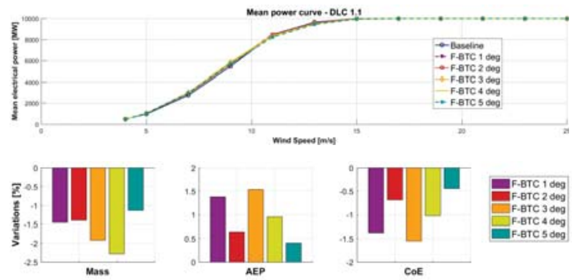

EERA DeepWind 2018

Lightweight redesign of the AVATAR rotor

Setup

Goals:

- Apply F-BTC to mitigate loads
- Redesign rotor to minimize the ICC
- Optimize collective pitch to increase AEP

Cp-Max modules:

- Structural Design Submodule (SDS)
- Finite Element Model
- Stability analysis tool

Design constraints:

- Same radius of the Baseline
- Same planform of the Baseline

Note: all rotors satisty the same design constraints!

EERA DeepWind 2018

Lightweight redesign of the AVATAR rotor

Final comparison

Results:

- All loads reduced. Best reduction for F-BTC of 5°
- AEP restored by optimal pitch scheduling
- COE reduction for all the parametric solutions

BR – Blade root
HC – Hub center
TT – Tower top
TB - Tower base

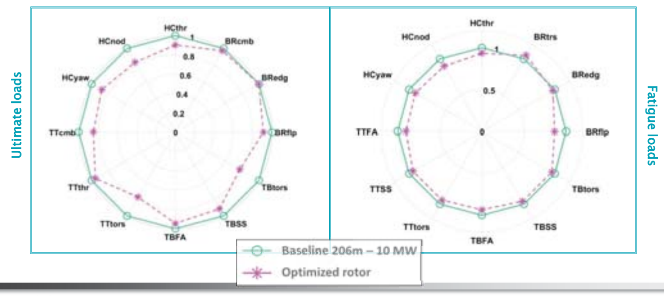

EERA DeepWind 2018

Lightweight redesign of the INNWIND.EU rotor

Setup

Goals:

- Apply F-BTC, O-BTC and IPC to mitigate loads
- Redesign rotor to optimize COE

Cp-Max modules:

- Aerodynamic Design Submodule (ADS)
- Structural Design Submodule (SDS)

Design constraints:

- Same hub thrust of the Baseline
- All loads at Hub, Tower Base < 1.10 than the Baseline
- Same rotor solidity of the Baseline

EERA DeepWind 2018

Conclusions

Remarks

- Several completed and ongoing activities about aero-structural rotor **tailoring**
- Application of **load mitigation** techniques to 10 MW concepts
- Important **loads reduction** (on hub and tower base)
- AEP losses could be limited by:
  - Elongating the blade (*Optimal-Cp* design)
  - Optimizing the collective pitch (*Low-Induction* design)
- Automated design procedures can help in identifying the **best trade-offs**

Outlook

- Application of additional load mitigation techniques (flap, VGs)
- Assessment of the effect of load alleviation techniques on the rotor stability
- Include airfoil shapes in the optimization loop
- **Add** module to analyze and **design the support structure**

EERA DeepWind 2018

Lightweight redesign of the INNWIND.EU rotor

Results:

- Longer blade
- Larger AEP
- Same thrust
- Loads at HC, TB do not exceed 10% more than Baseline

BR – Blade root
HC – Hub center
TT – Tower top
TB - Tower base

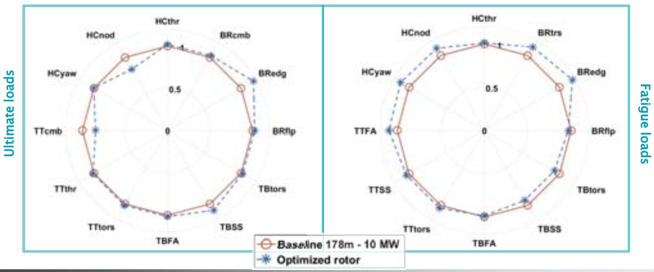

EERA DeepWind 2018

POLI-Wind Research Lab

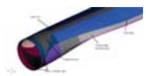

in collaboration with

Carlo L. Bottasso [†,*], Pietro Bortolotti [†], Luca Sartori [*]
[*] Department of Aerospace Science and Technology,Politecnico di Milano, Italy
[†] Technische Universität München, Germany

Presenting Author:

Prof. Alessandro Croce
Department of Aerospace Science and Technology
Politecnico di Milano

Phone: +39 02 2399 8322
E-mail: alessandro.croce@polimi.it
Web: www.poliwind.org

POLITECNICO MILANO 1863

EERA DeepWind 2018

Lightweight redesign of the INNWIND.EU rotor

	Baseline 178m - 10 MW	Optimized rotor	Variation %
Diameter [m]	178	188	+ 5 %
SC fiber angle [deg]	0	5	-
SC offset [cm]	0	20	
Max chord [m]	6.2	6.3	+ 1.6 %
Blade mass [ton]	42.4	48.9	+ 15.5 %
AEP [GWh]	46.4	48.3	+ 4.15 %
COE [€/MWh]	74.9	72.8	- 2.8 %

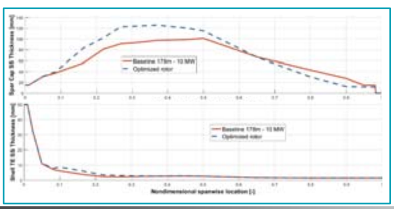

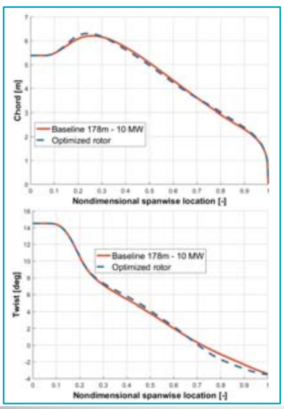

Initial Design of a 12 MW Floating Offshore Wind turbine

***Pham Thanh Dam**, Byoungcheon Seo, Junbae Kim, Hyeonjeong Ahn, Rupesh Kumar, Dongju Kim and Hyunkyoung Shin*[*†]

School of Naval Architecture & Ocean Engineering, University of Ulsan, Korea
EERA DeepWind'2018, JAN. 17, 2018, Trondheim, Norway

Outline

- 12MW FOWT design
- Numerical Simulation
- Design Load Cases
- Results
- Conclusion

12MW FOWT Design

UOU 12MW Wind Turbine Model

Design Process

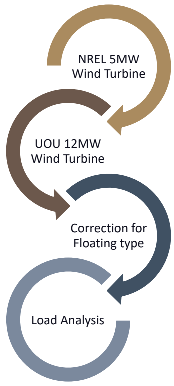

- Upscaling process SCSG/Flexible Shaft/Carbon Sparcap
- Blade (CFRP)
- Tower
- Control
- Platform
- Optimized platform
- Negative damping issue
- Tower 3P issue
- IEC61400-1
- IEC61400-3
- IEC61400-3-2

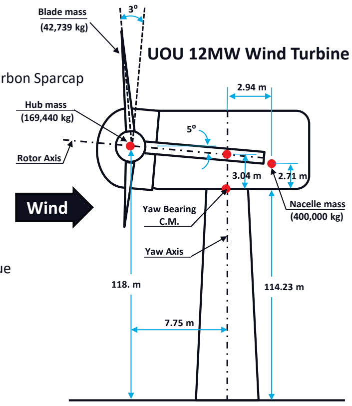

12MW Blade Scale ratio

- $P = C_p * \frac{1}{2}\rho A V^3$
- $\lambda_{Blade} = \sqrt{\frac{P_{12MW}}{P_{5MW}}} = 1.549$

P : Rotor power (kW)
ρ : Air density ($1.225\ kg/m^3$)
A : Rotor swept area (m^2)
V : Wind speed (m/s)
λ_{Blade} : Blade Scale Ratio

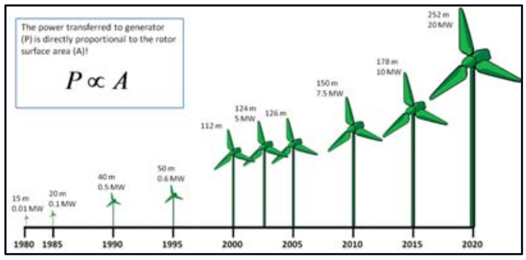

Source : EWEA, Wind energy—the facts: a guide to the technology, economics and future of wind power, 2009.

12MW Carbon blades

- **61.5 (m) 5MW glass blade : 17.7 ton**
  - **→ 95.28 (m) 12MW glass blade : 62.6 ton (Too heavy)**
  - **→ 95.28 (m) 12MW carbon (sparcap) blade : 42.7 ton**

Sparcap (43% of the total weight – 5MW class IIA)

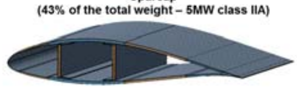

	0° Stiffness [Gpa]	Density [kg/m³]	Blade Weight [ton]	Center of Gravity [m]
CFRP	130	1572	42.7 (Carbon Sparcap)	31.8
GFRP	41.5	1920	62.6	31.8

Source : H. G. Lee, Korea Institute of Materials Science(KIMS)

N.F. [Hz]	1st Flapwise	2nd Flapwise	1st Edgewise	2nd Edgewise
12MW Blade	0.5770	1.6254	0.8920	3.2676

- Scale-up blade properties(deflection)

$$\frac{EI_{12}}{EI_5} = \left(\frac{L_{12}}{L_5}\right)^4$$

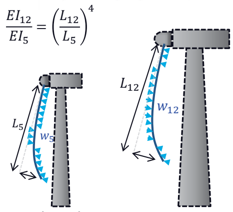

12MW Super conductor synchronous generator

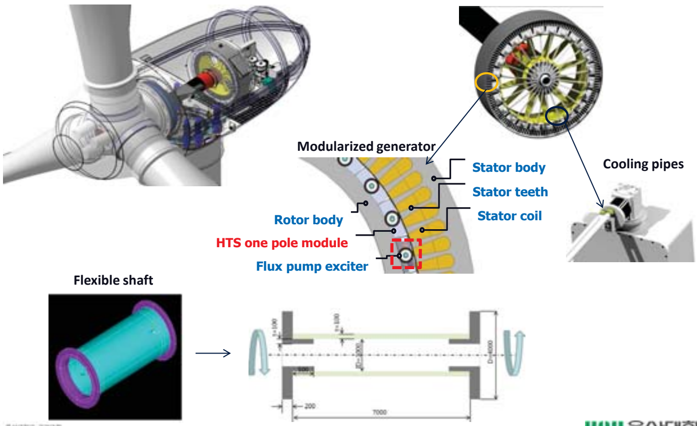

Design Summary

Rating	5 MW	12 MW
Rotor Orientation	Upwind, 3 Blades	Upwind, 3 Blades
Control	Variable Speed, Collective Pitch	Variable Speed, Collective Pitch
Drivetrain	High Speed, Multiple-Stage Gearbox	Low Speed, Direct Drive(gearless)
Rotor, Hub Diameter	126 m, 3 m	195.2 m, 4.64 m
Hub Height	90 m	118 m
Cut-In, Rated, Cut-Out Wind Speed	3 m/s, 11.4 m/s, 25 m/s	3 m/s, 11.2 m/s, 25 m/s
Cut-In, Rated Rotor Speed	6.9 rpm, 12.1 rpm	3.03 rpm, 8.25 rpm
Overhang, Shaft Tilt, Pre-cone	5 m, 5°, 2.5°	7.78 m, 5°, 3°
Rotor Mass	110,000 kg	297,660 kg
Nacelle Mass	240,000 kg	400,000 kg (*Target*)
Tower Mass (for offshore)	249,718 kg	735,066 kg

12MW Tower properties

▣ Scale up using offshore tower from OC4 definition

▣ 12MW "Material : steel, Height : 110.88 m, Weight : 781.964 ton (scale-up)"
[cf. UPWIND report 2011 : 983 ton (10MW), 2,780 ton (20MW)]

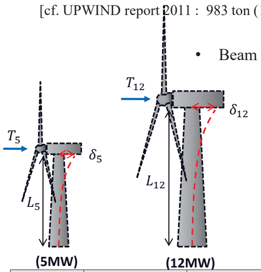

- Beam deflection $\delta = \frac{TL^3}{3EI}$ $\quad \frac{\delta_{12}}{\delta_5} = \frac{L_{12}}{L_5}$ $\quad \frac{T_{12}}{T_5} = \frac{12\ \text{MW}}{5\ \text{MW}}$
- Scale-up tower properties $\quad T = C_t * \frac{1}{2}\rho A V^2$

$$\boxed{\frac{EI_{12}}{EI_5} = \frac{12L_{12}^2}{5L_5^2} \text{ (Beam deflection)}}$$

- Tower scale ratio

$$\lambda_T = \sqrt[4]{\frac{EI_{12}}{EI_5}} = \sqrt[4]{\frac{12L_{12}^2}{5L_5^2}} = 1.482$$

	Tower height	Tower-base diameter	Tower-base thickness	Tower-top diameter	Tower-top thickness	Tower mass
5MW	77.6 m	6.5 m	0.027 m	3.87 m	0.019 m	249,718 kg
12MW	110.88 m	9.634 m	0.040 m	5.736 m	0.028 m	781,964 kg
12MW R1	104.23 m	9.634 m	0.040 m	5.736 m	0.028 m	735,066 kg

OC4 semi-submersible models

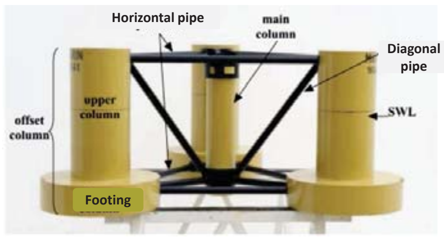

12MW Campbell diagram (Tower Redesign)

▣ **Tower Length : 104.23 m**

▣ **Tower Mass : 735,066 kg**

▣ **Rotor speed : 8.25 rpm**

➢ Rotor 3P-Excitation : 0.4125

➢ Tower 1st Side to Side Natural Frequency : 0.4337

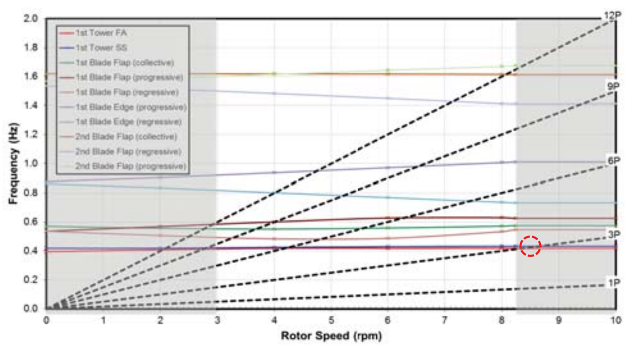

OC4 semi-submersible models

Elements	Parameters	Unit	OC4 semi Original	OC4 semi NTNU Optimal (*)	OC4 semi UOU-modified
Main column	Diameter	m	6.5	6.5	6.500
	Wall thickness	m	0.03	0.030	0.030
	Elevation above SWL	m	10	10.000	10.000
	Depth of base below SWL	m	20	20.000	20.000
Offset Column	Wall thickness	m	0.06	0.060	0.060
	Elevation above SWL	m	12	12.000	12.000
	Spacing between OCs	m	50	50.000	50.000
	Depth of base below SWL	m	20	20.000	20.000
Upper Column	Diameter	m	12	9.900	9.900
	Length	m	26	26.000	26.000
	Height of Ballast (water)	m	7.83	2.630	1.390
Footing Pontoon	Diameter	m	24	24.000	23.500
	Length	m	6	6.000	6.000
	Height of Ballast (water)	m	5.0478	5.625	5.880
Mass	Platform steel	kg	3,852,000	3,567,000	3,502,000
	Platform ballast	kg	9,620,820	8,350,000	8,068,000
	Platform total	kg	13,472,820	11,917,000	11,570,000
	Total system	kg	14,072,538	12,516,718	12,169,718
Bouyancy	Volume	m3	13,917	12,402	12,054
	CB below SWL	m	-13.15	-13.93	-13.48

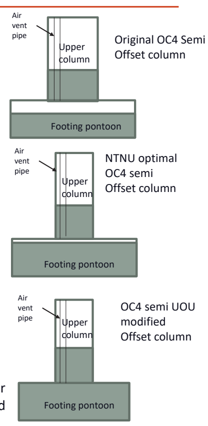

Fulfill ballast water in base column tanks (water level is on the top of air vent pipe) will reduce the difference of pressure between inside and outside footing ballast tank

(*) Leimeister,NTNU 2016 ,Rational Upscaling and Modelling of a Semi-Submersible Floating Offshore Wind Turbine

Principle of platform upscaling

Main column	Diameter	K1	Ratio tower base diameter upscale/original
	Wall thickness	K1	Ratio tower base diameter upscale/original
	Elevation above SWL	K	Ratio WT mass Upscale/original
	Depth of base below SWL	K	Ratio WT mass Upscale/original
Offset Columns	Wall thickness	K	Ratio WT mass Upscale/original
	Elevation above SWL	K	Ratio WT mass Upscale/original
	Spacing between OCs	K	Ratio WT mass Upscale/original
	Depth of base below SWL	K	Ratio WT mass Upscale/original
Upper Columns	Diameter	K	Ratio WT mass Upscale/original
	Length	K	Ratio WT mass Upscale/original
	Heigh of Ballast (water)	K	Ratio WT mass Upscale/original
Footing Pontoons	Diameter	K	Ratio WT mass Upscale/original
	Length	K	Ratio WT mass Upscale/original
	Heigh of Ballast (water)	K	Ratio WT mass Upscale/original
Pipes	Diameter	K	Ratio WT mass Upscale/original
	Wall thickness	K	Ratio WT mass Upscale/original

$$K = \sqrt[3]{\frac{12MW\_WT\_mass}{5MW\_WT\_mass}} \qquad K_1 = \frac{Tower\_base\_diameter_{12MW}}{Towe\_base\_diameter_{5MW}}$$

WT_mass includes: Rotor (blades and hub) mass, nacelle mass and tower mass

Platform steel mass reduction

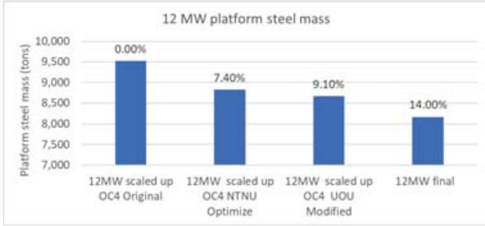

Parameters	Unit	12MW scaled up OC4 Original	12MW scaled up OC4 NTNU Optimize	12MW scaled up OC4 UOU Modified	12MW final
Platform steel	ton	9,525	8,822	8,661	8,168
Difference	%	0.0%	7.4%	9.1%	14.0%

12 MW platform upscaling

Elements	Parameters	Unit	12MW scaled up OC4 Original	12MW scaled up OC4 NTNU Optimize	12MW scaled up OC4 UOU modified	12MW final
Main column	Diameter	m	8.782	8.782	**8.782**	**9.634**
	Wall thickness	m	0.041	0.041	0.041	0.041
	Elevation above SWL	m	13.510	13.510	13.510	10.000
	Depth of base below SWL	m	27.020	27.020	27.020	27.020
Offset Column	Wall thickness	m	0.081	0.081	0.081	0.081
	Elevation above SWL	m	16.212	16.212	**16.212**	**12.000**
	Spacing between OCs	m	67.550	67.550	67.550	67.550
	Depth of base below SWL	m	27.020	27.020	27.020	27.020
Upper Column	Diameter	m	16.212	13.375	13.375	13.375
	Length	m	35.126	35.126	**35.126**	**30.914**
	Height of Ballast (water)	m	10.410	10.410	1.878	3.600
Footing Pontoon	Diameter	m	32.424	**32.424**	**31.716**	31.716
	Length	m	8.106	8.106	8.106	8.106
	Height of Ballast (water)	m	6.820	7.599	7.944	7.944
Mass	Platform steel	kg	9,501,600	8,798,600	8,638,267	8,168,000
	Platform ballast	kg	23,731,356	20,596,667	19,901,067	20,855,000
	Platform total	kg	33,232,956	29,395,267	28,539,333	28,978,000
	Total system	kg	34,712,260	30,874,571	30,018,638	30,457,418
Bouyancy	Volume	m3	34,329	30,592	30,049	30,049
	CB below SWL	m	-17.77	-18.81943	-18.21	-18.21

Checking structure strength

Calculate equivalence stress for the inner wall of bottom point of upper column

$$\sigma_{\mathrm{equ}} = \sqrt{\sigma_t^2 + \sigma_r^2 + \sigma_{\mathrm{ax}}^2 - \sigma_t\sigma_r - \sigma_t\sigma_{\mathrm{ax}} - \sigma_r\sigma_{\mathrm{ax}}}$$

Pressure checking point: inner wall of upper column at lowest position

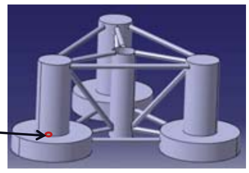

Elements	Parameters	Unit	5MW OC4 Original	12MW scaled up OC4 Original	OC4 NTNU Optimal	12MW scaled up OC4 NTNU Optimize	OC4 UOU-modified	12MW scaled up UOU OC4 modified	12MW final
Ptank min, Pwater max	σ_eq	Mpa	47.50	60.17	39.25	49.73	39.25	49.73	49.76
Steel AH36 (t~80mm)	Yield stress	Mpa	325	325	325	325	325	325	325
Steel SS400 (t~80mm)	Yield stress	Mpa	245	245	245	245	245	245	245

12 MW platform upscaling

OC4 semi UOU-modified scaled up for 12 MW FOWT

12 MW FOWT platform - final

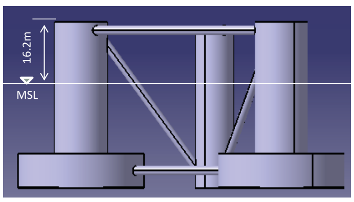

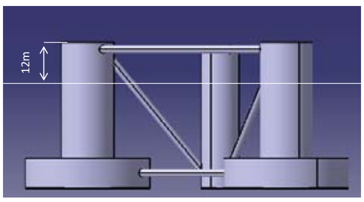

12 MW FOWT Platform modification based on:
- Reduced main column elevation above MSL to 10 m
- Reduced offset column elevation above MSL to 12 m

(the same as OC4 semi-submersible model)

12MW Stability analysis

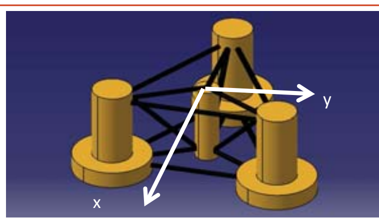

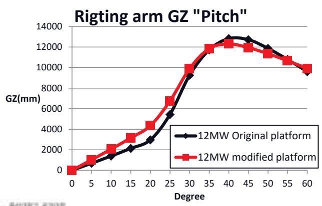

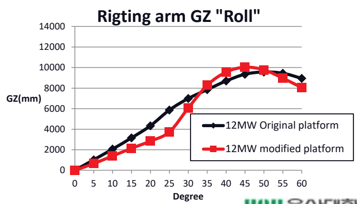

Reference location: West of Barra - Scotland

100m water depth

Main wind direction: SW

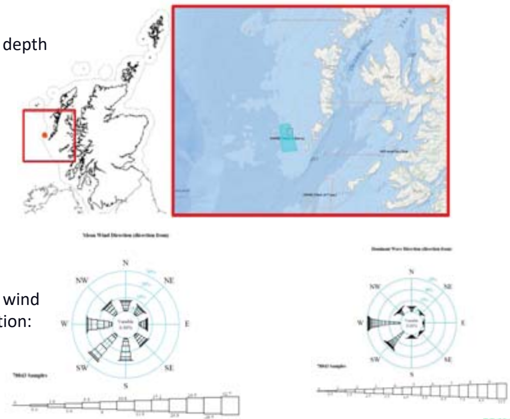

Source: LIFE50+ 'D1.1 Oceanographic and meteorological conditions for the design' 2015

Mooring line properties

Water Depth	m	100
Mooring Line Diameter (d)	mm	162
Number of Mooring Lines	-	3
Angle Between Adjacent Lines	deg	120
Depth to Anchors below SWL	m	100
Fairleads Location above SWL	m	10
Radius to Anchors from Platform Centerline	m	801.5
Radius to Fairleads from Platform Centerline	m	45.7
Equivalent Mooring Line Extensional Stiffness EA	N	2.360E+09
Minimum Breaking Load	N	2.600E+07
Segment 1 (top side) 162mm mooring stud chain, material class R5		
Un-stretched Mooring Line Length	m	385
Equivalent Mooring Line Mass Density	kg/m	522.73
Segment 2 (Anchor side) 2x162mm mooring stud chain, material class R5		
Un-stretched Mooring Line Length	m	400
Equivalent Mooring Line Mass Density	kg/m	1045.46
Equivalent Mooring Line Extensional Stiffness EA	N	2.360E+09
Minimum Breaking Load	N	2.600E+07

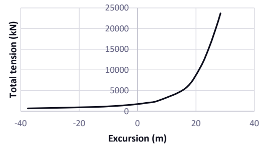

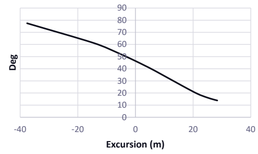

Mooring lines arrangement

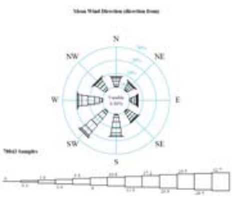

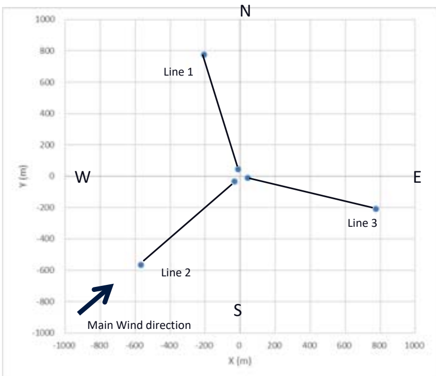

PI controller

- **Results using FAST Linearization with frozen wake assumption**

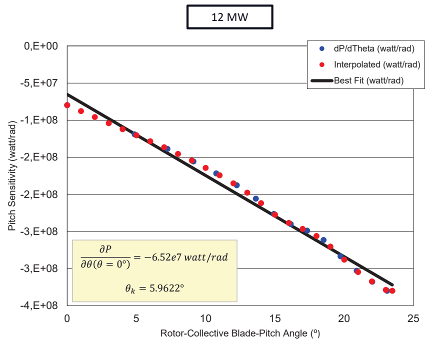

Parameters for pitch and VS control

Parameters	
ConerFreq	1.225221 rad/s
PC_DT	0.00125 s
PC_KI	0.19685052
PC_KK	0.0948646 rad
PC_KP	0.45931788 s
PC_MaxPit	1.5707963 rad
PC_MaxRat	0.139626 rad/s
PC_MinPit	0.0000000 rad
PC_RefSpd	0.8639 rad/s
VS_CtInSp	0.29636 rad/s
VS_DT	0.00125 s
VS_MaxRat	4900000 Nm/s
VS_MaxTq	15511547.75 Nm
VS_Rgn2K	19341827.070932 Nm/(rad/s)²
VS_Rgn2Sp	0.38537 rad/s
VS_Rgn3MP	0.0174533 rad
VS_RtGnSp	0.83802 rad/s
VS_RtPwr	12182741.1 W
VS_SlPc	15.0 %

Mooring lines arrangement

Stud common link

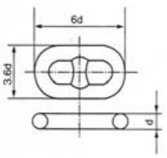

Mooring line components

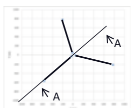

View A-A

Mooring lines configuration

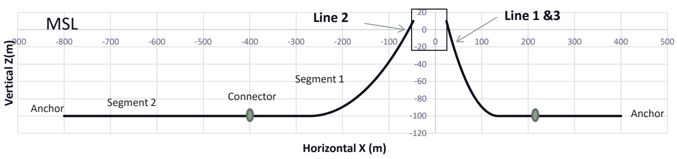

Numerical Simulation

Flow Diagram of UOU + FAST v8

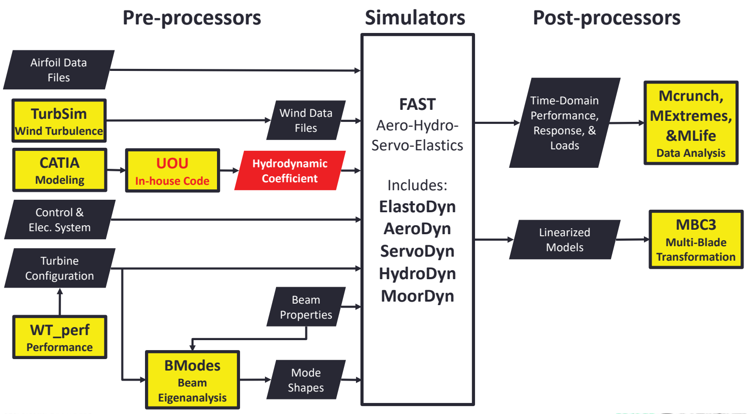

Source : J. Jonkman, FASTWorkshop, NREL

UOU in-house code

- **Hydrodynamic coefficients need for numerical simulation in hydro part**

Hydrodynamic in-house code modeling:
- Consider parts under water line
- Neglect pontoons and braces

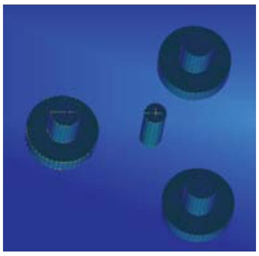

- UOU in-house code

3D panel method(BEM)
Element : 4000

Output
1. Added mass coefficients
2. Radiation Damping coefficients
3. Wave Excitation Forces/Moments

Design Load Cases(DLCs)

Design Load Cases (1/2)

DLC	Winds		Waves			Current	Controls/Events
	Model	Speed	Model	Height	Direction		
1) Power Production							
1.1	NTM	V_in<V_hub<V_out	NSS	Hs = E[Hs/V_hub]	0˚	NCM	Normal operation
1.2	NTM	V_in<V_hub<V_out	NSS	Hs = E[Hs/V_hub]	8 directions	NCM	Normal operation
1.4	EDC	V_hub = V_r, V_r+-2m/s	NSS	Hs = E[Hs/V_hub]	0˚	NCM	Normal operation
1.5	EWS	V_in<V_hub<V_out	NSS	Hs = E[Hs/V_hub]	0˚	NCM	Normal operation
1.6a	NTM	V_in<V_hub<V_out	SSS	Hsss	0˚	NCM	Normal operation
2) Power Production Plus Occurrence of Fault							
2.3	EOG	V_hub = V_r, V_r+-2m/s, V_out		Hs = E[Hs/V_hub]	0˚	NCM	Loss of load -> shutdown
6) Parked							
6.1a	EWM	V_hub = V50	ESS	Hs = Hs50	0˚ , +-45˚	ECM	Yaw = 0, +-8 Deg
9) Power production: Transient condition between intact and redundancy check condition: 1 mooring line lost							
9.1	NTM	V_in<V_hub<V_out	NSS		0˚	NCM	Normal operation
10) Parked: Transient condition between intact and redundancy check condition: 1 mooring line lost							
10.1	EWM	V-hub = V_50	ESS	Hs = Hs50	0˚	ECM	

Design Load Cases (2/2)

DLC1.1, DLC1.2, DLC9.1

Wave	NSS		
Current	NCM		
V-hub	Hs	Tp	Current
m/s	m	s	m/s
4	0.35	3.00	0.08
6	0.73	5.77	0.13
8	1.14	7.18	0.17
10	1.60	8.23	0.21
12	2.12	9.11	0.25
14	2.71	9.88	0.29
16	3.39	10.58	0.34
18	4.18	11.24	0.38
20	5.08	11.85	0.42
22	6.12	12.43	0.46
24	7.31	12.99	0.50

DLC1.6

Wind	ETM		
Wave	SSS		
Current	NCM		
V-hub	Hs	Tp	Current
m/s	m	s	m/s
10	11.5	14.4	0.21
11.2	11.5	14.4	0.25
12	15.6	15.2	0.50
24	15.6	15.2	0.50

DLC6.1, DLC10.1

Wind	EWM		
Wave	ESS		
Current	ECM		
V-hub	Hs	Tp	Current
m/s	m	s	m/s
50	15.6	15.2	1.82

Simulation time:
3 hours irregular waves (1h x 3 wave seed numbers)
DLC1.2: 1 hour simulation

Results

DLC1.1 Minimum, mean, and maximum values

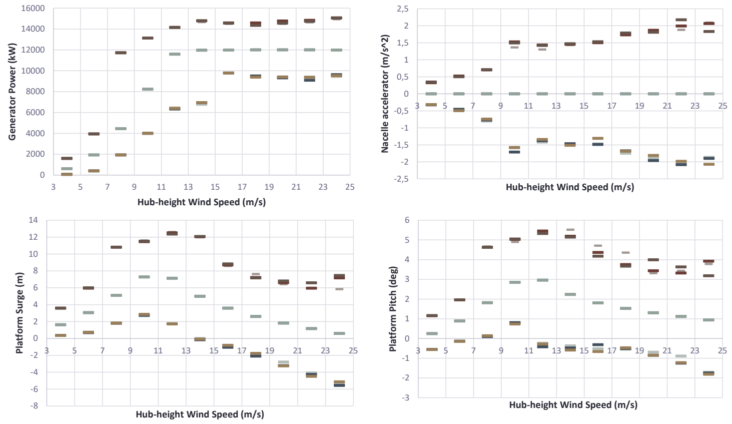

DLC1.1 Minimum, mean, and maximum values

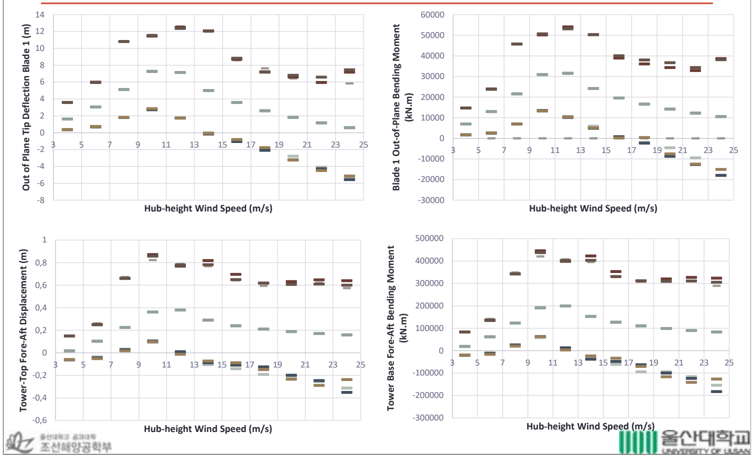

Extreme motions of the FOWT in operation conditions

Serviceability Limit States (SLS) during operational:
Max. tilt: 10 deg.
Nacelle acceleration: 0.3g

Parameter	Type	File Name	Unit	Calculated Extreme	Time (s)
PtfmSurge	Minimum	DLC1.6-25a.out	m	-1.23	3080.4
PtfmSurge	**Maximum**	**DLC1.6-12a.out**	**m**	**17.91**	761.1
PtfmSway	Minimum	DLC1.1-10c.out	m	-2.18	542.9
PtfmSway	Maximum	DLC1.1-10a.out	m	2.31	826.4
PtfmHeave	Minimum	DLC1.6-12c.out	m	-3.22	1306.2
PtfmHeave	Maximum	DLC1.6-25a.out	m	2.83	773.8
PtfmRoll	Minimum	DLC1.1-12c.out	deg	-0.33	3402.4
PtfmRoll	Maximum	DLC1.6-25a.out	deg	1.43	3504.3
PtfmPitch	Minimum	DLC1.6-25a.out	deg	-5.98	760.5
PtfmPitch	**Maximum**	**DLC1.6-12b.out**	**deg**	**8.69**	3365.5
PtfmYaw	Minimum	DLC1.1-24c.out	deg	-6.83	3548.6
PtfmYaw	Maximum	DLC1.1-12c.out	deg	5.16	3402.1
Nacelle acc. Fore-aft	Minimum	DLC1.6-12c.out	m/s^2	-3.12	1305.1
Nacelle acc. Fore-aft	**Maximum**	**DLC1.6-12b.out**	**m/s^2**	**3.37**	1300.0
Nacelle acc. Side-to-side	Minimum	DLC1.6-25b.out	m/s^2	-1.54	1959.9
Nacelle acc. Side-to-side	Maximum	DLC1.6-25b.out	m/s^2	1.59	1956.5

Extreme motions of the FOWT in parked conditions

Serviceability Limit States (SLS) during non-operational:
Max. tilt: 15 deg. (max. value)
Nacelle acceleration: 0.6g

Parameter	Type	File Name	Unit	Extreme Values	Time (s)
PtfmSurge	Minimum	DLC6.1-H0-Y8.out	m	9.40	2242.2
PtfmSurge	**Maximum**	**DLC6.1-H0-Y8.out**	**m**	**26.79**	2329.6
PtfmSway	Minimum	DLC6.1-H-45-Y-8.out	m	-14.28	3490.9
PtfmSway	Maximum	DLC6.1-H45-Y8.out	m	20.51	237.9
PtfmHeave	Minimum	DLC6.1-H45-Y8.out	m	-5.68	3198.4
PtfmHeave	Maximum	DLC6.1-H45-Y8.out	m	4.75	3206.3
PtfmRoll	Minimum	DLC6.1-H-45-Y8.out	deg	-10.27	1408.1
PtfmRoll	Maximum	DLC6.1-H-45-Y-8.out	deg	10.10	3490.5
PtfmPitch	**Minimum**	**DLC6.1-H0-Y8.out**	**deg**	**-11.12**	2559.0
PtfmPitch	Maximum	DLC6.1-H0-Y0.out	deg	0.35	1706.9
PtfmYaw	Minimum	DLC6.1-H45-Y8.out	deg	-3.13	288.6
PtfmYaw	Maximum	DLC6.1-H45-Y-8.out	deg	8.73	3507.4
Nacelle acc. Fore-aft	Minimum	DLC6.1-H0-Y8.out	m/s^2	-2.72	2908.8
Nacelle acc. Fore-aft	Maximum	DLC6.1-H0-Y8.out	m/s^2	2.34	2913.7
Nacelle acc. Side-to-side	**Minimum**	**DLC6.1-H-45-Y-8.out**	**m/s^2**	**-6.33**	3497.2
Nacelle acc. Side-to-side	Maximum	DLC6.1-H45-Y8.out	m/s^2	5.93	3128.1

Maximum Mooring line tensions

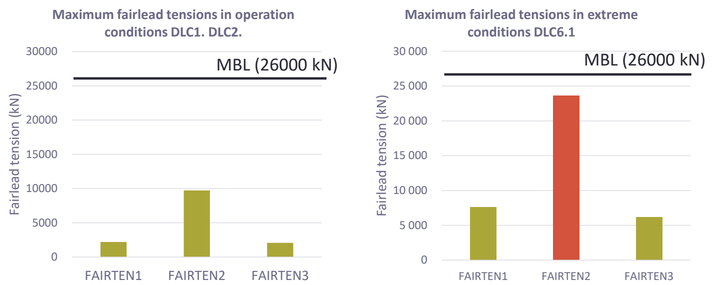

	Operation	Extreme (parked)
Max. Fairlead 2 Tension [kN]	9.727E+03	2.36E+04
Min. Breaking Load MBL [kN]	2.60E+04	2.60E+04
Ratio Max/MBL	0.374	0.908

Ratios of sea to land of absolute extreme values (all DLCs)

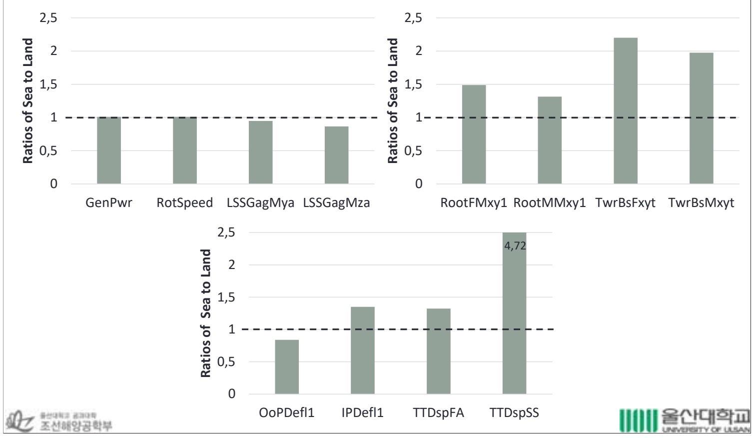

DLC1.2 Fatigue analysis

Comparison between sea and land wind turbine based on :
- The same wind conditions
- The same controller
- Root of blade m= 10, ultimate load L_Ult= 4600 kN
- Tower base m=4, ultimate load L_Ult= 8000 kN

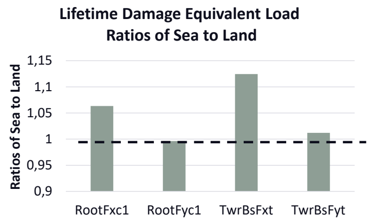

DLC9.1 Motions of the FOWT after a mooring line loss

Wind turbine trajectories after mooring line 2 was lost

Conclusion

Conclusion

- A design of the 12 MW FOWT was suggested.
- Lighting wind turbine mass such as super conductor generator, carbon fiber blade, short tower drive a smaller platform scale ratio.
- Strong wave and high current speed has a significant effect to the design of mooring system.
- Mooring line provided in 2 segments with heavier segment at anchor side to avoid the lift up force at the anchor.
- Loads and displacements of blades and tower in sea are higher than those in land
- Wind and wave misalignments have strong effects to nacelle side to side acceleration

Future work
- Consider 2nd order wave loads
- Optimize mooring system

THANK YOU!

ACKNOWLEDGMENTS

This work was supported by the Korea Institute of Energy Technology Evaluation and Planning(KETEP) and the Ministry of Trade, Industry & Energy(MOTIE) of the Republic of Korea (No. 20154030200970 and No. 20142020103560).

Added mass

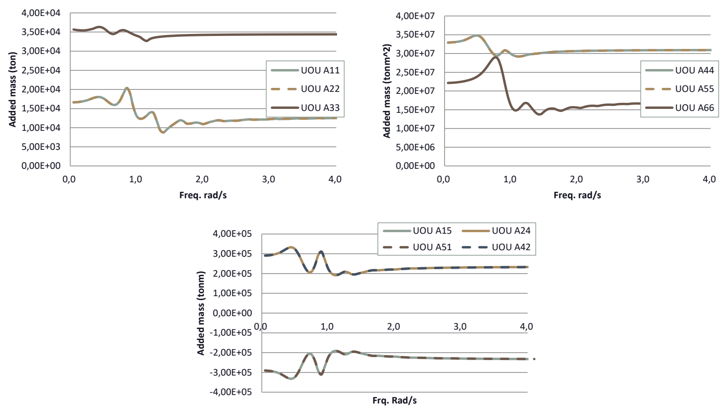

Damping

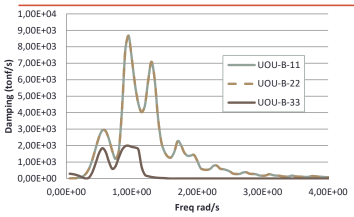

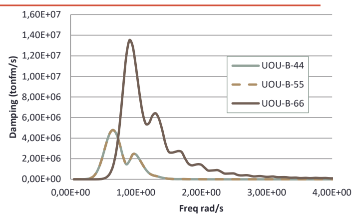

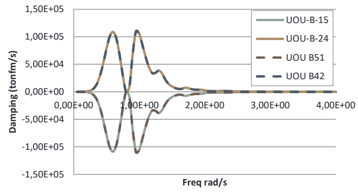

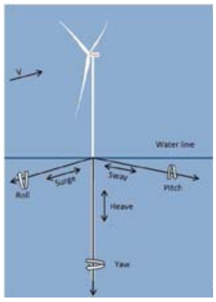

Surge	Translation along the longitudinal axis (main wind direction)
Sway	Translation along the lateral axis (transversal to the main wind direction)
Heave	Translation along the vertical axis
Roll	Rotation about the longitudinal axis
Pitch	Rotation about the lateral axis
Yaw	Rotation about the vertical axis

DOFs of a floating wind turbine (DNV-OS-J103)

Hydrodynamic coefficients(1/2)

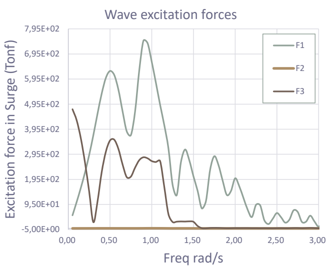

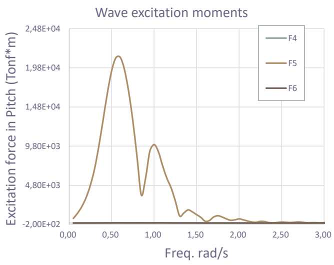

Design process for a floating offshore wind turbine

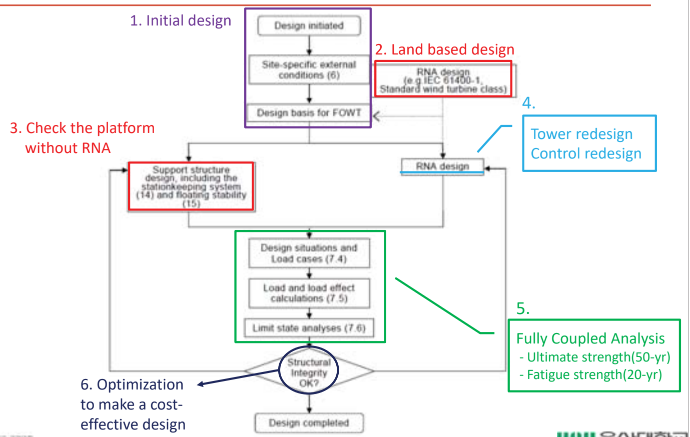

Source: IEC61400-3-2

EERA Deepwind 2018, Trondheim 17.01.2018

Grid Integration of High Definition MMC

Raymundo E. Torres-Olguin†, Michael Smailes, ‡ Chong Ng‡,, Jose Luis Domínguez-García□, Angel Perez Ŧ, Igor Gabiola Ŧ, Giuseppe Guidi†, Atsede Endegnanew†, Salvatore D'Arco†
†SINTEF Energy research
‡Offshore Renewable Energy Catapult
□Catalonia institute for energy research IREC
Ŧ Tecnalia
Presenter: Raymundo E. Torres-Olguin

Introduction

- MMC is emerging topology for offshore wind substations due to its black start capabilities, low Total Harmonic Distortion (THD) and high efficiency.
- The MMC uses a stack of identical modules.
- The multiple voltage steps make the MMC being capable of producing very small harmonic content

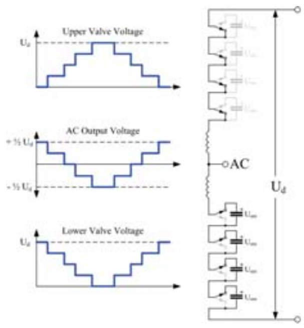

Content

- Introduction to the High Definition Modular Multilevel Converter
- Joint Experiments organized by IRP Wind
- HD-MMC on the performance in 3 phase converter+ high level control
- Concluding remarks

Introduction

- In the conventional MMC (C-MMC) each module create one level, so in order to produce a low THD many modules are required.
- What happen if MMC uses an uneven dc values?

Valve	u_c	Logic								
	V	t_0	t_1	t_2	t_3	t_4	t_5	t_6	t_7	t_8
4p	$U_{dc}/4$	1	1	1	1	1	0	0	1	0
3p	$U_{dc}/4$	1	1	1	0	0	0	0	0	1
2p	$U_{dc}/4$	0	1	1	1	1	1	0	0	0
1p	$U_{dc}/4$	0	0	1	1	0	0	0	0	1
1n	$U_{dc}/4$	1	1	0	0	0	1	1	1	0
2n	$U_{dc}/4$	1	0	0	1	1	1	1	1	1
3n	$U_{dc}/4$	0	0	0	0	0	0	1	1	0
4n	$U_{dc}/4$	0	0	0	0	1	1	1	0	1

Introduction

- The outcomes of this work is expected to contribute to the reduction of offshore wind platform costs.
- A platform-less system, recently proposed by ORE Catapult, aims to reduce the cost of HVDC substation by modularizing and miniaturizing the HVDC converter to integrate it within the wind turbine nacelle.
- A high power density, low Total Harmonic Distortion (THD) converter was required to realize this concept due to the tight space requirements within the turbine.
- This led to the development of the High Definition – Modular Multilevel Converter (HD-MMC) which can generate a lower THD than Conventional –MMCs (C-MMCs) helping to increase power density and efficiency.

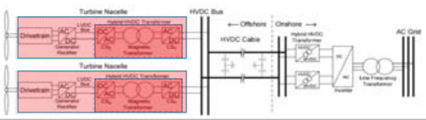

Introduction

By using uneven dc values in the C-MMC, the novel HD-MMC can produce 7 levels using the same number of modules.

.

Some potential advantages:

- It can reduce the THD with the same number of modules
- A more compact converter can be achieved reducing size and cost
- the utilization of the MMC's resources could be improved, since redundant states can be repurposed.

SM	u_c	Logic												
	V	t_0	t_1	t_2	t_3	t_4	t_5	t_6	t_7	t_8	t_9	t_{10}	t_{11}	t_{12}
1	u_{c1}	0	1	0	0	1	0	1	1	1	1	0	0	0
2	u_{c1}	1	1	1	0	0	0	0	1	0	1	1	0	1
3	$u_{c2}(2u_{c1})$	0	0	0	0	0	1	1	1	1	1	1	1	0
4	$u_{c2}(2u_{c1})$	1	0	0	0	0	0	0	0	1	1	1	1	1
5	u_{c1}	1	1	1	1	0	0	0	1	0	0	1	0	1
6	u_{c1}	0	1	0	1	1	0	1	1	1	0	0	0	0
7	$u_{c2}(2u_{c1})$	1	1	1	1	1	1	0	0	0	0	0	0	1
8	$u_{c2}(2u_{c1})$	0	0	1	1	1	1	1	0	0	0	0	1	0

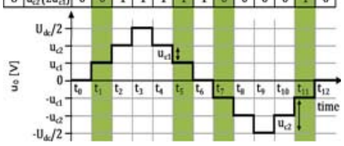

Joint Experiments within IRPWind

- This work is part of the **2nd call for Joint Experiments** organized within the Research Infrastructure WP of IRPWind.
- IRPWind is a European project, which it is aimed to foster better integration of European research activities in the field of wind energy research.
- In Europe, most large research facilities are being devoted to national activities that not necessarily matching the needs of Europe as a whole.
- **The Joint Experiments** has the objective of promoting alignment through joint experiments carried out in European research facilities and its effective use of resources.

Previous results (1st Joint experiments)

The figure shows switching events SE (efficiency) vs THD. C-MMC with PWM has the lowest THD but with the highest SE. C-MMC with NLM has the lowest SE, but the highest THD. HD-MMC is a good trade-off between THD and efficiency.

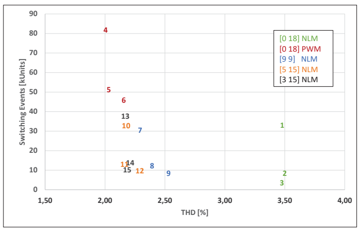

Joint Experiments within IRPWind

- The HD-MMC control algorithm concept was successfully demonstrated in a project granted in **the first IRPWind Joint Experiment** call using a single phase, 18 module, half bridge MMC under controlled laboratory conditions
- The high level control was omitted to quantify the performance of the HD-MMC without any unnecessary complication. A simple RL load was used on the AC bus in place of an AC grid.

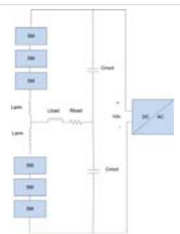

# of cells per arm	18
DC Voltage	776V
Rated power	60 kVA
Load power	5 kW
Cell capacitance per module	19.8mF
Arm inductance (Larm)	1.5 mH
Load resistance (Rload)	3.2 Ω
Load inductance (Lload)	33mH

2nd Joint Experiments within IRPWind

- This second project will build on the results of that project and it will focus on the real world application of the HD-MMC. The project will be split into two stages:
  - The first stage will evaluate the impact of the HD-MMC on the performance of a 3 phase converter with high level control integration.
  - The second stage will look at the real world application of the HD-MMC converter under two scenarios. One connected to an offshore wind turbine generator and the other one connected to an AC inter-array grid
- **SINTEF** is the host institution, and ORE Catapult and Tecnalia are users. The control algorithm for a HD-MMC was developed at **ORE Catapult** in a simulation environment. MMC implementation was made by **SINTEF. ORE Catapult, Tecnalia and SINTEF** performed the experiments in November. **Tecnalia/IREC** acts as an impartial referee during the comparison of both techniques C-MMC vs HD-MMC since it has no conflict of interest in the project.

Previous experiment setup

Access to SINTEF lab

SINTEF Energy Research has three different MMCs:

- MMC unit with half bridge cells with 18 cells per arm
- MMC unit with full bridge cells with 12 cells per arm
- MMC unit with half bridge cells with 6 cells per arm

HD-MMC on the performance in 3 phase converter

Objectives

- Ensure proper operation of the HD-MMC in 3-phases with high level power control
  - Correct voltage levels created
  - Module voltages are stable and correct
- Compare Efficiency/THD trade off compared to C-MMC using PWM and NLM

Set-Up

- GES creates constant, stable AC grid
- GES creates constant, stable DC bus
- MMC operates in PQ mode.

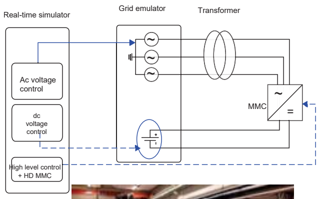

HD-MMC on the performance in 3 phase converter

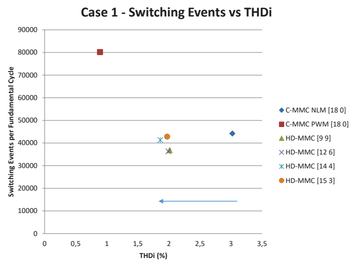

Weighting Factor0

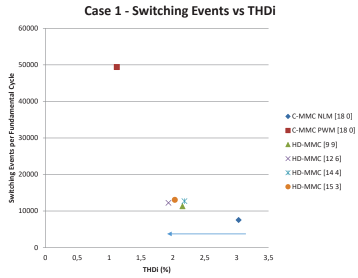

Weighting Factor 5000

HD-MMC on the performance in 3 phase converter

- 18 cases were performed.
- It includes C-MMC with NLM and PWM (As reference case)
- Different combination with HD-MMC
- The weight value is a mechanism that helps the sorting process by giving priority to capacitor voltage balancing or efficiency.

Experiment No	Converter	Configuration	Weighting Factor	Modulation Strategy
1.00	C-MMC	[18 00]	0	NLM
1.01	C-MMC	[18 00]	500	NLM
1.02	C-MMC	[18 00]	5000	NLM
1.03	C-MMC	[18 00]	0	PWM
1.04	C-MMC	[18 00]	500	PWM
1.05	C-MMC	[18 00]	5000	PWM
1.06	HD-MMC	[09 09]	0	NLM
1.07	HD-MMC	[09 09]	500	NLM
1.08	HD-MMC	[09 09]	5000	NLM
1.09	HD-MMC	[12 06]	0	NLM
1.10	HD-MMC	[12 06]	500	NLM
1.11	HD-MMC	[12 06]	5000	NLM
1.12	HD-MMC	[14 04]	0	NLM
1.13	HD-MMC	[14 04]	500	NLM
1.14	HD-MMC	[14 04]	5000	NLM
1.15	HD-MMC	[15 03]	0	NLM
1.16	HD-MMC	[15 03]	500	NLM
1.17	HD-MMC	[15 03]	5000	NLM

HD-MMC on the performance of a 3 phase converter with high level control integration

Objectives

- Determine stability of HD-MMC to sudden control point changes
- Determine the impact the HD-MMC has on the time taken to reach new operating point
- Ensure module voltages remain stable after each step change

Set-Up

- GES creates constant, stable AC grid
- GES creates constant, stable DC bus
- MMC operates in PQ mode. PQ references are used to create step changes in Apparent Power (S) magnitude or angle.

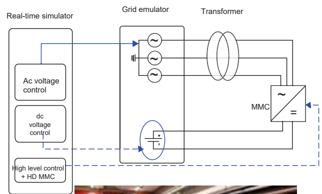

HD-MMC on the performance in 3 phase converter

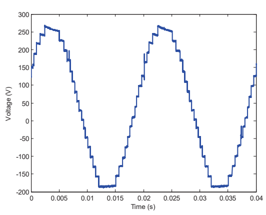

In C_MMC, 19 levels are produced in each arm voltage

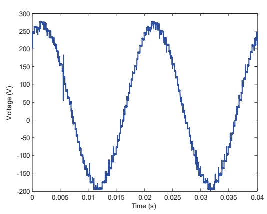

In HD-MMC [9, 9], 28 levels are produced in each arm voltage

HD-MMC on the performance of a 3 phase converter with high level control integration

No	Converter	Configuration	Weight	Modulation Strategy	Variable	Pattern
2.00	HD-MMC	[14 04]	0	NLM	S	1
2.01	HD-MMC	[14 04]	0	NLM	θ	1
2.02	HD-MMC	[14 04]	0	NLM	V	2
2.03	C-MMC	[18 00]	0	NLM	S	1
2.04	C-MMC	[18 00]	0	NLM	θ	1
2.05	C-MMC	[18 00]	0	NLM	V	2

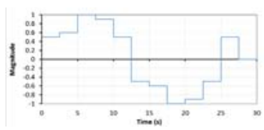

Profile for S, angle

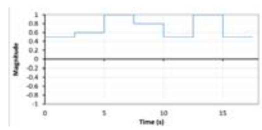

Profile for V

HD-MMC on the performance of a 3 phase converter with high level control integration

- Overshoot_Id (%) (ΔI_p in Figure):
- Overshoot_Iq (%) (ΔI_p in Figure):
- Peak Time Id (s) (t_p in Figure):.
- Peak Time Iq (s) (t_p in Figure):
- Rise Time Id (s) (t_r in Figure):
- Rise Time Iq (s) (t_r in Figure):
- Settling Time Id (s) ($t_{settling}$ in Figure):
- Settling Time Iq (s) ($t_{settling}$ in Figure):
- Steady State Mean Error Id (A) (ΔI_{mean} in Figure):
- Steady State Mean Error Iq (A) (ΔI_{mean} in Figure):
- Steady State Ripple Id Upper Level (A) (ΔI_u in Figure):
- Steady State Ripple Id Lower Level (A) (ΔI_l in Figure):
- Steady State Ripple Iq Upper Level (A) (ΔI_u in Figure):
- Steady State Ripple Iq Lower Level (A) (ΔI_l in Figure):

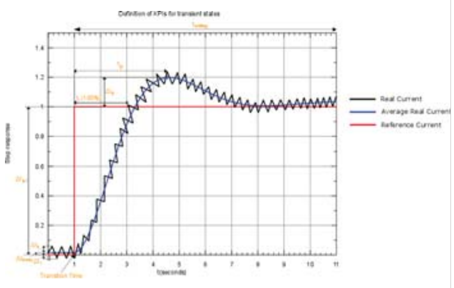

HD-MMC on the performance of a 3 phase converter in a more realistic scenario

Objectives

- This case determined the HD-MMC's performance when used as a generator facing converter.
- Using the non-dimensionalized generator output voltage and current waveforms saved by the Levenmouth Demonstration Turbine's (LDT's) SCADA.
- A time series with the voltages and frequencies to be produced by SINTEF's Grid Emulation System (GES) will be created.

Set-Up

- GES should follow the voltage magnitude and frequencies given to it in a csv file
- GES should create a stable DC voltage

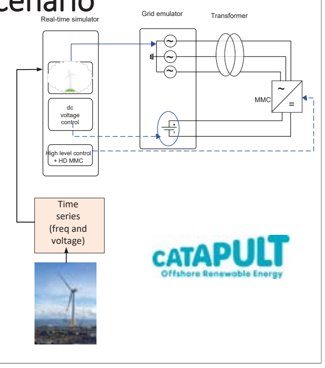

CATAPULT Offshore Renewable Energy

HD-MMC on the performance of a 3 phase converter with high level control integration

Experiment. No	2.00	2.01	2.03	2.04
Converter	HD-MMC	HD-MMC	C-MMC	C-MMC
Modulation	NLM	NLM	NLM	NLM
Configuration	[14 4]	[14 4]	[18 0]	[18 0]
Weighting Factor	0	0	0	0
OvershootId (%)	27.67	33.16	26.41	28.05
OvershootIq (%)	30.56	23.23	34.40	25.82
Peak Time Id (s)	0.026	0.017	0.021	0.019
Peak Time Iq (s)	0.006	0.035	0.010	0.034
Rise Time Id (s)	0.012	0.007	0.012	0.008
Rise Time Iq (s)	0.000	0.016	0.000	0.020
Settling Time Id (s)	0.058	0.066	0.052	0.056
Settling Time Iq (s)	0.062	0.063	0.061	0.055
Steady State Mean Error Id (A)	0.43	0.37	0.47	0.28
Steady State Mean Error Iq (A)	0.19	0.39	0.31	0.69
Steady State Ripple Id Upper Level (A)	1.93	2.25	3.14	3.20
Steady State Ripple Id Lower Level (A)	2.18	2.81	2.80	3.06
Steady State Ripple Iq Upper Level (A)	2.81	1.82	3.16	3.30
Steady State Ripple Iq Lower Level (A)	2.23	1.98	3.24	3.44

HD-MMC on the performance of a 3 phase converter in a more realistic scenario

HD-MMC should create an AC grid at the same voltage and frequency of that created by the GES

References

Produced by HD-MMC

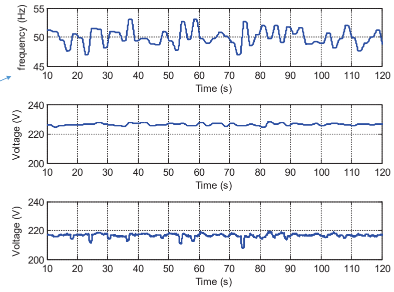

HD-MMC on the performance of a 3 phase converter with high level control integration

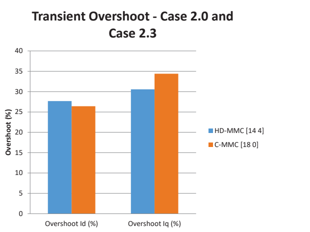

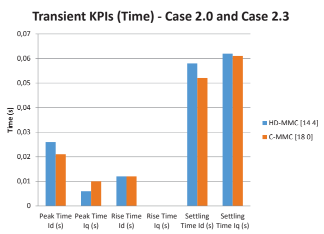

A similar dynamic behaviour between HD-MMC and C-MMC

Conclusions

This work was part of the **2nd call for Joint Experiments** organized within The Research Infrastructure WP of IRPWind.

The main goals were achieved:

(i) The performance of a 3 phase converter with HD-MMC with high level control integration was demonstrated. The performance of the HD-MMC to a C-MMC using THD and efficiency was verified. While the primary goal of HD-MMC, which is to reduce the THD was achieved.

(ii) The control stability and system response was verified through stepping the control set points and rapid changes in grid voltage and frequency to emulate potential grid variation and disturbances

(iii) The HD-MMC concept was tested in more real world conditions such as the connection of an emulated generated with real data.


CATAPULT
Offshore Renewable Energy
IREC
tecnalia
Inspiring Business
SINTEF
THANKS
IRPWind

REMS
RENEWABLE ENERGY MARINE STRUCTURES
Cranfield University

Load Mitigation through Advanced Controls for an Active Pitch to Stall Operated Floating Wind Turbine

Dawn Ward

Researcher, Offshore Energy Engineering Centre,
Cranfield University, Bedfordshire, UK

EPSRC

17 January 2018, EERA DeepWind 2018, Trondheim, Norway

*Third Generation Wind Power - DNV.GL

REMS
RENEWABLE ENERGY MARINE STRUCTURES
Cranfield University

1. Context and Problem Statement

- Usual to utilize offshore turbines designed for a fixed base on floating platforms
- FOWT experience increased tower base for-aft moments due to platform motion

EPSRC

17 January 2018, EERA DeepWind 2018, Trondheim, Norway 2

*Third Generation Wind Power - DNV.GL

REMS
RENEWABLE ENERGY MARINE STRUCTURES
Cranfield University

1. Context and Problem Statement
2. Aims, Objectives & Approach
3. Results
4. Conclusions
5. Q & A

EPSRC

17 January 2018, EERA DeepWind 2018, Trondheim, Norway 1

*Third Generation Wind Power - DNV.GL

REMS
RENEWABLE ENERGY MARINE STRUCTURES
Cranfield University

1. Context and Problem Statement

- Usual to utilize offshore turbines designed for a fixed base on floating platforms
- FOWT experience increased tower base for-aft moments due to platform motion
- All pitch-to-feather HAWTs experience 'negative damping' which can cause tower fore-aft oscillations that increase the loads on the tower

EPSRC

17 January 2018, EERA DeepWind 2018, Trondheim, Norway 2

*Third Generation Wind Power - DNV.GL

REMS
RENEWABLE ENERGY MARINE STRUCTURES
Cranfield University

1. Context and Problem Statement

- Usual to utilize offshore turbines designed for a fixed base on floating platforms

EPSRC

17 January 2018, EERA DeepWind 2018, Trondheim, Norway 2

*Third Generation Wind Power - DNV.GL

REMS
RENEWABLE ENERGY MARINE STRUCTURES
Cranfield University

1. Context and Problem Statement

- Advanced control strategies can reduce the platform motion and hence loads on the tower

EPSRC

17 January 2018, EERA DeepWind 2018, Trondheim, Norway 3

*Third Generation Wind Power - DNV.GL


REMS
RENEWABLE ENERGY MARINE STRUCTURES
Cranfield University
1. Context and Problem Statement
• Advanced control strategies can reduce the platform motion and hence loads on the tower
• Blades that pitch-to-stall cause a drag force which increases with wind speed, therefore avoid undesirable 'negative damping' effects.
EPSRC
17 January 2018, EERA DeepWind 2018, Trondheim, Norway
3
*Third Generation Wind Power - DNV.GL

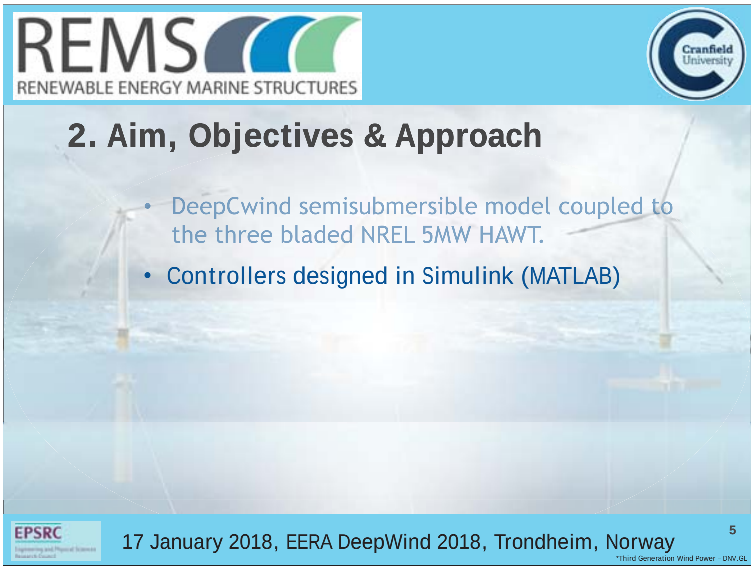
REMS
RENEWABLE ENERGY MARINE STRUCTURES
Cranfield University
2. Aim, Objectives & Approach
• DeepCwind semisubmersible model coupled to the three bladed NREL 5MW HAWT.
• Controllers designed in Simulink (MATLAB)
EPSRC
17 January 2018, EERA DeepWind 2018, Trondheim, Norway
5
*Third Generation Wind Power - DNV.GL


REMS
RENEWABLE ENERGY MARINE STRUCTURES
Cranfield University
2. Aim, Objectives & Approach
The aim is to assess whether pitching the turbine blades actively to stall in Region III, using advanced control strategies, could aid in reducing the loads on the tower of a turbine coupled to a semi-submersible platform design.
EPSRC
17 January 2018, EERA DeepWind 2018, Trondheim, Norway
4
*Third Generation Wind Power - DNV.GL

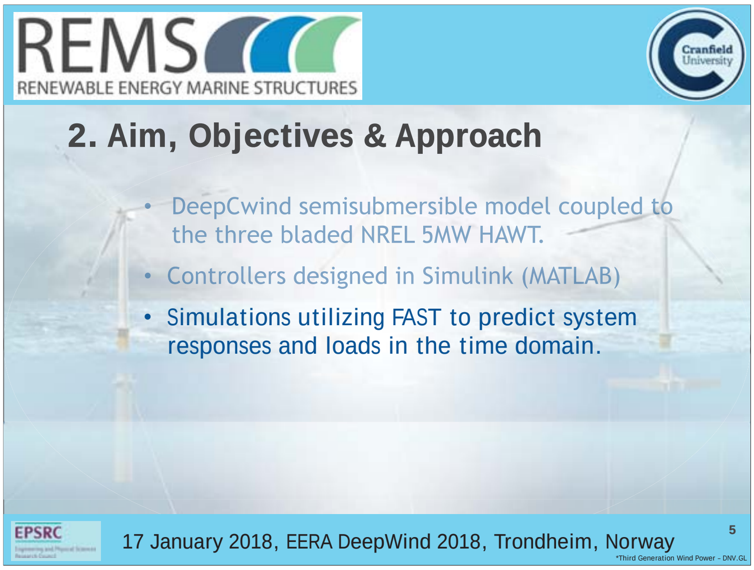
REMS
RENEWABLE ENERGY MARINE STRUCTURES
Cranfield University
2. Aim, Objectives & Approach
• DeepCwind semisubmersible model coupled to the three bladed NREL 5MW HAWT.
• Controllers designed in Simulink (MATLAB)
• Simulations utilizing FAST to predict system responses and loads in the time domain.
EPSRC
17 January 2018, EERA DeepWind 2018, Trondheim, Norway
5
*Third Generation Wind Power - DNV.GL

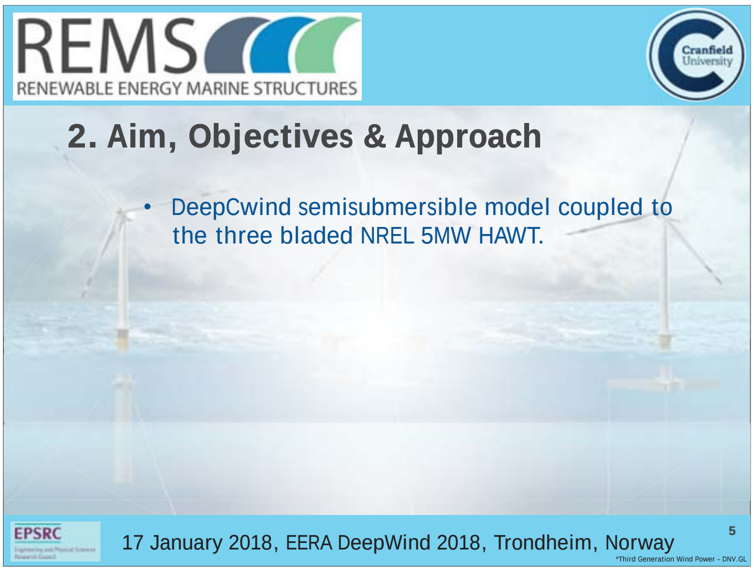
REMS
RENEWABLE ENERGY MARINE STRUCTURES
Cranfield University
2. Aim, Objectives & Approach
• DeepCwind semisubmersible model coupled to the three bladed NREL 5MW HAWT.
EPSRC
17 January 2018, EERA DeepWind 2018, Trondheim, Norway
5
*Third Generation Wind Power - DNV.GL

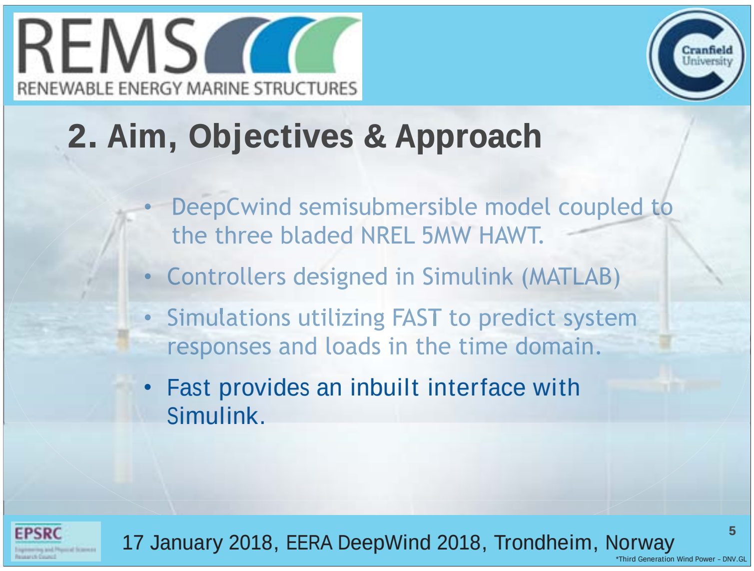
REMS
RENEWABLE ENERGY MARINE STRUCTURES
Cranfield University
2. Aim, Objectives & Approach
• DeepCwind semisubmersible model coupled to the three bladed NREL 5MW HAWT.
• Controllers designed in Simulink (MATLAB)
• Simulations utilizing FAST to predict system responses and loads in the time domain.
• Fast provides an inbuilt interface with Simulink.
EPSRC
17 January 2018, EERA DeepWind 2018, Trondheim, Norway
5
*Third Generation Wind Power - DNV.GL

REMS RENEWABLE ENERGY MARINE STRUCTURES — Cranfield University

2. Aim, Objectives & Approach

- DeepCwind semisubmersible model coupled to the three bladed NREL 5MW HAWT.
- Controllers designed in Simulink (MATLAB)
- Simulations utilizing FAST to predict system responses and loads in the time domain.
- Fast provides an inbuilt interface with Simulink.
- Identify fatigue reduction benefits available from different control strategies.

REMS RENEWABLE ENERGY MARINE STRUCTURES — Cranfield University

3. Results - Periodic steady wind responses

- Initially unstable and would not converge
- K_P & K_I gains increased
- Excessive blade deflections - striking the tower
- Blade flapwise stiffness increased
- A realistic active stall designed blade would be preferable

REMS RENEWABLE ENERGY MARINE STRUCTURES — Cranfield University

3. Results - Baseline pitch-to-stall controller

- Constant gain, closed-loop, feedback PI pitch controller
- Input = Error (the difference between the set-point (rated) and the actual rotor speed)
- Output = the summed results after K_P & K_I are applied & added to the equilibrium pitch value

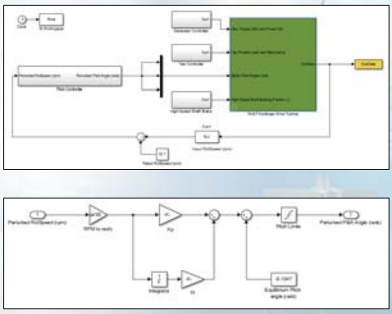

REMS RENEWABLE ENERGY MARINE STRUCTURES — Cranfield University

3. Results - Periodic steady wind responses

- Reduction in blade pitch angle in stall (-8.1˚ compared to 22.9˚)

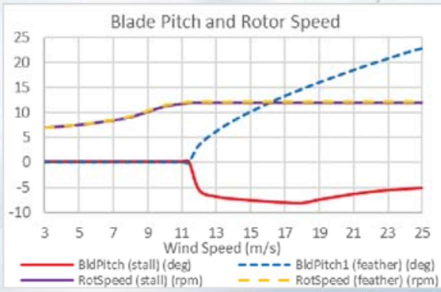

REMS RENEWABLE ENERGY MARINE STRUCTURES — Cranfield University

3. Results - Periodic steady wind responses

- Initially unstable and would not converge
- K_P & K_I gains increased

REMS RENEWABLE ENERGY MARINE STRUCTURES — Cranfield University

3. Results - Periodic steady wind responses

- Reduction in blade pitch angle in stall (-8.1˚ compared to 22.9˚)
- Positive thrust force i.e. avoiding the negative damping (891kN to 1361kN stall) (891kN to 402kN feather)

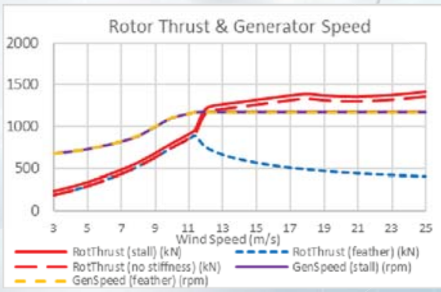

REMS RENEWABLE ENERGY MARINE STRUCTURES — Cranfield University

3. Results - Periodic steady wind responses

- Reduction in blade pitch angle in stall (-8.1˚ compared to 22.9˚)
- Positive thrust force i.e. avoiding the negative damping (891kN to 1361kN stall) (891kN to 402kN feather)
- Performance equal

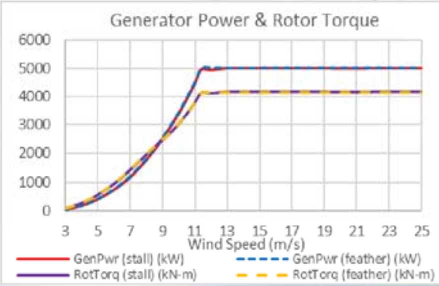

REMS RENEWABLE ENERGY MARINE STRUCTURES — Cranfield University

3. Results - Gain scheduling benefits

- 12mps mean turbulent winds irregular waves Hs 2m, Tp 7s
- Gain scheduling more complex in stall, may require 2 controller schedules

+ Faster response
+ Improved performance

Case ID	Control Regime	Natural Frequency, ωφn (rad/s)	Damping Ratio, ζφ	Proportional Gain, Kp (s)	Integral Gain, Ki
Case F1	Feather: Gain Scheduling	0.2*	0.7*	0.006275604*	0.000896015*
Case S1	Stall: Constant Gains at 12mps	0.6	0.7	-0.08555823	-0.03666824
Case S2	Stall: Constant Gains at 18mps	0.6	0.7	-0.00772205	-0.00330946

* at minimum pitch setting, Ref. Robertson A et al, 2014, Definition of the Semisubmersible Floating System for Phase II of OC4, NREL/TP-5000-60601

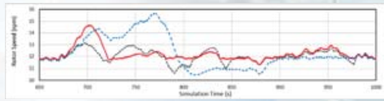

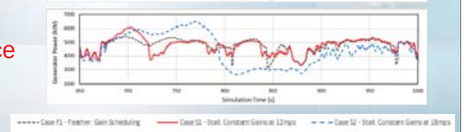

REMS RENEWABLE ENERGY MARINE STRUCTURES — Cranfield University

3. Results - Periodic steady wind responses

- Reduction in blade pitch angle in stall (-8.1˚ compared to 22.9˚)
- Positive thrust force i.e. avoiding the negative damping (891kN to 1361kN stall) (891kN to 402kN feather)
- Performance equal
- Increase in tower deflection

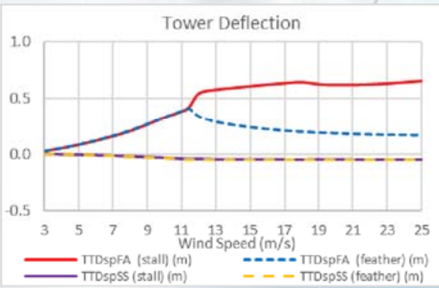

REMS RENEWABLE ENERGY MARINE STRUCTURES — Cranfield University

3. Results - Gain scheduling benefits

- 12mps mean turbulent winds irregular waves Hs 2m, Tp 7s
- Gain scheduling more complex in stall, may require 2 controller schedules

+ Faster response
+ Improved performance
+ Loads & motion reduced

Case ID	Control Regime	Natural Frequency, ωφn (rad/s)	Damping Ratio, ζφ	Proportional Gain, Kp (s)	Integral Gain, Ki
Case F1	Feather: Gain Scheduling	0.2*	0.7*	0.006275604*	0.000896015*
Case S1	Stall: Constant Gains at 12mps	0.6	0.7	-0.08555823	-0.03666824
Case S2	Stall: Constant Gains at 18mps	0.6	0.7	-0.00772205	-0.00330946

* at minimum pitch setting, Ref. Robertson A et al, 2014, Definition of the Semisubmersible Floating System for Phase II of OC4, NREL/TP-5000-60601

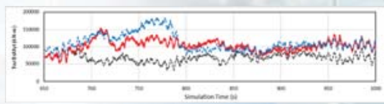

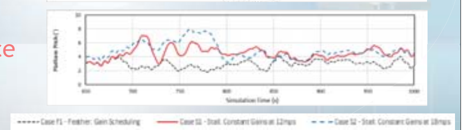

REMS RENEWABLE ENERGY MARINE STRUCTURES — Cranfield University

3. Results - Gain scheduling benefits

- 12mps mean turbulent winds irregular waves Hs 2m, Tp 7s
- Gain scheduling more complex in stall, may require 2 controller schedules

+ Faster response

Case ID	Control Regime	Natural Frequency, ωφn (rad/s)	Damping Ratio, ζφ	Proportional Gain, Kp (s)	Integral Gain, Ki
Case F1	Feather: Gain Scheduling	0.2*	0.7*	0.006275604*	0.000896015*
Case S1	Stall: Constant Gains at 12mps	0.6	0.7	-0.08555823	-0.03666824
Case S2	Stall: Constant Gains at 18mps	0.6	0.7	-0.00772205	-0.00330946

* at minimum pitch setting, Ref. Robertson A et al, 2014, Definition of the Semisubmersible Floating System for Phase II of OC4, NREL/TP-5000-60601

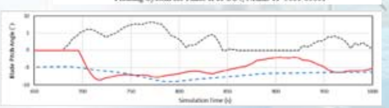

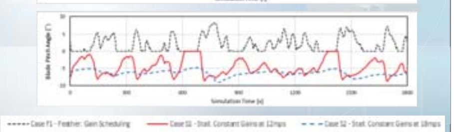

REMS RENEWABLE ENERGY MARINE STRUCTURES — Cranfield University

3. Results - Tower base fore-aft load mitigation

- 18mps mean turbulent winds irregular waves Hs 4m, Tp 10s
- Response too slow with calculated gains ∴ proportional gain too low

Case ID	Control Regime	Natural Frequency, ωφn (rad/s)	Damping Ratio, ζφ	Proportional Gain, Kp (s)	Integral Gain, Ki
Case F1	Feather: Gain Scheduling	0.2*	0.7*	[illegible]	[illegible]
Case F2	Feather: Constant Gains at 18mps	0.2	0.7	[illegible]	[illegible]
Case S3	Stall: Constant Gains at 18mps	0.6	0.7	[illegible]	[illegible]
Case S4	Stall: Constant Gains at 18mps x 10			[illegible]	[illegible]
Case S5	Stall: Constant Gains at 18mps x 100			[illegible]	[illegible]

* at minimum pitch setting, Ref. Robertson A et al, 2014, Definition of the Semisubmersible Floating System for Phase II of OC4, NREL/TP-5000-60601

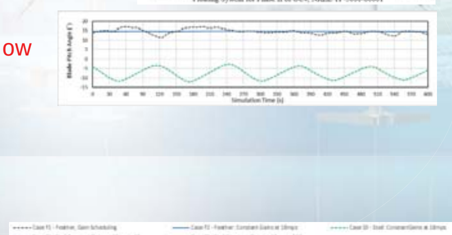

REMS RENEWABLE ENERGY MARINE STRUCTURES

Cranfield University

3. Results - Tower base fore-aft load mitigation

- 18mps mean turbulent winds irregular waves Hs 4m,Tp 10s
- Response too slow with calculated gains
  ∴ proportional gain too low
- Pitch actuation increased

Case ID	Control Regime	Natural Frequency, ωφ (rad/s)	Damping Ratio, ζφ	Proportional Gain, Kp (s)	Integral Gain, Ki
Case F1	Feather, Gain Scheduling	0.2*	0.7*	[illegible]	[illegible]
Case F2	Feather, Constant Gains at 18mps	0.2	0.7	[illegible]	[illegible]
Case S3	Stall, Constant Gains at 18mps	0.6	0.7	[illegible]	[illegible]
Case S4	Stall Constant Gains at 18mps x 10			[illegible]	[illegible]
Case S5	Stall Constant Gains at 18mps x 100			[illegible]	[illegible]

* at minimum pitch setting, Ref. Robertson A et al, 2014, Definition of the Semisubmersible Floating System for Phase II of OC4, NREL/TP-5000-60601

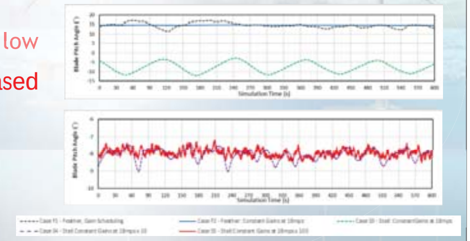

REMS RENEWABLE ENERGY MARINE STRUCTURES

Cranfield University

4. Conclusions

- A robust control system with gain scheduling for stall operation could be further enhanced when coupled to other advanced control strategies.

REMS RENEWABLE ENERGY MARINE STRUCTURES

Cranfield University

3. Results - Tower base fore-aft load mitigation

- 18mps mean turbulent winds irregular waves Hs 4m,Tp 10s
- Response too slow with calculated gains
  ∴ proportional gain too low
- Pitch actuation increased
- Performance improved

Case ID	Control Regime	Natural Frequency, ωφ (rad/s)	Damping Ratio, ζφ	Proportional Gain, Kp (s)	Integral Gain, Ki
Case F1	Feather, Gain Scheduling	0.2*	0.7*	[illegible]	[illegible]
Case F2	Feather, Constant Gains at 18mps	0.2	0.7	[illegible]	[illegible]
Case S3	Stall, Constant Gains at 18mps	0.6	0.7	[illegible]	[illegible]
Case S4	Stall Constant Gains at 18mps x 10			[illegible]	[illegible]
Case S5	Stall Constant Gains at 18mps x 100			[illegible]	[illegible]

* at minimum pitch setting, Ref. Robertson A et al, 2014, Definition of the Semisubmersible Floating System for Phase II of OC4, NREL/TP-5000-60601

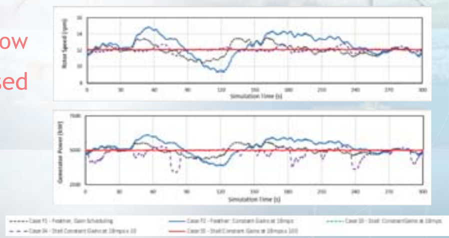

REMS RENEWABLE ENERGY MARINE STRUCTURES

Cranfield University

4. Conclusions

- A robust control system with gain scheduling for stall operation could be further enhanced when coupled to other advanced control strategies.
- Increasing the gains gave improved performance and reductions in the tower base fore-aft moment range

REMS RENEWABLE ENERGY MARINE STRUCTURES

Cranfield University

3. Results - Tower base fore-aft load mitigation

- 18mps mean turbulent winds irregular waves Hs 4m,Tp 10s
- Response too slow with calculated gains
  ∴ proportional gain too low
- Pitch actuation increased
- Performance improved
- Tower base fore-aft moment range & StD lower than F2

Case ID	Control Regime	Natural Frequency, ωφ (rad/s)	Damping Ratio, ζφ	Proportional Gain, Kp (s)	Integral Gain, Ki
Case F1	Feather, Gain Scheduling	0.2*	0.7*	[illegible]	[illegible]
Case F2	Feather, Constant Gains at 18mps	0.2	0.7	[illegible]	[illegible]
Case S3	Stall, Constant Gains at 18mps	0.6	0.7	[illegible]	[illegible]
Case S4	Stall Constant Gains at 18mps x 10			[illegible]	[illegible]
Case S5	Stall Constant Gains at 18mps x 100			[illegible]	[illegible]

* at minimum pitch setting, Ref. Robertson A et al, 2014, Definition of the Semisubmersible Floating System for Phase II of OC4, NREL/TP-5000-60601

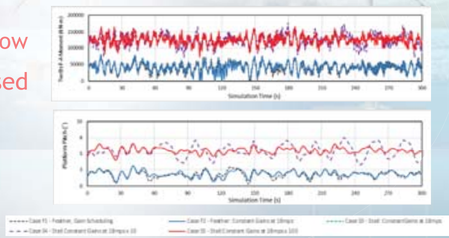

REMS RENEWABLE ENERGY MARINE STRUCTURES

Cranfield University

4. Conclusions

- A robust control system with gain scheduling for stall operation could be further enhanced when coupled to other advanced control strategies.
- Increasing the gains gave improved performance and reductions in the tower base fore-aft moment range
- The increase in positive mean of the platform pitch and tower fore-aft motions compared to feather indicate that this platform's stability would need increasing, for a pitch to stall operating regime.


REMS
RENEWABLE ENERGY MARINE STRUCTURES
Cranfield University
Thank you for your time
Questions and Advice welcome
Dawn.Ward@cranfield.ac.uk
EPSRC
17 January 2018, EERA DeepWind 2018, Trondheim, Norway
12
*Third Generation Wind Power – DNV.GL

A2) New turbine and generator technology

Integrated design of a semi-submersible floating vertical axis wind turbine (VAWT) with active blade pitch control, F.Huijs, GustoMSC

Evaluation of control methods for floating offshore wind turbines, W.Yu, University of Stuttgart

Impact of the aerodynamic model on the modelling of the behaviour of a Floating Vertical Axis Wind Turbine, V.Leroy, LHEEA and INNOSEA

GustoMSC

DESIGN OF A SEMI-SUBMERSIBLE FLOATING VAWT WITH ACTIVE BLADE PITCH CONTROL

17 JANUARY 2018, TRONDHEIM

Fons Huijs

THE PIONEERS OF OFFSHORE ENGINEERING

GustoMSC

INTRODUCTION - FLOATING VAWT

- Deeper waters
- Larger wind turbines
  - ⮡ Increasing interest for floating wind
- Low centre of gravity position
- Large allowable tilt angle
- Potential for scaling up
  - ⮡ VAWT promising for floating

GustoMSC

DESIGN OF A SEMI-SUBMERSIBLE FLOATING VAWT WITH ACTIVE BLADE PITCH CONTROL

17 JANUARY 2018, TRONDHEIM

Fons Huijs, Ebert Vlasveld, Maël Gormand	GustoMSC
Feike Savenije, Marco Caboni	ECN
Bruce LeBlanc, Carlos Simao Ferreira	TU Delft
Koert Lindenburg	WMC
Sébastien Gueydon, William Otto	MARIN
Benoît Paillard	EOLFI

TKI WIND OP ZEE Topsector Energie · S4VAWT · EOLFI · ECN · TU Delft · MARIN Knowledge Centre · WMC · GustoMSC

GustoMSC

INTRODUCTION - PREVIOUS WORK

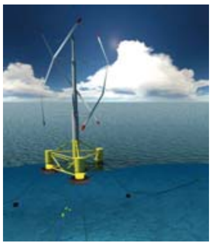

Technip, Nenuphar
Cahay et al, OTC 21704, 2011

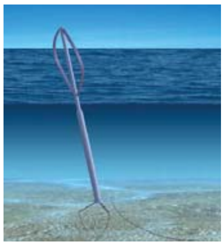

DeepWind project
Paulsen et al, DeepWind'2013

GustoMSC, TU Delft
Blonk, MSc thesis, 2010

GustoMSC

OUTLINE

- Introduction
- Floating VAWT design
- Coupled analysis
- Conclusions

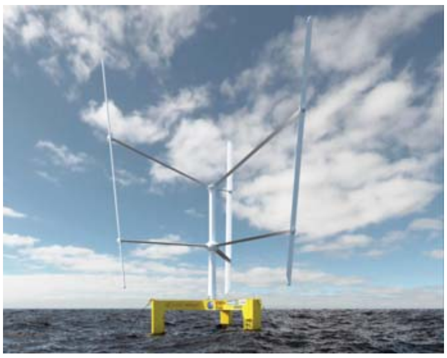

GustoMSC

INTRODUCTION - S4VAWT PROJECT

- Active blade pitch control for VAWT
  - Improved aerodynamic efficiency (power production)
  - Lower wind loads above rated (power production)
  - Lower survival loads (parked)
- Objectives S4VAWT project:
  - Verify & quantify VAWT advantages
  - Design semi-submersible floater
  - Verify design by simulations

S4VAWT
Semi-Submersible Support Structure for Vertical Axis Wind Turbines

GustoMSC

DESIGN - BASIS

- 6 MW VAWT
- Maximum static tilt during production < 10°

- French Mediterranean Sea
- Water depth ~ 100 m
- 50-year significant wave height ~ 6.5 m

- DNV GL standards

GustoMSC

DESIGN

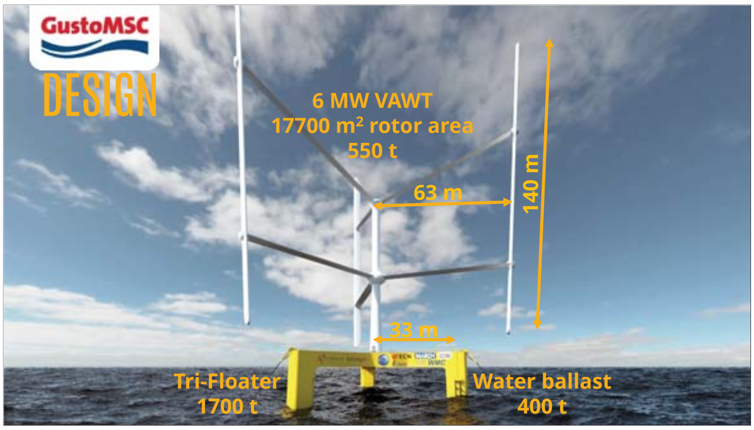

GustoMSC

DESIGN - 6 MW VAWT

- Active blade pitch control

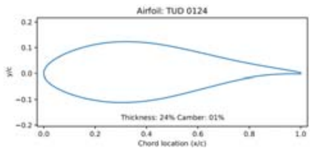

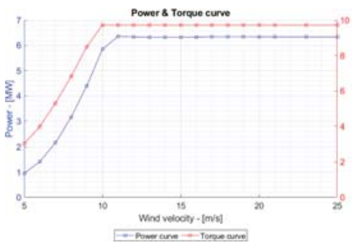

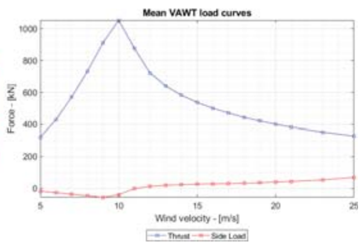

GustoMSC

COUPLED ANALYSIS - SOFTWARE

- Aerodynamics: Lifting line free vortex wake method
- Turbine and control: Structural dynamics, gyroscopic effects, etc.
- Hydrodynamics: Potential flow, full QTF, quadratic damping
- Mooring: Dynamic lumped-mass model

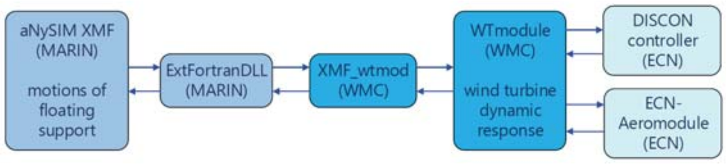

GustoMSC

DESIGN

GustoMSC

COUPLED ANALYSIS - MOTION RESULTS

		Rated	Cut-out	Survival
10-min mean wind velocity [m/s]		11	25	39
Significant wave height [m]		4.0	5.4	6.5
Floater surge [m]	mean	42	39	**42**
	max	46	43	**51**
Floater tilt (roll & pitch) [deg]	mean	**7**	3	2
	max	**11**	6	5
Floater yaw [deg]	mean	5	**6**	0
	max	8	**9**	6

GustoMSC

COUPLED ANALYSIS - PARKED SURVIVAL

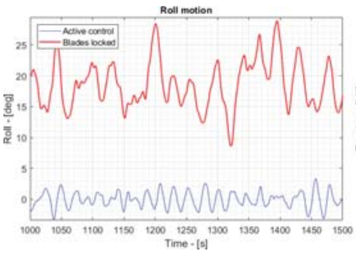

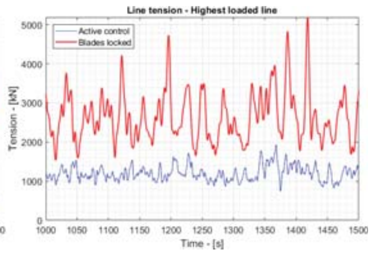

GustoMSC

THANK YOU FOR YOUR KIND ATTENTION

17 JANUARY 2018, TRONDHEIM

THE PIONEERS OF OFFSHORE ENGINEERING

GustoMSC

CONCLUSIONS - FLOATING VAWT DESIGN

- Active blade pitch control makes design drivers floater for VAWT more similar to HAWT:
  - Rated wind governing for floater tilt & tower base moment
  - Parked survival still governing for surge & mooring tensions
- Yaw induced by rotor torque no issue for Tri-Floater

GustoMSC

CONCLUSIONS - VAWT

- Known advantages VAWT for floating wind:
  - Low centre of gravity position
  - Large allowable tilt angle
  - Potential for scaling up

+

- Active blade pitch control:
  - Mitigate large loads above rated and parked

↓

- Floater for VAWT 20% lighter than for HAWT

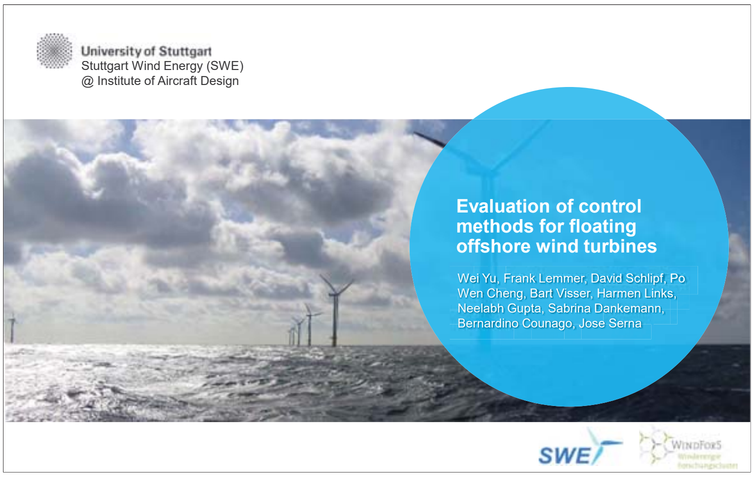
University of Stuttgart
Stuttgart Wind Energy (SWE)
@ Institute of Aircraft Design
Evaluation of control methods for floating offshore wind turbines
Wei Yu, Frank Lemmer, David Schlipf, Po Wen Cheng, Bart Visser, Harmen Links, Neelabh Gupta, Sabrina Dankemann, Bernardino Counago, Jose Serna
SWE
WINDFORS

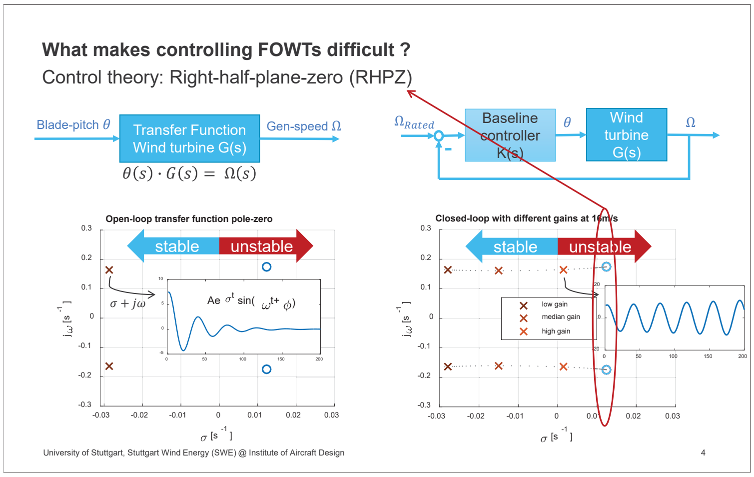
What makes controlling FOWTs difficult ?
Control theory: Right-half-plane-zero (RHPZ)
Blade-pitch θ
Transfer Function Wind turbine G(s)
Gen-speed Ω
θ(s) · G(s) = Ω(s)
Ω_Rated
Baseline controller K(s)
Wind turbine G(s)
Open-loop transfer function pole-zero
Closed-loop with different gains at 16m/s
stable
unstable
σ + jω
low gain
median gain
high gain
jω [s^-1]
σ [s^-1]
University of Stuttgart, Stuttgart Wind Energy (SWE) @ Institute of Aircraft Design
4

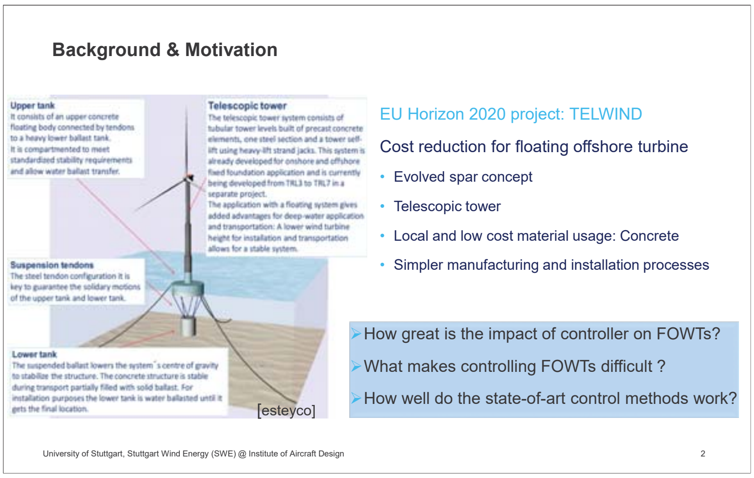
Background & Motivation
Upper tank
Telescopic tower
Suspension tendons
Lower tank
[esteyco]
EU Horizon 2020 project: TELWIND
Cost reduction for floating offshore turbine
Evolved spar concept
Telescopic tower
Local and low cost material usage: Concrete
Simpler manufacturing and installation processes
How great is the impact of controller on FOWTs?
What makes controlling FOWTs difficult ?
How well do the state-of-art control methods work?
University of Stuttgart, Stuttgart Wind Energy (SWE) @ Institute of Aircraft Design
2

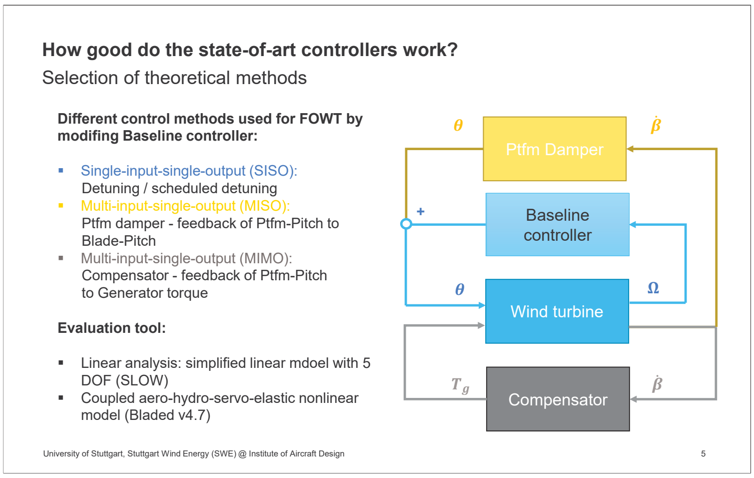
How good do the state-of-art controllers work?
Selection of theoretical methods
Different control methods used for FOWT by modifing Baseline controller:
Single-input-single-output (SISO): Detuning / scheduled detuning
Multi-input-single-output (MISO): Ptfm damper - feedback of Ptfm-Pitch to Blade-Pitch
Multi-input-single-output (MIMO): Compensator - feedback of Ptfm-Pitch to Generator torque
Evaluation tool:
Linear analysis: simplified linear mdoel with 5 DOF (SLOW)
Coupled aero-hydro-servo-elastic nonlinear model (Bladed v4.7)
Ptfm Damper
Baseline controller
Wind turbine
Compensator
University of Stuttgart, Stuttgart Wind Energy (SWE) @ Institute of Aircraft Design
5

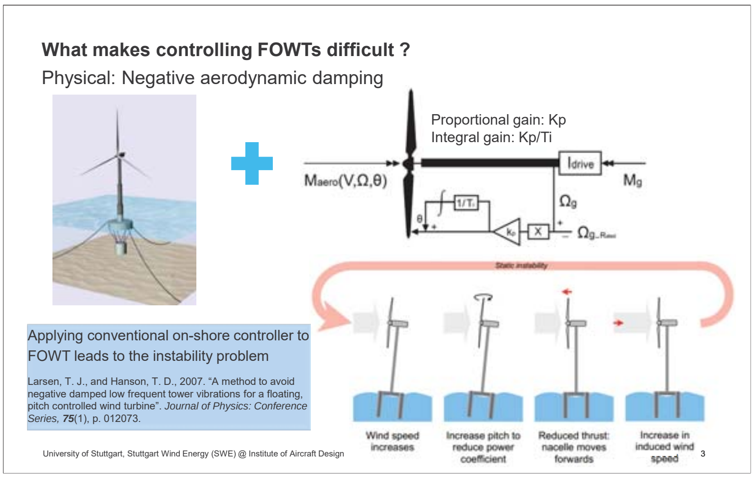
What makes controlling FOWTs difficult ?
Physical: Negative aerodynamic damping
Proportional gain: Kp
Integral gain: Kp/Ti
Maero(V,Ω,θ)
Idrive
Mg
Ωg
Applying conventional on-shore controller to FOWT leads to the instability problem
Larsen, T. J., and Hanson, T. D., 2007. "A method to avoid negative damped low frequent tower vibrations for a floating, pitch controlled wind turbine". Journal of Physics: Conference Series, 75(1), p. 012073.
Static instability
Wind speed increases
Increase pitch to reduce power coefficient
Reduced thrust: nacelle moves forwards
Increase in induced wind speed
University of Stuttgart, Stuttgart Wind Energy (SWE) @ Institute of Aircraft Design
3

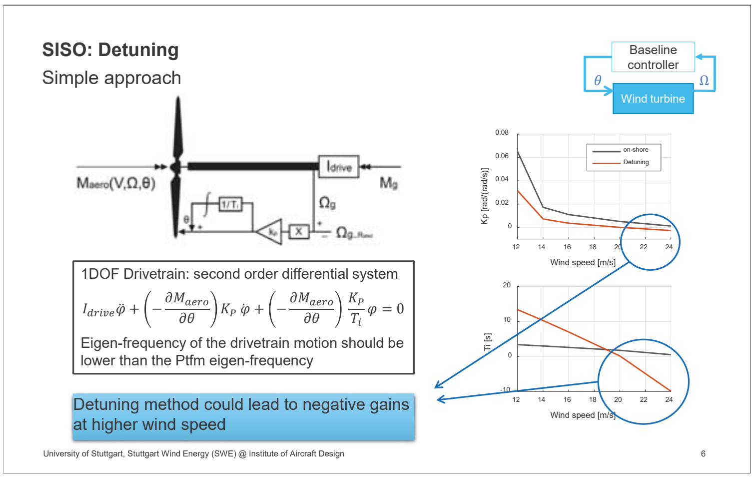
SISO: Detuning
Simple approach
Baseline controller
Wind turbine
Maero(V,Ω,θ)
Idrive
Mg
Ωg
1DOF Drivetrain: second order differential system
$I_{drive}\ddot{\varphi} + \left(-\frac{\partial M_{aero}}{\partial \theta}\right) K_P \dot{\varphi} + \left(-\frac{\partial M_{aero}}{\partial \theta}\right) \frac{K_P}{T_i} \varphi = 0$
Eigen-frequency of the drivetrain motion should be lower than the Ptfm eigen-frequency
Detuning method could lead to negative gains at higher wind speed
on-shore
Detuning
Kp [rad/(rad/s)]
Ti [s]
Wind speed [m/s]
University of Stuttgart, Stuttgart Wind Energy (SWE) @ Institute of Aircraft Design
6

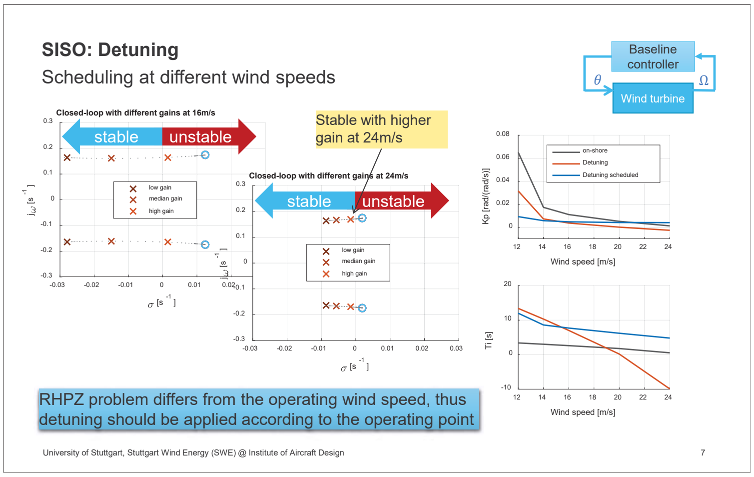
SISO: Detuning
Scheduling at different wind speeds
Baseline controller
Wind turbine
Closed-loop with different gains at 16m/s
stable
unstable
Stable with higher gain at 24m/s
Closed-loop with different gains at 24m/s
low gain
median gain
high gain
on-shore
Detuning
Detuning scheduled
Wind speed [m/s]
RHPZ problem differs from the operating wind speed, thus detuning should be applied according to the operating point
University of Stuttgart, Stuttgart Wind Energy (SWE) @ Institute of Aircraft Design
7

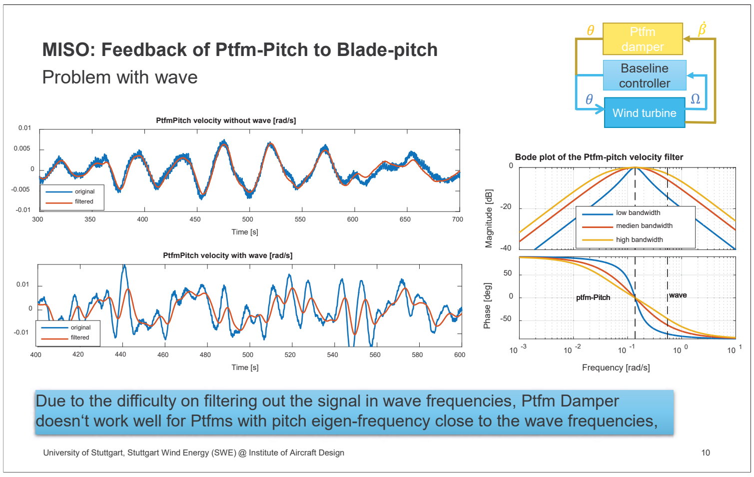
MISO: Feedback of Ptfm-Pitch to Blade-pitch
Problem with wave
Ptfm damper
Baseline controller
Wind turbine
PtfmPitch velocity without wave [rad/s]
PtfmPitch velocity with wave [rad/s]
original
filtered
Time [s]
Bode plot of the Ptfm-pitch velocity filter
low bandwidth
medien bandwidth
high bandwidth
Magnitude [dB]
Phase [deg]
ptfm-Pitch
wave
Frequency [rad/s]
Due to the difficulty on filtering out the signal in wave frequencies, Ptfm Damper doesn't work well for Ptfms with pitch eigen-frequency close to the wave frequencies.
University of Stuttgart, Stuttgart Wind Energy (SWE) @ Institute of Aircraft Design
10

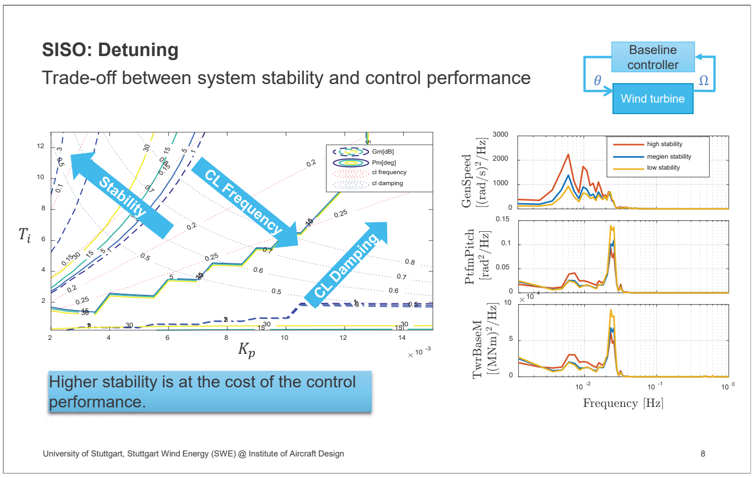
SISO: Detuning
Trade-off between system stability and control performance
Baseline controller
Wind turbine
Stability
CL Frequency
CL Damping
high stability
megien stability
low stability
Frequency [Hz]
Higher stability is at the cost of the control performance.
University of Stuttgart, Stuttgart Wind Energy (SWE) @ Institute of Aircraft Design
8

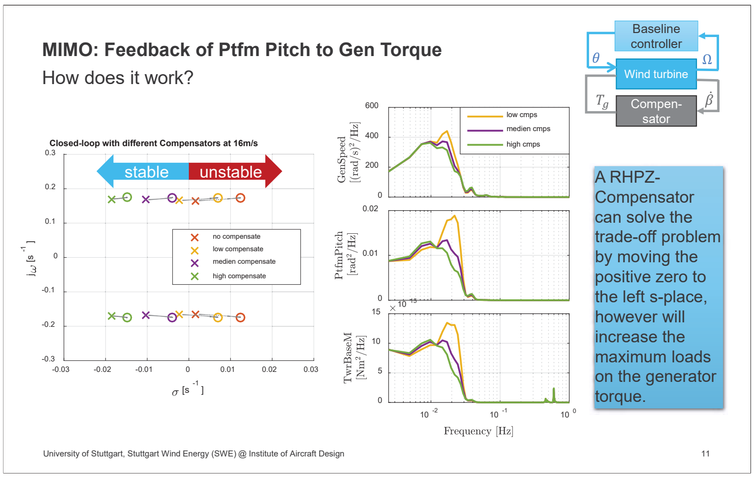
MIMO: Feedback of Ptfm Pitch to Gen Torque
How does it work?
Baseline controller
Wind turbine
Compen-sator
Closed-loop with different Compensators at 16m/s
stable
unstable
no compensate
low compensate
medien compensate
high compensate
low cmps
medien cmps
high cmps
Frequency [Hz]
A RHPZ-Compensator can solve the trade-off problem by moving the positive zero to the left s-place, however will increase the maximum loads on the generator torque.
University of Stuttgart, Stuttgart Wind Energy (SWE) @ Institute of Aircraft Design
11

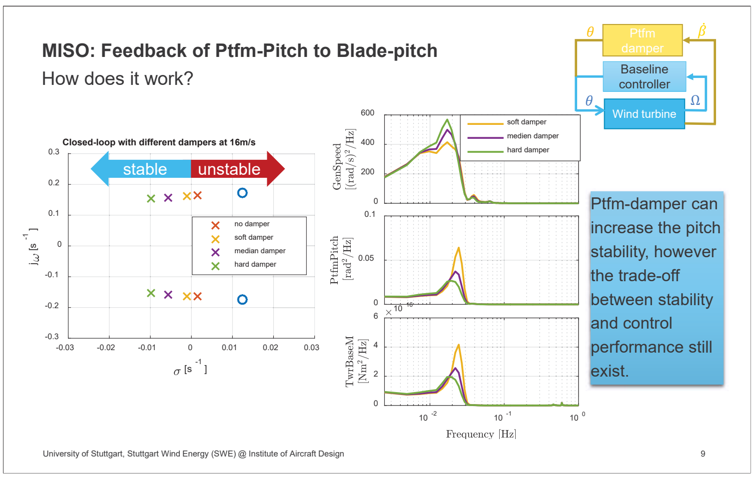
MISO: Feedback of Ptfm-Pitch to Blade-pitch
How does it work?
Ptfm damper
Baseline controller
Wind turbine
Closed-loop with different dampers at 16m/s
stable
unstable
no damper
soft damper
median damper
hard damper
medien damper
Frequency [Hz]
Ptfm-damper can increase the pitch stability, however the trade-off between stability and control performance still exist.
University of Stuttgart, Stuttgart Wind Energy (SWE) @ Institute of Aircraft Design
9

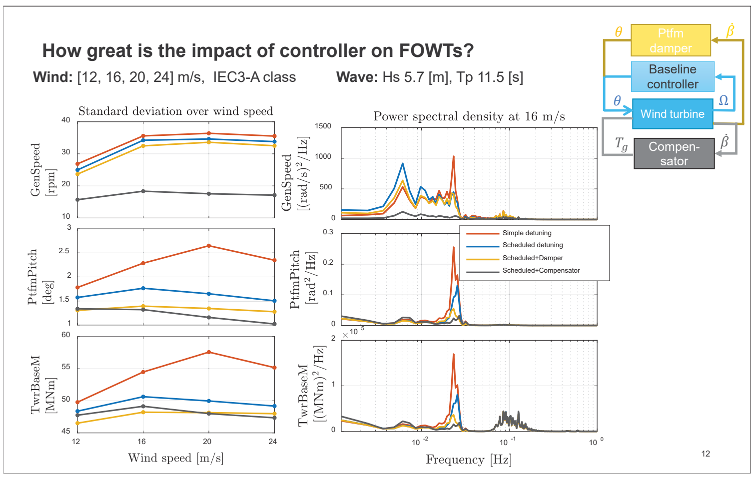
How great is the impact of controller on FOWTs?
Wind: [12, 16, 20, 24] m/s, IEC3-A class
Wave: Hs 5.7 [m], Tp 11.5 [s]
Ptfm damper
Baseline controller
Wind turbine
Compen-sator
Standard deviation over wind speed
Power spectral density at 16 m/s
Simple detuning
Scheduled detuning
Scheduled+Damper
Scheduled+Compensator
Wind speed [m/s]
Frequency [Hz]
12

Conclusion

- System motions and loads are strongly influenced by the controller. These can be significantly reduced by a well designed controller.
- Additional loops can improve the control performance. However, all of the state-of-art approaches have drawbacks.
- Improvement of control performance in wave frequency region is difficult with current sensor and actuators.

University of Stuttgart

Thank you!

Wei Viola Yu

e-mail yu@ifb.uni-stuttgart.de
phone +49 (0) 711 685-68240
fax +49 (0) 711 685-

University of Stuttgart

INNOSEA Ingénierie des Energies Marines — LHEEA CENTRALE NANTES — CNRS

Impact of the aerodynamic model on the modelling of the behaviour of a Floating Vertical Axis Wind Turbine

Vincent LEROY[1, 2]
PhD Student

J.-C. GILLOTEAUX[1], A. COMBOURIEU[2], A. BABARIT[1], P. FERRANT[1]

[1]LHEEA – Centrale Nantes – 1, rue de la Noë – 44321 Nantes - FRANCE
[2]INNOSEA – 1 rue de la Noë – 44321 Nantes - FRANCE

Unsteady aerodynamics of a VAWT at sea

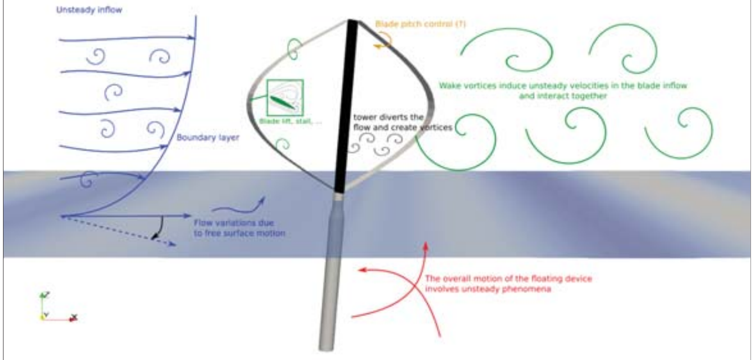

DeepWind VAWT (Paulsen et al., 2014)

Aerodynamic modelling of VAWTs

- Amongst other theories…
  - Inviscid models can usually account for viscous effects with **semi empirical models**

	Assumptions	Pros	Cons
DMS [1] *Double Multiple Streamtube*	**Steady** Inviscid flow Actuator disks	Fast State-of-the-art	Steady **Problems at high TSRs**
AC [2] *Actuator Cylinder*	Steady, 2D, Inviscid, Incompressible flow	Fast Accurate cylindrical swept surface Viscous models added	Steady flow Difficult to go 3D
FVW [3] *Free Vortex Wake + lifting line theory*	Potential flow Lifting line	**Unsteady** aerodynamics Inherent rotor/wake and wake/wake interactions	High CPU cost
CFD *Actuator line + RANS LES, …*	Var		Very high CPU cost

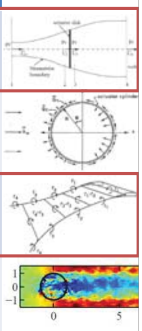

Which model can we use for a FVAWT ?

[1] (Paraschivoiu, 2002) [2] (Madsen, 1982) [3] (Murray et al., 2011)

Modular coupling

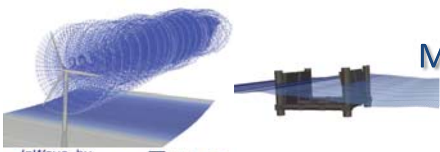

InWave by INNOSEA
Including NEMOH
(Babarit et al., 2015)

Hydrodynamics and multi-body solver

Moorings *MAP++* — NREL

Wind *constant/turbulent*

Rotor geometry

Aerodynamic solver FVW / DMS

Positions/velocities of blade elements

Forces and moments on the rotor

Control

A control module dedicated to **floating VAWTs** (Merz et al., 2013) and adapted as (Cheng, 2016) for our study, filtering $n * p$ frequencies. Or other DLL

CACTUS (SNL) *(Murray et al., 2011)*

In-house DMS solver

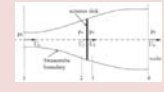

Skew correction (Wang, 2015)
Dynamic stall

Studied Floating HAWT and VAWTs

- NREL 5MW HAWT on the OC3Hywind SPAR (Jonkman, 2010)
- 2 and 3 bladed H-VAWTs of equal solidity, on the OC3Hywind SPAR
  - Designed by (Cheng, 2016)
- Same mooring system, with an added linear spring acting in Yaw (Jonkman, 2010)
- Rigid bodies (SPAR, tower and blades)
- Studied:
  - Motion RAOs with **"white noise"** waves and constant wind (DMS vs. FVW)
  - OC3 load cases in time domain for the VAWTs with **DMS vs. FVW** solvers
    - H2 presented today

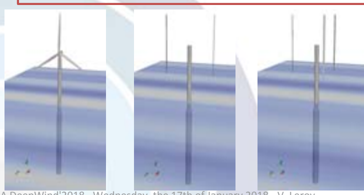

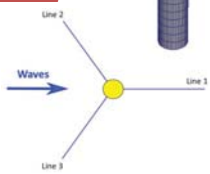

OC3 load cases on the H2 + OC3Hywind SPAR

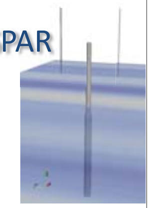

- Environmental conditions
  - $T_p = 10s, H_s = 6m$
  - Kaimal spectrum wind (x, y, t)
    - $U_\infty = 12m.s^{-1} \rightarrow TSR \approx 3.5$
    - $U_\infty = 18m.s^{-1} \rightarrow TSR \approx 2$
- Simulations run on $5000s$
  - Transient regime removed for analysis
- Relevant output data
  - Platform motions 6 DOFs
  - Aerodynamic loads and power on the rotor (F_x, F_y, P)
  - Aerodynamic loads on an equatorial blade element F_N, F_T

Power Spectral Densities: platform motions

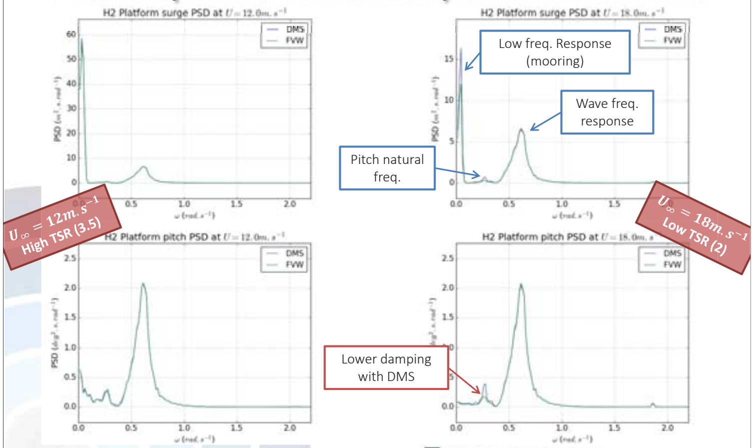

Power Spectral Densities: conclusions

- Similar motion PSDs in response to the two models: DMS and FVW
  - Surge, Heave, Pitch
  - Yaw (at natural frequency)
  - At waves and low frequencies
- Higher damping on the transversal motions with FVW
  - Differences in sway and roll at natural frequencies
- Important differences at high TSRs for the torque PSDs
  - At the $2p$ frequency
  - Similar behaviour at low frequencies

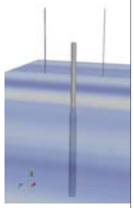

Power Spectral Densities: platform motions

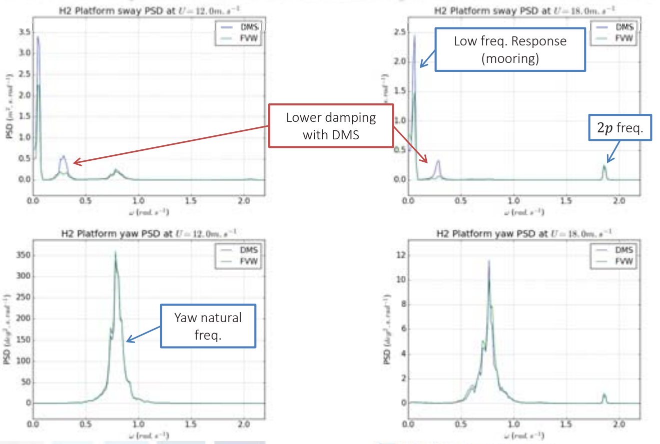

Mean and std: platform motions

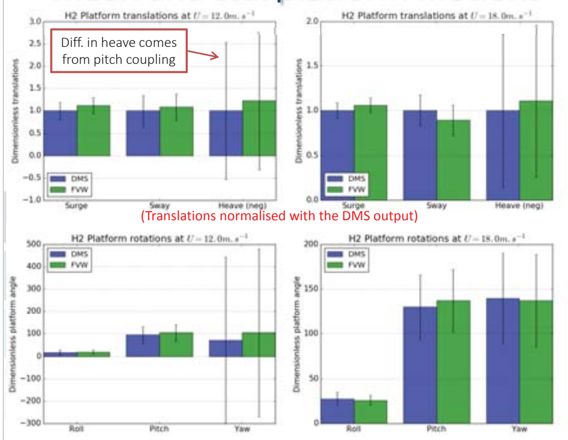

Relative differences: DMS vs. FVW

$U(m.s^{-1})$	12	18
$Mean(X)$	12%	6%
$Std(X)$	1%	6%
$Mean(Y)$	9%	11%
$Std(Y)$	14%	3%

$U(m.s^{-1})$	12	18
$Mean(\varphi)$	13%	6%
$Std(\varphi)$	14%	24%
$Mean(\theta)$	10%	5%
$Std(\theta)$	0%	2%
$Mean(\psi)$	19%	4%
$Std(\psi)$	1%	2%

Power Spectral Densities: aerodynamic loads

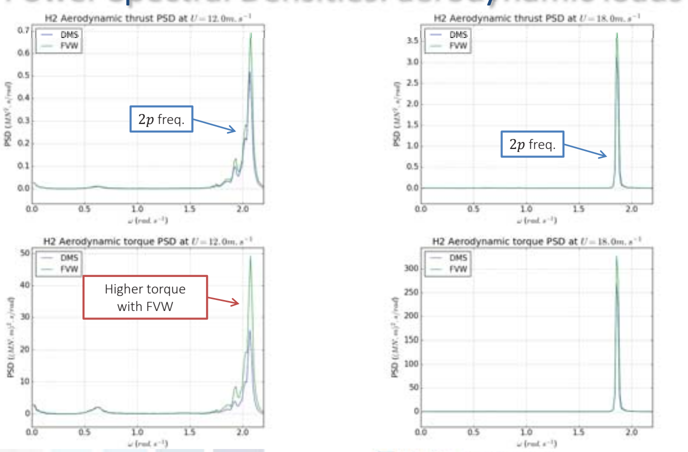

Mean and std: aerodynamics

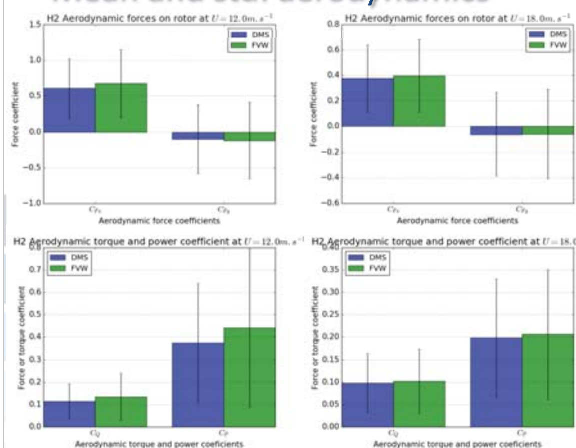

Relative differences: DMS vs. FVW

$U(m.s^{-1})$	12	18
$Mean(C_{Fx})$	12%	6%
$Std(C_{Fx})$	15%	9%
$Mean(C_{Fy})$	19%	5%
$Std(C_{Fy})$	11%	8%

$U(m.s^{-1})$	12	18
$Mean(C_P)$	17%	4%
$Std(C_P)$	33%	10%

Loads on a blade element

- Tangential load on equatorial blade element on a revolution
  - 25% relative difference on **mean load** at $12m.s^{-1}$
  - 37% relative difference on **std** at $12m.s^{-1}$
- Impact if considering flexible blades ?

$TSR = 3.5$

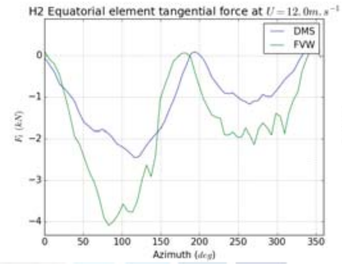

$TSR = 2$

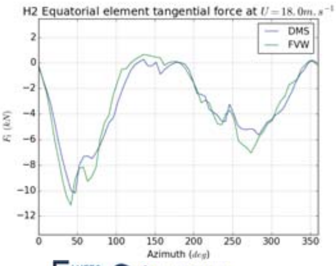

Takk !

Contact: vincent.leroy@ec-nantes.fr

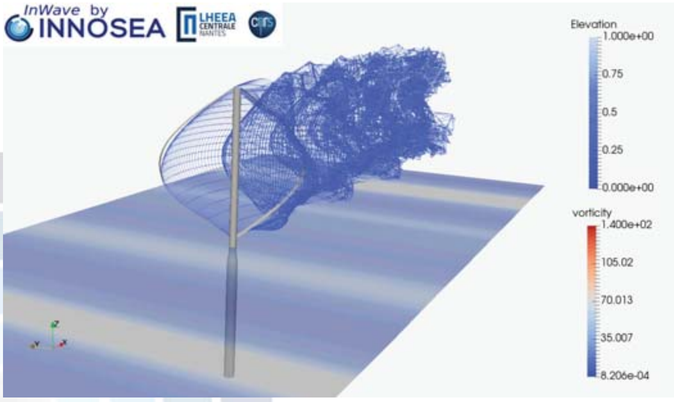

Conclusions

- On this case, with the OC3Hywind SPAR platform:
- Impact of the aerodynamic model on the H2 (OC3 load case): **DMS vs. FVW**
  - No substantial effect on PSDs (except transversal motions)
  - *Same conclusion on the motion RAOs with wind*
- Difficult to process mooring line tensions with this mooring model
  - Added linear stiffness in yaw, designed for a HAWT
  - A more detailed model could be important
- When focusing on mean and std:
  - At low TSR: models behave similarly
  - At high TSR: important differences on mean and std for
    - Aerodynamic loads
    - Motions

→ DMS seems to miss important aerodynamic unsteady effects due to strong rotor/wake interactions at high TSR
→ It could have a **strong impact** when looking at **blade design** (with **flexible blades**), for instance

- **Similar conclusions are obtained with the H3 VAWT** on the same load cases (not presented here…)
  - Comparative study to come

References

Paulsen et al., "DeepWind-from idea to 5 MW concept", *Energy Procedia*, 2014

I. Paraschivoiu, "Wind Turbine Design: With Emphasis on Darrieus Concept", *Presses Internationales Polytechniques*, 2002

H. A. Madsen, "The actuator cylinder - A flow model for vertical axis wind turbines", *Aalborg University Centre, Denmark*, 1982.

Murray et al., "The Development of CACTUS, a Wind and Marine Turbine Performance Simulation Code", *Proceedings of the 49th AIAA Aerospace Sciences Meeting including the New Horizons Forum and Aerospace Exposition, AIAA2011, 4 - 7 January 2011, Orlando, Florida,* 2011

A. Babarit and G. Delhommeau, "Theoretical and numerical aspects of the open source BEM solver NEMOH", *In Proceedings of the 11th European Wave and Tidal Energy Conference 6-11th Sept 2015, Nantes, France*, 2015

K. Merz and H. G. Svendsen, "A control algorithm for the DeepWind floating vertical-axis wind turbine", *Journal of Renewable and Sustainable Energy 5*, 2013

Z. Cheng, Integrated Dynamic Analysis of Floating Vertical Axis Wind Turbines, *Norwegian University of Science and Technology (NTNU)*, 2016

J. Jonkman et al., "Definition of the Floating System for Phase IV of OC3. Technical Report NREL/TP-500-47535", *National Renewable Energy Laboratory, National Renewable Energy Laboratory*, 2010

G. K. V. Ramachandran et al., "Investigation of Response Amplitude Operators for Floating Wind Turbines", *In Proceedings of 23rd International Ocean, Offshore and Polar Engineering Conference – ISOPE 2013, Anchorage, Alaska*, 2013

K. Wang, "Modelling and dynamic analysis of a semi-submersible floating Vertical Axis Wind Turbine", *Norwegian University of Science and Technology (NTNU)*, 2015

Coupled simulation tool: seakeeping

- *InWave* is developed at INNOSEA in collaboration with LHEEA Lab. of Centrale Nantes
- Key features:
  - Hydrodynamics: linear potential flow solver Nemoh (developed at Centrale Nantes)
  - Mechanics: multi-body solver
  - Quasi-steady mooring model (MAP++)
  - Accounts for Power Take Off (generator) and control laws (blade pitch and/or generator)
  - Solves the equations of motion in time domain using RK4 or Adams-Moulton scheme
  - Considers regular or irregular waves

Coupled simulation tool: FVW solver

- CACTUS
  - **C**ode for **A**xial and **C**ross-flow **TU**rbine **S**imulation
  - Developed at Sandia National Laboratories (BSD License)
- Free Vortex Wake theory – lifting line theory
  - Potential flow, unsteady
  - Either HAWT or VAWT
  - Works with known profiles (C_d, C_l, C_m)
  - Inherently accounts for tip vortices, rotor/wake interactions, skewed inflow
- Computes:
  - Unsteady aerodynamic loads, including the tower shadow
  - Including dynamic stall models:
    - Boeing-Vertol
    - Leishman-Beddoes
  - Pitch rate and added mass effects
- Validated on fixed horizontal and vertical rotors
- Added:
  - Parallel computing, turbulent inflow, visualizations, platform motions

SNL 34 m VAWT

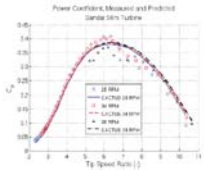

(Murray et al., 2011)

« Code-to-code » comparison

- First study on a floating HAWT with InWave + CACTUS
  - *OC3Hywind + NREL5MW (OC3)*
  - J. Jonkman et al., "Definition of the Floating System for Phase IV of OC3. Technical Report NREL/TP-500-47535", *National Renewable Energy Laboratory, National Renewable Energy Laboratory*, 2010

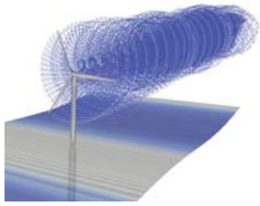

- Presented at OMAE2017 @Trondheim, Norway
  - V. Leroy, J.-C. Gilloteaux, M. Philippe, A. Babarit & P. Ferrant, "Development of a simulation tool coupling hydrodynamics and unsteady aerodynamics to study Floating Wind Turbines", *Proceedings of the ASME 2017 36th International Conference on Ocean, Offshore and Arctic Engineering, OMAE2017, June 25-30, 2017, Trondheim, Norway*, **2017**

Coupled simulation tool: DMS solver

- Theory from Paraschivoiu (2002)
  - Assumes steady and potential flow
  - Large number of double streamtubes
  - With actuator disks upwind and downwind
- Added:
  - Leishman-Beddoes dynamic stall model
  - Skew model as presented in Wang (2015)
  - Validated on a fixed turbine (SANDIA 17m) (Akins, 1986)
  - And in a skewed flow (Mertens, 2003)

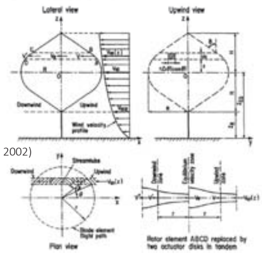

(Parachivoiu, 2002)

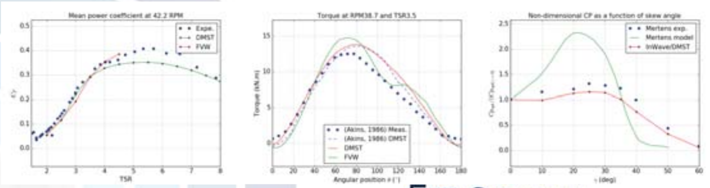

Studied Floating HAWT and VAWTs

- NREL 5MW HAWT on the OC3Hywind SPAR (Jonkman, 2010)
- 2 and 3 bladed H-VAWTs of equal solidity, on the OC3Hywind SPAR
  - Designed by (Cheng, 2016)
- Same mooring system, with an added linear spring acting in Yaw (Jonkman, 2010)
- Rigid bodies (SPAR, tower and blades)
- Studied:
  - Motions RAOs from "white noise" waves and wind (DMS vs. FVW)
  - OC3 load cases in time domain for the VAWTs with DMS vs. FVW solvers
    - H2 presented today

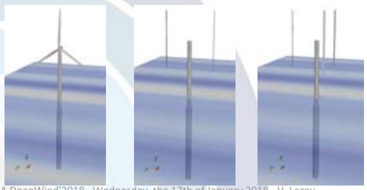

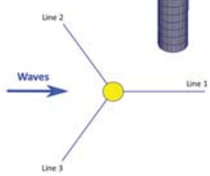

Control algorithm (Merz, 2013)

- Adapted by (Cheng, 2016)

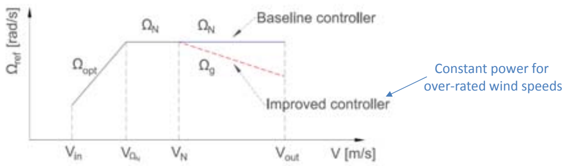

Constant power for over-rated wind speeds

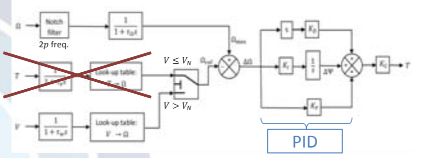

(Cheng, 2016)

Motion RAOs from time domain

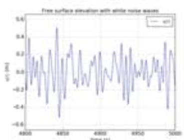

- Conditions:
  - White noise waves
  - Constant wind: $U_\infty = 0, 8, 12, 18\ m.s^{-1}$ (Only BEM (**FAST**) for HAWT or DMS for VAWTs)
- Post-processing:
  - PSD computation as in (Ramachandran et al., 2013)
  - $RAO(\omega) = \frac{S_{motion}(\omega)}{S_{waves}(\omega)}$, on the waves frequencies

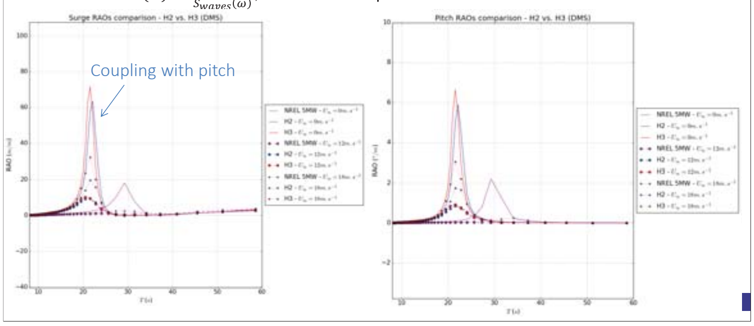

Impact of aero model and RAOs

- **Comparison of these RAOs for VAWTs: DMS vs. FVW**

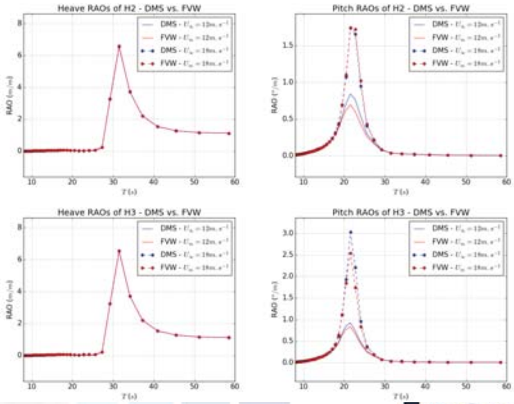

No effect on heave

Damping seems to be more important in FVW model

No other effect on RAOs

B1) Grid connection and power system integration

Ancillary services from wind farms, Prof W. Leithead, Strathclyde University

North Seas Offshore Network: Challenges and its way forward, P.Härtel, Fraunhofer IWES

Towards a fully integrated North Sea Offshore Grid: An engineering-economic assessment of a Power Link Island, M. Korpås, NTNU

Generic Future Grid Code regarding Wind Power in Europe, T.K.Vrana, SINTEF Energi

Ancillary Services from Wind Farms

Bill Leithead

Wind Energy and Control Centre
University of StrathClyde

The Faculty of Engineering

Wind Farm Control Structure

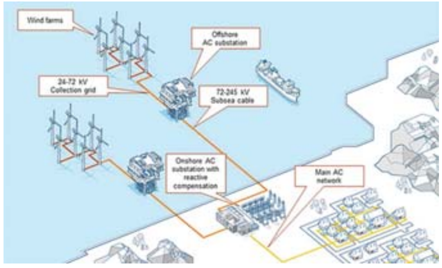

Context

To provide full range of Ancillary Services requires

- Flexible operation of array
- Flexible operation of turbines
- Delivery by wind farm control
- Robustness to comms delays
- Array to act as virtual plant

Wind Farm Control Structure

Ancillary Services are delivered by the controller

- Architecture provides full flexibility of operation
- It is distributed, hierarchical and scalable

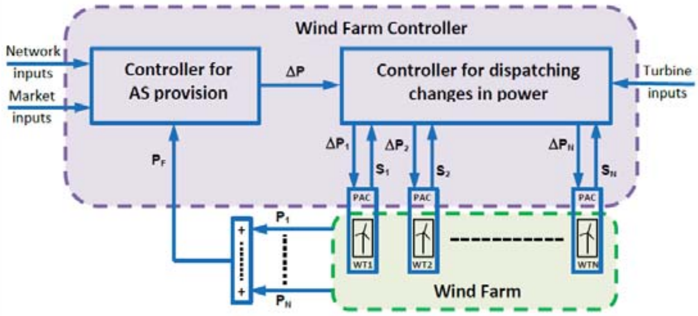

Context

Worst case scenario

- GW size array
- Far offshore
- HVDC connection-to-shore

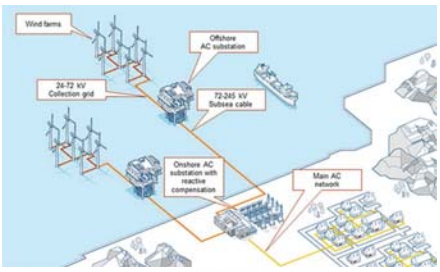

Wind Farm Control Structure

Controller for AS provision

- Determines total change in power, ΔP, required
- May or may not depend on current output, P_F

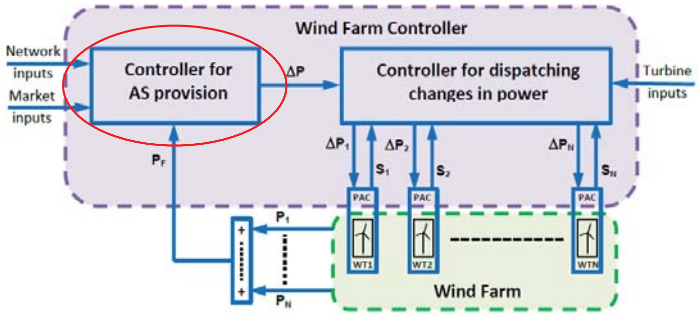

Wind Farm Control Structure

Controller for dispatching changes in power

- Determines change in output, ΔP_i, required from each turbine

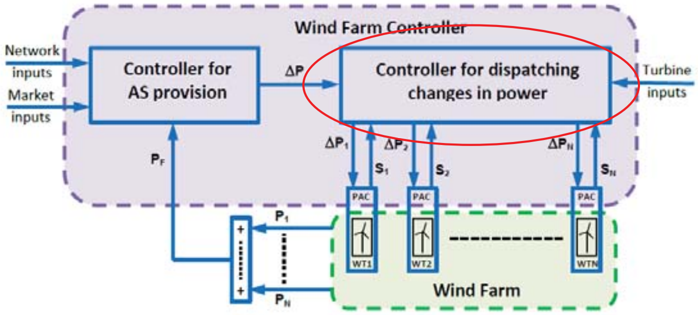

Wind Farm Control Structure

- 5MW wind turbine in 9m/s mean wind speed
- Output adjusted in increments of 100kW

Increase in output power

Full envelope controller mode switch

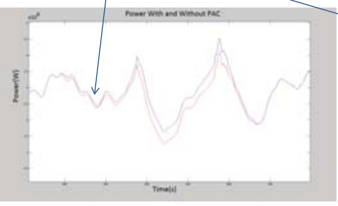

Power output with and without PAC

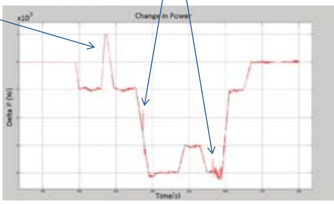

Difference in output with and without PAC

Wind Farm Control Structure

Power Adjusting Controller, **PAC**, is interface to turbine controller

- Adjusts output of turbine **i** by ΔP_i, as requested
- PAC passes back info on turbine state using flags, S_i

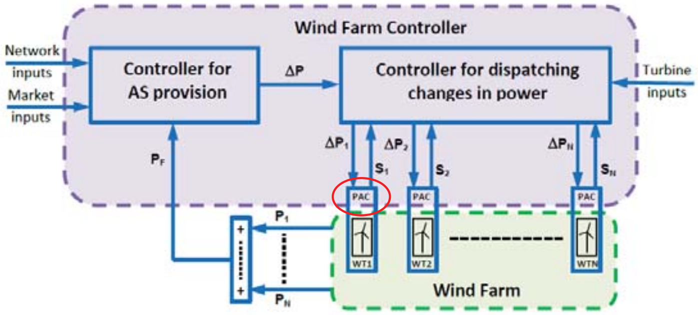

Wind Farm Control Structure

- Provision of synthetic inertia by PAC on 5MW wind turbine
- 7, 10 and 20m/s mean wind speed

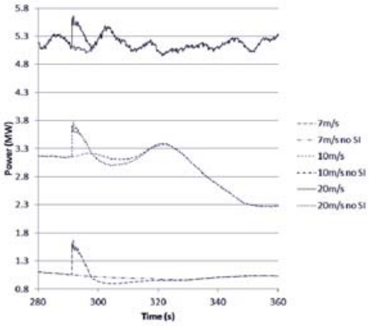

Absolute power outputs

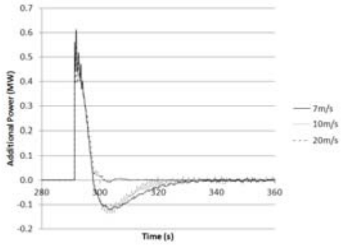

Relative power outputs

Wind Farm Control Structure

Power Adjusting Controller, **PAC**, is interface to turbine controller

- Adjusts output of turbine **i** by ΔP_i, as requested
- PAC passes back info on turbine state using flags, S_i

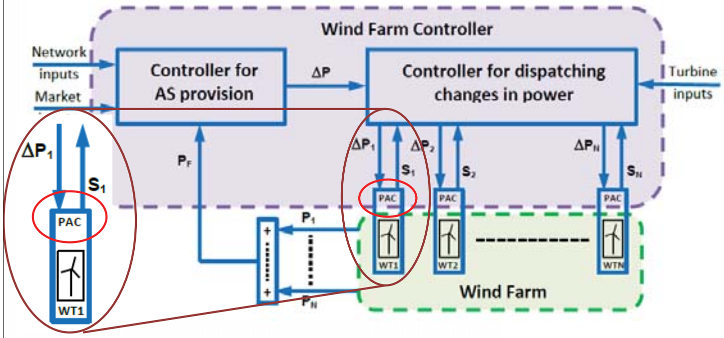

Wind Farm Simulation

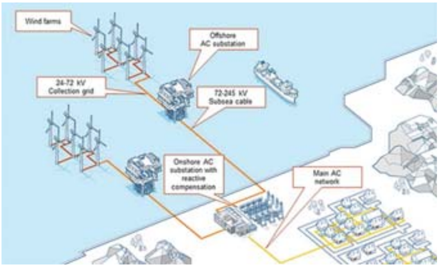

Wind Farm Simulation

- **StrathFarm**

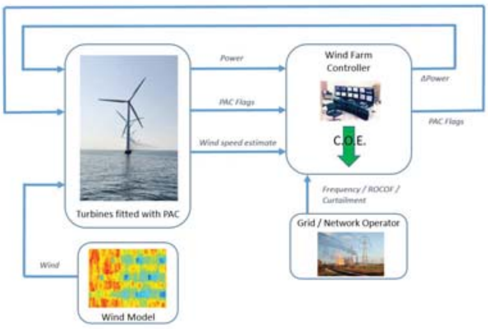

Farm Output Curtailment

- Controller for AS provision acts on (P_0- P_F)
- It has integral action
- ΔP is continuously updated to drive (P_0- P_F) to zero

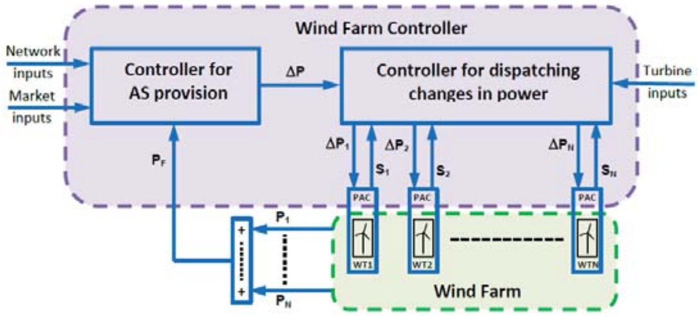

Wind Farm Simulation

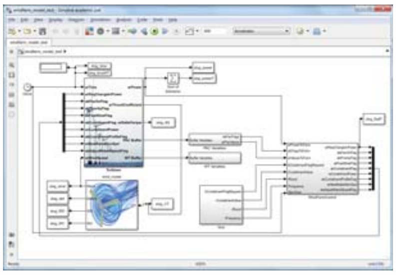

- Simulink model with compiled C++ elements
- Up to 100 turbines
- Run in real time on desk-top PC

Current simulation times (for 600s Simulation):

- 5WTs ~ 33s
- 20 WTs ~ 155s

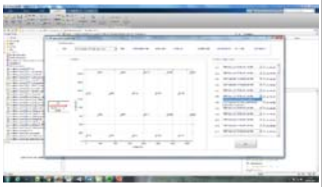

Farm Output Curtailment

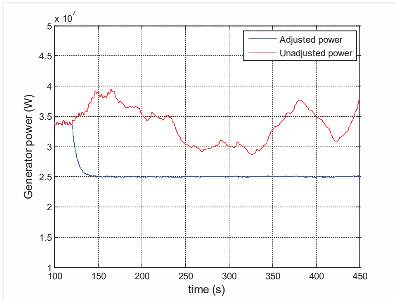

- Wind farm of 10x5MW turbines with mean wind speed of 10m/s.
- Farm output with and without curtailment

Farm Output Curtailment

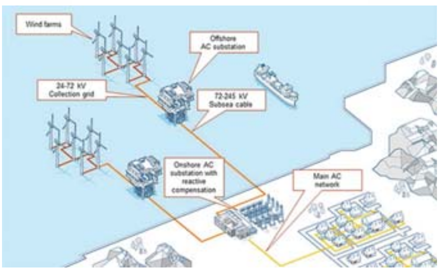

Farm Output Curtailment

- Individual turbine behaviour

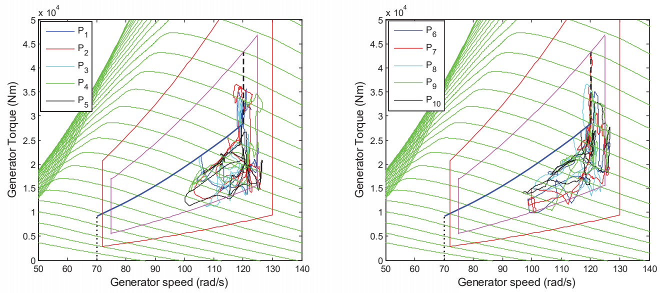

Farm Output Curtailment

- Wind farm output when turbines are curtailed individually.

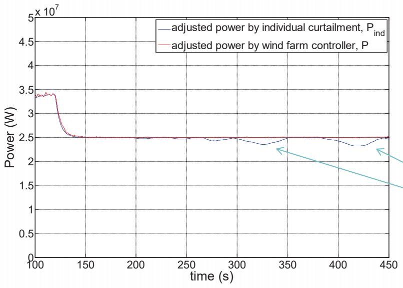

Reduction in wind farm output

Farm Level Frequency Support

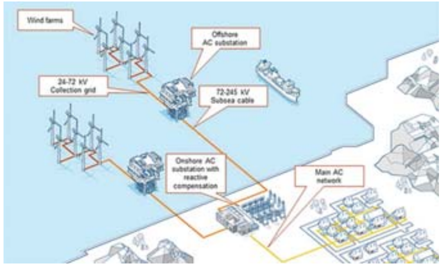

Farm Output Curtailment

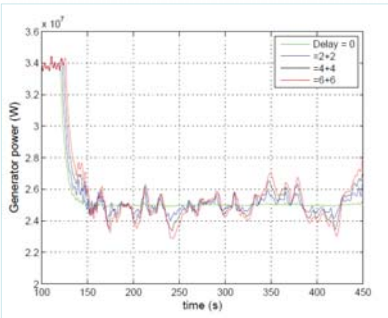

- Perturbations of power output about target of 25MW increases with time delay.
- Perturbations decrease as number of turbines in farm increases.
- Robustness to communication delays of 2, 4, and 6 seconds.

Farm Level Frequency Support

- Controller for AS provision does not act on $\mathbf{P_F}$
- $\mathbf{\Delta P}$ is continuously updated in response to grid frequency
- Provides both synthetic inertia and droop control

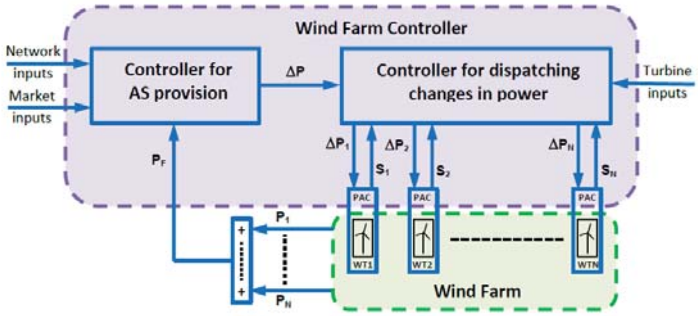

Farm Output Curtailment

No delay

4+4 delay

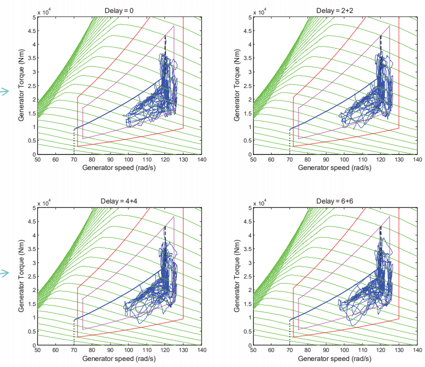

2+2 delay

6+6 delay

- Amber region safely cushions perturbations

Farm Level Frequency Support

- Provision of ancillary services at farm level

- 10x5MW turbines in 2 columns of 5
- Mean wind speed ~ 8m/s
- Turbulence ~10%
- Requested reserve ~ 2MW

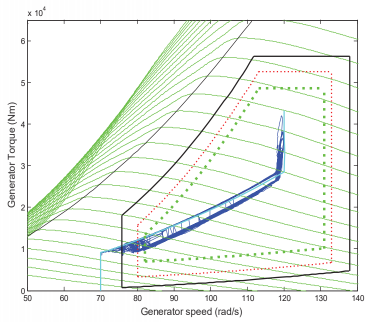

Provision of reserve power

Farm Level Frequency Support

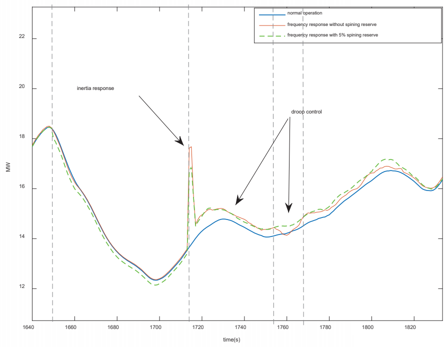

- Wind farm provision of frequency support with/without 2MW curtailment

Virtual Conventional Plant

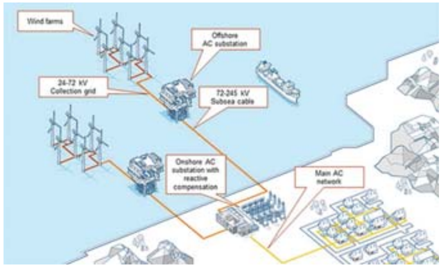

Farm Level Frequency Support

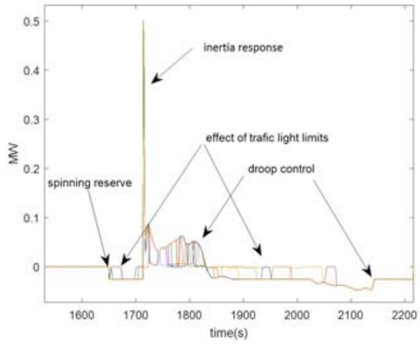

- Change in power for each turbine (with 2MW curtailment)
- Cross-compensation between turbines (needed as wind speed low)

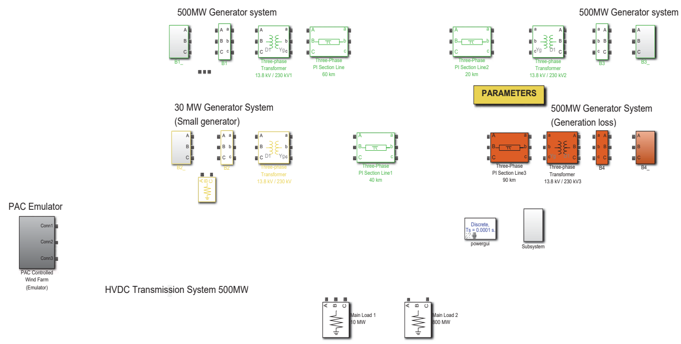

Farm Level Frequency Support

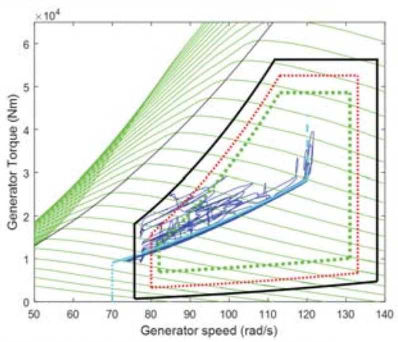

- Operation of each turbine

Virtual Conventional Plant

- Primary response provided by virtual plant

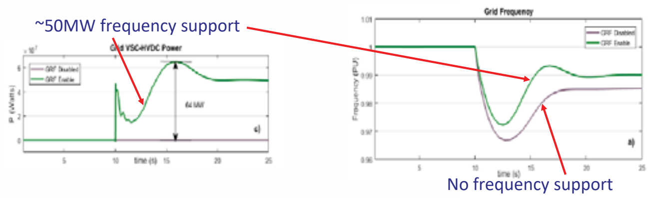

Virtual Conventional Plant

- Virtual plant with communication delay of 150ms

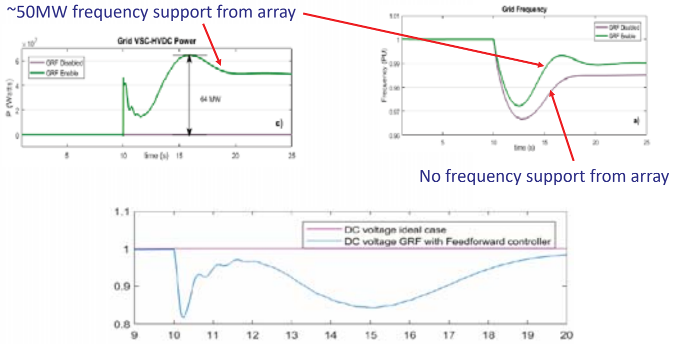

- DC voltage drop due to energy extraction

Virtual Conventional Plant

- GRF with communications delay of 150ms
- Feedforward control applied to HVDC sub-station
- Stability of grid is not compromised

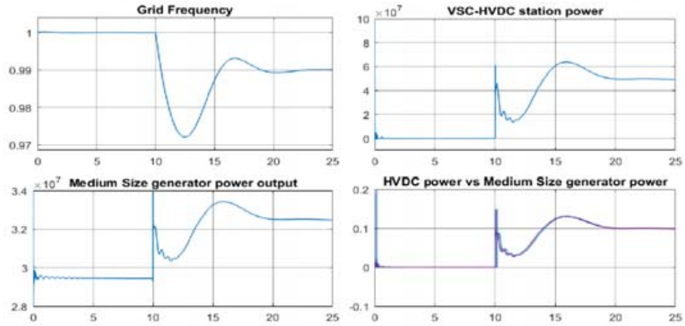

Virtual Conventional Plant

- Shorter delay reduces voltage drop
- Generator-response following control (GRP)

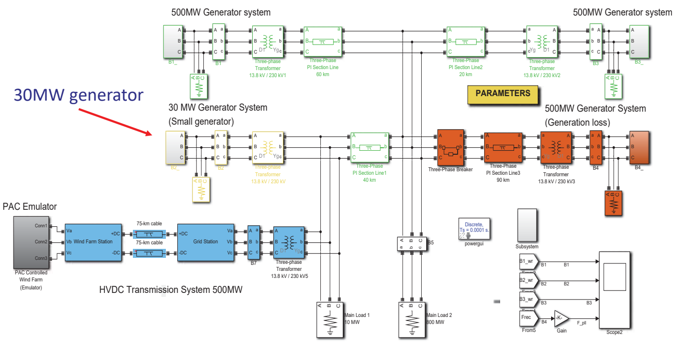

Virtual Conventional Plant

- GRF with communications delay of 150ms
- Feedforward control applied to HVDC sub-station
- Stability of grid is not compromised

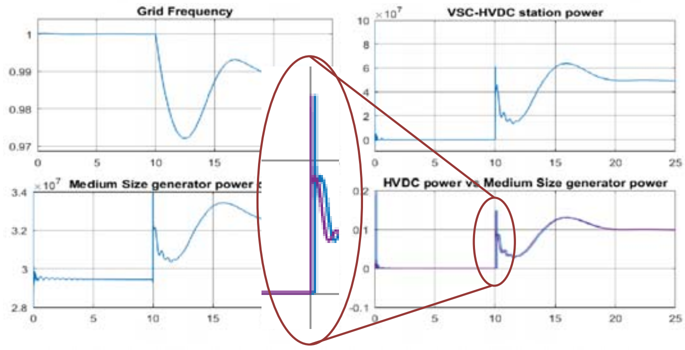

Virtual Conventional Plant

Generator-response following concept

- Fully instrumented small/medium synchronous generator is connect at the Point of Connection of the wind farm
- Power output of the wind farm is slaved to follow the output of the synchronous generator using the wind farm controller
- When the small/medium synchronous generator provides Ancillary Services, then so does the wind farm, albeit scaled-up

Potential advantages

- No direct power frequency measurements to reduce delays
- Provides a full range of Ancillary Services, inertia, governor-droop control, reserve, curtailment etc.
- Grid Code Compliant

Conclusion

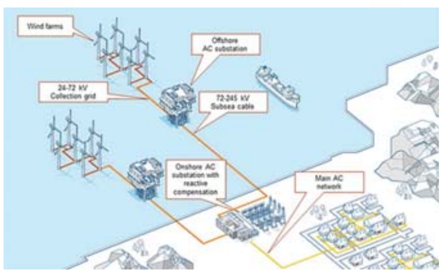

Conclusion

Provision of full range of Ancillary Services possible at wind farm level

Thank You

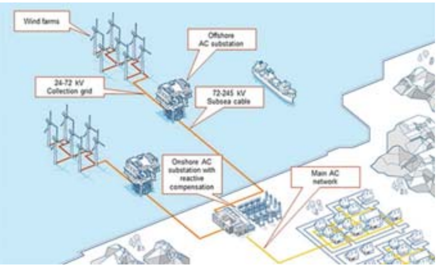

Northern Seas Offshore Network (NSON)

Challenges and its way forward

Philipp Härtel, Denis Mende, Kurt Rohrig, Energy Economics and Grid Operation, Fraunhofer IEE
Philipp Hahn, Andreas Bley, Institute of Mathematics, University of Kassel

Supported by:
Federal Ministry for Economic Affairs and Energy
on the basis of a decision by the German Bundestag

15th Deep Sea Offshore Wind R&D Conference, EERA DeepWind'2018
Trondheim, January 18, 2018

Agenda

Agenda

University of Kassel, IEH of Leibniz University Hannover and Fraunhofer IEE are the partners of the national project in Germany (NSON-DE)

Northern Seas Offshore Network (NSON) Initiative

- Pursuing an **offshore grid in the Northern Seas** region
- **Research, Development & Deployment Program**
- **Following the Berlin Model for cooperative research** activities in Europe: nationally funded projects which are guided by a simple and target-oriented implementation

Objectives of the NSON Initiative

- **Harnessing**, **sharing**, and **trading of offshore wind** resources
- Supporting the **utilisation** of **offshore** region's **wind resources**
- Making the **national markets more effient** by increasing connection capacities
- Providing **balancing from Nordic hydropower**

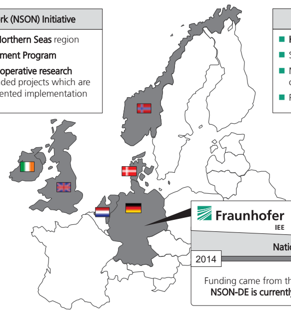

Fraunhofer IEE + UNIKASSEL VERSITÄT +

National NSON project in Germany (NSON-DE)

2014 → 2017

Funding came from the Federal Ministry for Economic Affairs and Energy (BMWi)
NSON-DE is currently being finalised - report to be published by June this year

Agenda

NSON-DE has four modelling stages to investigate potential NSON configurations and their impacts on both the German and European energy supply system with consistent data sets and feedback loops

Modelling stages		Geographical focus
Market-based grid planning	1	European energy market areas + offshore grid region (offshore hubs)
Technology-based grid planning	2	Offshore grid region (single wind farms)
Offshore grid validation	3	Offshore grid region (single wind farms)
Onshore grid repercussions	4	Onshore transmission system (German market area)

The market-based grid planning determines and assesses market-driven investment decisions in a potential NSON, adequately accounting for the directly and indirectly connected onshore market areas

Modelling stages		Geographical focus
Market-based grid planning	1	**European energy market areas + offshore grid region** (offshore hubs)
Technology-based grid planning	2	Offshore grid region (single wind farms)
Offshore grid validation	3	Offshore grid region (single wind farms)
Onshore grid repercussions	4	Onshore transmission system (German market area)

Consistent spatial and meteorological data is used to adequately capture the offshore grid region – final case studies will investigate three topology paradigms for NSON 2030 and 2050

Spatial and structural offshore wind data set

Single offshore wind farms[1] and **clustered offshore wind hubs** relevant **for offshore grid investment decisions** in the NSON 2050 scenario (values indicate installed generation capacity at offshore wind hubs in MW)

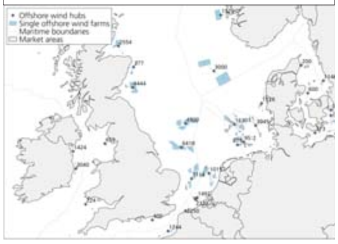

Meteorological data set

Meteorological data from the COSMO-EU model is used to obtain

- site-specific **offshore wind production profiles**
- site-specific **CAPEX , OPEX ,** and **LCOE data**

for **different investment periods** (5 year stages)

Final NSON case studies

NSON 2030	NSON 2050

Topology paradigms:

- **"Status Quo"** allowing radial offshore hub connections and no expansion on existing interconnector corridors
- **"Business as Usual"** allowing radial offshore hub connections and expansion on existing interconnector corridors
- **"Meshed Grid"** allowing meshed offshore hub connections and expansion on existing interconnector corridors

[1] Based on 4C Offshore 2017 Offshore Wind Farms Intelligence Database (Suffolk) https://www.4coffshore.com/.

Long-term NSON 2050 scenario features high level of decarbonisation due to coupled operation of energy sectors – capturing interaction and flexibility is essential in offshore grid expansion planning

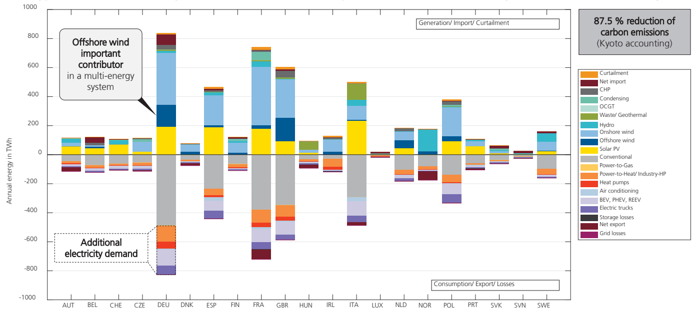

87.5 % reduction of carbon emissions (Kyoto accounting)

NSON scenarios were created with the cross-sectoral dispatch and investment model SCOPE at Fraunhofer IEE.

PRELIMINARY

Initial grid configuration shows realised and planned interconnector projects in Northern Europe – "Meshed Grid" shows investments in both interconnector and integrated offshore wind connections

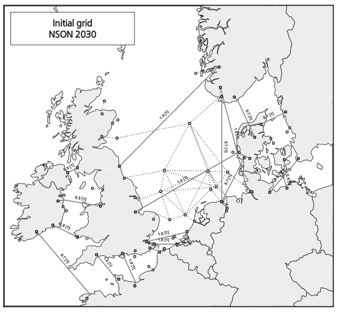

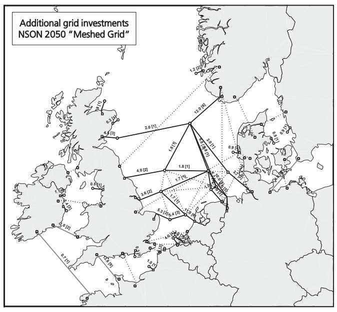

The large-scale offshore grid expansion planning model has a particular focus on capturing future energy system flexibility in the onshore market areas

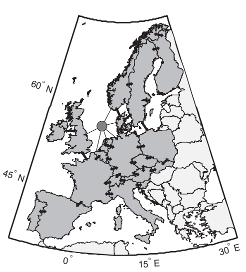

Multi Market Area Dispatch and Offshore Grid Expansion Model (static, deterministic TEP)

Onshore market area

- Load coverage of residual load
- Technical restrictions of the hydro-thermal plants
- Technical restrictions of other flexibility options (such as battery storage, heat pumps, flexible CHP, electric vehicles and trucks)

Offshore grid region (area)

- Load coverage/ node balance of offshore hubs with wind generation/ curtailment/ storage
- Investment decision variables in AC/DC offshore grid infrastructure (including integers for fixed costs of cables, converters, and platforms)[1]

Power exchange between areas

- Im-/ export between onshore market areas
- Im-/ export between onshore market areas and offshore grid region

! **Centralised/ closed solution of the full-year problem** (i.e. consecutive 8760 h) **with high unit** (blocks) and **investment details** (integer cable and platform costs) **is not tractable**

➡ **Careful aggregation of unit details + Regional decomposition approach (proximal bundle)** applied to improve the solvability of the offshore grid planning problem

[1] Härtel et al. 2017 Review of investment model cost parameters for VSC HVDC transmission infrastructure *Electric Power Systems Research* **151** 419.

The technology-based grid planning stage narrows the focus to the offshore grid region and investigates it with a higher level of detail

Modelling stages		Geographical focus
Market-based grid planning	1	European energy market areas + offshore grid region (offshore hubs)
Technology-based grid planning	2	**Offshore grid region** (single wind farms)
Offshore grid validation	3	Offshore grid region (single wind farms)
Onshore grid repercussions	4	Onshore transmission system (German market area)

Technology-based grid planning stage simultaneously optimises locations of future wind farms, their connection(s) to shore, and the main technical components

Market-based grid planning	Resulting output data ■ **Full-year time series data of power exchange** between offshore region and onshore market areas ■ Country-specific **offshore wind capacity targets**

Input

Technology-based grid planning	Goals ■ **Planning a detailed offshore grid** with its spatial and technical configuration ■ **Co-optimise single wind farm investments** ■ Considering **incremental expansion** of the offshore grid **for a long-term horizon** 2050 (multi-stage) ■ Satisfying **exchange demands** and offshore wind **capacity targets**

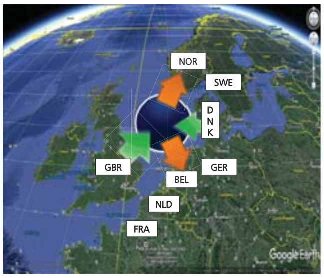

Planning aspects and technical requirements demand some simplifications when co-optimising grid planning and wind farm locations

Offshore region

Raster hubs

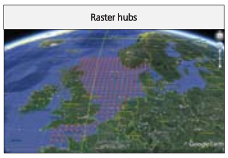

Potential wind farm locations

Planning aspects	
Vast number of potential locations	Incremental construction plan

Technical requirements		
Technical equipment (converters, transformers, switches)	Platforms for the equipment	Various line types (AC, DC, voltage levels, etc.)

Necessary simplifications
- Neglecting physical laws of power flow
- Temporal resolution (consider subset of weather year)

EXEMPLARY

A test grid instance was used to test the mixed-integer linear program and newly developed heuristics to quickly compute feasible initial solutions

Test grid instance

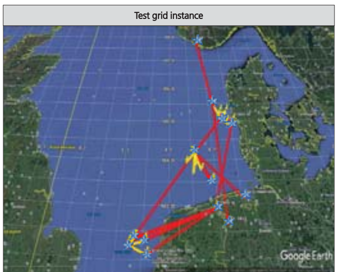

DC lines AC lines Converter

Benchmark test system for the offshore grid in the North Sea[1)]

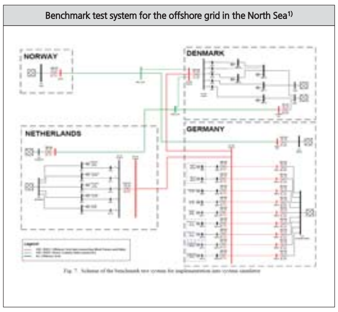

[1)] Rudion et al. 2010 Toward a Benchmark test system for the offshore grid in the North Sea *IEEE PES General Meeting*, Minneapolis, 1-8.

The offshore grid validation stage tests the grid planning results using power system analysis software assessing approximation errors

Modelling stages		Geographical focus
Market-based grid planning	1	European energy market areas + offshore grid region (offshore hubs)
Technology-based grid planning	2	Offshore grid region (single wind farms)
Offshore grid validation	**3**	**Offshore grid region (single wind farms)**
Onshore grid repercussions	4	Onshore transmission system (German market area)

Due to a large number of time steps and scenarios, an automated approach was developed to electrically validate the market- and technology-based grid planning results

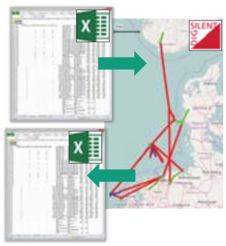

- Electrical data of components
- Grid topology & connection of elements
- Definition of node types and control schemes
- Power flow calculation
- Documentation of data and power flow results
- Comparison with grid planning assumptions
  - Component powers
  - Power flows in the grid
  - Losses of elements

Onshore grid repercussions induced by different offshore grid topologies are assessed for the onshore transmission system of the German market area

Modelling stages		Geographical focus
Market-based grid planning	1	European energy market areas + offshore grid region (offshore hubs)
Technology-based grid planning	2	Offshore grid region (single wind farms)
Offshore grid validation	3	Offshore grid region (single wind farms)
Onshore grid repercussions	**4**	**Onshore transmission system (German market area)**

Market simulation data and offshore grid planning data for the NSON 2030 scenario are combined with a detailed model representing the German part of the continental European transmission system

Assessment of onshore grid repercussions

- **Model** of the German transmission system **based on** the **German grid development plan** for 2030
- SCOPE model delivers **unit- and node-specific input data**
- **Implementation of offshore power flows into German grid** (due to market exchanges)
- Comparison of results and **impact analysis of market coupling through meshed offshore system**

Regionalised generation and consumption data sets

- **Renewable generation types:** onshore wind, offshore wind (i.e. offshore grid exchange), roof-top PV, utility-scale PV, flexible and inflexible biomass, waste, scrapwood, conventional and pumped hydro
- **Thermal generation types:** extraction condensing units (CHP), back-pressure units (CHP), condensing units, gas turbines
- **Traditional load types:** households, trade and services, industry, agriculture, public transport, pumped hydro
- **Additional load types:** battery and plug-in hybrid electric vehicles, electric overhead line trucks, industry heat pumps, decentralised air- and ground-source heat pumps, direct electric heating units (CHP and non-CHP), air-conditioning

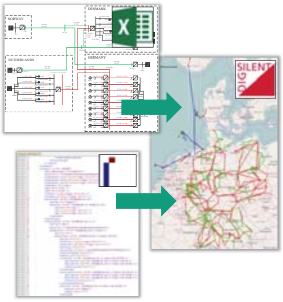

Agenda

- I Northern Seas Offshore Network (NSON)
- II Modelling stages of the national NSON project in Germany (NSON-DE)
- **III Challenges for future research**
- IV Summary

Over the course of the NSON-DE project a number of remaining challenges were identified for further research

Flexibility and uncertainty in future energy systems

- **Competition** of offshore grids **with future onshore flexibility options**
- **Uncertainty** from **bottom-up** developments and **top-down** target definitions
- **Simultaneous optimisation of generation and transmission expansion** for a highly decarbonised system heavily relying on wind and solar

Market integration and cost-benefit sharing

- **Harmonised cross-border rules of the involved market areas** (time-scales, market products)
- **Cost-benefit allocation** and **sharing methods** for both directly and indirectly connected market areas

Grid operation

- **Optimized grid and plant control** in normal operation
- **Dynamic control concepts** in normal operation as well as in fault and emergency situations

Grid planning

- Efficiently solving **optimisation problems capturing technical complexity** and **operational flexibility** in the grid planning stages
- **Handling time series data computationally more efficiently**
- Incorporate **statistically known data uncertainties** or **barely predictable** political, technological, or economic **uncertainties**

Power Link Islands (PLI)

- **Artificial island for transnational power exchange** and **distribution of offshore wind resources**, while hosting other services such as operation and maintenance for offshore wind farms
- **High uncertainty** associated with the **investment costs** and **potential locations**
- **Combined assessment of** the investment **costs and** the economic **benefits** a PLI offers

Agenda

- I Northern Seas Offshore Network (NSON)
- II Modelling stages of the national NSON project in Germany (NSON-DE)
- III Challenges for future research
- **IV Summary**

Conclusions

With a growing amount of offshore wind generation being deployed in Northern Europe, the relevance of a Northern Seas Oshore Network (NSON) increases
particularly in light of high cross-sectoral decarbonisation targets

The national NSON project in Germany (NSON-DE) developed a closely linked modelling chain involving several stages
market- and technology-based grid planning, offshore grid validation, and onshore grid repercussions

Flexibility and uncertainty in future (multi-)energy systems, market integration, cost-benefit sharing as well as robust grid planning and operation methods
are important issues for future research

Thank you very much for your attention!

Fraunhofer IEE

M.Sc. Philipp Härtel

Energy Economics and Grid Operation
Fraunhofer Institute for Energy Economics
and Energy System Technology IEE

Königstor 59 | 34119 Kassel
Phone +49 561 7294-471 | Fax +49 561 7294-260
philipp.haertel@iee.fraunhofer.de

Towards a fully integrated North Sea Offshore Grid

- An economic analysis of a Power Link Island / OWP hub

Martin Kristiansen
Magnus Korpås
Hossein Farahmand

Keywords: North Sea Offshore Grid, Grid Typologies, Market Integration, Optimization, TEP, GEP

Outline for the talk

1. **Main drivers for multinational TEP**
   - More renewables -> need for flexibility
2. **Motivation: Different grid topologies**
   - Radial // Meshed // Artificial Island (!)
3. **Added value of an artificial island**
   - "Power Link Island" versus radial solutions
4. **Conclusions and work in progress**

As we know: More renewables comes into the system

Quarterly Investments by Assets (ex. R&D)

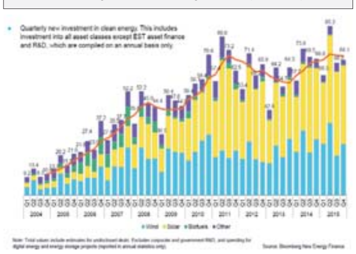

..causes a more volatile net-load

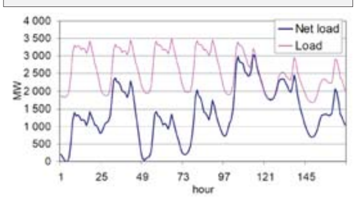

Ref: NREL, Holttinen (VTT)

...and the renewable resources are geographically spread

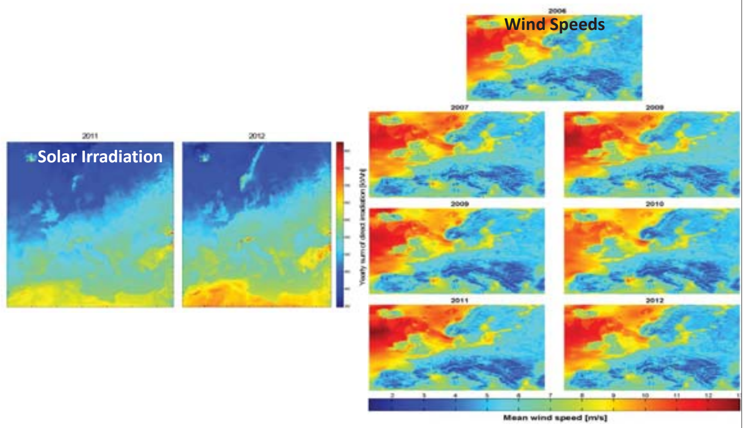

More RES yields a demand for infrastructure and flexibility

Increasing demand for spatial and temporal flexibility ➡ North Seas Offshore Grid (NSOG)

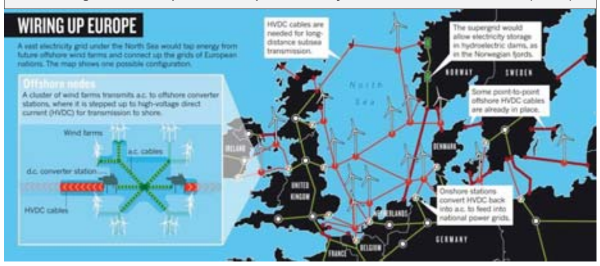

Power Link Island

Artificial island for transnational power exchange and distribution of offshore wind resources

Each PLI can include 30 GW offshore wind

Power Link VS radial

Assessing their performance with an optimization model for both investments and operation.

North Sea Offshore Grid 2030 Case study (ENTSO-E Vision 4)

…with expected cost savings due to economies of scale

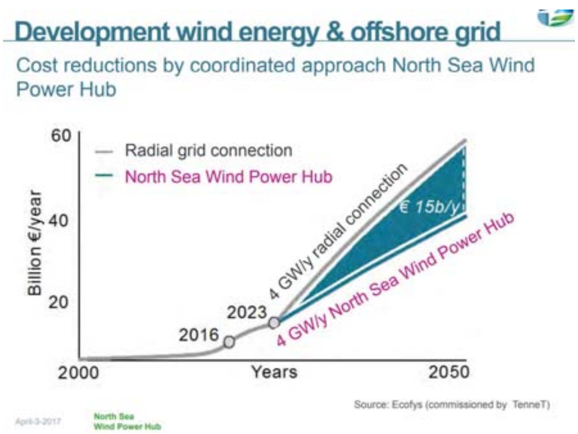

Base case including OWP grid integration costs

- Grid
  - 2030 planned infrastructure
  - Domestic grid restrictions (~5 to 15 GW)
- Supply and demand
  - ENTSO-E Vision 4 ("Green Revolution")
  - 65 GW OWP (Peak demand is 150 GW)
- Power flow modelling
  - Transport model due to HVDC connections
- Representation of hourly variability
  - Time series based on given geo coordinates
    - https://www.renewables.ninja/
  - Hydropower represented with hourly price series (water value)
    - Seasonal characteristics
  - Hourly load
    - ENTSO-E
- Goal
  - Include OWP to the lowest possible costs
    1. Radial solutions
    2. Power Link Island

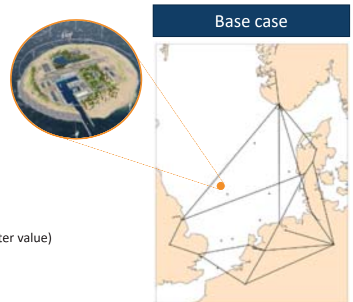

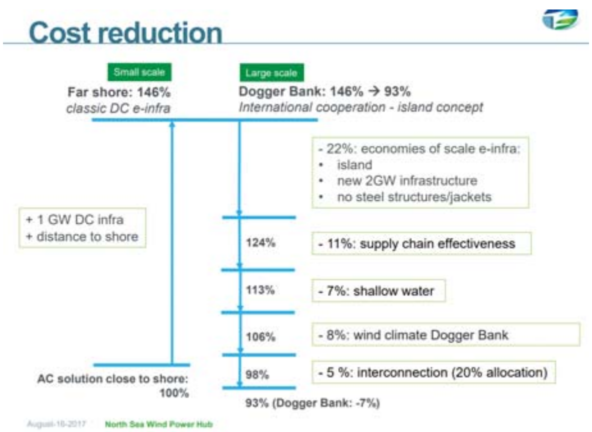

Value of having the possibility to invest in PLI

- Radial base case
  - PLI as a hub
  - No OWP capacity at the PLI

Total operation costs of the system (30 yrs)

- Radial: € 629 B
- PLI: € 610 B
- Cost savings: € 19

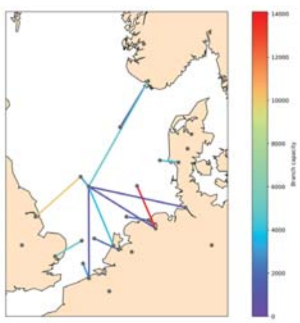

Value of connecting offshore wind to the island

What is the cost savings from adding OWP to PLI including the option to expand interconnectors even more than planned capacities?

Including generation expansion

Assuming planned interconnectors for 2030. What are the cost savings allowing for PLI when trying to anticipate changes in the generation mix? ENSTO-E V4 exogenous plus additional Generation Expansion Planning (GEP).

PLI without offshore wind allocated to it

- Radial expansion base case
  - No OWP at PLI
  - Allow interconnector expansion

Total operation cost of the system over 30 years

- €597 B

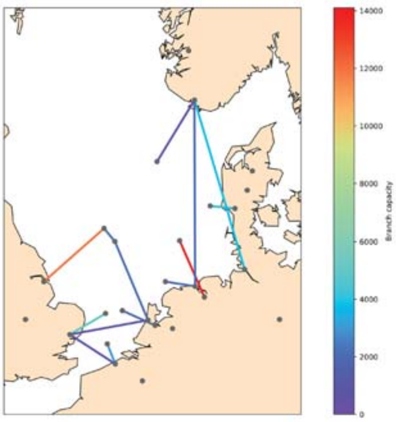

PLI with GEP base case as reference

- Radial base
  - OWP already integrated for free
  - GEP (except for hydro or nuclear)
  - TEP for a PLI
    - No additional interconnectors

Total operation costs of the system:

- € 507 B
- € 496 B
- Cost savings €11 B

- … significant cost savings also when accounting for GEP (i.e. a stable GTEP equilibrium before PLI TEP)

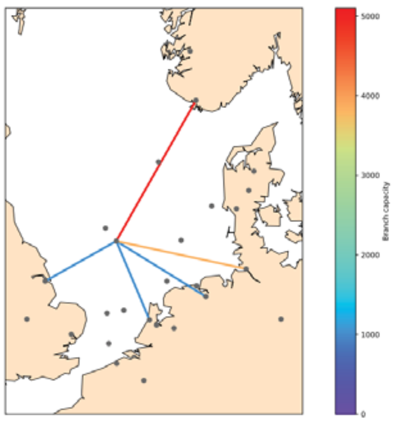

PLI with 30 GW allocated to it

- Compared to radial exp base case
  - Allow interconnector expansion
  - 30 GW at PLI (Reallocating from GB)

Total operation costs of the system

- Without PLI: €597 B
- With PLI: €589 B

- Cost savings = €8 B

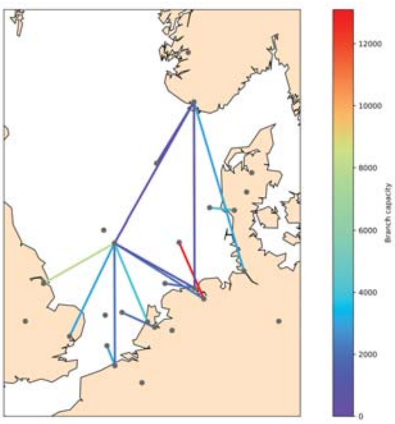

Meshed solutions

Some meshed alternatives to include offshore wind power

Base case incl costs for connecting OWP (meshed)

- Meshed base case (without interconnector expansion)

- Radial: €629 B
- Radial + PLI: €610 B
- Meshed: €611 B

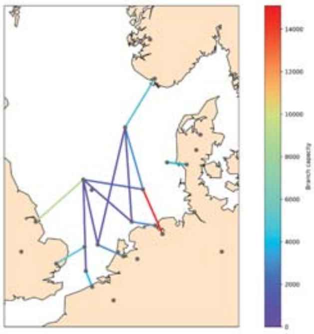

…it has an even more clear impact on CO2 emissions

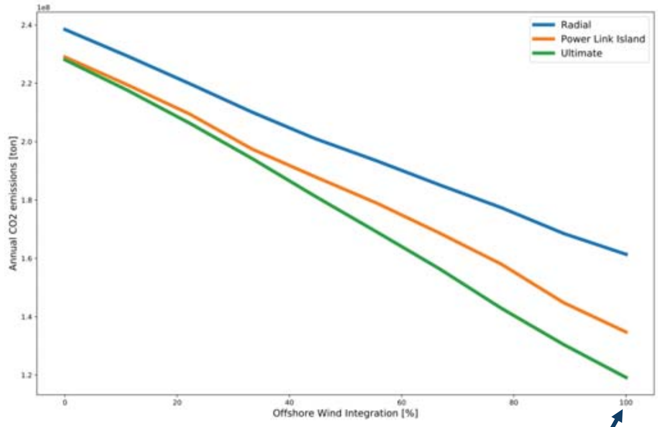

 Ultimate = Unlimited (free) capacity at candidate corridors

Base incl costs for including OWP (meshed) + PLI (as hub)

- Meshed base case
  - PLI as a hub (no wind allocated)
  - No additional interconnectors

- Radial: €629 B
- Radial + PLI: 610 B
- Meshed: 611 B
- Meshed + PLI: €609 B

- Cost savings: € 2 B

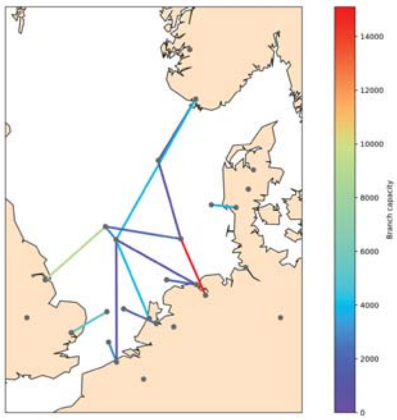

"PLI yields significant costs savings for an integrated NSOG"

Relevant findings from the optimization model:

Different comparisons of radial- and ***PLI integration of OWP capacity yields system cost savings up to €19 B over 30 years*** *depending on the degrees of freedom in the planning model.*

*When trying to anticipate the impact of generator expansion, the added value from the PLI is still significant (****~€11 B****).*

Assuming other flexible grid integration alternatives, such as a meshed grid, the added value of a PLI is expected to be around ***€ 2B****.*

Key takeaways so far:

The PLI provides a more ***cost-efficient OWP integration*** *than radial solutions,* ***reducing curtailment of wind*** *as well as increasing trade possibilities (****spatial flexibility*** *at a lower investment cost).*

It is shown that ***the relative value of a PLI increases when the level of offshore wind power capacity increases****.*

Limitations and future work:

cost uncertainty *// Unit commitment // multi-sector // onshore grid representation // local flexibility*

PLI shows increasing value when OWP capacity increases

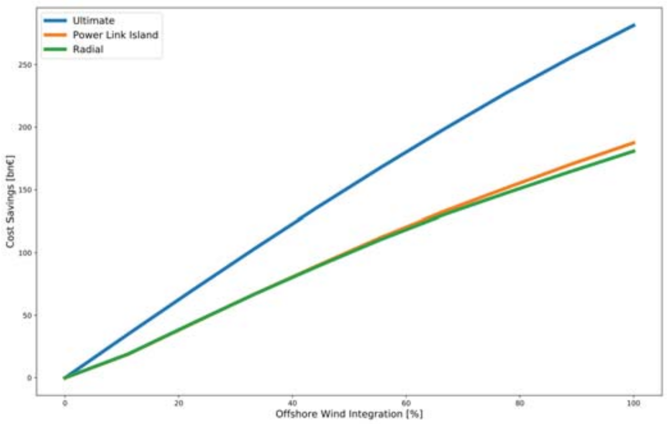

 Ultimate = Unlimited (free) capacity at candidate corridors

Contents

- **Introduction**
- Voltage Stability
- Frequency Stability
- Conclusion

Introduction
Real Grid Codes

- Are valid today – possibly not in the future
- Are valid for a specific TSO are – not generally valid
- Are readable for lawyers – not necessarily for engineers
- Contain many pages – not giving a easy overview

Introduction
Grid Codes Summaries

- Are valid today – possibly not in the future
- Are valid for a specific TSO are – not generally valid
- Are readable for lawyers – not necessarily for engineers
- Contain many pages – not giving a easy overview

Introduction
Grid Codes Summaries

- Are valid today – possibly not in the future
- Are valid for a specific TSO are – not generally valid
- ~~Are readable for lawyers – not necessarily for engineers~~
- ~~Contain many pages – not giving a easy overview~~

Introduction
ENTSO-E Grid Codes

- Are valid today – possibly not in the future
- Are valid for a specific TSO are – not generally valid
- Are readable for lawyers – not necessarily for engineers
- Contain many pages – not giving a easy overview

Introduction
ENTSO-E Grid Codes

- Are valid today – possibly not in the future
- ~~Are valid for a specific TSO are – not generally valid~~
- Are readable for lawyers – not necessarily for engineers
- Contain many pages – not giving a easy overview

Introduction
ENTSO-E Grid Codes

- Are valid today – possibly not in the future
- ~~Are valid for a specific TSO are – not generally valid~~
- Are readable for lawyers – not necessarily for engineers
- Contain many pages – not giving a easy overview
- Don't specify all the details – (...specified by the relevant TSO...)

Introduction
What does Academia need?

- Are valid today – possibly not in the future
- Are valid for a specific TSO are – not generally valid
- Are readable for lawyers – not necessarily for engineers
- Contain many pages – not giving a easy overview
- Don't specify all the details – (...specified by the relevant TSO...)

Introduction
What does Academia need?

- Are valid ~~today – possibly not~~ in the future
- Are ~~valid for a specific TSO are – not~~ generally valid
- Are readable ~~for lawyers – not necessarily~~ for engineers
- ~~Contain many pages – not~~ giving a easy overview
- ~~Don't~~ specify all the details ~~– (...specified by the relevant TSO...)~~

Introduction
Approach

- Develop a new generic grid code for Academic research purposes regarding wind power in Europe
  - Future oriented
  - Generic and general
  - readable for engineers
  - Few pages, no §s
  - specify the relevant details

An activity within IRPWind project

Introduction
Goal

- A most restrictive grid code as seen from turbine perspective
  - "worst case" for wind industry
  - Challenging to comply to
  - Not a proposal as WindEurope would come up with...
- Good for checking capabilities of new technology concepts
  - "if you can comply this, you likely can comply real codes too"

Introduction
Structure

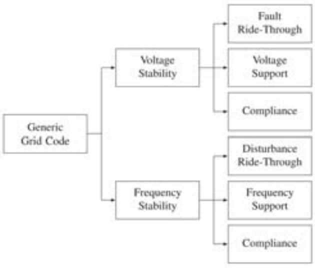

SINTEF

Contents

- Introduction
- **Voltage Stability**
- Frequency Stability
- Conclusion

SINTEF

Voltage Stability
Fault Ride Through

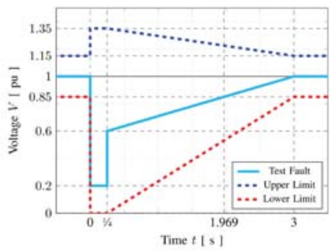

Fig. 3: Fault ride through requirement and test fault

TABLE II: FRT curve and test fault parameters

Parameter	Unit	Value
t_0	s	0.0
t_1	s	0.25
t_2	s	3.0
t_3	s	15.0
$V_{\text{lim+}}^{\text{fault}}$	pu	1.35
$V_{\text{lim+}}^{\text{norm}}$	pu	1.15
V_{nom}	pu	1.0
$V_{\text{lim-}}^{\text{norm}}$	pu	0.85
V_{test2}	pu	0.6
V_{test1}	pu	0.2
$V_{\text{lim-}}^{\text{fault}}$	pu	0.0

SINTEF

Voltage Stability
Voltage Support

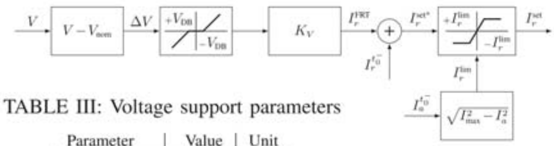

TABLE III: Voltage support parameters

Parameter	Value	Unit
V_{DB}	±0.15	pu
K_V	-3.00	—
I_{max}	1.12	pu
$I_r^{\text{lim}}(I_a = 1)$	0.50	pu

SINTEF

Voltage Stability
Support Tolerance Band

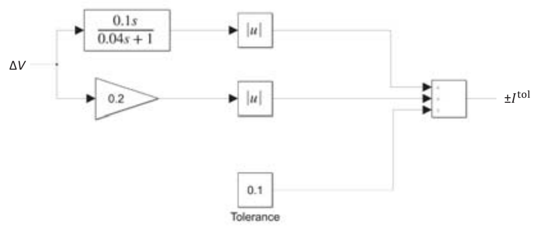

SINTEF

Voltage Stability
Compliance – Reactive Current

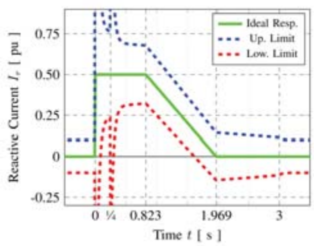

(a) Reactive current response compliance

SINTEF

Voltage Stability
Compliance – Active Current

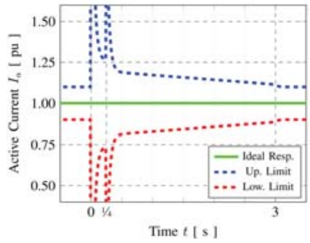

(b) Active current response compliance

SINTEF

Frequency Stability
Frequency Support

TABLE VII: Frequency support parameters

Parameter	Value	Unit
f_{DB}	±20 (±0.0004)	mHz (pu)
R	4	%
T_J	10	s
P^{D}_{max}	+10	% of P_{set}
P^{D}_{min}	−10	% of P_{set}
P^{P}_{max}	+10	% of P_{set}
P^{P}_{min}	−90	% of P_{set}

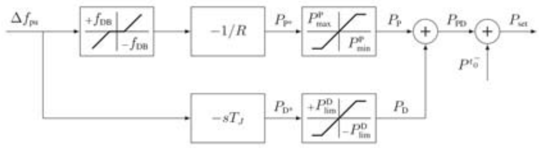

Fig. 8: Block diagram of the frequency support requirement

SINTEF

Contents

SINTEF

Frequency Stability
Support Tolerance Band

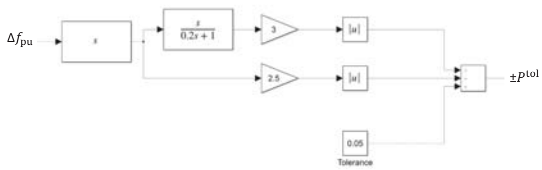

SINTEF

Frequency Stability
Disturbance Ride Through

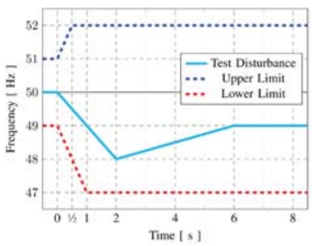

Fig. 6: Disturbance ride through requirement

TABLE VI: DRT curve and test disturbance parameters

Parameter	Value	Unit
t_0	0.0	s
t_1	0.5	s
t_2	1.0	s
t_3	2.0	s
t_4	6.0	s
f^{dist}_{lim+}	52	Hz
f^{norm}_{lim+}	51	Hz
f_{nom}	50	Hz
f^{norm}_{lim-}	49	Hz
f^{dist}_{lim-}	47	Hz
f_{test1}	48	Hz
f_{test2}	49	Hz

SINTEF

Frequency Stability
Compliance

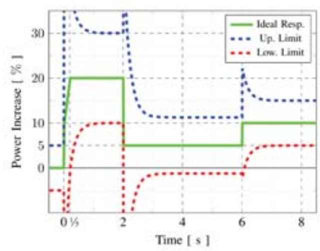

Fig. 9: The power response towards the test disturbance

SINTEF

Contents

- Introduction
- Voltage Stability
- Frequency Stability
- **Conclusion**

Conclusion
Outlook

- Overvoltage/Overfrequency

Conclusion
Summary

- Development of a strict but user-friendly generic grid code
- Helpful for academic studies regarding general future-oriented compliance
- Continuous definition of requirements
  - Determining the exact moment of a fault/disturbance event not necessary

Conclusion
Outlook

- Overvoltage/Overfrequency

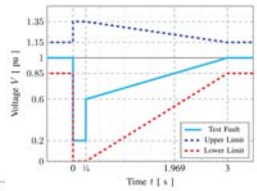

Fig. 3: Fault ride through requirement and test fault

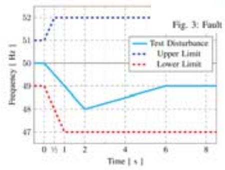

Fig. 6: Disturbance ride through requirement

Conclusion
Outlook

Conclusion
Outlook

- Overvoltage/Overfrequency
- Specification on voltage measurement

Conclusion
Outlook

- Overvoltage/Overfrequency
- Specification on voltage measurement
  - -> Asymmetric faults

31

SINTEF

Conclusion
Outlook

- Overvoltage/Overfrequency
- Specification on voltage measurement
  - -> Asymmetric faults
  - Simultaneous overvoltage and undervoltage on different phases?

32

SINTEF

SINTEF

Technology for a better society

B2) Grid connection and power system integration

Statistical Analysis of Offshore Wind and other VRE Generation to Estimate the Variability in Future Residual Load, M.Koivisto, DTU Wind Energy

A demonstrator for experimental testing integration of offshore wind farms with HVDC connection, S.D'Arco, SINTEF Energi

Optimal Operation of Large Scale Flexible Hydrogen Production in Constrained Transmission Grids with Stochastic Wind Power, E.F.Bødal, NTNU

Small signal modelling and eigenvalue analysis of multiterminal HVDC grids, Salvatore D'Arco, SINTEF Energi AS

Statistical Analysis of Offshore Wind and other VRE Generation to Estimate the Variability in Future Residual Load

Matti Koivisto
DTU Wind Energy

January 18th 2018
EERA DeepWind'18
Grid connection and power system integration
Trondheim, Norway

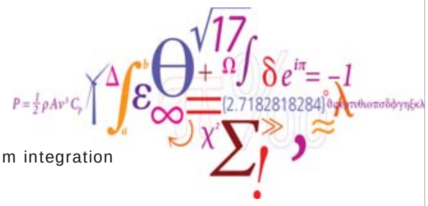

DTU Wind Energy
Department of Wind Energy

Simulated VRE generation

- The VRE generation time series are simulated using the CorRES tool developed at DTU Wind Energy
  - Based on meteorological data obtained from the mesoscale Weather Research and Forecasting (WRF) model
  - Reanalysis of past weather
- Mesoscale models tend to underestimate short-term variability in wind speeds, especially for offshore wind
  - To reach more realistic simulations, stochastic fluctuations are added on top of the mesoscale wind speed data
- VRE installation locations
  - When available, existing locations were used
  - For offshore, also planned locations were used
  - For solar PV, installations were assumed to be scattered through the analysed regions

Outline of the presentation

1. The analyzed base scenarios
2. The time series data used
3. Correlations between load and VRE generation
4. A modified 2050 scenario
5. Resulting residual loads in the scenarios
6. Discussion and future work
7. Conclusions

Historical load time series

- Four years of hourly historical load data (2012 to 2015) for the analysed countries were acquired from Nord Pool
  - https://www.nordpoolgroup.com/historical-market-data/
- A few clearly incorrect data points were fixed by using the data from the previous day of the same type (e.g., working day) from the same hour of the day

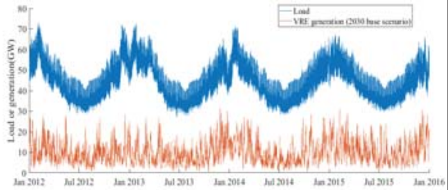

Time series of aggregate load and VRE generation with the 2030 base scenario installations for the four analysed years.

The analyzed base scenarios

- The base scenarios
  - Around 36 GW of VRE generation in 2030 for the analysed countries
  - Around 60 GW in 2050
  - From Nordic Energy Technology Perspectives (NETP) 2016
  - http://www.nordicenergy.org/project/nordic-energy-technology-perspectives/
- These are the base scenarios used in the Flex4RES project
  - http://www.nordicenergy.org/flagship/flex4res/
  - The authors would like to acknowledge support from the Flex4RES project and the NSON-DK (ForskEL) project

The analysed countries with regions marked. © EuroGeographics for the administrative boundaries (regions are combined of the EU NUTS classification).

Correlations in load time series

- Correlations are generally very high
- Countries further away (e.g., DK and FI) have lower correlations
- SD of the aggregate load is 9.01 GW
  - If all load time series would be fully correlated, the SD of the aggregate would be 9.41 GW
  - There is thus only about 4 % reduction in RSD due to loads not being fully correlated

Correlations between the load time series

	DK	EE	FI	LT	LV	NO	SE
DK		0.90	0.76	0.92	0.87	0.73	0.83
EE	0.90		0.90	0.87	0.85	0.87	0.93
FI	0.76	0.90		0.70	0.71	0.93	0.95
LT	0.92	0.87	0.70		0.89	0.62	0.74
LV	0.87	0.85	0.71	0.89		0.65	0.73
NO	0.73	0.87	0.93	0.62	0.65		0.96
SE	0.83	0.93	0.95	0.74	0.73	0.96	

	DK	EE	FI	LT	LV	NO	SE	Aggregate
Mean (GW)	3.82	0.91	9.42	1.13	0.80	14.6	15.6	46.3
SD (GW)	0.80	0.20	1.52	0.23	0.17	3.12	3.36	9.01
RSD	0.21	0.22	0.16	0.21	0.21	0.21	0.21	0.19

Relative standard deviation (RSD) is standard deviation (SD) divided by mean

Correlations in load time series ramp rates

- Ramp rates are analysed as first differences of hourly data
  - $\mathrm{diff}(y_t) = y_t - y_{t-1}$
- Correlations are generally very high
- SD of the aggregate load 1st difference is 1.59 GW/h
  - If all load time series would be fully correlated, the SD of the aggregate 1st difference would be 1.72 GW/h
  - There is thus about 8 % reduction in ramp rate SD due to loads not being fully correlated

Correlations between the load time series 1st differences

	DK	EE	FI	LT	LV	NO	SE
DK		0.80	0.66	0.79	0.71	0.86	0.90
EE	0.80		0.79	0.94	0.86	0.80	0.86
FI	0.66	0.79		0.78	0.70	0.65	0.71
LT	0.79	0.94	0.78		0.86	0.76	0.84
LV	0.71	0.86	0.70	0.86		0.70	0.76
NO	0.86	0.80	0.65	0.76	0.70		0.91
SE	0.90	0.86	0.71	0.84	0.76	0.91	

	DK	EE	FI	LT	LV	NO	SE	Aggregate
SD (GW/h)	0.24	0.05	0.27	0.07	0.05	0.45	0.60	1.59

Correlations between VRE generation sources and aggregate load (2/2)

- Both wind generation types are positively correlated with load
- As expected, solar PV is negatively correlated with load
- Solar generation is negatively correlated with wind generation
  - Can reduce residual load variability
  - $\mathrm{Var}(y_t + x_t) = \sigma_x^2 + \sigma_y^2 + 2\sigma_x\sigma_y\rho_{x,y}$

	Aggregate load	Offshore wind	Onshore wind	Solar PV
Aggregate load		0.12	0.17	-0.11
Offshore wind	0.12		0.36	-0.14
Onshore wind	0.17	0.36		-0.14
Solar PV	-0.11	-0.14	-0.14	

Behavior of different VRE generation types

- SDs are on average higher in offshore than onshore wind generation
- However, the higher mean generation causes the RSD to be on average 8 % lower in offshore than in onshore wind generation
- Hourly ramp rate SDs are much higher in offshore than in onshore generation
- Solar PV has higher RSD than either of the wind generation types

	Offshore wind	Onshore wind	Solar PV
Mean	0.36	0.27	0.10
SD	0.30	0.25	0.17
RSD	0.85	0.92	1.59
1st difference SD	0.09	0.04	0.05

Correlations between VRE generation and aggregate load 1st differences (1/2)

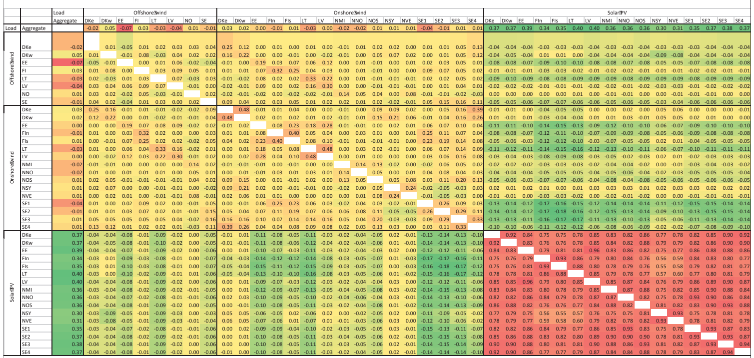

The colouring is based on how beneficial the correlations are for achieving a lower residual load 1st difference variance

Correlations between VRE generation sources and aggregate load (1/2)

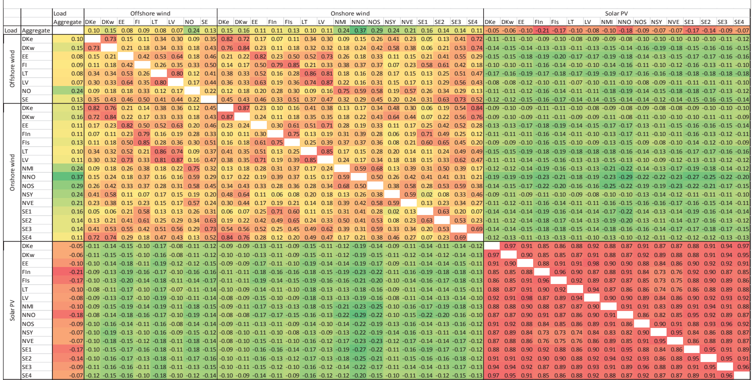

The colouring is based on how beneficial the correlations are for achieving a lower residual load variance

Correlations between VRE generation and aggregate load 1st differences (2/2)

- Wind generation 1st differences are much less correlated than the wind generation time series themselves
  - Wind ramping is thus expected to experience more geographical smoothening than is seen in wind generation itself
- Solar generation ramps are positively correlated with load ramps
  - Can reduce residual load ramp rates

	Offshore wind	Onshore wind	Solar PV
Correlation with aggregate load's 1st difference	-0.01	0.00	0.36

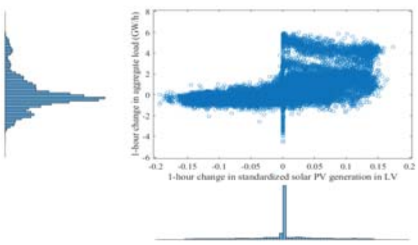

Example of solar PV ramps and aggregate load ramps

A modified 2050 scenario

- Modifications were tested for the base 2050 scenario
  - Expected yearly VRE energy generation was kept constant in all test scenarios
- Increasing the low offshore wind share in the baseline scenario up to 50 % resulted in a small reduction of the residual load SD (up to 2 %)
- Increasing the overall geographical distribution of wind decreased the residual load SD about 4 %
- A final modified 2050 scenario:
  - 30 % of wind energy from offshore, and solar share 10 %
  - Installations geographically more dispersed

Percentages of expected yearly energies coming from the different VRE types in the different scenarios

	Offshore wind	Onshore wind	Solar PV
2030 base scenario	15%	83%	2%
2050 base scenario	9%	90%	1%
2050 modified	27%	63%	10%

Future work

- Creating more years of load time series
  - To get different meteorological years into the analysis (e.g., very cold winters)
  - Either by acquiring more historical load data,
  - or by building stochastic time series models of load for the different countries and using past meteorological data to simulate load time series
  - VRE simulations are already available for 35 past meteorological years
- VRE technology development in the future
  - Changes, e.g., in hub heights and specific power will be implemented to model the capacity factors of future wind generation
- Optimizing the geographical distribution and VRE generation mix
  - E.g., by minimizing residual load variance

Resulting residual loads

- SD of the residual load increases only by a few percentages compared to only load in the 2030 base scenario
  - but notably in 2050 (22 % higher than the SD of load only)
- As the mean of residual load decreases at the same time, the RSD increases very significantly
- The modified 2050 scenario shows about 7% lower SD in residual load than in the base 2050 scenario

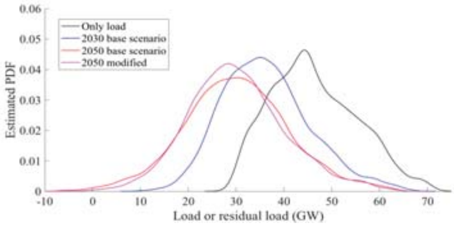

Scenario	Mean (GW)	SD (GW)	RSD	5th percentile (GW)	95th percentile (GW)
Only load	46.3	9.0	0.19	32.6	62.0
2030 base scenario	36.3	9.2	0.25	22.7	52.9
2050 base scenario	30.1	11.0	0.37	12.3	48.8
2050 modified	30.1	10.2	0.34	14.5	48.3

Conclusions

- SD of residual load in the 2050 base scenario expected to be 22 % higher than in load only
  - Mean decreases at the same time -> RSD increases significantly
  - There will be thus less energy to be generated by non-VRE generation types, but with higher needs of flexibility
- In the 2050 base scenario, the residual load ramp rate is expected to be 10% higher than in load only
- A modified scenario for 2050:
  - 7% lower SD in residual load than in the base 2050 scenario
  - Residual load ramp rate SD is expected to be even slightly lower than in load only
- During some high load hours of the year, there is only little VRE generation available in all scenarios

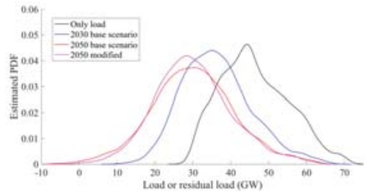

Resulting residual load ramp rates

- Hourly ramp rates in residual load increase only moderately
  - In the 2050 base scenario, the SD of the residual load ramp rate is 10% higher than in load only
- The modified scenario shows a much lower ramp rate SD compared to the base 2050 scenario
  - Especially the 95th percentile value is much lower
  - This is explained by the increased solar PV share, as solar up-ramping happens often at the same time as load up-ramping

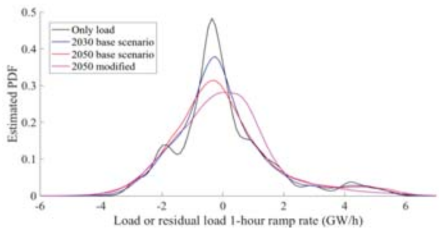

Scenario	Ramp rate SD (GW/h)	5th percentile (GW/h)	95th percentile (GW/h)
Only load	1.59	-2.24	3.54
2030 base scenario	1.62	-2.26	3.52
2050 base scenario	1.75	-2.42	3.64
2050 modified	1.57	-2.38	2.87

Extra material

	Offshore wind							
	DKe	DKw	EE	FI	LT	LV	NO	SE
Mean	0.43	0.45	0.29	0.31	0.35	0.30	0.41	0.34
SD	0.34	0.31	0.30	0.27	0.32	0.30	0.29	0.26
RSD	0.77	0.70	1.04	0.88	0.91	1.01	0.71	0.76
1st difference SD	0.10	0.08	0.11	0.08	0.10	0.10	0.07	0.08

	Onshore wind															
	DKe	DKw	EE	FIn	FIs	LT	LV	NMI	NNO	NOS	NSY	NVE	SE1	SE2	SE3	SE4
Mean	0.25	0.26	0.26	0.27	0.25	0.24	0.26	0.30	0.35	0.32	0.29	0.23	0.24	0.22	0.27	0.35
SD	0.25	0.24	0.24	0.26	0.22	0.24	0.26	0.29	0.25	0.24	0.30	0.25	0.22	0.20	0.22	0.28
RSD	1.00	0.95	0.93	0.98	0.87	1.00	1.00	0.95	0.70	0.75	1.03	1.09	0.90	0.89	0.83	0.81
1st difference SD	0.03	0.03	0.03	0.04	0.03	0.04	0.04	0.05	0.03	0.02	0.05	0.04	0.03	0.02	0.03	0.04

	Solar PV															
	DKe	DKw	EE	FIn	FIs	LT	LV	NMI	NNO	NOS	NSY	NVE	SE1	SE2	SE3	SE4
Mean	0.11	0.12	0.12	0.09	0.09	0.12	0.12	0.10	0.09	0.10	0.10	0.10	0.10	0.10	0.11	0.11
SD	0.18	0.18	0.19	0.14	0.14	0.18	0.18	0.15	0.14	0.16	0.16	0.16	0.17	0.17	0.17	0.17
RSD	1.54	1.55	1.57	1.64	1.63	1.54	1.54	1.61	1.63	1.60	1.60	1.59	1.65	1.61	1.57	1.56
1st difference SD	0.06	0.06	0.06	0.04	0.04	0.06	0.05	0.05	0.04	0.05	0.05	0.05	0.05	0.05	0.05	0.05

	Offshore wind							
Scenario	DKe	DKw	EE	FI	LT	LV	NO	SE
2030 base scenario	573	1443	250	1206	0	180	0	215
2050 base scenario	573	1443	250	1206	0	180	0	215
2050 modified	1000	2000	1000	1206	1000	950	3000	1500

	Onshore wind															
Scenario	DKe	DKw	EE	FIn	FIs	LT	LV	NMI	NNO	NOS	NSY	NVE	SE1	SE2	SE3	SE4
2030 base scenario	990	4219	635	533	1067	1677	2979	330	5033	124	1410	126	424	5488	4396	1206
2050 base scenario	1520	6480	400	533	1067	7046	2409	5033	5033	124	1410	126	5488	5488	10975	1206
2050 modified	990	4000	635	2100	1067	1677	2979	2000	5033	124	1410	126	5000	5000	4396	1206

	Solar PV															
Scenario	DKe	DKw	EE	FIn	FIs	LT	LV	NMI	NNO	NOS	NSY	NVE	SE1	SE2	SE3	SE4
2030 base scenario	268	624	0	0	40	750	2	0	0	0	0	0	0	0	0	79
2050 base scenario	268	624	0	0	40	740	2	0	0	0	0	0	0	0	0	79
2050 modified	1500	2000	1000	0	1500	1000	1000	0	0	1000	1000	1000	0	0	2000	2000

	Offshore wind							Onshore wind							Solar PV						
Year	DK	EE	FI	LT	LV	NO	SE	DK	EE	FI	LT	LV	NO	SE	DK	EE	FI	LT	LV	NO	SE
2014	1271	0	26	0	0	0	212	3603	303	607	279	62	819	5220	602	0.2	11	68	1.5	0	79

VRE installation in 2014 in total around 13 GW

Load TWhs

	DK	EE	FI	LT	LV	NO	SE	Aggregate
Annual TWh	33	8	83	10	7	128	137	405

VRE (all) annual TWhs

Scenario	TWh
2030 base scenario	87.57
2050 base scenario	141.80
2050 modified	141.78

SINTEF

A Demonstrator for Experimental Testing Integration of Offshore Wind Farms With HVDC Connection

S.D'Arco, A. Endegnanew, SINTEF Energi

DEMO 1 Objectives

- To investigate the **electrical interactions** between **HVDC link converters and wind turbine converters in offshore wind farms**.
- To **de-risk** the **multivendor and multiterminal schemes**: resonances, power flow and control.
- To **demonstrate** the results in a **laboratory environment** using scaled models (4-terminal DC grid with MMC VSC prototypes and a Real Time Digital Simulator system to emulate the AC grid).
- To use the validated use the validated models to simulate a **real grid with offshore wind farms connected in HVDC**.

BEST PATHS PROJECT

Best Paths
Transmission for sustainability

BEyond **S**tate-of-the-art **T**echnologies for re-**P**owering **A**C corridors and multi-**T**erminal **H**VDC **S**ystems

- Validate the technical feasibility, impacts and benefits of **novel grid technologies**,
- Five large-scale demonstrations
  - Deliver solutions that allow for transition from **High Voltage Direct Current (HVDC) lines to HVDC grids**;
  - **Upgrade and repower** existing Alternating Current (AC) parts of the network;
  - Integrate **superconducting high power DC links** within AC meshed network

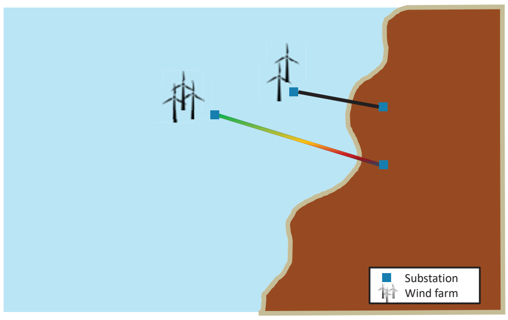

LARGE SCALE DEMONSTRATIONS

1. HVDC in offshore wind farms and offshore interconnections
2. HVDC-VSC multivendor interoperability
3. Upgrading multiterminal HVDC links
4. Innovative repowering of AC corridors
5. DC Superconducting cable

From HVDC lines to HVDC grid

Upgrading of existing AC grids

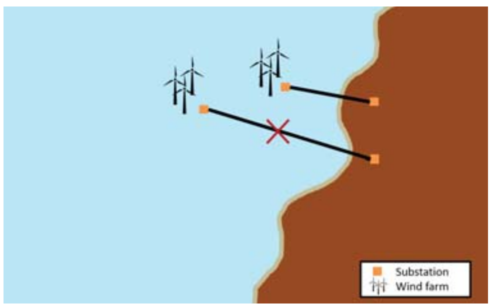

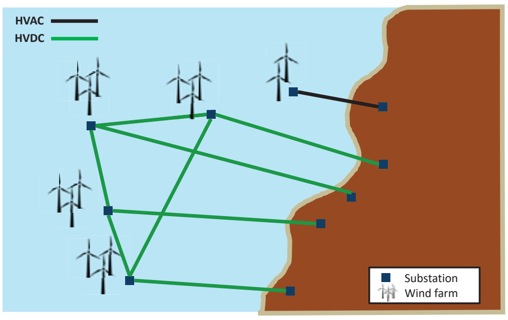

Demonstrator overview

- Three-terminal scheme MMC with
  - MMC with HB cells, 18 cells and 6 cells per arm,
  - MMC with FB cells, 12 cells per arm
- Wind farm emulator
- National smart grid laboratory

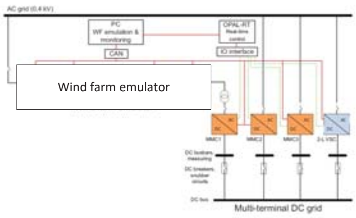

National Smart Grid Laboratory

- Laboratory formally opened in September 2016 after a major upgrade
- Jointly operated by NTNU and SINTEF
- Reconfigurable layout with multiple ac and dc bus
- Power electronics converters
  - 2 level VSC 60 kVA, MMC 60 kVA
- Electrical machines
  - Synchronous generators, Induction machines
- Real-time simulator

Real-time simulation and PHIL capabilities

- OPAL-RT based real time simulator platform
  - 5 parallel cores,
  - 2 FPGAs for IO and small time step simulation,
  - Fiber optic communication
- Egston Compiso Grid emulator
  - 200 kVA rated power
  - 6 individual outputs
  - > 10 kHz bandwidth
  - Connected to the OPAL-RT system via fiber optics with 4 µs update rate for measurements and references

Demonstration of HVDC transmission systems connected to offshore wind farms

- Designed and built 3 MMC prototypes
- Tested the converters in point to point and multiterminal configurations
- Planned PHIL experiments with real time model of a wind farm

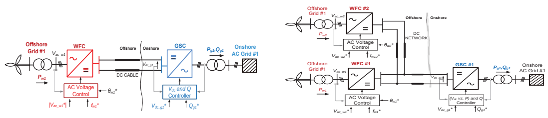

MMC Converters

- Three MMC converters were designed from scratch
  - MMC with HB cells, 18 cells per arm
  - MMC with FB cells, 12 cells per arm
  - MMC with HB cells, 6 cells per arm
- Built and successfully tested at full rating
  - 42 modules
  - 144 power cell boards
  - 1764 capacitors

Power cell boards

Assembling stages

Converter performance test

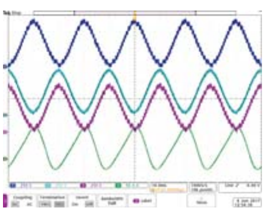

Conv12 700UDC, 100% active current I_d (-81.2A)
• Phase C upper arm voltage, • Phase C Lower arm voltage, • Phase C output voltage, • Phase C arm current

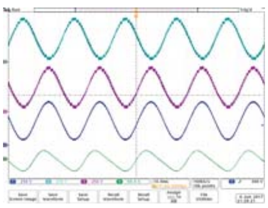

Conv18 700UDC, 24.3kW,7.8kVar
• Phase C upper arm voltage, • Phase C Lower arm voltage, • Phase C output voltage, • Phase C arm current

Point-to-point and multiterminal configurations

- Tests to **evaluate the accuracy of the models to represent the demonstrator**

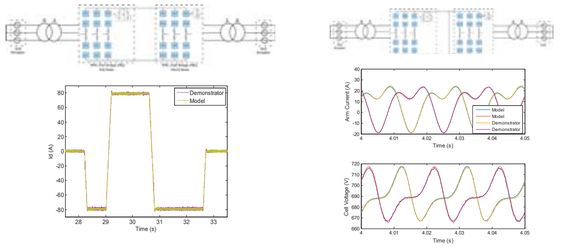

Wind farm emulator

- Wind farm model is adapted to run in the 200 kVA high-bandwidth grid emulator
- PHIL implementation combining the real time simulator and the grid emulator
  - Flexibility in the model simulated
  - Possibility to reproduce faster dynamics

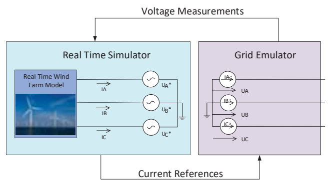

Interaction of an offshore wind farm with an HVDC

- Complex issues
  - Noise, randomness of event timings, and hardware design
- Numerical simulations are widely accepted and cost effective
  - Test a wide variety of different cases, however, the fidelity of the results is difficult to assess.
- Hardware power-in-the-loop (HIL) simulation offers a good balance between test coverage and fidelity.

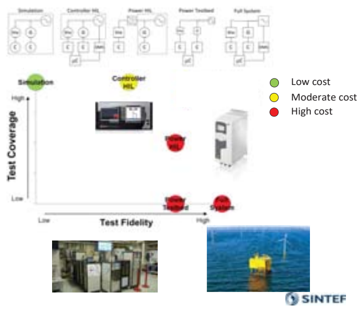

PHIL experiment: Wind farm connected to VSC-based HVDC

- Simulated wind farm
  - Input: Wind speed and measured voltage
  - Output: Grid emulator reference current
- Hardware
  - Two-level VSC generates a three-phase ac voltage with a fixed frequency
- The close-loop behaviour of the PHIL setup was stable

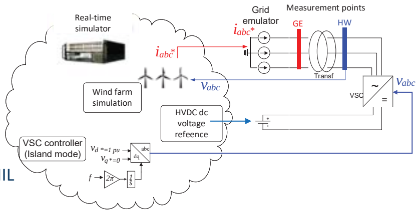

SINTEF

SINTEF

Teknologi for et bedre samfunn

Results

Simulation

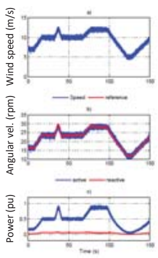

Hardware

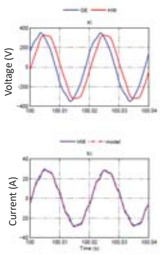

SINTEF

Conclusions

- Power hardware-in-the-loop (PHIL) approach combines hardware devices with software simulation.
- The hardware part allows a high fidelity of the results whereas, the software simulation part allows an extensive study of different cases at a reasonable cost
- Grid integration of wind farm using VSC-based HVDC system was evaluated in PHIL experiment as a proof of concept.
- In the future work ,PHIL implementation using modular multilevel concepts will be studied

SINTEF

Hydrogen Production from Wind and Hydro Power in Constrained Transmission Grids, Considering the stochasticity of wind power

Espen Flo Bødal and Magnus Korpås

Exploiting energy resources in remote regions

- Many good natural gas and wind resources are located in remote regions
- Lacking transmission capacity and long distances makes development of these resources expensive
- Raggovidda

Hyper Project

- Large scale production of hydrogen from natural gas with CCS, wind and hydro power
  - Storing CO_2 in depleted natural gas reservoirs
  - Producing hydrogen by electrolysis
- Liquefaction to liquid hydrogen and transportation to energy deficit area
- Creates a supply chain for hydrogen
- Flexible production of hydrogen can increase utilization and reduce need for new of transmission lines

Wind Power Stochasticity

- How important is it to include wind power stochasticity in the models?
  - How does it affect costs?
  - How does it affect storage strategies?
  - Does the effect of including hydrogen storage change?

Regional Power System Model

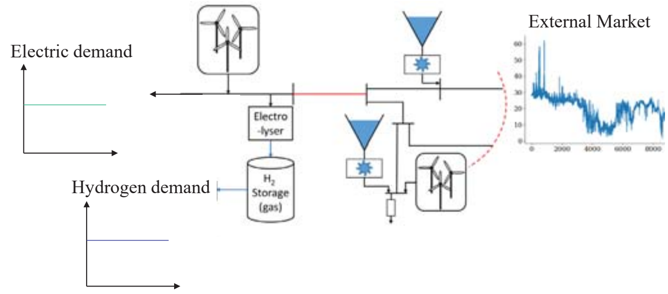

Wind Forecasting

- Meteorological forecasts and historic production
- Local quantile regression
- Sampling scenarios, including spatial and temporal correlations

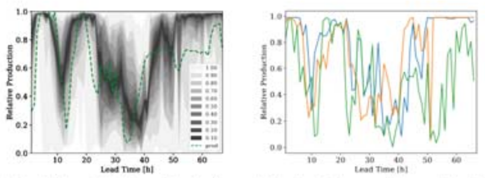

(a) Quantile forecast of relative production for Raggovidda wind farm in northern Norway.

(b) Scenarios of wind power production sampled from the quantile distribution.

Figure 1: Quantile forecasts are used to creating wind power scenarios for the stochastic model.

Rolling Horizon Model

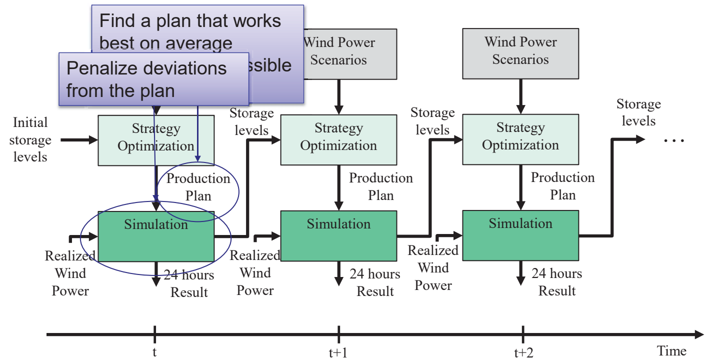

Lost Energy and Cost Breakdown

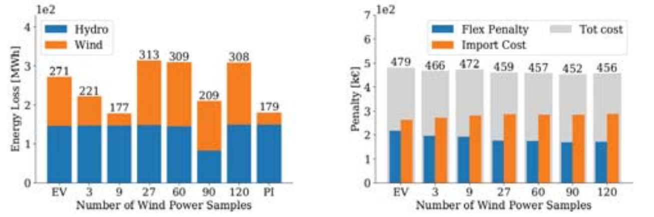

(a) Energy lost from spilling water in hydro power plants or curtailing wind power production.

(b) Penalty and import costs obtained in the different runs of the model. Values in excess of perfect information solution.

Figure 4: Energy lost and system costs in excess of the perfect information solution.

Case Study

- Finnmark in northern Norway
- Good wind potential and LNG production facility
- Weak transmission connection to the rest of the Nordic power system
- Modelled by a 9 bus system
- Simulated over a period of 10 days

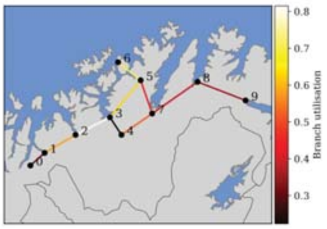

Figure 2: Case study system based on the power system in Finnmark, northern Norway. Lines are colored according to the line utilization in the run with 120 wind power samples. Power is on average flowing from both ends towards node 6.

Hydrogen Storage Strategy

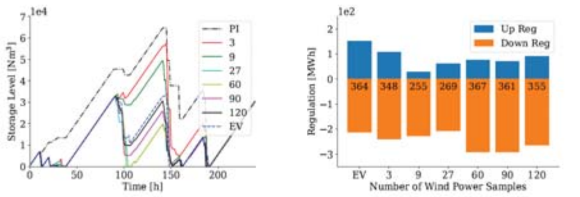

(a) Storage level in hydrogen storage in bus 6.

(b) Up and down regulation of the hydrogen load for the different cases. The total up and down regulation is stated inside the bars.

Figure 5: Hydrogen storage level and regulation of the hydrogen plant.

Model Performance

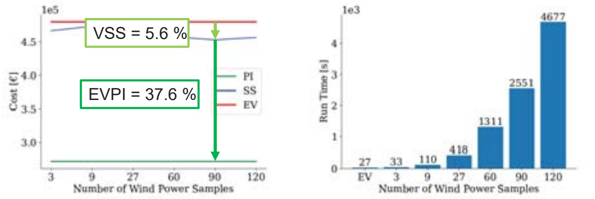

(a) Profi... informat... expected... Dependent on penalty cost which is high in this case ...ect ...the

(b) Run time of the strategy calculation, the run time in the simulator is negligible.

Figure 3: value of the solution and run time for the strategy calculation, showing the performance of the model.

Power Flow

- Hydrogen storage VS no hydrogen storage
- Slightly higher flow in storage case, increased flow on average by:
  - EV: 0.38 %
  - S120: 0.70 %
  - PI: 1.21 %
- The system already has high flexibility from hydro power
- Hydrogen load could be placed better or distributed to give more effect
- No storage results in rationing of 9.8 MW in all cases

Conclusion

- A rolling horizon model was developed for assessing the value of including stochastic wind power in a regional power system with hydrogen production
- Case study shows:
  - Reduced costs of 5.6% compared to deterministic solution
  - Potential of reducing costs in stochastic solution up to 37.6%
  - Lower regulation cost and higher import for the better solutions
  - Similar solutions for more than 60 wind samples
  - More flow on the transmission lines when storage is included, better improvement for better uncertainty representation
  - Storage helps to avoid very expensive rationing

SINTEF | NTNU – Trondheim Norwegian University of Science and Technology

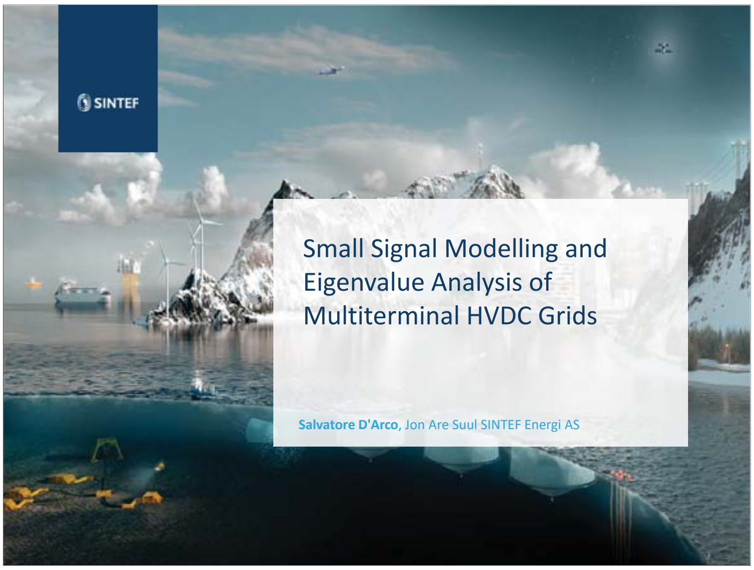

ProOfGrids

Overview of models and methods for stability analysis

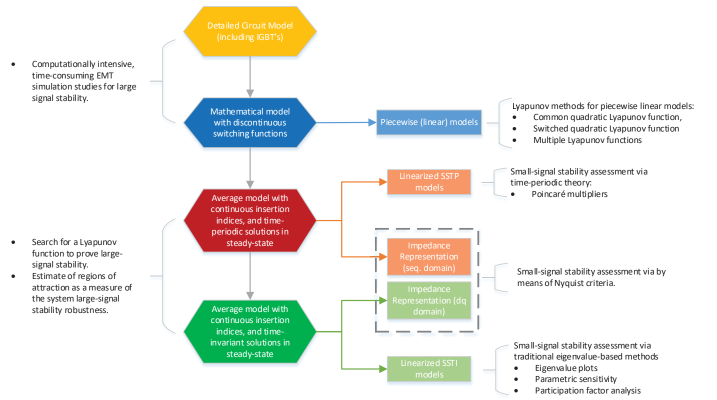

ProOfGrids

Eigenvalue based small signal analysis

- Power system stability is commonly assessed by eigenvalue analysis
  - Enables analysis and mitigation of oscillatory behaviour or instability due to system configuration, system parameters and controller settings
- VSC HVDC systems has different dynamics compared to traditional generators
  - Models of MMC HVDC terminals are currently under development
- State-space models for HVDC systems can be used for multiple purposes
  - Analysis, identification and mitigation of oscillations and small-signal instability mechanisms in HVDC transmission schemes
  - Analysis of controller tuning and interaction between control loops in HVDC terminals
  - Integration in larger power system models for assessment of how HVDC transmission will influence overall small signal stability and oscillation modes

ProOfGrids

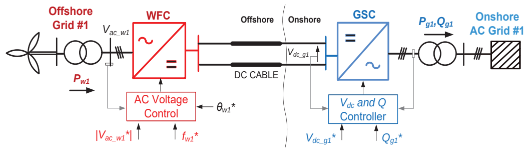

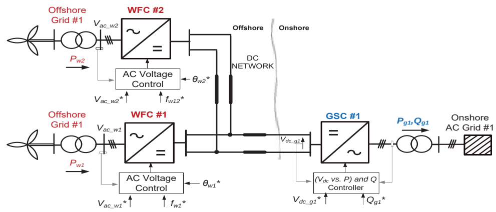

ProOfGrids

Protection and Fault Handling in Offshore HVDC grids

Objectives: Establish tools and guidelines to support the design of multi-terminal offshore HVDC grids in order to maximize system availability. Focus will be on limiting the effects of failures and the risks associated to unexpected interactions between components.

- Develop **models of offshore grid components** (cables, transformers, AC and DC breakers, HVDC converters) for electromagnetic transient studies.
- Define guidelines to reduce the risks of **unexpected interactions** between components during normal and fault conditions.
- Define strategies for **protection and fault handling** to improve the availability of the grid in case of failures.
- **Demonstrate** the effectiveness of these tools with numerical simulations (PSCAD, EMTP), real time simulations (RTDS, Opal-RT) and experimental setups.
- Expand the **knowledge** base on offshore grids by completion of two PhD degrees / PostDoc at NTNU and one in RWTH.

ProOfGrids Protection and Fault Handling in Offshore HVDC Grids

ProOfGrids

Frequency-Dependent State-Space modelling of HVDC cables

- The modelling approach is based on a lumped circuit and constant parameters
  - Parallel branches allow for capturing the frequency dependent behavior of the cable
  - Compatible with a state space representation in the same way as classical models with simple π sections
  - Model order depends on the number of parallel branches and the number of π sections

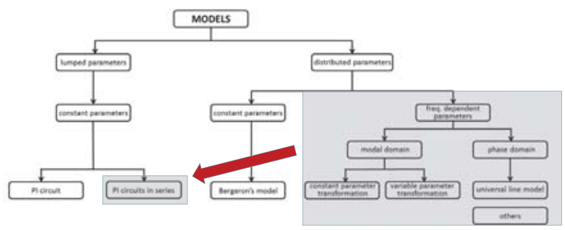

ProOfGrids

State-space frequency-dependent π section modelling

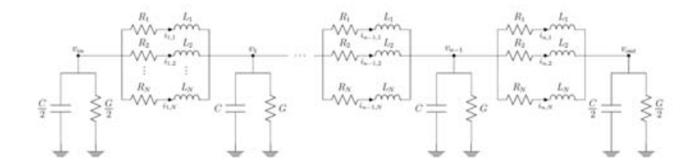

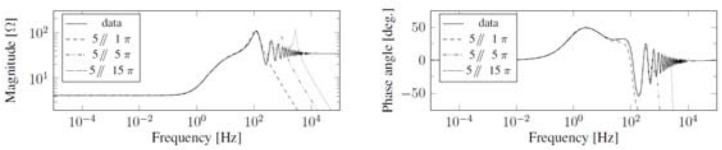

ProOfGrids

Behavior in a point to point HVDC transmission scheme

Eigenvalue trajectory for a sweep of dc voltage controller gain

All modes | Interaction modes

5 π sections
5 parallel branches

5 π sections
classical

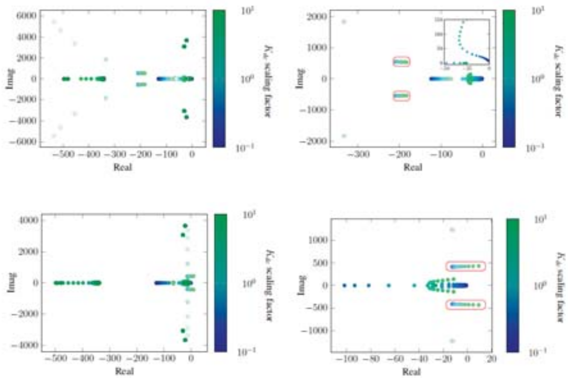

ProOfGrids

Main conclusions related to cable modelling

- ULM is established for EMT simulations
- Traditional π-section models of HVDC cables are not suitable for dynamic simulation or stability-assessment of HVDC systems
  - Single inductive branches imply significant under-representation of the damping in the system
- Frequency-dependent (FD) π-model for small-signal stability analysis
  - For simplified models, representation of cables by equivalent resistance and capacitance can be sufficient
- Developed Matlab-code and software tool for generating FD-π models

ProOfGrids

3-phase MMC Basic Topology

- Advantages
  - Modularity
  - Scalability
  - Redundancy
  - Low losses
  - DC-capacitor is not required
- Disadvantages
  - High number of switches
  - Large total capacitance
  - Complexity
  - **Sub-module Capacitors will have steady-state voltage oscillations and internal currents can have corresponding frequency components**

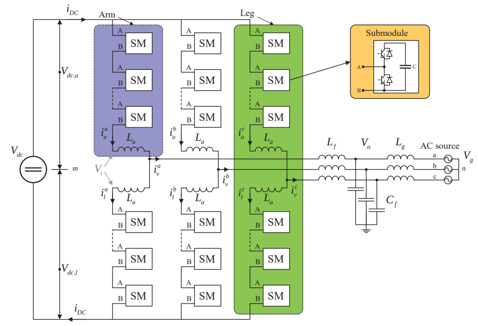

→ Main challenge for small-signal modelling

ProOfGrids

Classification of MMC Modelling for eigenvalue analysis

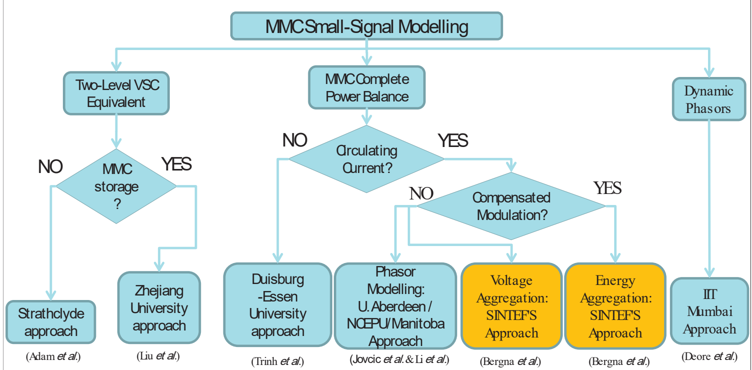

ProOfGrids

Compensated vs. Uncompensated Modulation

Compensated Modulation

Insertion Indexes

$$n_{uk} = \frac{-e_{vk}^* + u_{ck}^*}{u_{cu}^{\Sigma}} \qquad n_{lk} = \frac{e_{vk}^* + u_{ck}^*}{u_{cl}^{\Sigma}}$$

Voltage reference signals are divided by the actual arm voltage

$$u_{ck} \approx u_{ck}^* \qquad e_{vk} \approx e_{vk}^*$$

MMC output voltage component will be approximately equal to the reference

Appropriate for energy-based modelling

Uncompensated Modulation

Insertion Indexes

$$n_{uk} \approx \frac{-e_{vk}^* + u_{ck}^*}{V_{dc}} \qquad n_{lk} \approx \frac{e_{vk}^* + u_{ck}^*}{V_{dc}}$$

Voltage references are divided by a constant value

$$\begin{bmatrix} u_{ck} \\ e_{vk} \end{bmatrix} = \frac{1}{2V_{dc}} \begin{bmatrix} \left(\sqrt{w_{\Sigma k}+w_{\Delta k}}+\sqrt{w_{\Sigma k}-w_{\Delta k}}\right) & -\left(\sqrt{w_{\Sigma k}+w_{\Delta k}}-\sqrt{w_{\Sigma k}-w_{\Delta k}}\right) \\ -\left(\sqrt{w_{\Sigma k}+w_{\Delta k}}-\sqrt{w_{\Sigma k}-w_{\Delta k}}\right) & \left(\sqrt{w_{\Sigma k}+w_{\Delta k}}+\sqrt{w_{\Sigma k}-w_{\Delta k}}\right) \end{bmatrix} \begin{bmatrix} u_{ck}^* \\ e_{vk}^* \end{bmatrix}$$

Non-linear relationship between reference and "real" driving voltages

The control output is modified by the energy information in each arm/phase

Energy-based modelling is not suitable for this case

ProOfGrids

Main conclusions related to MMC modelling

- The internal energy storage dynamics of MMCs must be represented for obtaining accurate models
  - Established models of 2-Level VSCs should not be used for studying fast dynamics in HVDC systems
  - Models assuming ideal power balance between AC- and DC-sides can only be used for studying phenomena at very low frequency
- Two cases of MMC modelling
  - Compensated modulation with Energy-based modelling
  - Un-compensated modulation with Voltage-based modelling

Energy-based model

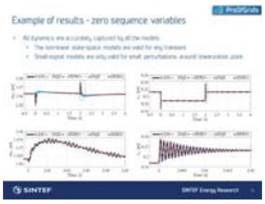

Voltage-based model

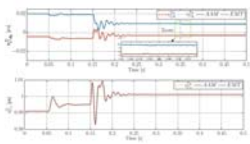

ProOfGrids

Generation of a small signal model for MT HVDC

- A modular approach was developed to generate the small signal model of MT HVDC transmission system
  - Decompose the HVDC MT into predefined modular blocks (cable, converters)
  - Modules can be customized by modifying the parameters but not the structure of the subsystem
  - Several blocks are developed for the converters reflecting the topology and the control
  - Steady state conditions (linearization points) for each block were precalculated as a function of the input
  - Steady state conditions for the entire system were obtained by implementing a dc loadflow

ProOfGrids

Definition of subsystem interfaces

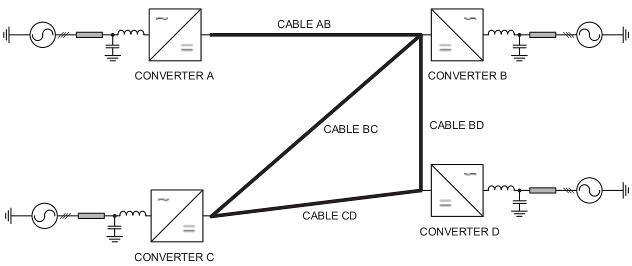

ProOfGrids

Definition of subsystem interfaces

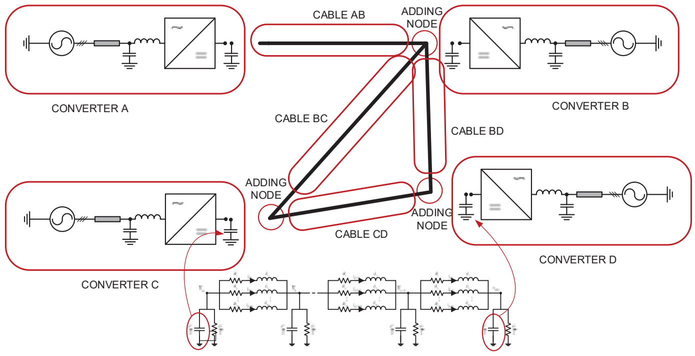

ProOfGrids

Workflow for generating the small signal model

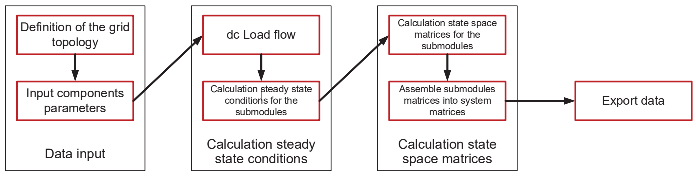

ProOfGrids

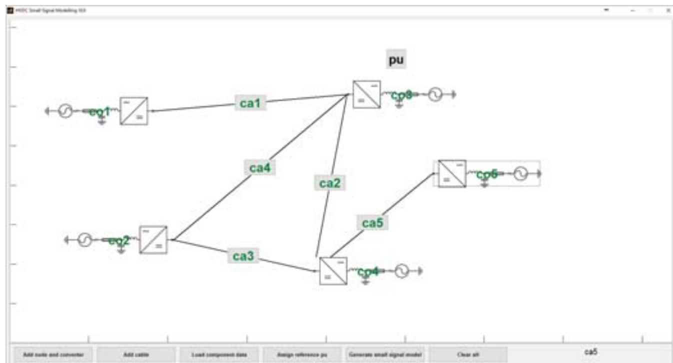

ProOfGrids

Screenshot of the GUI after generating the small signal model

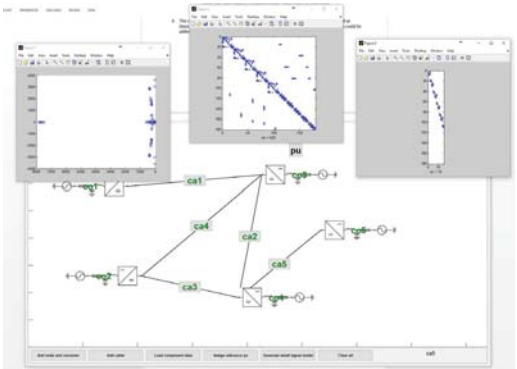

ProOfGrids

Aggregated participation factor analysis

- Approach proposed for identifying interactions in an interconnected system
  - An interaction mode is defined as an eigenvalue having participation ρ higher than a threshold χ from both parts of the interconnected system
- Interaction modes identified as shown below for $\chi = 0.20$
- Close correspondence can be identified between identified interaction modes and eigenvalues that are significantly influenced by the interconnection

$$\eta_{\alpha,i} = \frac{\left\| \mathbf{p}_{\alpha,i} \right\|}{\left\| \mathbf{p}_i \right\|}$$

$$\rho_{\alpha,i} = \frac{\eta_{\alpha,i}}{\sum_{\gamma \in S} \eta_{\gamma,i}}$$

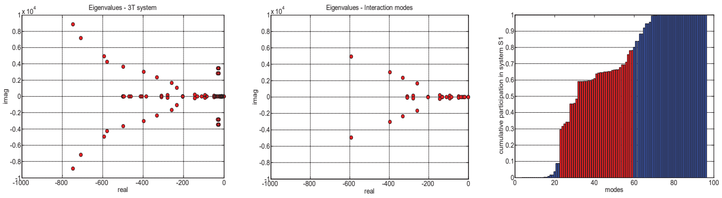

ProOfGrids

MMC-based point-to-point transmission scheme

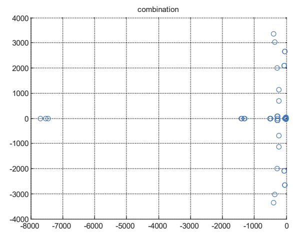

Eigenvalues of MMC HVDC point-to-point scheme

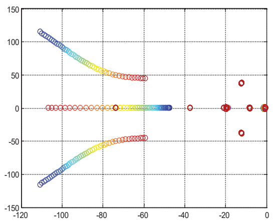

Trajectory of critical eigenvalue with power reference is varied from -1.0 to 1.0 pu

- Modes associated with the cable are quite quickly damped
- One oscillatory mode and one real pole are slightly dependent on operating conditions System is stable and well-damped in the full range of expected operating conditions

ProOfGrids

Interaction modes – MMC HVDC point-to-point scheme

- More interaction modes compared to case with 2L VSCs
  - In total 14 eigenvalues - 12 oscillatory modes (6 pairs) and two real poles.
- A first group is defined as those well damped oscillatory modes (real part smaller than -200).
- A second group of interaction modes is found much closer to the imaginary axis
  - Oscillatory mode (39-40)
  - Two real eigenvalues (48 and 49)

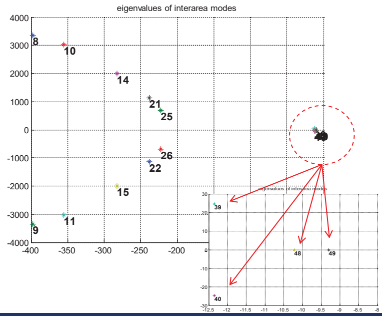

ProOfGrids

Time-domain verification of point-to-point MMC scheme

- Variables of small-signal model can accurately represent the nonlinear system model for variables at both terminals

DC voltage controlled terminal

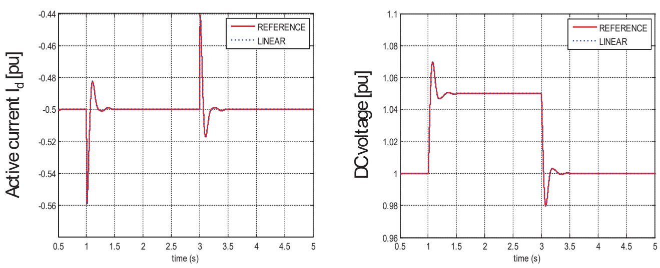

ProOfGrids

Interaction modes – Aggregated participation factor analysis

- For fast interaction modes:
  - Balanced participation from the two converter stations
  - High participation from the cable in the fastest modes
- Slow interaction modes
  - Dominant participation from the DC-voltage controlled terminal in oscillatory modes
  - Low participation from the cable, especially for the two real poles
- Depending on the eigenvalue, one station will have a higher participation

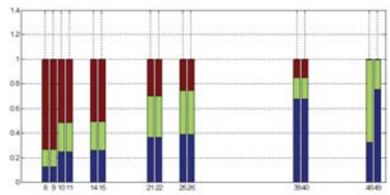

Aggregated participation factor analysis of interarea modes of the MMC-HVDC point-to-point scheme
– **blue**: DC Voltage controlling station
– **green**: power controlling station
– **brown**: dc cable

ProOfGrids

Participation Factor Analysis of Interaction Modes

- The fast oscillatory modes (8-9, 10-11, and 14-15)
  - Related to dc voltages at both cable ends
  - Associated with cable dynamics
- Modes 21-22 and 25-26
  - "DC-side" interactions
  - Almost no participation from the AC-sides
  - Associated with the MMC energy-sum w_{Σ} and the circulating current i_{cZ}

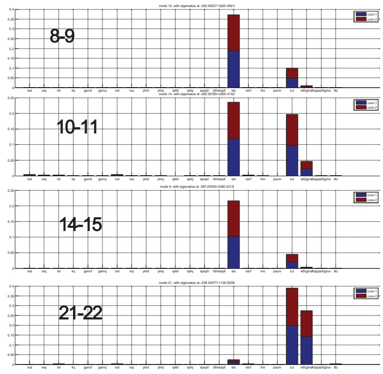

ProOfGrids

SINTEF

Technology for a better society

ProOfGrids

Participation Factor Analysis of Interaction Modes

- Oscillatory mode given by eigenvalues 39-40
  - Interaction modes associated with the power flow control in the system
  - Associated with the integrator state of the DC voltage controller, ρ
- Real poles 48 and 49
  - Associated with integrator states of the PI controllers for the circulating current, ξ_Z
  - The interaction of both stations in these eigenvalues is mainly due to the power transfer through the circulating current.
  - Small participation of the cable since the dynamics are slow and the equivalent parameters of the arm inductors dominate over the equivalent DC parameters of the cable

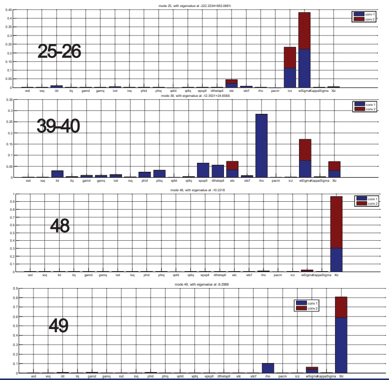

ProOfGrids

Main conclusions related to interaction analysis

- Small-signal eigenvalue analysis can be utilized to reveal the properties of modes and interactions in the system
  - Participation and sensitivity of all oscillations and small-signal stability problems can be analyzed
  - Suitable for system design, controller tuning and screening studies based on open models
- Aggregated participation factor analysis can reveal interaction between different elements or sub-systems

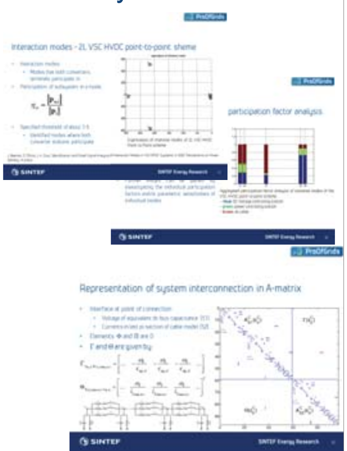

C1) Met-ocean conditions

Assessing Smoothing Effects of Wind Power around Trondheim via Koopman Mode Decomposition, Y. Susuki, Osaka Prefecture University

An interactive global database of potential floating wind park sites, L. Frøyd, 4Subsea AS

Offshore Wind: How an Industry Revolutionised Itself, M. Smith, Zephir Ltd

Assessing Smoothing Effects of Wind-Power around Trondheim via Koopman Mode Decomposition

Yoshihiko Susuki (JP)
Fredrik J. Raak (JP)
Harold G. Svendsen (NO)
Hans C. Bolstad (NO)

EERA DeepWind'2018
January 17

Purpose and Contents

Quantifying Smoothing Effects of Wind-Power around Trondheim via Koopman Mode Decomposition

1. Introduction of Koopman Mode Decomposition (KMD)
2. Review of KMD-based Quantification
   – F. Raak, Y. Susuki *et al.*, *NOLTA, IEICE*, vol.8, no.4, pp.342-357 (2017).
3. Application to Measured Data on Wind-Speed around Trondheim
   – Newly reported in this presentation

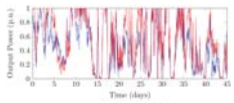

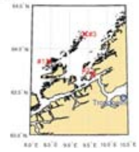

Outline of Presentation

- Introduction
  – About JST Project / Why Smoothing Effect?
- Koopman Mode Decomposition (KMD)
  – Brief summary of nonlinear time-series analysis
- KMD-based Quantification of Wind-Power Smoothing
  – F. Raak, Y. Susuki *et al.*, *NOLTA, IEICE*, vol.8, no.4, pp.342-357 (2017).
  – Definition and simple example
- Application to Wind-Data around Trondheim
  – Synthetic wind-power output
  – Quantification result
- Conclusion

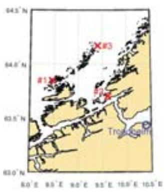

Outline of Presentation

- Introduction
  – About JST Project / Why Smoothing Effect?
- Koopman Mode Decomposition (KMD)
  – Brief summary of nonlinear time-series analysis
- KMD-based Quantification of Wind-Power Smoothing
  – F. Raak, Y. Susuki *et al.*, *NOLTA, IEICE*, vol.8, no.4, pp.342-357 (2017).
  – Definition and simple example
- Application to Wind-Data around Trondheim
  – Synthetic wind-power output
  – Quantification result
- Wrap-Up

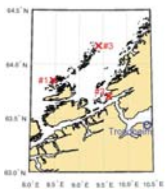

Smoothing Effects of Wind-Power

- Reduction of fluctuations in wind-power by aggregation
- Importance of its assessment (or quantification) for managing large-scale introduction of wind power:
  – *Large-term* use --- planning w/ use of **in-vehicle batteries**
  – *Short-term* use --- controlling turbines / maintaining power quality

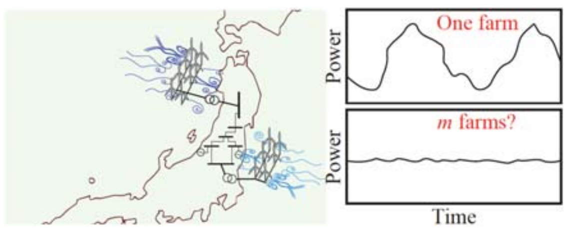

Koopman Mode Decomposition (KMD)

Novel technique to decompose multi-channel, complex time-series into **modes with single-frequencies**, conducted directly from ***data***

$\{g_0, \dots, g_m\}$ Finite-time data obtained in experiments or simulations under uniform sampling

Koopman Eigenvalue, determining freq./damping

Koopman Mode, determining amplitude/phase

$$g_k = \sum_{j=1}^{m} \boxed{\tilde{\lambda}_j^k} \tilde{V}_j, \quad g_m = \sum_{j=1}^{m} \tilde{\lambda}_j^m \boxed{\tilde{V}_j} + \eta_m$$

$$k = 0, \dots, m-1$$

For details, see the paper [C. Rowley, I. Mezic, *et al.*, *J. Fluid Mech.*, vol.641, pp.115-127 (2009)].

KMD-based Quantification (1/3) -- Derivation

Ref.) F. Raak, Y. Susuki *et al.*, *NOLTA, IEICE*, vol.8, no.4, pp.342-357 (2017).

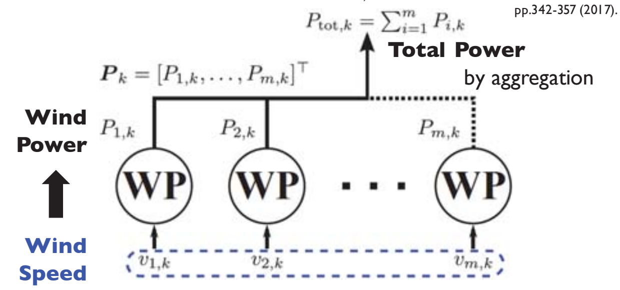

$$\boldsymbol{P}_k = \sum_{i=1}^{N} \tilde{\lambda}_i^k \tilde{\boldsymbol{v}}_i, \quad k = 0, \ldots, N \qquad P_{\mathrm{tot},k} = \sum_{i=1}^{N} \tilde{\lambda}_i^k \sum_{j=1}^{m} [\tilde{\boldsymbol{v}}_i]_j =: \sum_{i=1}^{N} \tilde{\lambda}_i^k \overline{\boldsymbol{v}}_i$$

KMD of Wind-Power

KMD-based Quantification (2/3) -- Definition

KMD of Wind-Power (again):

Ref.) F. Raak, Y. Susuki *et al.*, *NOLTA, IEICE*, vol.8, no.4, pp.342-357 (2017).

$$\boldsymbol{P}_k = \sum_{i=1}^{N} \tilde{\lambda}_i^k \tilde{\boldsymbol{v}}_i, \quad k = 0, \ldots, N \qquad \tilde{\boldsymbol{v}}_i = \boldsymbol{A}_i \angle \boldsymbol{\alpha}_i$$

Complex-valued vectors

Proposed Index:

$$\mathrm{coh}_{i,\mathrm{KMD}} = \frac{1}{m(m-1)} \sum_{j=1}^{m} \sum_{\substack{l=1 \\ l \neq j}}^{m} [\hat{\boldsymbol{A}}_i]_j [\hat{\boldsymbol{A}}_i]_l \cos(\Phi_{jl}^i)$$

Normalized Moduluses

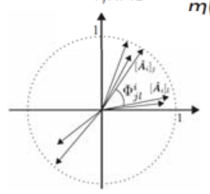

- Total sum of **similarity** for every pair of components of a single Koopman mode
- Index computed for each **single** frequency
- Generalization of the conventional Power Spectrum Density (PSD)-based index

KMD-based Quantification (3/3) -- Example

Ref.) F. Raak, Y. Susuki *et al.*, *NOLTA, IEICE*, vol.8, no.4, pp.342-357 (2017).

$$x_1(t) = a_1 \cdot \sin(2\pi f_1 t) + b_1 \cdot \cos(2\pi f_2 t),$$
$$x_2(t) = -\left\{a_2 \cdot \sin(2\pi f_1 t + \varphi) + b_2 \cdot \cos\left(2\pi f_2 t - \frac{\pi}{3} + \varphi\right)\right\} \qquad f_1 = 2\,\mathrm{Hz}, \; f_2 = 7\,\mathrm{Hz}$$

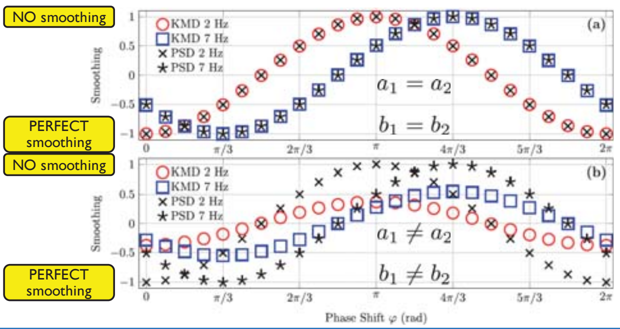

Outline of Presentation

- Introduction
  - About JST Project / Why Smoothing Effect?
- Koopman Mode Decomposition (KMD)
  - Brief summary of nonlinear time-series analysis
- KMD-based Quantification of Wind-Power Smoothing
  - F. Raak, Y. Susuki *et al.*, *NOLTA, IEICE*, vol.8, no.4, pp.342-357 (2017).
  - Definition and simple example
- Application to Wind-Data around Trondheim
  - Synthetic wind-power output
  - Quantification result
- Wrap-Up

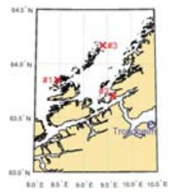

Measurement Data around Trondheim

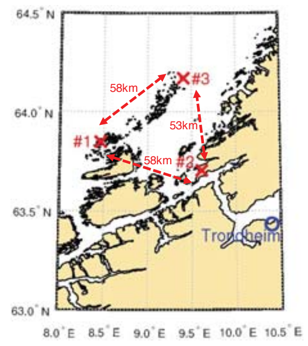

Three Hypothetical Wind-Farm Sites

- 92-days long time-series of hourly wind speeds
  - 10 meters above ground / Mmean value for last 10 minutes before time of observation
- Converted into wind-power (in per-unit) via the static nonlinear power curve below

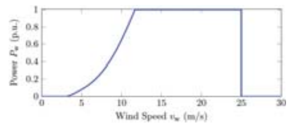

Data on Aggregated Wind-Power

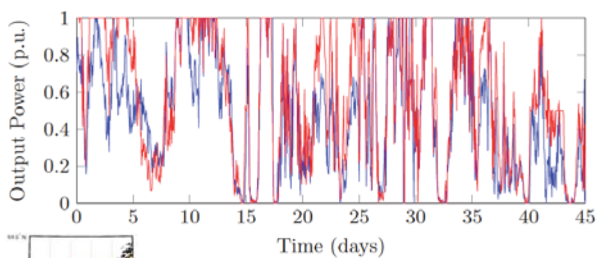

Aggregation of #1 and #2

Aggregation of #2 and #3

Original Data and Reconstructed Data via KMD

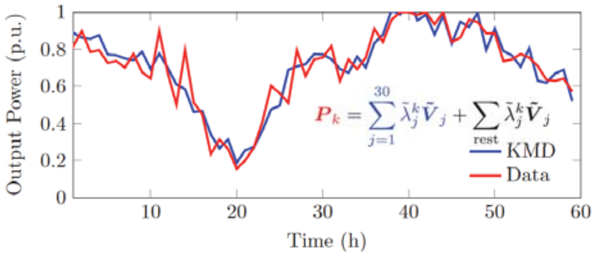

Table 1. Variances of total powers P and of reconstructed time-series via KMD $\tilde{P}$

Case		$P_{\text{tot,first}}$	$P_{\text{tot,last}}$	$\tilde{P}_{\text{tot,first}}$	$\tilde{P}_{\text{tot,last}}$
Case 1	#1 and #2	0.10	0.08	0.12	0.06
Case 2	#1 and #3	0.11	0.09	0.12	0.08
Case 3	#2 and #3	0.12	0.10	0.12	0.09

Lower Value of Variance!

Summary and Take-Home Messages

Quantifying Smoothing Effects of Wind-Power around Trondheim via Koopman Mode Decomposition (KMD)

1. KMD enables an extraction of dominant feature w/ clear time-scale separation directly from complex wind-power data.
2. KMD enables a quantification of smoothing effects of wind-power around Trondheim
   ---how the smoothing is engineered by the choice of locations.

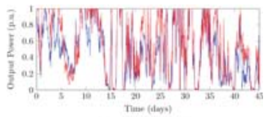

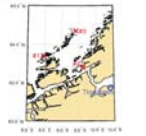

Quantification Result

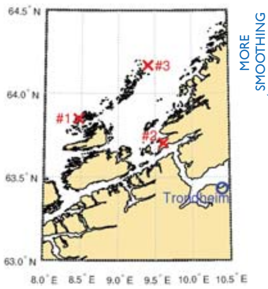

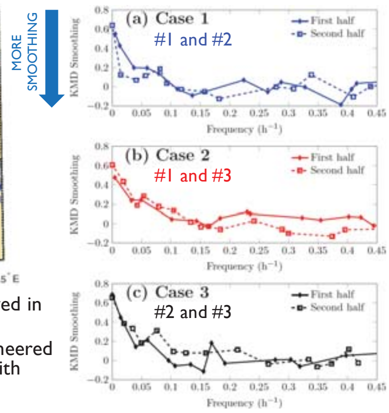

- More smoothing archived in high frequencies
- Better smoothing engineered in Case:1, consistent with the variance test

Thank You for Your Attention!

susuki@eis.osakafu-u.ac.jp

Outline of Presentation

- Introduction
  - About JST Project / Why Smoothing Effect?
- Koopman Mode Decomposition (KMD)
  - Brief summary of nonlinear time-series analysis
- KMD-based Quantification of Wind-Power Smoothing
  - F. Raak, Y. Susuki *et al.*, *NOLTA, IEICE*, vol.8, no.4, pp.342-357 (2017).
  - Definition and simple example
- Application to Wind-Data around Trondheim
  - Synthetic wind-power output
  - Quantification result
- Wrap-Up

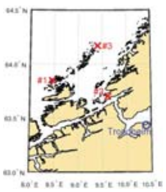


4subsea
An interactive global database of potential floating wind park sites
EERA DeepWind 2018
Trondheim 2017-01-17
Lars Frøyd
lars.froyd@4subsea.com

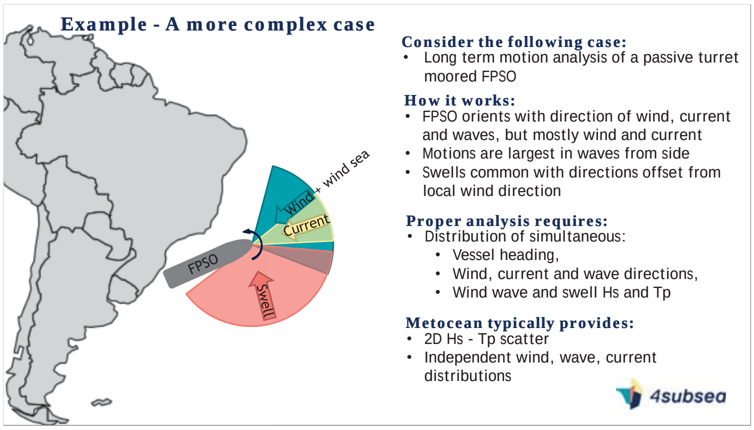
Example - A more complex case
Consider the following case:
• Long term motion analysis of a passive turret moored FPSO
How it works:
• FPSO orients with direction of wind, current and waves, but mostly wind and current
• Motions are largest in waves from side
• Swells common with directions offset from local wind direction
Proper analysis requires:
• Distribution of simultaneous:
• Vessel heading,
• Wind, current and wave directions,
• Wind wave and swell Hs and Tp
Metocean typically provides:
• 2D Hs - Tp scatter
• Independent wind, wave, current distributions
Wind + wind sea
Current
FPSO
Swell
4subsea

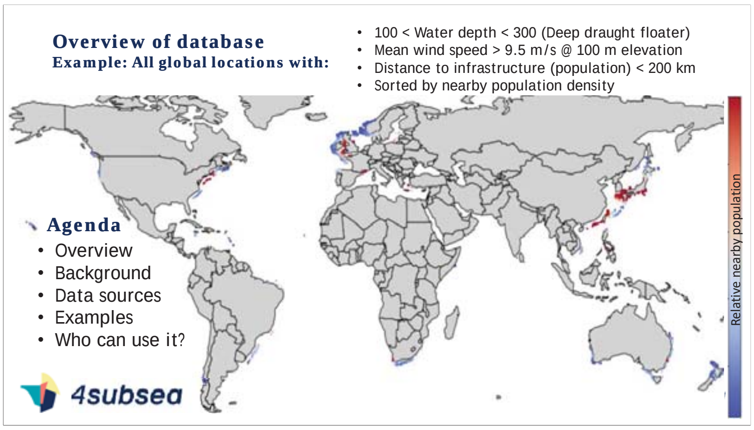
Overview of database
Example: All global locations with:
• 100 < Water depth < 300 (Deep draught floater)
• Mean wind speed > 9.5 m/s @ 100 m elevation
• Distance to infrastructure (population) < 200 km
• Sorted by nearby population density
Relative nearby population
Agenda
• Overview
• Background
• Data sources
• Examples
• Who can use it?
4subsea

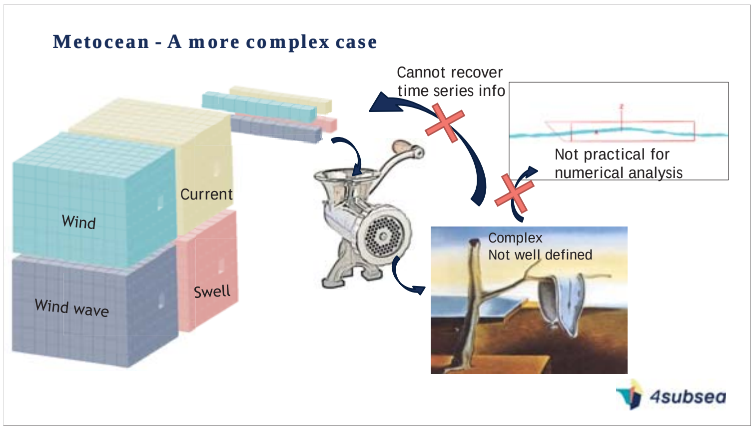
Metocean - A more complex case
Cannot recover time series info
Not practical for numerical analysis
Wind
Current
Wind wave
Swell
Complex
Not well defined
4subsea

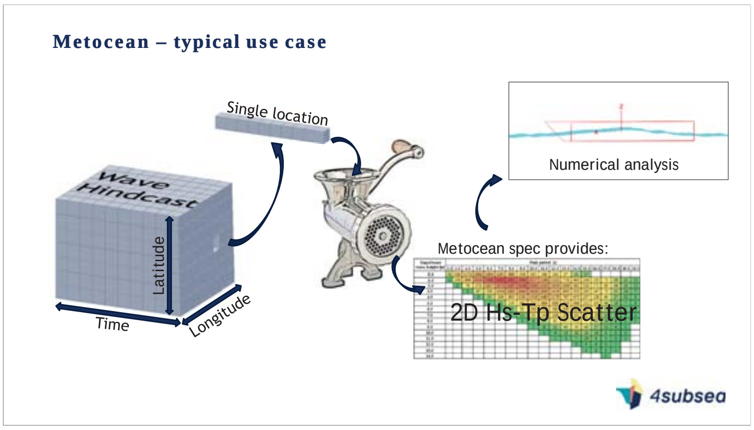
Metocean – typical use case
Single location
Numerical analysis
Wave Hindcast
Latitude
Time
Longitude
Metocean spec provides:
2D Hs-Tp Scatter
4subsea

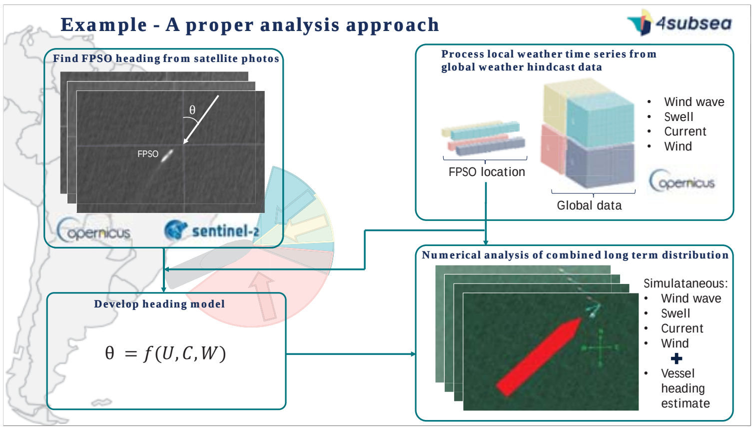
Example - A proper analysis approach
4subsea
Find FPSO heading from satellite photos
FPSO
θ
copernicus
sentinel-2
Process local weather time series from global weather hindcast data
• Wind wave
• Swell
• Current
• Wind
FPSO location
Global data
copernicus
Develop heading model
θ = f(U, C, W)
Numerical analysis of combined long term distribution
Simultaneous:
• Wind wave
• Swell
• Current
• Wind
+
• Vessel heading estimate

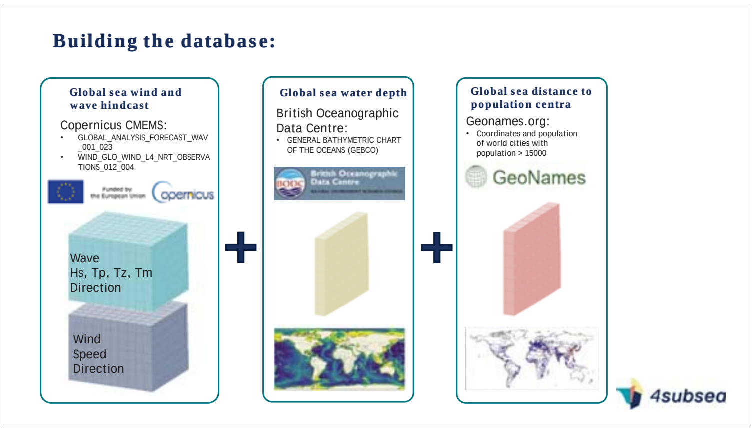
Building the database:
Global sea wind and wave hindcast
Copernicus CMEMS:
GLOBAL_ANALYSIS_FORECAST_WAV_001_023
WIND_GLO_WIND_L4_NRT_OBSERVATIONS_012_004
Copernicus
Wave
Hs, Tp, Tz, Tm
Direction
Wind
Speed
Direction
+
Global sea water depth
British Oceanographic Data Centre:
GENERAL BATHYMETRIC CHART OF THE OCEANS (GEBCO)
British Oceanographic Data Centre
+
Global sea distance to population centra
Geonames.org:
Coordinates and population of world cities with population > 15000
GeoNames
4subsea

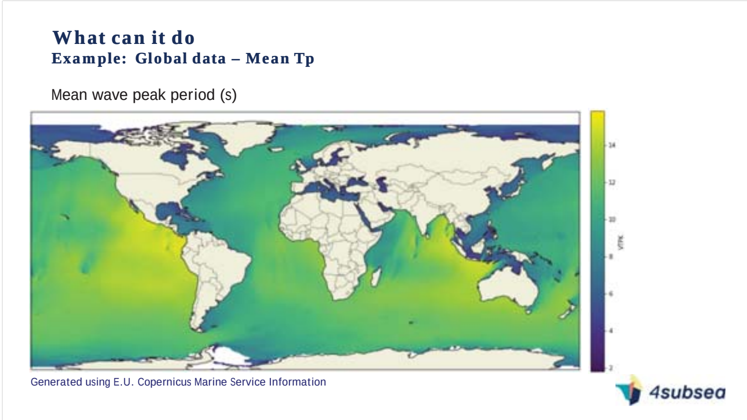
What can it do
Example: Global data – Mean Tp
Mean wave peak period (s)
Generated using E.U. Copernicus Marine Service Information
4subsea

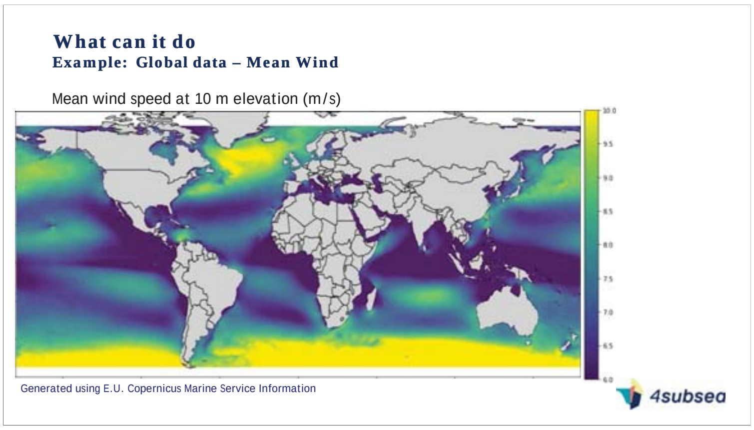
What can it do
Example: Global data – Mean Wind
Mean wind speed at 10 m elevation (m/s)
Generated using E.U. Copernicus Marine Service Information
4subsea

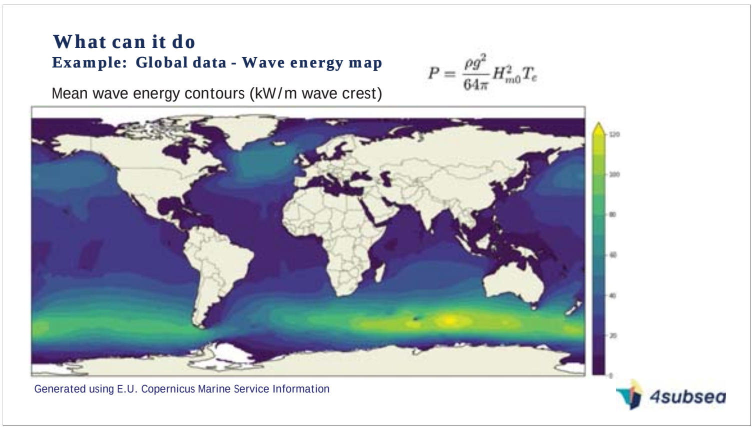
What can it do
Example: Global data - Wave energy map
$P = \frac{\rho g^2}{64\pi} H_{m0}^2 T_e$
Mean wave energy contours (kW/m wave crest)
Generated using E.U. Copernicus Marine Service Information
4subsea

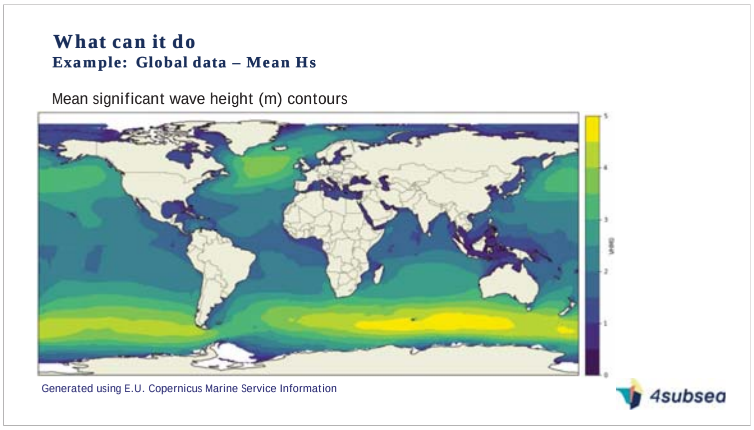
What can it do
Example: Global data – Mean Hs
Mean significant wave height (m) contours
Generated using E.U. Copernicus Marine Service Information
4subsea

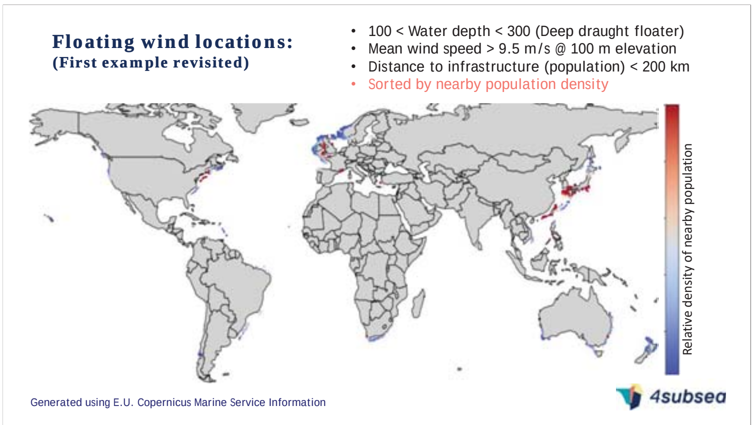
Floating wind locations:
(First example revisited)
100 < Water depth < 300 (Deep draught floater)
Mean wind speed > 9.5 m/s @ 100 m elevation
Distance to infrastructure (population) < 200 km
Sorted by nearby population density
Relative density of nearby population
Generated using E.U. Copernicus Marine Service Information
4subsea

Floating wind locations:

- 100 < Water depth < 300 (Deep draught floater)
- Mean wind speed > 9.5 m/s @ 100 m elevation
- Distance to infrastructure (population) < 200 km
- Sorted by annual mean wind speed (10 m elevation)

Generated using E.U. Copernicus Marine Service Information

4subsea

Who can use it:

- All data sources are publically available
- In principle, the combined product can be made publically or comercially available:
  - E.g. complete global coverage
  - .. or on a location by loaction basis
  - Full hindcast time series
  - .. or aggregated properties (e.g. mean, max)
- Access and availablilty is not yet decided
  - (Remember, dataset more or less a bi-product of another work)
  - Please make contact if the dataset can be useful for you – we will arrange something! lars.froyd@4subsea.com

4subsea

Floating wind locations:
Some interesting areas

- 100 < Water depth < 300 (Deep draught floater)
- Mean wind speed > 9.5 m/s @ 100 m elevation
- Distance to infrastructure (population) < 200 km
- Sorted by annual mean wind speed (10 m elevation)

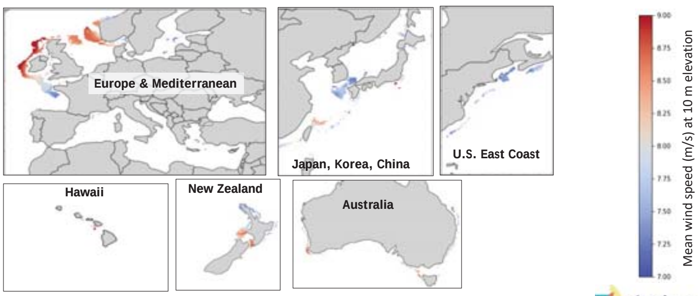

Generated using E.U. Copernicus Marine Service Information

4subsea

Sources – Wind/wave hindcast

- This study has been conducted using E.U. Copernicus Marine Service Information
- Copernicus CMEMS: http://marine.copernicus.eu/

copernicus sentinel-2

4subsea

Example of possible data views:
- With the magic of Python (and some patience)

Simple aggregated views:
- Sorting based on mean or annual max: Hs, Tp, wind speed, water depth, etc..
- Ranking sites by some fitness function (high wind, low wave, near shore, etc)

Utilizing the full hindcast:
- Seasonal waiting times for marine operation with some operational limit (Hs, Tp, Wind speed)
- Power factor of some specific wind turbine (based on binning of wind speeds)
- Estimated site LCOE (with some clever cost model)
- Etc..

Proposed use cases:
- Resource assessment
- Feasibility studies
- Preliminary site optimization / analyses
- Operational/maintenence planning
- Etc..

4subsea

Sources – Water depth:

British Oceanographic Data Centre

- GEBCO 2014 water depth database:
  - https://www.bodc.ac.uk/data/hosted_data_systems/gebco_gridded_bathymetry_data/

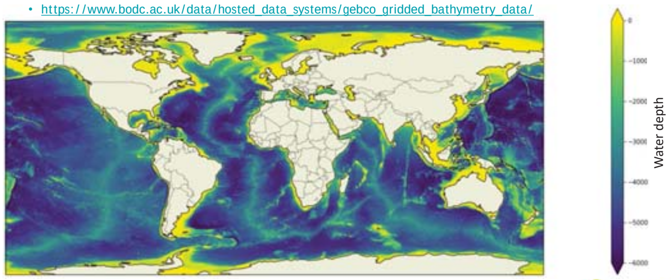

4subsea

Sources – Population density:

- Geonames.org database of world cities with population > 15000:
  - http://download.geonames.org/export/dump/cities15000.txt

GeoNames

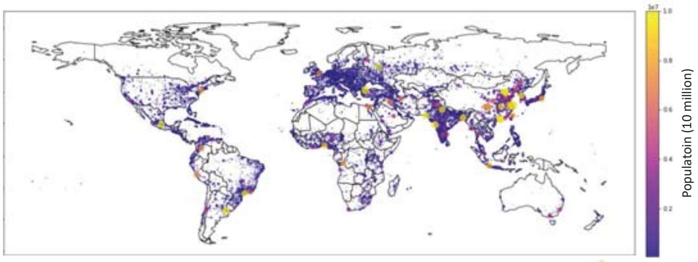

4subsea

Offshore Wind

How an Industry Revolutionised Itself

Matt Smith — Offshore Lidar Expert

EERA DeepWind 2018

2002 **Garrad Hassan introduction to lidar by ZephIR / QinetiQ**

July 2006 — **Remote Sensing Positioning Statement – Issue A**
First statement globally assessing and evaluating the acceptance of remote sensing. ZephIR enters Stage 1, completes Milestone 1, enters Stage 2:

"Provided suitable off-site and/or onsite validation steps as defined above are carried out, and the results of these validations are positive, then GH consider that data recorded using the ZephIR device may be used in a quantitative sense for the formal assessment of the wind speed and energy production of a potential wind farm site."

Advice stated to provide tall mast verification - ZephIR launch UK Remote Sensing Test Site.

July 2007 — **Remote Sensing Positioning Statement – Issue B**
ZephIR demonstrates Stage 2 progress with body of evidence being developed for Stage 3.
ZephIR 'Best practice verification methodology' endorsed by Garrad Hassan.

August 2010 — **Remote Sensing Positioning Statement – Issue C**
ZephIR enters Stage 3:

"For relatively simple terrain sites… data from the ZephIR device may be used in a quantitative sense with reasonable error bars for the purpose of the assessment of the wind regime at a potential wind farm site."

October 2012 — **Remote Sensing Positioning Statement – Revised document**
ZephIR achieves Stage 3 acceptance:

"DNV GL considers ZephIR 300 to be at Stage 3 under "benign" conditions - accepted for use in bankable / finance-grade wind speed and energy assessments with either no or limited on-site met mast comparisons. "

10 years to receive formal approval for ground-based wind resource assessment with Lidar…

A disclaimer!

Please note:

- As many of you know, I am a Lidar salesperson!
- This is less of a scientific and more of an overview of various activities that occurred over the last decade that have revolutionised the wind industry.
- I hope it's an interesting story and many of you will have been involved along the way.
- Feel free to leave now on this basis or submit your thoughts to me after the presentation!

So how did the offshore industry differ?

Not so much 'how' but 'why' - the then only available option for wind recourse assessment offshore – an offshore met mast:

- Massive "at risk" investment if looking at installing a new platform
- Mast anemometry is difficult to achieve at modern offshore hub heights
- Increased interest in the full rotor swept area
- Ongoing maintenance, health & safety inspections and calibration of anemometry
- Impact on Levelised Cost of Energy
- Time to get to results – planning etc.
- Representation of wind resource at a single point across the site
- … Floating Wind!

Let's just say Lidar was knocking on an already open door!

15 years ago… in a galaxy not so far away

The response? Go and prove yourselves! And at this time, there were no clear standards, no IEC guidance on remote sensors, no authorities in this area.

Project needs and adoption

What did that open door look like?

- Time to market for a disruptive technology vs. rate of industry growth
- Quality of wind data
- Quantity of wind data
- Data across a site
- Health & Safety improvements
- Through-life risks – Day 1, Day 100, Day 1000, Day 10,000?
- Through-life costs

The first movers / innovators

ZephIR Lidars were the first to be deployed offshore on fixed platforms.




2005, Beatrice Platform, North Sea
2006, NaiKun, Hecate Strait
2010, Robin Rigg, Solway Firth
2014, Bell Rock Offshore Windfarm, Dundee

The rise of the truly floating Lidar

Roadmap to acceptance

NaiKun demonstrated a low-cost Lidar platform could work but only went part of the way to reducing cost and time to water.

But in 2010 Deepwater Wind demonstrated that a floating Lidar could work just as well.

Just 3 years later - 2013 – a range of floating Lidars were tested and validated as part of the UK's Carbon Trust Offshore Wind Accelerator (OWA) programme.

Knowing the time pressures / scale of offshore wind growth, the OWA published a set of recommendations to give the industry the formal framework needed to accelerate the commercial deployment of the technology while standards were being developed. The IEA build on this work to offer recommendations for using floating lidar including wider considerations; H&S, Deployment, Moorings,..

Commercial deployments of floating Lidars accelerated significantly!

The industry pulls sideways

Lidar is now accepted as a proven technology by the wind industry from a practical, contractual and, increasingly, from an industry standards' perspective.

Perfect timing as the hub height and swept area of offshore wind turbines surpasses using mast anemometry as an economically viable option.

- Use of Lidar for Resource Assessment demonstrates Best in Class data
- Reliability demonstrated on industry firsts with floating lidars going into their third year of continuous operation
- Known boundaries of use through research studies – important! And help to define new areas of research and validation
- Cost advantages demonstrated on projects coming to fruition
- … Look at the US market, there are no masts and most sites will progress without one

Research Council of Norway

[Picture from lidar comparison test (CMR)]

One of the earlier publicly available assessments was conducted here in Norway.

Financed by NRC and Statoil with in-kind support from Fugro Oceanor, UiB and CMR.

This directly led to the further development and adoption of the Fugro Seawatch buoy (based 5 minutes walk from this event)

Operational Assessments

No platform to use from met mast?
Deploy Lidars on wind farm substations!

Merkur Offshore Windfarm
- Lidar is coupled to met data acquisition systems, data is transmitted to client platform for access.
- Data is integrated with SCADA systems.
- Lidar is used for power performance analysis using hub height measurements.
- Combined with other sensors to support helicopter landing ops including personnel winching.


Energisation and Start of Warranty

Offshore, contractual power curve verification tests according to IEC 61400-1-12 standards remains highly impractical as they require the installation of a met mast and this only permits the testing of one turbine in such large arrays.

The March 2018 update permits the combination use of Lidar and mast and whilst this has progressed the use of verifications onshore it still requires significant investment offshore to accommodate the requirements.

Nacelle mounted Lidar delivers accurate measurements, across multiple turbines, at a significantly lower cost point, with high availability and low uncertainties.

2014 – A project conducted by a consortium made of DTU Wind Energy (formerly Risø Wind Energy Department), DONG Energy, Siemens Wind Power and Avent Lidar Technology, and funded by the Danish Energy Technology Development and Demonstration Program (EUDP). The procedure provides the basis for a new, industry-wide best-practice for performance verification with nacelle LIDARs.

The shear size and cost of offshore wind projects is focussing more on commercial agreements than IEC standards whereby development wind specialists are defining power curve verification tests with the turbine OEM's.

Many leading OEM's now accepting a nacelle mounted Lidar power curve test (Lidar calibrations, test methodologies and result analysis has already been defined)

2017 – Look at where we were

London, 18 July 2017. Leading wind measurement experts gathered in London claimed that LiDARs have been replacing met masts to become the sole wind measurement tool used for offshore resource assessment and power curve verification purposes

Deutsche WindGuard, Klause Franke, Project Engineer: *"Application of Nacelle Based Lidar for Offshore Power Curve Tests"*
ECN, Hans Verhoef, Project Leader Measurements: *"Offshore wind development with standalone Lidar"*
EDF EN, Cedric Dall'Ozo, Senior Wind Resource Assessment Engineer: *"Reducing uncertainties: vertical profiler, floating, scanning and nacelle Lidars"*
MHI Vestas, Tue Hald, Senior Specialist: *"Power curve verification with nacelle two-beam Lidar on V164-8.0 MW"*
RES, Iain Campbell, Technical Analyst and Wind Resource Manager: *"Lidar: Just better than a mast?"*
Siemens, Pedro Salvador, rotor Performance engineer: *"From R&D to Plug & Play: 8 years of nacelle Lidar experience"*
SSE, Gordon Day, Offshore Wind Analyst: *"Replacing masts with Lidar for financing and performance assessment"*
UL DEWI, Beatriz Canadillas, Senior Researcher: *"Offshore Wind Lidar since 2009: from R&D to commercial applications"*

Construction Monitoring

Block Island Windfarm

ZephIR 300 was installed on Fred. Olsen Windcarrier's Brave Tern jack-up vessel - used to compare wind speeds against those measured with the main boom tip crane wind sensor.

Measurements were used as a "live" instrument during all phases of construction and specifically during critical points of component lift. 1 second live data was displayed with wind shear curves in the user interface.

Where wind behaviour was difficult to explain i.e. when wind at the tip of the crane was lower than on the crane A-frame, or bridge level, ZephIR 300 could identify and explain the difference across the full lift height.

During WOW (Waiting-On-Weather) downtime, ZephIR 300 provided a very accurate picture of the wind conditions to enable effective decision making.

During high winds when the crane was in the boomrest, ZephIR 300 was used to confirm when it was worth lifting the crane out of the boomrest again before making any unnecessary movements.

Today we see Lidar included as standard in offshore tenders for vessels operating on wind farm construction

The industry has revolutionised itself

In the space of 5 years since the first OWA analysis of offshore Lidars, there is adoption for fixed and floating platforms with Lidar, across all project phases – something not even achieved onshore yet!

What next?

- The full range of capabilities offered by Lidar in any format continues to be developed and validated.
- This will lead to further pull sideways in to other applications and project phases.
- The industry continues to drive down LCOE.
- Safety First across everything we do.
- Innovation time is getting faster.

The industry has revolutionised itself

Our guess?

All of these drivers, particularly offshore, will move towards:

- Turbine control (passive, i.e. look and learn, and active) and load management to allow for life extension, asset sweating or opportunities for repowering with new innovations e.g. blade extensions
- Wake effects will be quantified and strategies implemented to better manage power loss / irregular loading
- Wind sector management will be more appropriately applied with Best in Class wind sensors
- Power forecasting will be more inline with new grid and trading requirements

Lidar is 'just' a sensor – others need to build systems around this technology – through partnerships the value can be realised

It certainly hasn't finished yet.....

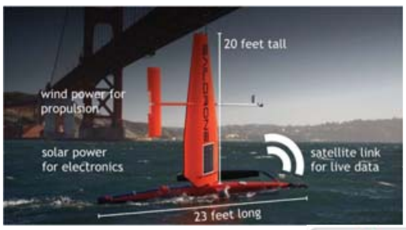

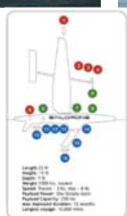

ZephIR Lidar

Contact

The Old Barns, Fairoaks Farm,
Hollybush, Ledbury, HR8 1EU

Phone: +44 (0)1531 651 004

Email: matt@zephirlidar.com

Web: www.zephirlidar.com

ZephIR Lidar

Terms and Conditions

C2) Met-ocean conditions

Wind conditions in a Norwegian fjord derived from tall meteorological masts and synchronized doppler lidars, H. Agustsson, Kjeller Vindteknikk

Complementary use of wind lidars and land-based met-masts for wind characterization in a wide fjord, E. Cheynet, University of Stavanger

Simulation and observations of wave conditions in Norwegian fjords, B.R. Furevik, Meteorologisk institutt

Wind conditions in a Norwegian fjord derived from tall meteorological masts and synchronized doppler LIDARs

Hálfdán Ágústsson, Martin S. Grønsleth, Ola Kaas Eriksen, Ove Undheim, Finn K. Nyhammer, Øyvind Byrkjedal, Kjeller Vindteknikk, Norway
halfdan.agustsson@vindteknikk.no

Lidar campaign in Halsafjorden: Sept. '17 - '18

Eastern side: Åkvika

Minni
WC400s-6
IP: 192.168.30.35

Klara Ku
Camera

Dolly
WC400s-12
IP: 192.168.30.36

Western side: Myrahaugen

Mikke
WC400s-10
IP: 192.168.30.38

Langbein
Camera

Donald
WC400s-13
IP: 192.168.30.37

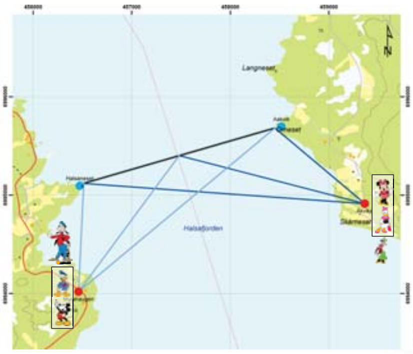

Ferry free E39 in West/Norway

Statens vegvesen

- Eight fjords to cross
- Fjord widths 2-7.5 km
- Fjord depths 300-1300 m
- High and variable climate loads
- What are the appropriate design loads?

Concept bridge Halsafjorden (Statens Vegvesen)
Suspension bridge, 1 span @ 2050 m

Lidar campaign in Halsafjorden: Sept. '17 - '18

Eastern side: Åkvika

Minni
WC400s-6
IP: 192.168.30.35

Klara Ku
Camera

Dolly
WC400s-12
IP: 192.168.30.36

Western side: Myrahaugen

Mikke
WC400s-10
IP: 192.168.30.38

Langbein
Camera

Donald
WC400s-13
IP: 192.168.30.37

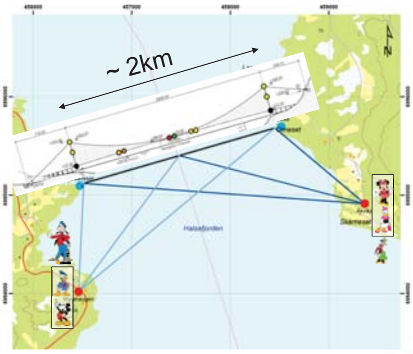

Extensive observational campaign

Statens vegvesen

- A 50 – 100 m high met mast at ends of each crossing.
- Min. 4 years of 10 Hz obs. of 3D wind at 3-4 elevations in masts.
- Additional masts to investigate horizontal coherence
- Wave and current buoys
- **Two pairs of synchronized LIDARs**

Observational data in the open domain. Corroborated by up to 10 years of meso-scale (500 m X 500 m) and CFD simulations (~100 m X ~100 m).

LIDARs on west side of fjord

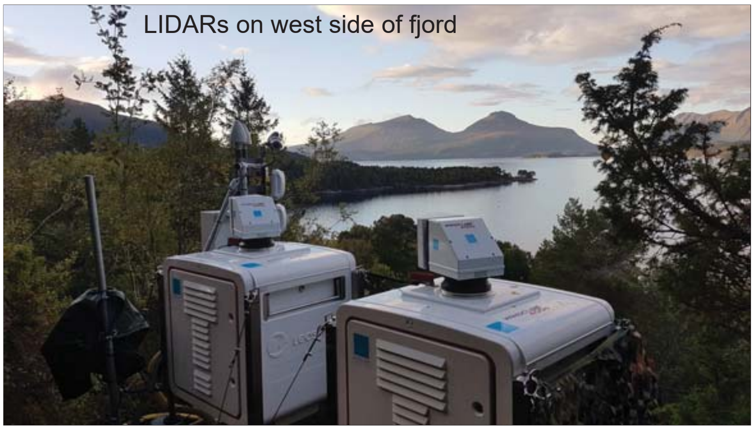


LIDARs on east side of fjord

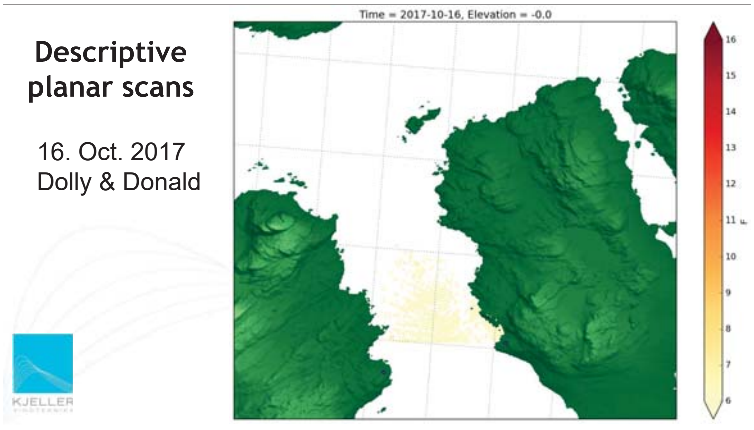
Descriptive planar scans
16. Oct. 2017
Dolly & Donald
Time = 2017-10-16, Elevation = -0.0
KJELLER

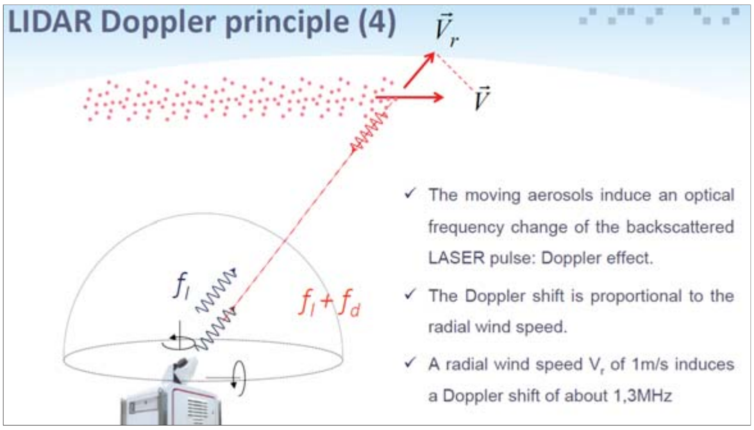
LIDAR Doppler principle (4)
$\vec{V}_r$
$\vec{V}$
f_l
$f_l + f_d$
✓ The moving aerosols induce an optical frequency change of the backscattered LASER pulse: Doppler effect.
✓ The Doppler shift is proportional to the radial wind speed.
✓ A radial wind speed V_r of 1m/s induces a Doppler shift of about 1,3MHz

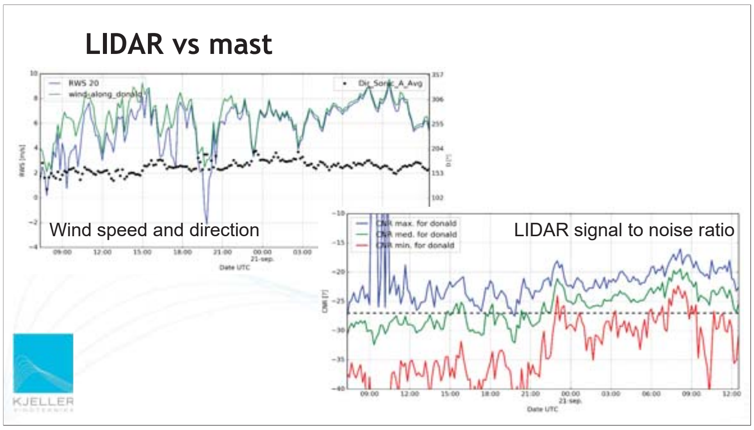
LIDAR vs mast
RWS 20
wind_along_donald
Dir_Sonic_A_Avg
Wind speed and direction
CNR max. for donald
CNR med. for donald
CNR min. for donald
LIDAR signal to noise ratio
Date UTC
KJELLER

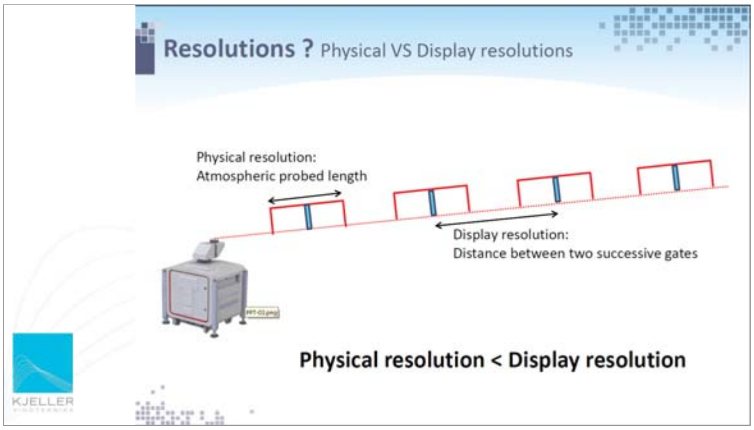
Resolutions ? Physical VS Display resolutions
Physical resolution:
Atmospheric probed length
Display resolution:
Distance between two successive gates
Physical resolution < Display resolution
KJELLER

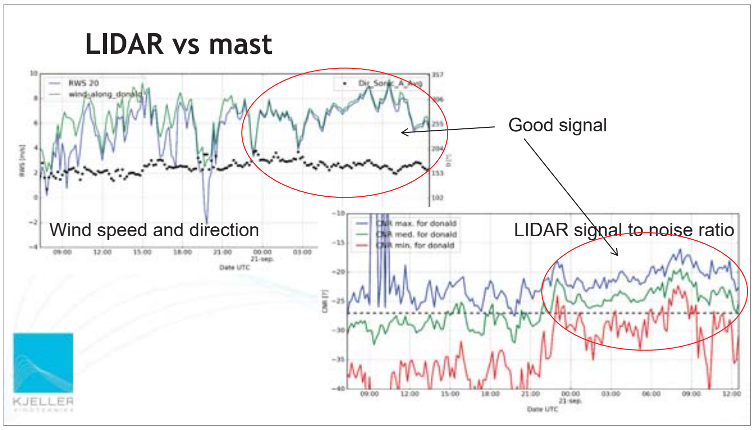
LIDAR vs mast
RWS 20
wind_along_donald
Dir_Sonic_A_Avg
Good signal
Wind speed and direction
CNR max. for donald
CNR med. for donald
CNR min. for donald
LIDAR signal to noise ratio
Date UTC
KJELLER

Radial wind speed - LIDAR vs mast

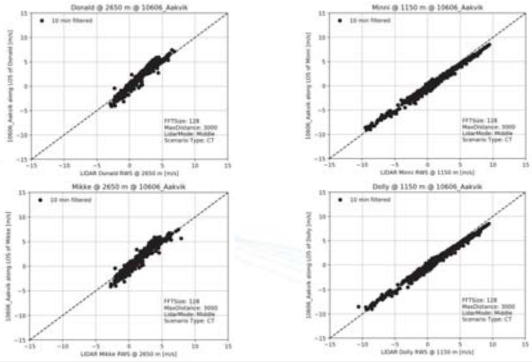

Example turbulence spectra – Mast vs LIDAR

1 Hz / 10 Hz temporal resolution, 20 min period, **50.3 m.**

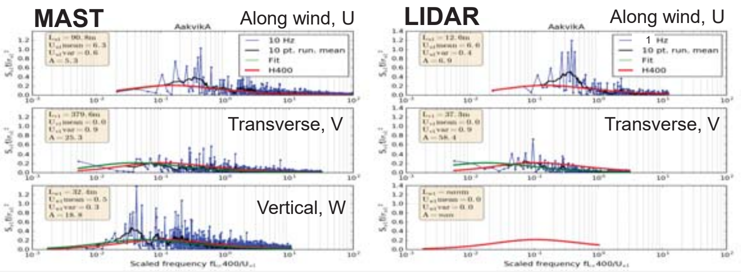

True wind - LIDAR vs mast

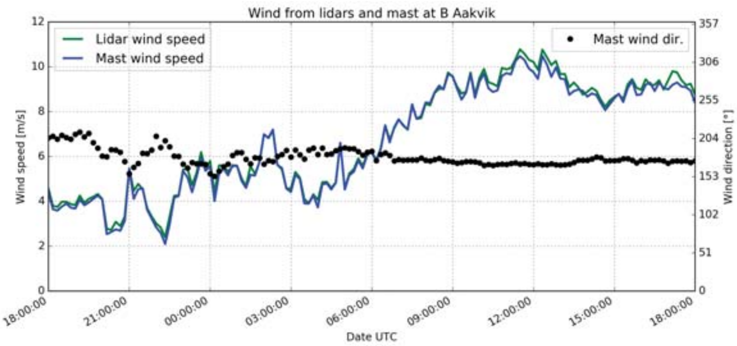

Example turbulence co-spectra – Mast vs lidar

1 Hz / 10 Hz temporal resolution, 20 min period

Vertical co-coherence of along wind variation U, 50.3 m vs. 31.8 m

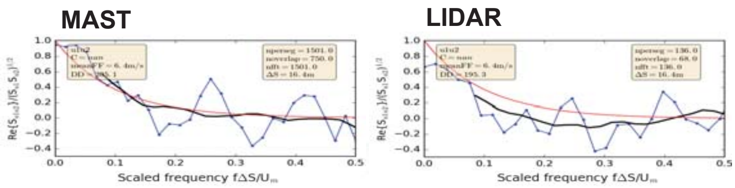

True wind - LIDAR vs mast

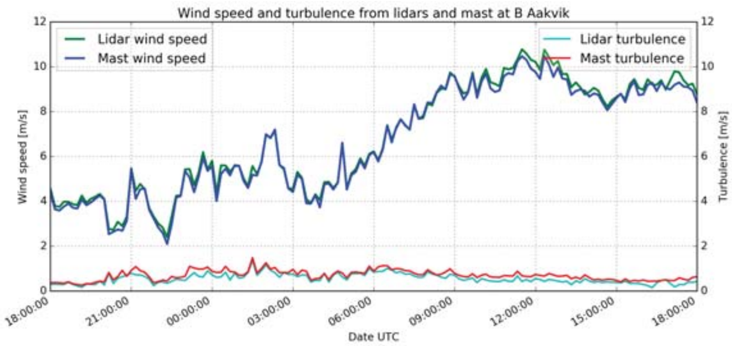

Example turbulence co-spectra – Mast vs lidar

1 Hz / 10 Hz temporal resolution, 20 min period

Vertical co-coherence of transverse wind variation V, 50.3 m vs. 31.8 m

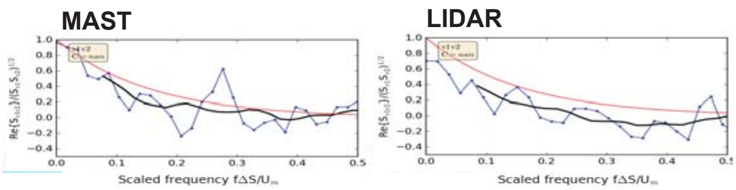

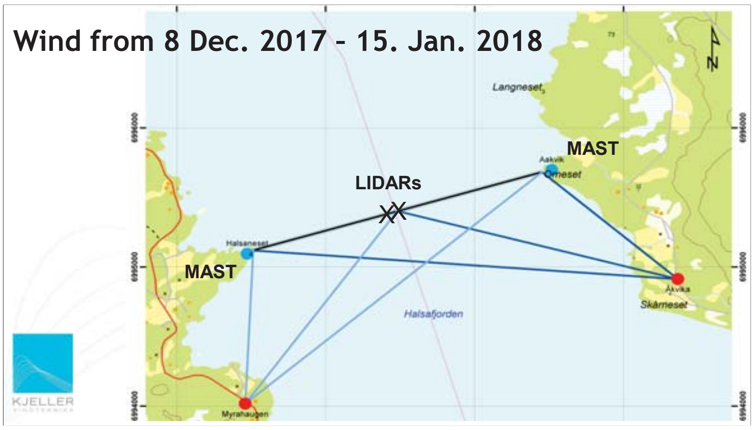

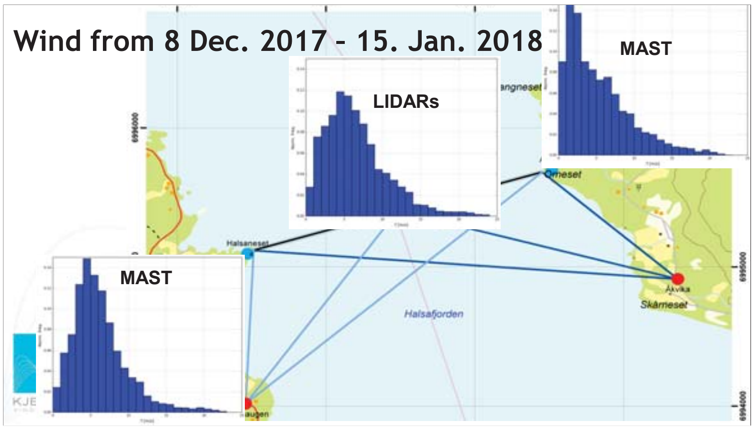

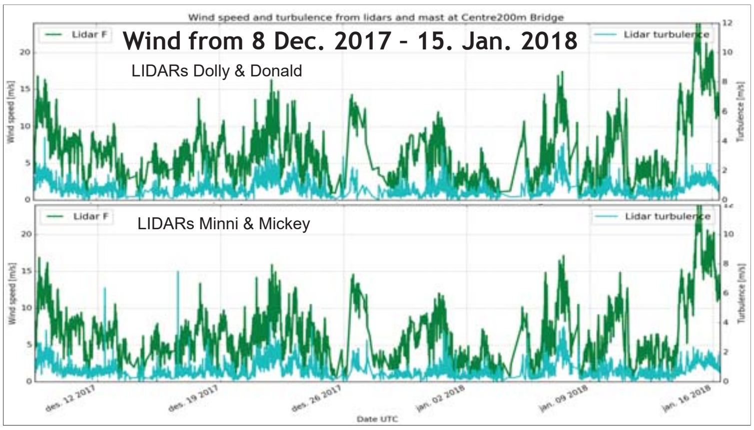

Concluding remarks

- First results and examples from from four LIDARs observing atmospheric flow in Halsafjorden since autumn 2017.
- The synchronized LIDARs are a part of the extensive observation campaign pertaining to the ferry-free E39 project.
- Detailed description of key parameters of atmospheric flow away from the shore, here surrounded by complex orography

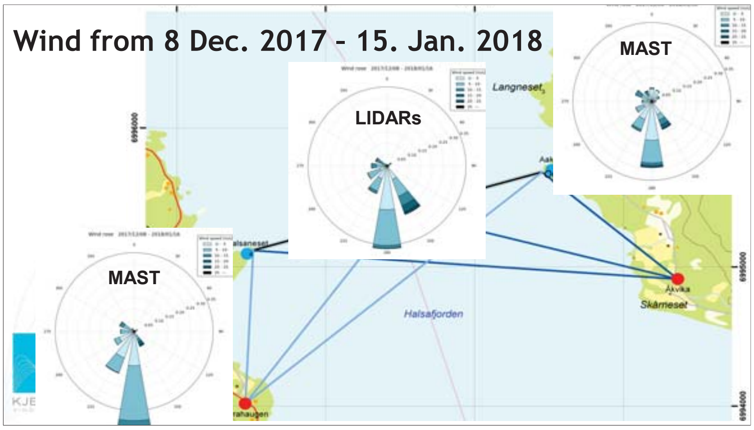

Acknowledgments

Important contributions and expert advice from:

- Michael Courtney and Guillaume Lea from the Danish Technical University
- Jasna Bogunovic Jakobsen and Etienne Francois Cyprien Cheynet from the University in Stavanger

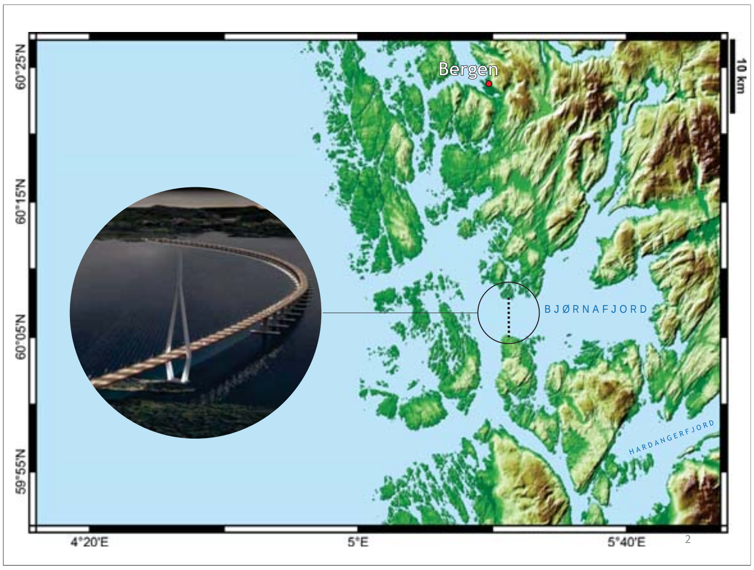

2

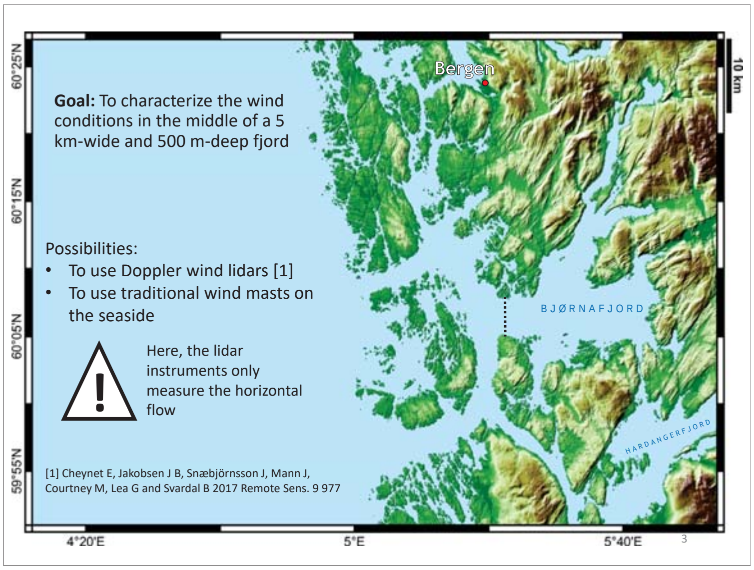

3

Main questions

Are the lidar records and anemometer measurements consistent ?

To what extent are the wind velocity data on the shores of the fjord affected by the surrounding terrain ?

4

Location of the Sensors (1/2)

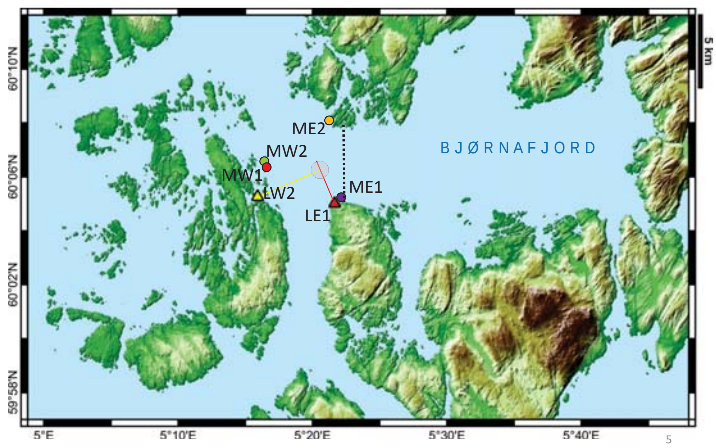

5

Location of the Sensors (2/2)

Each contour line corresponds to a height of 5 m

MW1 and MW2: One sonic anemometers at 33 m, and two at 49 m above the ground.

ME1 and ME2: Sonic anemometers at 12 m, 32 m and 48 m above the ground.

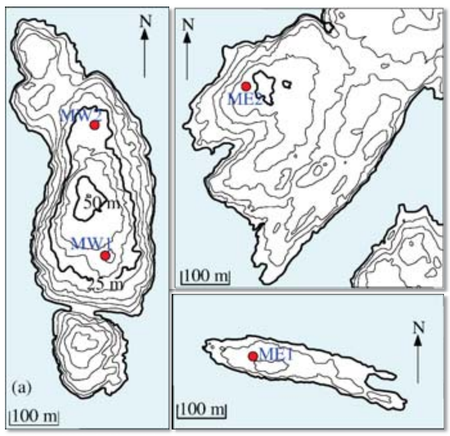

Overall wind conditions (1/2)

Record period: Mai-June 2016

Lidar records
(z = 25 m above sea level)

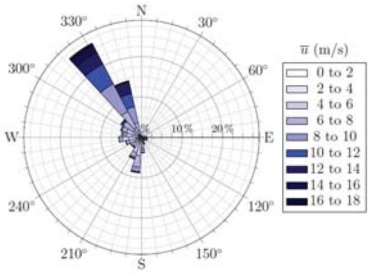

Anemometer records on MW1
(z = 33 m above ground)

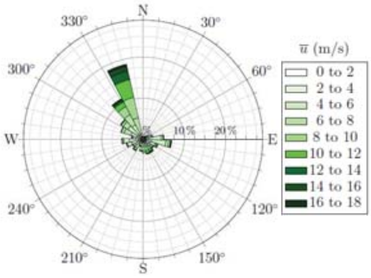

Mast MW1 vs Lidar records (2/3)

Relative difference on the mean wind direction

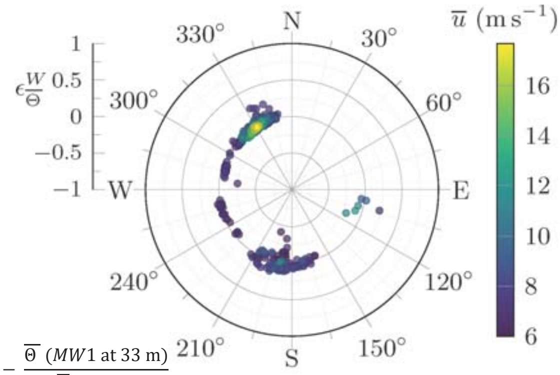

$$\epsilon^W_\Theta = 1 - \frac{\overline{\Theta}\ (MW1 \text{ at } 33 \text{ m})}{\overline{\Theta}\ (Lidar)}$$

Overall wind conditions (2/2)

Record period: Mai-June 2016

Lidar records
(z = 25 m above sea level)

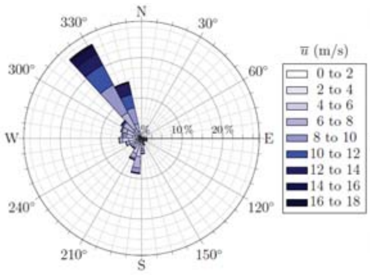

Anemometer records on ME1
(z = 32 m above ground)

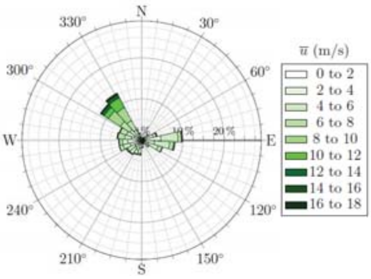

Mast MW1 vs Lidar records (3/3)

Relative difference on the standard deviation of the along-wind velocity component

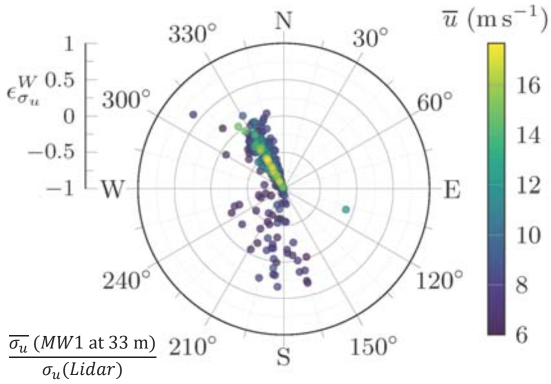

$$\epsilon^W_{\sigma_u} = 1 - \frac{\overline{\sigma_u}\ (MW1 \text{ at } 33 \text{ m})}{\sigma_u (Lidar)}$$

Mast MW1 vs Lidar records (1/3)

Relative difference on the mean wind velocity

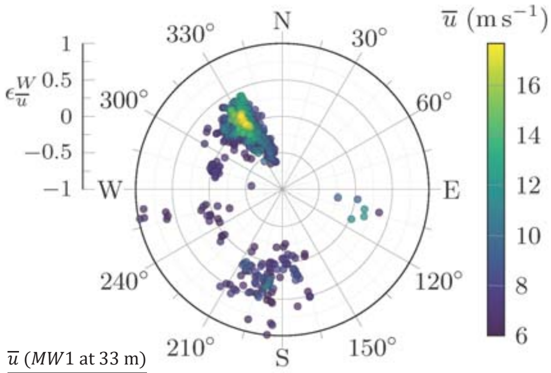

$$\epsilon^W_{\overline{u}} = 1 - \frac{\overline{u}\ (MW1 \text{ at } 33 \text{ m})}{\overline{u}\ (Lidar)}$$

Mean incidence angle

Relative difference on the mean wind velocity

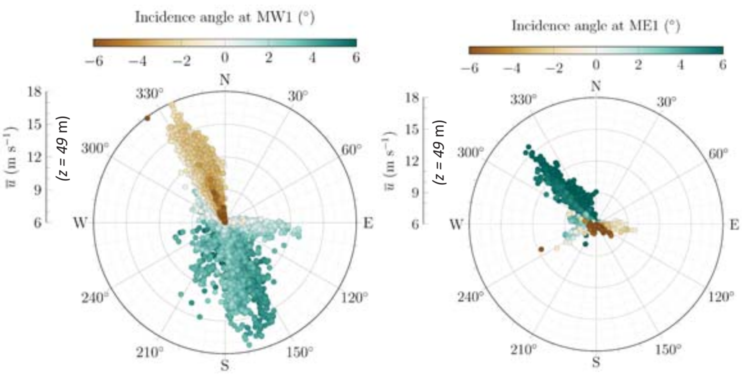

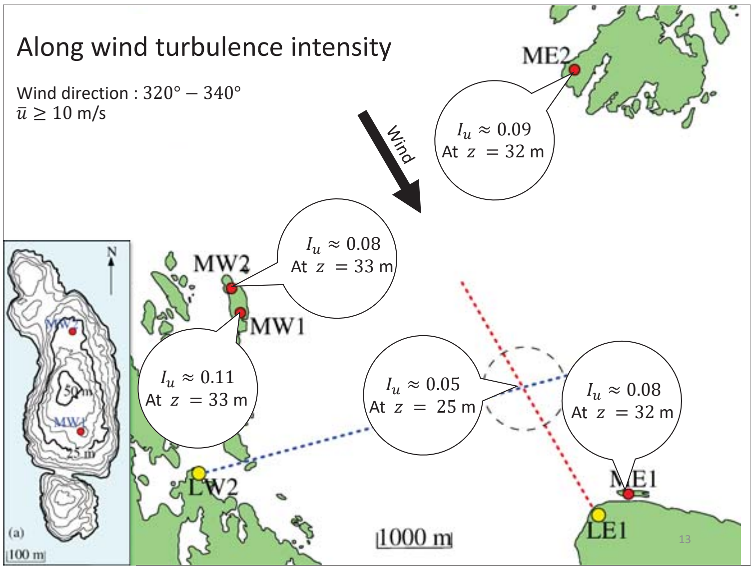

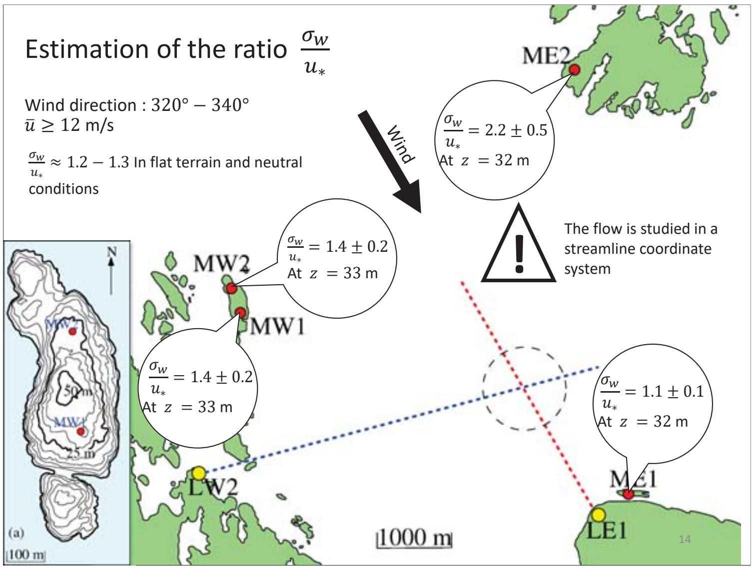

Conclusions

1. The lidar records are consistent with those from the anemometers for a limited number of sectors only.

2. There is a clear influence of the local topography on the anemometer measurements.

3. The combined use of Doppler Wind lidar with Sonic anemometer data is relevant for wind characterization in a wide fjord.

15

Simulation and observations of wave conditions in Norwegian fjords

Birgitte R. Furevik, Konstantinos Christakos (MET Norway), Øyvind Byrkjedal, Hálfdán Ágústsson, (Kjeller Vindteknikk), Lasse Lønseth, (Fugro Oceanor)

17/01/18

Meteorologisk institutt

Statens vegvesen
Norwegian Public Roads Administration

Measurements in Sulafjord - unique data set, freely available

Tall met-masts with sonic wind measurements in three heights, around 100m, 70m and 50m (red)

Wave buoys (A, B, D) and under water rigs for oceanographic measurements (blue)

Data are available on http://thredds.met.no/thredds/obs.html

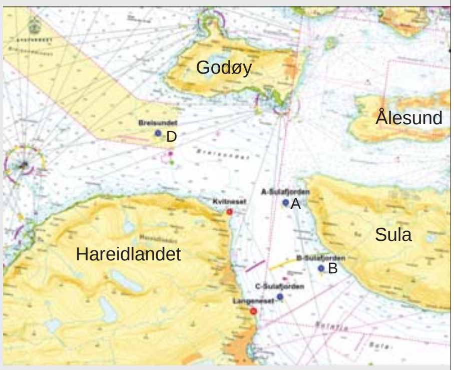

Outline

- Background and motivation
- Observations
- Operational forecast models of wind and waves
  - Setup and forcing
  - Verification
- SWAN hindcast
  - Setup for ferry-free E39
  - NORA10
  - Atmosphere model
- Results
  - Statistics
  - Case
- Summary

Forecast models at MET

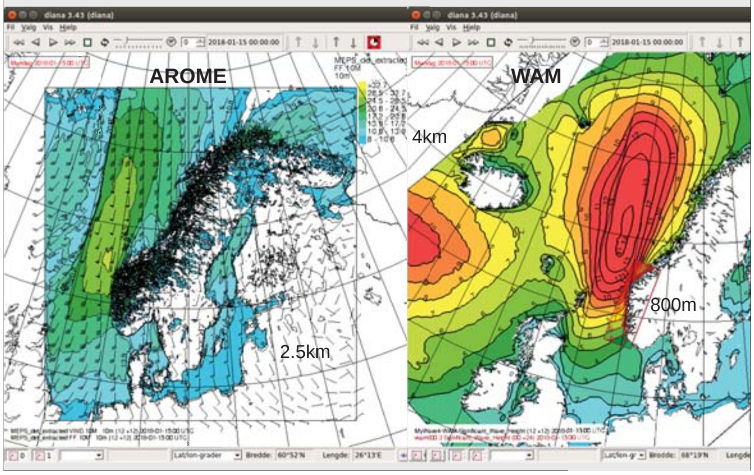

Ferry-free E39

Verification of forecasts in Sulafjord

AROME wind speed

WAM significant wave height

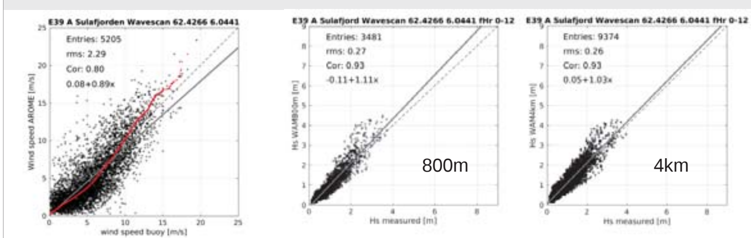

Wave hindcast using SWAN

- Version 41.10
- 3rd generation wave model
- Temporal and spatial development of 2D wave spectra in each grid point
- Variable wind input and spectra on the open borders

- 36 directions, 31 frequencies (0.04-1Hz)
- Domain with 250mx250m grid cells nested into outer grid (1kmx1km)

- Wind from *Kjeller Vindteknikk* hindcast with WRF (500mx500m)
- Border spectra from the Norwegian wind and wave hindcast (10-11km)
- January 2007 – june 2017

- Hourly output of integrated wave parameters (Hs, Tp, Tm02, Peak dir., Mdir etc.) and spectra in selected locations

Wave model setup with SWAN

- SWAN 41.10 – with van der Westhuysen (2007) dissipation
  - 1 January 2007 – 30 June 2017
  - 1km to 250m nesting
  - Wind from WRF (500m), Spectra on border from NORA10

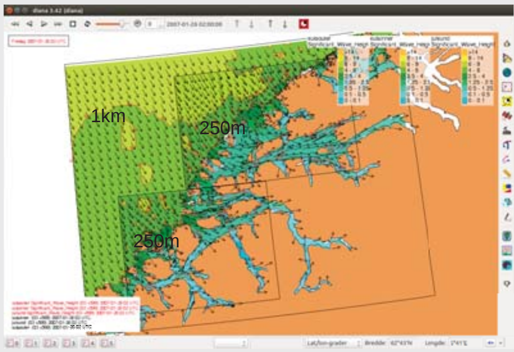

Norwegian Reanalysis 10 km (NORA10)

dynamical downscaling of ERA-40 and standalone wave hindcast

Atmospheric component – HIRLAM 10 km:
- ERA-40 on boundaries (6-hourly)
  - 40 levels: temp, wind, humidity, cloud water
  - Surface: pressure
- Blended with ERA-40 in interior (digital filter)
  - Maintain large-scale features
  - Preserve mesoscale features (polar lows)
- Sequence of 9-hour model runs (3 hourly data)
- 248 x 400 grid points

Wave component – nested WAM-model
- WAM 50 km forced by ERA-40 winds
- WAM 10 km forced by HIRLAM10 winds
  - 2D spectrum: 24 by 25 directional/frequency bins
- September 1957 onwards

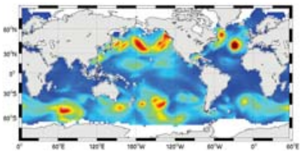

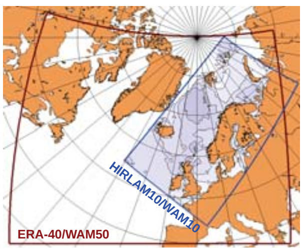

WAM and SWAN wave height

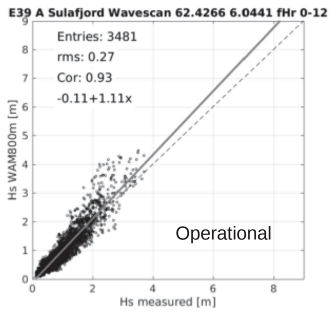

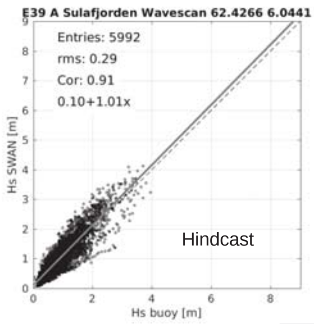

Similar performance
Slight overestimation in Hs

Wind input to SWAN

- WRF nested 1500m to 500m

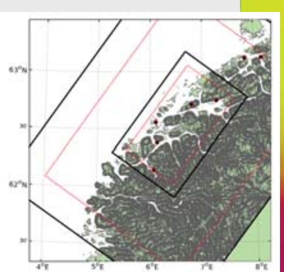

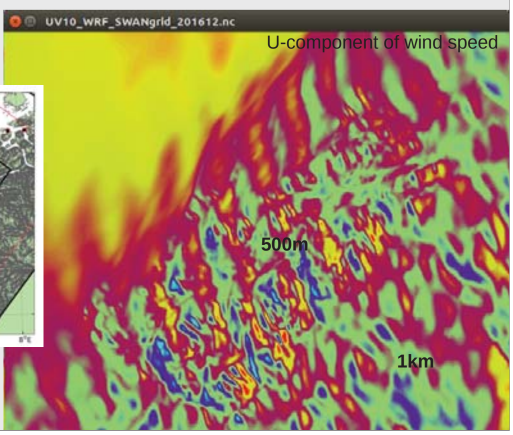

SWAN wave height – statistics

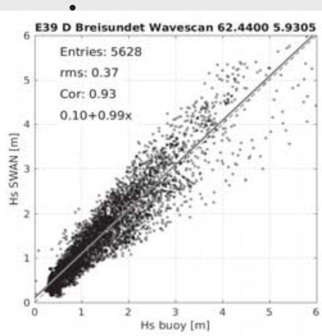

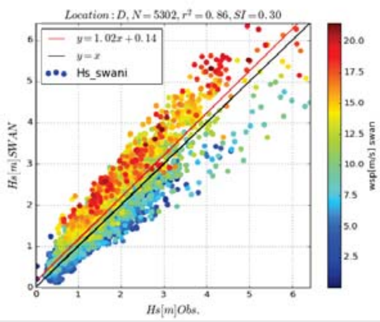

Relation between overestimation in Hs and high wind speeds

AROME and WRF wind speeds

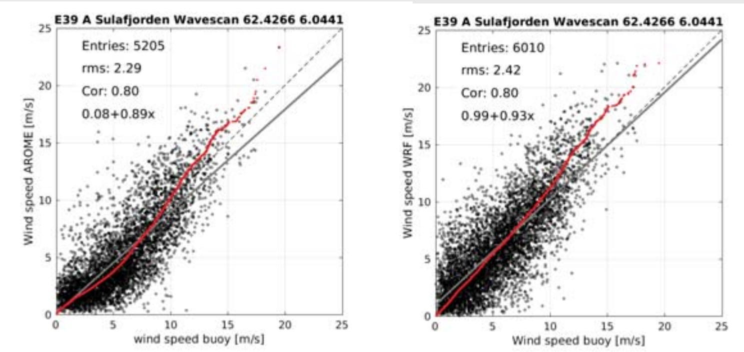

Too weak winds in AROME at low wind speeds

Wave statistics in Sulafjord

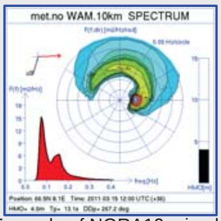

Example of NORA10 mixed sea spectrum

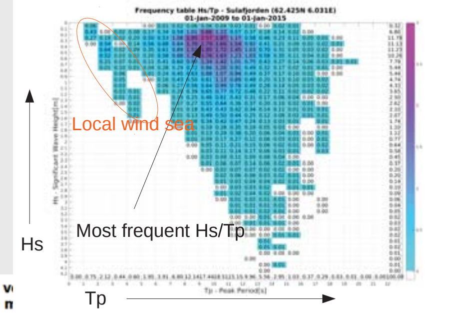

Tabell 7-3 Beregnet 100 års v
Sulafjorden Nord, Sulafjorden m
skravert.

Sector	360	30	60	90	120	150	180	210	240	270	300	330	All
Hs Sulafj_Nord	1.0	1.0	0.5	0.3	1.0	1.9	2.2	2.2	2.5	2.8	5.2	1.7	5.2
Hs Sulafj_midt	1.2	1.2	1.1	1.4	1.6	2.0	1.9	1.7	1.6	1.7	3.1	2.9	3.2
Hs Vartdalsfjorden	0.4	1.0	0.9	0.4	0.4	0.9	1.6	1.9	0.7	0.3	0.3	0.2	1.9

Example of uncertainty due to parameter-based wave spectra

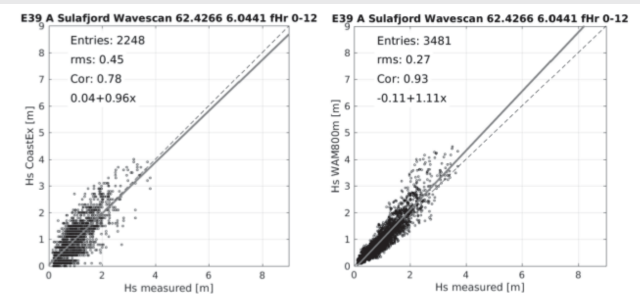

JONSWAP spectrum based on Hs/Tp
Forecasts from barentswatch.no

Wave model with 2D wave spectra
Forecasts from MET

Wave spectra

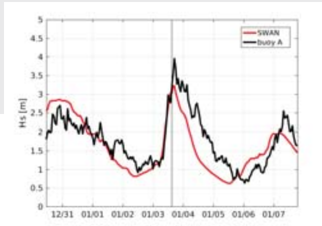

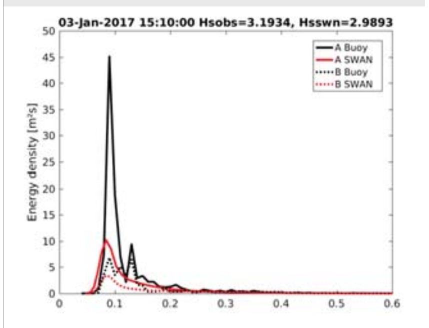

Model may be right for the wrong reason

Marine radar image 2017.01.03 15:14

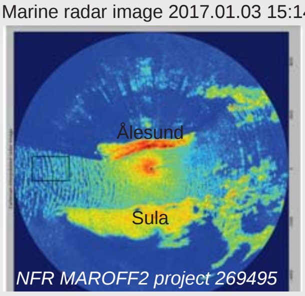

AROME compared to satellite SAR

Weak winds and low correlation in fjords

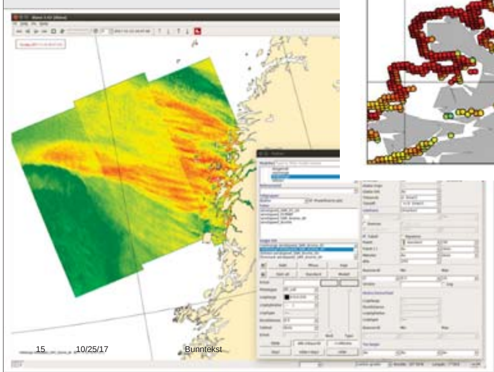

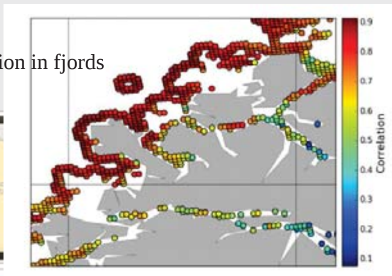

Final report from project FjordVind funded by the Norwegian Space Center

Summary and comments

- Large measurement program in several fjords in mid-Norway
- Data freely available, but access is temporarily closed at the moment (until May)

- Working to improve wave and wind modelling in the fjords
- Three PhD students started last year
  - Poster on wind shear by Midjiyawa Zakari outside

D1) Operations & maintenance

Wind Turbine Gearbox Planet Bearing Failure Prediction Using Vibration Data, S. Koukoura, University of Strathclyde

Data Insights from an Offshore Wind Turbine Gearbox Replacement, A.K. Papatzimos, University of Edinburgh

Further investigation of the relationship between main-bearing loads and wind field characteristics, A. Turnbull, University of Strathclyde

Damage Localization using Model Updating on a Wind Turbine Blade, K. Schröder, University of Hannover

Wind turbine gearbox planet bearing failure prediction using vibration data

Sofia Koukoura, James Carroll & Alasdair McDonald

Department of Electronic & Electrical Engineering
University of Strathclyde, Glasgow
sofia.koukoura@strath.ac.uk

EERA DeepWind'18, Trondheim, 17 - 19 January 2018

Paper Objective

Create an automated failure prediction framework for wind turbine gearbox bearing faults. This framework is based on two stages:

Vibration Analysis and Feature Extraction

Find trends at varying times prior to component failure.

Extract features based on those trends.

Classification

Use features as inputs to a pattern recognition model.

Learn the behaviour characteristics of the trends for prognosis of degradation and failure prediction.

Motivation

- Wind turbines are machines that operate under harsh conditions and therefore component failures happen before the end of the expected life of the turbine.
- Catastrophic failures increase O&M costs and consequently the LCOE.
- Predictive maintenance is applied in wind turbine industry so that O&M actions are optimised accordingly.

Figure: Wind Turbine on fire.[1]

[1] Source

Bearing Vibration Theory

- Bearing faults introduce a shock that excites high frequency resonances.
- Bearing signatures:
  - masked by other components in the gearbox.
  - stochastic.
- Planetary stage hard to diagnose.
- Ball passing frequency (repetition frequency) depends on:
  - speed (f).
  - dimensions.

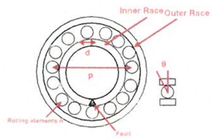

Figure: Bearing with an inner race fault and its significant dimensions.

$$\text{BPFI} = f\frac{n}{2}\left(1 + \frac{d}{p}\cos(\theta)\right)$$

Average Repair Time and Costs in Offshore Wind

Average repair times and costs for major replacements are given per failure category [2].

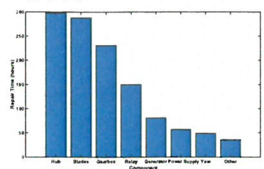

Figure: Average repair time.

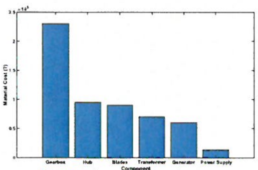

Figure: Average repair cost.

- The top three average repair times occur in the hub, blades and gearbox.
- The gearbox has the highest average cost per failure.
- From the CM perspective, a wind turbine gearbox consists of three major components: **bearings**, gears and lubricant.

Vibration Signal Pre-processing

- Deterministics (gear) and random (bearing) components need to be separated. This can be done using an adaptive filter.
- Envelope analysis -often used in bearing diagnostics- demodulates the signal in a high frequency band.
- In order to choose the right band, spectral kurtosis indicates how kurtosis is distributed in the frequency domain and shows the impulsiveness of the signal. Thus it can be used as a filter [3].

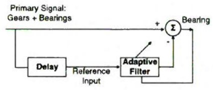

Figure: Adaptive filter.

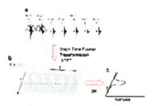

Figure: Spectral Kurtosis [3].

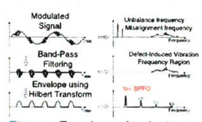

Figure: Envelope Analysis.

Classification: k Nearest Neighbours

kNN

- kNN classifier classifies unlabelled observations by assigning them to the class of the most similar labelled examples [1].
- Non parametric and instance based.
- k tuning using cross validation.
- Features used as input in a bearing fault case could be energy around ball passing frequency and its harmonics.

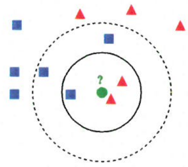

Figure: Example of kNN classification.

Signal Processed Vibration Data Analysis Results

Envelope spectra of vibration signal for similar loading conditions. Only 3s of each signal are used and where they are assumed to be stationary.

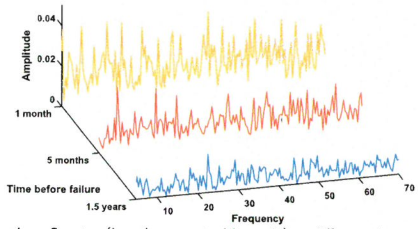

Figure: Envelope Spectra (based on spectral kurtosis) at different times prior to failure.

Wind Turbine Considered in This Study

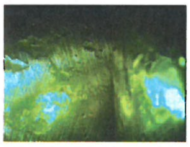

Figure: Faulty bearing.

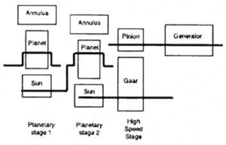

Figure: Gearbox internal structure.

- Wind turbine rated between 2.5-3.5MW.
- Double planetary stage gearbox, commonly found offshore.
- Inner race spalling.
- 95 samples collected at various times prior to failure (2.5 years to 1 week before).
- Acceleration data collected on a sampling rate between 20-30kHz for 10-15s. [2]

[2] Ranges are given for confidentiality reasons

Classification Results

	Predicted Class		
Actual Class	1-2 months	5-6 months	healthy
1-2 months	**75%**	18%	7%
5-6 months	21%	**69%**	9%
healthy	6%	12%	**79%**

Table: 3 Class Classification Results

	Predicted Class	
Actual Class	5-6 months	healthy
5-6 months	**89%**	11%
healthy	17%	**83%**

Table: 2 Class Classification Results

- Classes are assigned based on the acquisition time of the signal with respect to failure.
- 5-fold cross validation used

Raw Vibration Data Analysis Results

RMS of the data as a function of load at different times before the component failure.

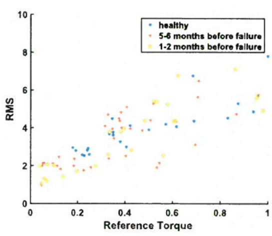

Figure: RMS of raw vibration signals.

Conclusion and Future Work

Conclusion

Low speed stage bearing faults may not be diagnosed through raw vibration data.

Signal processing can help enhance the bearing fault impulses.

Given sufficient samples, features can be extracted from vibration data and given as inputs to machine learning classification models.

Classification models are able to classify signals based on their health state, useful for diagnosis and prognosis.

Conclusion and Future Work

Future work

Other types of classification methods, e.g. neural networks could increase accuracy.

Order tracking techniques can improve the filter and the overall accuracy results.

More historic data samples will train more robust models.

References I

- Christopher M Bishop.
  Pattern recognition and machine learning (information science and statistics) springer-verlag new york.
  Inc. Secaucus, NJ, USA, 2006.
- James Carroll, Alasdair McDonald, and David McMillan.
  Failure rate, repair time and unscheduled o&m cost analysis of offshore wind turbines.
  Wind Energy, 2015.
- Robert B Randall and Jerome Antoni.
  Rolling element bearing diagnosticsa tutorial.
  Mechanical systems and signal processing, 25(2):485–520, 2011.

January 18, 2018

EERA DeepWind 2018
15th Deep Sea Offshore Wind R&D Conference
Trondheim, Norway

Data Insights from an Offshore Wind Turbine Gearbox Replacement

Alexios Koltsidopoulos Papatzimos[1,2]
Tariq Dawood[2]
Philipp R. Thies[3]

[1]*Industrial Doctorate Centre for Offshore Renewable Energy (IDCORE), Edinburgh, EH9 3JL*
[2]*EDF Energy R&D UK Centre, London, CR0 2AJ*
[3]*University of Exeter, Cornwall, TR10 9FE*

Contents

1. Introduction and Motivation
2. Wind Turbine Gearbox Failures
3. Wind Turbine Gearbox Monitoring
4. Data Pre-processing
5. Failure Detection & Diagnosis
6. Data-Driven Models
7. Conclusions & Future Work

1. Introduction and Motivation

Introduction- EDF Group Offshore Assets

- Teesside Offshore Wind Farm
  - 27 2.3MW turbines
  - 1.5 km offshore
  - 7-15m water depth
  - Installation completed in June 2013
- Blyth Demonstrator Project
  - 5 Vestas 8.3MW turbines
- Future assets
  - Totalling 1.5GW

Motivation

- Gearbox replacement @ Teesside
- Gearboxes are designed to last for the lifetime of the asset- IEC 61400-4
- Majority of onshore and offshore wind turbines have a geared drivetrain
- Currently largest installed wind turbine (V164-8.0 MW) has a gearbox
- Early detection by OEM
  - Reduce downtime
  - Reduce component lead time
  - Understand component reliability
- Perform future fault prediction and diagnosis

2. Wind Turbine Gearbox Failures

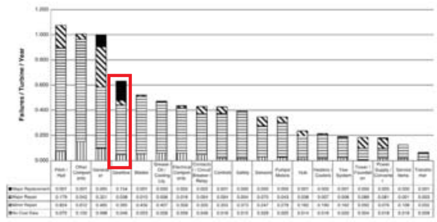

[1]

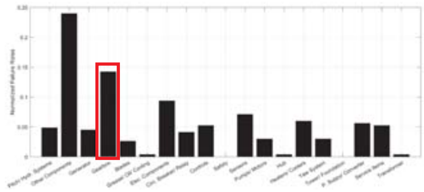

[2]

2. Wind Turbine Gearbox Failures

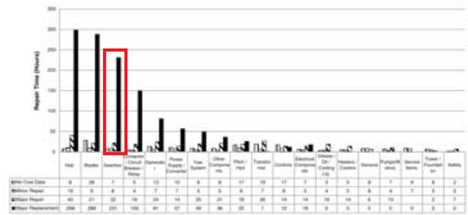

[1]

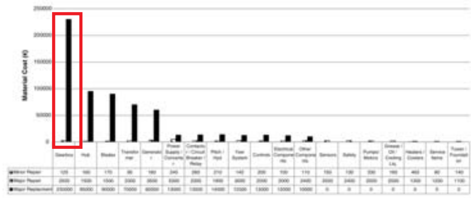

[1]

2. Wind Turbine Gearbox Failures

Most common failure causes [3, 4]:
- Fundamental gearbox design errors
- Manufacturing or quality issues
- Underestimation of operational loads
- Variable and turbulent wind conditions
- Insufficient maintenance

Most common failure locations [4-8]:
- HS Bearing
- IMS bearing
- Planet bearing

Most common failure modes:

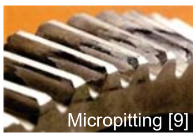

Micropitting [9]

Tooth breakage [10]

Pitting [11]

Spalling [12]

Scuffing [11]

2. Wind Turbine Gearbox Failures

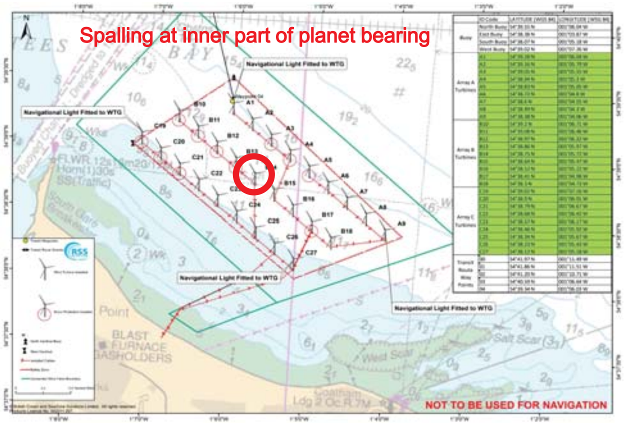

3. Wind Turbine Gearbox Monitoring

- SCADA
  - Temperature, pressure, vibration, current, rotational speed, etc.
    - Timeseries
- CMS
  - Vibration
    - Sampling in time instances
    - Pre-processed (Envelopes, FFTs, Cepstrum, RMS, etc)
  - Oil Particle Counter

3 stage planetary/ helical gearbox

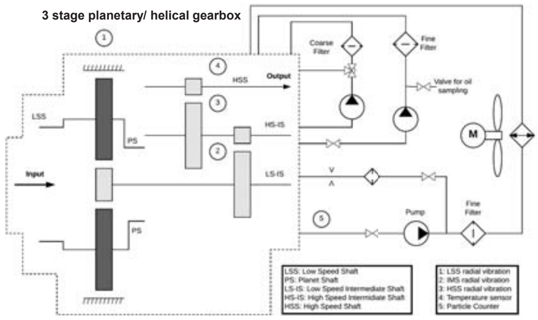

4. Data Pre-processing

Filtering

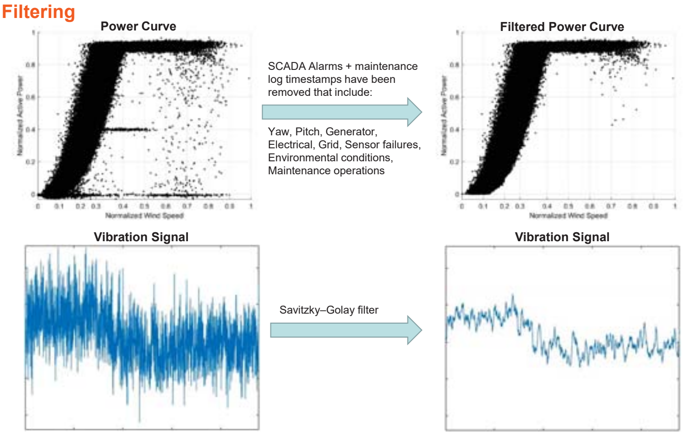

4. Data Pre-processing

Filtering

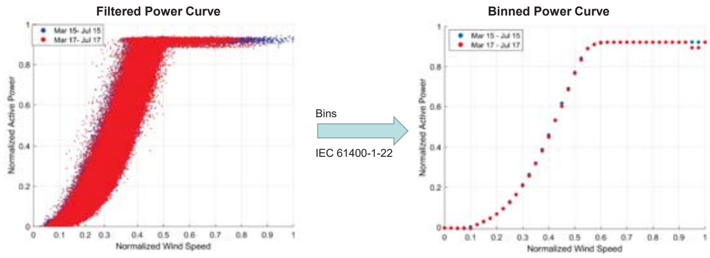

5. Failure Detection & Diagnosis

SCADA

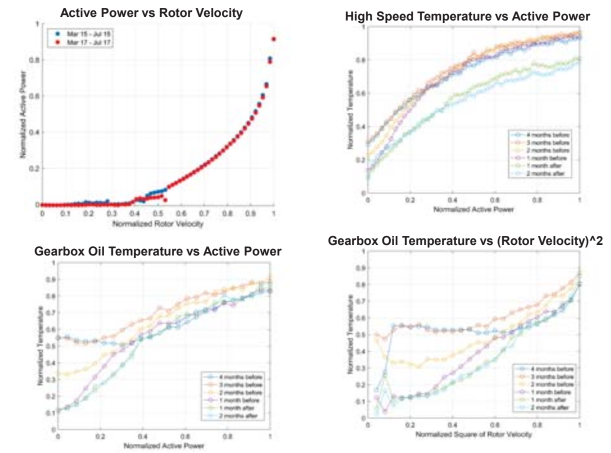

5. Failure Detection & Diagnosis

SCADA

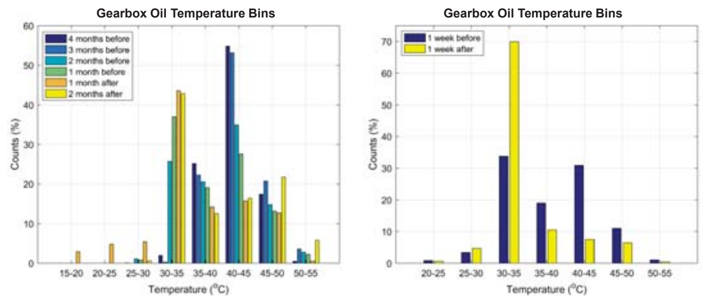

5. Failure Detection & Diagnosis

CMS

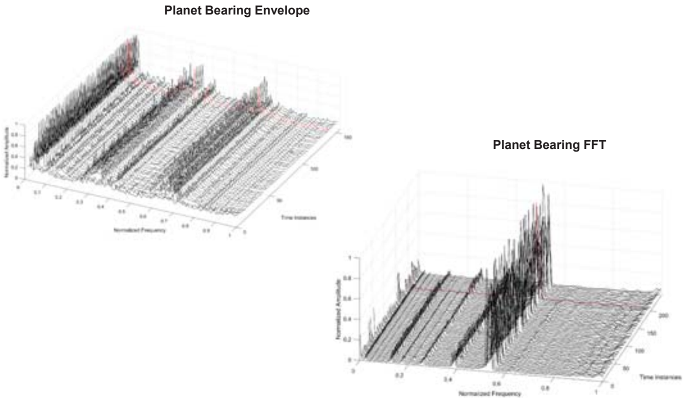

5. Failure Detection & Diagnosis

CMS

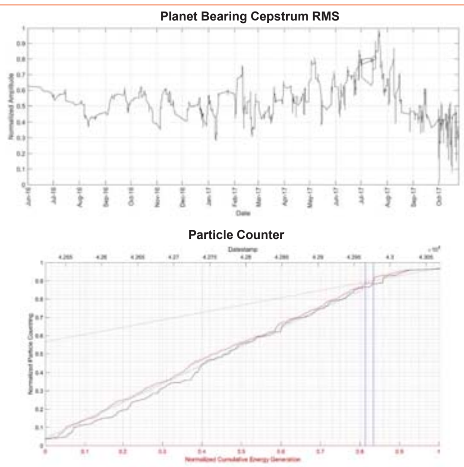

5. Failure Detection & Diagnosis

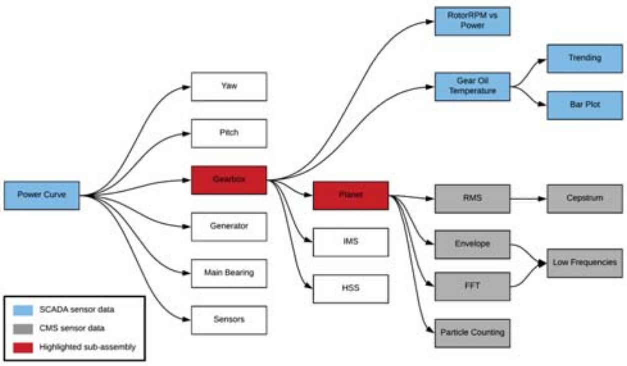

6. Data-Driven Models

SCADA

- "Healthy" state for data 4 months after replacement (orange)
- "Warning" state for data 4 months prior to replacement (blue)

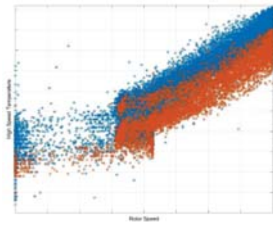

Algorithm	Specifications	True Pos. (Healthy)	True Positive Rate (Warning)
SVM	Gaussian, Scale:0.26	97%	92%
Ensemble	Bagged Trees, Split: 10, learners: 30	96%	91%
KNN	Mahalanobis, NN=10	96%	92%
Decision Tree	Gini's index, max number of splits: 400	95%	86%
SVM	Quadratic, box constraint: 1	93%	81%

6. Data-Driven Models

CMS

- Not constantly monitored systems
- Automation of forecasting models
- Autoregressive model for RMS signal
    - Predicted same slope for 26 out of 27 turbines

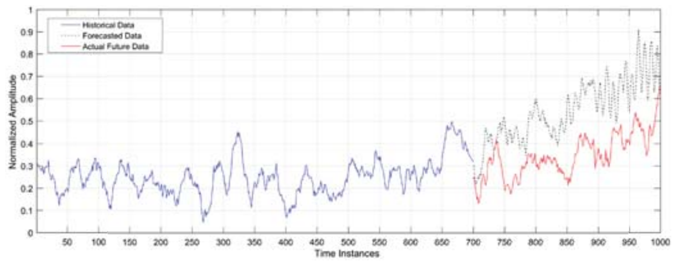

7. Conclusions and Future Work

Conclusions

- Planet stage bearing spalling on a 3-stage 2.3MW turbine gearbox
- Similar studies investigated catastrophic gearbox failures
- Identify and diagnose the failure by using SCADA and CMS data
    - Temperature readings
    - RMS vibration
- Data driven models to predict future failures

Future Work

- Further test the models in other failure modes and wind turbine models
- Investigate the environmental conditions' impact on the results

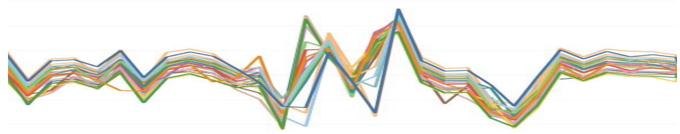

References

[1] Carroll J, McDonald A and McMillan D 2016 Failure rate, repair time and unscheduled O&M cost analysis of offshore wind turbines *Wind Energy* **19** 6 1107-19

[2] Koltsidopoulos Papatzimos A, Dawood T and Thies PR 2017 An integrated data management approach for offshore wind turbine failure root cause analysis *Proc. 36th Int. Conf. on Ocean, Offshore and Arctic Engineering* (Trondheim) vol. 3B (New York: ASME)

[3] Qiu Y, Chen L, Feng Y and Xu Y 2017 An Approach of Quantifying Gear Fatigue Life for Wind Turbine Gearboxes Using Supervisory Control and Data Acquisition Data *Energies* **10** 1084

[4] Musial W, Butterfield S, McNiff B 2007 Improving Wind Turbine Gearbox Reliability *European Wind Energy Conference*

[5] Nejad AR, Gao Z, Moan T 2014 Fatigue Reliability-Based Inspection and Maintenance Planning of Gearbox Components in Wind Turbine Drivetrains *Energy Procedia* **53** 248-57

[6] Nejad AR, Gao Z and Moan T 2015 Development of a 5MW reference gearbox for offshore wind turbines *Wind Energy* **19** 6 1089–1106

[7] McVittie D 2006 *Wind turbine gearbox reliability* Online: https://goo.gl/gqLSv8

[8] Smolders K, Long H, Feng Y and Tavner PJ 2010 Reliability Analysis and Prediction of Wind Turbine Gearboxes *Proc. European Wind Energy Conference* (Warsaw: EWEA)

[9] https://www.gearboxfailure.com/wp-content/uploads/2016/07/MicropittingOn_Misaligned_Gear.jpg

[10] http://media.noria.com/sites/archive_images/Backup_200101_Gear3.jpg?__hstc=108323549.07430159d50a3c91e72c280a7921bf0d.1514764800116.1514764800117.1514764800118.1&__hssc=108323549.1.1514764800119&__hsfp=528229161

[11] https://www.novexa.com/en/intervention/gears/defects-treated.html

[12] http://www.rttech.com.au/wp-content/uploads/2010/06/mt6.jpg

Questions

Alexios.Koltsidopoulos@edfenergy.com

Acknowledgement:
This work is funded by the Energy Technology Institute and the Research Council Energy Programme as part of the IDCORE programme (grant EP/J500847).

Further investigation of the relationship between main-bearing loads and wind field characteristics

A Turnbull[1], E Hart[1], D McMillan[1], J Feuchtwang[1], E Golysheva[2] and R Elliott[2]

[1]University of Strathclyde, Glasgow, UK
[2]Romax InSight, Nottingham, UK

Motivation

- Main-bearings seldom reach design life of roughly 20 years.
- Some failing after as little as 6 years [1].
- Reasons for this are still not fully understood.
- Cost associated with the repair is expensive.
- As we move further offshore, these effects are amplified due to cost of support vessels, weather and access restrictions.

Research aims

1. Create a simple model which focuses on realistic input loads from which cause and effect can be easily separated.
2. Understand loading across wind turbine operating envelope and link this to wind field conditions.
3. Provide evidence to support claims that axial to radial load ratio is a key factor in main bearing failure.

Aeroelastic model

- GH Bladed software used for aeroelastic wind turbine simulations.
- Wind field characteristics
  - 4 wind speeds (10, 12, 16, 20m/s)
  - 2 shear profiles (shear exponent 0.2, 0.6)
  - 3 turbulence intensities (high, med, low as described in IEC standards [2])
- 144 different wind fields to define operating envelope.
- Hub forces and bending moments extracted in all three degrees of freedom.

Drivetrain model

- Drivetrain models generated for both double and single main bearing configuration.
- Separate model for radial and axial loads.
- Lengths and spring stiffness's determined by ROMAX Insight FEA modelling software for commercially available wind turbine of rated power around 2MW.
- Bearing type dependent on the configuration.

Drivetrain model

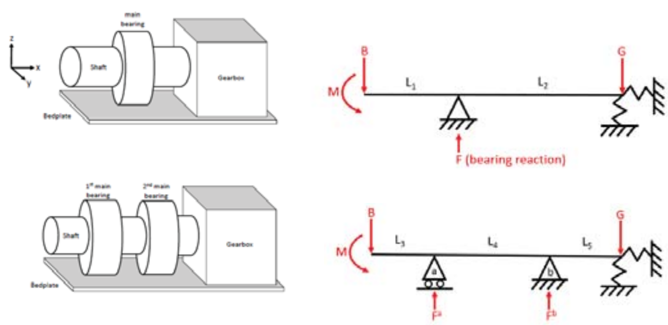

Results – Peak axial loads

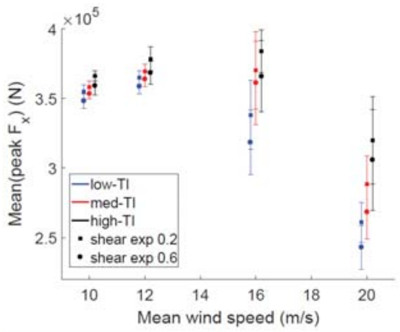

Results – Peak radial loads

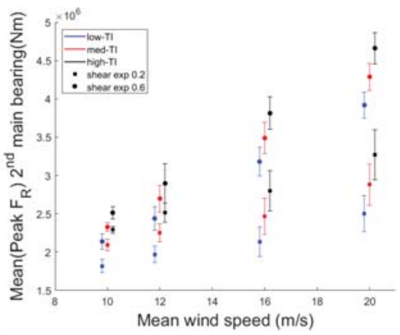

Results – Load ratio

Medium turbulence intensity and high shear

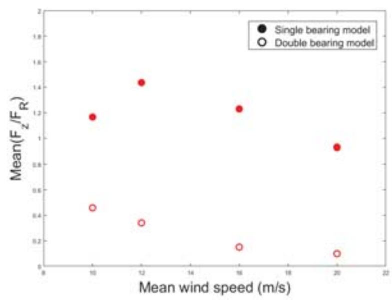

Results – Load ratio

Effects of shear profile

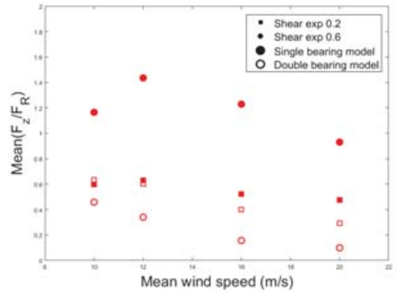

Results – Load ratio

Effects of turbulence intensity

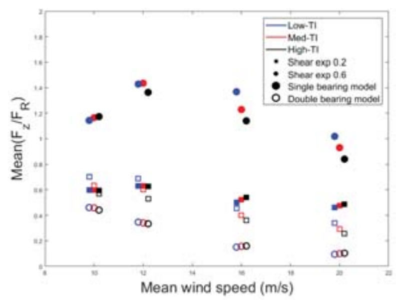

Conclusions

- Strong link between wind conditions and main bearing loads for both configuration – wind shear highest sensitivity factor.
- In general it can be observed that the double bearing configuration experiences a significant decrease in load ratio.
- Highest load ratio occurs in the single main bearing configuration in high shear and low turbulent conditions.
- With single main bearing configuration observed to fail more often, evidence suggests there could be link with load ratio.

Potential impact of research

- Develop ways in which to bring the relationship into design stage when calculating component life, steering away from traditional methods of steady cyclic loading.
- Use relationship as a factor to support decision making of wind turbine type/configuration at particular site.

Thank you for your attention, any questions?

K. Schröder, S. Grove, S. Tsiapoki, C.G. Gebhardt and R. Rolfes

Structural Change Identification at a Wind Turbine Blade using Model Updating

EERA DeepWind'18, 18.01.18

Content

I. Motivation

II. Optimization based model updating

III. Rotor blade test

IV. Model updating at the rotor blade
   1. Damage localization
   2. Ice accretion

V. Conclusion and Outlook

Motivation

- Remote location
- Rotor blades: costly and time-consuming repair
- Ice accretion: - Risk of ice throw
  - Undesired loads

⇨ Localization and quantification of structural changes using model updating

Finite Element Model Updating

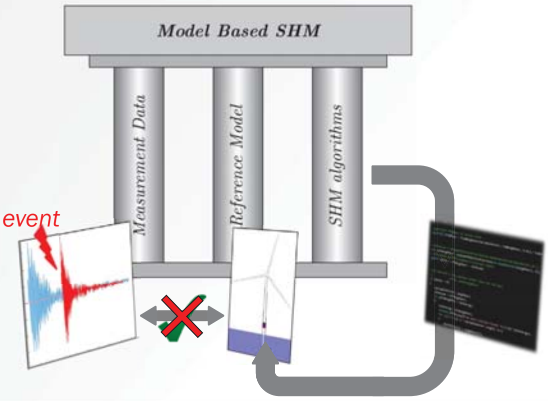

Deviation between numerical model and measured data

⇨ Quantification of the „difference" between model and measurement

Modal parameters

- Eigenvalues
- Mode shapes

$$\varrho(\theta) = \left\|\frac{\omega_m - \omega_s(\theta)}{\omega_m}\right\|_2 + \sum_{i\in\mathcal{Y}} \|\phi_m^i - \phi_s^i(\theta)\|_2$$

Transmissibility functions

$$\varrho(\theta) = \sum_{i=1}^{n} \frac{\|TF^m_{xy,i} - TF^s_{xy,i}(\theta)\|_2}{\|TF^m_{xy,i}\|_2}$$

Minimization of the deviation

$$\min_{\theta}\ \varrho(\theta)$$
$$\text{subject to } c_i(\theta) \geq 0\ \forall\, i \in \mathcal{I}$$

- Nonlinear
- Constrained
- Nonconvex
- Several local minima

Global optimization algorithm:
⇨ Simulated Quenching

Local optimization algorithm:
⇨ Sequential Quadratic Programming

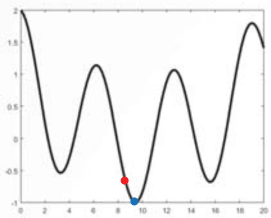

Rotor blade test

- Hammer excitation
- 12 measurement channels

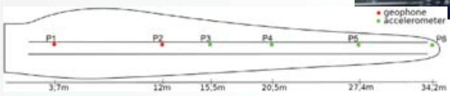

Rotor blade test

- Hammer excitation
- 12 measurement channels
- Ice mass
- Damage

Trailing edge bondline: Spot of damage initiation

Trailing edge – Pressure Side (outside)

Numerical Modeling

- Rectangular Cross Section
- Known: EI and mass
- 26 Timoshenko beam elements
- Clamping at blade root
- Material damping

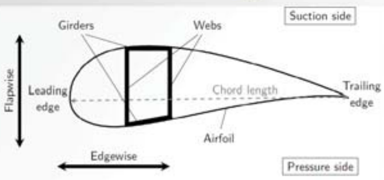

	ω_m in Hz	ω_s in Hz	$\pm$ in %	Dir.	MAC
1.	1.069	1.048	2.0	flap	0.99957
2.	1.679	1.726	2.7	edge	0.99747
3.	3.113	3.128	0.5	flap	0.99731
4.	5.643	5.390	4.5	edge	0.99727
5.	6.644	6.811	2.5	flap	0.99847
6.	11.536	11.999	3.9	flap	0.99712
7.	13.140	12.383	5.8	edge	0.99118
$\mathcal{M}$			4.58		0.99682

Numerical validation

Stiffness reduction

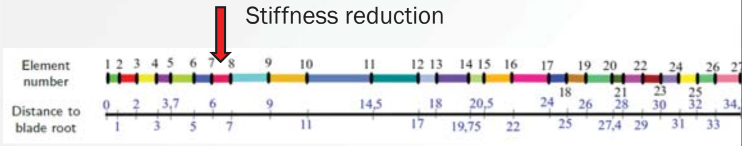

$$\min_{\theta} \varrho(\boldsymbol{\theta})$$

$$\text{subject to} \quad \theta_i \geqslant 0,5 \; \forall \; i \in \boldsymbol{\theta}$$

$$\theta_i \leqslant 1,01 \; \forall \; i \in \boldsymbol{\theta}$$

$$\sum_i (1 - \theta_i) \leqslant 0,5$$

Numerical validation– Modal Parameters

Parameter number

	$\varrho(\boldsymbol{\theta})$	1	2	3	4	5	6	7	8	9	10	11	12	13
1	$3,975 \cdot 10^{-06}$	1,00	1,00	1,00	1,00	1,00	1,00	1,00	1,000	0,999	1,000	1,00	1,00	1,00
2	$5,032 \cdot 10^{-08}$	1,00	1,00	0,992	0,985	1,001	1,00	1,00	1,00	1,00	1,00	1,00	1,00	1,00
3	$3,494 \cdot 10^{-06}$	1,00	1,00	1,00	1,00	1,00	[illegible]	[illegible]	[illegible]	[illegible]	[illegible]	[illegible]	[illegible]	[illegible]
4	$4,007 \cdot 10^{-06}$	1,00	1,00	1,00	1,00	1,00	[illegible]	[illegible]	[illegible]	[illegible]	[illegible]	[illegible]	[illegible]	[illegible]
5	$1,510 \cdot 10^{-08}$	1,00	1,00	1,00	0,978	1,001	[illegible]	[illegible]	[illegible]	[illegible]	[illegible]	[illegible]	[illegible]	[illegible]
6	$5,032 \cdot 10^{-08}$	1,00	1,00	0,992	0,985	1,001	[illegible]	[illegible]	[illegible]	[illegible]	[illegible]	[illegible]	[illegible]	[illegible]
7	$3,272 \cdot 10^{-06}$	1,00	1,00	1,00	1,00	1,00	[illegible]	[illegible]	[illegible]	[illegible]	[illegible]	[illegible]	[illegible]	[illegible]
8	$1,496 \cdot 10^{-08}$	1,00	1,00	1,00	0,978	1,001	[illegible]	[illegible]	[illegible]	[illegible]	[illegible]	[illegible]	[illegible]	[illegible]

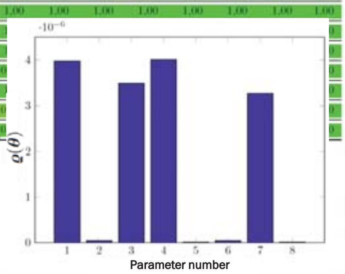

Numerical validation – Transmissibility Functions

Parameter number

	$\varrho(\boldsymbol{\theta})$	1	2	3	4	5	6	7	8	9	10	11	12	13
1	0,0537	1,00	1,00	0,996	0,982	1,001	1,00	1,00	1,00	1,00	1,00	1,00	1,00	1,00
2	0,0869	1,00	1,004	0,994	0,982	1,00	1,00	1,00	1,00	1,00	1,00	1,00	1,00	1,00
3	2,3264	1,00	1,00	1,00	1,00	1,010	1,010	0,952	1,00	1,00	1,00	1,00	1,00	1,00
4	0,4932	1,010	0,983	1,00	1,00	[illegible]	[illegible]	[illegible]	[illegible]	[illegible]	[illegible]	[illegible]	[illegible]	[illegible]
5	0,0540	1,00	1,00	0,996	0,982	[illegible]	[illegible]	[illegible]	[illegible]	[illegible]	[illegible]	[illegible]	[illegible]	[illegible]
6	0,0538	1,00	1,00	0,996	0,982	[illegible]	[illegible]	[illegible]	[illegible]	[illegible]	[illegible]	[illegible]	[illegible]	[illegible]
7	0,5321	1,00	1,00	1,00	1,00	[illegible]	[illegible]	[illegible]	[illegible]	[illegible]	[illegible]	[illegible]	[illegible]	[illegible]
8	2,2413	1,00	1,00	1,00	1,00	[illegible]	[illegible]	[illegible]	[illegible]	[illegible]	[illegible]	[illegible]	[illegible]	[illegible]
9	0,2233	1,00	1,010	0,987	0,978	[illegible]	[illegible]	[illegible]	[illegible]	[illegible]	[illegible]	[illegible]	[illegible]	[illegible]
10	2,0297	1,00	1,00	1,00	1,00	[illegible]	[illegible]	[illegible]	[illegible]	[illegible]	[illegible]	[illegible]	[illegible]	[illegible]

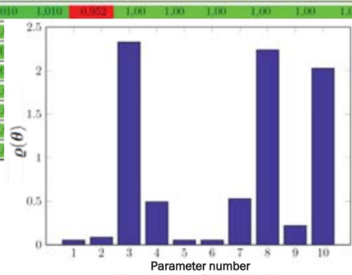

Ice accretion

- 4 steps
- Variation of density
- Optimization problem: $\min_{\theta} \varrho(\theta)$

$$\text{mit } \theta_i \geqslant 0,99 \ \forall \ i \in \theta$$

$$\theta_i \leqslant 1,75 \ \forall \ i \in \theta$$

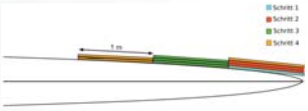

- Step 3: 14,4kg at 32m-33m and 33m-34m

Ice localization – Modal Parameters

	$\varrho(\theta)$	1	2	3	4	5	6	7	8	9	10	11	12	13
1	0,0165	1,00	1,00	1,00	1,00	1,00	1,00	1,00	1,00	1,00	1,00	1,00	1,093	1,224
2	0,0199	1,00	1,00	1,00	1,00	1,00	1,00	1,029	1,077	1,046	1,00	1,00	1,00	1,00
3	0,0167	1,00	1,00	1,00	1,00	1,00	1,00	1,00	1,00	1,00	1,00	0,990	1,190	1,197
4	0,0199	1,00	1,00	1,00	1,00	1,00	1,00	1,040	1,170	1,111	1,00	1,00	1,00	1,00
5	0,0197	1,00	1,00	1,00	1,00	1,00	1,00	1,00	1,00	1,062	1,103	1,024	1,00	1,00
6	0,0196	1,00	1,00	1,00	1,00	1,00	1,00	1,00	1,00	1,020	1,113	1,051	1,00	1,00
7	0,0166	1,00	1,00	1,00	1,00	1,00	1,00	1,00	1,00	1,00	1,00	1,00	1,126	1,200
8	0,0199	1,057	1,147	1,023	1,00	1,00	1,00	1,00	1,00	1,00	1,00	1,00	1,00	1,00
9	0,0168	1,00	1,00	1,00	1,00	1,00	1,00	1,00	1,00	1,00	1,00	1,004	1,231	1,158
10	0,0200	1,082	1,023	1,00	1,00	1,00	1,00	1,00	1,00	1,00	1,00	1,00	1,00	1,00
11	0,0165	1,00	1,00	1,00	1,00	1,00	1,00	1,00	1,00	1,00	1,00	1,00	1,093	1,224

Parameter number

- Correct Localizations in runs 1, 3, 7, 9 und 11
- Verification using objective function value
- Ice localization using modal parameters is possible

Ice quantification – Modal Parameters

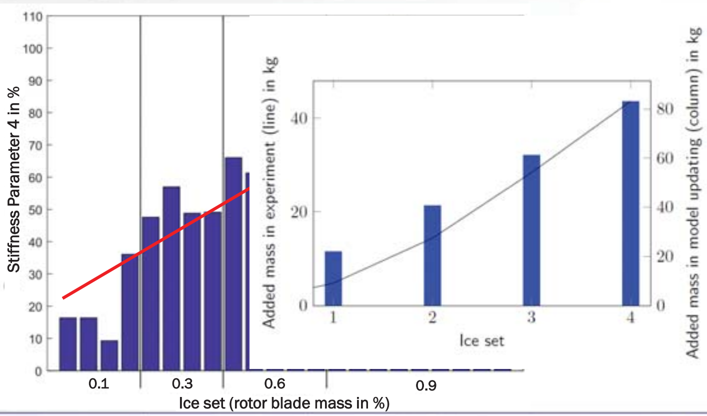

Conclusion & Outlook

Conclusion

- Updating in numerical examples and for ice quantification successful
- Minimization using global two-step optimization algorithm
- No success for damage localization using measured data
- Modal parameters superior to transmissibility functions

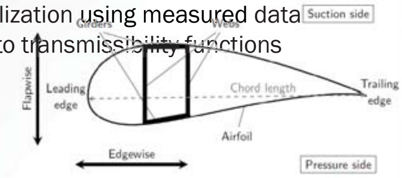

Outlook

- Investigate more advanced metrics for model updating
- Application to changing conditions (in situ)

Thank you for your attention!

ISD
INSTITUT FÜR STATIK
UND DYNAMIK

Leibniz Universität Hannover
Institute of Structural Analysis (ISD)
Appelstraße 9a, 30167 Hannover
+49 511 762 8063
k.schroeder@isd.uni-hannover.de

D2) Operations & maintenance

Using a Langevin model for the simulation of environmental conditions in an offshore wind farm, H.Seyr, NTNU

The LEANWIND suite of logistics optimisation and full life-cycle simulation models for offshore wind farms, F.D. McAuliffe, Univeristy College Cork

Analysis, comparison and optimization of the logistic concept for wind turbine commissioning, M. Wiggert, Fraunhofer IWES

Using a Langevin model for the simulation of environmental conditions in an offshore wind farm

Helene Seyr and Michael Muskulus

January 18, 2018

Langevin process

Deterministic contribution

$$F = D^{(1)}$$

Stochastic contribution

$$G = \sqrt{D^{(2)}}\Gamma_t$$

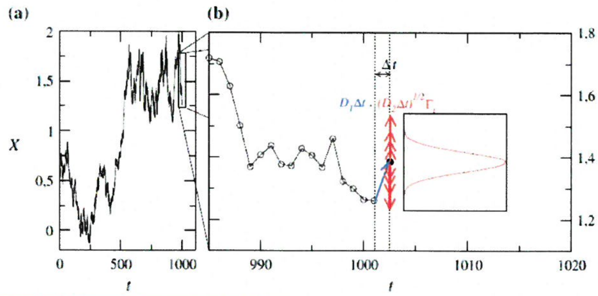

Outline

- Introduction
- Methodology
- Data
- Results
- Conclusions

Data

ECMWF:

- Re-analysis
- 6h resolution
- Dogger Bank wind farm
- 37 years

Fino 1:

- Measurement from met-mast and buoy
- 10min/30min means
- Alpha Ventus wind farm
- 6 years

Introduction

- O&M (cost) optimization is focus of research
- Many simulation models/optimizations rely on artificially generated weather time series to test different strategies
- Novel approach to model significant wave height and wind speed
- Langevin process:
  - Equations fitted to the data
  - Used to generate artificial weather

Results I

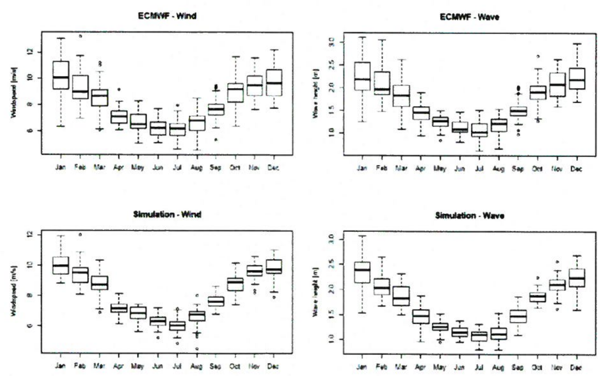

Results II

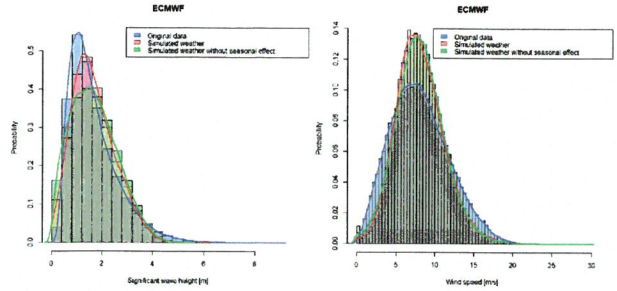

Results V

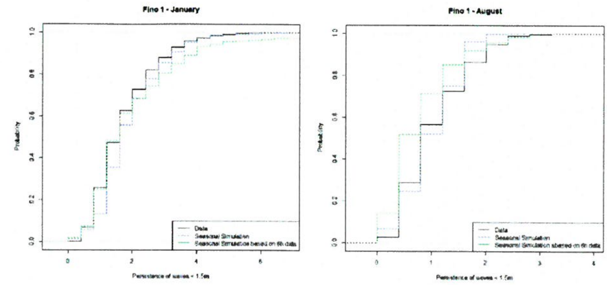

Results III

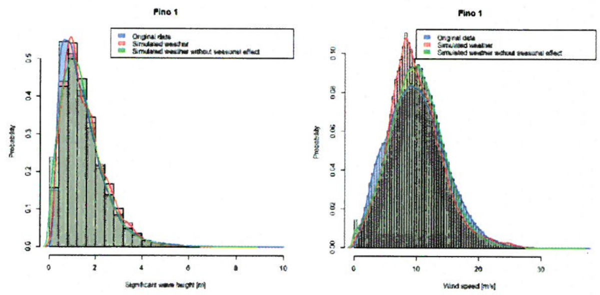

Results VI

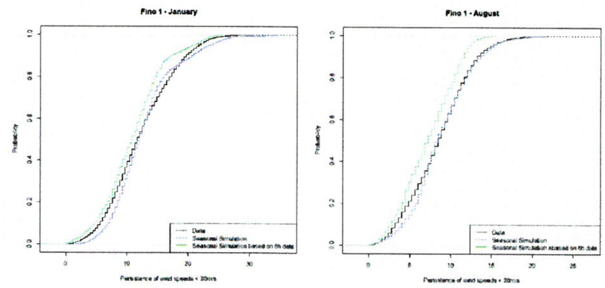

Results IV

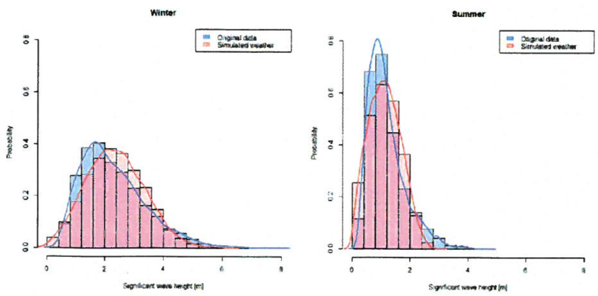

Conclusions

- Langevin process is a good alternative
- Properties of waves represented very well (Distribution, Persistence)
- Higher sampling frequency → better model
- 2D Langevin process for correlation (?)

AWESOME

Thank you for your attention

Helene Seyr
PhD Candidate
helene.seyr@ntnu.no
+47 400 86 761

NTNU
Norwegian University of Science and Technology

EERA DeepWind'18 conference

Trondheim, Norway

The LEANWIND suite of logistics optimisation & full lifecycle simulation models for offshore wind farms

leanwind

Presenter: Fiona Devoy McAuliffe

Project supported within the Ocean of Tomorrow call of the European Commission Seventh Framework Programme

Introduction

leanwind

What progress needs to be made?

Turbine	Foundation & tower	Transmission	Installation	OMS	Development
Technology contributions to reducing LCOE					
10%	1.5%	3%	1.5%	2%	2%
Supply chain contributions to reducing LCOE					
2%	1.5%	2%	1.5%	1%	1%

Source: BVG Associates 2016 The supply-chain's role in LCOE reduction, Belgo-British offshore wind farm supply-chain seminar Brussels

Presentation overview

leanwind

- Introduction
- Methodology
- Logistics optimisation models
- Financial simulation model
- Combined use
- Potential end-users

Introduction

leanwind

Logistic Efficiencies And Naval architecture for Wind Installations with Novel Developments

OBJECTIVE: *to provide cost reductions across the offshore wind farm lifecycle and supply chain through the application of lean principles and the development of state of the art technologies and tools.*

- UCC is coordinator
- 31 partner organisations
  - 52% industry partners
  - Representing 11 countries;
- €14.9m total funding;
- €10m EC funding;
- 4 year duration
  - December 2013-November 2017

Project Partners

Introduction

leanwind

Significant cost reductions to date:

Vattenfall's 2016 offshore wind price bid of €49.9/MWh for the Kriegers Flak project set a record LCOE forecast of €40/MWh

Current and future challenges to maintain & surpass savings:

- Increased industry competition to find cost reductions
- New markets yet to achieve LCOE forecasts
- Sites further from shore in deeper waters and harsher conditions
- Larger turbines and farms with new equipment and logistical requirements
- Facing the unknown – the decommissioning phase

Introduction

leanwind

Modelling is a safe and cost-effective way to evaluate and optimise operations. However, there is a lack of comprehensive decision-support tools, detailed enough to provide insight into the effects of technological innovations and novel strategies.

They can reduce costs by identifying potential savings and fostering effective decision-making for a wide range of stakeholders.

LEANWIND developed a suite of logistics and financial tools, which can optimise the entire supply-chain and simulate the full wind farm lifecycle, providing in-depth cost and time analysis.

Introduction

leanwind

LEANWIND developed a suite of <u>logistics</u> and financial tools, which can **optimise the entire supply-chain** and simulate the full wind farm lifecycle, providing in-depth cost and time analysis.

Methodology

leanwind

Introduction

leanwind

LEANWIND developed a suite of logistics and <u>financial tools,</u> which can optimise the entire supply-chain and **simulate the full wind farm lifecycle, providing in-depth cost and time analysis.**

Methodology

leanwind

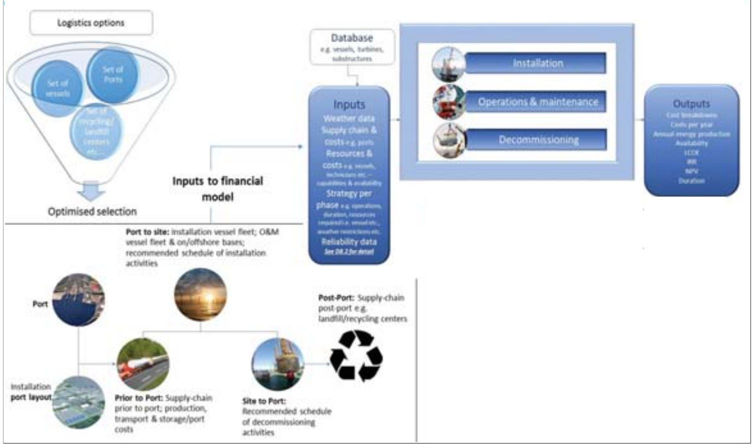

Methodology

leanwind

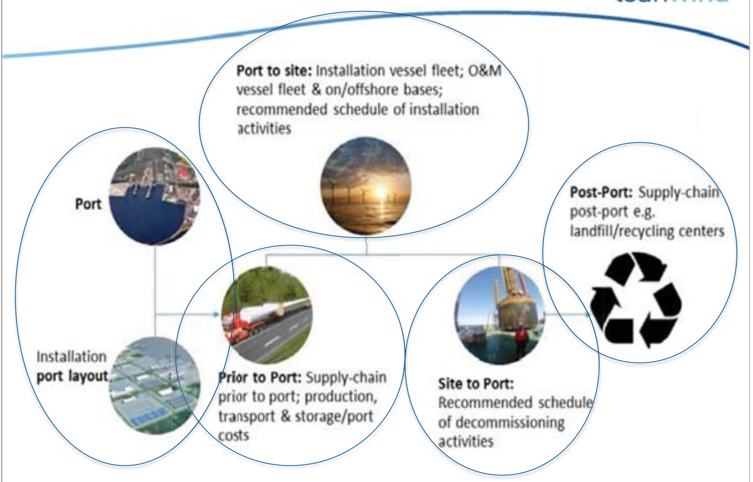

Logistics optimisation models

leanwind

	Installation	O&M	Decommissioning
Prior to/post port	PTPIns	PTPOM	IntDis
At port	Portlay, PortIns	PortOM	PortDis
To/from offshore site	VMIns	VMOM	IntDis

- **<u>Prior to/post port:</u> manufacturing, transportation, storage, and assembly.**
- **<u>At port:</u> selection of the port(s) for each lifecycle phase & optimal layout (installation phase).**
- **<u>Supply to/from offshore site:</u> transportation of parts to/from the port to the site.**

PTPIns PTPOM – prior to port models

leanwind

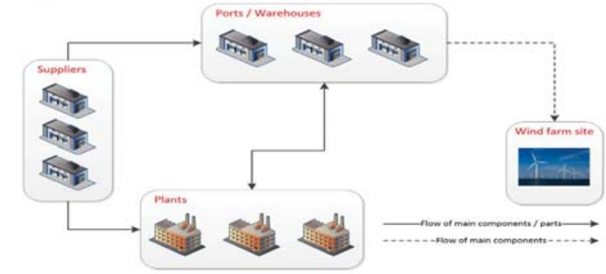

Optimal arrangement of supply chain (suppliers, manufacturers/plants, and warehouses (ports)) and schedule from the production of turbine parts to delivery at port.

VMIns VMOM – port to site models

leanwind

VMIns - optimal vessel fleet and schedule of installation activities i.e. the number of components to be installed per day.

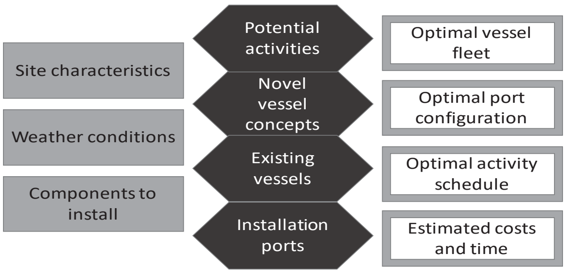

PortIns PortOM PortDis – port selection

leanwind

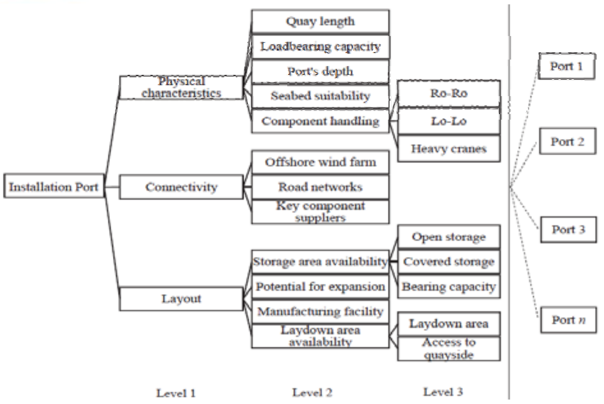

Source: Akbari N, Irawan C, Jones D and Menachof D 2017 A multi-criteria port suitability assessment for developments in the offshore wind industry Renewable Energy 102 pp 118-133

VMIns VMOM – port to site models

leanwind

VMOM - Based on the generated corrective & preventive maintenance patterns, the model chooses the *number and type of vessels and* the corresponding *infrastructure (bases, platform, mothership)* needed in the offshore transport system.

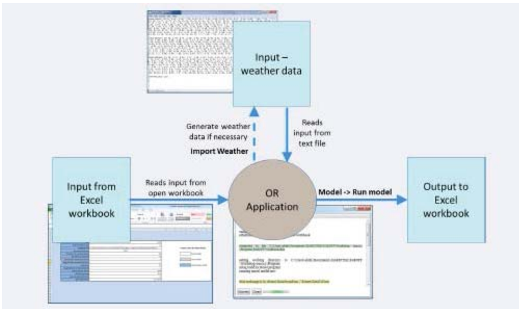

Source: Nonås L, Halvorsen-Weare E E and Stålhane M 2015 *Finding cost-optimal solutions for the maritime logistic challenges for maintenance operations at Offshore Wind Farms* (Denmark: Poster presentation at EWEA Offshore Wind Conference)

Portlay - port layout

leanwind

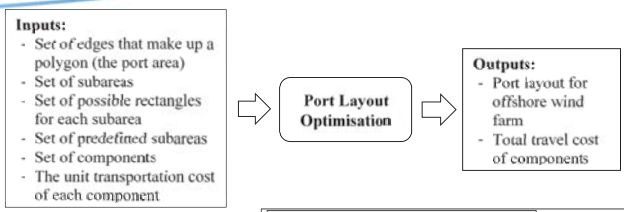

Optimal layout of the port given the dimensions and travel costs

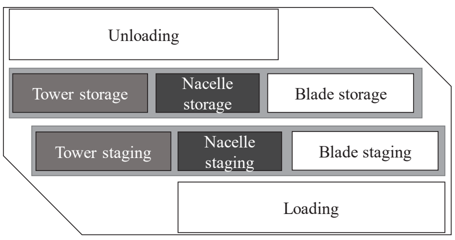

IntDis – integrated dismantling model

leanwind

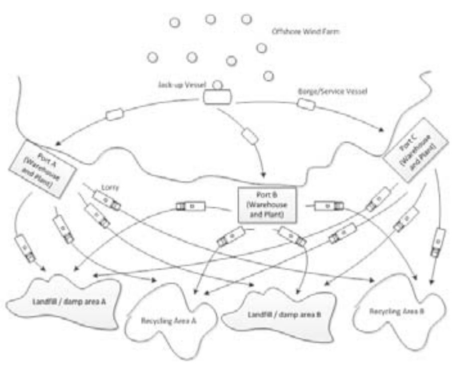

Vessel schedule and flow of components for decommissioning. The objective function is to minimise the total cost of activities.

Financial simulation model

leanwind

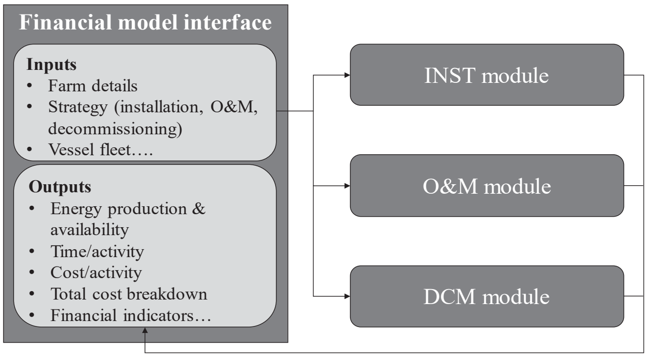

O&M module

leanwind

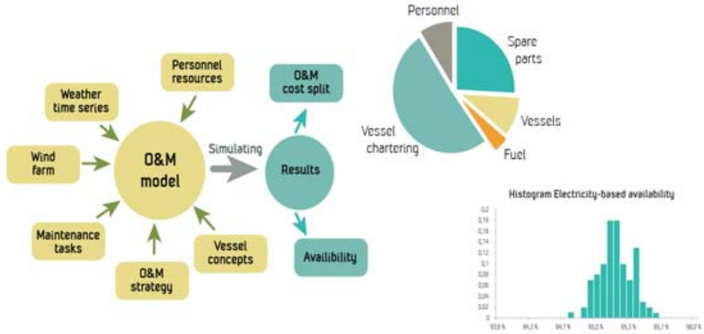

Financial simulation models

leanwind

Key Outputs

- Full project timeline i.e. duration of activities across the lifecycle
- Energy yield and availability
- Detailed breakdown of
  - capital & installation costs (CAPEX)
  - operation & maintenance costs (OPEX)
  - decommissioning costs (DECEX)
- LCOE, NPV, IRR and payback period
- Cashflow with project profit and loss sheet
- Balance sheet to evaluate debt and equity

O&M module

leanwind

1. Hofmann M and Sperstad I B 2013 NOWIcob – A tool for reducing the maintenance costs of offshore wind farms *Energy Procedia* **35** pp 177–186
2. Sperstad I B, Kolstad M and Hofmann M 2017 *Technical Documentation of Version 3.3 of the NOWIcob Tool Report no. TR A7374, v. 4.0* (Trondheim: SINTEF Energy Research)
3. Sperstad I B, Stålhane M. Dinwoodie I, Endrerud O.-E. V., Martin R and Warner E 2017 Testing the robustness of optimal access vessel fleet selection for operation and maintenance of offshore wind farms Ocean Engineering **145** pp 334–343
4. Sperstad I B, Devoy McAuliffe F, Kolstad M L and S Sjømark 2016 Investigating Key Decision Problems to Optimize the Operation and Maintenance Strategy of Offshore Wind Farms Energy Procedia **94** pp 261-268

INST module

leanwind

Scope: the turbine, foundation, substation, substation foundation, export and inter-array cabling. The user can specify or use a pre-defined selection of assets. Different operations are then associated with the installation of each asset e.g.

Installation method	Lifts
2 tower parts, nacelle and hub pre-assembled	6
Tower parts and nacelle and hub pre-assembled	5
Blades and hub pre-assembled	4
Nacelle, hub and 2 blades (bunny ears) pre-assembled	4
Tower parts and nacelle, hub and 2 blades (bunny ears) pre-assembled	3
Pre-assembled	1
Pre-installed on substructure	0

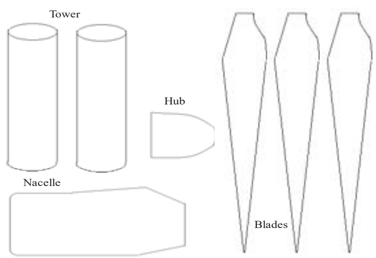

DCM module

leanwind

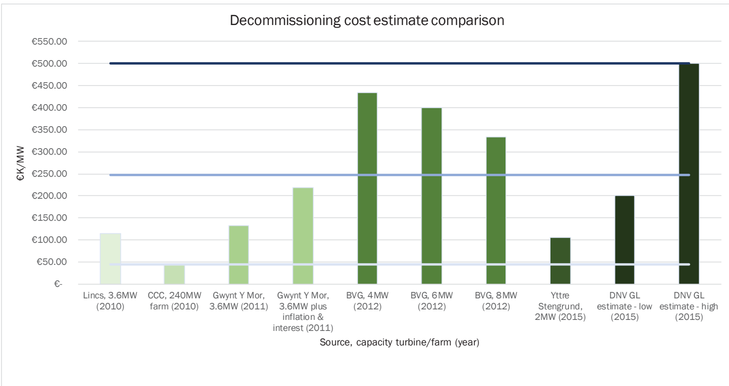

DCM module

Scope: Turbine and foundation.

Inputs: The component (e.g. blades, nacelle, gearbox etc.) and order in which they are dismantled; component materials and weight; operation durations; up to three destination ports; landfill or recycling centre locations; number of technicians; vessels available etc.

Outputs: Costs; time and revenue e.g. salvage

Validation: Results for the C-Power OWF were €513,000 per MW within range estimated by DNV GL of €200,000-€600,000/MW
(Source: Chamberlain K 2016 *Offshore Operators Act on Early Decommissioning* (http://newenergyupdate.com/wind-energy-update/offshore-operators-act-early-decommissioning-data-limit-costs; New Energy Update)

Conclusion

1. Comprehensive and complementary set of logistics and financial models
2. Can foster significant cost-savings in the industry through effective decision-support.
3. Fill a significant gap in the current models available.
4. They can be used individually or together to optimise and simulate the full supply-chain and lifecycle of an OWF project.
5. Combined use can save considerable computational time.
6. Designed primarily for the project planning and design phase but also useful during operational period.
7. They can address current and future challenges faced by a wide range of stakeholders.

Combined use – the benefits

Different objectives and methodologies but complementary:
- Very time-consuming to optimise a scenario with simulation models & not humanly possible to consider all possible solutions.
- The optimisation models determine the key supply-chain configurations and the financial models examine the top ranking options in further detail.
- Simulation models can assess a scenario in detail and the Monte Carlo method considers the uncertainty of key risk factors e.g. failures and weather.
- Combined they can obtain the most economically viable and time efficient solutions to a wide range of logistical and strategic issues.

Potential end-users

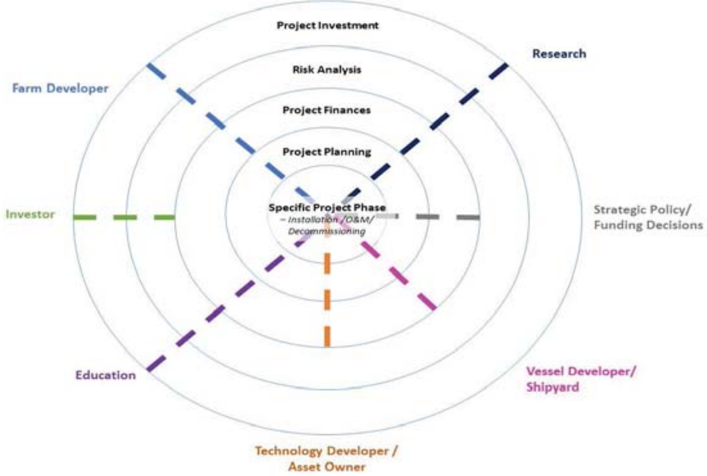

Thank you very much
for your attention

Welcome

WIND. ASSURING CONFIDENCE THROUGH COMPETENCE

Analysis, comparison and optimization
of the logistical concept for wind turbine commissioning

Dr. Marcel Wiggert

Fraunhofer IWES

Agenda & Goals

- Topic and challenges
- Introduction WaTSS concept
- Approach
- Case study: Commissioning
- Conclusions

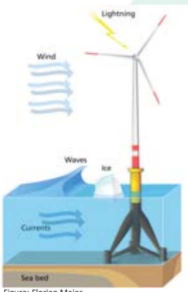

Figure: Florian Meier

Topic

- Title:

Analysis, comparison and optimization of the logistical concept for wind turbine commissioning

- Conditions:
  - Weather risk of the WTG installation
  - Optimization of the number of commissioning teams
  - Comparison of 3 different logistical concepts
- Decision criteria: lowest cost and risks

Challenge

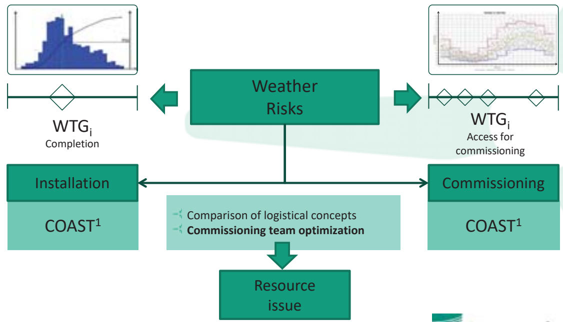

¹ COAST – Comprehensive Offshore Analysis and Simulation Tool

IWES Modeling Approaches

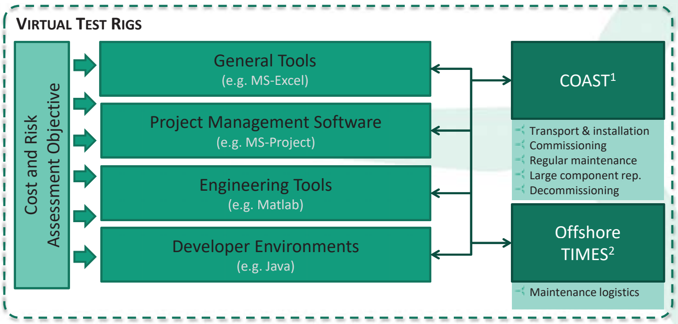

¹ COAST – Comprehensive Offshore Analysis and Simulation Tool
² Offshore TIMES – Offshore Transport, Inspection an Maintenance Software

Information Profile

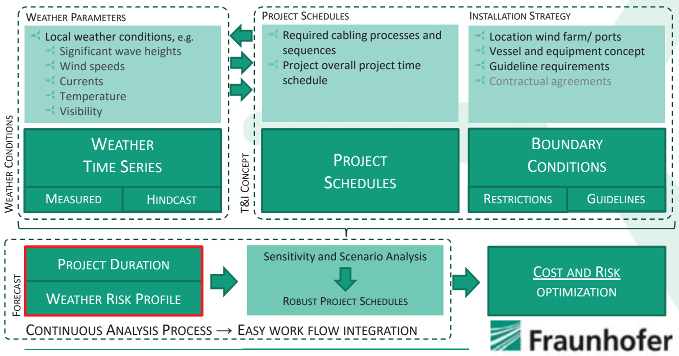

WaTTS – Method
Weather Time Series Scheduling

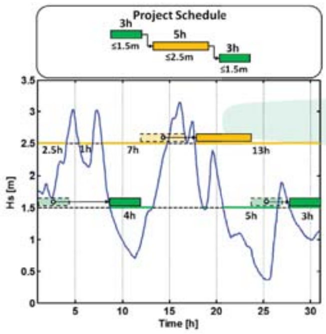

- Consideration of:
  - Task sequence
  - Contingencies in guidelines
  - Different weather restrictions
- Calculation of project durations and their probabilities

Fraunhofer IWES

Virtual Project Test Center
Yearly Simulation

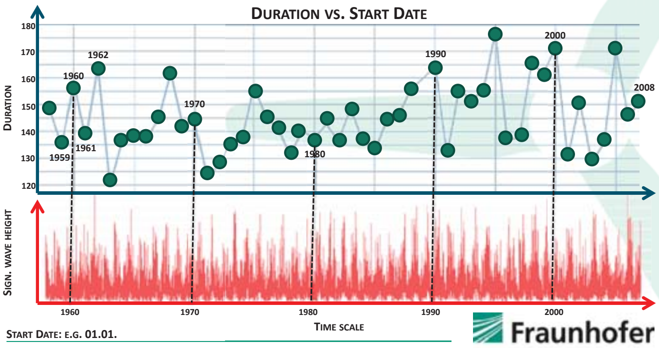

Start Date: e.g. 01.01.

Fraunhofer IWES

Virtual Project Test Center
Continuous Simulation

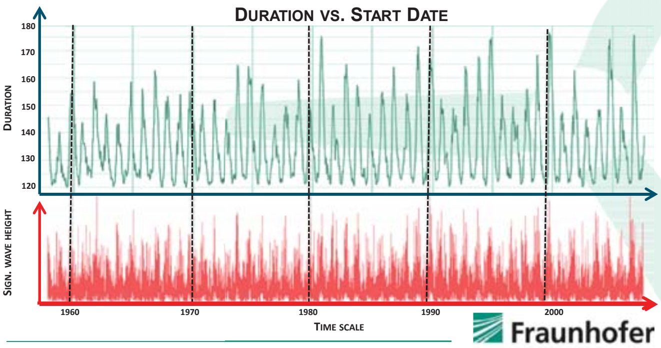

Fraunhofer IWES

Duration vs. Start Day

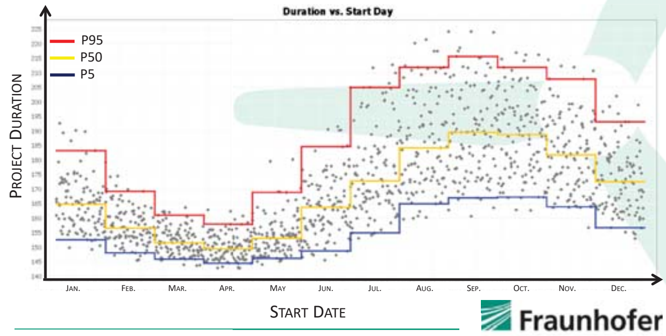

Fraunhofer IWES

COAST – Software

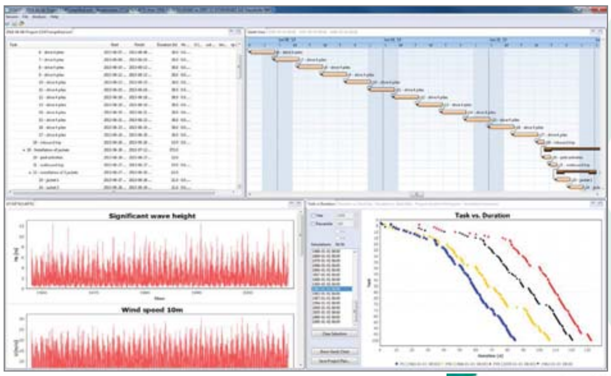

Fraunhofer IWES

Simulation Concept

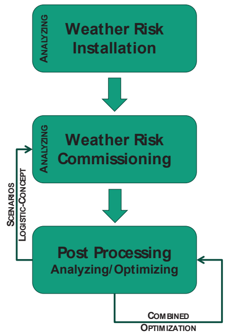

1. Installation dates of the wind turbines per analyzed year
   Goal: Definition commissioning start dates
2. Success of the commissioning work for every day
   Goal: Definition of the turbine accessibility
3. Post Processing: e.g., MS Excel or MATLAB
   Goal: Analyzing the scenarios
   1. Calculation of the commissioning duration per turbine and year under consideration of weather and resource constraints
   2. Calculation of the required vessel days and costs
   3. Evaluation and presentation of the results

Fraunhofer IWES

Case Study: IWES Baltic Introduction

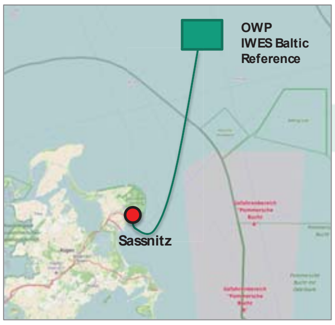

IWES OWP Baltic

Boundary conditions	Assumption
Number of turbines	60
Port distance	40km
Start date	2020-07-01
Commissioning (1 Team)	160h/turbine (net)
Team costs	3,000 Euro/day
Opportunity costs	3,000 Euro/day per turbine
Weather data	coastDat v1 (1958–2002) [4]
Duration of installation incl. weather risks (P50)	100 days (COAST)

- Weather parameters:
  - Significant Wave Height (h_s)
  - Wind Speed (U)

Scenario Analysis

Scenario CTV — Crew Transfer Vessel

Vorgangsname	Dauer
12/7 CTV Base Case	12 Std.
1. WTG - Fahrt 1	12 Std.
Transfer to site	2 Std.
Comm Works	8 Std.
Transfer back to harbour	2 Std.

Scenario HV — Hotel Vessel

Vorgangsname	Dauer
Accommodation Vessel 24/7	24 Std.
1. WTG - Fahrt 1	24 Std.
Transfer to site	1 Std.
Comm Works	10 Std.
Transfer back to Vessel	1 Std.
Transfer to site	1 Std.
Comm Works	10 Std.
Transfer back to Vessel	1 Std.

Scenario SOV — Service Operation Vessel

Vorgangsname	Dauer
DP2 Vessel	24 Std.
Fahrt 1	24 Std.
Transfer to site	1 Std.
Comm Works	10 Std.
Transfer back to V	1 Std.
Transfer to site	1 Std.
Comm Works	10 Std.
Transfer back to V	1 Std.

Assumptions

- CTV: H_s = 1.5m; 3 Teams on board; 12h/7 days; Costs: 4,000 €/d; 8h/day on turbine
- HV: H_s = 1.5m; 20 Teams; 24h/7 days; Costs: 20,000 €/d; 10h/day on turbine
- SOV: H_s = 2.5m, U = 10 m/s; 20 Teams; 24h/7 days; Costs: 24,000 €/d; 10h/day on turbine

WTG Installation Strategy

WTG Installation Strategy only

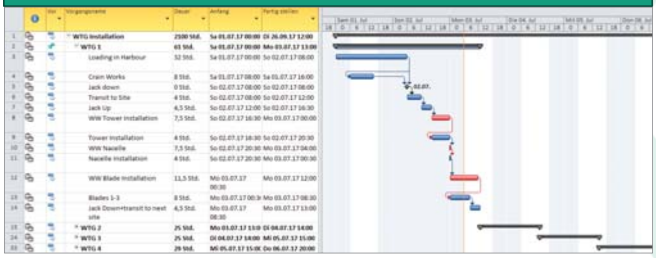

Case Study: IWES Baltic – Results

Costs (P50) | Risk Profile

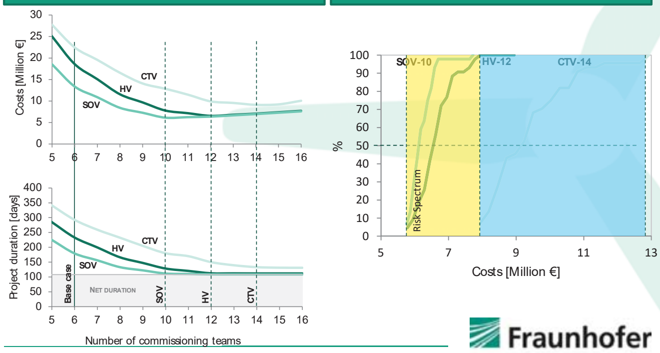

Scenario Analysis

Scenario CTV — Crew Transfer Vessel


www.pomaritime.com

Scenario HV — Hotel Vessel


https://c-bed.nl

Scenario SOV — Service Operation Vessel


www.siemens.com/windpower

Assumptions

- CTV: H_s = 1.5m; 3 Teams on board; 12h/7 days; Costs: 4,000 €/d; 8h/day on turbine
- HV: H_s = 1.5m; 20 Teams; 24h/7 days; Costs: 20,000 €/d; 10h/day on turbine
- SOV: H_s = 2.5m; 20 Teams; 24h/7 days; Costs: 24,000 €/d; 10h/day on turbine

Conclusion

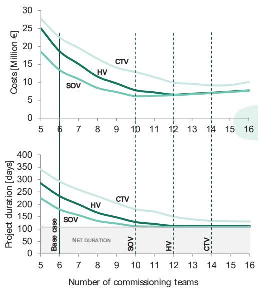

- Post processing extends capabilities of the WaTSS method
- Approach to consider the availability of transport (resources) for the commissioning teams
- Important to consider risks and cost simultaneously
- Case Study: "IWES Baltic"

Acknowledgements
Fraunhofer IWES is funded by the:

Federal Republic of Germany

Federal Ministry for Economic Affairs and Energy

Federal Ministry of Education and Research

European Regional Development Fund (ERDF):

Federal State of Bremen
- Senator of Civil Engineering, Environment and Transportation
- Senator of Economy, Labor and Ports
- Senator of Science, Health and Consumer Protection
- Bremerhavener Gesellschaft für Investitions-Förderung und Stadtentwicklung GmbH

Federal State of Lower Saxony

Free and Hanseatic City of Hamburg

Fraunhofer IWES

Background

DETAILED INFORMATION

Fraunhofer IWES

References

Fraunhofer IWES

Detailed Analysis

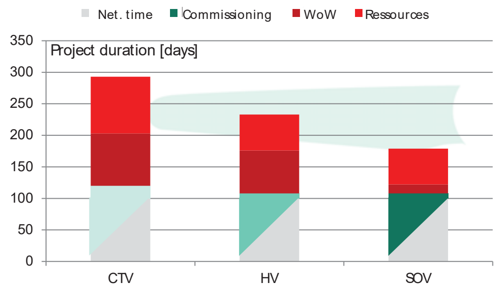

Fraunhofer IWES

Thank You For Your Attention

Any questions?

marcel.wiggert@iwes.fraunhofer.de

Fraunhofer IWES

Risk Efficiency

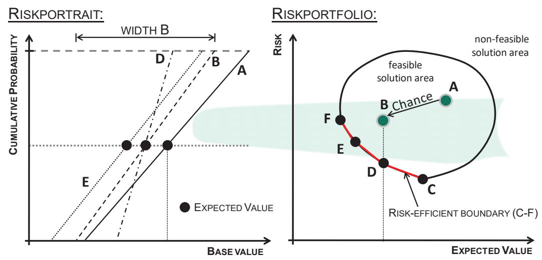

- Risk efficiency concept by CHAPMAN/WARD 2003, based on MARKOWITZ portfolio theory
- Rule: *„that the investor does (or should) consider expected return a desirable thing <u>and</u> variance of return an undesirable thing“* (MARKOWITZ 1952, S.77)

Fraunhofer IWES

Primary and Secondary Weather Risks Duration vs. Start Day

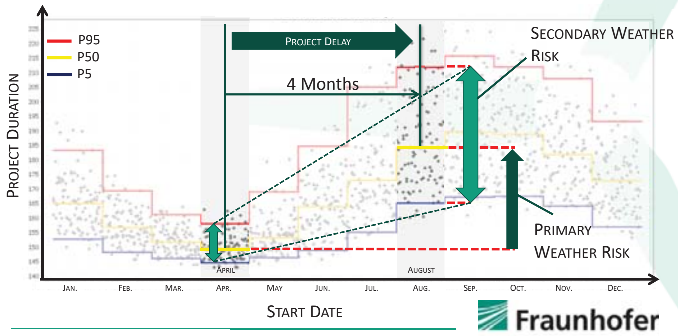

Fraunhofer IWES

Weather Impact – Example Accessibility (July – December)

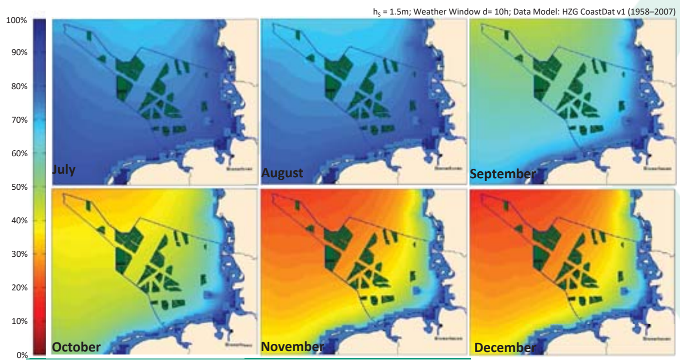

E1) Installation and sub-structures

Floating offshore wind turbine design stage summary in LIFES50+ project, G. Pérez, TECNALIA

A comprehensive method for the structural design and verification of the INNWIND 10MW tri-spar floater, D. Manolas, NTUA

Reducing cost of offshore wind by integrated structural and geotechnical design, K. Skau, NGI and NTNU

Catenary mooring chain eigen modes and the effects on fatigue life, T.A.Nygaard, IFE

Floating offshore wind turbine design stage summary in LIFES50+ project

Germán Pérez (TECNALIA)

DeepWind 2018
Trondheim, 18 January 2018

Qualification of innovative floating substructures for 10MW wind turbines and water depths greater than 50m

The research leading to these results has received funding from the European Union Horizon2020 programme under the agreement H2020-LCE-2014-1-640741.

Outline

- LIFES50+ project overview
- WP1 Concepts Design
- Design Basis
- Concepts Design process
- Conclussions & Challenges

LIFES50+ project overview

Qualification of innovative floating substructures for 10MW wind turbines and water depths greater than 50m
Grant Agreement: H2020-LCE-2014-1-640741
OBJECTIVES:
- Optimize and qualify to a TRL 5, of two innovative substructure designs for 10MW turbines
- Develop a streamlined KPI-based methodology for the evaluation and qualification process of floating substructures

FOCUS:
- Floating wind turbines installed in water depths from 50m to 200m
- Offshore wind farms of large wind turbines (10MW) – identified to be the most effective way of reducing cost of energy in short term

BUDGET:
- 7.3 MM€

40 months duration staring June 1, 2015
Project leader MARINTEK, Partners:

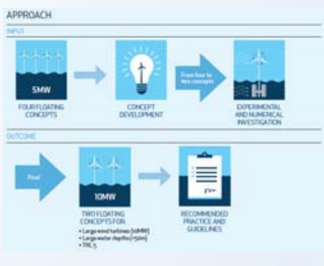

LIFES50+ project overview

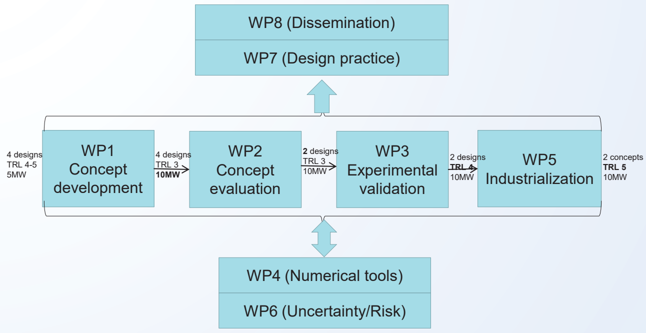

First stage of the project: design and evaluation of four concepts, for three sites, 10 MW reference wind turbine and considering 500 MW wind farm.

WP1 Concepts Design

WP1 - Concept development and optimization

M1-M40

176 PM, 23% of total budget

Work organized in three stages:

1. Design Basis
2. Concepts design
3. Selected concepts optimization

Stage 2 focused on the concepts design for their assessment

WP1 Concepts Design

MS1: Design Basis ready for starting design (June-November 2015)

Task 1.1 Definition of the target locations: business cases.

Results: D1.1 Oceanographic and meteorological conditions for the design (Public)

Task 1.2 Wind turbine specification.

Result: D1.2 Wind turbine models for the design (Public)

MS2: Concepts design ready (December 2015 – March 2017)

Task 1.3 Concepts development for a 10MW wind turbine.

Results:
D1.3 Concepts design.
D1.4 Wind turbine controller adapted to each concept.
D1.5 Marine operations.
D1.6 Upscaling procedure (Public)

Task 1.4 Concepts design assessment.

D1.7 Information for concepts evaluation.

MS4: Phase 1 qualification performed

Public deliverables available on the project`s web site www.lifes50plus.eu

Design Basis

- Oceanographic and meteorological conditions for the three selected sites.
  - Site A (moderate met-ocean conditions), offshore of **Golfe de Fos**, France
  - Site B (medium met-ocean conditions), the **Gulf of Maine**, United States of America
  - Site C (severe met-ocean conditions) **West of the Isle of Barra**, Scotland

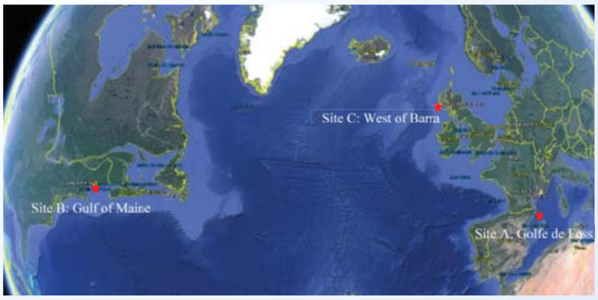

Design Basis

- Information collected:
  - Sites location
  - Water Depth and Water Levels
  - Wind climate, wave climate and wind-wave combined conditions
  - Currents Data
  - Soil Conditions
  - Other Environmental Conditions (ice, sea water characteristics, marine growth…)

	50-year wind at hub height [m/s]	50-year significant wave height [m]	50-year sea-state peak period [s]	50-year current [m/s]	Extreme water level range [m]	Design Depth [m]	Soil Type
Site A	37	7.5	8-11	0.9	1.13	70	Sand/Clay
Site B	44	10.9	9-16	1.13	4.3	130	Sand/Clay
Site C	50	15.6	12-18	1.82	4.2	100	Basalt

Design Basis

- FAST model of DTU 10MW reference wind turbine.
- Generic controller for the wind turbine.
- Tower reference design.

Concepts Design process

Concepts design, driven by the information required for the evaluation:

- KPIs.
- LCOE and LCA figures. Forms for 50 wind turbines wind farms -3 excel sheets-, one wind turbine -1 excel sheet- and 5 wind turbines -1 excel sheet-
- Uncertainty forms for each of the sites.
- Information for risk analysis.

LIFES50+ Design Process conditioned for the concepts assessment and evaluation:

1. Onshore benchmark to validate WT models.
2. 'Design references' to select an justify the Load Cases for each site and each concept.
3. Design Briefs to validate the design process and the assumptions.

Concepts Design process

Numerical tools used in LIFES50+ consortium

	WAMIT	AQWA	FAST	BLADED	OrcaFlex	3DFloat	Flex5	HAWC2	SIMA (SIMO/ RIFLEX)	Sesam/ Wadam	Simpack Wind	SLOW
DNVGL	X			X								
DTU	X		X				X	X				
IBER		X	X									
IDEOL		X	X		X							
MARINTEK	-*								X			
OO	-*					X	X		X	X		
TECN		X	X		X							
USTUTT		X	X	X							X	X
POLIMI		X	X									

*WAMIT data is incorporated in the software tools SIMA, Sesam/Wadam and 3DFloat

Ref.: D4.4 – Overview of the numerical models used in the consortium and their qualification. Public deliverable.

Concept developers followed their own design procedures and codes, validated at different levels in the consortium, to ensure a common framework for their assessment

Concepts Design process

Design Basis
- Met-ocean condictions - DLCs
- Wind Turbine model, including WTG controller
- Standards
- Design restrictions and assumptions

SW becnhmark
- Definition of the benchmark: Load Cases
- Comparison of model results

Design Briefs
- Review of the design procedures
- Qualitative assessment of the modelling approach

Concepts Design
- Design for the three sites
- Concept Developer provide figures: KPI, LCOE, LCA
- Evaluation Comittee review results and provide feedback
- Design summary collected in D1.3 to D1.5 deliverables

Concepts Design process

Concept developers considered all the **design topics**:

- Sizing and structural design –subtask 1.3.1-
- Mooring design –subtask 1.3.2-
- Aero-hydrodynamic simulations –subtask 1.3.3-
- Adaptation of the WT controller –subtask 1.3.4-
- Analysis of marine operations, including manufacturing strategy –subtask 1.3.5-

Several information submissions were stablished in order to facilitate the concepts evaluation and improve concepts design

Evaluation Committee gave feedback after each submission, and requested more information for specific topics.

Concepts Design process

Concepts Design results

No	Deliverable Name	Lead Beneficiary	Type	Dissemination Level
D1.3	Concepts design	5 – TECNA	Report	CO
D1.4	Wind turbine controller adapted to each concept	5 – TECNA	Report	CO
D1.5	Marine operations	8 – IBER	Report	CO
D1.6	Upscaling procedure	5 – TECNA	Report	PU

Conclussions & Challenges

Concepts design and design workshop main highlights:

- Same design methodology and considerations as for 5 MW-scale conceptual designs.
- The main challenge arisen by the four concept developers is related to tower natural frequencies and the challenge to avoid coupling with the 3P frequency of the WTG.
- Working in direct collaboration with a turbine manufacturer is critical for the optimum design of a floating structure for offshore wind.
- Control has been highlighted by all partners as a very important part of the design that might need additional attention.
- Logistics can be a bottleneck for the deployment of large wind farms, using next generation of large wind turbines. Working with the industry is very important for reaching a concept design that keeps on 'standard' industry elements.
- A global vision of the wind farm may be critical for reaching the optimum design. Aspects which were out of LIFES50+ scope like wind farm layout, wake effects, power production or O&M strategy may influence the substructure and moorings design.

Conclussions & Challenges

Specific to LIFES50+ work in the first stage of the project.

- It was difficult to establish the framework to assess and compare different types of substructures –technical point of view, KPIs-

General to the floating offshore wind design.

- Precise and clear information from the very beginning: design basis.
  - Wind turbine features and restrictions for the substructure developer
  - Site information
  - Standards
- Close collaboration between the different parties involved in the wind farm development, in order to ensure a global view of the project.
- Design and simulation tools adapted to each project stage.

NATIONAL TECHNICAL UNIVERSITY of ATHENS (NTUA)

A comprehensive method for the structural design and verification of the INNWIND 10MW tri-spar floater

DI Manolas, CG Karvelas, IA Kapogiannis, VA Riziotis, KV Spiliopoulos and SG Voutsinas

EERA DEEPWIND'18, Trondheim, January 18th 2018

Outline

- Scope
- Numerical Tools
- Method for detailed design and verification
- INNWIND 10MW tri-spar concrete floater
- Conclusions

Scope

- Cost effective method for floater detailed design and verification
- 3D "complex" geometry (i.e. semi-submersible, tri-spar etc)
- Concrete!
- Account for ULS and FLS
- Environmental excitation (wind & wave/current)
- Realistic modeling
- Application: INNWIND 10MW tri-spar concrete floater

Numerical Tools

SAP2000: 3D FEM Solver

General purpose commercial software for analyzing any type of structures.

- Solution: Static, frequency domain and time domain
- Elements: Beam, shell thick, solid
- Design is fully integrated for both steel and concrete members, based on American or European standards

Numerical Tools

hGAST: hydro-servo-aero-elastic tool

General in-house simulation platform for analyzing the fully-coupled dynamic behavior of WT

Simulates all support structures

Modules

- Dynamics: Multi-body formulation
- Elasticity: beam theory
- Aerodynamics: BEM or Free wave
- Hydrodynamics: Potential theory or Morison's equation
- Moorings: dynamic modeling
- Control: variable speed/pitch
- Environmental Excitation according IEC

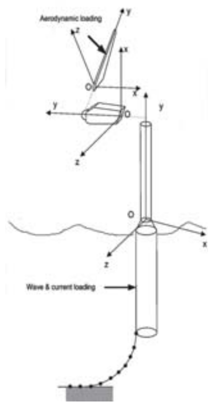

Numerical Tools

freFLOW: Hybrid integral equation method

General in-house hydrodynamic solver for analyzing and designing floating structures

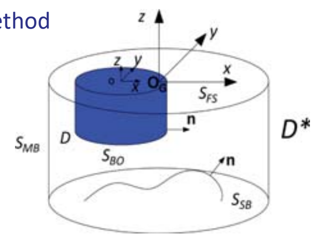

- Solution: 3D Laplace equation in frequency domain
- Method: BEM – indirect formulation with constant source distribution
- Radiation condition: Matching with Garrett's analytic solution
- Provides: Exciting loads, Added mass & damping coefficients, RAOs, total hydrodynamic loads and total hydrodynamic pressure

Method for detailed design and verification

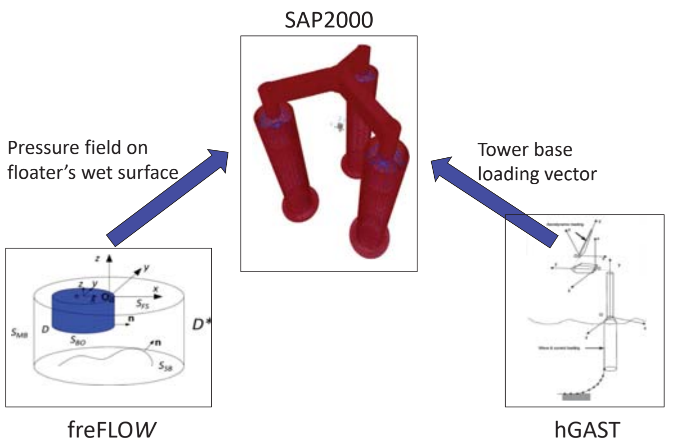

Method for detailed design and verification

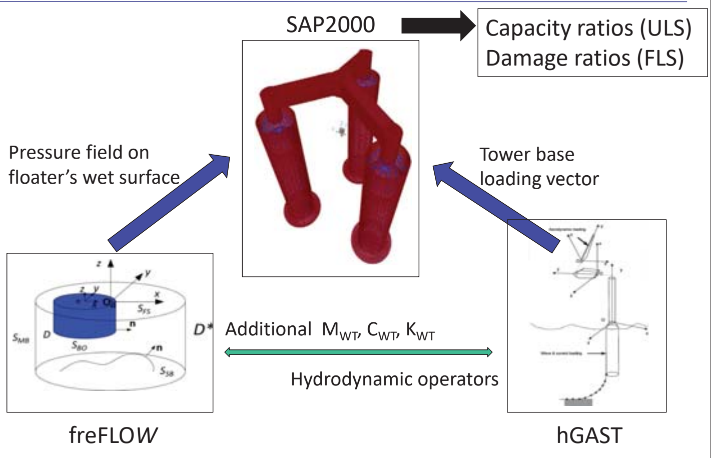

Method for detailed design and verification

- Detailed Analysis in 3D FEM
  - ULS: static solution
  - FLS: frequency domain stochastic solution
- Input: Preliminary design
- Checking (stress level)
  - ULS: capacity ratios (max σ / material yield σ)
  - FLS: σ PSD → Time series → RFC → damage ratios (S-N curve data)
- hGAST (IEC DLCs)
  - ULS: maximum loading
  - FLS: lifetime PSD
- freFLOW

$$p_{PSD}(\mathbf{x},\omega)=[p(\mathbf{x},\omega)/A]^2\, S(\omega;T_p,H_s)$$

$$p_{\max}(\mathbf{x})=1.86\cdot 2\sqrt{\int_0^\infty [p(\mathbf{x},\omega)/A]^2\, S(\omega;T_p,H_s)\,d\omega}$$

  - FLS: pressure PSD
  - ULS: max pressure
    - Simultaneously applied
    - Generating the max moment at critical points

INNWIND 10MW tri-spar concrete floater

WT: DTU 10MW RWT

Rotor D : 178.3m
Hub Height : 119.0m
Tower base : 25.0m

Floater: tri-spar concrete

Concrete : 11478tn
Steel : 1138tn
Ballast : 15653tn
Total : 28268tn

Water Depth : 180m

Catenary mooring lines

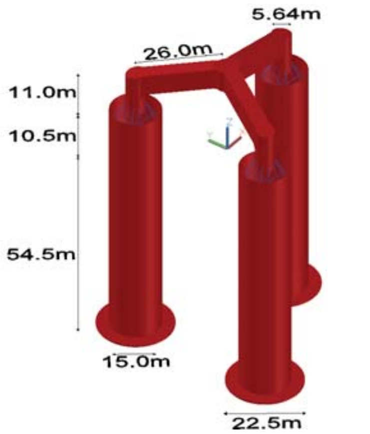

Method for detailed design and verification

(Realistic) Modeling

- SAP2000: Introduce the 6 rigid body motions (Stiffness Matrix)
- hGAST: simulations for the off-shore WT
- freFLOW: total pressure field (RAOs for floater & M_{WT}, C_{WT}, K_{WT})

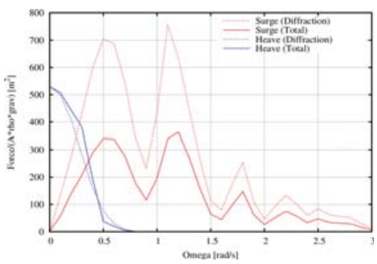

INNWIND 10MW tri-spar concrete floater

DLCs definition for time domain simulations

DLC	Wind	Wave	Seeds	Bins [m/s]	Yaw	Wave	SF
1.2	NTM	NSS	1	5, 7, 9, 11, 13, 15, 17, 21, 23, 25	0	0	
1.3	ETM	NSS	3	11, 25	0	0	1.35
1.6	NTM	ESS	3	11, 13, 17, 21, 25	0	0	1.35
6.1	EWM	SSS	3	41.8	0	0, 30	1.35
6.2	EWM	SSS	3	41.8	0,+/-30	=Yaw	1.10

Maximum tower base loading applied on the tri-spar floater (DLC1.6 at 13m/s, Hs=10.9m, Tp=14.8s. SF=1.3).

Fx [kN]	Fy [kN]	Fz [kN]	Mx [kNm]	My [kNm]	Mz [kNm]
7472	168	-9736	-5186	621000	3679

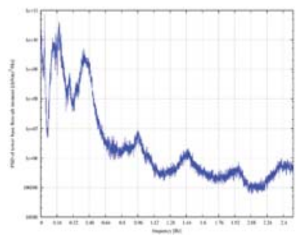

Lifetime PSD of tower base fore-aft moment, Weibull C=11/s, k=2.

Detailed design and verification

- Heave plates (HP): steel → concrete
- Concrete Column (CC): reinforcement
- Connection (steel legs-concrete columns)
- Steel Tripod

Materials:

- Steel : S450 , t=0.0564m
- Concrete : C50/60 , t=0.40m
- Rebar : Reinforcement

Reinforcement (DLC1.6 - max pressure)

- CC Vertical : Φ25/180
- CC Horizontal : Φ20/250
- HP Radial : double Φ36/65
- HP Horizontal : double Φ36/75

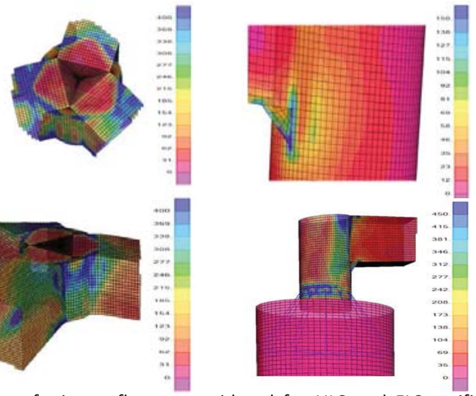

Critical points of tri-spar floater considered for ULS and FLS verification. Stress contours from ULS case II (max moment at gamma connection).

Tripod Design Modifications

Bracket width (5.64m → 4.62m)

Local reinforcements

- Central cylinder : t=0.0564-0.175m
- Brackets : 3 diaphragms
- Legs : 4 diaphragms
- Legs : t-top =0.0564m
- t-bottom=0.175m
- gamma connection: triangular plate

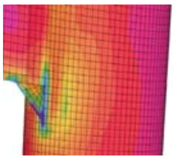

ULS verification: capacity ratios at critical positions (DLC1.6 at 13m/s, Hs=10.9m, Tp=14.8s)

Critical Position	Capacity ratios	
	I**	II
1. Central Cylinder -Horizontal Leg Connection	0.64	0.68
2. Horizontal Leg-Vertical Leg Connection	0.26	0.28
3. Vertical Leg –Inclined Rods Connection	0.64	0.78
4. Inclined Rods	0.46	0.54
5. Ties	0.08	0.09

FLS verification: 20 years damage ratios at critical positions.

Connection	S-N curve parameters			Damage
	Type	log(a)	m	Ratio
1. Central Cylinder – Horizontal Leg	B2	16.856	5	0.31
2. Horizontal Leg at inclination point	C	16.320	5	0.93
3. Horizontal Leg –Vertical Leg	B2	16.856	5	0.86

****I: max pressure, II: max moment at gamma- connection**

Steel – Concrete connection

- 12 inclined steel rods (inclination =60°)
- 12 horizontal steel ties
- a steel ring

Rods - Ties

- D= 0.50m
- t = 0.02m
- Pinned connection

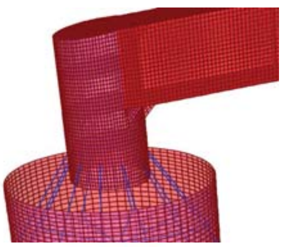

Conclusions

- A comprehensive method for floater detailed design and verification has been presented.
- The isolated floater is analyzed in 3D FEM solver, by performing static (ULS) and frequency domain (FLS) simulations
- WT loads: hydro-servo-aero-elastic tool (hGAST)
- Wave loads: frequency domain potential solver (freFLOW)
- Application on INNWIND 10MW tri-spar floater; the present designs seems to be FLS driven.

Outlook

- More design loops (mainly for FLS)
- Detailed modeling for mooring lines connection point
- Verification of the method vs fully coupled analysis

Thank you for your attention

Acknowledgements:
This work was funded by the European Commission under INNWIND.EU project. The authors would like to thank all INNWIND WP4 colleagues and especially José Azcona, Frank Lemmer and Feike Savenije who provided expertise that greatly assisted this research.

NGI

REDWIN – REDucing cost in offshore WINd by integrated structural and geotechnical design

EERA DEEPWIND January 2018

Load frequencies and eigen frequncy

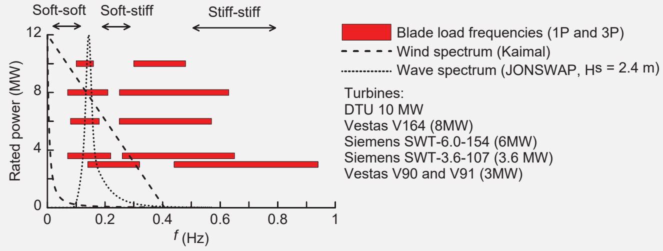

NGI Source: Arany, L., Bhattacharya, S., Macdonald, J. H. G. and Hogan, S. J. (2016)

NGI

Skau, K.S., Senior engineer, NGI and PhD candidate, NTNU
Kaynia, A.M., Technical Expert and Professor II, NTNU
Page, A.M., PhD Candidate, NTNU
Løvholt, F., Senior Specialist, NGI
Norén-Cosgriff, K., Head of Section CGM, NGI
Sturm, H., Discipline leader Offshore renewables, NGI
Jostad, H.P., Technical director offshore energy NGI and Professor II, NTNU
Nygard, T.A., Senior researcher IFE and Professor, NMBU
Andersen, H.S., Structural Engineer, Dr. Tech Olav Olsen
Eiksund, G., Professor, NTNU
Havmøller, O., Senior researcher, Statoil ASA
Strøm, P., Lead Geotechnical Engineering, Statoil ASA
Eichler, D., Senior Lead Structural Engineer, Vattenfall

The importance of the foundation

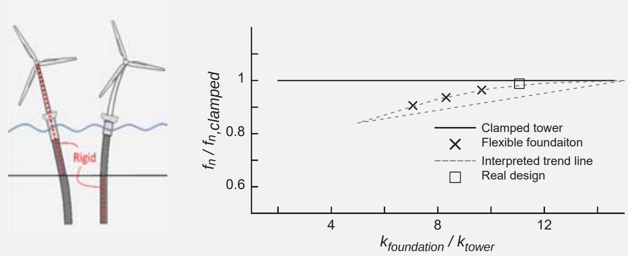

NGI

REDWIN

- 4-year research project
- Sponsors: NFR, Statoil, Vattenfall, Statkraft
- Partners: NGI, NTNU, IFE, Dr. Tech. Olav Olsen
- 16 mill NOK
- Bottom fixed OWT
- 1 year left

NGI

The importance of the foundation

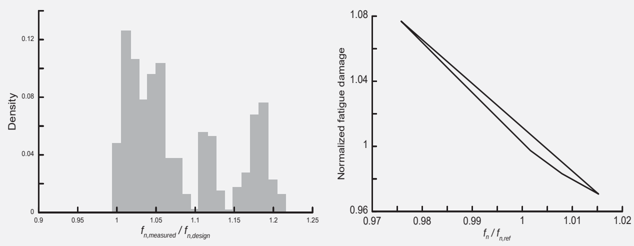

NGI Source: Kallehave, D., Byrne, B. W., LeBlanc Thilsted, C. and Mikkelsen, K. K. (2015)

Adapted from: Schafhirt, S., Page, A., Eiksund, G. R. and Muskulus, M. (2016)

Integrated dynamic analyses

- Aero dynamics
- Hydro dynamics
- Struktural dynamic
- Turbine controller (pitch)
- Soil/foundation respons

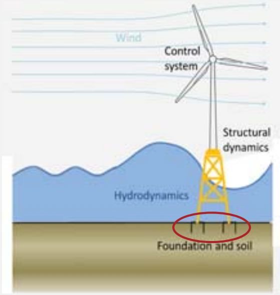

REDWIN model principles

- Application oriented models, such that the choice of model appear intuitive.
- User interface understandable for practitioners.
- General models, adaptable to different ground conditions.
- The models have to work in time domain analyses.

Geotechnical involvment

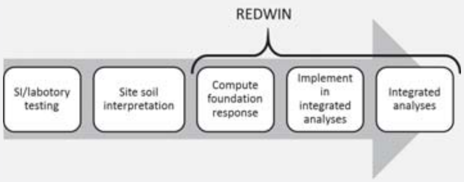

Current practise

- *p-y* springs (API, PISA) for monopiles
- Linear elastic springs for shallow fundations

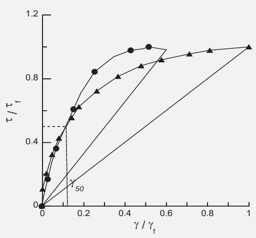

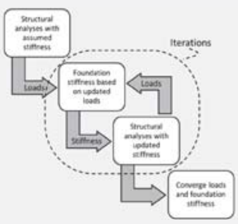

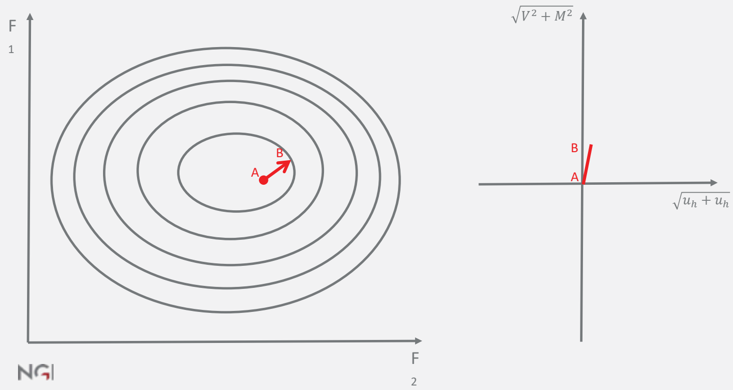

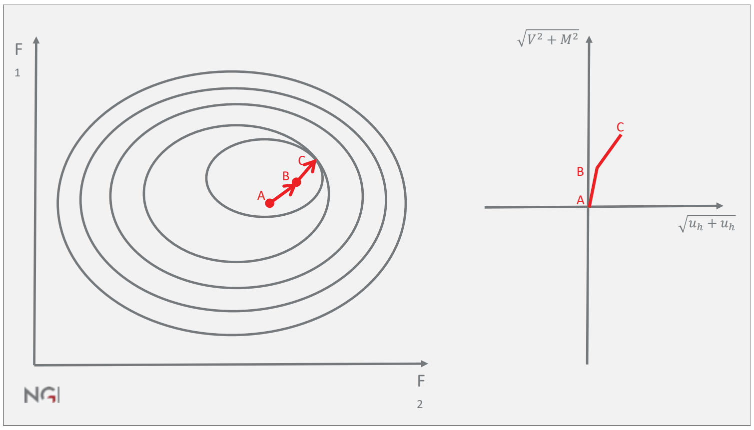
F
1
F
2
A
B
C
$\sqrt{V^2+M^2}$
$\sqrt{u_h+u_h}$
NGI

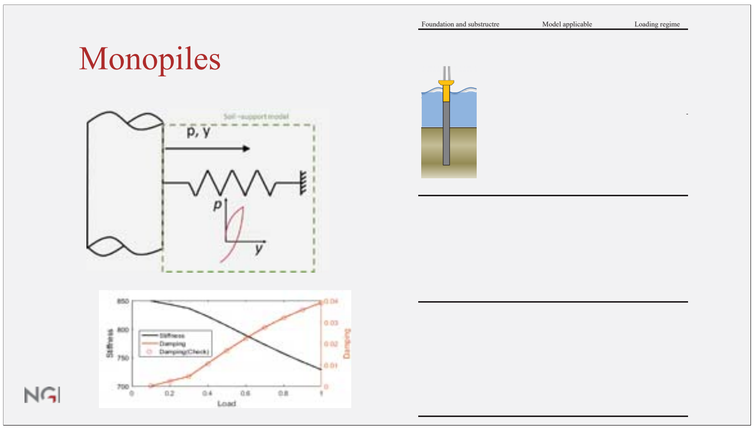
Monopiles
Soil-support model
p, y
p
y
Stiffness
Damping
Damping(Check)
Load
Foundation and substructre
Model applicable
Loading regime
NGI

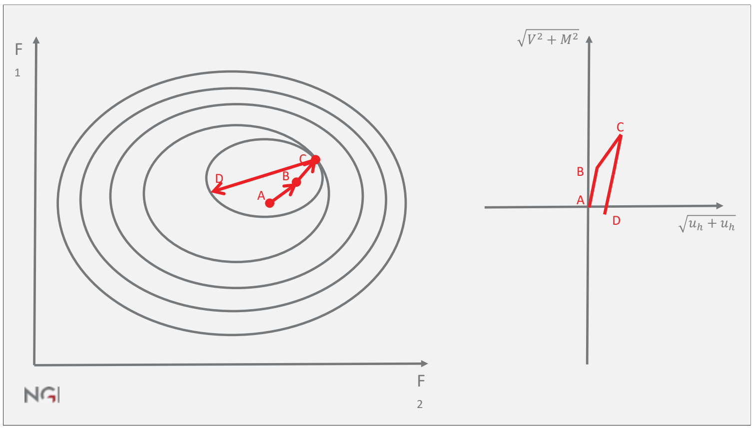
F
1
F
2
A
B
C
D
$\sqrt{V^2+M^2}$
$\sqrt{u_h+u_h}$
NGI

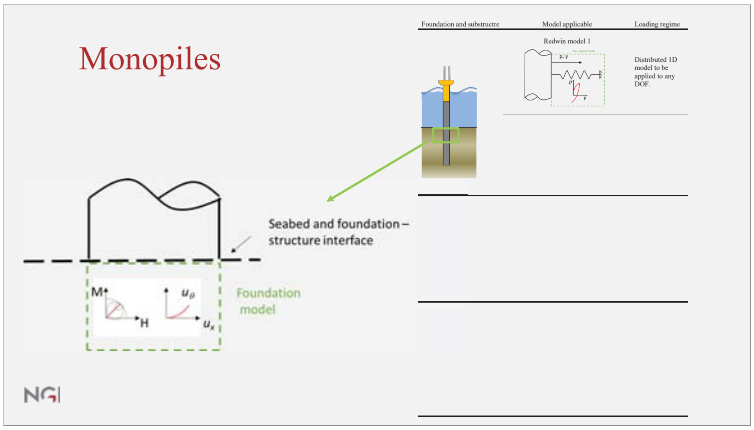
Monopiles
Seabed and foundation – structure interface
Foundation model
M
H
u_θ
u_x
Foundation and substructre
Model applicable
Loading regime
Redwin model 1
Distributed 1D model to be applied to any DOF.
NGI

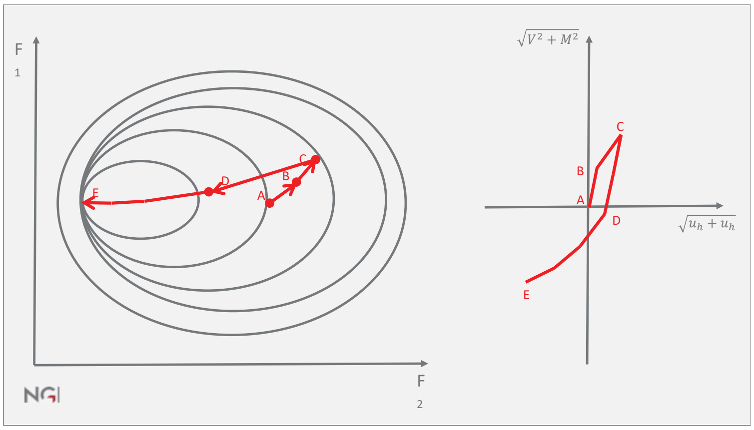
F
1
F
2
A
B
C
D
E
$\sqrt{V^2+M^2}$
$\sqrt{u_h+u_h}$
NGI

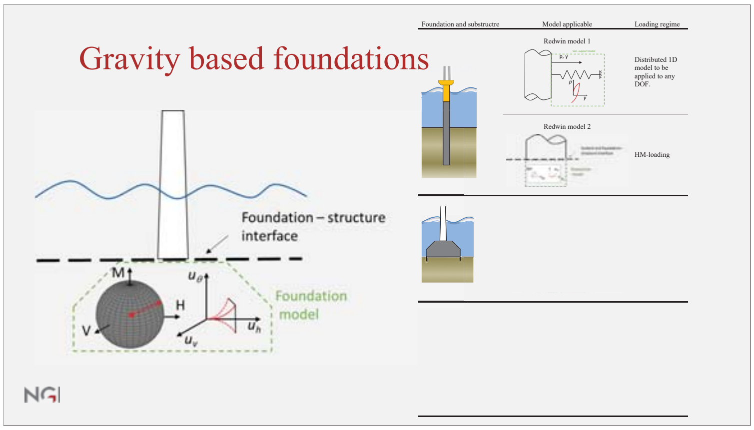
Gravity based foundations
Foundation – structure interface
Foundation model
M
H
V
u_θ
u_h
u_v
Foundation and substructre
Model applicable
Loading regime
Redwin model 1
Distributed 1D model to be applied to any DOF.
Redwin model 2
HM-loading
NGI

Bucket foundations

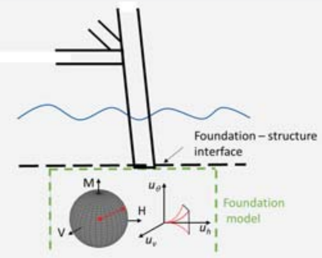

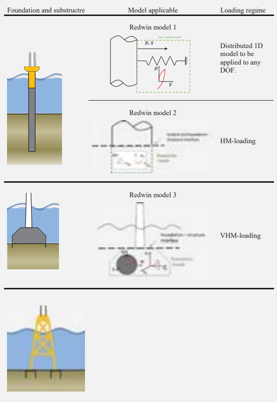

Foundation damping

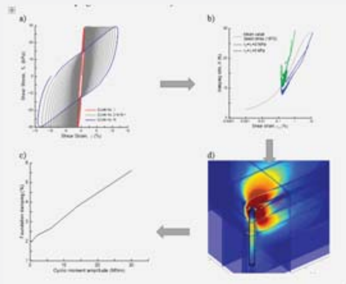

$$D_{found} = \frac{\sum(V \cdot E_h)}{4\pi \sum(V \cdot E_p)}$$

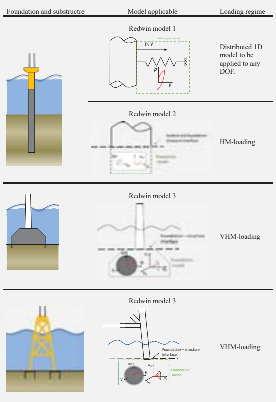

Effect of foundation behaviour on fatigue

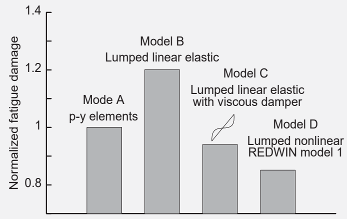

Aasen, S., Page, A. M., Skau, K. S. and Nygaard, T. A. (2017)

Model demonstration

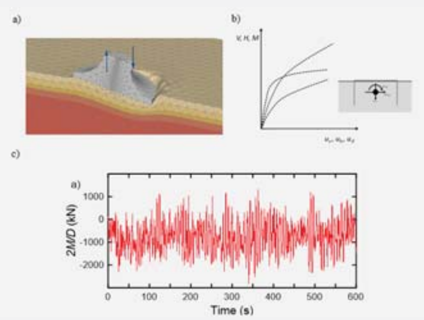

Comparison of model and measured response

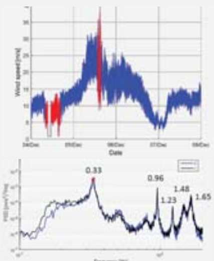

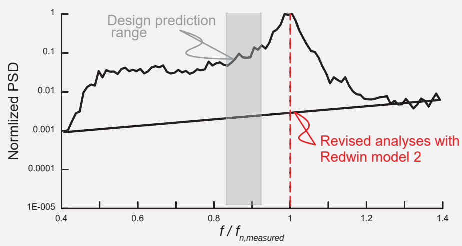

Summary and conclusions

- The models and tools developed in REDWIN seems to contribute to more accurate descriptions of foundations in design
- They include damping, which is often neglected.
- The knowledge of soil and site can be better utilized in design
- Improved accuracy reduce costs
- Currently working om cost reduction effects in more detail.

NGI

NGI

@infoNGI

NORWEGIAN GEOTECHNICAL INSTITUTE
NGI.NO

Thanks to:

The Norwegian research council, Statoil, Vattenfall og Statkraft

..and co-authors and contributors !

NGI

And thanks for your attention !

NGI

Catenary Mooring Chain Eigen Modes and the Effects on Fatigue Life

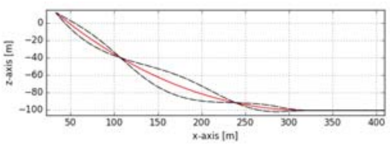

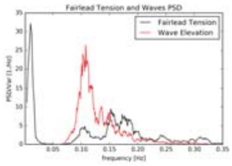

Tor Anders Nygaard and Jacobus de Vaal, IFE
Morten Hviid Madsen and Håkon Andersen, Dr.techn Olav Olsen AS
Jorge Altuzarra, Vicinay Marine Innovacion

IFE   DR. TECHN. OLAV OLSEN   VICINAY marine innovacion

Effects of Water Depth

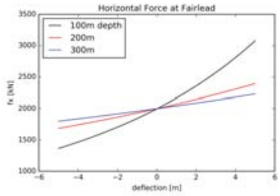

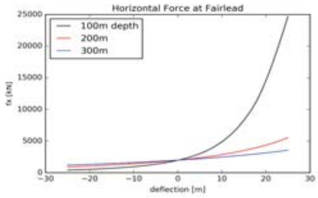

Decreasing water depth gives decreasing catenary effect and increasing force amplitudes for given floater motions

Sharp rise in force when the entire chain is lifted off the seafloor

Catenary Mooring

- Soft station-keeping, keep platform within envelope for current, drift forces and mean rotor thrust
- Should ideally not restrict platform first order wave motions. Platform inertia is averaging wave force peaks
- Restoring force by geometric stiffness of the catenary shape
- Possible conflict with maximum deflection of power cable

Typical Results for Fatigue

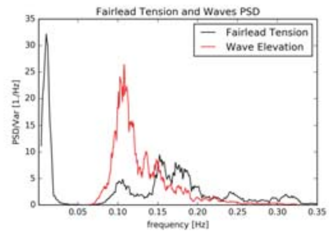

- First order wave excitation between 0.05 and 0.3Hz
- Fairlead Motions (not shown in figure) closely follow first order wave excitation + surge eigen mode
- Fairlead tension response is shifted towards higher frequencies
- The response above 0.12 Hz accounts for a significant part of the fatigue damage
- **Aim for work in progress: Understand the response , and make sure we compute this correctly.**

Baseline Fatigue Case

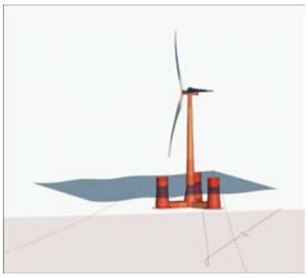

OO-Star Wind Floater with 6MW rotor, baseline FLS case, 3DFloat Animation

- OO-Star Wind Floater with 6MW rotor
- 100m water depth, anchor radius 750m
- 147mm chain with marine growth and hydrodynamic coefficients according to DNV-GL recommendations
- Wind (16 m/s), waves (Hs 3.7m) and current (0.15m/s) aligned with upstream mooring line

Contributions to fatigue, Rainflow Counting, 1

- Identify turning points
- Split in full- and half cycles
- Each cycle has a stress range, that together with the S-N curve and Miner rule correspons to fatigue damage
- Each stress cycle also has a frequency
- We have binned the stress cycles accoording to stress range and frequency, and can then sort out the contributions from different frequencies and stress ranges

Contributions to fatigue, Rainflow Counting, 2

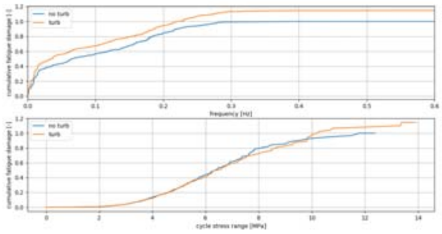

Important contributions to fatigue from frequencies up to 0.3Hz

Important stress ranges 2 – 10 MPa

Frequencies above 0.12Hz contribute to about 40% of the fatigue damage

These low stress ranges are commonly ignored on dry land. The standard does not recommend a cut-off in sea-water

Single Line, Fixed Fairlead, Waves Only

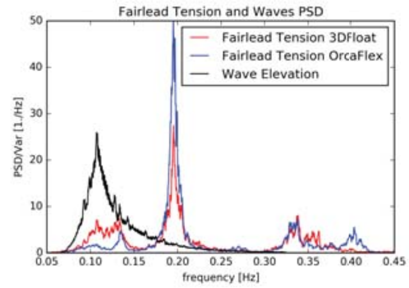

- Standard deviation of stress is around 0.2MPa, compared to 2MPa for FLS with floater, waves, current and wind.
- Stress due to direct wave loading on line is therefore not important compared to floater motions
- This case is useful also for identifying possible eigen frequencies

Models

- 3DFloat(IFE), SIMA(Sintef Ocean) and OrcaFlex(Orcina)
- Morison's equation on relative form.
- Nonlinearities: Co-rotated in 3DFloat and SIMA, direct specification of element matrices in global frame in OrcaFlex
- Chain eigen modes by linearization and eigen analysis in SIMA, and by bandpass-filtering of time-domain motions in 3DFloat

Forced Motion Sweep 0.15 – 0.6 Hz

3DFloat

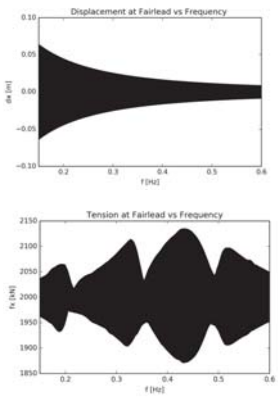

Single mooring line, pre-tension 2000kN

Harmonic inline horizontal motion of fairlead, increasing frequency slowly from 0.10Hz to 0.6Hz (shown from 0.15Hz due to initial transient)

Amplitude is decreased with increasing frequency to keep peak acceleration of fairlead constant

Peaks at approx. 0.19Hz, 0.33Hz and 0.42Hz

This corresponds relatively well with the waves only case shown in the previous slide

Eigen Modes Identification

- Single mooring line similar to baseline, but with constant properties. The results are simular, but the eigen frequencies change somewhat
- Pre-tension by positioning of fairlead to obtain 2000kN tension at fairlead.
- Apply irregular waves as in baseline case.
- Compare peaks in PSD plots with eigen analysis and forced fairlead motion results.
- Visualization of motions

Forced Motion of Fairlead

Comparison of models

Horizontal harmonic motion, 10cm amplitude

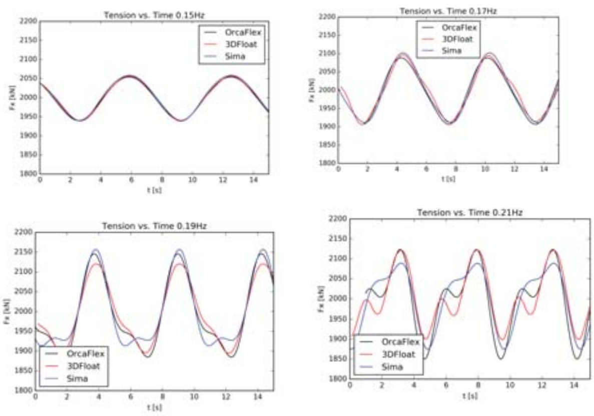

Forced Motion of Fairlead, 2

Horizontal harmonic motion, 10cm amplitude

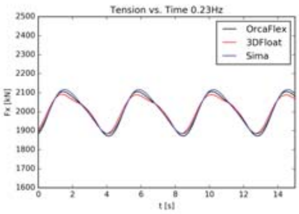

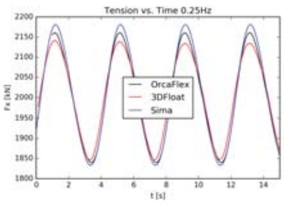

- Good agreement for 0.15 and 0.17Hz
- 0.19 and 0.21Hz are close to eigen frequency at 0.2Hz, some differences and sensitivity to model parameters
- Some differences at 0.23 and 0.25Hz, increased influence of inertial loads.
- At 0.2Hz, the dynamic response compared to the quasi-static response correspond to an «amplification factor of 10

Conclusions

- Computations of fatigue in a catenary mooring system applied at intermediate water depth with three state-of-the art integrated models show similar results, that are very different from quasi-static mooring line characteristics
- A mode with three half-waves between fairlead and touch-down shifts the response to higher frequencies than what is expected from the wave spectrum
- Important contributions to fatige are from stress ranges 2 – 10 MPa and frequencies up to 0.3Hz
- More experimental results are needed for model validation; previous succeseful validation was at a water depth corresponding to 200m, and with different influence of inertial forces relative to gravity and drag forces.

Model validation against experiments

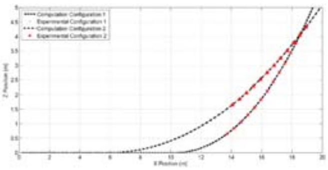

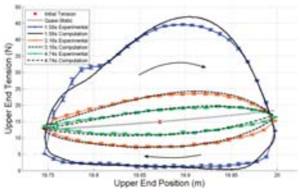

Azcona, J., Munduate, X., González, L., and Nygaard, T.A. (2017). *Experimental Validation of a Dynamic Mooring Lines Code with Tension and Motion Measurements of a Submerged Chain.* Ocean Engineering 2017, Vol. 129 , pg. 415-427.

- The models OPASS (CENER) and 3DFloat (IFE) were successfuly validated, but this was for 200m depth, and no marine growth.
- We have not found experimental results corresponding to our case study.

Acknowledgements - Innovative mooring systems

- Scope: Innovative Solutions for Shallow Water Mooring Systems
- RCN project under ENERGIX, project number: 256364
- Project Responsible: Dr.techn. Olav Olsen
- Partners: IFE, Statoil, Rolls Royce, Vicinay, OTS, Aibel, Servi
- External advisors: DNV-GL, NGI, FMGC

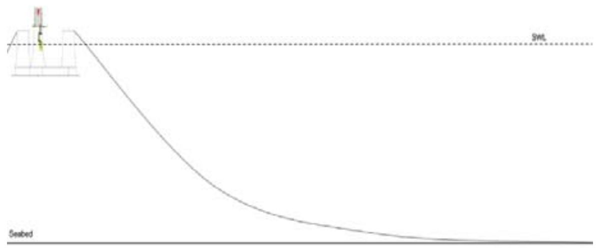

Sensitivity Studies

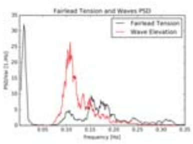

- Sensitivity studies on parameters regarding numerics and load models, with respect to response, in particular above 0.12Hz.
- Limited sensitivity, except the inertial coefficient in the Morison equation and marine growth.
- Extreme current can limit the response through increased viscous damping

E2) Installation and sub-structures

A numerical study of a catamaran installation vessel for installing offshore wind turbines, Z. Jiang, NTNU

FSFound – Development of an Instrumentation System for novel Float / Submerge Gravity Base Foundations, P. McKeever, ORE Catapult

Integrated conceptual optimal design of jackets and foundations, M. Stolpe, Technical University of Denmark

EERA DeepWind'18, Trondheim, 17 - 19 January 2018

A numerical study of a catamaran installation vessel for installing offshore wind turbines

Zhiyu Jiang
January 18, 2018

Postdoctoral researcher
Department of Marine Technology
Centre for Marine Operations in Virtual Environments (SFI MOVE)
Norwegian University of Science and Technology

Outline

1. Introduction
2. The catamaran installation concept
3. Numerical simulation
4. Conclusion

Outline

1. Introduction
2. The catamaran installation concept
3. Numerical simulation
4. Conclusion

Background

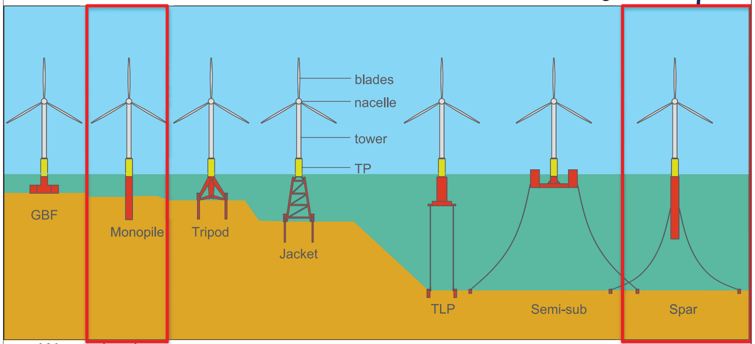

Water depth:
<20m<40m 50-70m >50-100m

Capital expenditure of offshore wind

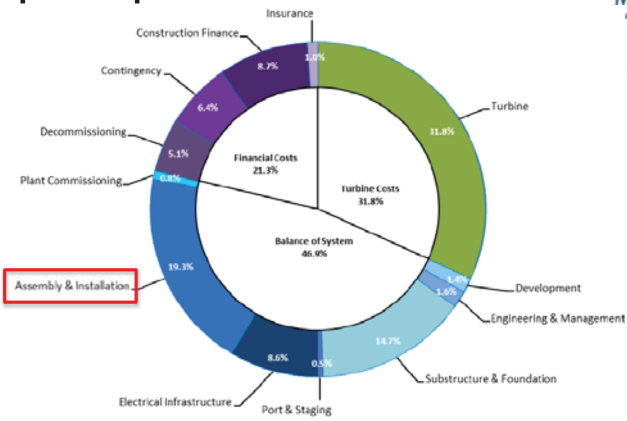

C. Mone et al. (2015) 2015 Cost of Wind Energy Review, NREL

Installation methods - foundation

Tripod installation using a jack-up vessel
(http://worldmartimenews.com)

Jacket installation using a floating vessel
(https://www.boskalis.com)

Monopile installation
(www.seawayheavylifting.com.cy)

Installation methods - rotor blade

Bunny ear
Vatenfall

Full rotor
Dong Energy

Single-blade installation
Fred Olsen Wind Carrier

Installation methods - full assembly

Saipem 7000
Statoil AS

Novel installation vessel
Ullstein AS

Purpose of numerical simulation

- Design and testing of novel installation methods
- Response-based prediction of limiting operational conditions
- Online decision support for offshore installations

Outline

1. Introduction
2. The catamaran installation concept
3. Numerical simulation
4. Conclusion

The catamaran installation concept

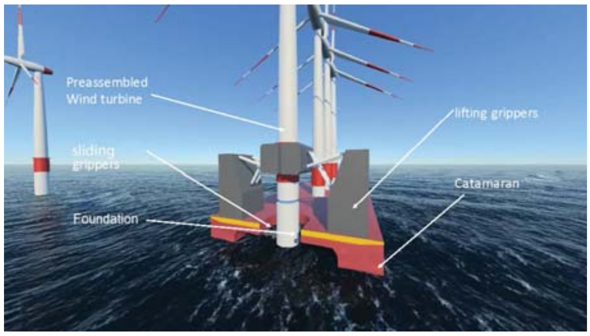

L.I. Hatledal et al. (2017)

Challenges of the concept

- Hydrodynamics
  hydrodynamic coupling, sloshing, viscous effect
- Structural dynamics
  coupled motion modes, mechanical coupling
- Automatic control
  station keeping of the vessel, active ballast system
  motion tolerance and control, landing force control

Installation procedure

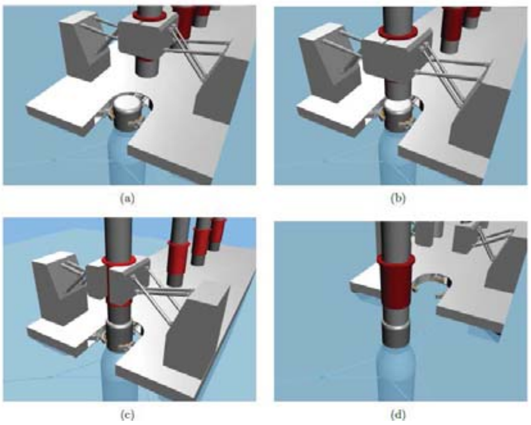

Monitoring the relative motions

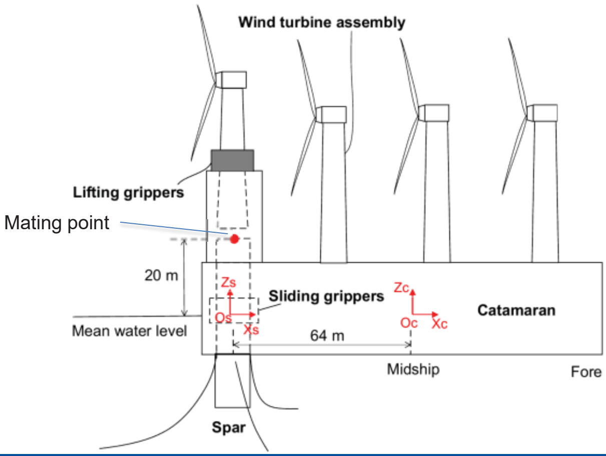

Properties of the catamaran

Catamaran with four wind turbines

Length overall (m)	L_{OA}	144
Breath moulded (m)	B	60
Spacing between monohulls at waterline (m)	L_{hull}	38
Draft (m)	T_c	8.0
Displacement mass (tonnes)	D	18502.9
Vertical center of gravity above baseline (m)	KGc	28.6
Transverse metacentric height (m)	GMt	66.4

Properties of the spar

Diameter at top (m)	L_{bd}	9.5
Diameter at waterline (m)	M_{bd}	14
Draft (m)	T_s	70
Displacement mass (tonnes)	D	11045
Vertical center of gravity above baseline (m)	KGs	30
Vertical fairlead position below waterline (m)	Z_f	15
Body origin in global coordinate system	(X_s,Y_s,Z_s)	(0,0,0)
Total length of mooring line (m)	L_{moor}	680
Diameter of upper chain segments (mm)	D_{up}	132
Diameter of lower chain segments (mm)	D_{low}	147

Outline

1. Introduction

2. The catamaran installation concept

3. Numerical simulation
   - Time-domain simulation
   - Frequency-domain simulation

4. Conclusion

Time-domain simulation

WADAM: Hydrodynamic analysis of the two-body system

HAWC2: Calculation of the wind forces on the turbine assemblies

SIMO: Time-domain coupled analysis
Catamaran with dynamic positioning system; spar with mooring lines;
sliding grippers between catamaran and spar

Modelling of the hydrodynamics

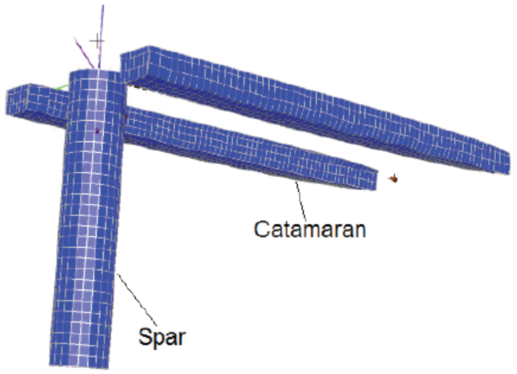

Modelling of the sliding grippers

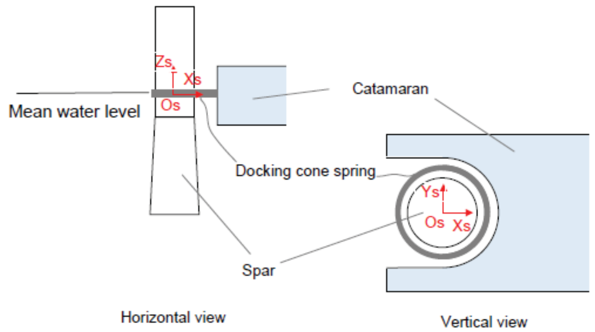

Modelling of the mooring system

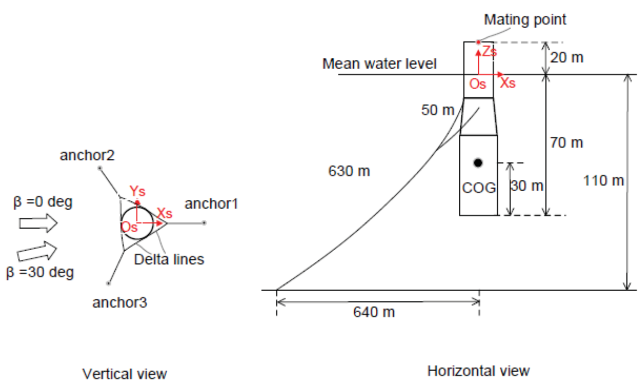

Frequency-domain approach

1. Hydrodynamic analysis of the two-body system

2. Short-term motion prediction of the mating point by using Response Amplitude Operators

Magnitude of the pitch RAOs

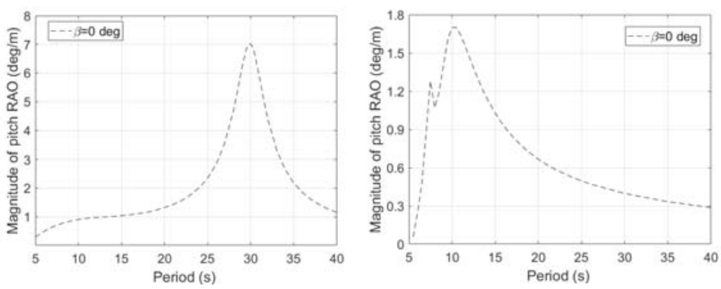

Spar Catamaran

Environmental conditions

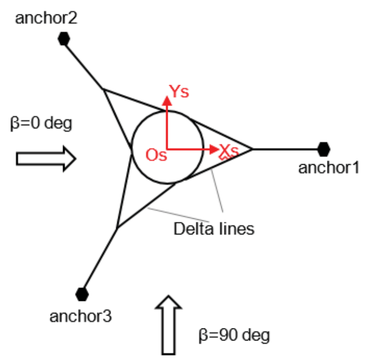

Hs=2.0 m Tp=6, 8,...,12 s β=0, 90 deg

Results - relative surge motion

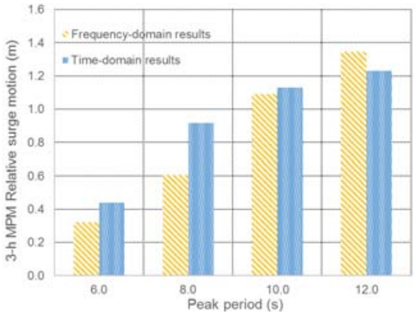

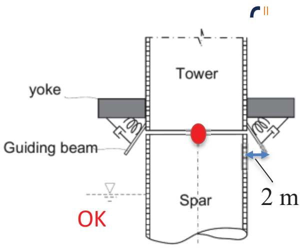

Hs=2.0 m, β=0 deg

Results - relative roll motion

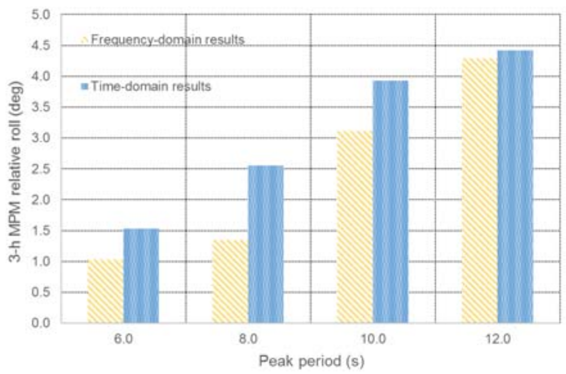

Hs=2.0 m, β=90 deg

Conclusion

- A numerical modelling approach of the catamaran installation concept is introduced.
- Future work is needed for implementing the active heave compensator, dimensioning of the catamaran, active ballast system, etc.

Acknowledgements

- Zhen Gao
- Karl Henning Halse
- Peter Christian Sandvik
- Zhengru Ren

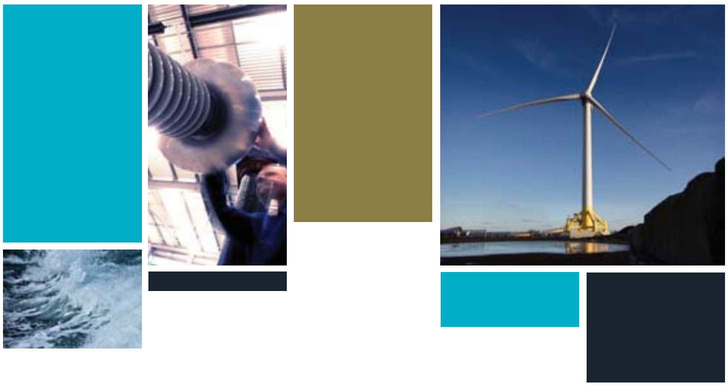

Instrumenting the Gravity base foundations for the Blyth Offshore Demonstration wind farm

January 2018 | Jonathan Hughes and Paul McKeever

CATAPULT Offshore Renewable Energy

ORE Catapult

Our Vision:
Abundant, affordable energy from offshore wind, wave and tide

- Reduce the cost of offshore renewable energy
- Deliver UK economic benefit
- Engineering and research experts with deep sector knowledge
- Independent and trusted partner
- Work with industry and academia to commercialise new technologies

80+ technical experts

ore.catapult.org.uk
@orecatapult

CATAPULT Offshore Renewable Energy

Agenda

- ORE Catapult
- Demowind and the FSFound Project
- The Blyth Offshore Demonstration Wind Farm
- The Project
- Instrumentation in the Marine Environment
- Future Work

ore.catapult.org.uk
@orecatapult

CATAPULT Offshore Renewable Energy

ORE Catapult Business Model

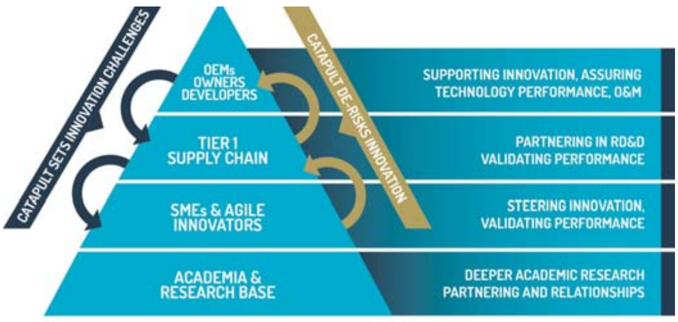

THE WORLD'S LARGEST PORTFOLIO OF OPEN-ACCESS FACILITIES:
£250M capital investment in assets dedicated to research and product validation

ore.catapult.org.uk
@orecatapult

CATAPULT Offshore Renewable Energy

The catapult network: A long-term vision for innovation & growth

11 Catapults

- Established by InnovateUK
- Designed to transform the UK's capability for innovation
- Core grant leveraged with industry and other public funding

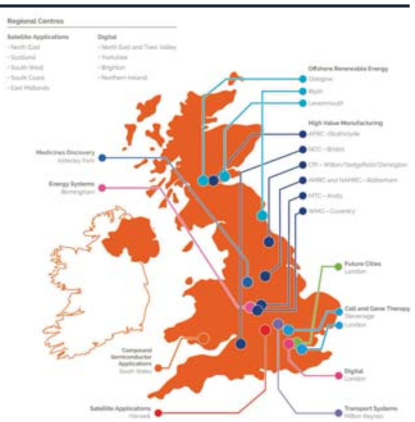

ore.catapult.org.uk
@orecatapult

CATAPULT Offshore Renewable Energy

Blyth Offshore Demonstrator Wind farm

- 5x 8.3MW turbines
- 6.5km off the coast of Blyth
- 191.5m Tip Height (AOD)
- Approx 40m Water Depth

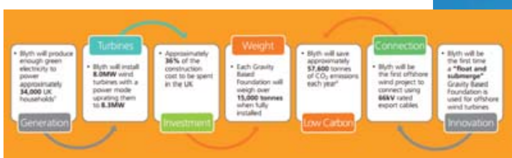

Installation of GBFs at Blyth – Satellite Imagery

Image from Aeronet-OC Project

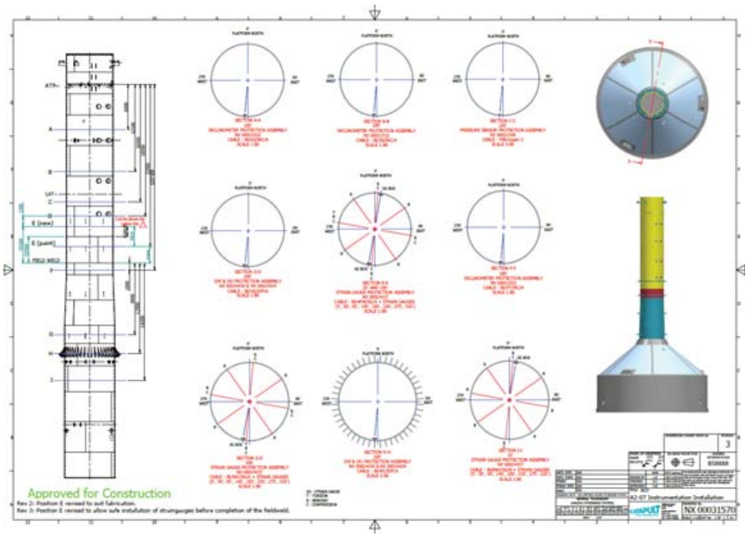

FSFound Project Aims

To validate the FS GBF solution as an alternative solution to energy provision by proving that FS GBF performs as intended and can be installed cost-effectively;

- *To conduct a range of simulation and modelling studies to minimise the uncertainties and inefficiencies in the deployment process and in various weather windows;*
- *To compare the actual costs and performance with the cost-benefit analysis performed;*
- *To assess structural response to extreme and fatigue loads on the FS GBF and compare theoretical loads with real ones;*
- *To establish the effect of cyclic loadings on the seabed through monitoring and measurement and verify/calibrate models for differential settlements in the soil;*
- *To establish the optimal seabed preparation requirements (i.e. minimum preparation depth).*

Caisson Pressure Sensors

- Upper sensor mounted near vent (sea reference)
- Lower sensor mounted near top of slipform
- 3 sets of 2 mounted at 120° spacing
- 4Hz sample rate

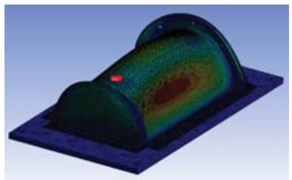

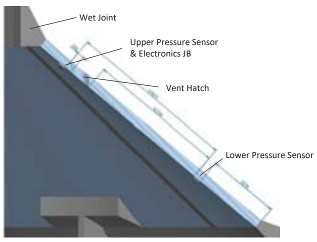

- Indirect measurement of depth
- Also can calculate period
- Triangulation may permit direction measurement
- Comparison after calculation with other wave data on site.
- Data corrected for Atmospheric variation

Aims of the measurement campaign?

1. Validation of the design, including input to verifying simulation models
2. Providing feedback to the design limits of the structure, such that an updated life expectancy can be calculated (if required)
3. Understanding the interaction between:
   - GBF and Seabed (e.g. settlement)
   - GBF and WTG (e.g. modal interaction, load transfer)
   - GBF/WTG combination and the Environment (e.g. wind/wave misalignment loads)
   - Effect of internal divisions on the displacement of the caisson outer walls
4. Provide inputs to the design of a Structural Health Monitoring system for GBF system
5. Provide inputs to the cost model, in the form of estimated O&M OPEX costs
6. Provide a platform for the development of a prognostic methodology for NDT of GBFs

Inclination and Mode Shapes

- High stability servo inclinometers
- Measurement range of +/-14.5°
- Resolution of 0.001°
- Positioned to match ANSYS AQWA modelling nodes
- Positioning is critical to interpretation of data

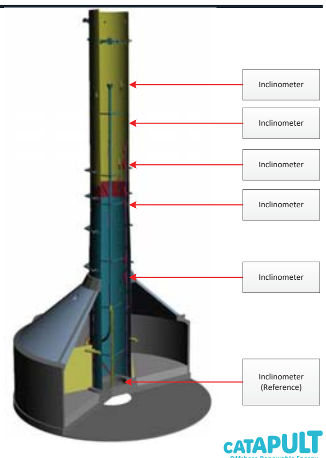

Load Paths

- Initially aimed to installed SGs into Concrete, however not possible
- Structure can be analysed through load paths rather than direct loads
- Bending, Compression and Torsion are independently assessed
- Loads measured above and below "Wet Joint" – calculation of loads into caisson roof
- Loads measured at field weld to establish effect of loads from turbine and torsional loads

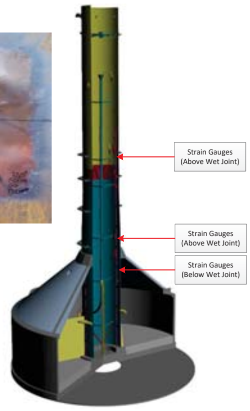

Installation Challenges

- Vertical installation requires significant additional time and risk management
- Installing delicate sensors; to fine tolerances; in the wet; hanging from a rope…
- Horizontal installation challenging without the ability to roll or traverse
- Location Referencing
- Novel and Evolving design
- Fitting research into a complex and time-critical construction project

Corrosion

- Structures are filled ballasted with sand and seawater flooded below LAT
- Water is expected to have slow transit rate through structure, leading to oxygen depletion
- Dissolved Oxygen sensors are installed to monitor
- Water level in shaft is monitored for comparison
- DO Sensors use dynamic luminescence quenching rather than an EC sensor

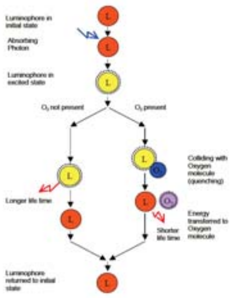

From AADI 4330 manual

How close are models to their physical counterparts?

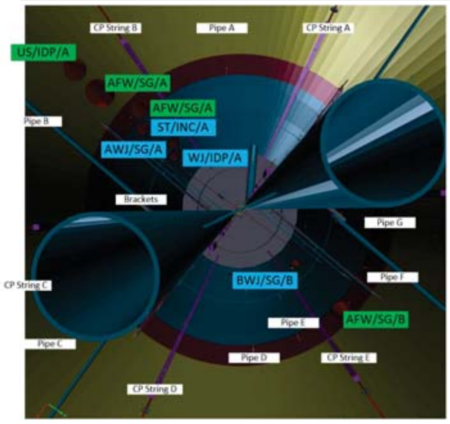

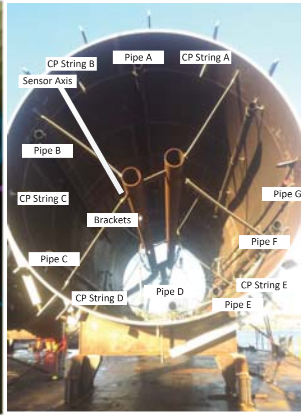

Connection and Protection

- Instruments are useless if they don't work or give questionable data
- Welding and Bolting were not permitted by the designer
- All instruments are permanently bonded, but need a temporary method of attachment until the adhesive "grabs"
- Protection needed against ballasting force
- Protection against settlement
- Subsea-grade cables and connectors
- Full epoxy fill to instrumentation systems

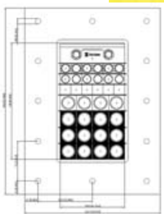

Software Systems

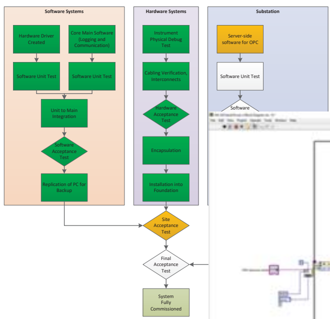

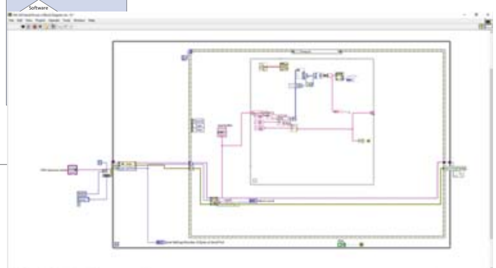

Example Data – Inclinometer Profile

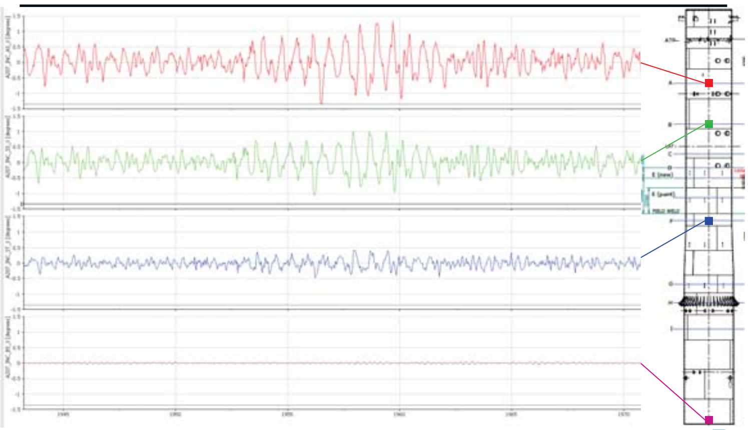

Contact us

GLASGOW
ORE Catapult
Inovo
121 George Street
Glasgow
G1 1RD

T +44 (0)333 004 1400
F +44 (0)333 004 1399

BLYTH
ORE Catapult
National Renewable Energy Centre
Offshore House
Albert Street
Blyth, Northumberland
NE24 1LZ

T +44 (0)1670 359 555
F +44 (0)1670 359 666

LEVENMOUTH
ORE Catapult
Fife Renewables Innovation Centre (FRIC)
Ajax Way
Leven
KY8 3RS

T +44 (0)1670 359 555
F +44 (0)1670 359 666

info@ore.catapult.org.uk
ore.catapult.org.uk

Planning for Analysis

- Flowcharts convert theory into algorithm for processing

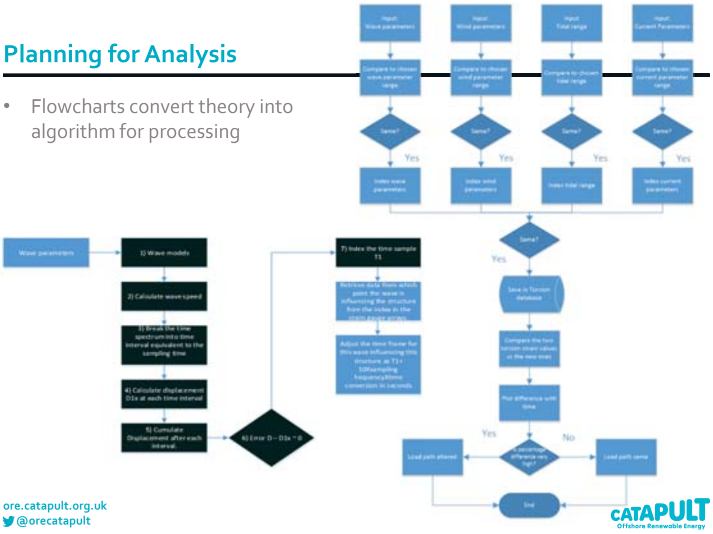

Why is Research in a Commercial Project so challenging?

Commercial Ideals

- Strong "proven" technical solution
- Warrantable performance allowing for "tight" contracts
- No unexpected outcomes

Research Ideals

- Cutting Edge "novel" technical solution
- Project technical output comes before programme
- Unexpected outcomes are interesting (isn't that why we do it?)

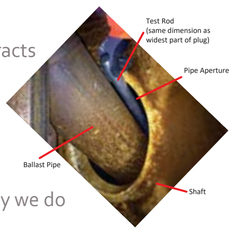

The best common outcomes only come through

- Close collaboration between practical and theoretical work
- Novel techniques but proven technologies and strong theoretical base
- Trial and error (more trials, fewer errors!)

DTU

Integrated design optimization of jackets and foundations for offshore wind turbines

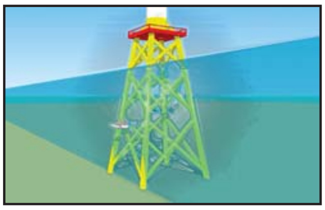

Kasper Sandal
Chiara Latini
Varvara Zania
Mathias Stolpe

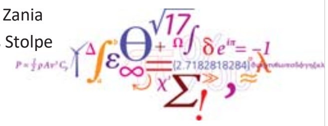

DTU Wind Energy
Department of Wind Energy

ABYSS – *Advancing BeYond Shallow waterS*
funded by Innovation Fund Denmark

DTU

This is how optimization can become a valuable tool for structural engineers in offshore wind

Design considerations

minimize $f(x)$
subject to $Ax - b \leq 0$
$\underline{\sigma} \leq \sigma(x) \leq \overline{\sigma}$
$\underline{\omega} \leq \omega(x) \leq \overline{\omega}$

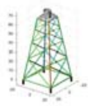

Optimal design problem

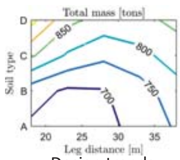

Design trends

DTU

This is how optimization can become a valuable tool for structural engineers in offshore wind

ENGINEERING **SCIENCE**

Design considerations

minimize $f(x)$
subject to $Ax - b \leq 0$
$\underline{\omega} \leq \omega(x) \leq \overline{\omega}$

Optimal design problem

ADDED VALUE

Design trends

DTU

How to formulate a numerical optimization problem: Let *x* be a vector of variables, where we want to minimize *f*(*x*)

Objective function

minimize $f(x)$
subject to $g(x) \leq 0$

Constraint functions

DTU

How to design a jacket and its foundation with optimization: Let *x* describe the design, *f*(*x*) the cost, and *g*(*x*) the engineering limits

Cost ≈ Jacket + foundation mass

minimize $f(x)$
subject to $g(x) \leq 0$

Engineering limits:

1. Fatigue limit state
2. Ultimate limit state
3. Soft-stiff frequency range

x = design variables:

1. Diameters & wall thickness
2. Diameters, wall thickness, & length

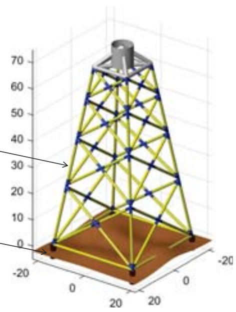

DTU

The optimization problem has very few design variables, but a high number of nonlinear constraints

minimize $f(x)$
subject to $g(x) \leq 0$

- 24 design variables for the jacket
- 3 design variables for the foundation
- 7k constraints for each static load
  - Stress along all tubular welds
  - Shell buckling & column buckling
  - Foundation capacity
- 2 frequency constraints

The problem is implemented in the special purpose software JADOP (Jacket Design Optimization)

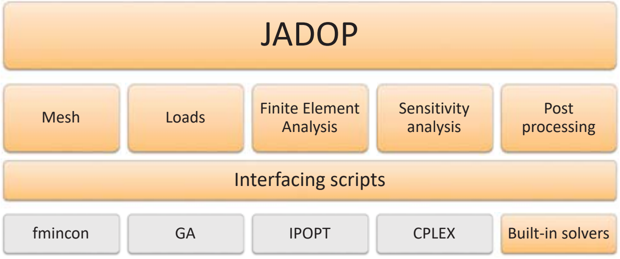

We make assumptions in the structural analysis which are suitable for the conceptual design phase

- **Timoshenko beam elements** for the support structure
- **Linear 6-dof response** for each foundation
- **4 Damage equivalent loads** for the fatigue limit state
- **3 Extreme static loads** for the ultimate limit state
- **Conservative analysis** of column buckling
- **Stress concentration factors** in welded tubular joints

<u>**No safety factors are applied in the following examples**</u>

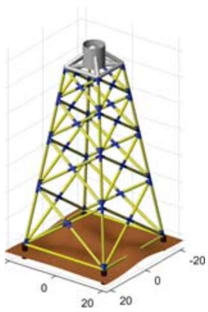

For a given design problem (10 MW turbine, 50 m depth, piles), the total mass was minimized to 631 tons (in 5 minutes on a laptop)

Jacket	
Mass:	491 tons

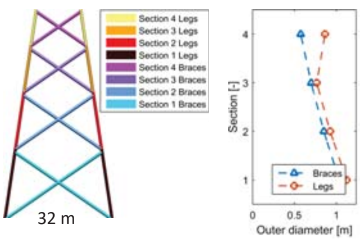

Piles in sand	
Diameter:	1.41 m
Length:	50 m
Mass:	140 tons

Soil:	Medium stiff sand
Foundation:	Piles
Design procedure:	API

JADOP has a parameterized mesh which makes it a quick task to modify for example the leg distance

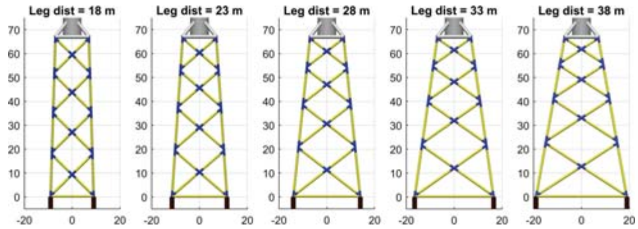

When support structures with different leg distance are optimized, jacket mass and foundation mass show opposite design trends

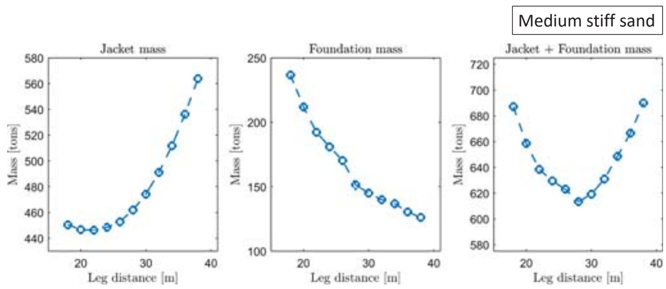

The optimal leg distance will depend on for example the soil stiffness

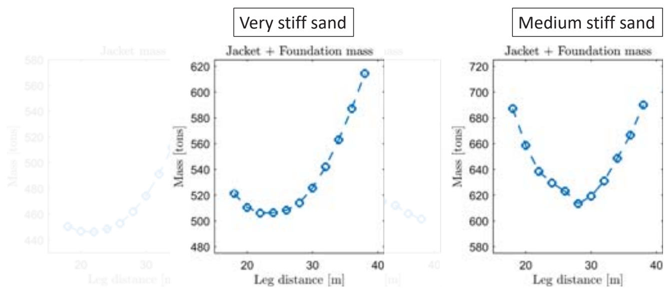

But several other aspects of the anchoring will also influence the design problem

We have looked at:

- Piles & suction caissons
- Sand & clay
- Varying soil stiffness
- Different design procedures for piles

Piles

Source: 4coffshore

Suction caisson

Source: SPT Offshore

The design considerations are "translated" into an optimization problem, and it is now a quick task to generate design trends

Design considerations

minimize $f(\boldsymbol{x})$

subject to $\boldsymbol{A}\boldsymbol{x} - \boldsymbol{b} \leq \boldsymbol{0}$

$\underline{\boldsymbol{\sigma}} \leq \boldsymbol{\sigma}(\boldsymbol{x}) \leq \overline{\boldsymbol{\sigma}}$

$\underline{\boldsymbol{\omega}} \leq \boldsymbol{\omega}(\boldsymbol{x}) \leq \overline{\boldsymbol{\omega}}$

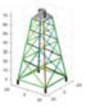

Optimal design problem

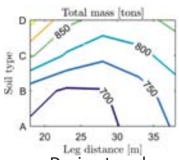

Design trends

The figure below shows how jacket mass and foundation mass change as functions of both leg distance and soil stiffness (A=stiff, D=soft)

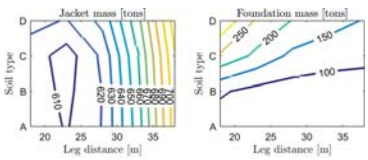

Soil = sand

Foundation = piles

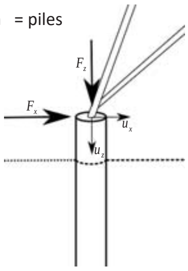

The preferred leg distance now depends on the soil stiffness, and perhaps also the desired fundamental frequency

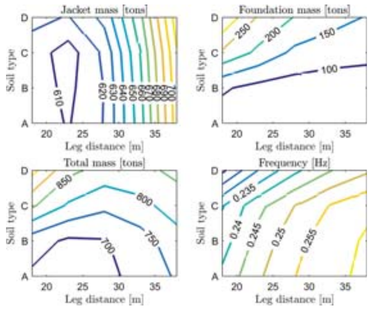

Soil = sand

Foundation = piles

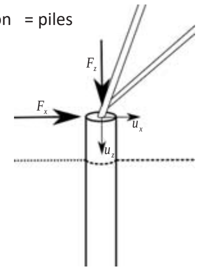

Structural optimization is used to automate the "well-defined" engineering tasks of conceptual support structure design

Cost function

minimize $f(\boldsymbol{x})$

subject to $\boldsymbol{g}(\boldsymbol{x}) \leq \boldsymbol{0}$

$\boldsymbol{x}$ = design variables

Engineering limits:

1. Fatigue limit state
2. Ultimate limit state
3. Soft-stiff frequency range

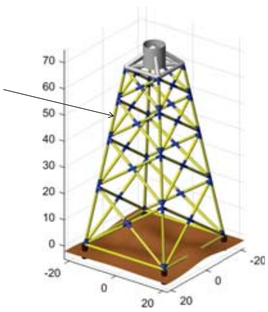

With a tool like JADOP it is then quick & easy to investigate how input conditions influences the design

minimize $f(\boldsymbol{x})$

subject to $\boldsymbol{g}(\boldsymbol{x}) \leq \boldsymbol{0}$

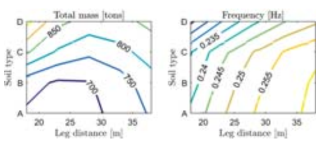

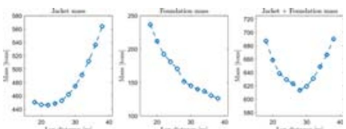

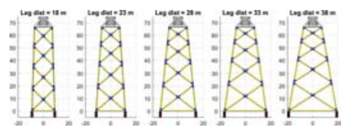

F) Wind farm optimization

The DIMSELO Project (Dimensioning Sea Loads for Offshore Wind Turbines), F. Pierella, IFE

A savings procedure based construction heuristic for the offshore wind inter-array cable layout optimization problem, S. Fotedar, University of Bergen

Calibration and Initial Validation of FAST.Farm Against SOWFA, J.Jonkman, National Renewable Energy Laboratory

An Experimental Study on the Far Wake Development behind a Yawed Wind turbine, F. Mühle, NMBU

DIMSELO KPN Project

Fabio Pierella

Wave models

- Deep water
  - Low steepness (A/λ) of the wave
  - Linear solution is satisfactory
- Shallower waters
  - $h = 25m - 40m$
  - High steepness
  - Nonlinear effects
- **Bottom-fixed wind farms are positioned at this depth**

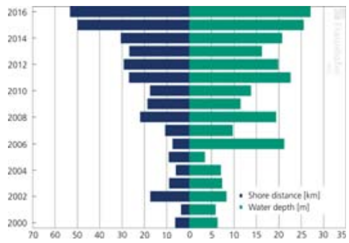

IWES (2016)

DIMSELO

<u>Dim</u>ensioning <u>Se</u>a <u>Lo</u>ads (2014-2017)

- Knowledge Building Project
  - Awarded by NFR
- Challenge standard design practice for Offshore Wind Turbines
- Consequences of advanced engineering models
- IFE
  - Project responsible
- DTU, NTNU
  - Academic Partners
- Statoil, Statkraft
  - Industrial partners

Diffraction of waves

- Large structures scatter incoming waves
- Leads to reduction in loads
- **Important for large monopiles**
  - $T = 2.5\ s$
  - $h = 30\ m$

$D = \lambda = 10\ m$

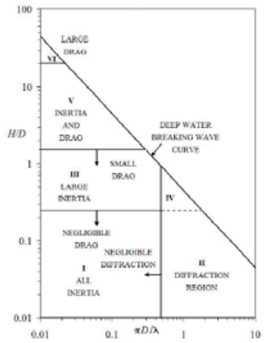

Chakrabarti (1987)

Wave models

- Deep water
  - Low steepness (A/λ) of the wave
  - Linear solution is satisfactory
- Shallower waters
  - $h = 25m - 40m$
  - High steepness
  - Nonlinear effects
- **Bottom-fixed wind farms are positioned at this depth**

Le Mehaute (1976)

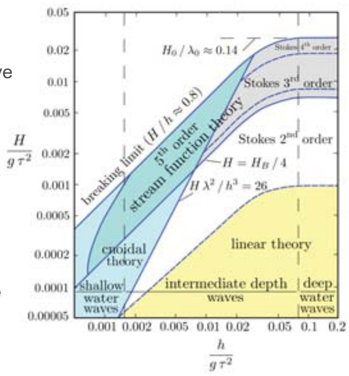

Design calculations via integrated models Current practice

	Fatigue	Extreme loads
Kinematics model	Linear irregular waves	Embedded 50-yr nonlinear wave
Load Model	Morison equation LPT	Morison equation
Challenges	Non-linearity Wave diffraction	Accuracy of non-linearity Directionality

Questions at the base of DIMSELO

Kinematic loads can drive the design

1. How conservative are standard kinematics and force models?
2. Are the better engineering models? Can they be used?
3. *Can we quantify* the consequences of applying them?

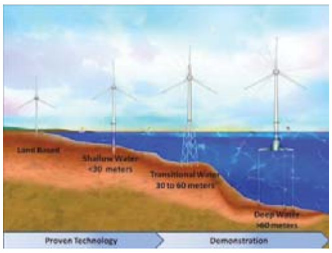

NREL (2016)

DIMSELO

Structure of the project:

WP1 Sea Load Modeling	WP2 Wave Modeling	WP3 Aerodynamics VLR
• Slender body models • Large cylinders (First order Diffraction)	• Irregular 2nd order waves • Embedment of nonlinear waves	• Coherence of turbulence spectra • 6p and 2nd order bending moment interaction

WP1
Rainey slender body model

- Based on an energy balance methodology and not on pressure integration considerations
- Three contributions on a submerged structure
  - Distributed force F_d
  - Distributed moment M_d
  - Force on free end F_{pfe}
  - Force on piercing point F_{pfs}

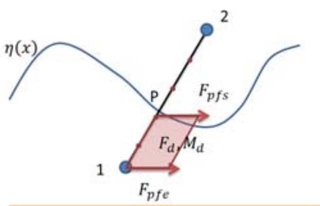

WP1
McCamy-Fuchs load model

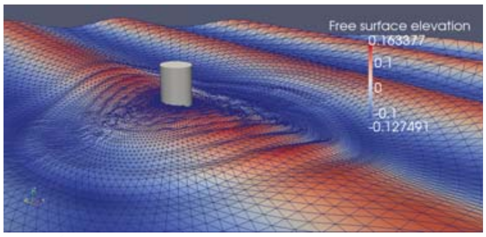

Scatter of waves by cylinder

WP1
McCamy-Fuchs load model

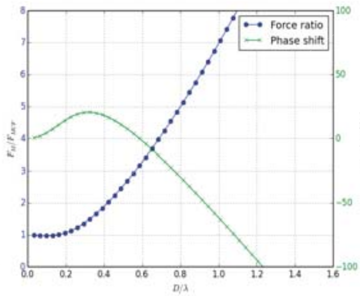

Ratio of force predicted by Morison force model over MacCamy-Fuchs force model

WP2
Embedment of streamfunction waves

- **Standard**: 50-yr wave «cut-and-paste» in irregular linear waves
- **DIMSELO:** «Find and replace» highest linear wave with nonlinear SF wave
- Use of the Hilbert transfer to calculate the embedment period
  - Pierella, F., Stenbro, R., Oggiano, L., de Vaal, J., Nygaard, T. A., & Krokstad, J. (2017, July). Stream Function Wave Embedment into Linear Irregular Seas: A New Method Based on the Hilbert Transform. In *The 27th International Ocean and Polar Engineering Conference.* (ISOPE 2017)

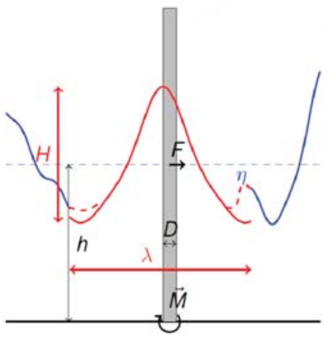

WP2
Second-order irregular short-crested

- Full second-order short-crested waves
  - Sharma and Dean (1981)
- **Standard**: not possible without simplifications
- **DIMSELO**: Full theory implemented
  - 2D FFT calculation in space

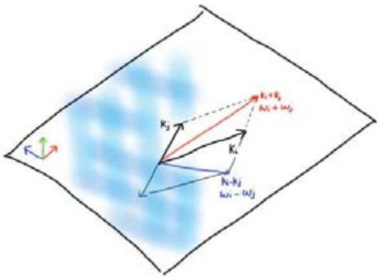

10 MW Monopile 25m: design characteristics

- 1st bending natural frequency
  - $f = 0.23\ [Hz]$
  - Between 1p and 3p
- Transition piece
  - Point mass $z = 19\ [m]$
- Pile
  - Steel

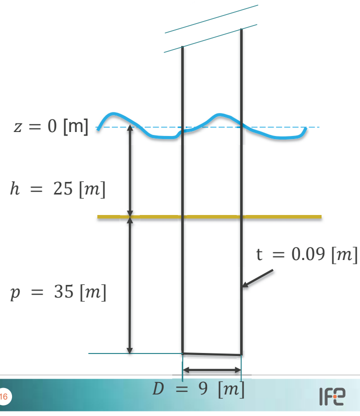

DIMSELO Reference wind turbines

- Site
  - Dogger Bank
- Water depth
  - $h = 25m\ ;\ h = 35m$
- Metocean conditions: Statoil
- Foundations
  1. XL Monopile 25m
  2. XL Monopile 35m
  3. Jacket 35m
     - Designed by Kasper Sandal (DTU)

Monopile 25m: Soil model

- P-y soil springs
- Logarithmic decrement of 1st tower bending oscillation
  - $\delta = \frac{1}{n} \ln \frac{x_n}{x_{n+1}}$
- 1.5 % damping as a fraction of critical
  - $\zeta = \frac{\delta}{2\pi} = 0.015$
- Achieved by installing dampers at the mudline

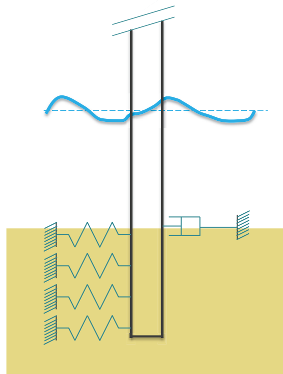

Monopile 25m 10MW

- Turbine
  - DTU 10MW reference wind turbine
  - $H_{hub} = 119.\ [m]$
- DTU controller
- Tower
  - Steel, onshore tower
- Substructure
  - Designed ad-hoc
- **Fatigue and Extreme loads**

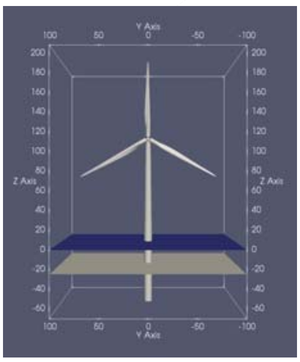

Monopile 25m

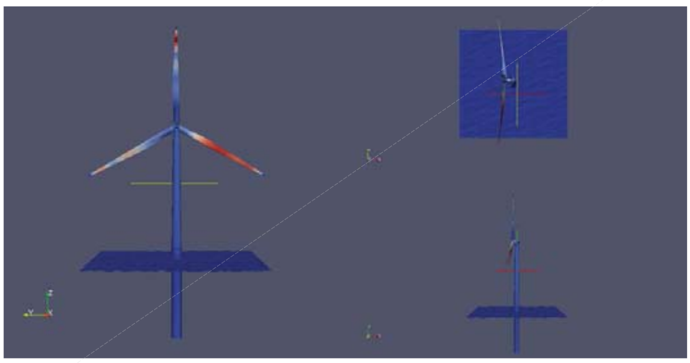

Jacket Model

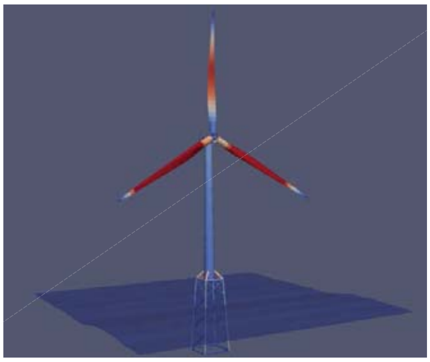

Monopile 25m
Tower side-to-side bending

- $f = 0.23\,Hz$

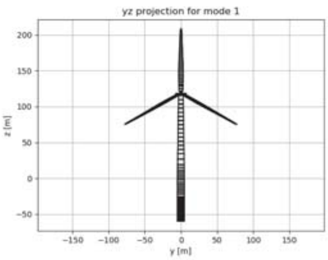

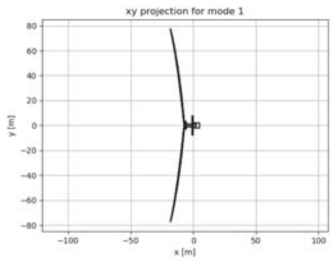

Monopile 25m
Rotor edgewise bending

- $f = 0.48\,Hz$

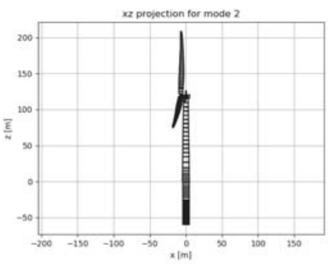

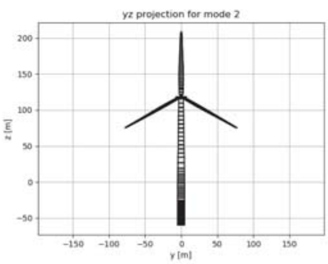

Monopile 25m
Rotor flapwise with yaw

- $f = 0.57\,Hz$

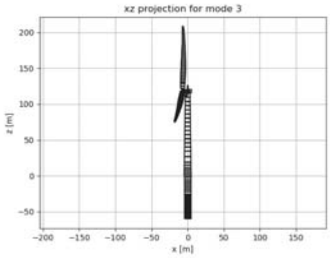

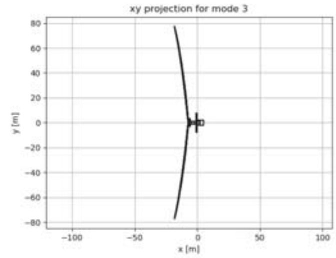

Monopile 25m
Rotor flapwise with tilt

- $f = 0.59\,Hz$

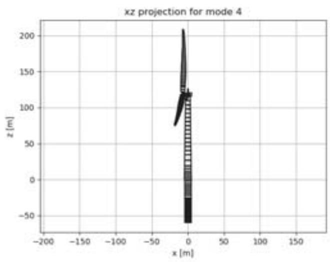

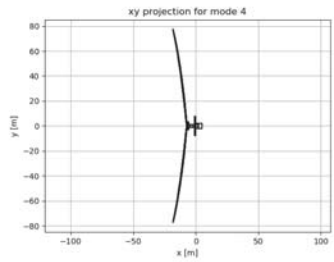

Monopile 25
Collective flapwise

- $f = 0.62\,Hz$

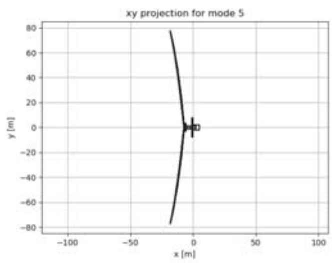

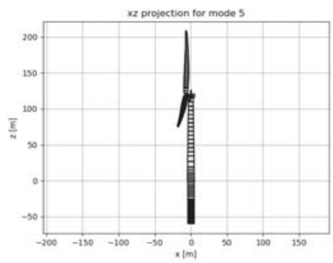

MetOcean conditions for DIMSELO structures

- Northern sea location
  - Dogger Bank
- Wind speed
  - conditional on H_S
  - Aligned with waves
- Turbulence
  - IEC-61400-1
- $\sum P(H_S, T_P) = 100$

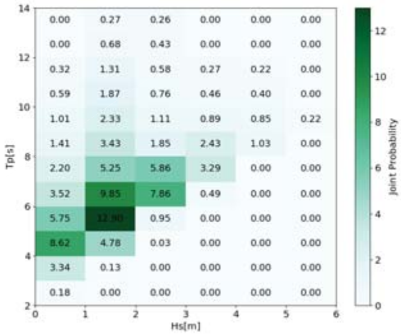

Wind Speed@100 [m] [m/s] 5.8 9.1 13.5 17.6 21.0 23.8

Example: effect of kinematics 1st vs 2nd order

- Histogram
- Sea state
  - $H_S = 3.5\,[m], T_P = 7.5[m]$
- Mudline x-wise force

	1	2
Kinematics	1st order	2nd order
Load Model	Morison	Morison
Directonal spread	Long crested	Long crested

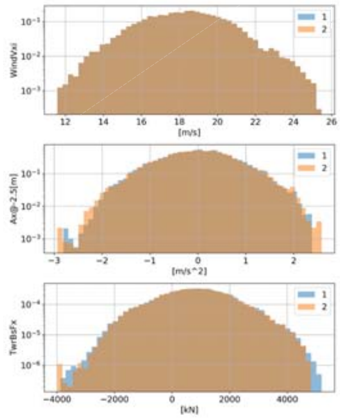

Combination of models

- Force models
  - Rainey force model
  - McCamy-Fuchs force model
  - Morison force model
- Wave kinematics
  - First-order irregular waves
  - Second-order irregular waves
- Directional Spread
  - Short crested
  - Long crested

= 10 simulations per (H_S, T_P) Jonswap spectrum

Example: effect of kinematics 1st vs 2nd order

- Exceedance probability
- Sea state
  - $H_S = 3.5\,[m], T_P = 7.5[m]$
- Mudline x-wise force

	1	2
Kinematics	1st order	2nd order
Load Model	Morison	Morison
Directonal spread	Long crested	Long crested

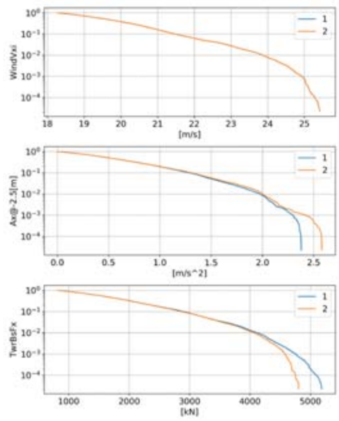

Example: effect of kinematics 1st vs 2nd order

- Time series 30 min
- Sea state
  - $H_S = 3.5\,[m], T_P = 7.5[m]$
- Mudline x-wise force

	1	2
Kinematics	1st order	2nd order
Load Model	Morison	Morison
Directional spread	Long crested	Long crested

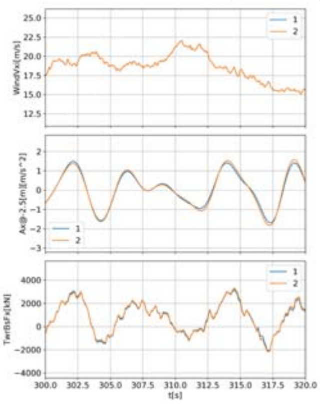

A more compact view

- Fatigue IEC-61400-1
  - LC 1.6 → operation with NTM
- Simulate N series of 30 minutes
- Extract timeseries of important parameters
  - Mudline Fx [kN]
  - Mudline My[kNm]
  - Blade root Flapwise Mf[kNm]
- DAMAGE EQUIVALENT LOAD (DEL)
  - Regular load that would do the same damage as the irregular one if applied in a 1-min sinusoid

$$D \propto DEL^m$$

- **D :** damage (inverse of lifetime)
- **DEL :** damage equivalent load
- **m** : Wöhler exponent (m=3 for steel)

Morison – 1st order – Long Crested (Base case)

Fatigue due to Mudline Fx

(H_S, T_P) joint probability

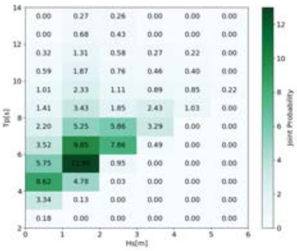

Example: effect of force model

- Histogram
- Sea state
  - $H_S = 3.5\,[m], T_P = 7.5[m]$
- Mudline Fx

	Morison	Maccamy
Kinematics	1st order	1st order
Load Model	Morison	MacCamy-Fuchs
Directonal spread	Long crested	Long crested

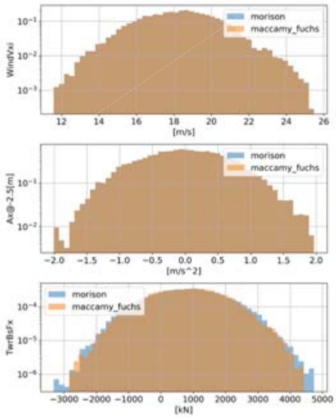

MacCamy-Fuchs – 1st order – Long crested

Fatigue due to Mudline Fx

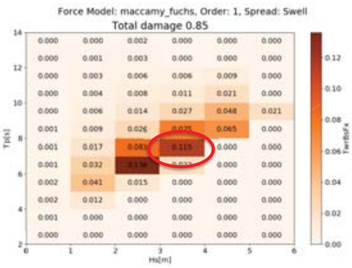

Example: effect of force model

- Exceedance probability
- Sea state
  - $H_S = 3.5\,[m], T_P = 7.5[m]$
- Mudline Fx

	Morison	Maccamy
Kinematics	1st order	1st order
Load Model	Morison	MacCamy-Fuchs
Directonal spread	Long crested	Long crested

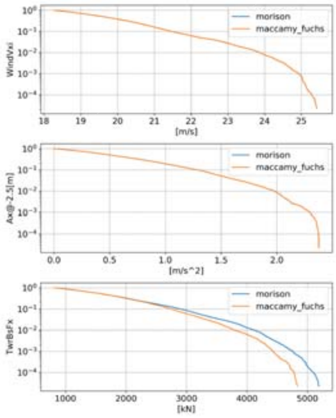

Example: effect of force model

- Time series
- Sea state
  - $H_S = 3.5\,[m], T_P = 7.5[m]$
- Mudline Fx

	Morison	Maccamy
Kinematics	1st order	1st order
Load Model	Morison	MacCamy-Fuchs
Directonal spread	Long crested	Long crested

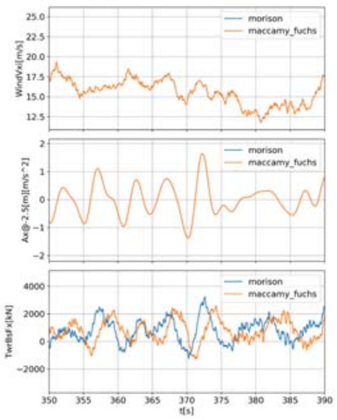

Example: effect of force model

- Power spectral density
- Sea state
  - $H_S = 3.5\,[m], T_P = 7.5[m]$
- Mudline Fx

	Morison	Maccamy
Kinematics	1st order	1st order
Load Model	Morison	MacCamy-Fuchs
Directonal spread	Long crested	Long crested

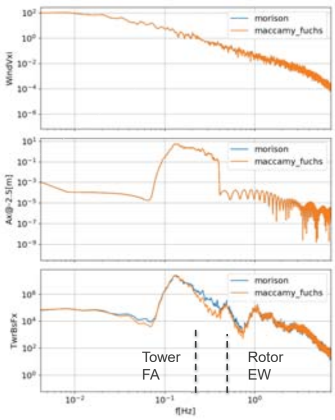

Rainey – 2nd order – Swell

Fatigue due to Mudline Fx

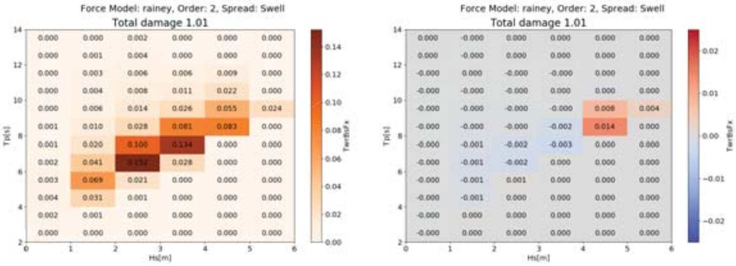

Rainey – 2nd order – Long crested waves

Fatigue due to Blade Root Flapwise moment

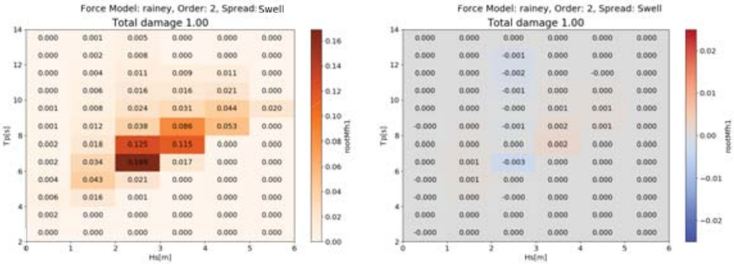

MacCamy-Fuchs – 1st order – Swell

Fatigue due to Blade Root Flapwise moment

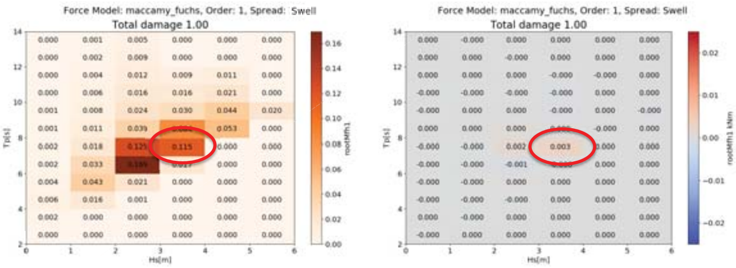

Morison – 1st order – Short vs Long crested

Fatigue due to Mudline moment around y-axis

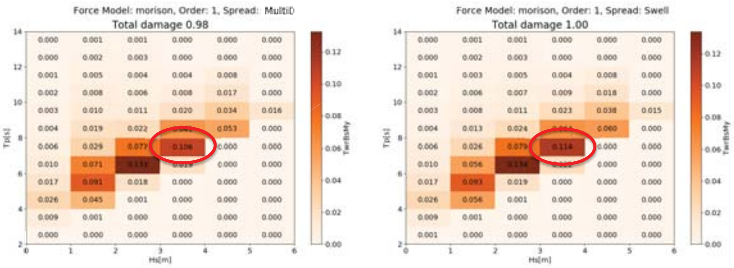

Example: effect of force model

- Power spectral density
- Sea state
  - $H_S = 3.5\,[m], T_P = 7.5[m]$
- Blade root Flapwise moment

	Morison	Maccamy
Kinematics	1st order	1st order
Load Model	Morison	MacCamy-Fuchs
Directonal spread	Long crested	Long crested

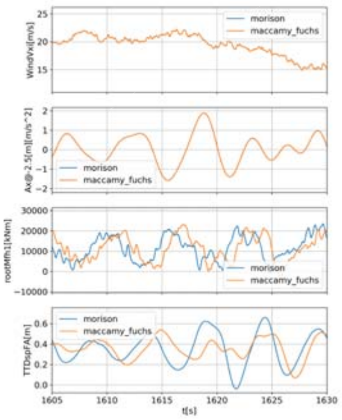

Effect of wave spreading

- Time series
- Sea state
  - $H_S = 3.5\,[m], T_P = 7.5[m]$
- Mudline x-wise force

	5	20
Kinematics	1st order	1st order
Load Model	Morison	Morison
Directonal spread	Short crested	Long crested

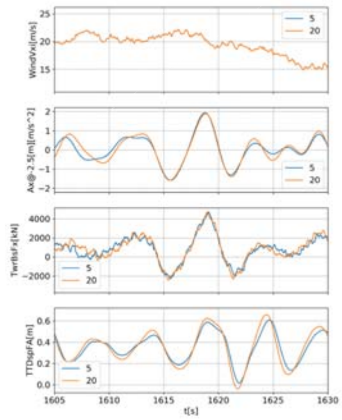

Effect of wave spreading

- Histogram
- Sea state
  - $H_S = 3.5\,[m], T_P = 7.5[m]$
- Mudline x-wise force

	5	20
Kinematics	1st order	1st order
Load Model	Morison	Morison
Directonal spread	Short crested	Long crested

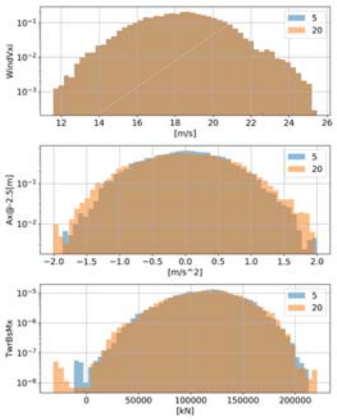

Conclusions

- DIMSELO has shed light into effect of improved models on OWT dimensioning loads
- It helped understand when it is useful to adopt a more complex wave **force** or **kinematics** model
- For example, on a 25m Monopile fatigue load case:
  - 1st order diffraction made a difference on tower base fatigue
  - the blade loads were insensitive to wave load models
  - 2nd order waves do not significantly influence fatigue loads
- Timeline: Complete the calculations and deliver final report

Effect of wave spreading

- Power spectral density
- Sea state
  - $H_S = 3.5\,[m], T_P = 7.5[m]$
- Mudline x-wise force

	5	20
Kinematics	1st order	1st order
Load Model	Morison	Morison
Directonal spread	Short crested	Long crested

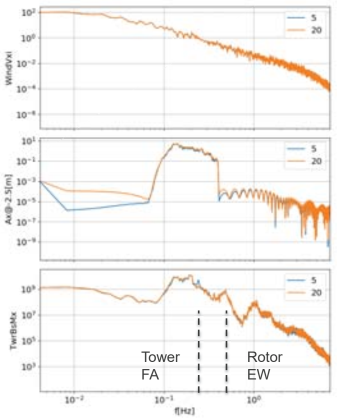

MacCamy-Fuchs – 1st order – MultiD

Mudline moment My

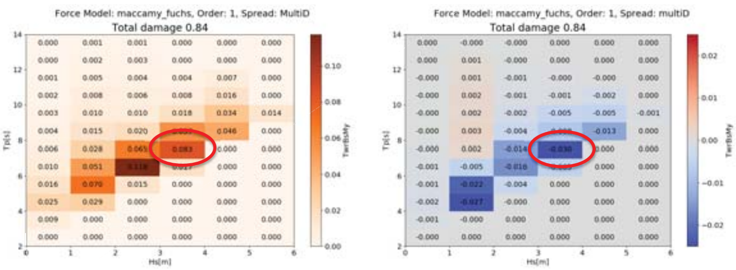

Effect of wave spreading

- Exceedance probability
- Sea state
  - $H_S = 3.5\,[m], T_P = 7.5[m]$
- Mudline x-wise force

	5	20
Kinematics	1st order	1st order
Load Model	Morison	Morison
Directonal spread	Short crested	Long crested

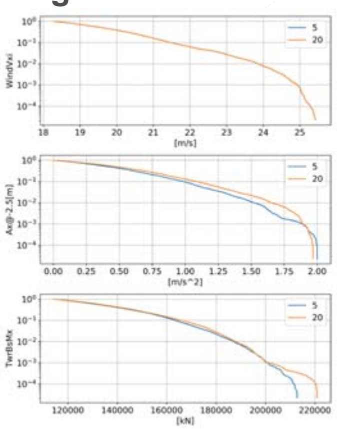

Design calculations: today's practice

- Fatigue calculations
- Linear irregular waves
- Morison equation
- Some critical points
  - Non-linearity in irregular waves
  - Non-linearity in the force model
  - What about wave diffraction of large monopiles?

- Extreme loads
- Embedment of a 50-yr nonlinear wave in long-crested waves
- Morison equation
- Some critical points
  - Directionality in the extreme loads?
  - Non-linearity of the force?
  - Statistical significance of extreme load?

A savings procedure based construction heuristic for the offshore wind cable layout optimization problem

Sunney Fotedar (B.Eng. Mechanical)
MSc. Candidate in Energy
Department of Informatics, University of Bergen, Norway
sunney.fotedar@student.uib.no
2018
Supervisors: Prof. Dag Haugland (UiB) and Ahmad Hemmati ,PhD.

Deep Wind Conference 2018, Trondheim, Norway

Offshore Wind Cable Layout Optimization

- Offshore wind or inter-array cable layout (OWCL) optimization problem is a NP hard problem
- There is similarity between OWCL and capacitated miniumum spanning tree (CMST) problem with unit demand which has also been proved to be NP hard (Papadimitriou, 1978)
- With increasing number of turbine nodes and additional restricted areas in the wind farm , exact methods in solving large instances become inefficient
- Due to the inefficiencies of the exact methods in solving large instances, heuristics can be used to attain good and feasible solutions
- Construction, improvement and hybrid heuristics are classical heuristics exploring a limited search space as opposed to large search space in metaheuristics , but using some unique strategies can be used to attain small optimality gap even with classical approaches

Table of Content

Offshore wind cables

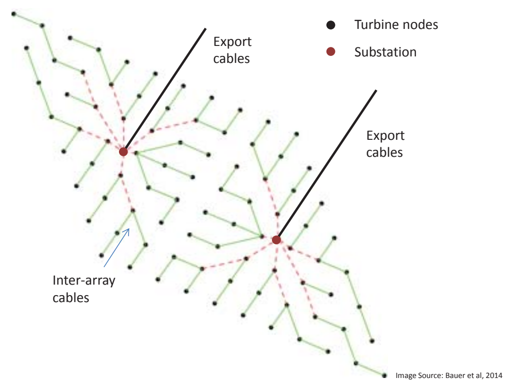

Each node must be connected to one of the substation

Table of Content

Problem Statement and Assumption

<u>Problem</u> :

Input:
1. Location of the turbines and substations
2. Location of the restricted areas and obstacles in the sea-bed
3. Cable capacity (maximum power flow or number of turbines allowed on a single cable)

Output: Minimum cable length layout such that there is a unique path from each turbine to one of the substation

Constraints:
1. Cable crossing/Node crossing not allowed
2. Cable capacity must be satisfied
3. Outdegree of each turbine is one (no splitting of power cables)

Assumption:
Cable cost is directly proportional to the length of the cables and doesnot depend on any other parameter.

This is similar to a **capacitated minimum spanning tree problem (NP hard) with some additional constraints**

Problem Statement and Assumption

Problem :

Input:
1. Location of the turbines and substations
2. Location of the restricted areas and obstacles in the sea-bed
3. Cable capacity (maximum power flow or number of turbines allowed on a single cable)

Output: Minimum cable length layout such that there is a unique path from each turbine to one of the substation

Constraints:
1. Cable crossing/Node crossing not allowed
2. Cable capacity must be satisfied
3. Outdegree of each turbine is one (no splitting of power cables)

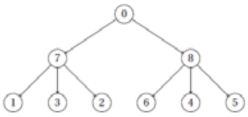

Capacity = 4

Assumption:
Cable cost is directly proportional to the length of the cables and doesnot depend on any other parameter.

This is similar to a **capacitated minimum spanning tree problem (NP hard) with some additional constraints**

Constraint 3: Restricted areas

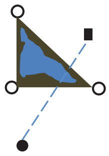

- Steiner nodes\optional nodes
- Turbine nodes
- Substation node
- Convex hull around the obstacle
- Cables
- Restricted area

- Direct links are sometimes not possible due to restricted areas in the sea-bed
- Number of steiner nodes is a design parameter and can be more than the extreme points of the convex hull
- We are making an assumption that any concave and convex restricted area can be represented by a convex hull without compromising on optimality

Constraint 1: Cable crossing and Node crossing

Node crossing

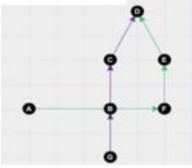

Cable crossing

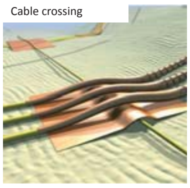

Image Source: Fischetti et al 2016

Node crossing free

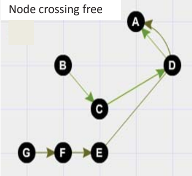

The main reasons behind such a constraint are:
1. Need for expensive bridge structure
2. Thermal interference between the two cables results in reducing the cable capacity
3. In case of failure of one of the cable both the cables are affected while reparing

Constraint 3: Restricted areas

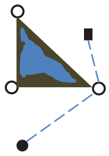

- Steiner nodes\optional nodes
- Turbine nodes
- Substation node
- Convex hull around the obstacle
- Cables
- Restricted area

- Direct links are sometimes not possible due to restricted areas in the sea-bed
- Number of steiner nodes is a design parameter and can be more than the extreme points of the convex hull
- We are making an assumption that any concave and convex restricted area can be represented by a convex hull without compromising on optimality

Constraint 2: Power cables cannot be splitted

Allowed

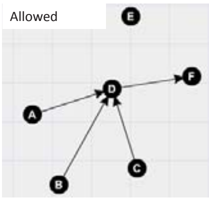

Not Allowed

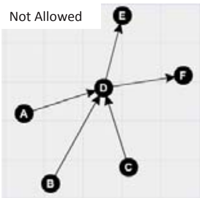

The out-degree of each turbine node must be one. However, in-degree can be more which is refered to as **branching** .

Allowed: Branching and parallel cables

Both branching and parallel cables provide flexibility to the final layout and may lead to reduction in the total cable length

No-Branching

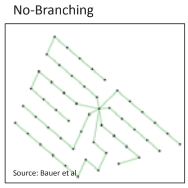

Branching

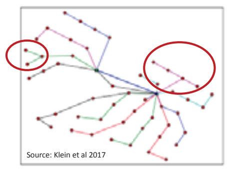

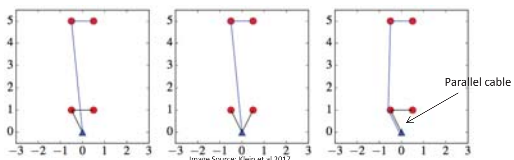

Image Source: Klein et al 2017

Table of Content

INTRODUCTION
- Offshore Wind Cable Layout (OWCL)Optimization
- Problem Statement and Assumptions
- Constraints: Node crossing/cable crossing, obstacles and out-degree
- Features: Parallel cables and branching
- MILP model used for benchmarking heuristic solutions

HEURISTIC
- Basic idea
- Pseudocode (Esau-Williams)
- Ideas to tackle cable crossing
- Ideas to identify node crossing
- Pseudocode (Obstacle-Aware Esau Williams)

Experimental Results and Modified Algorithm
- Initial results from the Modified Esau-Williams (Wind farms: Walney 1 , Walney 2 and Barrow)
- Parametrization and introducing a shape factor
- Improved results
- From construction heuristic to Meta-Heuristic : Future activities (Very large Neighborhood search (VLNS) and GRASP)

Pseudocode of Esau-Williams' heuristic

Algorithm 1 Esau Williams

Data: G=(V, A, c, K)
Result: M: set of $|V|-1$ arcs spanning G
$M \leftarrow \emptyset$
for *node* $i \in V\backslash 0$ **do**
  $M \leftarrow M \cup \{(0,i)\}$; // set of links in spanning tree
  $X_i \leftarrow \{i\}$
  $R_i = .1$; // any value except 0
end
while $(\exists i \in V : R_i > 0)$ **do**
  for *node* $i \in V$ **do**
    $j(i) \leftarrow$ nearest neighbouring node ; // using (2.2.9)
    compute R_i ; // Reduction value using (2.2.10)
  end
  find $i^* \in \operatorname{argmax}_{i \in V} R_i$
  if $R_{i^*} > 0$ **then**
    $M \leftarrow M \cup \{(j(i^*), i^*)\}$
    $M \leftarrow M \backslash \{(0, i^*)\}$
    $X_{j(i^*)} \leftarrow X_{i^*} \leftarrow X_{i^*} \cup X_{j(i^*)}$
  end
end
return M

V: set of vertices
A: $A \subseteq (V \times (V \backslash \{0\}))$
0: root node
c: cost of the arcs
K: cable capacity
R_i: reduction fuction value of node i
X_i: connected component containing node i

$$S(i) = \{j \in V \backslash 0 : j \notin X_i, (j,i) \in A, |X_i| + |X_j| \leq K\} \quad (2.2.8)$$

$$j(i) = \begin{cases} \text{one of the } j \in \operatorname{argmin}_{j \in V \backslash \{0\}} \{c_{ji} : j \in S(i)\}, & S(i) \neq \emptyset \\ 0, & S(i) \neq \emptyset \end{cases} \quad (2.2.9)$$

$$R_i = \begin{cases} c_{0i} - \min\{c_{ji} : j \in S(i)\}, & S(i) \neq \emptyset \\ 0, & S(i) \neq \emptyset \end{cases} \quad (2.2.10)$$

Basic idea behind the heuristic

- **Esau-Williams'** heuristic is a well known heuristic for the capacitated minimum spanning tree problem.
- Start with a costly, feasible star layout
- In each iteration remove one link connecting the non-root node with the root node (substation node) resulting in cost saving.

Final output of the Esau-Williams' Heuristic

Capacity = 3

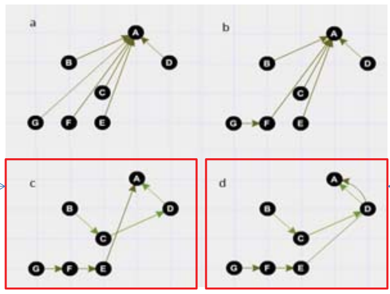

Feasible layout

Although CMST and cable layout problems are quite similar but there are additional constraints which are to be satisfied in the offshore wind cable layout problem

Pseudocode of Esau-Williams' heuristic

Algorithm 1 Esau Williams

Data: G=(V, A, c, K)
Result: M: set of $|V|-1$ arcs spanning G
$M \leftarrow \emptyset$
for *node* $i \in V\backslash 0$ **do**
  $M \leftarrow M \cup \{(0,i)\}$; // set of links in spanning tree
  $X_i \leftarrow \{i\}$
  $R_i = .1$; // any value except 0
end
while $(\exists i \in V : R_i > 0)$ **do**
  for *node* $i \in V$ **do**
    $j(i) \leftarrow$ nearest neighbouring node ; // using (2.2.9)
    compute R_i ; // Reduction value using (2.2.10)
  end
  find $i^* \in \operatorname{argmax}_{i \in V} R_i$
  if $R_{i^*} > 0$ **then**
    $M \leftarrow M \cup \{(j(i^*), i^*)\}$
    $M \leftarrow M \backslash \{(0, i^*)\}$
    $X_{j(i^*)} \leftarrow X_{i^*} \leftarrow X_{i^*} \cup X_{j(i^*)}$
  end
end
return M

V: set of vertices
A: $A \subseteq (V \times (V \backslash \{0\}))$
0: root node
c: cost of the arcs
K: cable capacity
R_i: reduction fuction value of node i
X_i: connected component containing node i

$$S(i) = \{j \in V \backslash 0 : j \notin X_i, (j,i) \in A, |X_i| + |X_j| \leq K\} \quad (2.2.8)$$

$$j(i) = \begin{cases} \text{one of the } j \in \operatorname{argmin}_{j \in V \backslash \{0\}} \{c_{ji} : j \in S(i)\}, & S(i) \neq \emptyset \\ 0, & S(i) \neq \emptyset \end{cases} \quad (2.2.9)$$

$$R_i = \begin{cases} c_{0i} - \min\{c_{ji} : j \in S(i)\}, & S(i) \neq \emptyset \\ 0, & S(i) \neq \emptyset \end{cases} \quad (2.2.10)$$

Reduction function value (R_i)at each non-root node is the difference of the cost of the central link with the root node and cost of forming a link with the nearest feasible connected component (satisfying the cable capacity limitation)

Basic idea behind the heuristic

- **Esau-Williams'** heuristic is a well known heuristic for the capacitated minimum spanning tree problem.
- Start with a costly, feasible star layout
- In each iteration remove one link connecting the non-root node with the root node (substation node) resulting in cost saving.

Can't use Esau-Williams' heuristic alone!

Final output of the Esau-Williams' Heuristic

Capacity = 3

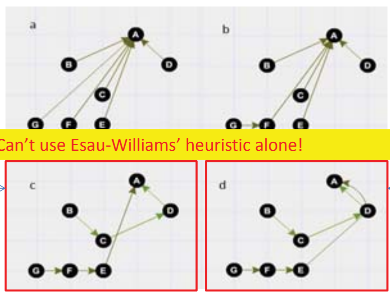

Feasible layout

Although CMST and cable layout problems are quite similar but there are additional constraints which are to be satisfied in the offshore wind cable layout problem

Idea to tackle cable crossing

Non- crossing procedure and Dijkstra are used subsequently to identify shortest feasible path between two nodes i_0 and i_n

$DJ \leftarrow$ Dijkstra(G, i_0, i_n) /* shortest path between i_0 and i_n */
for *each arc* (i_k, i_{k+1}) *in the shortest path DJ* **do**
  if *Non-Crossing(IntersectionArray,* i_k, i_{k+1}*)* == *FALSE* **then**
    $c_{i_k i_{k+1}} \leftarrow \infty$; // any high value
  end
end

Continues until a shortest feasible (non-crossing) path is found between i_0 and i_n

So, the basic idea is that once we have identified the two turbine nodes to be connected using the max reduction function value, we try to use the above idea to find the shortest non-crossing path between them

Obstacle-Aware Esau Williams Heuristic(1/2)

```
Algorithm 2 Obstacle Aware Esau Williams
Data: G=(V,A,c,K),L,C,PointArray
Result: M: set of rooted trees spanning |T ∪ S|
L2 ← ∅,  M ← ∅
while any(R) do
    /* #1                                                        */
    FirstTime ← 0
    while FirstTime≠ 1 do
        /* #2                                                    */
        for node i ∈ T do
            compute R_i ;          // Reduction value using (2.2.10)
            minIndex[i] ← j(i);                 // equation (2.2.9)
        end
        for each line segment e in L2 do
            IntersectionArray.add(e)
        end
        for each line segment s in L do
            IntersectionArray.add(s)
        end
        i_0 ← i* ∈ argmax_{i∈T} R_i
        i_n ← minIndex[i*];     // Now we have arc (i_0,i_n) to be
        checked in pre-processing stage
        crossingSwitch ← TRUE
```

- **L** : stores line segments related to the obstacles
- **PointArray**: stores coordinates of all the nodes
- **L2**: stores the arcs/line segments formed during the procedure
- **IntersectionArray**: stores both L2 and L
- **While loop #1**: continues unless all the reduction values become zero
- **While loop #2**: continues unless the node with highest reduction values gets linked with another node

Non-Crossing procedure's output

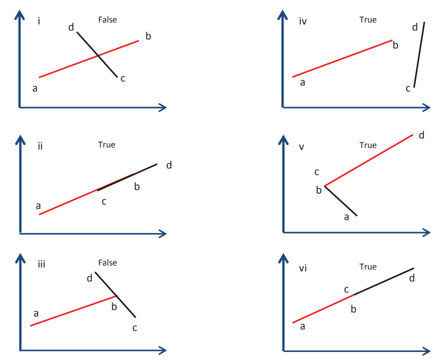

Obstacle-Aware Esau Williams Heuristic(1/2)

```
Algorithm 2 Obstacle Aware Esau Williams
Data: G=(V,A,c,K),L,C,PointArray
Result: M: set of rooted trees spanning |T ∪ S|
L2 ← ∅,  M ← ∅
while any(R) do
    /* #1                                                        */
    FirstTime ← 0
    while FirstTime≠ 1 do
        /* #2                                                    */
        for node i ∈ T do
            compute R_i ;          // Reduction value using (2.2.10)
            minIndex[i] ← j(i);                 // equation (2.2.9)
        end
        for each line segment e in L2 do
            IntersectionArray.add(e)
        end
        for each line segment s in L do
            IntersectionArray.add(s)
        end
        i_0 ← i* ∈ argmax_{i∈T} R_i
        i_n ← minIndex[i*];     // Now we have arc (i_0,i_n) to be
        checked in pre-processing stage
        crossingSwitch ← TRUE
```

- **L** : stores line segments related to the obstacles
- **PointArray**: stores coordinates of all the nodes
- **L2**: stores the arcs/line segments formed during the procedure
- **IntersectionArray**: stores both L2 and L
- **While loop #1**: continues unless all the reduction values become zero
- **While loop #2**: continues unless the node with highest reduction values gets linked with another node

We have selected node i_0 having the maximum reduction function value and its nearest node i_n . Now, in pre-processing stage the shortest feasible path between them is searched which may or may not be a direct arc

Non-Crossing procedure's output

Note: Non-crossing procedure always assesses pair of line segments (one from IntersectionArray and one of the edge in the shortest path given by Dijkstra)

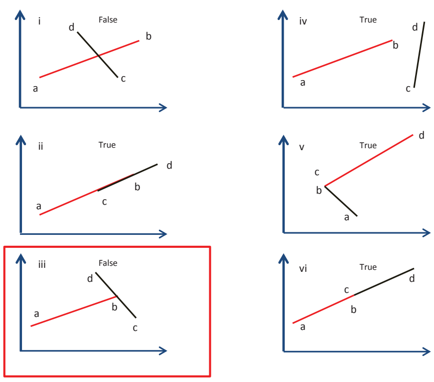

Obstacle-Aware Esau Williams Heuristic(2/2)

```
        /* #3                                                    */
        while crossingSwitch == TRUE do
            FirstTime ← FirstTime + 1
                crossingSwitch ← FALSE
                DJ  ←  Dijkstra(G,i_0,i_n)  /* shortest path between
                i_0 and i_n                                      */
            for each arc (i_k,i_{k+1}) in the shortest path DJ do
                if Non-Crossing(IntersectionArray,i_k,i_{k+1}) == FALSE
                 then
                    c_{i_k i_{k+1}} ← ∞;              // any high value
                    crossingSwitch ← TRUE
                end
            end
            if !crossingSwitch&&FirstTime ≠ 1 then
                C[i_0][i_n] ← c_{i_0 i_1} + c_{i_1 i_2} + ··· + c_{i_{n-1} i_n} ;   // exit loop #3
            end
        end
    end
    post node joining steps and updates of connected components, L2, M
end
forming shortest feasible paths from an active node in each connected
 component to the substation
 return M
```

Pre-processing stage

Challange: Non-Crossing procedure is unable to identify node crossing

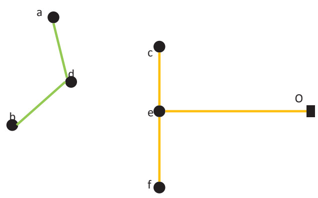

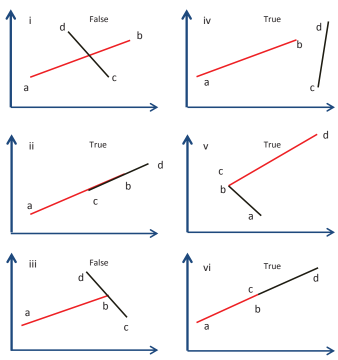

Challange: Non-Crossing procedure is unable to identify node crossing

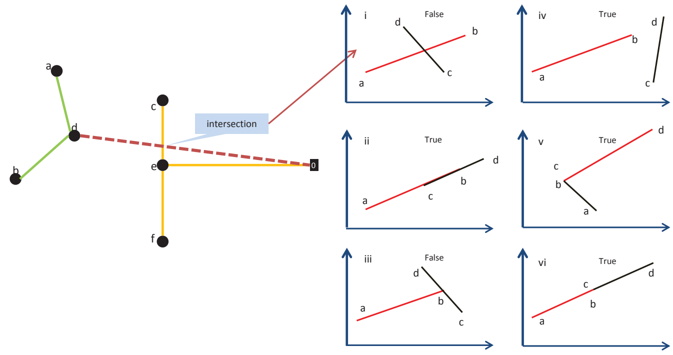

Solution(1/4): Add new line segments such that node crossings are detected by Non-crossing procedure

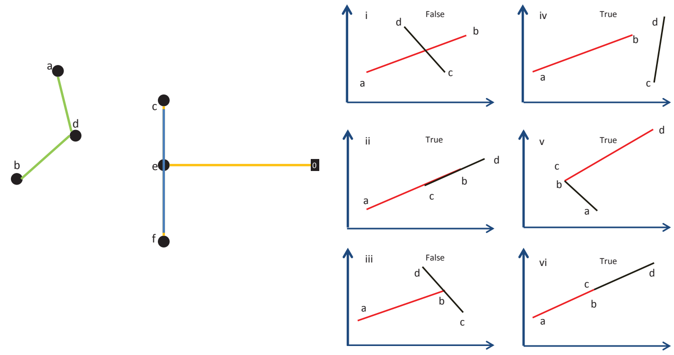

Challange: Non-Crossing procedure is unable to identify node crossing

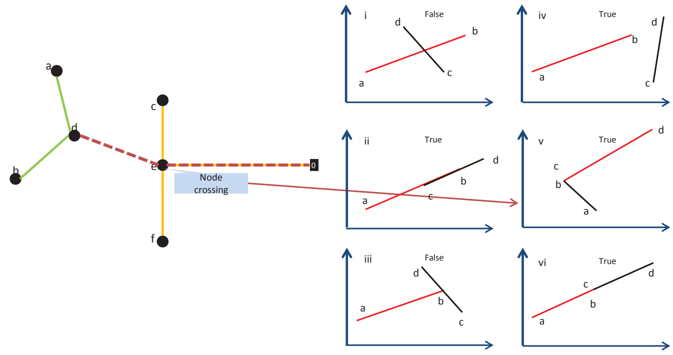

Solution(2/4): Add new line segments such that node crossings are detected by Non-crossing procedure

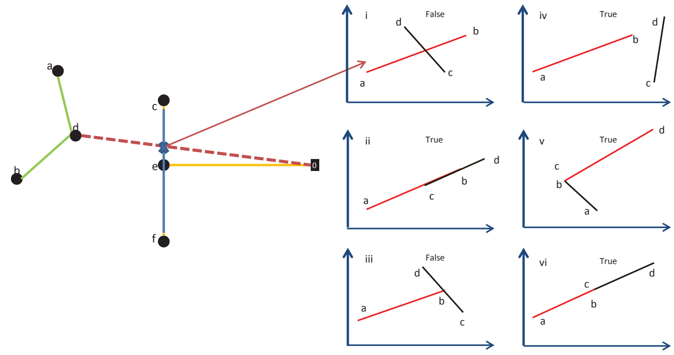

Challange: Non-Crossing procedure is unable to identify node crossing

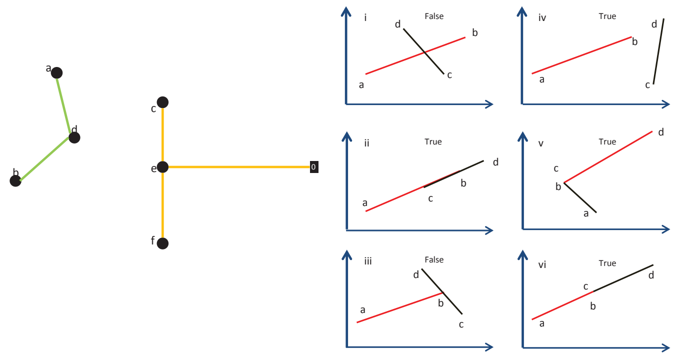

Solution(3/4): Add new line segments such that node crossings are detected by Non-crossing procedure

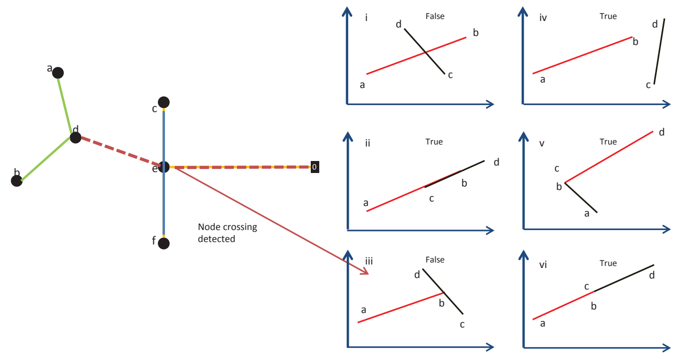

Solution(4/4): Add new line segments such that node crossings are detected by Non-crossing procedure

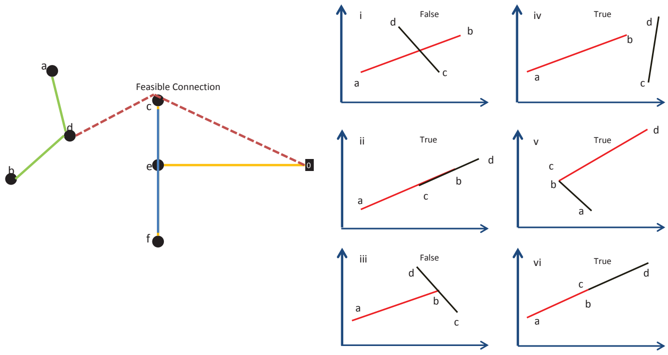

Solution(2/2): Where to add the line segments?

Partitioning of turbine nodes in different connected components

Output from 1st part of the algorithm

Post joining step

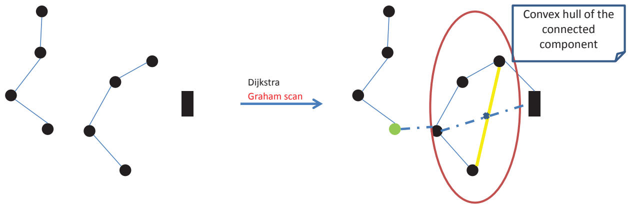

Solution(1/2): Where to add the line segments?

Partitioning of turbine nodes in different connected components

Output from 1st part of the algorithm

Post partitioning step

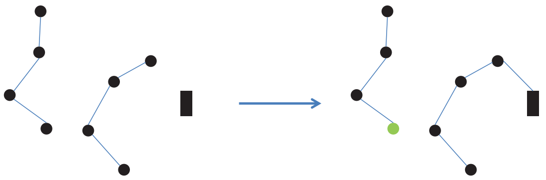

Solution(2/2): Where to add the line segments?

Partitioning of turbine nodes in different connected components

Output from 1st part of the algorithm

Post joining step

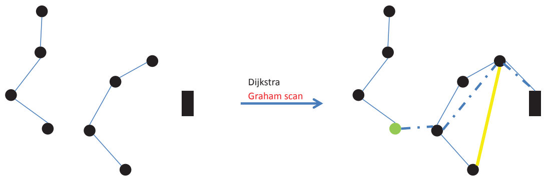

Solution(1/2): Where to add the line segments?

Partitioning of turbine nodes in different connected components

Output from 1st part of the algorithm

Post partitioning step

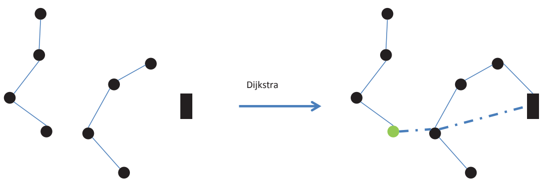

Solution(2/2): Where to add the line segments?

Partitioning of turbine nodes in different connected components

Output from 1st part of the algorithm

Post joining step

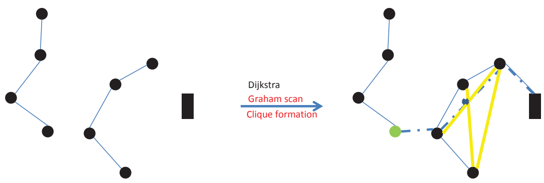

Solution(2/2): Where to add the line segments?

Partitioning of turbine nodes in different connected components

Output from 1st part of the algorithm

Post joining step

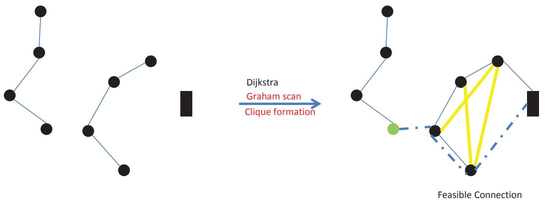

Assumption: All the nodes are in the convex hull of their own connected component and not in the convex hull of others'

Experimental Results-2

K	Barrow(T=30)			Walney-1(T=51)			Walney-2(T=51)		
	Exact	Alg 2	gap	Exact	Alg 2	gap	Exact	Alg 2	gap
2	36990	38115	1.03	70286	75105	1.07	97885	117849	1.20
4	23208	23243	1.00	47411	49534	1.04	63496	73374	1.15
5	20691	21815	1.05	43420	44444	1.02	56904	62739	1.10
6	18374	20980	1.14	41418	43858	1.05	52981	63568	1.19

K= cable capacity , Alg2 = Obstacle-Aware Esau Williams

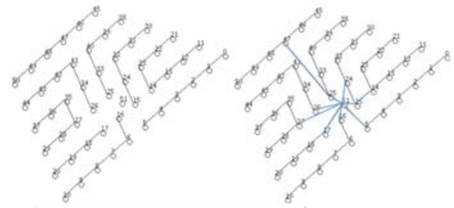

Walney 1 final layout for K=6

Table of Content

INTRODUCTION

- Offshore Wind Cable Layout (OWCL)Optimization
- Problem Statement and Assumptions
- Constraints: Node crossing/cable crossing, obstacles and out-degree
- Features: Parallel cables and branching
- MILP model used for benchmarking heuristic solutions

HEURISTIC

- Basic idea
- Pseudocode (Esau-Williams)
- Ideas to tackle cable crossing
- Ideas to identify node crossing
- Pseudocode (Obstacle-Aware Esau Williams)

Experimental Results and Modified Algorithm

- Initial results from the Modified Esau-Williams (Wind farms: Walney 1 , Walney 2 and Barrow)
- Parametrization and introducing a shape factor
- Improved results
- From construction heuristic to Meta-Heuristic : Future activities (Very large Neighborhood search (VLNS) and GRASP)

Experimental Results-3

Walney 2 final layout for K=6

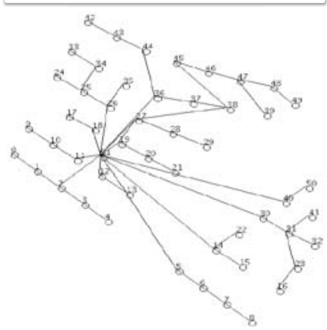

- There is a large optimality gap for Walney 2
- The partitioning of the turbine nodes leads to extremely long paths connecting connected components to the substation
- For example, the connected component containing nodes 45, 46, 47, 48, 49, 39 is linked with the substation using a long path 45->38->27->51

Experimental Results-1

Existing Model:

- We have compared our results to the optimal solutions attained from an existing MILP model developed by our colleague Arne Klein, UiB,Norway
- The model presented in [Klein and Haugland, 2017] is implemented using CPLEX 12 Python 3.4 API. All the experiments were carried out on a fast computer - Intel Xenon with 72 logical cores and 256GB RAM
- The experiments were carried out for Walney 1, Walney 2, Barrow wind farms and for different cable capacities

Developed Heuristic :

- All the experiments involving the heuristics (Obstacle Aware Esau-Williams) in this work are carried out on a personal computer using 2.5 GHz Intel Core i5 processor and 4GB RAM
- Programming language used is Java and without use of any commercial solver
- The ambition of the first version of the obstacle-aware heuristic is to find good, feasible solutions with less optimality gap **[cost(heuristic)/cost(optimal solution)]**

Experimental Results-3

Walney 2 final layout for K=6

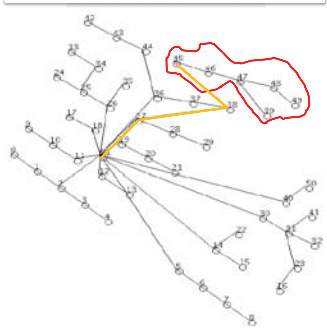

- There is a large optimality gap for Walney 2
- The partitioning of the turbine nodes leads to extremely long paths connecting connected components to the substation
- For example, the connected component containing nodes 45, 46, 47, 48, 49, 39 is linked with the substation using a long path 45->38->27->51

Ideas/Activities to reduce the opt. gap

- Modifying the reduction function and the algorithm such that radial topologies are encouraged and thus, long paths to the substation are avoided

- Using a multi-exchange large neighbourhood search for finding the locally optimal solution

Results from exact, obstacle aware Esau Williams and algorithm with weight parameter

Wind Farm	Exact	Obstacle-Aware		Parametric	
K=6		value	gap	value	gap
Walney 1	41418	43858	1.05	42580	1.028
Barrow	18374	20980	1.14	18900	1.0286
Walney 2	52981	63568	1.19	53214	1.004
K=5		value	gap	value	gap
Walney 1	43420	44444	1.0235	43498	1.002
Barrow	20691	21815	1.054	21105	1.02
Walney 2	56904	62739	1.1	57816	1.016
K=4		value	gap	value	gap
Walney 1	47411	49534	1.044	48396	1.02
Barrow	232208	23243	1.001	23243	1.001
Walney 2	63496	73374	1.15	63579	1.001

Introducing weight parameter in reduction function

$$S(i) = \{j \in V\backslash 0 : j \notin X_i, (j,i) \in A, |X_i| + |X_j| \leq K\} \quad (2.2.11)$$

$$j(i) = \begin{cases} \text{one of the } j \in \operatorname{argmin}_{j\in V\backslash\{0\}} \{c_{ji} + \frac{W}{1000} \times c_{0j} : j \in S(i), W \in [1,1000], W \in \mathbb{Z}\}, & S(i) \neq \emptyset \\ 0, & S(i) = \emptyset \end{cases} \quad (2.2.12)$$

$$R_i = \begin{cases} c_{0i} - \min\{c_{ji} + \frac{W}{1000} \times c_{0j} + : j \in S(i)\}, & S(i) \neq \emptyset \\ 0, & S(i) = \emptyset \end{cases} \quad (2.2.13)$$

Improved result for Walney 2

Walney 2 (Modified Esau Williams Algorithm-Parametric) | Walney 2 (Modified Esau Williams Algorithm)

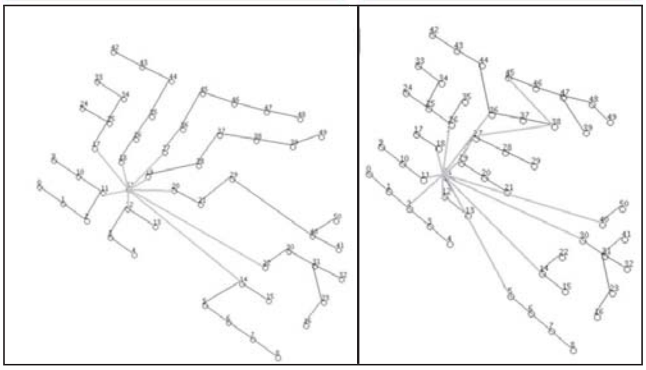

Introducing weight parameter in reduction function

$$S(i) = \{j \in V\backslash 0 : j \notin X_i, (j,i) \in A, |X_i| + |X_j| \leq K\} \quad (2.2.11)$$

$$j(i) = \begin{cases} \text{one of the } j \in \operatorname{argmin}_{j\in V\backslash\{0\}} \{c_{ji} + \frac{W}{1000} \times c_{0j} : j \in S(i), W \in [1,1000], W \in \mathbb{Z}\}, & S(i) \neq \emptyset \\ 0, & S(i) = \emptyset \end{cases} \quad (2.2.12)$$

$$R_i = \begin{cases} c_{0i} - \min\{c_{ji} + \frac{W}{1000} \times c_{0j} : j \in S(i)\}, & S(i) \neq \emptyset \\ 0, & S(i) = \emptyset \end{cases} \quad (2.2.13)$$

As the value of weight parameter W increases , turbine nodes closer to the substation will be preferred.

Change in cable length with weight parameter

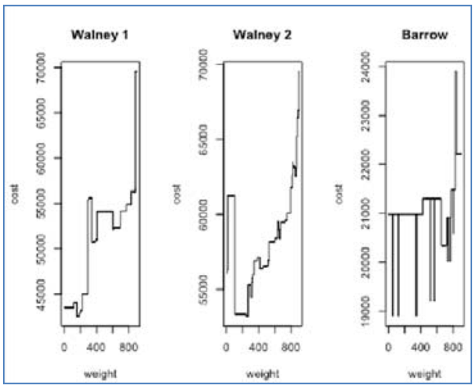

Ideas/Activities to reduce the opt. gap

- Modifying the reduction function and the algorithm such that radial topologies are encouraged and thus, long paths to the substation are avoided

- Using a multi-exchange large neighbourhood search for finding the locally optimal solution

Questions?

Thank You!

Project is supported by Hordaland fylkeskommune.

NREL
NATIONAL RENEWABLE ENERGY LABORATORY

Calibration & Initial Validation of FAST.Farm Against SOWFA

Jason Jonkman, Ph.D. – NREL
Paula Doubrawa, Ph.D. – NREL
Jennifer Annoni, Ph.D. – NREL
Aditya Suresh Ghate – Stanford University

EERA DeepWind'2018
17-19 January, 2018
Trondheim, Norway

The Challenge

- Wind industry plagued by underperformance, failures, & expenses:
  - Improvements required in wind-farm performance & reliability, together w/ reduced uncertainty & expenditures to achieve cost targets
  - Improvements eluded by complicated nature of wind-farm design, especially interaction between atmospheric phenomena & wake/array effects
- Range of wind-farm tools exist, but none fully meet engineering needs, e.g.:
  - **FLORIS**: Steady-state wind-farm performance & controls, but no turbine loads
  - **DWM**: Both performance & loads, including dynamics, but individual or serial solution limits accuracy & usefulness
  - **SOWFA**: Large-eddy simulation (LES CFD) computational demand means very few runs

Example ***SOWFA*** *Simulation*

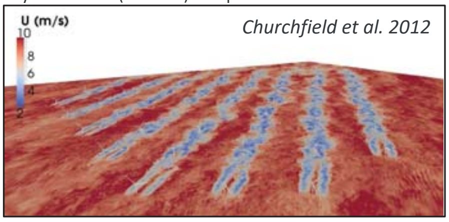

Churchfield et al. 2012

Objective & Approach

- *Objective*: Develop, validate, & demonstrate new multiphysics tool (**FAST.Farm**) applicable to engineering problems involving wind-farm design
  - This presentation focuses on calibration
- **FAST.Farm** aims to balance need for:
  - Accurate modeling of relevant physics for predicting performance & structural loads
  - Maintain low computational cost to support highly iterative & probabilistic design process & system-wide optimization
- **FAST.Farm**:
  - Relies on some **DWM** modeling principles
  - Avoids many limitations of existing **DWM** implementations
  - Compliments controls capability of **FLORIS**
  - Functions more like **SOWFA/Nalu**
- Insight from **SOWFA** simulations being used to support development, parameter calibration, & validation of **FAST.Farm**

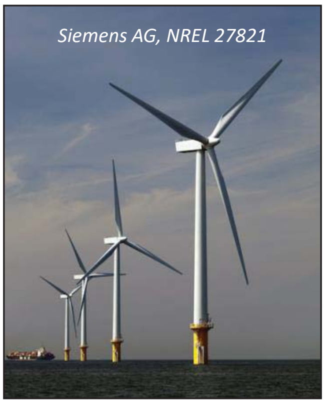

Siemens AG, NREL 27821

FAST.Farm Submodel Hierarchy

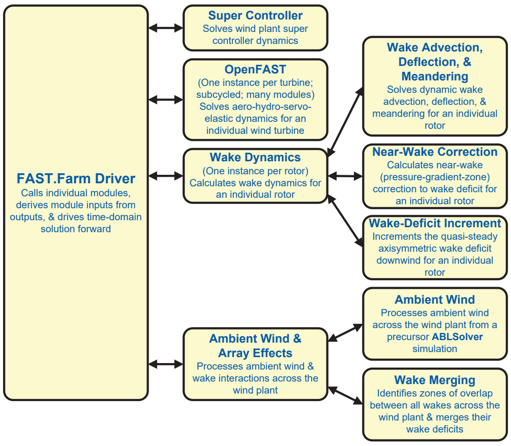

- **FAST.Farm** functions nonlinearly in time-domain
- **FAST.Farm** follows requirements of **OpenFAST** modularization framework
- Unique innovations:
  - Use LES precursor for ambient wind
  - Developed new models for wake advection, deflection, & merging
  - Inclusion of a super controller
  - Solve entire wind farm in serial or parallel
  - Calibration of model parameters against HFM

Wake Planes, Wake Volumes, & Zones of Overlap

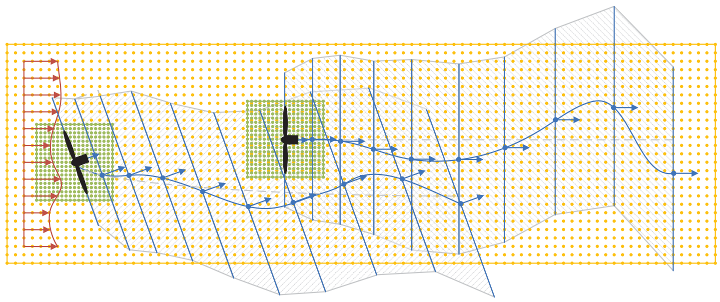

FAST.Farm-Generated w/ Stepped Yaw – 8m/s Neutral

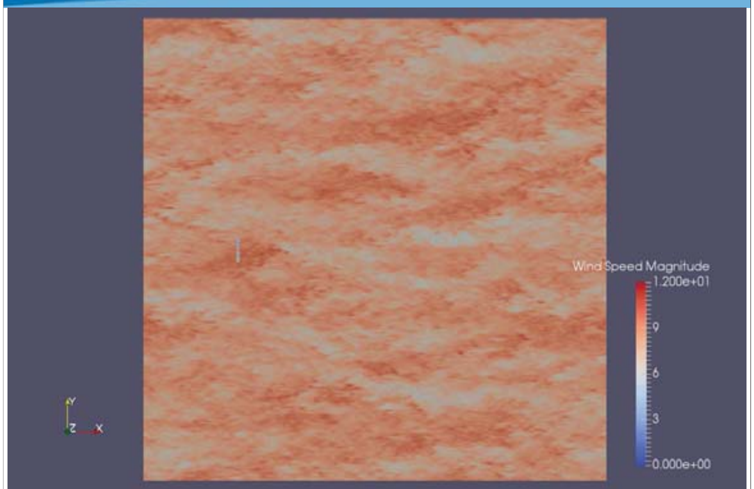

Calibration of FAST.Farm Against SOWFA

- **FAST.Farm** contains many (20) parameters that can be used to influence wake dynamics
- A calibration approach is used to set default parameter values
- Approach:
  - Identify calibration cases & approach
  - Identify starting values of calibration parameters
  - Run **SOWFA** & extract wake characteristics
  - Run **FAST.Farm** w/ varied parameters (sequenced grid search)
  - Identify parameters that minimize wake-deficit & wake-meandering error between **FAST.Farm** & **SOWFA**

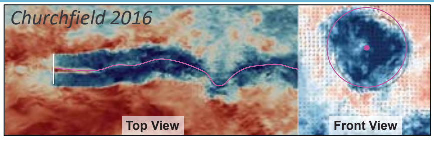

***SOWFA**-Derived Wake Deficit & Centerline*

Case	Name	Description
1	N	8 m/s, neutral, 10% TI, 0.2 shear, normal operation
2	U	8 m/s, unstable, 10% TI, 0.1 shear, normal operation
3	S	8 m/s, stable, 5% TI, 0.2 shear, normal operation
4	SHS	8 m/s, stable/high shear, 10% TI, 0.4 shear, normal operation
5-8	N_{-25}, N_{-10}, N_{+10}, N_{+25}	8 m/s, neutral, 10% TI, 0.2 shear, operation under fixed yaw error
9	N_{Step}	8 m/s, neutral, 10% TI, 0.2 shear, operation with yaw steps

Calibration Approach

Step	Name	Cases Run	Parameters Calibrated
1	Fixed Yaw	N, N_{-25}, N_{-10}, N_{+10}, N_{+25} (5)	Wake deflection (4)
2	Eddy	N, U, S, SHS (4)	Near-wake correction & eddy viscosity (3)
3	Eddy - Amb	N, U, S, SHS (4)	Eddy viscosity for ambient turbulence(4)
4	Eddy - Shr	N, U, S, SHS (4)	Eddy viscosity for wake-shear layer (4)
5	Meander	N, U, S, SHS (4)	Spatial averaging (2)
6	Step Yaw	N, N_{step} (2)	Low-pass filter (1)

SOWFA Solutions

Neutral
8 m/s, 10% TI, 0.2 shear

Unstable
8 m/s, 10% TI, 0.1 shear

Stable
8 m/s, 5% TI, 0.2 shear

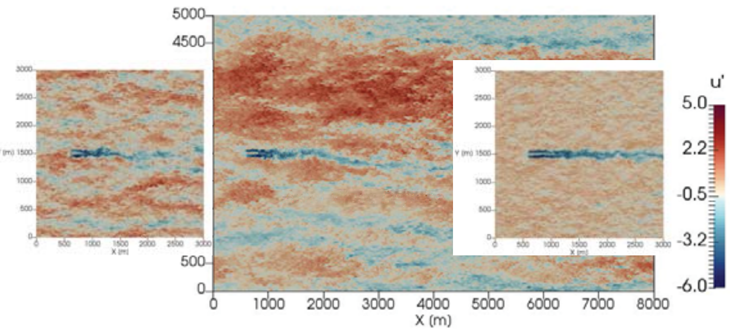

***SOWFA** Solutions*

Calibration Results

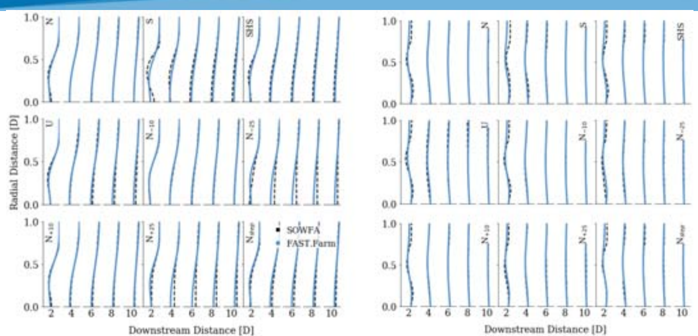

Axial Wake Deficits *Radial Wake Deficits*

- **FAST.Farm** captures change in wake-deficit evolution w/ downstream distance, but doesn't fully capture change predicted by **SOWFA** across different stability conditions or yaw errors
- Still reviewing, but think **SOWFA** predicts fast wake recover in U due to anisotropic turbulence
- Results suggest that **FAST.Farm** would benefit from:
  - Different calibration parameters for different stability conditions or yaw errors
  - Improved physics in the eddy-viscosity formulation

Calibration Results

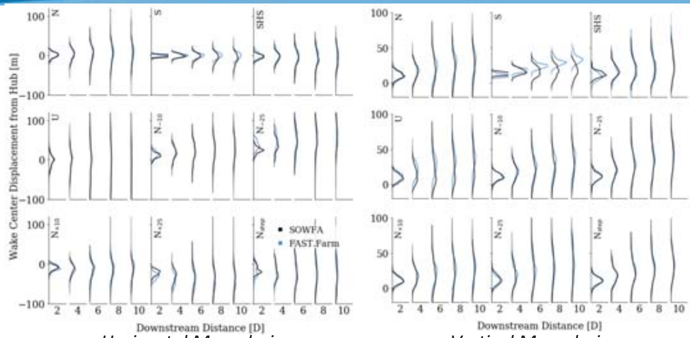

Horizontal Meandering *Vertical Meandering*

- **FAST.Farm** captures overall wake-meandering statistics predicted by **SOWFA** across different stability conditions, w/ some underprediction for S
  - Meandering in **SOWFA** for S likely driven by more than just large-scale ambient turbulence (e.g. smaller scales or wake-induced turbulence & boundary layer)
- Comparisons hampered by lack of statistical convergence (30-min/case)

Ongoing Work – Validation of FAST.Farm Against SOWFA

- Currently running **SOWFA** simulations—w/ modest variations in inflow & control, independent from those used to support calibration—to validate **FAST.Farm**
- **FAST.Farm** calibration parameters are untouched to check their robustness & range of applicability
- Results will be presented at TORQUE 2018

Validation Cases

Case	Number of turbines	Turbine spacing	Mean hub-height wind speed	Atmospheric stability	Turbulence intensity	Shear exponent	Yaw error
N^6	1	-	6	Neutral	10%	0.2	0°
N^{18}	1	-	18	Neutral	10%	0.2	0°
N_{+15}	1	-	8	Neutral	10%	0.2	15°
S_{+10}	1	-	8	Stable	5%	0.2	10°
N3	3	8D	8	Neutral	10%	0.2	0°
$N3_{+10/+10/0}$	3	8D	8	Neutral	10%	0.2	10°/10°/0°
S3	3	8D	8	Stable	5%	0.2	0°
U3	3	8D	8	Unstable	10%	0.1	0°

Next Steps

- Complete initial validation of **FAST.Farm**
- Release **FAST.Farm** as public, open-source software through **OpenFAST**
- Apply **FAST.Farm** by including turbine loads in wind-farm controls design/ testing
- Use **FAST.Farm** with HFM symbiotically in a multi-fidelity approach to support validation, UQ, & design
- Host a meeting of experts (likely @ TORQUE 2018) to discuss current capabilities & uses of mid-fidelity wind-farm engineering tools such as **FAST.Farm** & to outline their limitations, needs, & future development direction
- Address **FAST.Farm** limitations through more development

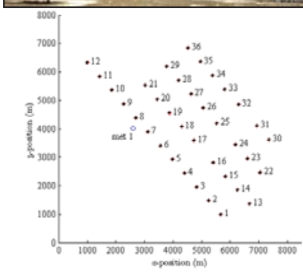

OWEZ Offshore Wind Farm
[Churchfield et al 2014]

Carpe Ventum!

Jason Jonkman, Ph.D.
+1 (303) 384 – 7026
jason.jonkman@nrel.gov

www.nrel.gov

NREL
NATIONAL RENEWABLE ENERGY LABORATORY

Yawed Wind Turbines

An Experimental Study on the Far Wake Development behind a Yawed Wind Turbine

F. Mühle, M. Vatn, J. Bartl, M.S. Adaramola, L. Sætran

19. January 2018, Trondheim, Norway

Norwegian University of Life Sciences

Yawed Wind Turbine Project

Influence of yaw misalignment on the wake developement

Collaboration project

NTNU ForWind

Experimental Campaign
- Different rotor designs
- Same wind tunnel
- Single turbine and multiple turbine arrays

Motivation

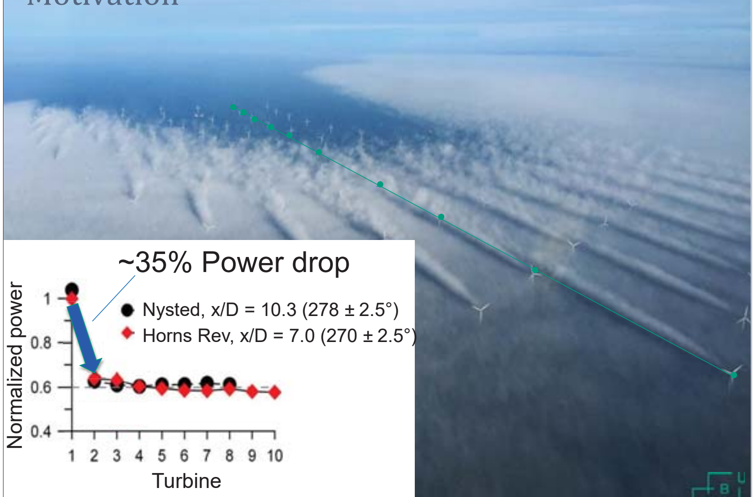

Barthelmie et al. "Modelling the impact of wakes on power output at Nysted and Horns Rev." EWEC, 2009.

Yawed Wind Turbine Project

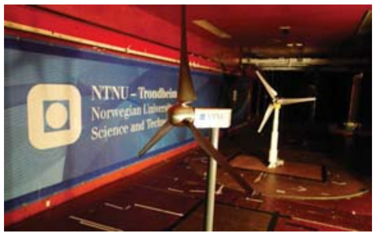

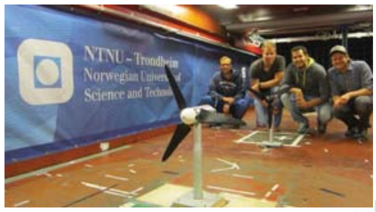

What can be done to limit wake effects?

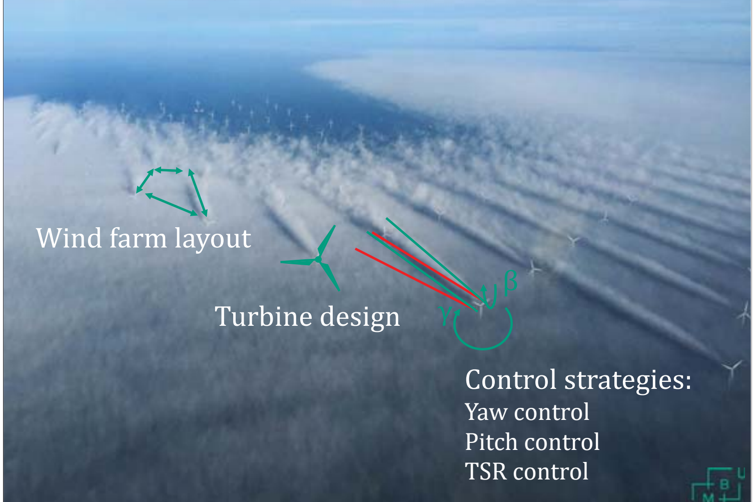

Picture: Bel Air Aviation Denmark – Helocopter Services

Model wind turbines

NTNU

D=0.89m
NREL S826
Small hub & tower
CCW rotation

Small NTNU

D=0.45m
NREL S826
Relative Big hub & tower
CCW rotation

ForWind

D=0.58m
SD 7003
Low blockage
CW rotation

Model wind turbines

Streamwise velocity 6D behind +30° yawed turbine

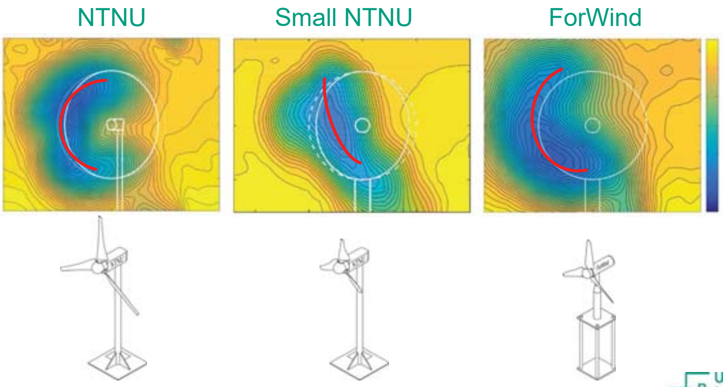

Model wind turbines

Streamwise velocity 6D behind +30° yawed turbine

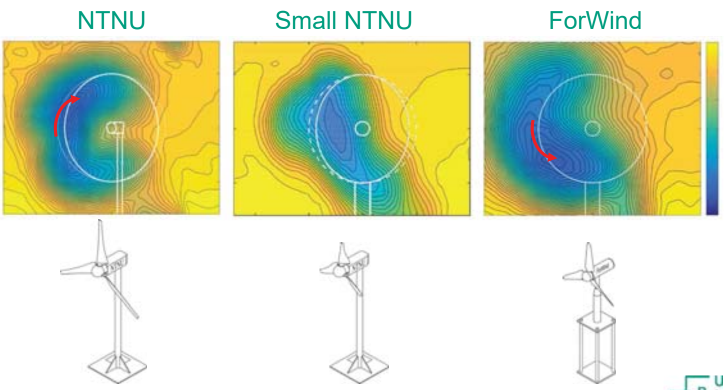

Publications

"Comparative study on the wake deflection behind yawed wind turbine models"
Published in Journal of Physics: Conf. Series

"Wind tunnel experiments on wind turbine wakes in yaw: Effects of inflow turbulence and shear"
Posted as discussion paper on Wind Energy Science

"Wind tunnel experiments on wind turbine wakes in yaw: Redefining the wake width"
Posted as discussion paper on Wind Energy Science

"Blind test 5 - The wake behind a yawed model wind turbine"
In process

"Performance and loads of two interacting wind turbines operated at different yaw"
In process

"An Experimental Study on the Far Wake Development behind a Yawed Wind Turbine"

Experimental setup

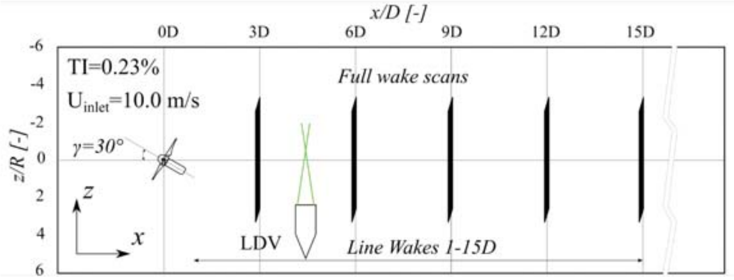

Experimental setup

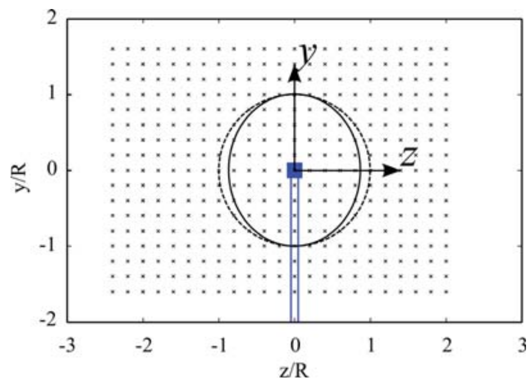

Results

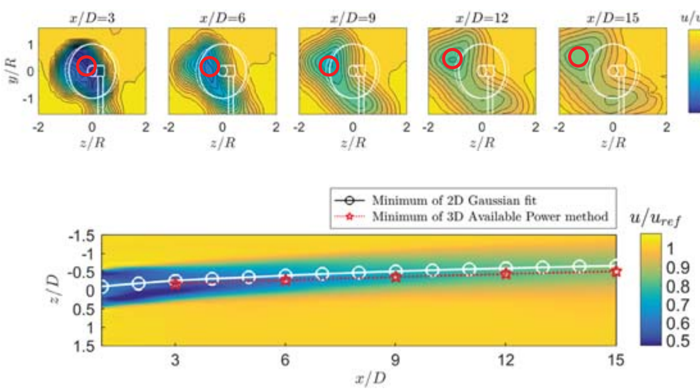

Results

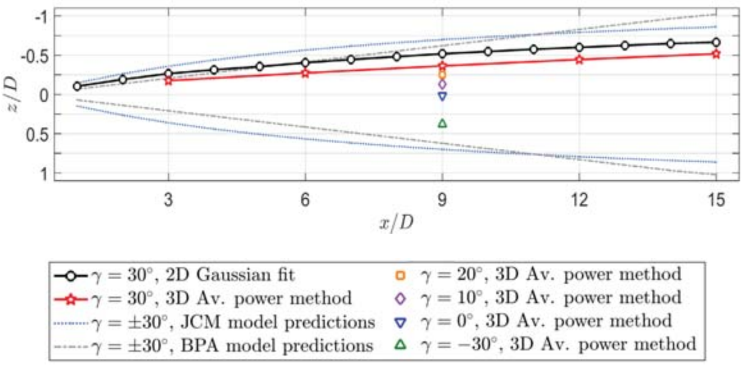

Conclusions

Rotor size and turbine dimension have large influence on wake shape

Wake behind yawed turbine is complex and asymetric

Larger wake deflection from line wake analysis

Analytical wake models over predict wake deflection

Thank you for the attention!

I'm looking forward to your Questions

Norwegian University of Life Sciences

G1) Experimental Testing and Validation

Wind tunnel experiments on wind turbine wakes in yaw: Redefining the wake width, J.Schottler, ForWind, University of Oldenburg

A Detached-Eddy-Simulation study, J.Göing, Technische Universität Berlin

BOHEM (Blade Optical HEalth Monitoring), P. McKeever, ORE Catapult

Scaled Wind Turbine Setup in Turbulent Wind Tunnel, F. Berger, CvO University of Oldenburg

Wind tunnel experiments on wind turbine wakes in yaw: Redefining the wake width

J. Schottler[1], J.Bartl[2], F. Mühle[3], J. Peinke[1,4], L. Sætran[2], M. Hölling[1]

[1] ForWind, Institute of Physics, University of Oldenburg, Germany
[2] Norwegian University of Science and Technology, (NTNU), Trondheim, Norway
[3] Norwegian University of Life Sciences, As, Norway
[4] Fraunhofer IWES, Oldenburg, Germany

jannik.schottler@forwind.de

Motivation

Field measurements
- expensive
- limited availability
- uncontrolled boundary conditions

Numerics
- computational costs
- turbulence models
- validation?

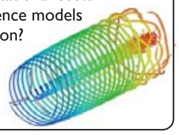

Experiments
- inexpensive
- controlled environment
- **tunable boundary conditions**
- upscaling?

Motivation

Field measurements
- expensive
- limited availability
- uncontrolled boundary conditions

Motivation

Field measurements
- expensive
- limited availability
- uncontrolled boundary conditions

Numerics
- computational costs
- turbulence models
- validation?

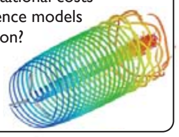

Experiments
- inexpensive
- controlled environment
- **tunable boundary conditions**
- upscaling?

Motivation

Field measurements
- expensive
- limited availability
- uncontrolled boundary conditions

Numerics
- computational costs
- turbulence models
- validation?

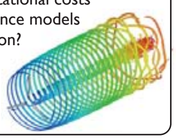

Motivation

Field measurements
- expensive
- limited availability
- uncontrolled boundary conditions

Numerics
- computational costs
- turbulence models
- validation?

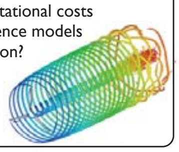

Experiments
- inexpensive
- controlled environment
- **tunable boundary conditions**
- upscaling?

Wakes Experimentally

- turbine models are **not** standardized
  - varying blade design / geometry / control...

Wakes Experimentally

- turbine models are **not** standardized
  - varying blade design / geometry / control...
- how sensitive are results to facility/turbine model/...?
- experiments lack systematics and comparability

Here:

2 turbines, 2 geometries, 2 scales
1 facility/setup


Neunaber, ForWind
60 cm


Schottler, ForWind
58 cm


Medici, KTH Mechanics
25 cm


Campagnolo, Politec Milano
2 m

Wakes Experimentally

- turbine models are **not** standardized
  - varying blade design / geometry / control...


Neunaber, ForWind
60 cm


Schottler, ForWind
58 cm


Medici, KTH Mechanics
25 cm


Campagnolo, Politec Milano
2 m

Wakes Experimentally

- turbine models are **not** standardized
  - varying blade design / geometry / control...
- how sensitive are results to facility/turbine model/...?
- experiments lack systematics and comparability

Here:

2 turbines, 2 geometries, 2 scales
1 facility/setup

Thorough analyses of wakes
from mean velocity to **two-point statistics**,
including **yaw misalignment**


Neunaber, ForWind
60 cm


Schottler, ForWind
58 cm


Medici, KTH Mechanics
25 cm


Campagnolo, Politec Milano
2 m

Wakes Experimentally

- turbine models are **not** standardized
  - varying blade design / geometry / control...
- how sensitive are results to facility/turbine model/...?
- experiments lack systematics and comparability


Neunaber, ForWind
60 cm


Schottler, ForWind
58 cm


Medici, KTH Mechanics
25 cm


Campagnolo, Politec Milano
2 m

Two-point statistics

time series

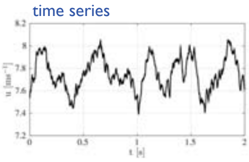

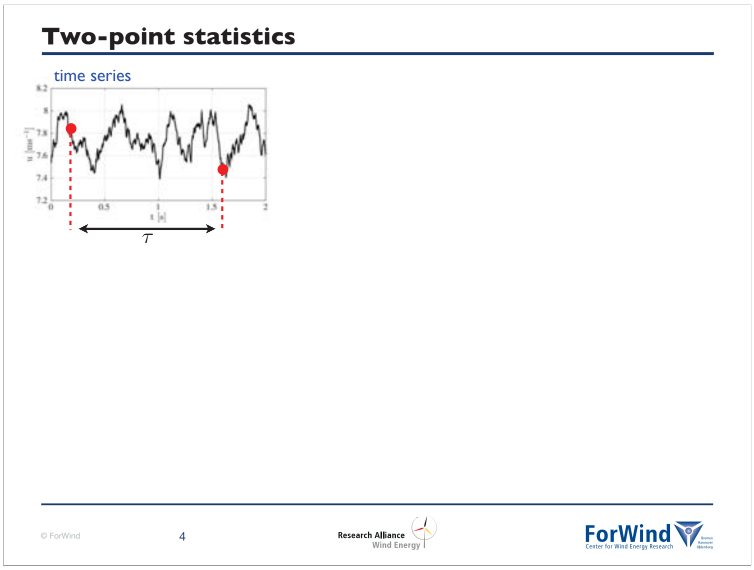
Two-point statistics
time series
t [s]
τ
© ForWind
4
Research Alliance Wind Energy
ForWind
Center for Wind Energy Research

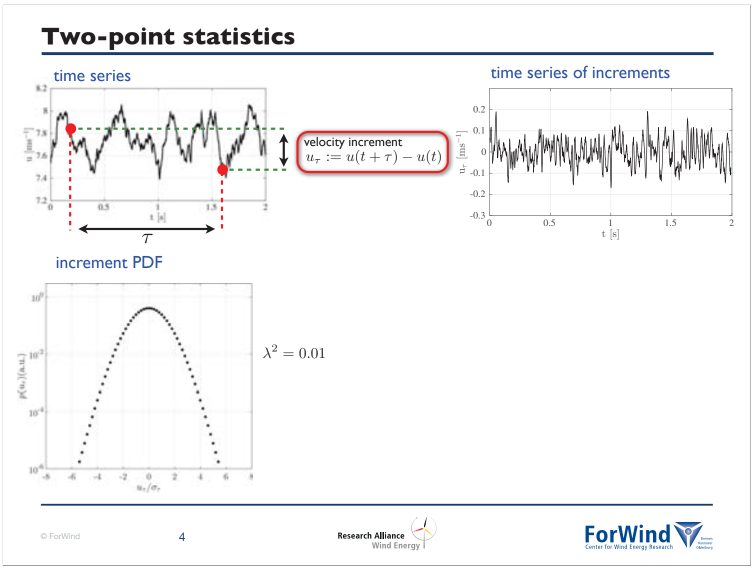
Two-point statistics
time series
velocity increment
$u_\tau := u(t+\tau) - u(t)$
time series of increments
τ
increment PDF
$\lambda^2 = 0.01$
© ForWind
4
Research Alliance Wind Energy
ForWind
Center for Wind Energy Research

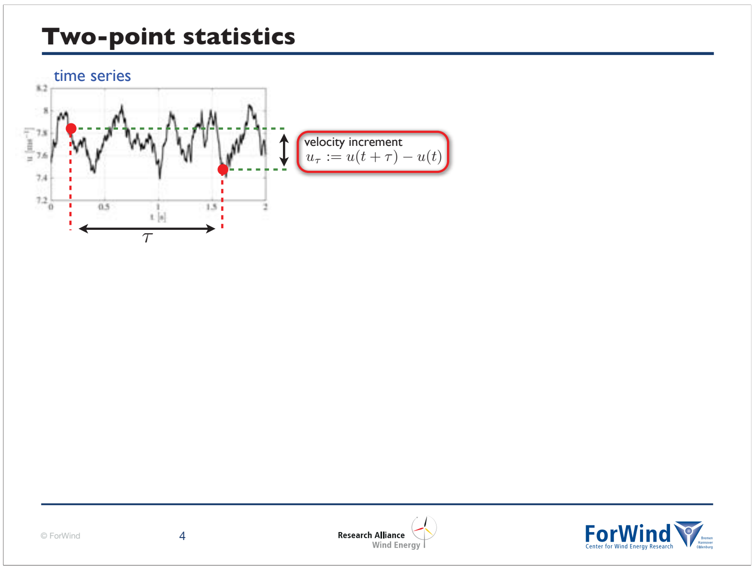
Two-point statistics
time series
velocity increment
$u_\tau := u(t+\tau) - u(t)$
τ
© ForWind
4
Research Alliance Wind Energy
ForWind
Center for Wind Energy Research

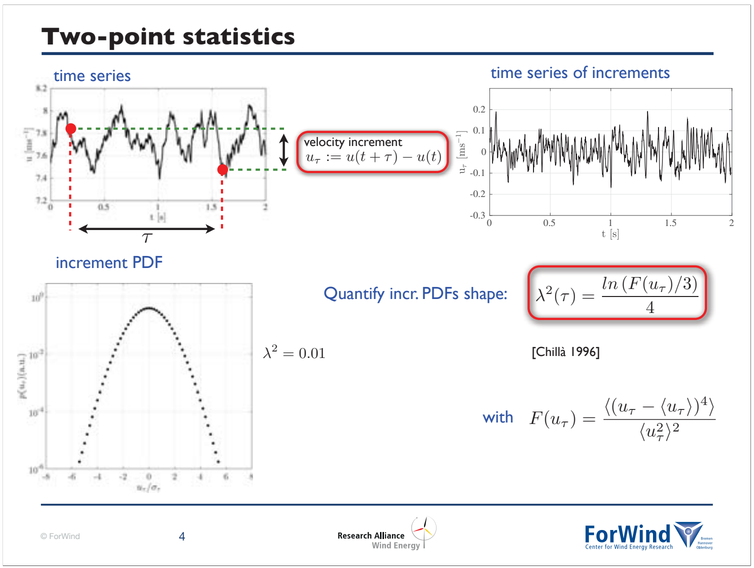
Two-point statistics
time series
velocity increment
$u_\tau := u(t+\tau) - u(t)$
time series of increments
τ
increment PDF
Quantify incr. PDFs shape:
$\lambda^2(\tau) = \frac{ln\,(F(u_\tau)/3)}{4}$
$\lambda^2 = 0.01$
[Chillà 1996]
with $F(u_\tau) = \frac{\langle (u_\tau - \langle u_\tau \rangle)^4 \rangle}{\langle u_\tau^2 \rangle^2}$
© ForWind
4
Research Alliance Wind Energy
ForWind
Center for Wind Energy Research

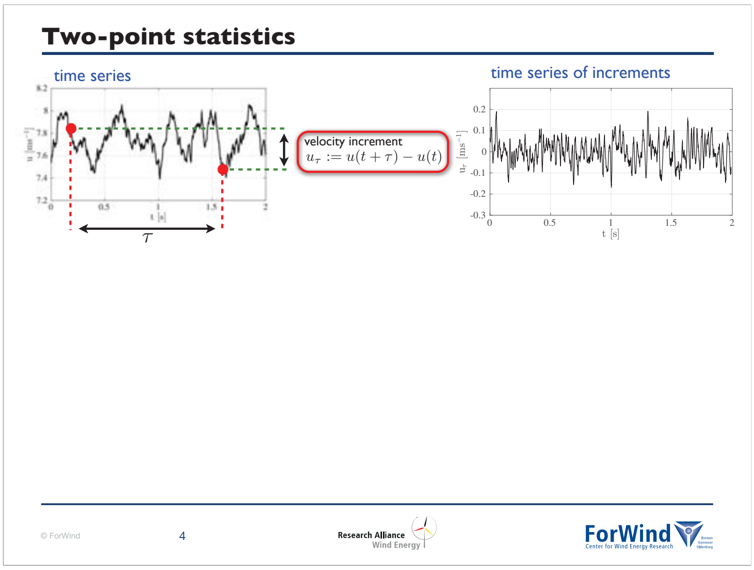
Two-point statistics
time series
velocity increment
$u_\tau := u(t+\tau) - u(t)$
time series of increments
τ
© ForWind
4
Research Alliance Wind Energy
ForWind
Center for Wind Energy Research

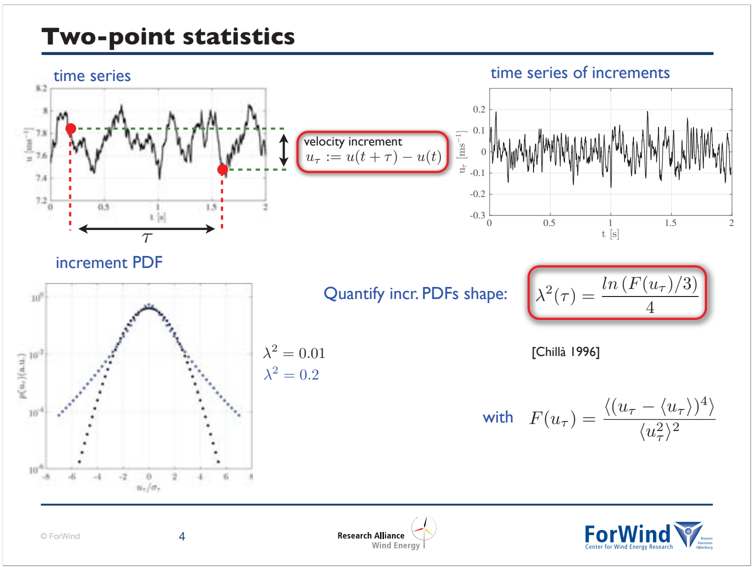
Two-point statistics
time series
velocity increment
$u_\tau := u(t+\tau) - u(t)$
time series of increments
τ
increment PDF
Quantify incr. PDFs shape:
$\lambda^2(\tau) = \frac{ln\,(F(u_\tau)/3)}{4}$
$\lambda^2 = 0.01$
$\lambda^2 = 0.2$
[Chillà 1996]
with $F(u_\tau) = \frac{\langle (u_\tau - \langle u_\tau \rangle)^4 \rangle}{\langle u_\tau^2 \rangle^2}$
© ForWind
4
Research Alliance Wind Energy
ForWind
Center for Wind Energy Research

Two-point statistics

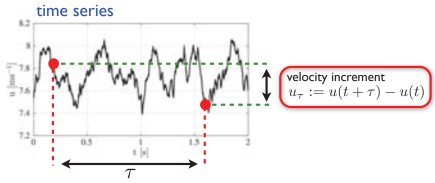

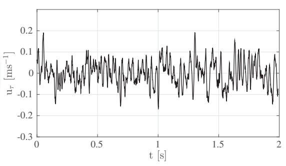

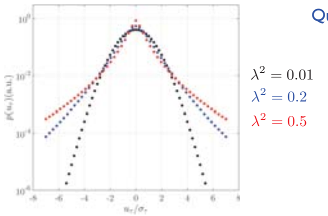

Quantify incr. PDFs shape: $\boxed{\lambda^2(\tau) = \frac{ln\left(F(u_\tau)/3\right)}{4}}$

[Chillà 1996]

with $F(u_\tau) = \frac{\langle (u_\tau - \langle u_\tau \rangle)^4 \rangle}{\langle u_\tau^2 \rangle^2}$

Setup & Overview

Turbine	Rotor diameter	Hub diameter	Blockage	TSR	Re_{tip}	Rotation	c_T
ForWind	0.580 m	0.077 m	5.4 %	6	$\approx 6.4 \times 10^4$	cw	0.97
NTNU	0.894 m	0.090 m	13 %	6	$\approx 1.1 \times 10^5$	ccw	0.87

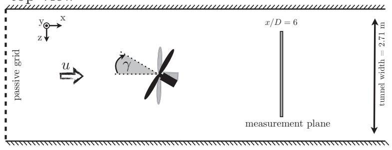

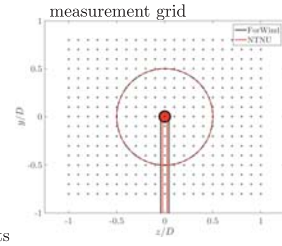

Full plane, Laser Doppler Anemometer measurements

Setup & Overview

Turbine	Rotor diameter	Hub diameter	Blockage	TSR	Re_{tip}	Rotation	c_T
ForWind	0.580 m	0.077 m	5.4 %	6	$\approx 6.4 \times 10^4$	cw	0.97
NTNU	0.894 m	0.090 m	13 %	6	$\approx 1.1 \times 10^5$	ccw	0.87

Full plane, Laser Doppler Anemometer measurements

The non-yawed wakes

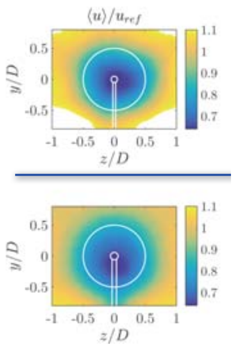

NTNU

ForWind

Setup & Overview

Turbine	Rotor diameter	Hub diameter	Blockage	TSR	Re_{tip}	Rotation	c_T
ForWind	0.580 m	0.077 m	5.4 %	6	$\approx 6.4 \times 10^4$	cw	0.97
NTNU	0.894 m	0.090 m	13 %	6	$\approx 1.1 \times 10^5$	ccw	0.87

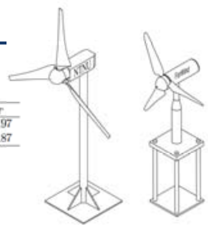

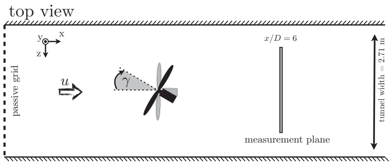

Full plane, Laser Doppler Anemometer measurements

The non-yawed wakes

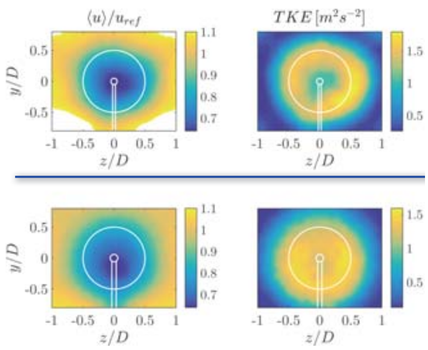

NTNU

ForWind

The non-yawed wakes

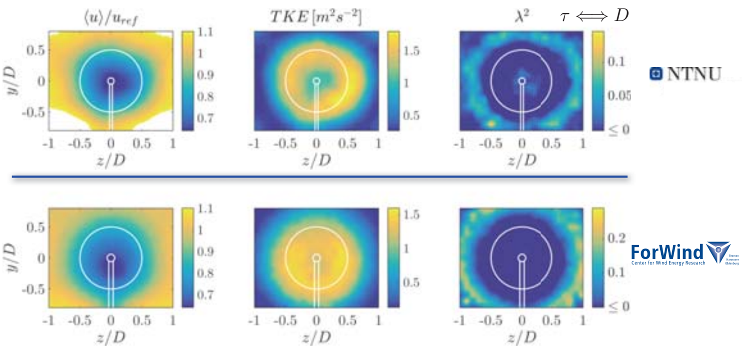

Shape parameter $\lambda^2(\tau)$

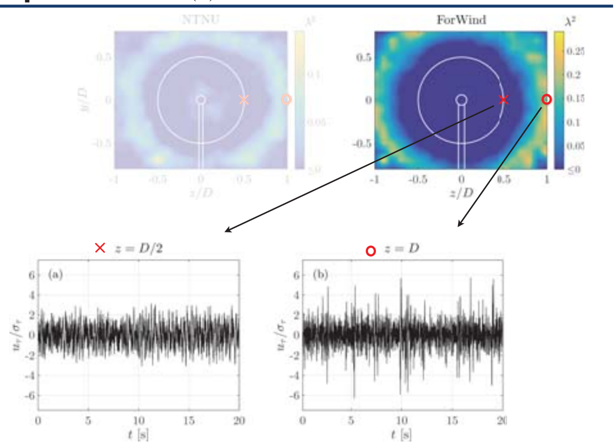

Shape parameter $\lambda^2(\tau)$

qualitative

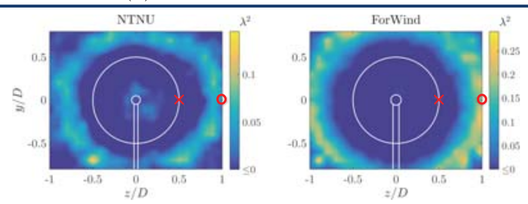

Radial wake areas

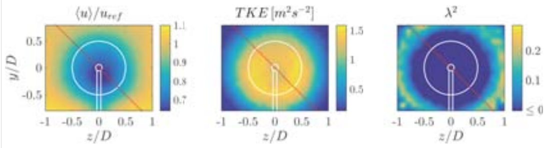

Different radial areas of interest !

Shape parameter $\lambda^2(\tau)$

qualitative

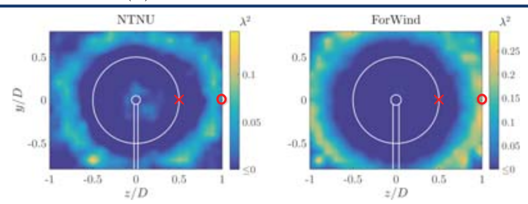

quantitative

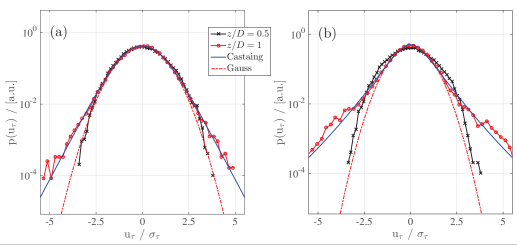

Radial wake areas

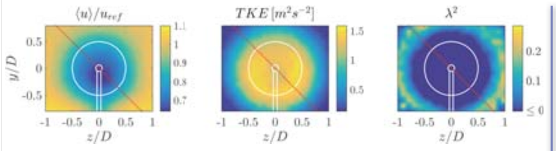

Different radial areas of interest !

Radial wake areas

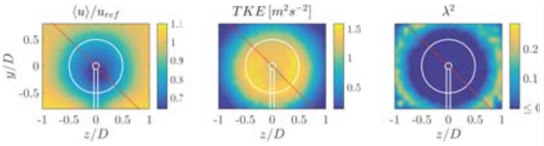

Different radial areas of interest !

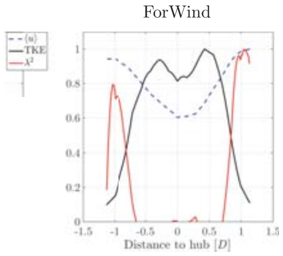

Radial wake areas

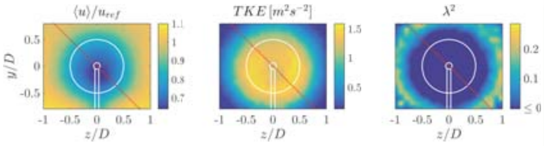

Different radial areas of interest !

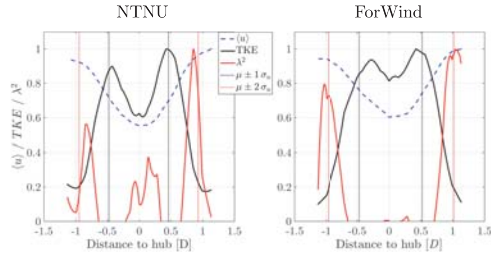

Areas of heavy-tailed increment PDFs (high λ^2) where <u> already recovered!

Approximation of high λ^2 values by $\mu \pm 2\sigma_u$

Radial wake areas

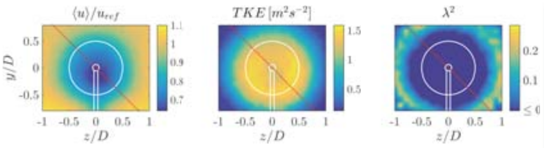

Different radial areas of interest !

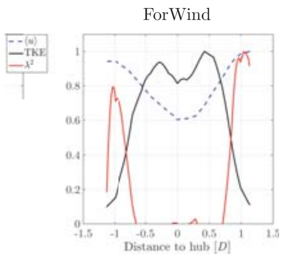

Areas of heavy-tailed increment PDFs (high λ^2) where <u> already recovered!

So far:

Radial wake areas

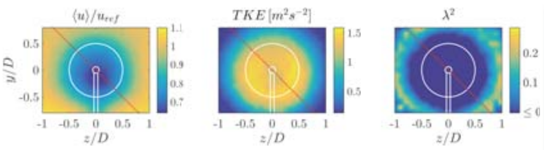

Different radial areas of interest !

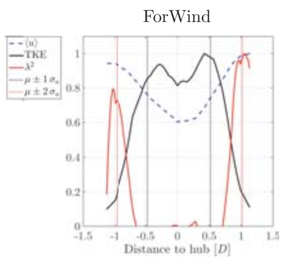

Areas of heavy-tailed increment PDFs (high λ^2) where <u> already recovered!

Approximation of high λ^2 values by $\mu \pm 2\sigma_u$

So far:

- circular wake shape
- intermittent flow regions surrounding the velocity deficit
- increased wake width
- qualitatively comparable results for both turbines

So far:

- circular wake shape
- intermittent flow regions surrounding the velocity deficit
- increased wake width
- qualitatively comparable results for both turbines

yaw misalignment:

$$\gamma = \pm 30°$$

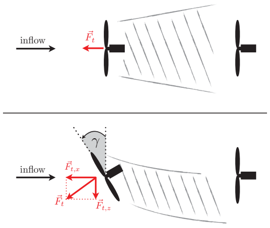

Yaw misalignment y/D

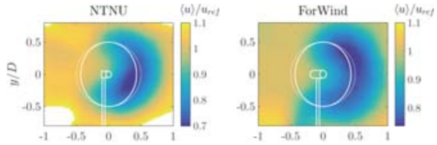

- lateral deflection
- curled shape

Yaw misalignment y/D

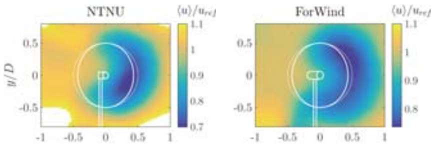

Yaw misalignment y/D

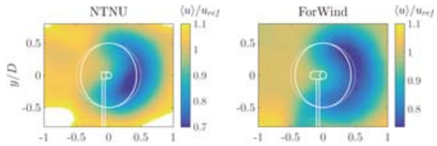

- lateral deflection
- curled shape
- vertical transport

Yaw misalignment y/D

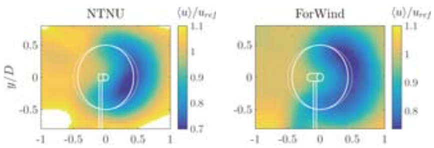

- lateral deflection

Yaw misalignment y/D

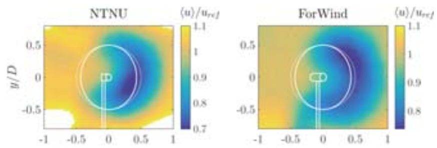

- lateral deflection
- curled shape
- vertical transport
  - depends on rotational direction !

Yaw misalignment y/D

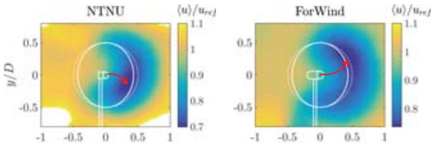

- lateral deflection
- curled shape
- vertical transport
  - depends on rotational direction !

Curled Wake in yaw - towards quantification

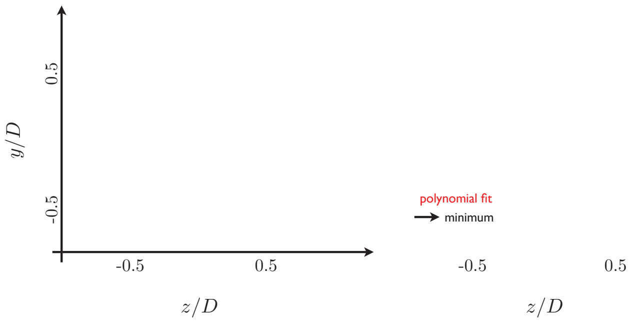

Yaw misalignment y/D

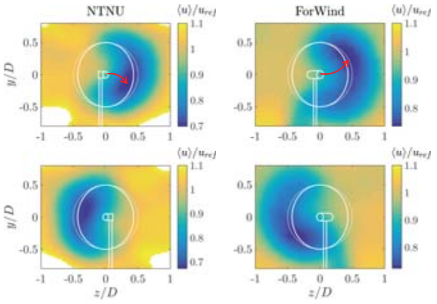

- lateral deflection
- curled shape
- vertical transport
  - depends on rotational direction !

Curled Wake in yaw - towards quantification

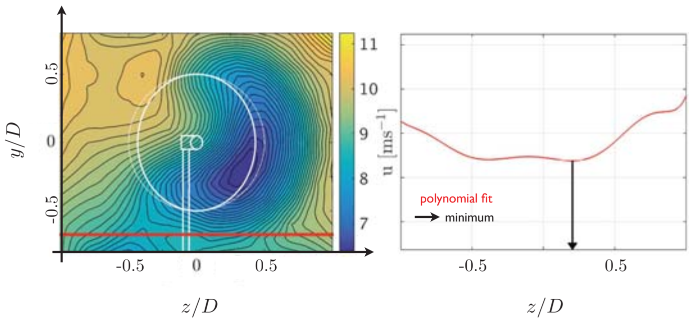

Yaw misalignment y/D

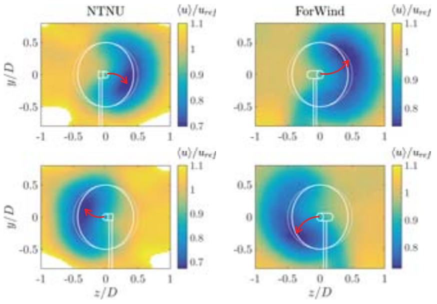

- lateral deflection
- curled shape
- vertical transport
  - depends on rotational direction !

Curled Wake in yaw - towards quantification

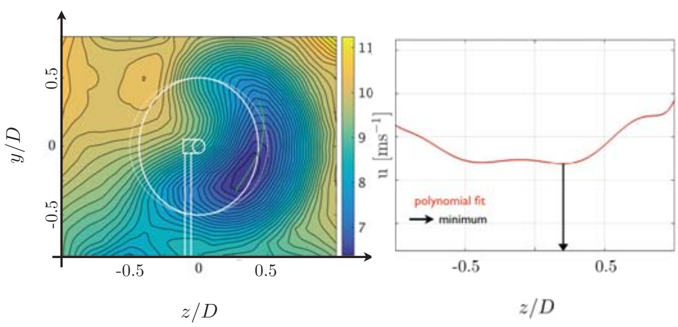

Curled Wake in yaw - towards quantification

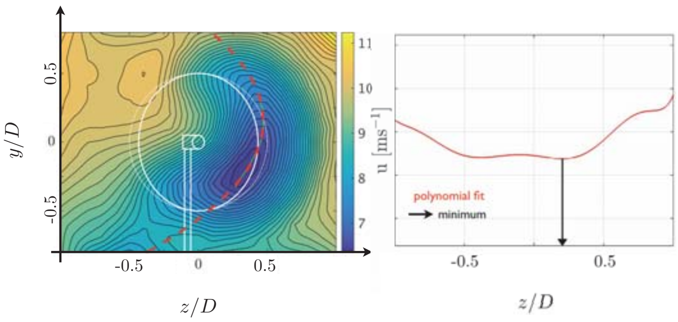

Yaw misalignment: Curl and asymmetry

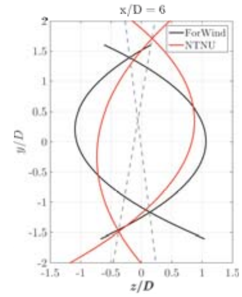

- 'curl' observed for all wakes where $\gamma \pm 30°$
- tilt in opposite direction
  - different direction of rotation!
  - interaction with the ground/tower shadow

in accordance with
[Bastankhah & Porté-Agel 2016]

Yaw misalignment: Curl and asymmetry

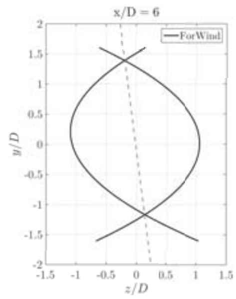

Yaw misalignment: Curl and asymmetry

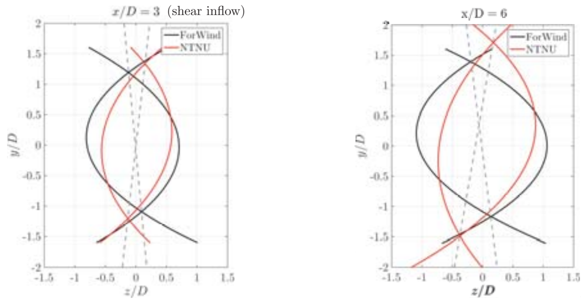

- 'curl' observed for all wakes where $\gamma \pm 30°$
- tilt in opposite direction
  - different direction of rotation!
  - interaction with the ground/tower shadow

in accordance with
[Bastankhah & Porté-Agel 2016]

Yaw misalignment: Curl and asymmetry

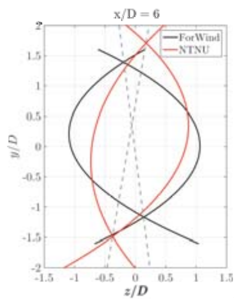

Parameter comparison at $\gamma = -30°$

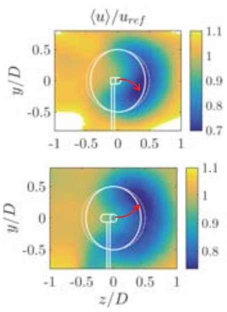

- lateral deflection
- curled shape
- vertical transport

Parameter comparison at $\gamma = -30°$

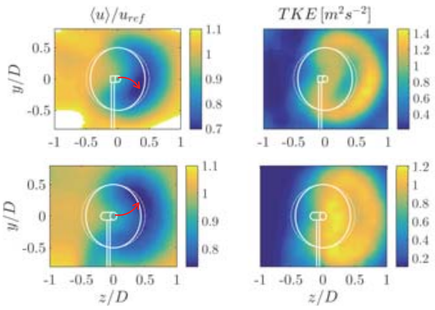

- lateral deflection
- curled shape
- vertical transport

- similar shape as <u>
- pronounced outer ring
(turbine specific)

Parameter comparison at $\gamma = -30°$

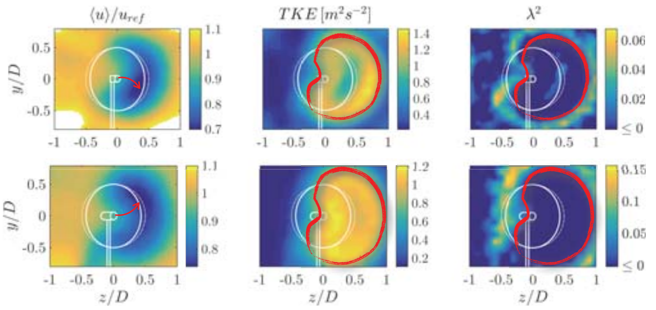

- lateral deflection
- curled shape
- vertical transport

- similar shape as <u>
- pronounced outer ring
(turbine specific)

- distinct ring surrounding TKE
- broader wake area !
- not included in models !

Parameter comparison at $\gamma = -30°$

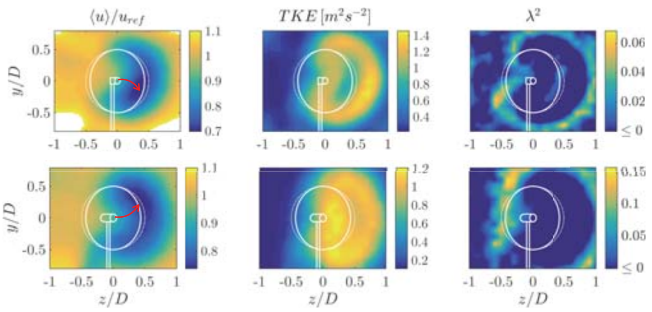

- lateral deflection
- curled shape
- vertical transport

- similar shape as <u>
- pronounced outer ring
(turbine specific)

- distinct ring surrounding TKE
- broader wake area !
- not included in models !

Summary & conclusion

Parameter comparison at $\gamma = -30°$

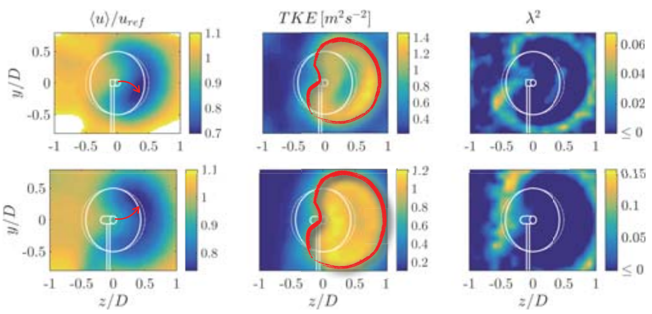

- lateral deflection
- curled shape
- vertical transport

- similar shape as <u>
- pronounced outer ring
(turbine specific)

- distinct ring surrounding TKE
- broader wake area !
- not included in models !

Summary & conclusion

- wake measurements with focus on yaw misalignment
  - full plane LDA data
  - 2 model wind turbines, differing in size/design
  - 3 yaw angles, 3 inflow conditions
  - > 20 wakes total

project

Summary & conclusion

- wake measurements with focus on yaw misalignment
  - full plane LDA data
  - 2 model wind turbines, differing in size/design
  - 3 yaw angles, 3 inflow conditions
  - > 20 wakes total

project

- wake analysis including two-point statistics
- radial wake extension significantly larger when including two-point statistics !
- important for downstream turbine loads
  -> affecting wake steering application and wind farm layout

this talk

Curl parametrization

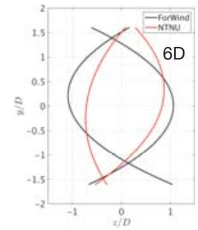

Summary & conclusion

- wake measurements with focus on yaw misalignment
  - full plane LDA data
  - 2 model wind turbines, differing in size/design
  - 3 yaw angles, 3 inflow conditions
  - > 20 wakes total

project

- wake analysis including two-point statistics
- radial wake extension significantly larger when including two-point statistics !
- important for downstream turbine loads
  -> affecting wake steering application and wind farm layout

this talk

- Blind test 5 coming up
- data available for cooperation/validation

outlook

Curl parametrization

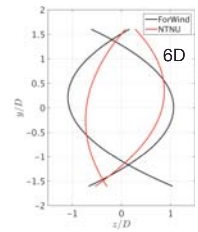

- 'curl' observed for all wakes where $\gamma \pm 30^\circ$
- further deflection of 'ForWind'-wake
- tilt in opposite direction
  - different direction of rotation!
  - interaction with the ground/tower shadow

in accordance with [Bastankhah & Porté-Agel 2016]

Thank you!

Partly funded by the Reiner Lemoine Foundation

jannik.schottler@forwind.de

Curl parametrization

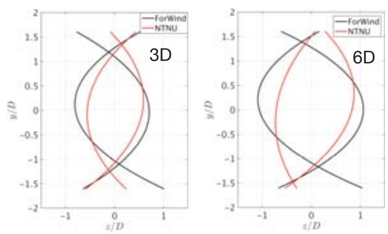

- 'curl' observed for all wakes where $\gamma \pm 30^\circ$
- further deflection of 'ForWind'-wake
- tilt in opposite direction
  - different direction of rotation!
  - interaction with the ground/tower shadow

in accordance with [Bastankhah & Porté-Agel 2016]

Shape parameter $\lambda^2(\tau)$

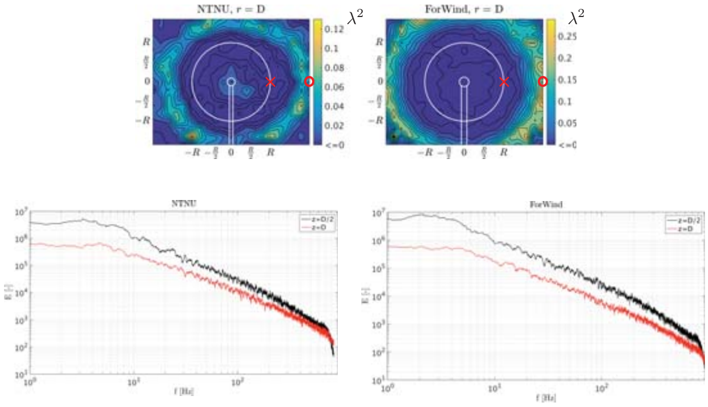

Wake center detection

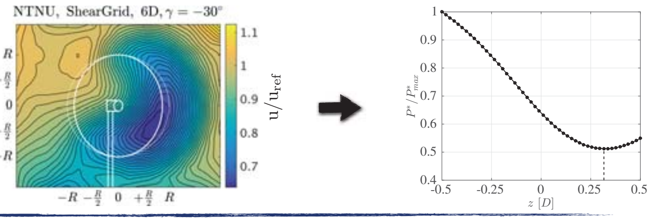

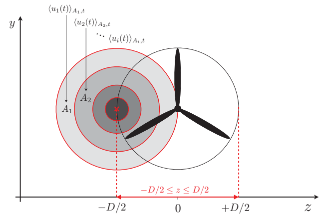

For $-D/2 \le z \le D/2$

$$P^* = \sum_{i=1}^{10} \rho A_i \langle u_i(t) \rangle^3_{A_i,t}$$

Wake center detection

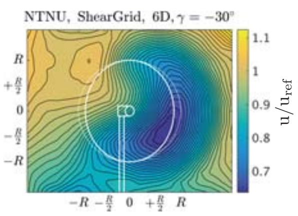

Wake center detection

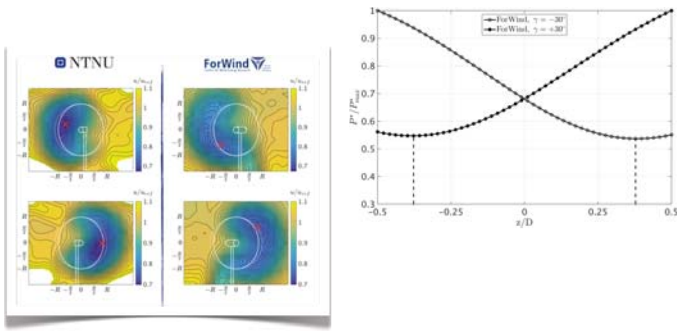

Wake center detection

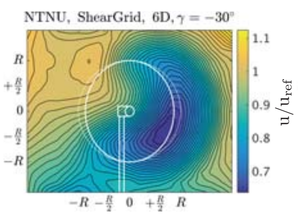

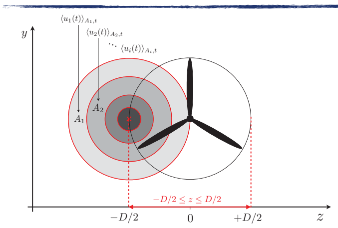

For $-D/2 \le z \le D/2$

$$P^* = \sum_{i=1}^{10} \rho A_i \langle u_i(t) \rangle^3_{A_i,t}$$

Wake center detection

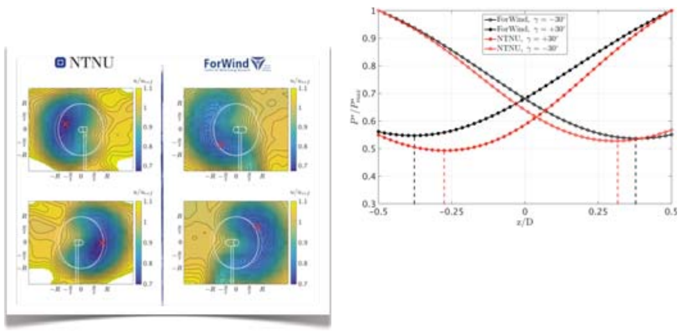

Wake center detection

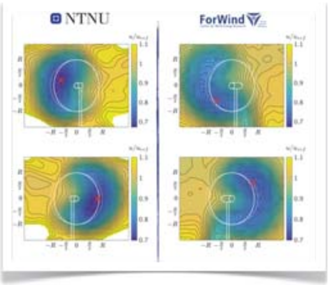

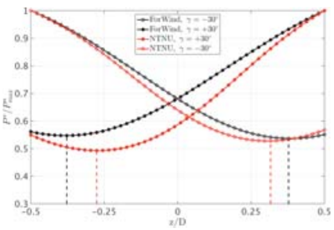

Turbine	γ	Wake center	Skew angle
NTNU	$30°$	$-0.28D$	$\approx -2.6°$
NTNU	$-30°$	$0.32D$	$\approx 3.0°$
ForWind	$30°$	$-0.38D$	$\approx -3.6°$
ForWind	$-30°$	$0.38D$	$\approx 3.6°$

Curled wake in yaw - a general effect ?

ForWind

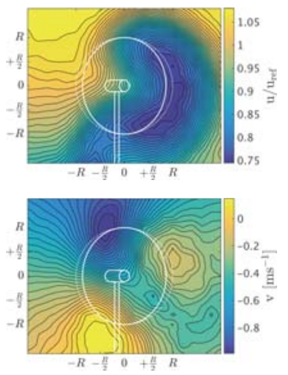

NTNU

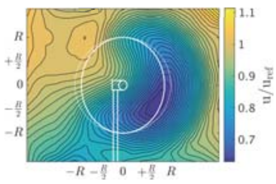

Curled wake in yaw - a general effect ?

ForWind

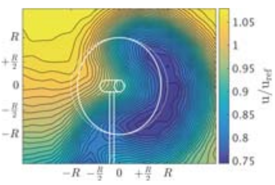

NTNU

Curled wake in yaw - a general effect ?

ForWind

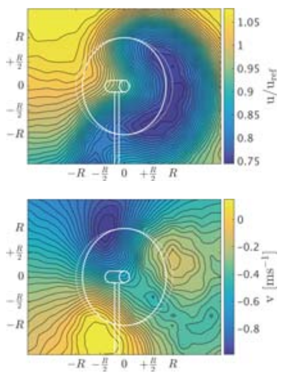

NTNU

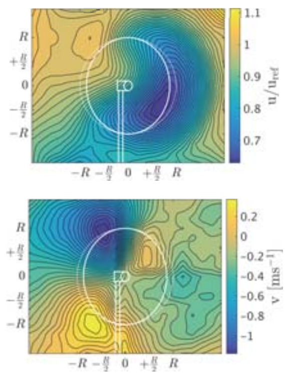

Curled wake in yaw - a general effect ?

ForWind

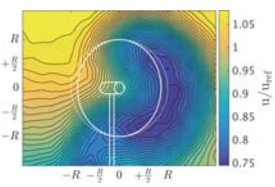

NTNU

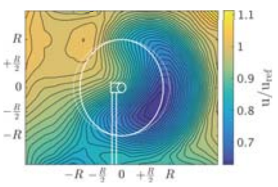

Curled wake in yaw - a general effect !

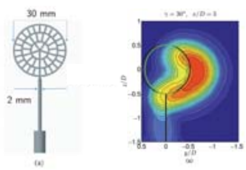

[Howland et al. 2016]

Curled wake in yaw - a general effect !

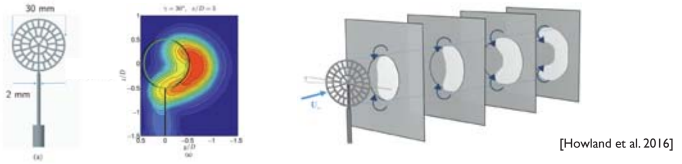

[Howland et al. 2016]

Curled wake in yaw - a general effect !

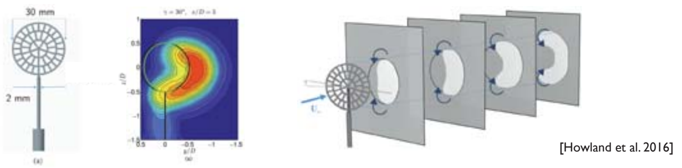

[Howland et al. 2016]

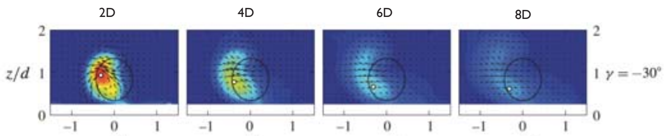

[Bastankhah & Porté-Agel 2016]

Curled wake in yaw - a general effect !

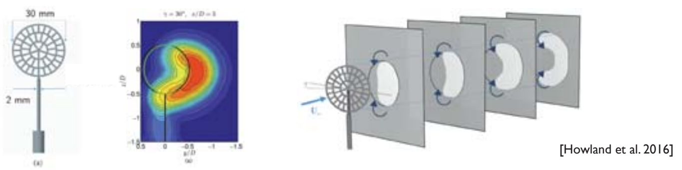

[Howland et al. 2016]

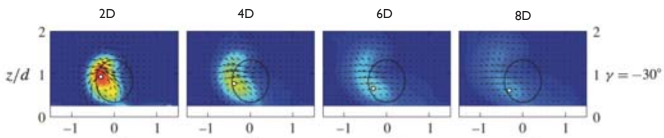

[Bastankhah & Porté-Agel 2016]

Curled wake observed for drag disc (30mm) model wind turbines (150mm, 580mm, 890mm)

A Detached-Eddy-Simulation study

Proper-Orthogonal-Decomposition of the wake flow behind a model wind turbine

J. Göing[1], J. Bartl[2], F. Mühle[3], L. Sætran[2], P.U. Thamsen[1]

Technical University of Berlin[1], Norwegian University of Science and Technology[2], Norwegian University of Life Sciences[3]

Introducing the UT2 (Circulating tank 2) at the TU Berlin

- One of the biggest circulating water tanks worldwide
- Built in 70´s and recently renovated
- Suitable for studies of ship properties as well as of floating wind turbine models

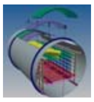

- Drive: 2 motors, 1.6 MW each
- Pump: Q = 60000 l/s at H= 2 m
- Flow speed up to 9 m/s

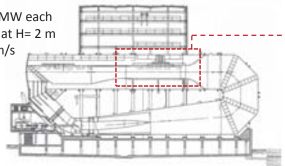

Real problem in the wind park optimization?

(1)

LDA-Experiment conditions

(a) Test wind turbine

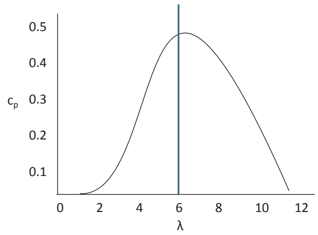

(b) Tip speed ratio

Simulation conditions

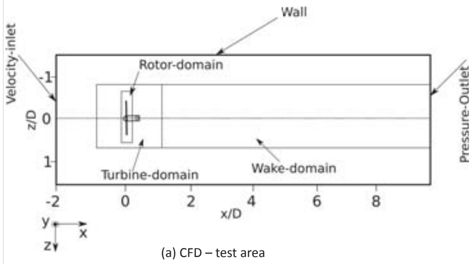

(a) CFD – test area

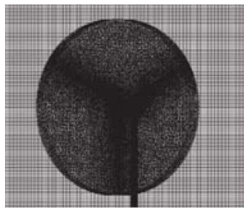

(b) Sliding mesh and grid size

Detached-Eddy-Simulation (DES)

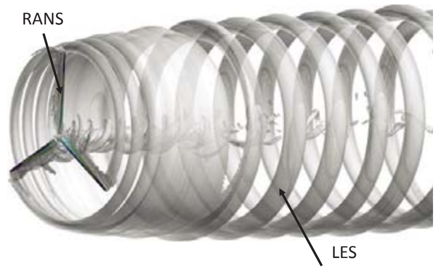

(2)

CFD Methods	Simulation properties
Reynolds-Averaged-Navier-Stokes	Mean values
Large-Eddy-Simulation	Large eddies

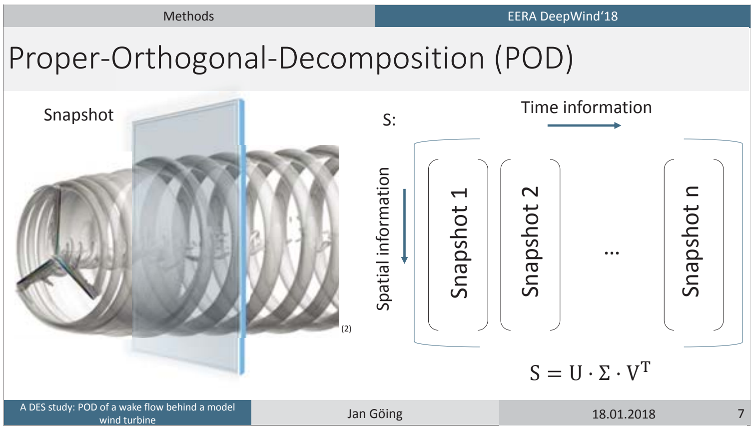
Methods
EERA DeepWind'18
Proper-Orthogonal-Decomposition (POD)
Snapshot
S:
Time information
Spatial information
Snapshot 1
Snapshot 2
...
Snapshot n
(2)
S = U · Σ · V^T
A DES study: POD of a wake flow behind a model wind turbine
Jan Göing
18.01.2018
7

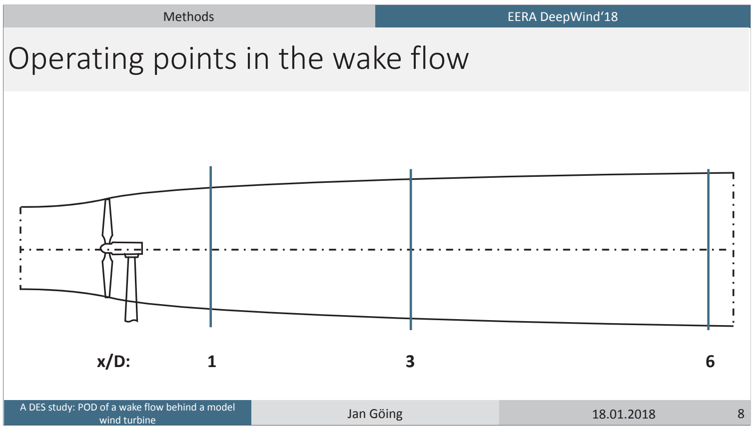
Methods
EERA DeepWind'18
Operating points in the wake flow
x/D:
1
3
6
A DES study: POD of a wake flow behind a model wind turbine
Jan Göing
18.01.2018
8

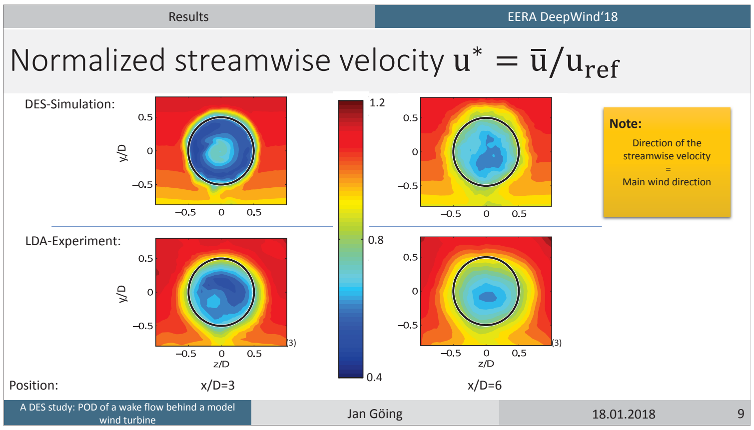
Results
EERA DeepWind'18
Normalized streamwise velocity u* = ū/u_ref
DES-Simulation:
LDA-Experiment:
y/D
z/D
1.2
0.8
0.4
(3)
Note:
Direction of the streamwise velocity
=
Main wind direction
Position:
x/D=3
x/D=6
A DES study: POD of a wake flow behind a model wind turbine
Jan Göing
18.01.2018
9

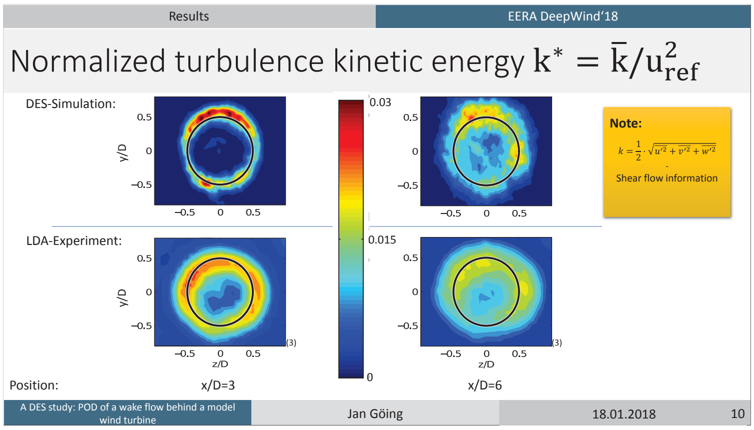
Results
EERA DeepWind'18
Normalized turbulence kinetic energy k* = k̄/u_ref^2
DES-Simulation:
LDA-Experiment:
y/D
z/D
0.03
0.015
0
(3)
Note:
Shear flow information
Position:
x/D=3
x/D=6
A DES study: POD of a wake flow behind a model wind turbine
Jan Göing
18.01.2018
10

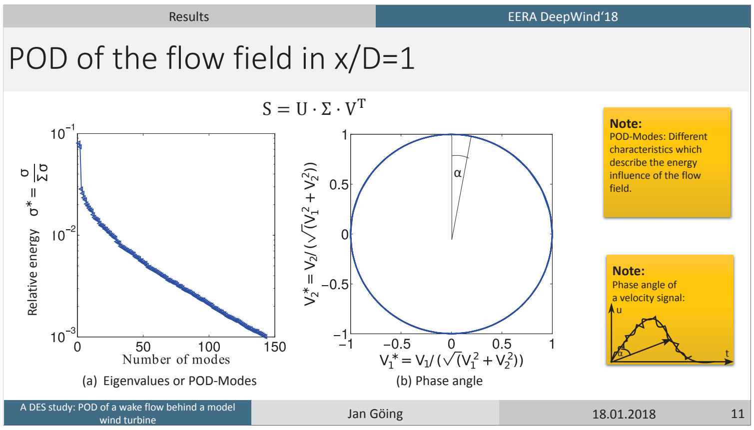
Results
EERA DeepWind'18
POD of the flow field in x/D=1
S = U · Σ · V^T
Relative energy σ* = σ/Σσ
Number of modes
(a) Eigenvalues or POD-Modes
V2* = V2/(√(V1² + V2²))
V1* = V1/(√(V1² + V2²))
α
(b) Phase angle
Note:
POD-Modes: Different characteristics which describe the energy influence of the flow field.
Note:
Phase angle of a velocity signal:
A DES study: POD of a wake flow behind a model wind turbine
Jan Göing
18.01.2018
11

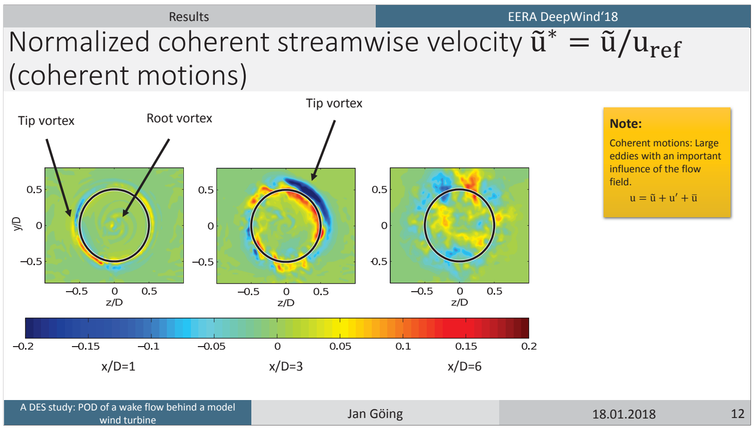
Results
EERA DeepWind'18
Normalized coherent streamwise velocity ũ* = ũ/u_ref (coherent motions)
Tip vortex
Root vortex
Tip vortex
y/D
z/D
x/D=1
x/D=3
x/D=6
Note:
Coherent motions: Large eddies with an important influence of the flow field.
u = ū + u' + ũ
A DES study: POD of a wake flow behind a model wind turbine
Jan Göing
18.01.2018
12

Fluctuation loads (significant frequencies)

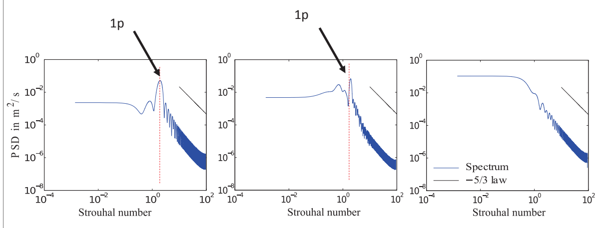

x/D=1 x/D=3 x/D=6

Note:

1p: Interaction between the rotation frequency of one blade and the tower.

Validation of the frequency

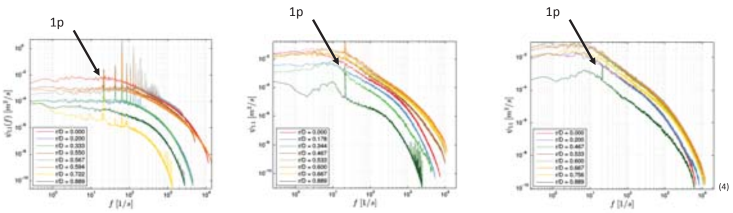

x/D=1 x/D=3 x/D=5

Conclusion

1. DES and POD
   a. Velocity components, turbulence kinetic energy
   b. Coherent motions (tip vortex, root vortex)
   c. Fluctuation load (1p frequency)
2. Future studies
   a. Different inflow/boundary conditions
   b. Wake flow analyses for more than one turbine
   c. Optimization of the wind park planning

Thank you for your attention…

…Questions?

References:

(1) http://www.envision-energy.com/2016/08/17/optimizing-energy-production/ 14.01.2018

(2) https://www.windpowerengineering.com/simulation/seeing-the-unseeable-in-a-rotor-wake/ 14.01.2018

(3) Bartl, J., Mühle, F., Schottler, J., Sætran, L. Peinke, J., Adaramola, M. and Hölling M. [2017], Experiments on wind turbine wakes in yaw: Effects of inflow turbulence and shear. *Manuscript submitted to Wind Energy Science.*

(4) Eriksen, P. E. [2016] Rotor wake turbulence: An experimental study of a wind turbine wake, *Doctoral thesis at NTNU 2017*: 2017:34, isbn: 978-82-326-1408-0

BOHEM – Blade Optical Health Monitoring

18/01/2018 | Paul McKeever

CATAPULT Offshore Renewable Energy

ORE Catapult

Our Vision:

Abundant, affordable energy from offshore wind, wave and tide

- Reduce the cost of offshore renewable energy
- Deliver UK economic benefit
- Engineering and research experts with deep sector knowledge
- Independent and trusted partner
- Work with industry and academia to commercialise new technologies

80+ technical experts

ore.catapult.org.uk
@orecatapult

CATAPULT Offshore Renewable Energy

Agenda

- Project partners
- Project objectives
- How BOHEM works
- BOHEM initial results
- Latest BOHEM results
- Summary

ore.catapult.org.uk
@orecatapult

CATAPULT Offshore Renewable Energy

Blade Cross-Sectional Deformation

- The current generation of large wind turbines have blades in excess of 80m long, with a typical chord length of 6m
- This means that there are extremely large unsupported panels around the max chord region of the blade which can deform out of plane when the blade bends
- These deformations stress the panels in the transverse direction (potentially causing delamination and create peeling stresses at the trailing edge bond line)

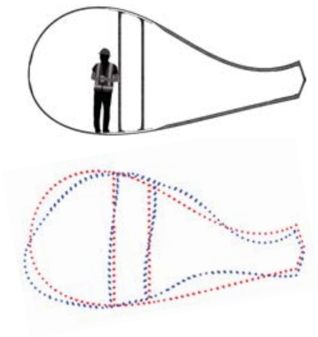

ore.catapult.org.uk
@orecatapult

wideblue making technology happen | CATAPULT Offshore Renewable Energy

About the BOHEM Partners

wideblue making technology happen

WideBlue Ltd is multi-disciplinary product design and product development consultancy based in Glasgow. WideBlue's team of product, mechanical, electronic and software engineers, physicists and optical designers have years of experience of taking products from design through to successful manufacture and commercialisation.

CATAPULT Offshore Renewable Energy

The Offshore Renewable Energy Catapult is the UK's flagship technology innovation and research centre for advancing wind, wave and tidal energy. ORE Catapult participates in large-scale collaborative R&D and innovative commercial and public funded projects, amassing vast technical knowledge and know-how.

ore.catapult.org.uk
@orecatapult

wideblue making technology happen | CATAPULT Offshore Renewable Energy

Blade Cross-Sectional Deformation

- In addition to this phenomenon of panel deformation, the whole blade cross-section can shear as a result of combined torsional and shear loading, which generates stresses at the bond between the shear webs and the spar cap or the blade shell, depending on blade architecture.
- The use of large flatback aerofoils further compounds this issue.

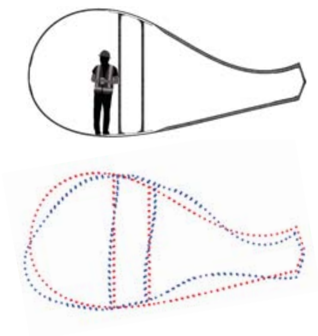

ore.catapult.org.uk
@orecatapult

wideblue making technology happen | CATAPULT Offshore Renewable Energy

Blade Cross-Sectional Deformation (Flap Max)

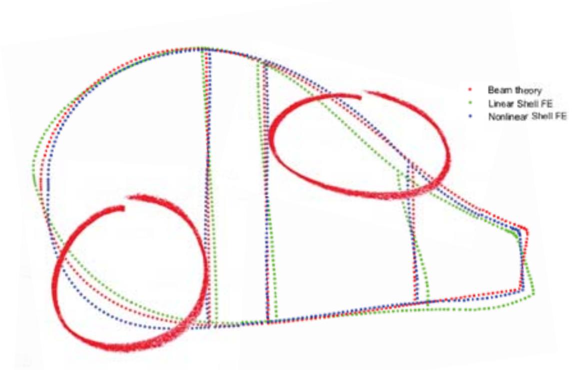

Nonlinear and linear deflections are in opposite directions!

BOHEM Concept

BOHEM's robust root mounted vision system tracks the displacement of a series of reflective markers installed in the blade's most critical areas. The reflective markers are passive, low cost, easy to install and can be removed without damage to the blade.

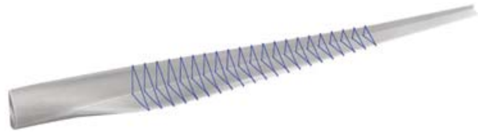

Blade Cross-Sectional Deformation (Edge Min)

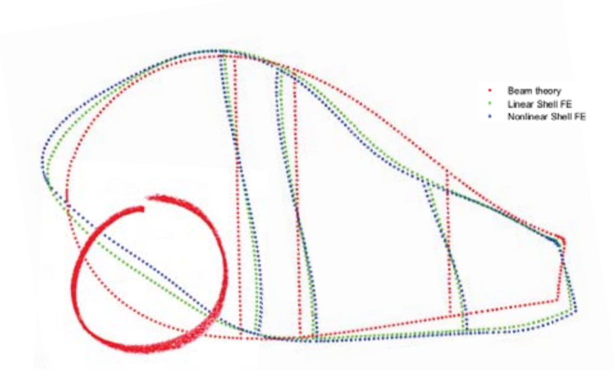

Nonlinear deflections are much larger than linear

BOHEM Process

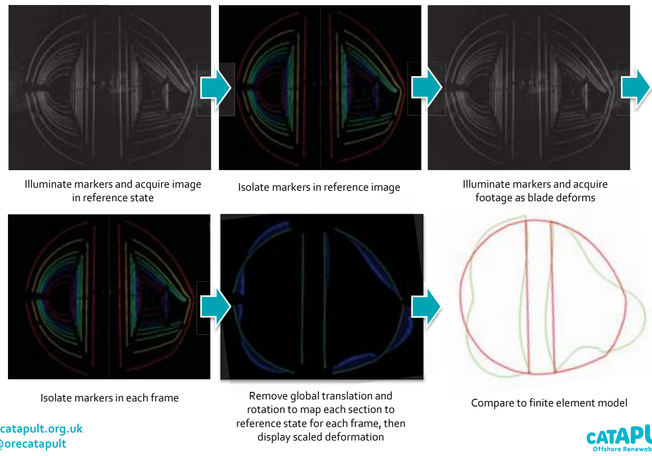

Blade Cross-Sectional Deformation

- It is clear that, whilst blades are beam like structures, their hollow structure means that the cross section can deform and the assumption of 'plane sections remaining plane' cannot be used. The structural designer must use nonlinear shell or brick based 3D FE (finite element) models to characterize how panels deform, and these models must be validated.
- ORE Catapult and Wideblue Ltd have developed the BOHEM system to monitor blade cross-sectional deformation

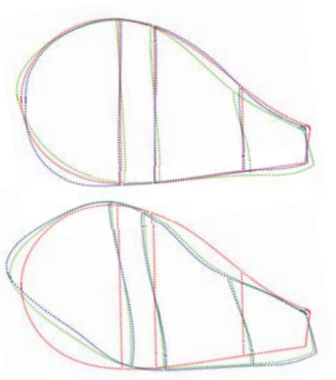

Raw Footage
Reflectors 5m - 20m in a 40m Blade

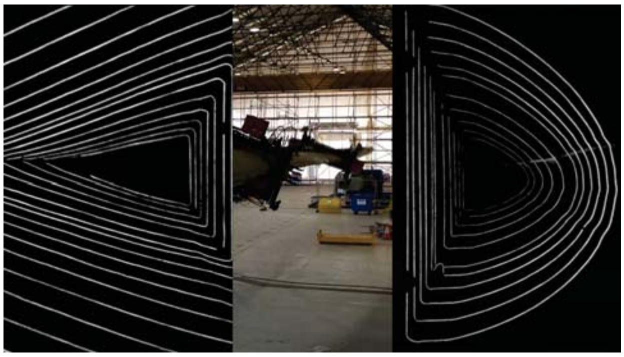

Footage Processing

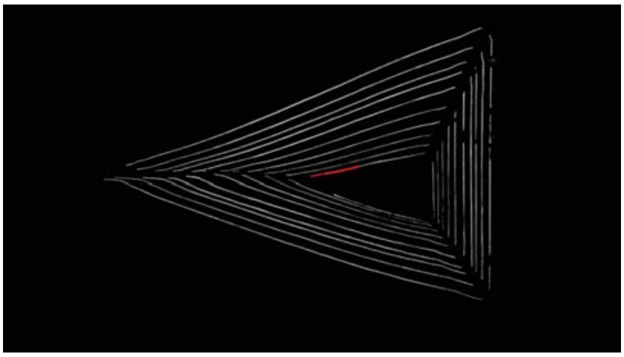

BOHEM Validation

- BOHEM can be used as a 'virtual stringpot' to measure the displacement between two points
- It has been validated against stringpot measurements during static blade testing
- Unfortunately, the stringpot measurements were not reliable so in the final test laser measurement mounted on telescopic poles was used
- Overall, good agreement was achieved but it is hard to say whether measurement inaccuracy is responsible for discrepancies…
- A lot of lessons have been learnt for next time!

	Measurement Location	BOHEM Prediction (mm)	FE Prediction (mm)	Test value Stringpot (mm)	Test Value Laser (mm)
Test 1	Leading edge 11m	100%	108%	81%	
	Trailing edge 8m	100%	114%	91%	
Test 2	Leading edge 11m	100%	186%	-17%	
	Trailing edge 8m	100%	186%	110%	
Test 3	Leading edge 11m	100%	87%	71%	103%
	Trailing edge 8m	100%	254%	181%	181%

Footage Processing

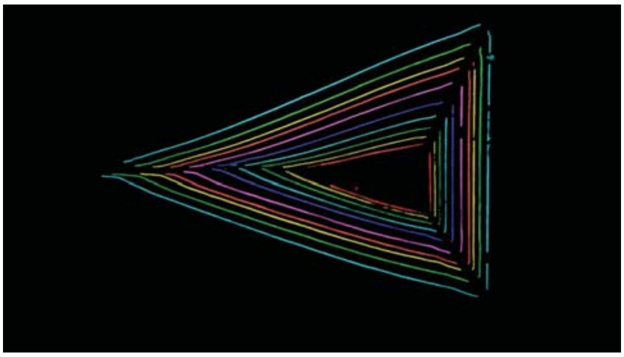

Summary and Further Work

- BOHEM is a novel method of monitoring cross-sectional deformation based on acquiring images of reflective markers
- It has been proven to give useful results during full scale blade tests
- The long term goal of the BOHEM project is to develop a low cost health monitoring mechanism for blades in service
- By tracking the deflection envelope and how it changes over time for a given wind speed (known from SCADA data) BOHEM could act as an early warning system for panel delamination or trailing edge debonding

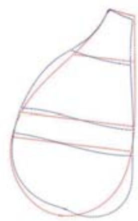

Post Processing

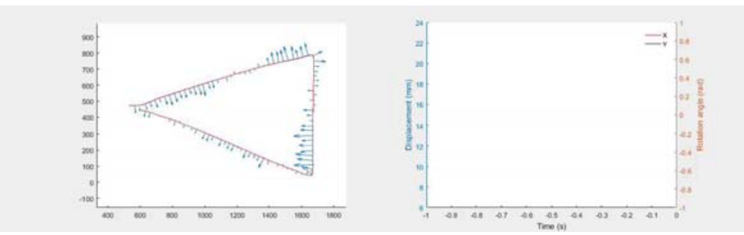

Contact us

GLASGOW
ORE Catapult
Inovo
121 George Street
Glasgow
G1 1RD

T +44 (0)333 004 1400
F +44 (0)333 004 1399

BLYTH
ORE Catapult
National Renewable Energy Centre
Offshore House
Albert Street
Blyth, Northumberland
NE24 1LZ

T +44 (0)1670 359 555
F +44 (0)1670 359 666

LEVENMOUTH
ORE Catapult
Fife Renewables Innovation Centre (FRIC)
Ajax Way
Leven
KY8 3RS

T +44 (0)1670 359 555
F +44 (0)1670 359 666

info@ore.catapult.org.uk
ore.catapult.org.uk

Scaled wind turbine setup in turbulent wind tunnel

MoWiTO 1.8 (Model Wind Turbine Oldenburg 1.8 m)

Frederik Berger, Lars Kröger, David Onnen, Vlaho Petrović and Martin Kühn

ForWind – Carl von Ossietzky University Oldenburg

Trondheim – EERA DeepWind conference
January 18, 2017

Motivation

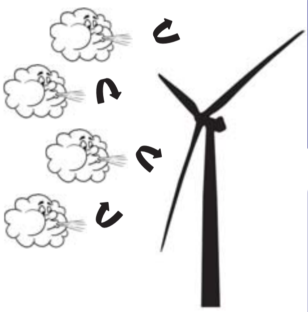

- Interaction of turbulent wind w/ wind turbine in controlled wind tunnel environment:
  - Loads
  - Aerodynamics
  - Control

- Scaling objectives:
  1. Representative aerodynamic response in turbulence
  2. Realistic characteristic curves
  3. Characteristics Re insensitive

Scaling: Global Parameters

Parameters

- Based on NREL 5MW
- Keep design TSR (~7.5)
- Scaling parameters:
  - Length scaling

$$n_L = \frac{D_{\text{scaled}}}{D_{\text{refernce}}} = \frac{1.8\ \text{m}}{126\ \text{m}} = \frac{\mathbf{1}}{\mathbf{70}}$$

  - Time scaling

$$n_T = \frac{n_{\text{scaled}}}{n_{\text{reference}}} = \frac{600\ \text{rpm}}{12.1\ \text{rpm}} = \mathbf{49.6}$$

Rated values	Scaling factor	Reference	Scaled
Revolutions	$1 * n_T$	12.1 rpm	600 rpm
Power	$n_L^5 * n_T^3$	5 MW	363 W
Wind speed	$n_L * n_T$	11.4 m/s	8.1 m/s
Reynolds number	$n_L^2 * n_T$	$\sim 10^7$	$\sim 10^5$

Scaling: Aerodynamics

Exchange of airfoils

Root airfoil exchange

original	scaled
DU 99-W-350	SG6040
0.25 R – 0.32 R	0.2 R – 0.38 R
35 % thickness	16 % thickness

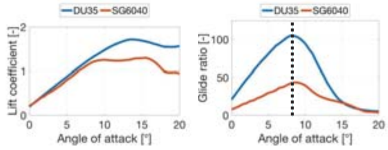

Tip and midspan airfoil exchange

original	scaled
NACA 64618	SG6041
0.7 R – 1 R	0.5 R – 1 R
18 % thickness	10 % thickness

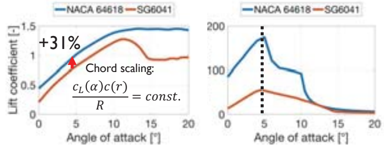

Blade design

- Carbon fiber with foam spar
- Composite blade weight ~160 g ($m_{\text{blade NREL 5MW}} / 70^3 = 52$ g)
- Glued on metal inlet
  - Flapwise strain gauge
  - Pitch motor housing
  - Pitch bearing shaft surface
- First eigenfrequency ~39 Hz

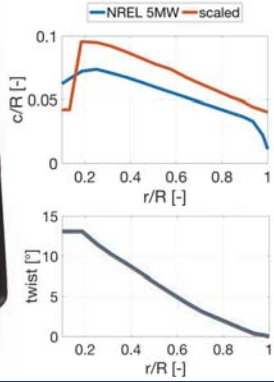

Objective 1: Aerodynamic response in turbulence ✓

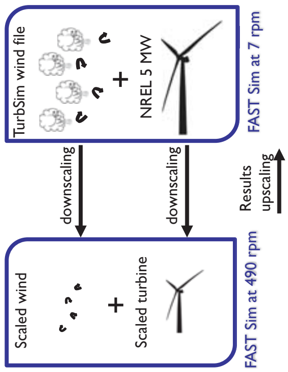

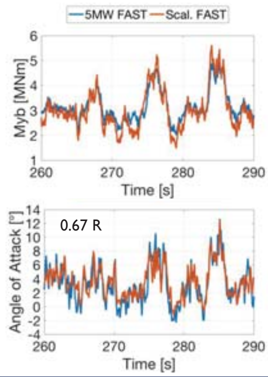

Turbine key facts

- **Sensors and actuators**:
  - Strain gauges at blade root (flapwise)
  - Strain gauges at tower base (fore–aft, side–side)
  - Torque meter with encoder
  - Individual pitch motors
  - Real time control and data acquisition
- **Operation**:
  - 400 – 600 rpm
  - Rated wind 8.1 m/s

Active Grid

20 split axes with flaps in each, horizontal and vertical, direction

80 servomotors driving the axes

Reproduce turbulent wind patterns, e.g. based on free field measurements

Nacelle layout

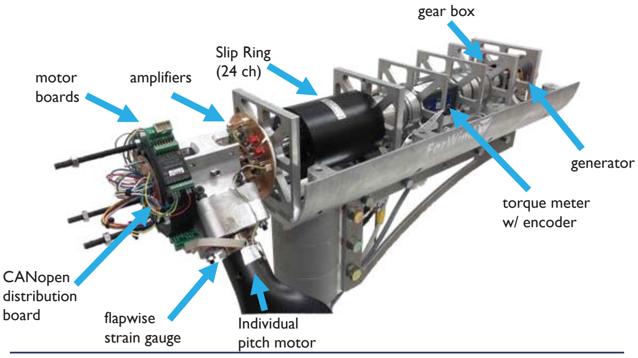

Aerodynamic characterisation in wind tunnel

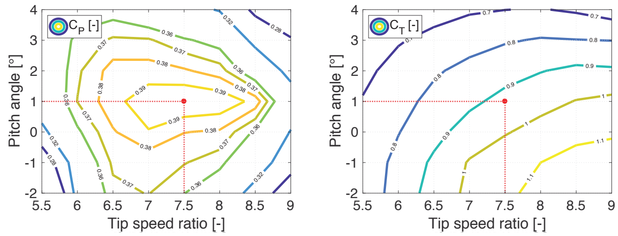

Wind Tunnel at University Oldenburg

- WindLab; Dimensions (H x W x L) 3 x 3 x 30 m^3
- Open test section or closed test section
- V_{Wind} up to 42 m/s (closed) or 30 m/s (open)

Objective 2:
C_p and C_t characteristic° ✓

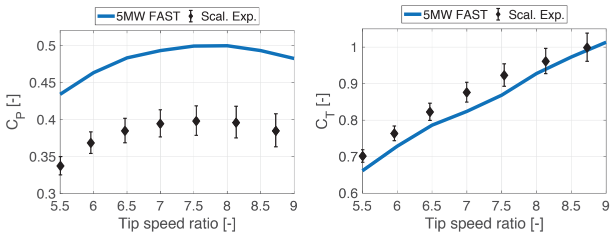

- Slope matches
- Offset due to difference in glide ratio of profiles

- Good match

Error bars indicate influence of ± 0.1 m/s in reference wind

Objective 3: Influence of Reynolds number ✓

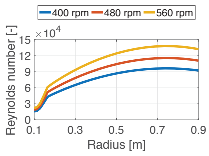

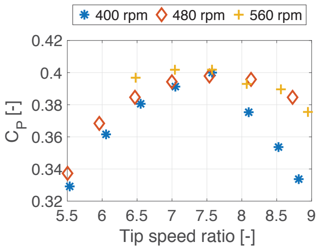

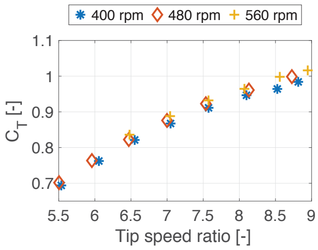

Experiments: Turbulent Inflow

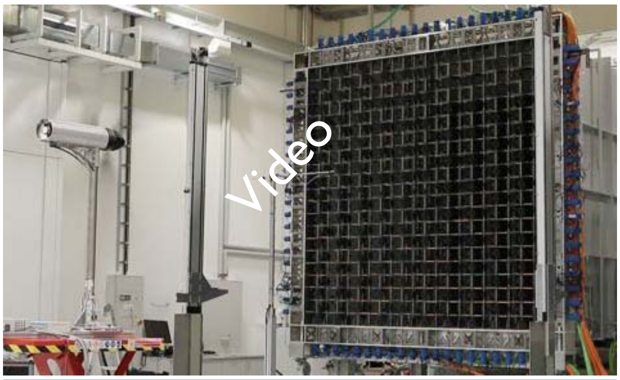

Experiments: Turbulent Inflow

- Turbulent protocol based on free field measurement
- Mean wind velocity 5.7 m/s
- Turbulence intensity 10.4 %

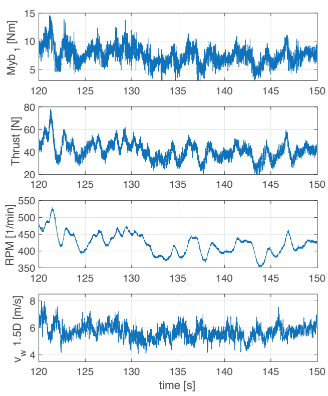

Summary

- **Introduction of test setup** :
  - Model wind turbine (D=1.8 m)
    - Fully equipped with sensors
    - Blade aerodynamics and loads scalable to NREL 5 MW turbine
  - Wind tunnel with active turbulence grid
    - Reproduceable turbulent patterns
- **Planned experiments**:
  - Engineering models (e.g. dyn. inflow)
  - Turbulent inflow (temporal/spatial)
  - PIV investigations
  - Controller testing

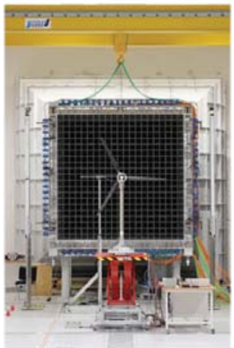

Acknowledgements

This work was partially funded by the German Federal Ministry for Economic Affairs and Energy (BMWi) in the Smart Blades 2.0 project (0324032D) and the state of Lower Saxony (ZN3092).

Supported by:
Federal Ministry for Economic Affairs and Energy
on the basis of a decision by the German Bundestag

G2) Experimental Testing and Validation

SINTEF

DOCUMENTATION VERIFICATION AND VALIDATION OF REAL-TIME HYBRID MODEL TESTS WITH THE 10MW OO-STAR WIND FLOATER

Maxime Thys (SINTEF Ocean)
Lene Eliassen (SINTEF Ocean)
Petter A. Berthelsen (SINTEF Ocean)
Valentin Chabaud (SO/NTNU)
Thomas Sauder (SO/AMOS)

HYBRID KPN LIFES50+

Layout

- Model testing: motivation and limitations
- Real-Time Hybrid Model testing
- OO-Star Wind Floater ReaTHM tests
- Verification
- Conclusion

HYBRID KPN LIFES50+

Motivation for model tests

- Common to all offshore structures
  - Significant investments should be de-risked and optimized
  - Some physical effects are not modelled correctly by engineering tools yet
  - Some physical effects are not known yet
- Specific to FOWT
  - Complex coupling between wind and wave loads, structure and blade dynamics.
  - → Issue: the experiments must capture these couplings correctly



HYBRID KPN LIFES50+

Limitations of classical approaches

- Tests in wave tanks, using fans to generate the aerodynamic loading
  - *Challenge 1:* ensure a correct wind field above the wave field → accuracy, repeatability, traceability
  - *Challenge 2:* ensure a correct mass distribution of the RNA model
  - *Challenge 3:* Froude/Reynolds scaling conflict, and rotor re-design by "Performance scaling"

Hywind demo, 2005

Politecnico Milano / 2016

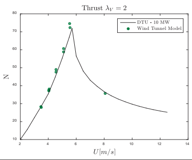

HYBRID KPN LIFES50+

Real-Time Hybrid Model (ReaTHM®) testing

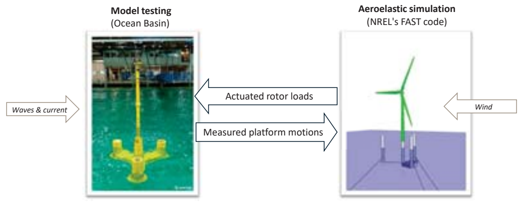

HYBRID KPN LIFES50+

ReaTHM® testing

Strong points of ReaTHM® testing?

- Realistic and controlled rotor loads
- Possibility to test extreme conditions
- Cost-effective and flexible

Any challenges?

Multidisciplinary

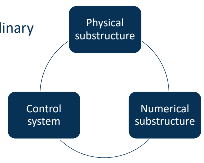

How to ensure high quality testing?

OO-Star Wind Floater model tests

- Lifes50+ H2020 project (http://lifes50plus.eu/)
- OO-Star Wind Floater with DTU 10MW turbine
- Tested in Nov 2017 in the Ocean Basin at SINTEF Ocean
- Scale 1/36
- Environmental conditions of Gulf of Main (depth 130m)
- Objectives:
  - Concept performance verification
  - Data for num. calibration
  - Develop hybrid methods

7

Verification: Sensitivity study

- How important are each of the turbine load components for operational and parked conditions?
- Realized by use of Riflex-SIMO-Aerodyn, where rotor loads are modified one by one.
- Sensitivity to
  - aerodynamic sway, heave, pitch, and yaw
  - Gyro moments/centrifugal forces
  - Vertical and horizontal directionality
- 16 loading conditions

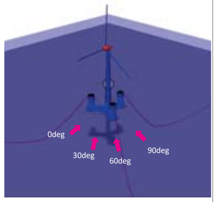

Description	Unit	EC1	EC2	EC3	EC4
Wind	m/s	8.0	11.4	20.0	44.0
TI	%	12.7	12.4	9.5	11.0
Wind model	-	NTM	NTM	NTM	NTM (EWM)
Power law coeff.	-	0.14	0.14	0.14	0.11
H_s	m	2.3	2.5	3.6	10.9
T_p	s	9.7	9.8	9.9	16.0
Wave spectrum	-	PM	PM	PM	PM

10

OO-Star Wind Floater model tests

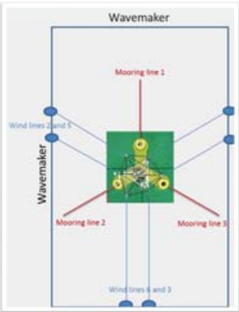

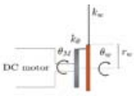

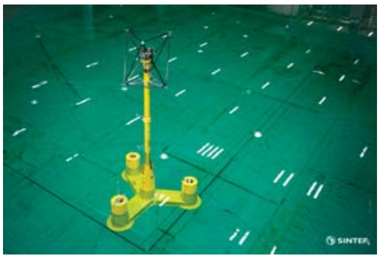

Verification: Sensitivity study

- Influence on standard deviation for quantities of interest (DOF1-6, mooring line tensions, BM and SF)

Removed	Operating (EC1-3)	Parked (EC4)
Aerodynamic sway	small	15% tension and 8% yaw and pitch
Aerodynamic heave	small	12% tension
Aerodynamic pitch	+18% pitch and +10% SF	+22% pitch and +22% BM
Aerodynamic yaw	-85% on yaw (small)	small
Vertical directionality	small	7% pitch and 15% tension

11

=> 6 actuators in two parallel horizontal planes to apply all loads except heave

SINTEF

Verification: Stepwise approach

- General: Sensitivity study
- Substructure Verification
- Verification of complete system

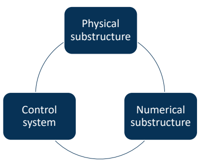

9

SINTEF

Verification of Physical Substructure

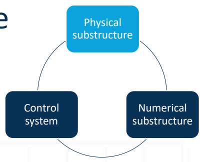

- Pullout
- Decay
- Repetitions

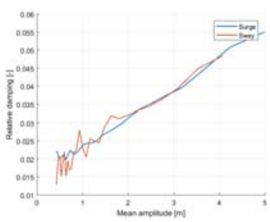

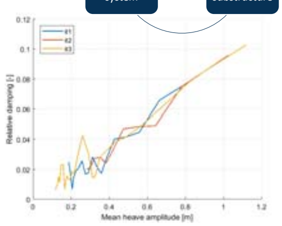

12

HYBRID KPN LIFES50+

Verification of Numerical Substructure

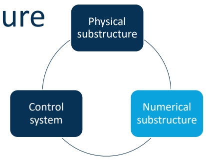

Physical part of the experiments emulated in SIMA for verification of

- Allocation (rotor loads->forces on actuators 1-6)
- Scaling
- Applied actuators forces

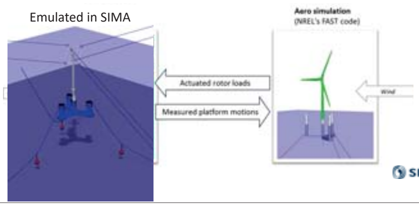

 SINTEF

HYBRID KPN LIFES50+

Verification of Control System

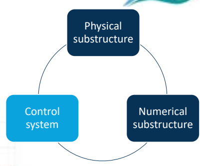

Main objectives:

- Reference tracking
- Disturbance rejection

Through:

- Chirp tests
- Following tests

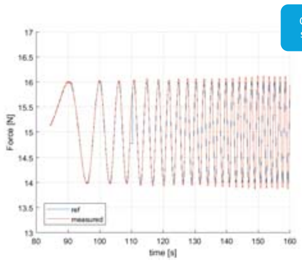

 SINTEF

HYBRID KPN LIFES50+

Verification of Complete System: Decay

Pitch decay test without ReaTHM system and with the system in following mode

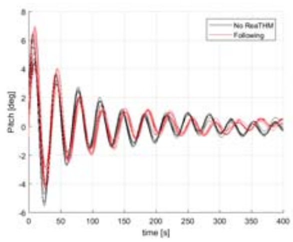

	Tn Pitch [s]
No ReaTHM	34.9
Following	35.8
Rel. Diff [%]	2.5

 SINTEF

HYBRID KPN LIFES50+

Verification of Complete System: Decay

Pitch decay test without ReaTHM system and with the system in following mode

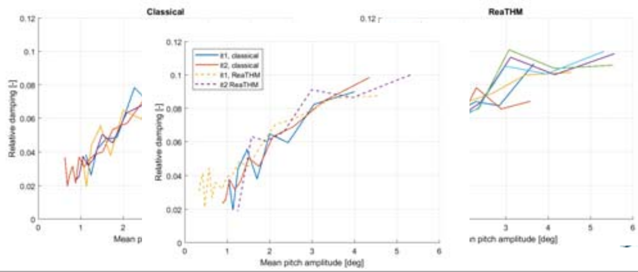

HYBRID KPN LIFES50+

Verification of Complete System: Repetition

Test repetition:

- DLC 1.6
- Waves: Pierson-Moskowitz Hs=7.7m and Tp=12.4s
- Wind: NTM 8m/s

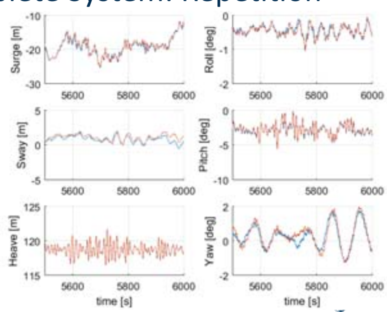

Collinear wind and waves

HYBRID KPN LIFES50+

Conclusions

- ReaTHM® testing is a multidisciplinary method
- Sensitivity analysis is key in the design process
- New verification and documentation methods developed for substructures and complete system
- Examples shown from Lifes50+ with OO-Star Wind Floater
- More work needed to address experimental uncertainty of hybrid tests -> Phase 2 of Lifes50+ in March 2018 *(Nautilus-DTU10)*

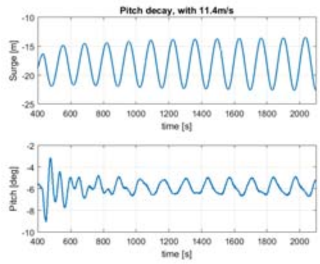

 SINTEF

HYBRID KPN LIFES50+

Acknowledgments

LIFES50+

The research leading to these results has received funding from the European Union Horizon2020 programme under the agreement H2020-LCE-2014-1-640741

HYBRID KPN

"The present work was part of the "HYBRID KPN" project supported by the Maritime Activities and Offshore Operations Program" (MAROFF) of the Research Council of Norway (grant No. 254845/O80).

SINTEF NTNU

Also, we are grateful to Dr. techn. Olav Olsen AS for the permission and contribution to set up the public 10MW semi-submersible design based on their concept of the OO-Star Wind Floater (www.olavolsen.no).

19 SINTEF

SINTEF

Teknologi for et bedre samfunn

Validation of the real-time-response ProCap system for full field wake scans behind a yawed model wind turbine

Jan Bartl[1], Andreas Müller[2], Andrin Landolt[3], Franz Mühle[4], Mari Vatn[1], Luca Oggiano[1,5], Lars Sætran[1]

EERA DeepWind2018, January 17-19, 2018, Trondheim, Norway

1 NTNU 2 ETH zürich 3 STREAMWISE 4 NMBU 5 IFE

Norwegian University of Science and Technology

Wake model validation across the scales

Full-scale measurements

Alpha ventus, Picture: Martina Nolte, Licence: Creative Commons by-sa-3.0 de

PREDICTION

SCALING?? BLOCKAGE??

Simulations

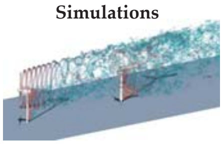

Picture: Steve Evans, CD-adapco/Siemens

VALIDATION

Wind tunnel experiments

Picture: Jan Bartl, NTNU

2

Turbine interaction & Wake flow prediction

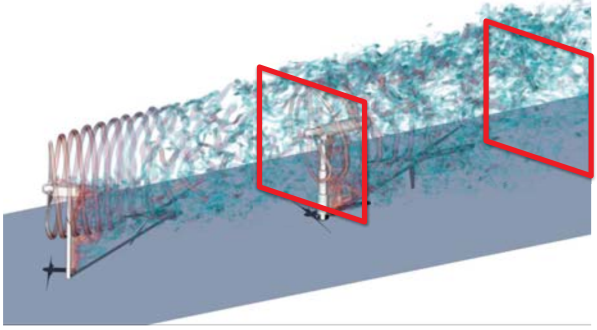

© Simulation by Siemens/CD-Adapco

This presentation: Comparsion of two flow measurement techniques

Laser-Doppler Anemometry (LDA) *vs* Probe Capture (ProCap)

3

Wake velocity measurement techniques

Single point measurements

- Pressure measurements (Pitot tube)
- Hot-wire measurements
- Laser-Doppler measurements (LDA)

➢ Traverse of single grid points
➢ Interpolation in post-processing
➢ ***Measurement time full wake (2m x 1m) ≈ 5 hours***

Flow field measurements

- Particle Image Velocimetry (PIV)

➢ Limited measurement window

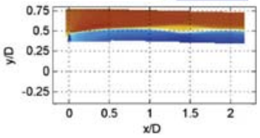

L.E.M. Lignarolo et al. / Renewable Energy 70 (2014) 31–46

4

Experimental setup ProCap

➢ Developed at ETH Zürich and its spin-off ***streamwise***

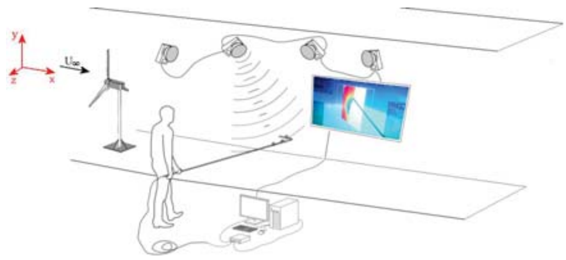

The ProCap system consists of

- a hand-guided 5-hole pressure probe equipped with three markers
- a motion capture camera system
- a real-time data processing and visualization system

5

ProCap: Experimental setup

6

Real-time response data acquisition

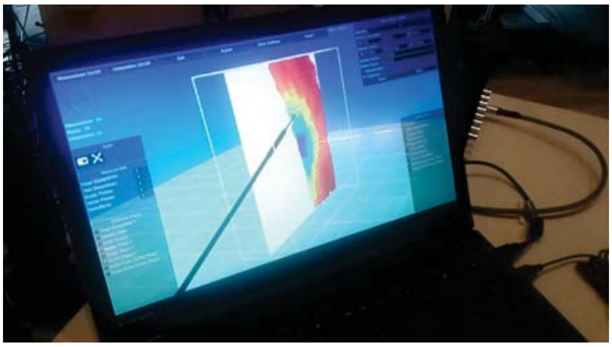

➢ *Measurement time full wake (2m x 1m) ≈ 10 minutes*

7

Comparison of results: u and v at 3D, γ=30°

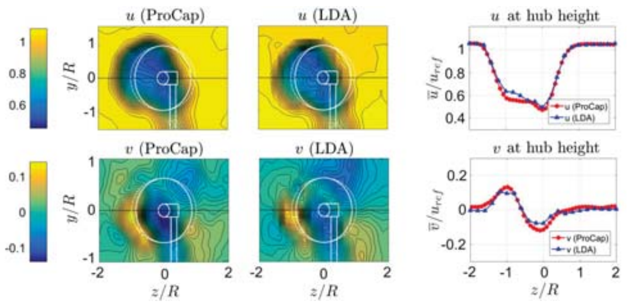

Comparison of the measured flow component u and v at x/D = 3 and γ= 30°. First column: ProCap results. Second column: LDA results.

8

Comparison of results: u and v at 9D, γ=30°

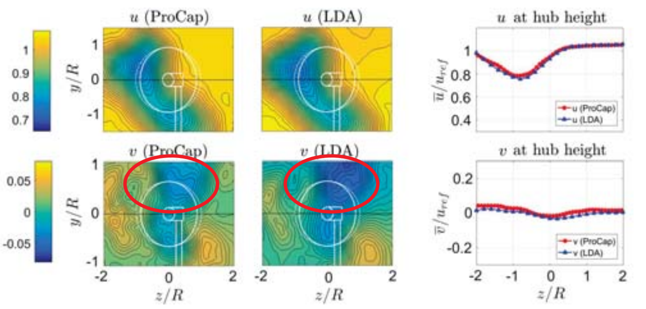

Comparison of the measured flow component u and v at x/D = 6 and γ= 30°. First column: ProCap results. Second column: LDA results.

9

Further results: wake flow at 9D for different yaw angles

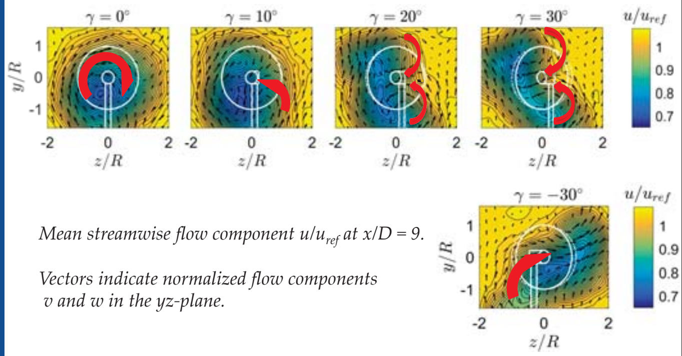

Mean streamwise flow component u/u_{ref} at $x/D = 9$.

Vectors indicate normalized flow components v and w in the yz-plane.

10

Conclusions

- Successfully validation of ProCap measurement system for multiple wake scans
- Precise capture of strong velocity gradients and flow circulation
- Significantly shorter recording time

  t_{ProCap}= 10 min vs t_{LDA}= 6 h.
- Real-time data acquisition

  + Review and discussion of the results during measurement

➡ **Fast & accurate system for wind turbine wake measurements**

11

Experimental Study on Slamming Loads by Simplified Substructures

EERA DeepWind`18
[17th ~19th /Jan/2018]
University of Ulsan, Wide Tank

Junbae Kim, Pham Thanh Dam, Hyeonjeong Ahn, Dac Dung Truong
Professor : Hyunkyoung Shin
Presenter : Byoungcheon Seo

Contents

Introduction

Area : 99,720㎢, 109th in the world
Population : 51,778,544 people, 27th in the world
(CIA, The World Factbook)

Introduction

Introduction

Breaking Wave

Horizontal Slamming

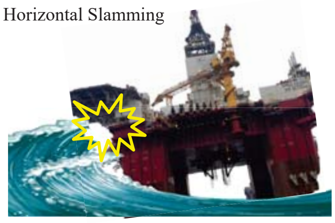

Wave Run-up

Bottom Slamming

Introduction

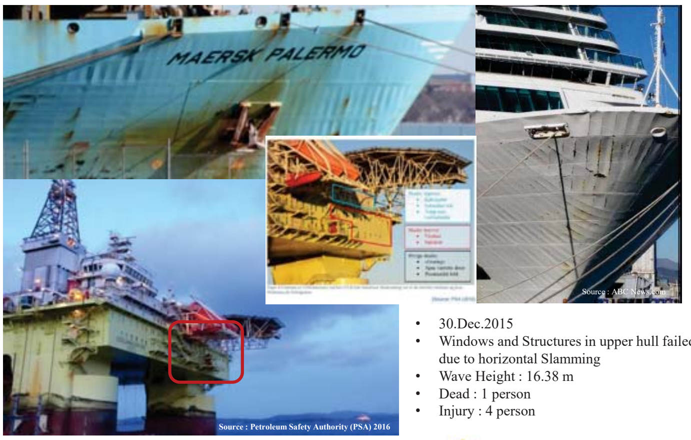

- 30.Dec.2015
- Windows and Structures in upper hull failed due to horizontal Slamming
- Wave Height : 16.38 m
- Dead : 1 person
- Injury : 4 person

Introduction

- Test model in wide tank, UOU -
- Freeboard : 6 m(full scale), 150 mm(model scale)
- Condition : Irregular wave, sea state 6(extreme)

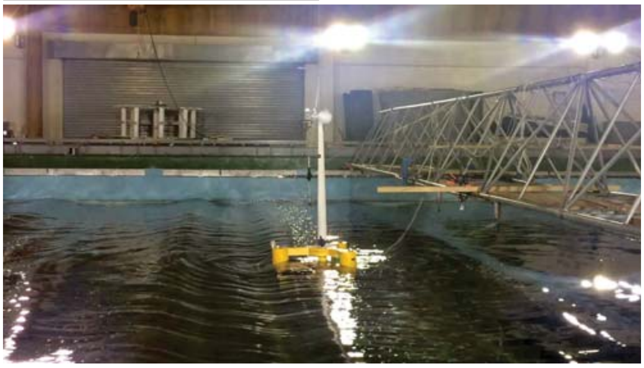

Introduction

➢ Information of impulsive pressure

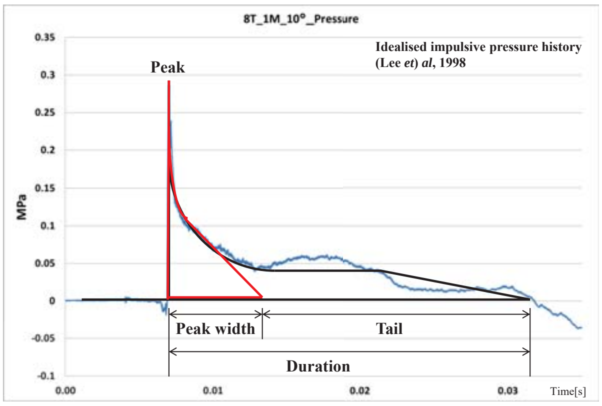

Experimental System (UOU Trimming Tank)

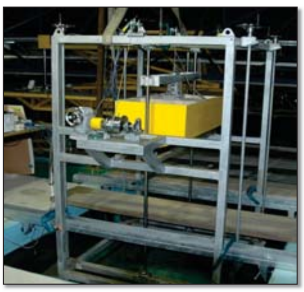

- ◆ **Trimming Tank**
- **Width = 2,170mm**
- **Water depth = 1,000 mm**
- **Max. drop height = 1,000mm**

Experimental System (UOU Slamming Tank)

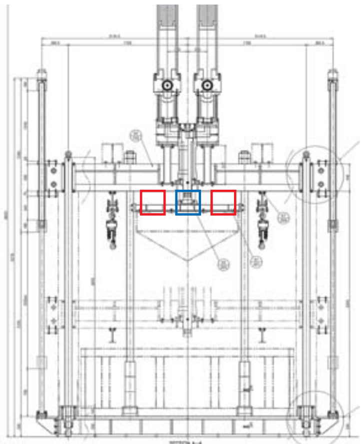

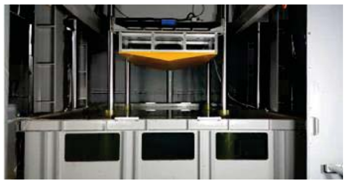

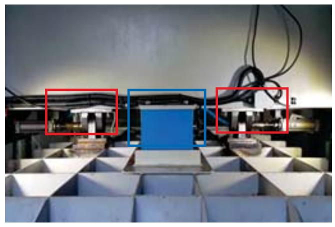

Test model (UOU Trimming Tank)

Model	Wood	Steel
Dead-rise angle [deg.]	0, 3,10	
Length [mm]	1,000	
Width [mm]	600	
Height [mm]	400	
Mass [kg]	60	
Bottom plate thickness [mm]	50	3,4,5

Test Model (Production process at UOU Trimming Tank)

Wood

Steel

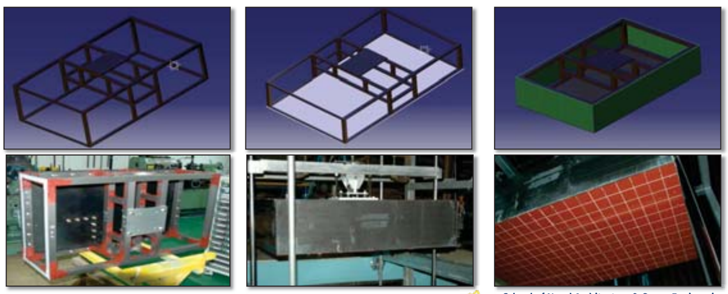

Test model (UOU Slamming Tank)

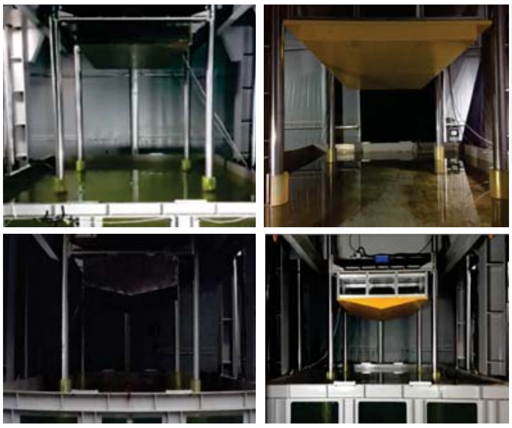

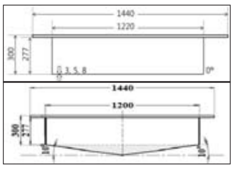

Model	Steel / Wood
Bottom plate thickness [mm]	3, 5, 8 / 100
Height [mm]	300
Length [mm]	2,000
Width [mm]	1,200
Mass [kg]	820
Dead-rise angle [deg.]	0, 10

Test model (UOU Slamming Tank)

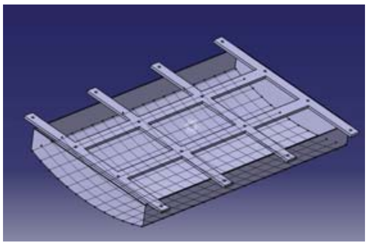

Model	Steel
Bottom plate thickness [mm]	8
Height [mm]	300
Length [mm]	2,000
Width [mm]	1,200
Mass [kg]	820
Dead-rise angle [deg.]	Cylindrical

Measurement (Sensor location)

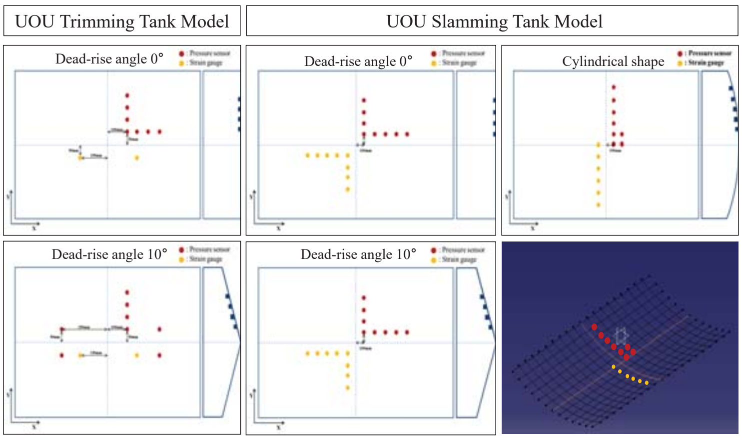

Measurement

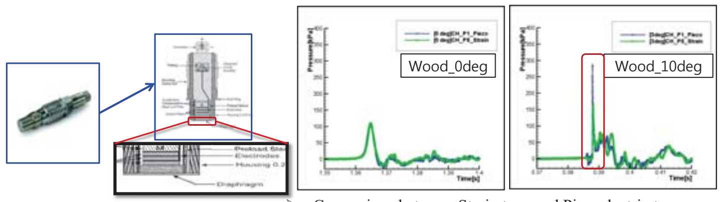

➢ Comparison between Strain type and Piezoelectric type sensor

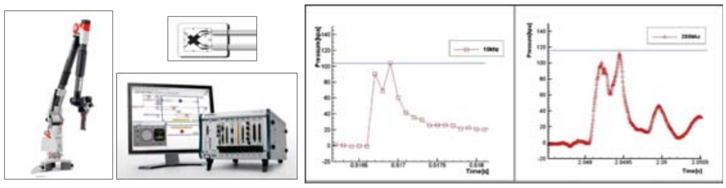

➢ Comparison sampling rate

Free wet drop test (UOU Trimming Tank)

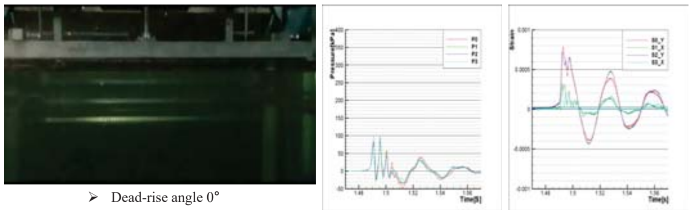

➢ Dead-rise angle 0°

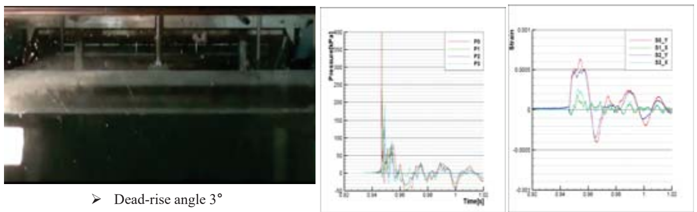

➢ Dead-rise angle 3°

0° - 500mm Free drop test (UOU Trimming Tank)

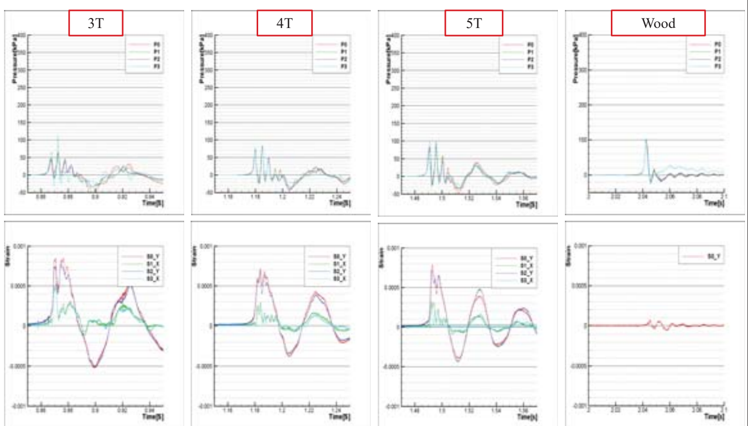

3° - 500mm Free drop test (UOU Trimming Tank)

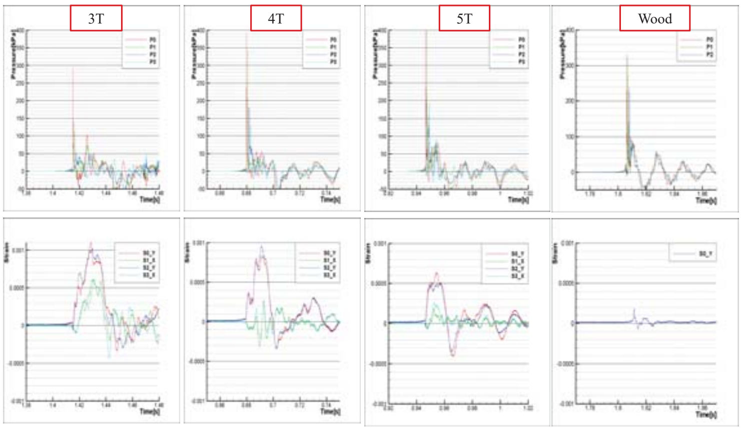

Experimental Results - 3T_0°

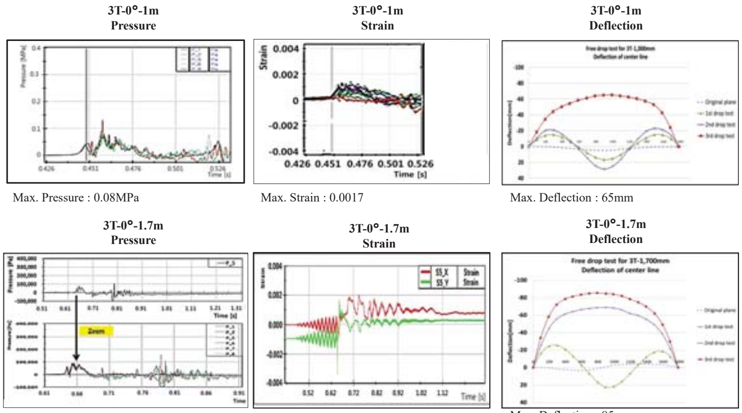

Max. Pressure : 0.08MPa
Max. Strain : 0.0017
Max. Deflection : 65mm

Max. Pressure : 0.10MPa
Max. Strain : 0.0020
Max. Deflection : 85mm

10° - 500mm Free drop test (UOU Trimming Tank)

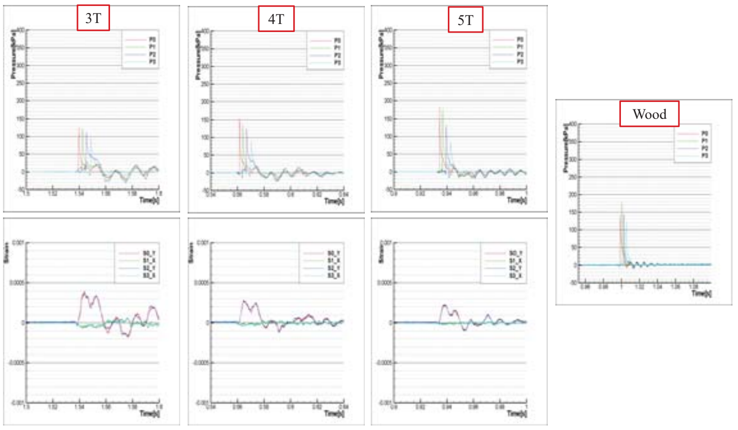

Experimental Results - 5T_0°

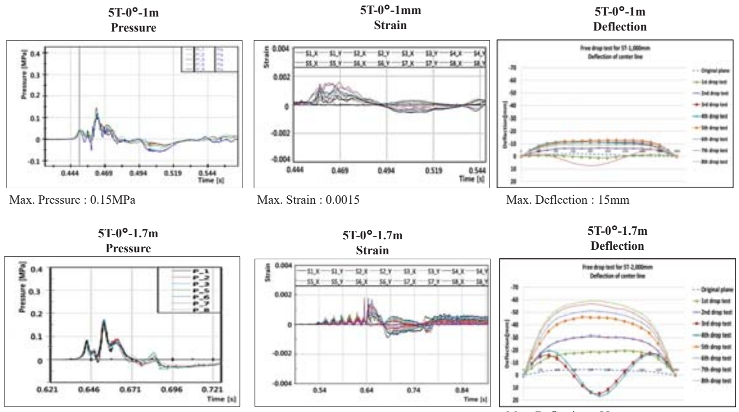

Max. Pressure : 0.15MPa
Max. Strain : 0.0015
Max. Deflection : 15mm

Max. Pressure : 0.17MPa
Max. Strain : 0.0018
Max. Deflection : 55mm

Free wet drop test (Wood & Steel_0° in UOU Slamming Tank)

- Wood - Dead-rise angle 0°, Drop height : 1m

- Wood - Dead-rise angle 0°, Drop height : 1.7m

- Steel - Dead-rise angle 0°, Drop height : 1m

- Steel - Dead-rise angle 0°, Drop height : 1.7m

Experimental Results - 8T_0°

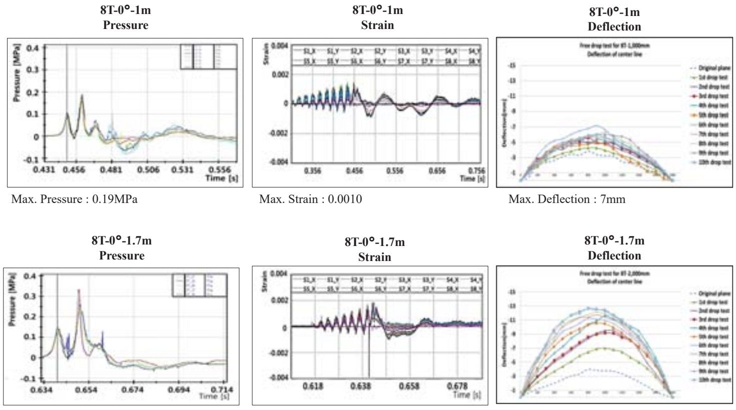

Max. Pressure : 0.19MPa
Max. Strain : 0.0010
Max. Deflection : 7mm

Max. Pressure : 0.33MPa
Max. Strain : 0.0015
Max. Deflection : 9mm

Free wet drop test (Wood & Steel_0° in UOU Slamming Tank)

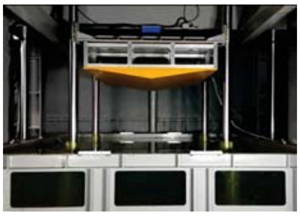

➢ Wood - Dead-rise angle 10°, Drop height : 1m

➢ Wood - Dead-rise angle 10°, Drop height : 1.7m

➢ Steel - Dead-rise angle 10°, Drop height : 1m

➢ Steel - Dead-rise angle 10°, Drop height : 1.7m

Experimental Results - 3T_10°

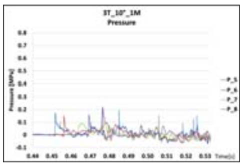

Max. Pressure : 0.18MPa

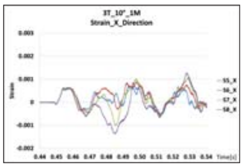

Max. Strain : 0.0007

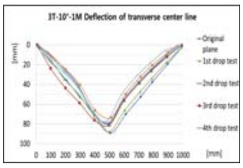

Max. Deflection : 30mm

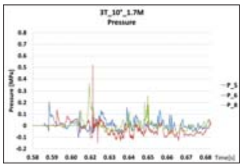

Max. Pressure : 0.22MPa

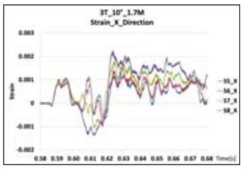

Max. Strain : 0.0012

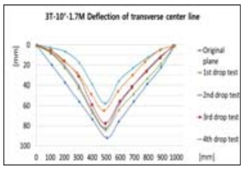

Max. Deflection : 40mm

Experimental Results - 5T_10°

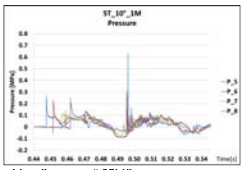

Max. Pressure : 0.27MPa

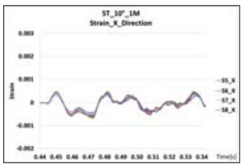

Max. Strain : 0.0005

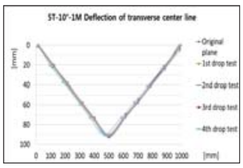

Max. Deflection : 4mm

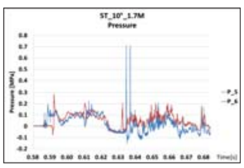

Max. Pressure : 0.29MPa

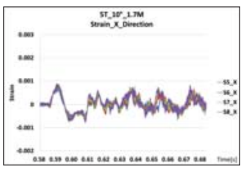

Max. Strain : 0.0008

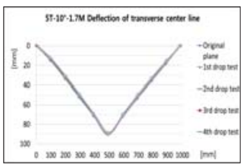

Max. Deflection : 5mm

Experimental Results - 8T_10°

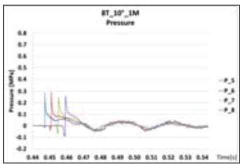

Max. Pressure : 0.29MPa

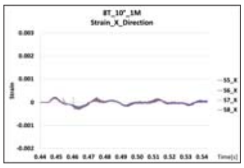

Max. Strain : 0.0003

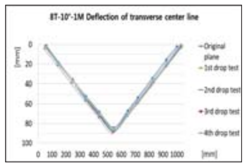

Max. Deflection : 2mm

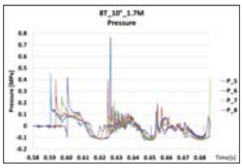

Max. Pressure : 0.45MPa

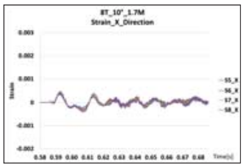

Max. Strain : 0.0005

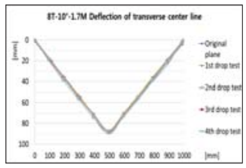

Max. Deflection : 4mm

Experimental Results - 8T_10°_Damped Wave

➢ Steel - Dead-rise angle 10°, Drop height : 1.7m

Experimental Results - 8T_10°_Pressure and Strain (Damped Wave)

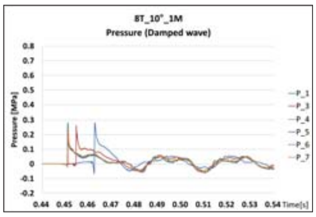

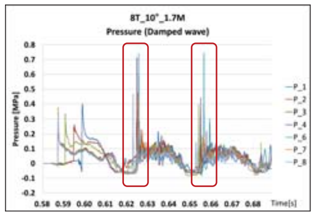

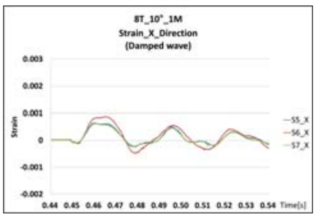

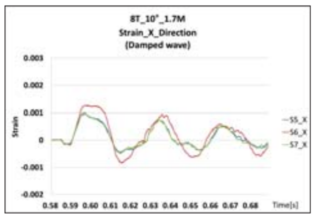

Experimental Results (Wood)

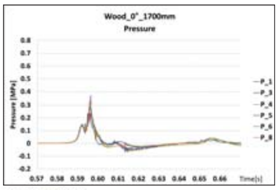

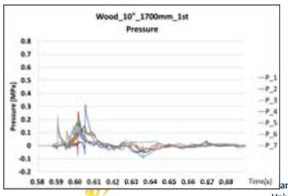

Numerical analysis

1. Finite element modelling of tested models
   - Using shell elements
   - Mesh / plate thickness =1.88
   - Fully fixed at upper supporting frame

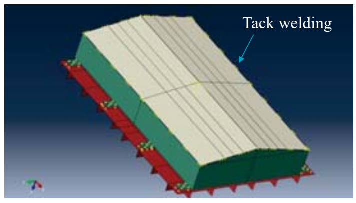

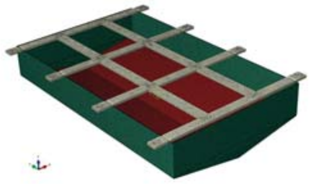

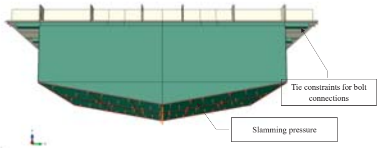

Free wet drop test (Steel_Cylindrical shape in UOU Slamming Tank)

➢ Steel – Cylindrical shape, Drop height : 1m

➢ Steel – Cylindrical shape, Drop height : 1.7m

Numerical analysis

2. Simplified impulsive pressure shape : Triangular shape

   Three presentative parameters:
   - Peak pressure
   - Rising time
   - Decaying time

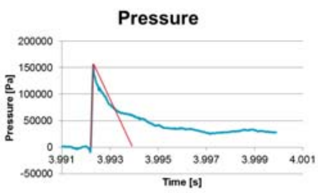

Process of simplified slamming pressure history

Free wet drop test (Steel_Cylindrical shape in UOU Slamming Tank)

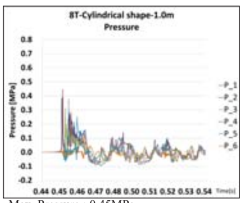

Max. Pressure : 0.45MPa

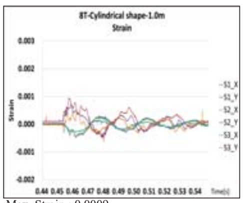

Max. Strain : 0.0009

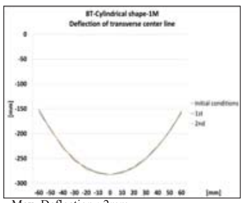

Max. Deflection : 2mm

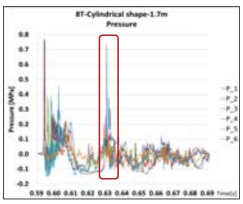

Max. Pressure : 0.78MPa

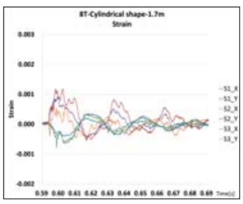

Max. Strain : 0.0012

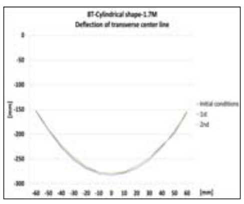

Max. Deflection : 4mm

Numerical analysis

3. Material property definition
   - Strain hardening: Use tensile test data
   - Strain rate hardening: Cowper-Symonds Eq. (D=40.4 & q=5)

$$\sigma_{YD} = \sigma_Y \left[1 + \left(\frac{\dot{\varepsilon}_p}{D} \right)^{\frac{1}{q}} \right]$$

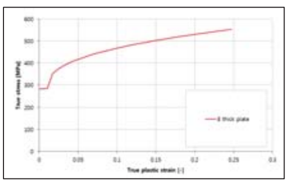

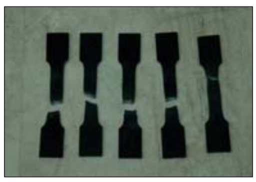

Thickness		Yield stress	Ultimate strength	Ultimate strain
Nominal [mm]	Actual [mm]	[MPa]	[MPa]	[-]
8	7.84	280.8	433.2	0.2151

Numerical analysis results

4. Deflection: SU-10-8T-1.7m

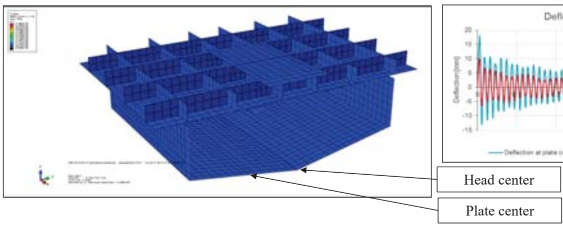

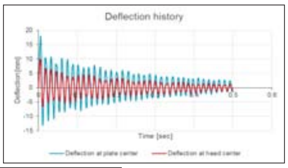

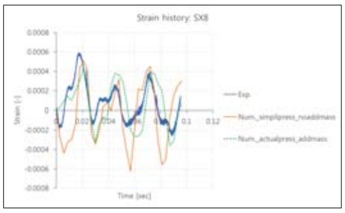

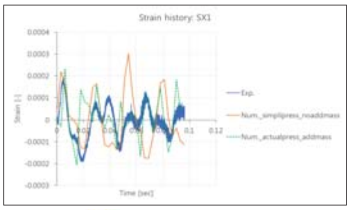

Discussions & Future work

1. The slamming load characteristics were investigated through experiments with numerical analysis.
2. In case of dead-rise angle 0°, the slamming pressure value is smaller than dead-rise angles 3° and 10° due to the air effect.
3. Air effect comes from the elastic effect, so the model size is made bigger that can be applied to the actual design.
4. The same air effect occurred at dead-rise angle 0°.
5. Pressure increase is directly proportional to the increase of drop height, weight and thickness.
6. It was confirmed that several peak pressures were generated in one drop at dead-rise angle 10° and cylindrical shape models.
7. The largest slamming pressure was observed in the cylindrical shape model.
8. Considering the slamming load in the elastic region, it was taken into consideration that several slamming loads are applied to a single wave load rather than a single pressure value.
9. Further study is necessary to improve its accuracy and reliability, and additional experiments under the same test conditions are required for the uncertainty.

THANK YOU

ACKNOWLEDGMENTS

This work was supported by the Korea Institute of Energy Technology Evaluation and Planning(KETEP) and the Ministry of Trade, Industry & Energy(MOTIE) of the Republic of Korea(No. 20154030200970 & 20163010024620).

Physical model testing of the TetraSpar floater in two configurations

M Borg[a], H Bredmose[a], H Stiesdal[b], B Jensen[c], RF Mikkelsen[a], M Mirzaei[a], A Pegalajar-Jurado[a], FJ Madsen[a], TRL Nielsen[a], AK Lomholt[a]

[a]*DTU Wind Energy, Kgs. Lyngby, Denmark*
[b]*Stiesdal Offshore Technologies, Odense, Denmark*
[c]*DHI, Hørsholm, Denmark*

EERA DeepWind'2018
18th January 2018
Trondheim, Norway

DTU Wind Energy
Department of Wind Energy
Stiesdal
DHI

Outline

- Introduction
- TetraSpar concept
- Experimental setup
- Example Results
- Conclusions

Introduction

Scientific ambitions
Improving SoA wind-wave testing
Detailed hydrodynamic testing
Fault & transient conditions

Tech. development ambitions
Proof-of-concept
De-risk concept

DTU Wind Energy
Department of Wind Energy
Stiesdal

Collaborative research project

DHI

The TetraSpar concept

- Concept developed by Stiesdal Offshore Technologies
- Rationale:

Mindset
- Conventional thinking
  - We have designed this structure – now, how do we build it?
- TetraSpar thinking
  - We need to manufacture this way – now, how do we design it?

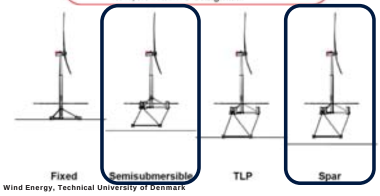

Experimental setup: wave basin

- DHI deep-water wave basin with 4 x 4 m2 wind generator

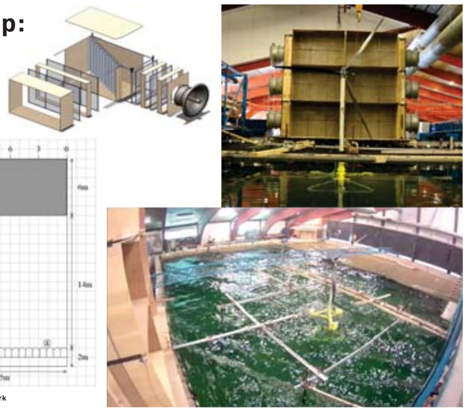

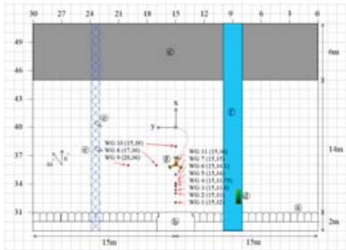

Experimental setup: floater configurations

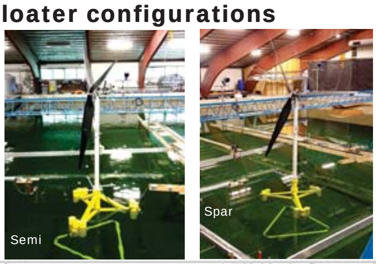

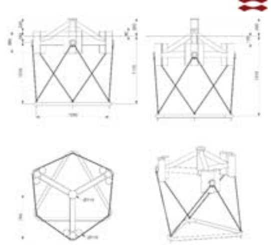

Item	1:60 Model scale	Prototype scale
Floater mass (incl. instrumentation)	15.66 kg	3383 t
Floater vertical centre of gravity below MSL	0.231 m	13.9 m
Water depth	3 m	180 m
Draft, semi configuration	1.12 m	67.2 m
Draft, spar configuration	1.32 m	79.2 m
Transition piece mass	1.08 kg	233 t
Counterweight mass, semi configuration	20.98 kg	4532 t
Counterweight mass, spar configuration	35.66 kg	7703 t

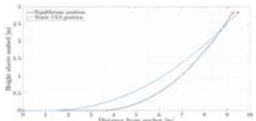

Experimental setup: wind turbine model

- DTU 10MW RWT 1:60 scale model from previous campaigns [1-3]
  - Match steady thrust curve – 75% increased chord → Rotor I
  - Collective blade pitch control
- New rotor design
  - Match $d(C_T)/d\theta$ – 30% increased chord → Rotor II
  - Steady thrust mismatch
  - ***Improve aerodynamic damping***

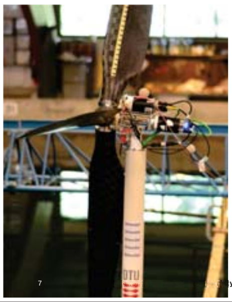

Dimension	Prototype Scale	Froude Model Scale	Actual Model Scale (incl. instrumentation)	
Tower			**Rotor I**	**Rotor II**
Diameter	7.82m-5.50m	130mm-92mm	80mm	80mm
Tower length	95.6m	1594mm	1692mm	1692mm
Hub height above MSL	119m	1983mm	2070mm	2070mm
Mass	408t	2.12kg	2.250kg	2.250kg
Nacelle and rotor			**Rotor I**	**Rotor II**
Rotor diameter	178.3m	2972mm	2972mm	2972mm
Blade Length	86.7m	1440mm	1440mm	1440mm
Blade mass	41.7t	0.189kg	0.198kg	0.192kg
Nacelle+hub mass	552t	2.45kg	2.806kg	2.806kg
Nacelle+hub+rotor mass	677t	3.06kg	3.400kg	3.172kg

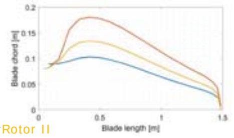

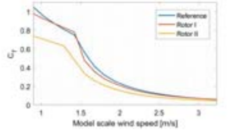

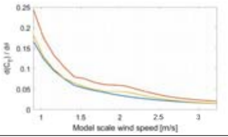

Experimental program – selected results

Test matrix

Type	Direction [deg]	Duration [full scale minutes]	No wind	With wind
Free decays	-	variable (10 repetitions)	x	semisub only
Wind only	-	190		x
2D regular	0	20	x	x
2D irregular	0	190	x	x
2D focused	0	100 (8 repetitions)	x	x
2D regular	30	20	x	x
2D irregular	30	190	x	x
White noise	0	190	x	x
Start-up/shut-down	0	100 (5 repetitions)		x
Start-up/shut-down	30	100 (5 repetitions)		semisub only
Skewed inflow condition - semisub only				
2D regular	0	20	x	x
2D irregular	0	190	x	x
2D focused	0	100 (8 repetitions)	x	x
2D regular	30	20	x	x
2D irregular	30	190	x	x

Environmental conditions

EC	Type	Full scale U_{hub} [m/s]	H.H. [m]	T.T_p [s]	Model scale U_{hub} [m/s]	H.H. [m]	T.T_p [s]	Turbine operation
3	below-rated	8.5	3.3	6.5	1.10	0.055	0.839	yes
5	rated	11.4	4.16	7.3	1.47	0.069	0.942	yes
6	above rated	18.0	6.18	8.9	2.32	0.103	1.149	yes
64	above rated	18.0	6.18	18.0	2.32	0.103	2.324	yes
11	ULS	18.0	10.5	14.2	2.32	0.175	1.833	idling
12	ULS	18.0	10.5	14.2	2.32	0.175	1.833	yes
W03	white noise	0.0	3.3	n/a	1.10	0.055	n/a	idling

- System damping
- Dynamic response of both configurations in ULS condition (EC11)
- Dynamic response of spar in focused wave group

Experimental setup - instrumentation

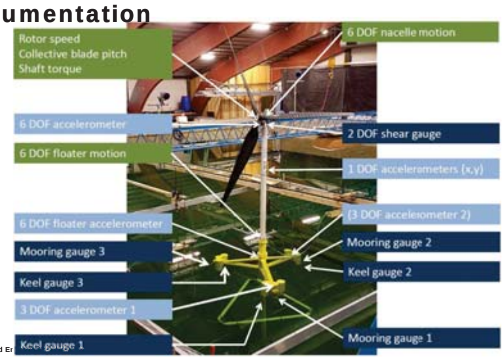

Results – system damping

- Identification of system damping – free decay tests in 6 DOF, 10 repetitions
- Roll example:

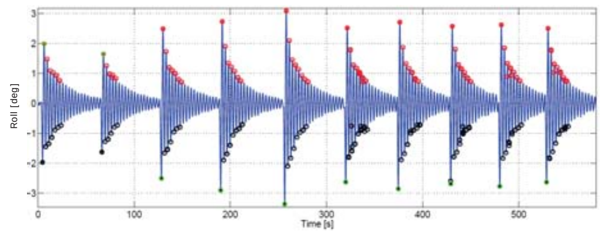

Experimental program

Test matrix

Type	Direction [deg]	Duration [full scale minutes]	No wind	With wind
Free decays	-	variable (10 repetitions)	x	semisub only
Wind only	-	190		x
2D regular	0	20	x	x
2D irregular	0	190	x	x
2D focused	0	100 (8 repetitions)	x	x
2D regular	30	20	x	x
2D irregular	30	190	x	x
White noise	0	190	x	x
Start-up/shut-down	0	100 (5 repetitions)		x
Start-up/shut-down	30	100 (5 repetitions)		semisub only
Skewed inflow condition - semisub only				
2D regular	0	20	x	x
2D irregular	0	190	x	x
2D focused	0	100 (8 repetitions)	x	x
2D regular	30	20	x	x
2D irregular	30	190	x	x

Environmental conditions

EC	Type	Full scale U_{hub} [m/s]	H.H. [m]	T.T_p [s]	Model scale U_{hub} [m/s]	H.H. [m]	T.T_p [s]	Turbine operation
3	below-rated	8.5	3.3	6.5	1.10	0.055	0.839	yes
5	rated	11.4	4.16	7.3	1.47	0.069	0.942	yes
6	above rated	18.0	6.18	8.9	2.32	0.103	1.149	yes
64	above rated	18.0	6.18	18.0	2.32	0.103	2.324	yes
11	ULS	18.0	10.5	14.2	2.32	0.175	1.833	idling
12	ULS	18.0	10.5	14.2	2.32	0.175	1.833	yes
W03	white noise	0.0	3.3	n/a	1.10	0.055	n/a	idling

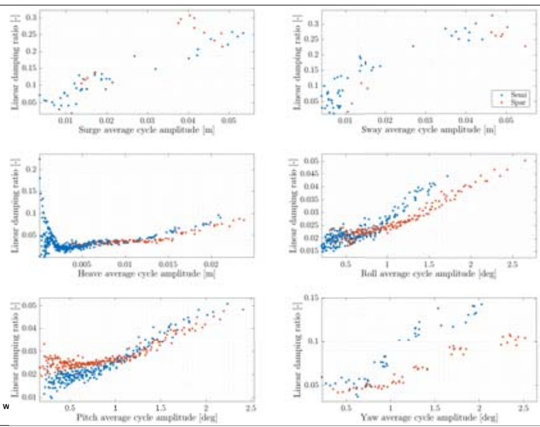

Results
ULS waves only
Motion response

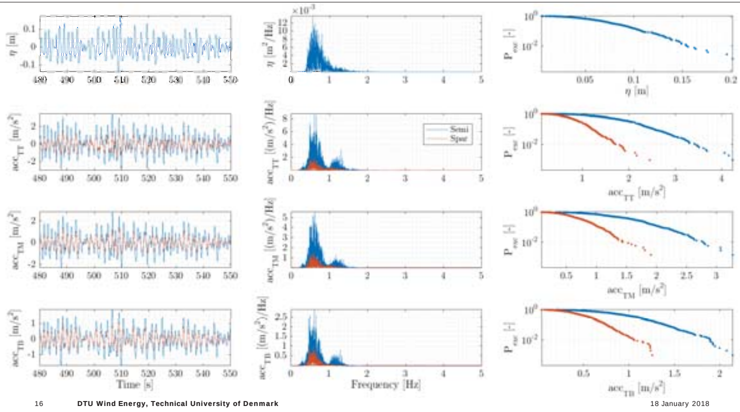

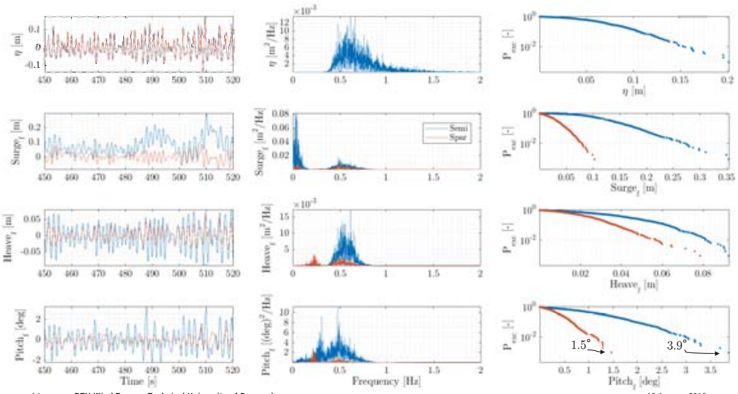

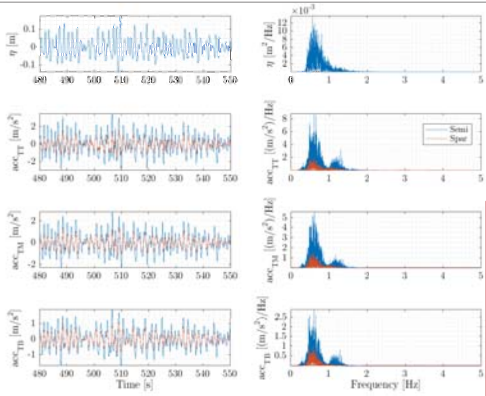

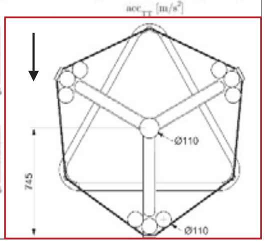

Results
ULS waves only
Acceleration response

Results
ULS waves only
Counterweight line tensions

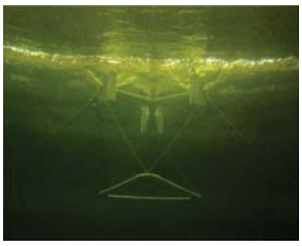

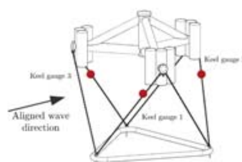

Results
ULS waves only
Counterweight line tensions

DTU

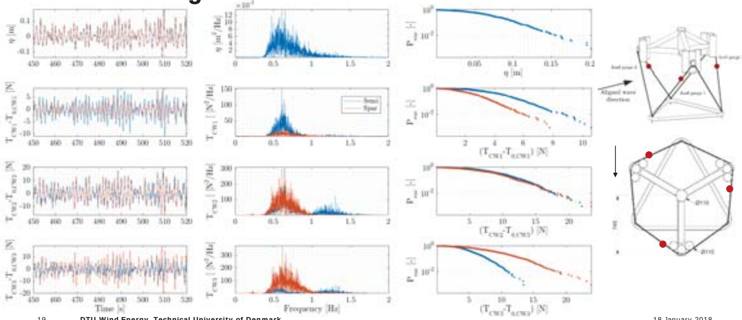

Conclusions

- Testing of TetraSpar in semi and spar configurations
- Nonlinear system damping
- Significant subharmonic wave forcing
- C/W tensions dominated by inertia loads
- WT operation observed to reduce max acceleration

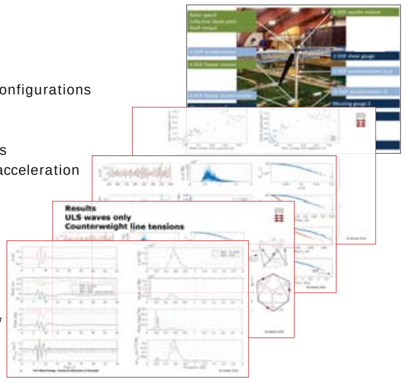

References

[1] A. M. Pegalajar Jurado, A. M. Hansen, R. Laugesen, R. F. Mikkelsen, M. Borg, T. Kim, N. F. Heilskov, H. Bredmose, Experimental and numerical study of a 10MW TLP wind turbine in waves and wind, Journal of Physics: Conference Series (online) 753 (2016) 092007

[2] H. Bredmose, F. Lemmer, M. Borg, A. Pegalajar-Jurado, R. Mikkelsen, T. Larsen, T. Fjelstrup, W. Yu, A. Lomholt, L. Boehm, J. Azcona, The Triple Spar campaign: Model tests of a 10 MW floating wind turbine with waves, wind and pitch control, Energy Procedia (2017), 137, pp.58-76.

[3] F. J. Madsen, T. R. L. Nielsen, Experimental and numerical study of the scaled DTU 10MW floating wind turbine on a TLP platform, MSc thesis, Department of Wind Energy, Technical University of Denmark, (2017).

Results
Focused wave group – EC11 – H = 0.33m (19.5m)
Spar response

DTU

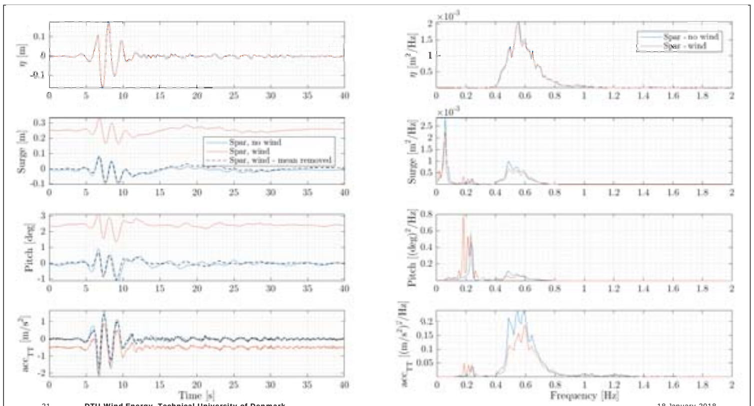

H) Wind farm control systems

Real-time wind field estimation & model calibration using SCADA data in pursuit of closed-loop wind farm control, B.Doekemeijer, Delft University of Technology

Mitigating Turbine Mechanical Loads Using Engineering Model Predictive Wind Farm Controller, J.Kazda, DTU Wind Energy

Local stability and linear dynamics of a wind power plant, K.Merz, SINTEF Energi

Wind farm control, Prof William Leithead, Strathclyde University

Closed-loop control of wind farms

Real-time wind field estimation & model calibration using SCADA data

*B.M. Doekemeijer
Delft University of Technology

S. Boersma
Delft University of Technology

J.W. van Wingerden
Delft University of Technology

L.Y. Pao
University of Colorado Boulder

January 19th, 2018

TU Delft

CL-Windcon

INTRODUCTION

TU Delft

Introduction

The problem in wind farms: wake interaction

The Horns Rev offshore wind farm (Vattenfall) under foggy conditions. Photograph by C. Steiness, February 2008

TU Delft

Introduction

The problem in wind farms: wake interaction

The Horns Rev offshore wind farm (Vattenfall) under foggy conditions. Photograph by C. Steiness, February 2008

TU Delft

Introduction

Axial induction control for wind farms

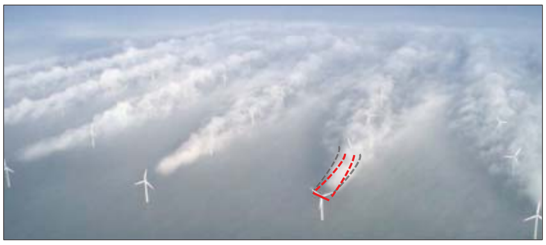

The Horns Rev offshore wind farm (Vattenfall) under foggy conditions. Photograph by C. Steiness, February 2008

TU Delft

Introduction

Wake redirection control in wind farms

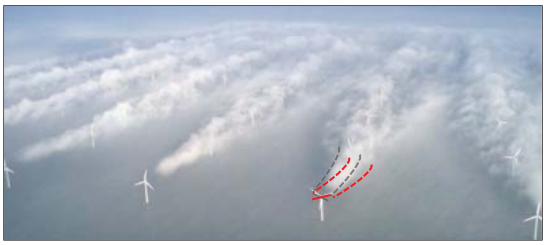

The Horns Rev offshore wind farm (Vattenfall) under foggy conditions. Photograph by C. Steiness, February 2008

TU Delft

Introduction

Wake redirection control in wind farms

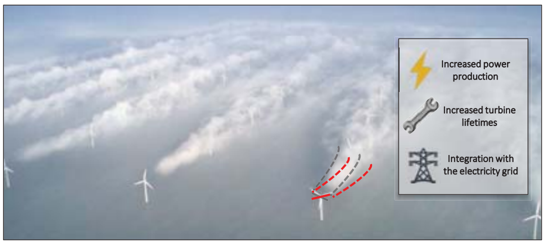

The Horns Rev offshore wind farm (Vattenfall) under foggy conditions. Photograph by C. Steiness, February 2008

TUDelft

7

Introduction

Wind farm control: current practice in existing farms

TUDelft

8

Introduction

Wind farm control: state of the art – open-loop wind farm control

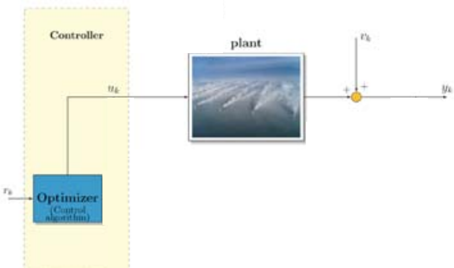

TUDelft

9

Introduction

Wind farm control: bleeding edge – closed-loop wind farm control

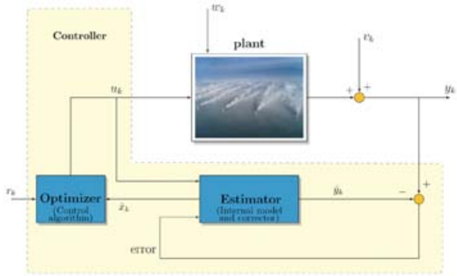

TUDelft

10

Introduction

Wind farm control: bleeding edge – closed-loop wind farm control

TUDelft

11

OUR RESEARCH

TUDelft

12

Our research
An estimator for a dynamic surrogate wind farm model

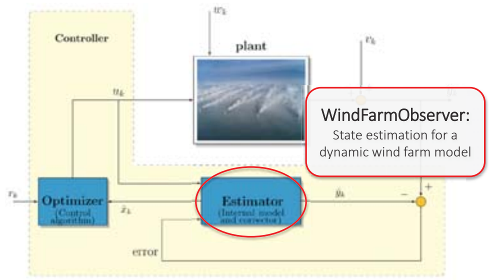

TUDelft

13

Our research
WindFarmSimulator (WFSim)[1,2]

- 3D LES model simplified to 2D (assumption of axisymmetry)
- Nonlinear, medium-fidelity dynamical wind farm model
- Mixing length turbulence model with spatial variations
- Validated to high-fidelity LES data in 2-turbine and 3 x 3-turbine case

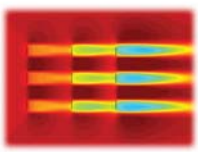

1. Boersma, S., Doekemeijer, B., Vali, M., Meyers, J., and van Wingerden, J.-W.: A control-oriented dynamic wind farm model: WFSim, Wind Energ. Sci. Discuss., https://doi.org/10.5194/wes-2017-44, in review, 2017.
2. WFSim is publically available on Github: https://github.com/TUDelft-DataDrivenControl/WFSim

TUDelft

14

Our research
WindFarmSimulator (WFSim)[1,2]

- 3D LES model simplified to 2D (assumption of axisymmetry)
- Nonlinear, medium-fidelity dynamical wind farm model
- Mixing length turbulence model with spatial variations
- Validated to high-fidelity LES data in 2-turbine and 3 x 3-turbine case

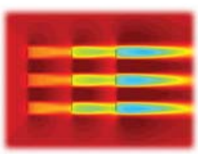

" How far can we push the accuracy of a wind farm model while maintaining computational tractability? "

1. Boersma, S., Doekemeijer, B., Vali, M., Meyers, J., and van Wingerden, J.-W.: A control-oriented dynamic wind farm model: WFSim, Wind Energ. Sci. Discuss., https://doi.org/10.5194/wes-2017-44, in review, 2017.
2. WFSim is publically available on Github: https://github.com/TUDelft-DataDrivenControl/WFSim

TUDelft

15

Our research
WindFarmObserver (WFObs)[1,2]

- Employs an *Ensemble Kalman filter* for state and parameter estimation
- Follows a power inversion rule to estimate the freestream wind speed
- Computationally superior to state of the art in the literature

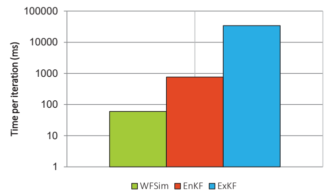

1. B. M. Doekemeijer, S. Boersma, L. Y. Pao and J. W. van Wingerden, "Ensemble Kalman filtering for wind field estimation in wind farms," 2017 American Control Conference (ACC), Seattle, WA, 2017, pp. 19-24.
2. WFObs is publically available on Github: https://github.com/TUDelft-DataDrivenControl/WFObs

TUDelft

16

SIMULATIONS

TUDelft

17

Results
Calibration of 2D flow field, TI_∞ and U_∞

- WFSim meshed at approx. 12000 states
- WFSim initialized with poor TI_∞ and U_∞
- Measurements exclusively SCADA data
- Reality modelled by LES with ALM rotor models
- Extremely low computational cost
- Accuracy comparable to the best in the literature (UKF)

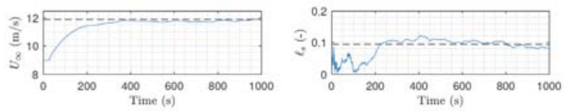

TUDelft

18

Results

WindFarmObserver (WFObs)

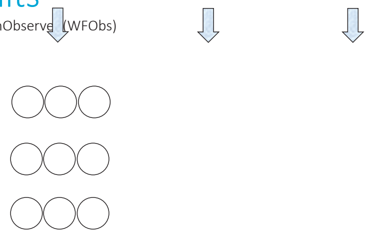

TUDelft

19

CONCLUSIONS

TUDelft

20

Conclusions

- Real-time calibration of a dynamic wind farm model
  - Freestream wind speed and turbulence intensity
  - Modeling errors within the wind farm
- High accuracy at very low computational cost
  - Comparable accuracy to the Unscented Kalman filter
  - Two orders of magnitude lower computational cost
- Using only SCADA data
- Ongoing work: optimization using the calibrated model

TUDelft

21

Thank you!

TUDelft

CL-Windcon

This project has received funding from the European Union's Horizon 2020 research and innovation program under grant agreement No 727477.

22

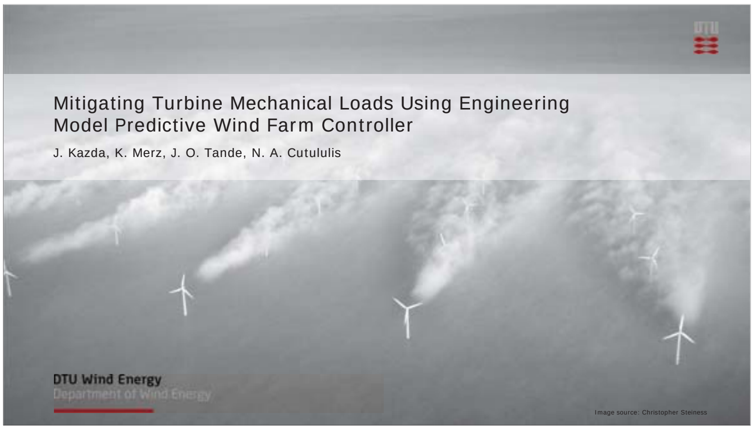

Mitigating Turbine Mechanical Loads Using Engineering Model Predictive Wind Farm Controller

J. Kazda, K. Merz, J. O. Tande, N. A. Cutululis

DTU Wind Energy
Department of Wind Energy

Image source: Christopher Steiness

Contents

- Motivation and objectives
- Wind farm controllers
- Case studies

Motivation

- Interaction of wakes with downstream turbines causes up to 80% higher fatigue loads
- O&M costs amount for large share of offshore wind farm lifetime costs

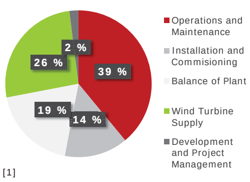

[1]

- Wake-induced fatigue loads can be reduced using optimal wind farm controller (WFC)

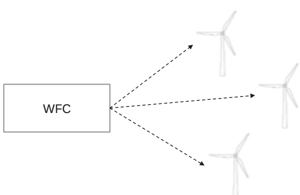

[1] "Wind Energy Update", 2015. [Online]. Available: http://analysis.windenergyupdate.com/

Objectives

Reduce wind turbine fatigue loads during wind farm ancillary services

- Develop model predictive wind farm controller (MPC) for this operational objective
- Compare performance of MPC with other commonly used wind farm controllers

Wind Farm Controllers: PI-Controller

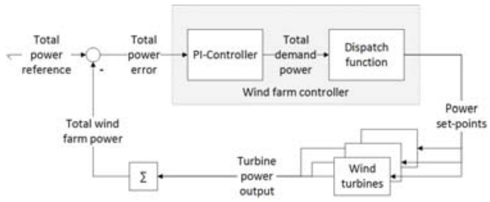

- Dispatch function sets distribution of total demanded power to individual turbines

Wind Farm Controllers: Engineering Model Predictive Controller

- MPC cost function objectives are to
  - follow total wind farm power reference
  - follow optimum turbine operation point derived from statistical fatigue load models
  - reduce gust-driven mechanical loads
- Model predictive controller estimates wind farm operation using
  - linear, dynamic wind farm flow model
  - statistical and deterministic turbine load model

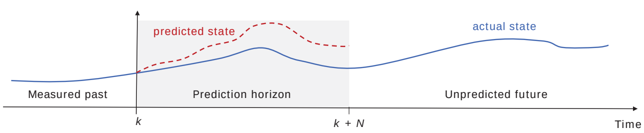

Controllers Tested in SimWindFarm Simulation Tool

- SimWindFarm can perform simultaneous, dynamic simulations of
  - wind turbines
  - wind farm controller
  - aerodynamic interaction of wind turbines
- Controllers are tested through DTU Wind Farm Control framework
- All simulations use wind conditions of
  - mean wind speed of 8m/s
  - turbulence intensity of 6%
  - constant wind direction along turbine row

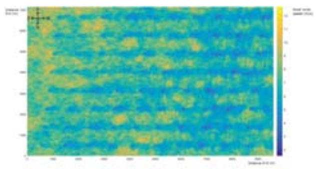

Turbine Fatigue Load Model Developed

- Turbine tower fatigue load model is derived from SimWindFarm simulations of two turbine array

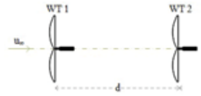

- MPC uses optimum operation point determined from fatigue load model

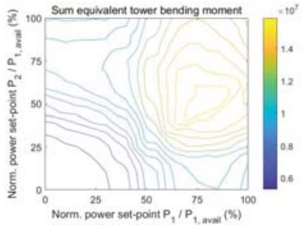

Design of Linear Dynamic Wind Farm Operation Model

- Inlet wind speed at downstream turbine is obtained as

$$u_{inl,i} = u_{\infty} - \sum_{j=1}^{N} \delta\tilde{u}_j$$

- Wind speed deficit from upstream turbine is calculated as

$$\delta\tilde{u}_j = \delta u_{j,0} + \frac{\partial \delta u_j}{\partial u}_{x_0} \Delta u + \frac{\partial \delta u_j}{\partial P}_{x_0} \Delta P$$

- State space delay model is used to account for duration of wake propagation

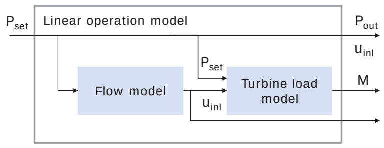

- Resulting total system description of flow model is

$$\begin{bmatrix} \underline{u}_{del,all} \\ \underline{u}_0 \end{bmatrix} [n+1] = \begin{bmatrix} \underline{\underline{A}}_{del,all} + \underline{\underline{B}}_{u,inl}\underline{\underline{C}}_{u,inl} & \underline{\underline{B}}_{u_0} \\ 0 & I \end{bmatrix} \begin{bmatrix} \underline{u}_{del,all} \\ \underline{u}_0 \end{bmatrix} [n] + \begin{bmatrix} \underline{\underline{B}}_{\Delta P} \\ 0 \end{bmatrix} \underline{\Delta P}[n]$$

Two-Turbine Case Study

- Performance of MPC and PI-controller are compared in simulations of two turbine array

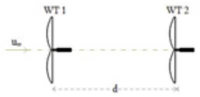

- Dispatch functions used in PI-controller are
  - static dispatch (WT1: 20%, WT2: 80 %)
  - proportional dispatch

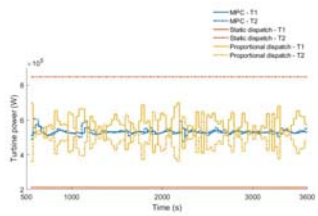

Successful Validation of Linear Operation Model

- Linear operation model compares well with SimWindFarm
- Comparison is conducted on array of 8 turbines

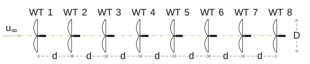

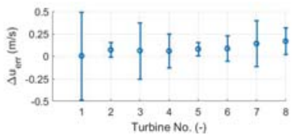

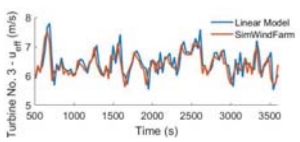

Two-Turbine Case Study: Results

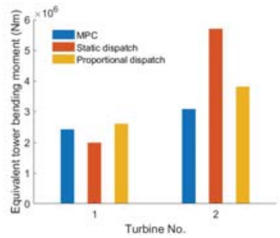

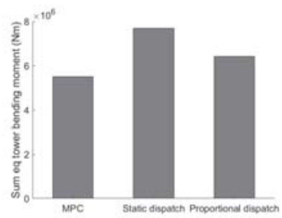

- Model-predictive control approach reduces total turbine fatigue loads by up to 28% in this case study

Eight-Turbine Case Study: Set-up

- Performance of MPC and PI-controller are compared in simulations of eight turbine array

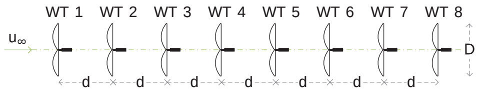

- Eight turbine array configuration is representative of common offshore wind farms
- Dispatch functions used in PI-controller are
  - static dispatch
  - proportional dispatch

Eight-Turbine Case Study: Results

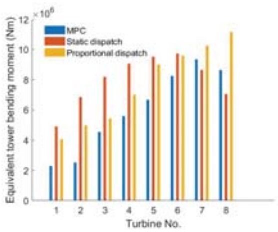

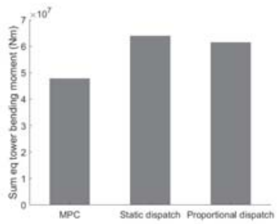

- Model-predictive control approach reduces total turbine fatigue loads by up to 25% in this case study

Conclusions

- Developed linear wind farm operation model is successfully validated against SimWindFarm
- Developed turbine fatigue load model can be used in total power reference following WFC to reduce turbine fatigue
- Simulations of developed model predictive controller show up to 28% lower fatigue loads than with other commonly used wind farm controllers

Acknowledgements

- CONCERT project fundet by ForskEl and with partners Siemens Gamesa and Vattenfall
- OPWIND project funded by Research Council of Norway, Statoil, Vattenfall and Vestas

Backup

Two Turbine Case Study

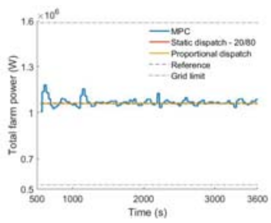

- Variations of total power are within Danish grid code limits
- Danish grid code specifies limit of 5% of rated wind farm power as maximum deviation from total power reference

An approach to linear analysis of wind power plant dynamics, stability, and control

Karl Merz
SINTEF Energy Research

Deepwind, January 19, 2018.

Characterization of nonlinearity in wind power plant dynamics

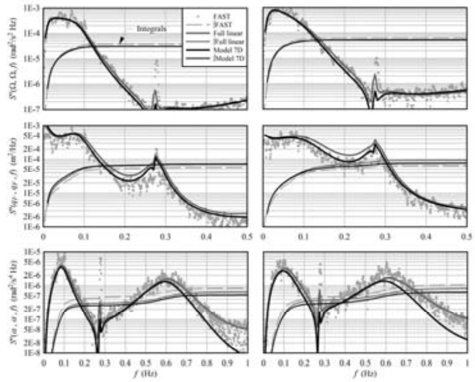

STAS WPP: Unified state-space model of a wind power plant

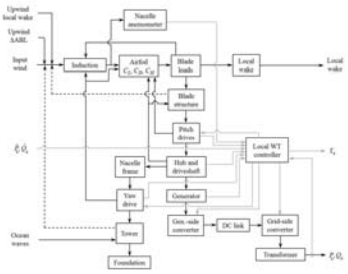

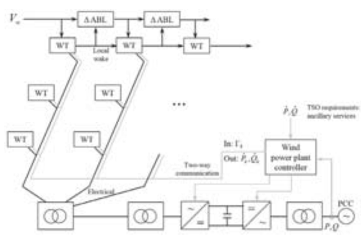

Characterization of nonlinearity in wind power plant dynamics

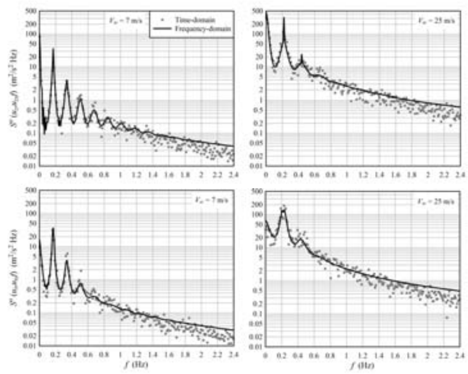

Tangent dynamics

$$\frac{d\mathbf{x}}{dt} = \mathbf{f}(\mathbf{x}, \mathbf{u}, t) \qquad \mathbf{y} = \mathbf{g}(\mathbf{x}, \mathbf{u}, t)$$

Nonlinear trajectory

$$\frac{d\mathbf{x}_1}{dt} = \mathbf{f}(\mathbf{x}_1, \mathbf{u}_1, t_1) \qquad \mathbf{y}_1 = \mathbf{g}(\mathbf{x}_1, \mathbf{u}_1, t_1)$$

Initial condition

$$\frac{d(\delta\mathbf{x})}{dt} = \left.\frac{\partial \mathbf{f}}{\partial \mathbf{x}}\right|_1 \delta\mathbf{x} + \left.\frac{\partial \mathbf{f}}{\partial \mathbf{u}}\right|_1 \delta\mathbf{u} + \left.\frac{\partial \mathbf{f}}{\partial t}\right|_1 \delta t = \mathbf{A}\,\delta\mathbf{x} + \mathbf{B}\begin{bmatrix}\delta\mathbf{u}\\ \delta t\end{bmatrix}$$

$$\delta\mathbf{y} = \left.\frac{\partial \mathbf{g}}{\partial \mathbf{x}}\right|_1 \delta\mathbf{x} + \left.\frac{\partial \mathbf{g}}{\partial \mathbf{u}}\right|_1 \delta\mathbf{u} + \left.\frac{\partial \mathbf{g}}{\partial t}\right|_1 \delta t = \mathbf{C}\,\delta\mathbf{x} + \mathbf{D}\begin{bmatrix}\delta\mathbf{u}\\ \delta t\end{bmatrix}$$

Perturbation

$\mathbf{x}_1$, $\mathbf{u}_1$, t_1 is an initial condition. It does not need to be an equilibrium point.

Characterization of nonlinearity in wind power plant dynamics

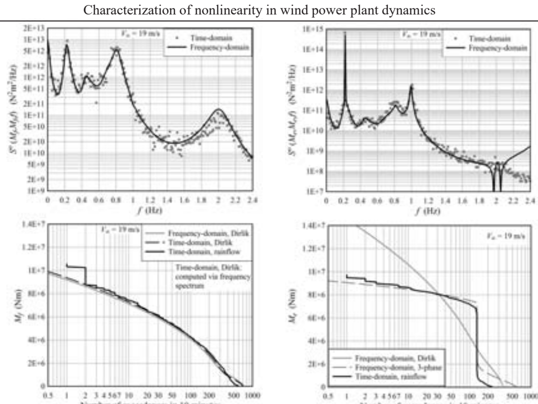

Characterization of nonlinearity in wind power plant dynamics

Two different codes, models built by two different analysts.

What is nonlinearity and what is modelling error?

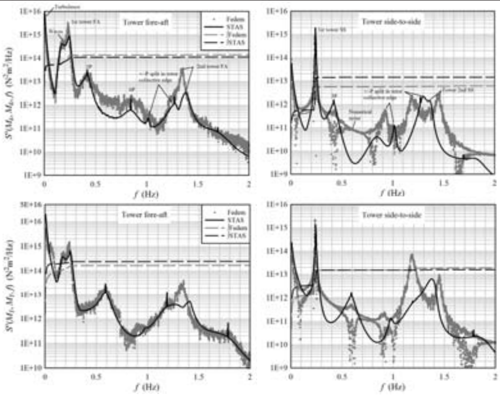

The new version of STAS provides nonlinear and linear equation sets that agree, at the point of linearization, to machine precision. Perturbed solutions will show explicitly the influence of nonlinearity.

Stochastic dynamics of linear systems

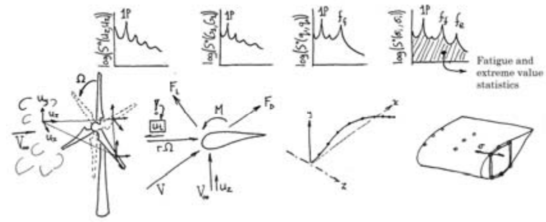

In the frequency domain, stochastic loads and fatigue cycle counts are numerically smooth and deterministic: no random numbers!

Modal analysis, explanations of cause and effect in WPP dynamics

	Tower side-to-side mode $\lambda = -0.049 \pm i\,1.508$		(Tower fore-aft mode) $\lambda = -0.095 \pm i\,1.557$		SS damping filter mode $\lambda = -0.090 \pm i\,1.449$	
States	$\lvert a \rvert$	θ/π	$\lvert a \rvert$	θ/π	$\lvert a \rvert$	θ/π
$\dot{q}_s$	1.000	0.000	0.244	-0.966	1.000	0.000
$\dot{q}_F$	1.230	0.428	1.000	0.000	1.487	-0.931
Ω	0.039	0.410	0.003	0.707	0.032	0.670
$\tilde{\Omega}$	0.035	0.239	0.003	0.524	0.028	0.465
β	0.016	-0.344	0.005	-0.414	0.025	0.030
ϑ_s	1.432	-0.065	0.396	0.759	2.178	0.189
ϑ_F	1.695	0.579	2.565	0.020	1.780	-0.562
Outputs	$\lvert a \rvert$	θ/π	$\lvert a \rvert$	θ/π	$\lvert a \rvert$	θ/π
$\hat{P}_e$	8.048	-0.025	2.233	0.800	12.174	0.229
T_g	8.889	-0.092	2.405	0.753	13.182	0.175
P_e	8.034	-0.120	2.217	0.705	12.004	0.140
T_a	2.982	-0.657	2.565	0.826	3.809	0.016
F_T	0.134	-0.899	0.181	0.790	0.097	0.130

$\dot{q}_s$: Side-to-side velocity of the nacelle (m/s). $\dot{q}_F$: Fore-aft velocity of the nacelle (m/s). Ω: Rotor speed, measured at the generator (rad/s). ϑ_s: Band-pass filtered side-to-side nacelle velocity (m/s). $\hat{P}_e$: Commanded electrical power (MW). T_g: Generator air gap torque (MN). P_e: Electrical power at the network-side terminals of the wind turbine's transformer (MW).

	Tower side-to-side mode		Tower fore-aft mode		Damping filter mode	
K_s (MN)	f_n (Hz)	ζ	f_n (Hz)	ζ	f_n (Hz)	ζ
0	0.236	0.007	0.245	0.052	0.236	0.100
1	0.237	0.011	0.245	0.054	0.236	0.094
2	0.237	0.016	0.245	0.055	0.235	0.087
5	0.240	0.028	0.247	0.059	0.231	0.069
10	0.244	0.030	0.251	0.056	0.224	0.065
40	0.247	0.036	0.263	0.033	0.207	0.068
5 + lead	0.240	0.032	0.248	0.061	0.231	0.062

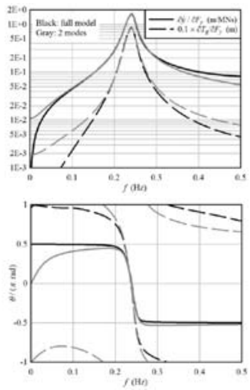

Tangent dynamics: applications in the optimization of wind power plants

$$\Pi = \int_0^T P(\mathbf{x},\mathbf{u})\,dt \qquad \frac{d\mathbf{x}}{dt} = \mathbf{f}(\mathbf{x},\ldots,t)$$

$$\Pi = \int_0^T P + \boldsymbol{\lambda}^T\left(\frac{d\mathbf{x}}{dt} - \mathbf{f}\right) dt$$

$$\delta_u \Pi = \int_0^T \left(\frac{\partial P}{\partial \mathbf{u}} - \boldsymbol{\lambda}^T \frac{\partial \mathbf{f}}{\partial \mathbf{u}}\right)\delta\mathbf{u} - \underbrace{\left(\frac{d\boldsymbol{\lambda}^{\mathbf{T}}}{dt} + \boldsymbol{\lambda}^T\frac{\partial \mathbf{f}}{\partial \mathbf{x}} - \frac{\partial P}{\partial \mathbf{x}}\right)}_{\text{Define } \boldsymbol{\lambda}}\delta\mathbf{x}\,dt + \boldsymbol{\lambda}^T\delta\mathbf{x}\Big|_0^T$$

$$\frac{d\boldsymbol{\lambda}}{dt} = -\left(\frac{\partial \mathbf{f}}{\partial \mathbf{x}}\right)^T \boldsymbol{\lambda} + \left(\frac{\partial P}{\partial \mathbf{x}}\right)^T \qquad \frac{\partial P}{\partial \mathbf{u}} = \boldsymbol{\lambda}^T \frac{\partial \mathbf{f}}{\partial \mathbf{u}}$$

Evolution equation for the gradient of the cost with respect to some parameters **u**.

Formal model reduction

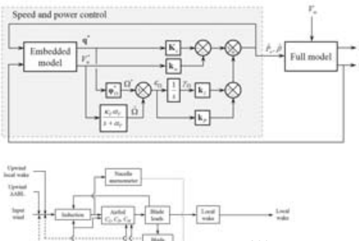

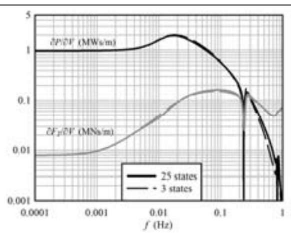

STAS: ~300 states → Modal reduction: 22 states → LQG optimal controller: 25 states → Reduced-order controller: 3 states

Starting high-resolution and reducing, we can check that we don't miss any important dynamics.

Wind Farm Control

Bill Leithead

Wind Energy and Control Centre
University of StrathClyde

The Faculty of Engineering

General Purpose Farm Controller

A generic wind farm controller architecture has been adopted with the following attributes.

- It is hierarchical, decentralised and scalable.
- Top layer responds to grid requirements to determine an adjustment in the power output from the wind farm.
- It may operate open-loop, eg to reduce the power output by a fixed amount, or closed-loop, e.g to curtail the output from the farm to a fixed power level. The latter feedback is based on feedback of the total farm output.
- Second layer determines change in power required from each turbine.
- Bottom layer is a generic interface to each turbine, the PAC.
- The only feedback permitted from each turbine to the first and second layers are flags containing information on the state of the turbines and an estimate of the local wind speed.

Contents

- General purpose farm controller
- Wind farm simulation for control

General Purpose Farm Controller

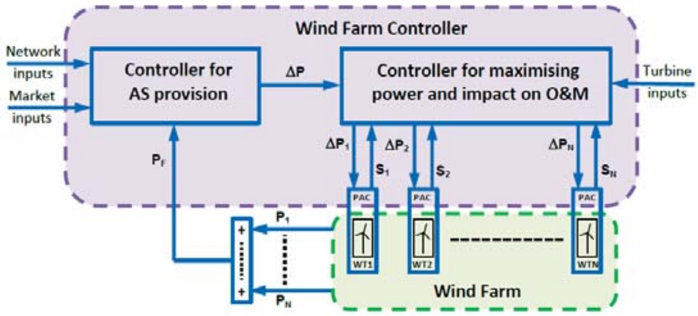

General Purpose Farm Controller

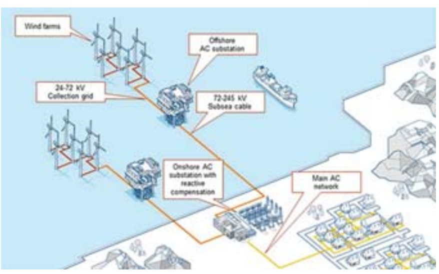

General Purpose Farm Controller

This hierarchical structure of the wind farm controller ensures that the turbine controllers are not compromised

- The wind speed estimation is sufficiently good not to be influenced by the state of the turbine
- The use of flags avoids the introduction of feedbacks based on the state of the turbine
- The farm level feedback acting on the total power introduces feedback round a single turbine but weakened by the inverse in the number of turbines

Tight control at the wind farm level can, thus, be achieved with very weak control of each turbine.

General Purpose Farm Controller

Simplified top layer feedback loop

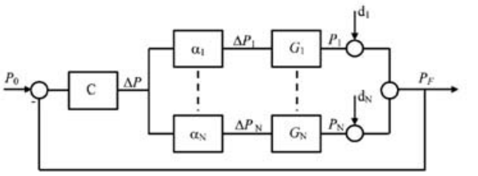

Feedback loop for single turbine

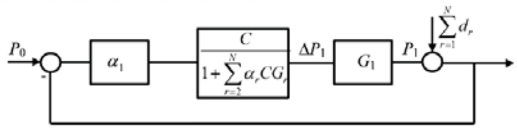

Power Adjusting Controller (PAC)

PAC jackets full envelope controller

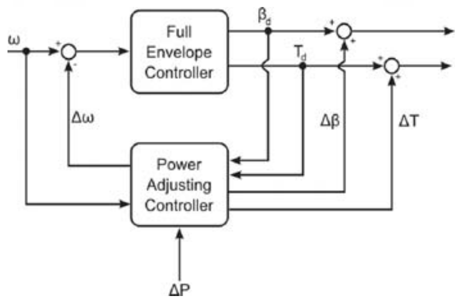

Power Adjusting Controller (PAC)

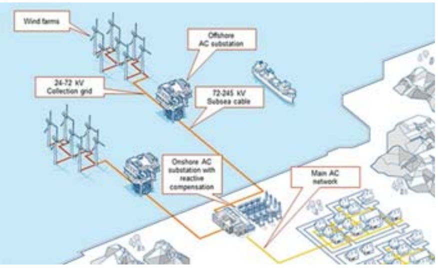

Power Adjusting Controller (PAC)

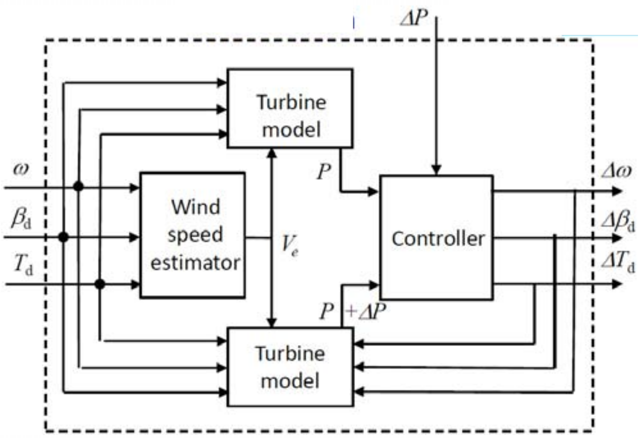

Power Adjusting Controller (PAC)

The PAC has the following attributes.

- The PAC does not compromise the turbine controller since it is essentially feed forward in nature
- It can be interpreted as changing the set point or operational strategy of the wind turbine albeit in a continuous and dynamic manner.
- The turbine is kept within a safe operating region through the use of the flags
- The change in output power from the turbine matches very accurately the change in power requested
- Response of the turbine to the requested change can be very fast.
- Very little information about the turbine is required. No information is required on turbine dynamics or the turbine controller.
- It is easily retrofitted.

Power Adjusting Controller (PAC)

Transmittance from pitch demand to generator speed with/without PAC

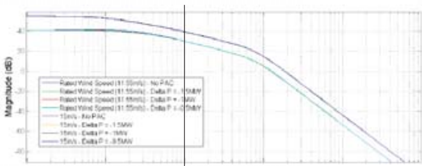

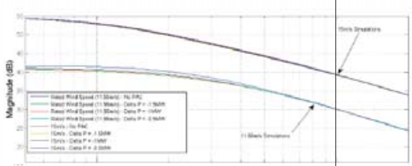

- 5MW turbine
- Wind speeds of 11.5 and 15m/s
- ΔP of 0.5, 1.0 and 1.5MW

1rad/s

- Maximum difference is -0.2dB
- So PAC acts as feedforward

Power Adjusting Controller (PAC)

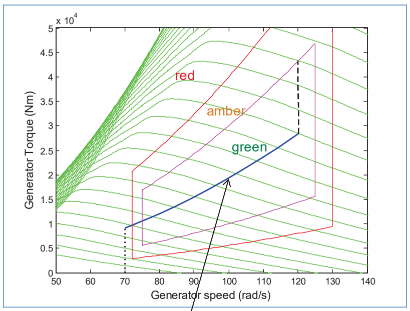

Normal operating strategy

- Flexibility of operation achieved by continuously varying the operating strategy
- The operating strategy curve has been replaced by a region.
- Traffic light system used to keep within safe operating region

Power Adjusting Controller (PAC)

Provision of synthetic inertia

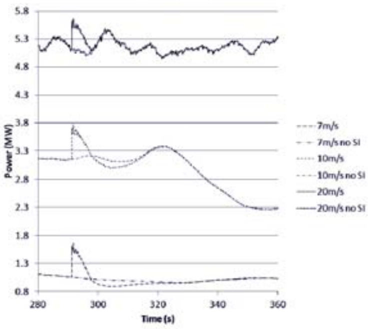

Absolute power outputs

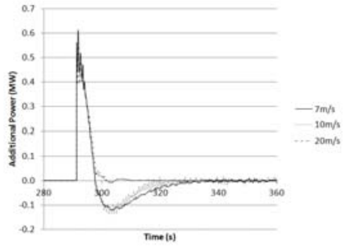

Relative power outputs

Power Adjusting Controller (PAC)

- Individual turbine behaviour
- Traffic light boundaries constrain operational state

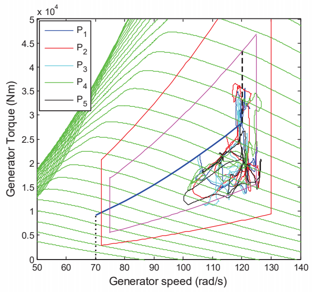

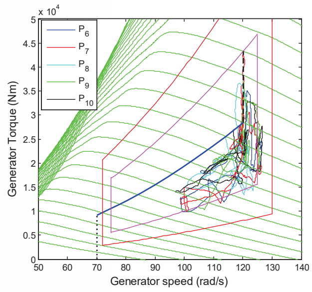

Applications

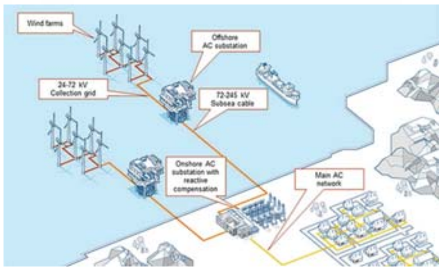

Power Adjusting Controller (PAC)

Increase in output power

Full envelope controller mode switch

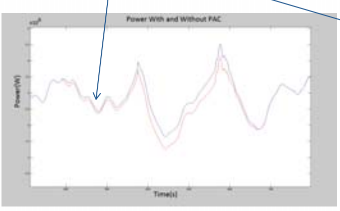

Power output with/without PAC

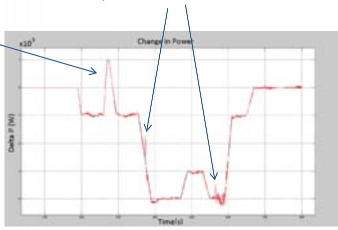

Difference in output with/without PAC

- 5MW wind turbine in 9m/s mean wind speed

Applications

Ancillary Services

- Delivery of full range of ancillary services at the wind farm level has been demonstrated
  - Curtailment, droop control and synthetic inertia, etc
- No recourse to modifying turbine's converter or controller
- Advantages compared to single turbine provision of AS
  - Turbines can compensate each other
  - Only very weak feedback round turbines required
- No significant increase observed but more detailed assessment required
- Issues related to communications delays and grid frequency measurement addressed by Generator-Response Following concept
- Lab based demonstration of GRF being conducted

Applications

Power optimisation and minimisation of loads

- Extent of benefits not clear
- More detailed assessment required
- Need a suitable wind simulation tool – **StrathFarm**

Wind Farm Simulation Tool

- **StrathFarm**

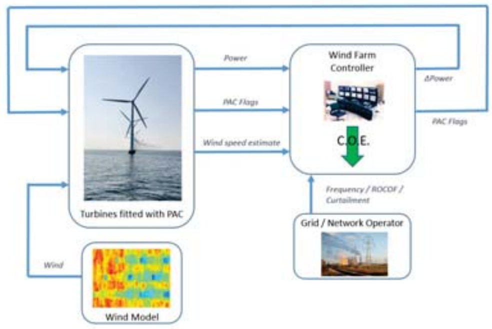

Wind Farm Simulation Tool

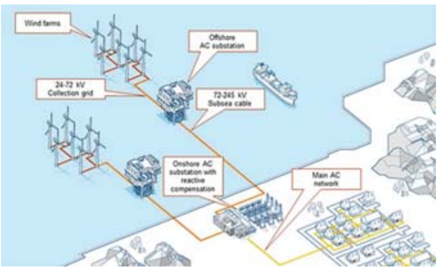

Wind Farm Simulation Tool

- Comparison of blade RBMs to Bladed (——) at 15m/s

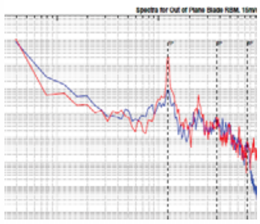

Out-of-plane blade RBM

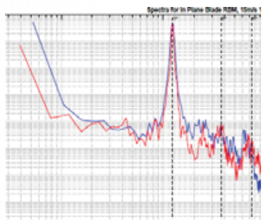

In-plane blade RBM

Wind Farm Simulation Tool

An analysis and design wind farm model and simulation tool is required with the following requirements

- Model wakes and wake interactions
- Model turbines in sufficient detail that tower, blade and drive-train loads are sufficiently accurate to estimate the impact of turbine and farm controllers on loads.
- Include commercial standard turbine controllers.
- Include wind farm controller and interface to turbine controllers.
- Very fast simulation of large wind farms; run in real time with 100 turbines on a standard PC.
- Flexibility of choice of farm layout, turbines & controllers and wind conditions direction, mean wind speed and turbulence intensity.

All above requirements have been met by StrathFarm

Wind Farm Simulation Tool

- Comparison of tower loads to Bladed (——) at 15m/s

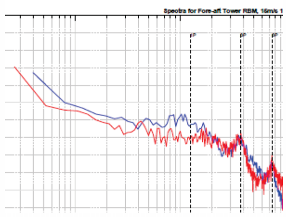

Fore-and-aft tower RBM

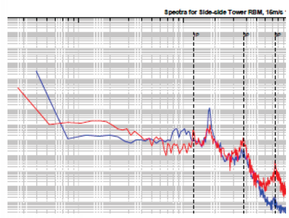

Side-to-side, tower RBM

Wind Farm Simulation Tool

The generic controller architecture has been tested

Example
- 5x5MW turbines curtailed to 9MW
- Mean wind speed 9m/s, TI 2%

Strategy 1

Strategy 2

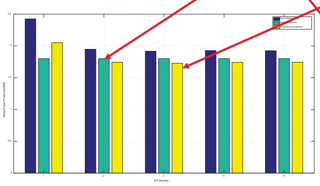

Average power

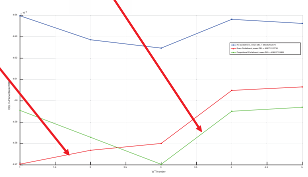

DEL tower fore-aft RBM

Conclusion

- A general purpose controller architecture has been developed and demonstrated to be very effective.
- It's hierarchical, decentralised and scalable
- A fast wind farm simulation tool has been developed for wind farm control design studies
- Capable of simulating 100 turbines in real time on a standard PC

Wind Farm Simulation Tool

- Next steps
  - Enhance its batch processing capability
  - Add power systems aspects to cater for grid events
  - Improve the modelling of wakes

Acknowledgements

The following funding is gratefully acknowledged
- EPSRC EP/G037728/1 DTC Wind Energy Systems
- EPSRC EP/L016680/1 DTC Wind and Marine Energy Systems
- EPSRC EP/H018662/1 Supergen Wind Phase2
- EPSRC EP/L014106/1 Supergen Wind Hub
- EPSRC EP/N006224/1 MAXFARM
- FP-ENERGY-2013.10.1.6: 609795 IRPWind

and the contributions from
- Adam Stock, Victoria Neilson, Lourdes Gala Santos, Saman Poushpas, Sung-Ho Hur, Giorgio Zorzi, Lindsey Amos, Velissarios Kourkoulis and David Campos-Gaona

Conclusion

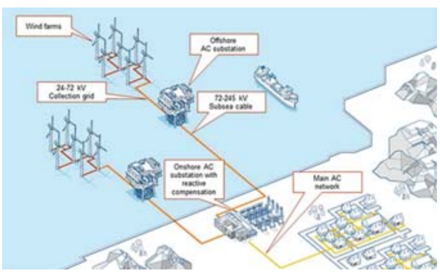

Closing session – Strategic Outlook

WindBarge: floating wind production at intermediate water depths, J. Krokstad, NTNU

OO-Star Wind Floater – The cost effective solution for future offshore wind developments,Trond Landbø, Dr.techn.Olav Olsen

The first floating wind turbine in France: Status, Feedbacks & Perspectives, I. Le Crom, Centrale Nantes

Progress of EERA JPwind towards stronger collaboration and impact; Peter Hauge Madsen, DTU Wind Energy

EERA DeepWind'2018 – Closing remarks, J.O.Tande, SINTEF Energi


WINDBARGE

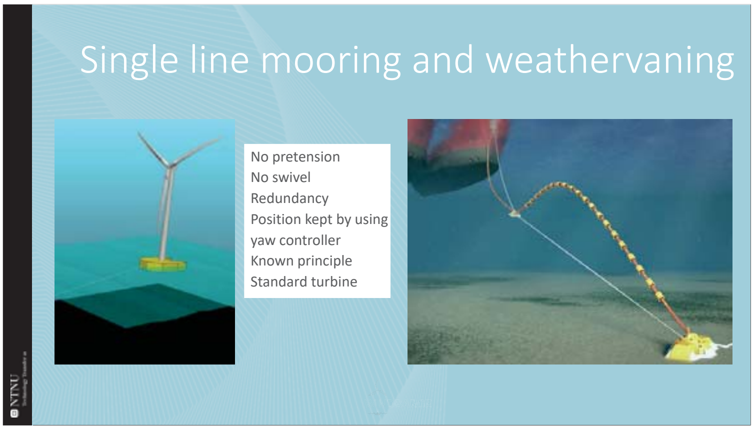
Single line mooring and weathervaning
No pretension
No swivel
Redundancy
Position kept by using yaw controller
Known principle
Standard turbine
NTNU

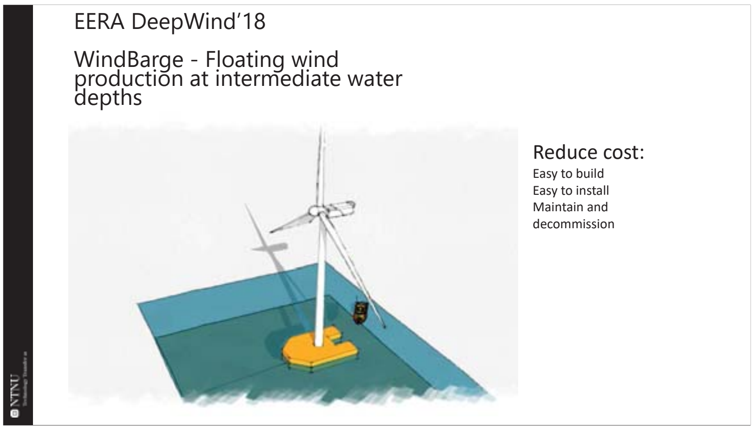
EERA DeepWind'18
WindBarge - Floating wind production at intermediate water depths
Reduce cost:
Easy to build
Easy to install
Maintain and decommission
NTNU

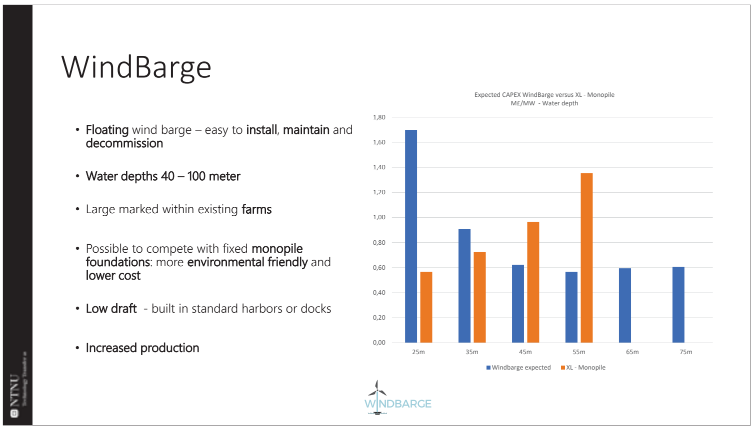
WindBarge
• Floating wind barge – easy to install, maintain and decommission
• Water depths 40 – 100 meter
• Large marked within existing farms
• Possible to compete with fixed monopile foundations: more environmental friendly and lower cost
• Low draft - built in standard harbors or docks
• Increased production
Expected CAPEX WindBarge versus XL - Monopile
M£/MW - Water depth
1,80
1,60
1,40
1,20
1,00
0,80
0,60
0,40
0,20
0,00
25m
35m
45m
55m
65m
75m
Windbarge expected
XL - Monopile
WINDBARGE
NTNU


TEAM
Jørgen Ranum Krokstad
Inventor, Prof II at Dep. Marin Technology. 32 yr. of experience in hydrodynamic and wind
Synne Nybø
M.S.c in offshore construction from Dep. Marin Technology. Research on fatigue and global analysis of WindBarge
Jan Tore Horn
PhD at Dep. Marin Technology. Focusing on hydrodynamics and reliability.
Fredrik S. Moen
Project Manager
International rig management and shipyard experience
NTNU

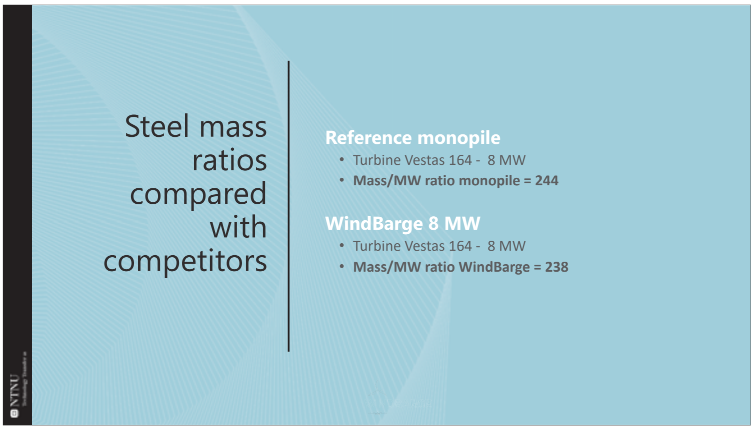
Steel mass ratios compared with competitors
Reference monopile
• Turbine Vestas 164 - 8 MW
• Mass/MW ratio monopile = 244
WindBarge 8 MW
• Turbine Vestas 164 - 8 MW
• Mass/MW ratio WindBarge = 238
NTNU

WindBarge – Sheltered access

- **Sheltered access** in the stern of the floater for maintenance vessels (example ESNA – daughter ship (SES))
- Increased weather window
- Target 2.5m Hs

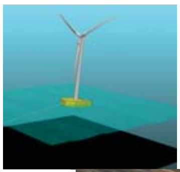

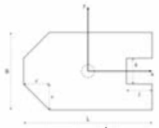

WINDBARGE

Single Mooring Line (SML – system)

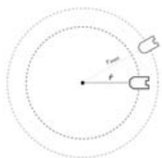

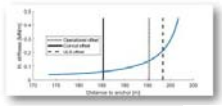

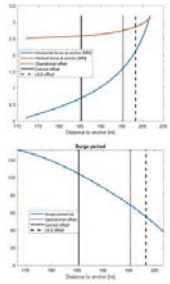

WINDBARGE

Suction anchor – not new to the wind industry

- High vertical load capacity
- Safety factor of 2 -> 6 MN vertical load
- Anchor mass in order of 100 tonn
- Towing installation method

WINDBARGE

Accept criteria	Comments	Status
Intact stability	DNV OS-J103. Different in roll/pitch due to weather vaning.	OK
Restoring moment	Max mean pitch angle < 5 deg	OK
Nacelle acceleration	RMSE < 0.2g , MPMV < 0.6g	OK
High pitch-period	Maximized during optimization	OK
Yaw stability	Avoid fishtailing and maintain heading passively/actively	In progress
Mooring system	Single mooring line with buoys and electrical cable + suction anchor for unobstructed rotation	Initial design
Turbine support	5-8MW	OK
Maintenance access	Sheltered docking < 2.5m Hs	Not verified
Structural capacity	Wave- and wind bending moments within the capacity of a simple barge design	In progress
ULS simulations	Verify barge behavior in extreme conditions	In progress
FLS simulations	Long-term FLS analyses with SCFs – find damage equivalent loads	Not started

WINDBARGE

Main dimensions – 5 MW version (could be scaled to 8 MW – estimated 1700 ton steel)

Natural Periods
- Heave 7s
- Pitch 17s
- Roll 24.4s

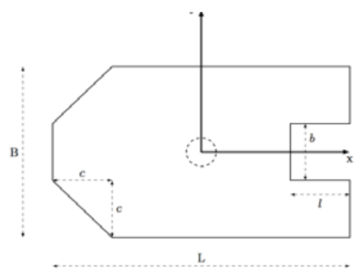

WINDBARGE

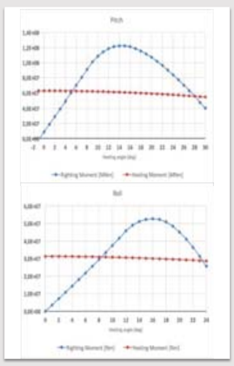

Intact stability

- DNV requirements satisfied in pitch.
- In roll, it is assumed that 50% of the capacity is sufficient due to limited wind overturning moment.

WINDBARGE

Planed Projects

- Verification from simulations/model tests
- General design improvements
- Technology qualification
- LCOE – documentation

Metocean parameters

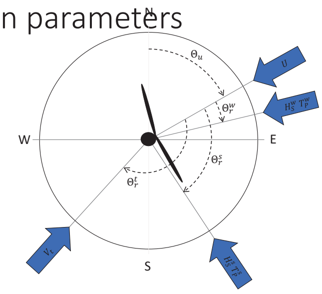

1

EERA DEEPWIND 2018
RADISSON BLU ROYAL GARDEN HOTEL, TRONDHEIM

OO-STAR WIND FLOATER
THE FUTURE OF OFFSHORE WIND?

Trondheim, January 19th. 2018

Trond Landbø
Manager Business Area Energy/Renewable
Dr.techn.Olav Olsen AS

DR. TECHN. OLAV OLSEN

2

INTRODUCTION - MAIN MESSAGES

> We believe floating wind will beat onshore wind as well as bottom fixed offshore wind in the future
> We believe that in the future there will be three different segments within the wind industry:
– **Onshore wind**; WTGs limited to typically **5 MW** due to transport and installation limitations on land
– **Offshore wind, bottom fixed**; WTGs limited to typically **10 MW** due to installation cost
– **Offshore wind, floating**; WTGs typically **20 MW**, no size limitations related to assembly and installation
> We believe Olav Olsen has developed a very cost effective floating solution with the OO-Star Wind Floater, with all the qualities required by the future floating offshore wind market

DR. TECHN. OLAV OLSEN

3

DR.TECHN.OLAV OLSEN AS INTRODUCTION

DR. TECHN. OLAV OLSEN

4

DR.TECHN. OLAV OLSEN – COMPANY PROFILE

> Norwegian independent Structural and Marine consulting company founded in 1962
> Offices in Oslo and Trondheim (Norway)
> Approximately 90 employees
> Contributes in all project phases, from concept development to decommissioning
> Active in research and development projects

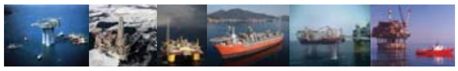

DR. TECHN. OLAV OLSEN

5

OFFSHORE CONCRETE STRUCTURES

> World leading designer of offshore concrete structures
> Shallow to deepwater
> Gravity Base Structures (GBS)
> Floating concrete platforms
> Arctic applications

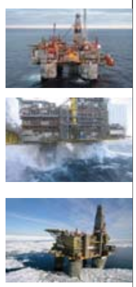

DR. TECHN. OLAV OLSEN

6

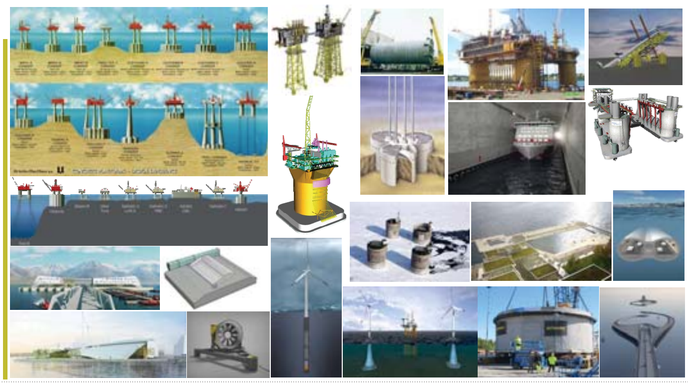

DR. TECHN. OLAV OLSEN

7

BUSINESS AREAS

- Buildings onshore
- Offshore Oil & Gas
- Renewable energy
- Infrastructures
- Harbours and Industry
- OO «Futurum»

Core business: Structural & Marine engineering

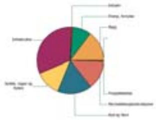

Adding value to company and clients

DR. TECHN. OLAV OLSEN

8

DR.TECHN.OLAV OLSEN AS OFFSHORE WIND

DR. TECHN. OLAV OLSEN

9

OLAV OLSEN - OFFSHORE WIND

DR. TECHN. OLAV OLSEN

10

OLAV OLSEN - CAPABILITIES OFFSHORE WIND

- Substructures
  - Bottom fixed and floating
  - Steel and concrete
  - Concept development
  - Design and analysis (ShellDesign)
  - Geotechnics
- Mooring and anchors
  - System configuration
  - System design
  - Geotechnics
- Installation
  - Method development
  - Installation concepts
- Fully coupled simulations:
  - SIMA
  - 3DFloat
  - Deeplines
  - (Orcaflex, Ashes, FEDEM Windpower)
- Cost models
  - Fabrication and Installation
    - Substructure
    - Mooring
    - Anchors
- Third party verification

DR. TECHN. OLAV OLSEN

11

FLOATING OFFSHORE WIND TURBINES

Hywind

Hydro/Statoil

HiPRWind

EU project

OO Star Wind Floater

Patented concept

DR. TECHN. OLAV OLSEN

12

OO-STAR WIND FLOATER

DR. TECHN. OLAV OLSEN

13

THE OO-STAR WIND FLOATER HISTORY

- Few realistic WTG floaters before 2010
- Hiprwind (2010) – questions to scalability and fatigue

- What does the optimal floater look like?
- OO-Star Wind Floater developed 2010/11, presented at ONS2012
- Preferred concept (steel) for EU project Floatgen – Acciona part 3 MW WTG
- NFR project 2013-2014: Designed for 6MW, WD 100 m, North Sea
- LIFES50+ 2015-2018: Up-scaling to 10 MW, WD 70-130 m, Hs=7.0 -15.6 m

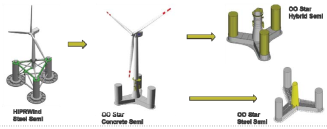

DR. TECHN. OLAV OLSEN

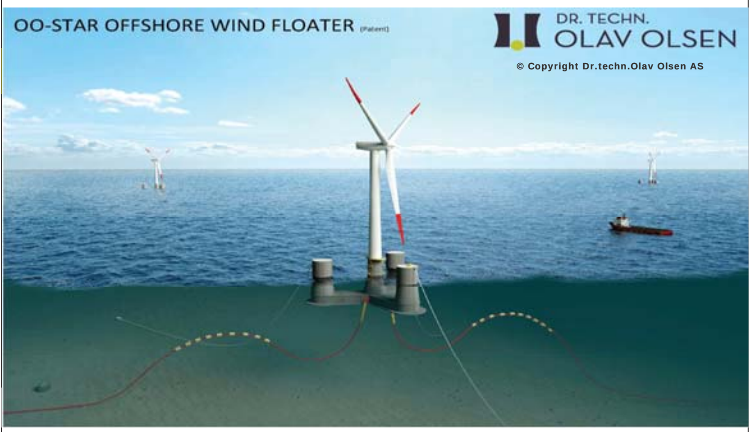

15

OO-STAR WIND FLOATER – GENERAL DESCRIPTION

- Robust, stable and very simple 3-leg semisubmersible floater.
- Passive ballast system
- Water depth potential from 50 m
- Concrete, steel or a combination (hybrid). Material selection according to optimal design, cost, fabrication facilities etc.
- Concrete best suited for large wind turbines. Not fatigue sensitive and long design life, 100 years +. Possible to reuse floater.
- The OO-Star Wind Floater consists of a central shaft supporting the WTG, and a tri-star shaped pontoon supporting 3 buoyancy cylinders for optimal stability.
- Permanent buoyancy in the columns and shaft. The pontoons provide structural support of the columns, weight stability, damping/added mass and temporary buoyancy for inshore assembly.
- Fabrication in a dock, on a barge or on a quay. The structure is well suited for modular fabrication.
- The substructure can float with very small draft and the unit can be fully assembled at quay-side before tow to site. No requirements for deep waters at assembly site.
- Transport to site by towing. No requirements for expensive offshore heavy lifts.

DR. TECHN. OLAV OLSEN

16

MOORING - BASIC CONFIGURATION

- 3 line system

GoF and GoM: Chain catenary with Clump weight

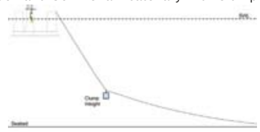

WoB: Pure chain catenary

- Focus on new development
  - Line configurations
  - Number of lines
  - Line materials
  - Anchor types and sharing

DR. TECHN. OLAV OLSEN

17

HORIZON 2020 - LIFES 50+

- Horizon 2020 project, total budget 7.3 MEuro
- Project lead by SINTEF Ocean
- OO Star Wind Floater selected as one of two concepts for Phase 2 (model testing and further development)
- Project web page: http://lifes50plus.eu/

DR. TECHN. OLAV OLSEN

This project has received funding from the *European Union's Horizon 2020 research and innovation programme* under grant agreement No 640741

18

LIFES 50+ MODEL TESTS

- Modell tests planned in Phase 2:
  - Ocean Basin at SINTEF Ocean, November 2017 (Scale 1:36)
  - Wind tunnel at Polimi, Spring 2018 (Scale 1:75)

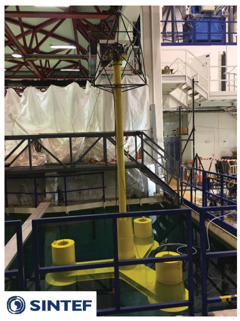

DR. TECHN. OLAV OLSEN

This project has received funding from the *European Union's Horizon 2020 research and innovation programme* under grant agreement No 640741

19

FABRICATION/INSTALLATION OO-STAR WIND FLOATER

20

FABRICATION SET-UP

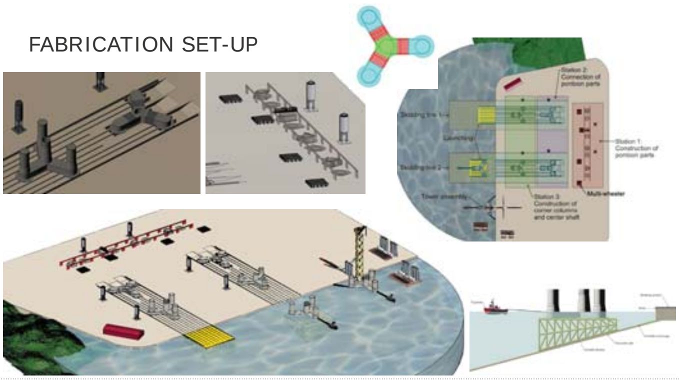

21

FABRICATION 25 UNITS/YEAR – TYPICAL SCHEDULE

		...	W 1	W 2	W 3	W 4	W 5	W 6	W 7	W 8	W 9	W 10	W 11	W 12	W 13	W 14	W 15	W 16	W 17	W 18	W 19	...
For sk. line 1	Construction of pontoon parts	...	4 weeks				4 weeks															...
For sk. line 2		...			4 weeks				4 weeks													...
Skidding line 1	Connection of pontoon parts	...					4 weeks				4 weeks											...
	Columns construction	...									4 weeks				4 weeks							...
	Central shaft construction	...									4 weeks				4 weeks							...
	Launching	...																				...
Skidding line 2	Connection of pontoon parts	...							4 weeks				4 weeks									...
	Columns construction	...											4 weeks				4 weeks					...
	Central shaft construction	...											4 weeks				4 weeks					...
	Launching	...																				...
Total launched units		...	L1		L2		L1		L2		L1		L2		L1		L2		L1		L2	...

22

ASSEMBLY AT QUAYSIDE – CURRENT WTG's

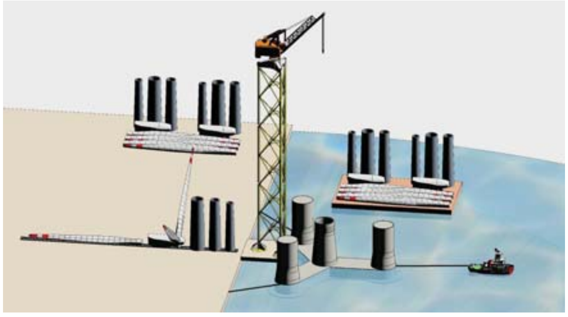

23

ASSEMBLY AT QUAYSIDE – FUTURE LARGE WTG's

24

BOTTOM FIXED WTGs (FOR COMPARISON)

FABRICATION/INSTALLATION - CHALLENGES

25

OFFSHORE WIND - BOTTOM FIXED

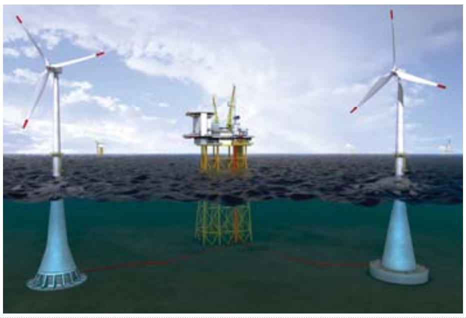

26

GBS Production Facilities – Large Scale

Main challenges:

- Variations in GBS configuration
- Flexibility of yard wrt. water depth at site and soil conditions
- Water depth at keyside and towing draft – stability issues
- Large site investment required, few sites suited

Conclusion:

- Difficult to industrialize fabrication process
- Full inshore assembly is not cost effective for GBS since floating stability will be the main design parameter, not the operation phase.
- Alternative: Offshore assembly

27

SPACE FRAME TOWER (SFT)

> Foundation - different solutions
  - Gravity base
  - Suction buckets
  - Piles

> 3 main element types:
  - Vertical legs, constant diameter
  - X and K nodes with uniform design. Cost effective fabrication, superior fatigue capacity.
  - Uniform X-bracing system

> Transition structures are standardized for turbine type

Gravity/Skirt piles · Gravity Base · Piled foundation frame · Suction buckets · Pre installed piles

28

SFT - NODE FABRICATION

Hot forming with hydraulic press

Welding two halves together to an X-node

Splitting X-node into two K-nodes

29

Proposed Fabrication scheme for SFT substructure

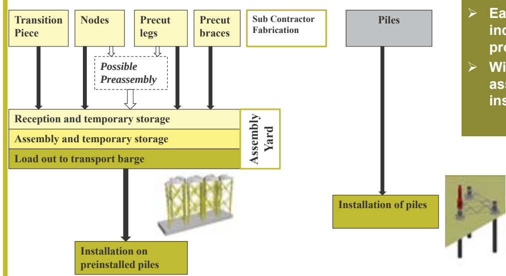

Conclusion:

- Easier (than GBS) to industrialize the fabrication process
- Will depend on offshore assembly or special installation vessels

30

SUMMARY BOTTOM FIXED

- Monopiles have been dominating the market for bottom fixed offshore wind – highly industrialized
- Jacket structures becoming more popular for deeper water and larger WTGs, less steel than monopoles give potential for cost savings.
- Use of concrete can increase the operational life of substructures
- Difficult to standardize bottom fixed substructures due to variation in water depth, soil conditions and environmental loading
- Monopiles and jackets have higher potential for standardization and industrialization than concrete GBS
- Installation of bottom fixed WTGs requires offshore assembly or costly measures to solve temporary conditions.
- Future large WTGs (20 MW) will require expensive new installation tools. Likely that bottom fixed WTGs will be limited in size.

31

OFFSHORE WIND CHALLENGES

DR. TECHN. OLAV OLSEN

32

OFFSHORE WIND CHALLENGES

- The main and overall challenge is to reduce cost of energy (LCOE) – cannot rely on subsidies in the future
- *Requirements:*
- Consistent frame conditions (political, consenting, tendering process, environment etc.)
- Development of consistent rules and regulations
- Development of business tools (financing, insurance etc.)
- Development of supplier industry (competition, effectivity, market stability)
- Development of new and better technology
  - Economy of scale, larger turbines
  - Increase effectivity, robustness and operation life
  - Reduce CAPEX, OPEX
- Development of fabrication and installation methods (reduce CAPEX, risk)

DR. TECHN. OLAV OLSEN

33

OFFSHORE WIND CHALLENGES

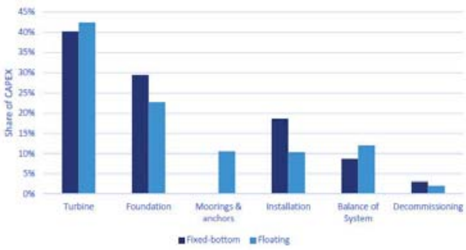

Source Carbon Trust 2015

DR. TECHN. OLAV OLSEN

34

WHY

FLOATING OFFSHORE WIND

WILL OUTBEAT

BOTTOM FIXED OFFSHORE WIND

IN THE FUTURE

DR. TECHN. OLAV OLSEN

35

FLOATING WIND – KEY ADVANTAGES

- Floating wind has larger energy potential than bottom fixed.
- In some areas floating wind is the only way to go. This will ensure development of a floating market.
- Floating substructures have higher potential for standardization than bottom fixed (not very sensitive to water depth and soil conditions). Efficient and cost effective mass fabrication of substructures
- Shallow draft floaters - Quayside assembly and testing prior to tow out
- Installations without offshore heavy lift – tow to site
- Simple removal – reverse installation
- Large potential for reuse – 2nd hand value of floater will reduce energy cost
- Large potential for efficient supply chain and significant cost reductions

- Robust execution program suitable for future large WTGs
- Next generation 20 MW floating WTGs can be assembled without expensive new offshore cranes

- Specific for Norway:
  - Norway do not have suitable sites for bottom fixed offshore wind (with a couple of exceptions).
  - Floating wind has a significant future potential in Norway

DR. TECHN. OLAV OLSEN

36

WHY

OO-STAR WIND FLOATER

HAS THE QUALITIES REQUIRED BY THE

FUTURE OFFSHORE WIND MARKET

DR. TECHN. OLAV OLSEN

37

OO-STAR - ADVANTAGES

- OO-Star Wind Floater is a simple and robust floater concept, with favourable motions for WTG and cable
- Adaptive to «all» environmental conditions and WTG sizes
- Very good «scalability-factor» for increase of WTG size
- Concrete is less sensitive to fatigue than steel (WTGs are fatigue machines) and requires minimum maintenance
- Concrete substructure has long design life, 100+ years with minor cost increase (concrete cover, cathodic protection and outfitting)
- Concrete is fabricated in all countries, limited number of skilled workers required
- Shallow minimum draft - can be fully assembled and tested at quayside
- No offshore heavy lifts – WTG assembly by land cranes onto fixed substructure (resting at seabed)
- Mooring connections above water – easy access and «artificial» increase of water depth (benefit for mooring in shallow water)
- Fixed mooring points at 2 columns, fairlead/chain stopper at 3rd column. Tensioning from vessel, no winch.
- Possible to improve cost and durability by lifting interface between concrete and steel and to reduce steel tower fatigue (crucial for future large WTGs)

38

DISCLAIMER & COPYRIGHT

SHAKE THE FUTURE.

CENTRALE NANTES SEM-REV - LHEEA

FLOATGEN is co-financed by the European Commission's 7th Framework Programme for Research and Technological Innovation.

The first Floating Wind Turbine in France (SEM-REV)

I. Le Crom, ECN, EERA Deepwind 19/01/2018

FOW: 1st pre-Commercial Farms in France (EOLFLO)

Commissionning expected in 2020

3 floater technologies

Perspective: 6GW in 2030

SHAKE THE FUTURE.

Offshore Wind Ressource in France

01/2018
Installed Onshore:
> 13.7 GW
Forecasted Offshore:
> 3.1 GW

France is investing

Fixed offshore wind turbine:
> 80 GW over 10 000 km²

Floating wind turbine:
> 140 GW over 25 000 km²

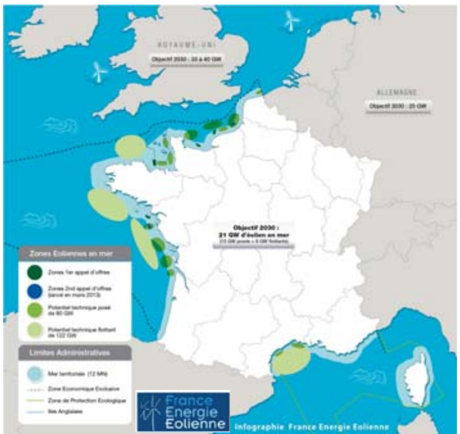

SHAKE THE FUTURE.

Introduction

CENTRALE NANTES and SEM-REV Test Site
- LHEEA Laboratory
- SEM-REV

Floatgen Project
- Floatgen FWT
- Status

LHEEA R&D Roadmap
- Research Program
- Feedback & Perspectives

SHAKE THE FUTURE.

BFOW: 1st Commercial Farms in France

1st Call : commisionning expected in 2020-2022

2nd Call : commisionning expected in 2021-2023

Perspective: 15GW in 2030

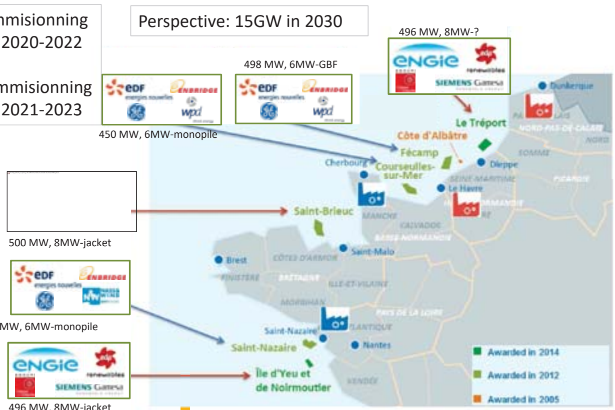

SHAKE THE FUTURE.

SHAKE THE FUTURE.

CENTRALE NANTES SEM-REV - LHEEA

CENTRALE NANTES & SEM-REV Test Site

Centrale Nantes

- Graduate engineering programs, Masters and PhDs, to French and international students (2000 students)
- Mechanics, Materials, Energy, Cybernetics, Architecture
- 250 teaching and research staff, 38 partners countries
- 50% R&D budget in collaborative projects with industry

« Widespread recognition of the institute by firms and R&D organizations has enabled graduates to assume positions of responsibility in every sector... »

SHAKE THE FUTURE.

CENTRALE NANTES SEM-REV - LHEEA

SEM-REV

- General view of marine social sciences : consenting, permitting, environment, safety
- Responsible for the procurement & installation of Electrical connection + Moorings
- Design by IDEOL

Actual State

Instrumentation
> DWR West

Electrical Connexion
> Export Cable
> Junction Box
> Hub
> Umbilical

Moorings (6 lines)
> Drag embedded Anchor – chain - - synthetic rope)

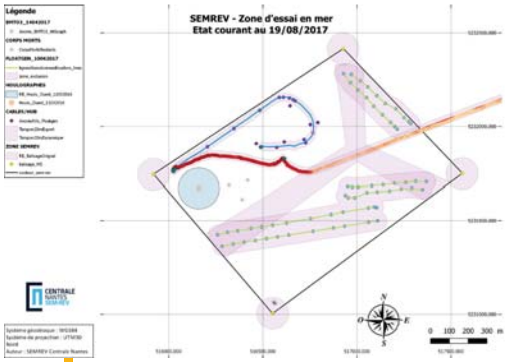

SHAKE THE FUTURE.

CENTRALE NANTES SEM-REV - LHEEA

LHEEA

Strategy to support R&D projects and technology development to make the MRE economically viable

- By using large scale numerical and testing facilities
- Validation of numerical methods and model tests vs results in real conditions

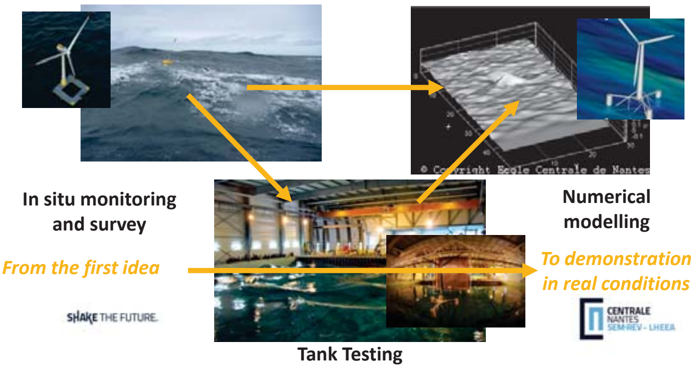

SHAKE THE FUTURE.

CENTRALE NANTES SEM-REV - LHEEA

SHAKE THE FUTURE.

CENTRALE NANTES SEM-REV - LHEEA

Floatgen Project

SEM-REV : Overview

- CAPEX: 20 M€
- 12nm from Le Croisic
- 1 km² restricted area
- 35m LAT

Main steps :
2009 – Test site monitoring,
2012 – Export cable,
2015 – Subsea hub

SHAKE THE FUTURE.

CENTRALE NANTES SEM-REV - LHEEA

Floatgen

FLOATGEN is co-financed by the European Commission's 7th Framework Programme for Research and Technological Innovation.

Demonstrate the technical and economic feasibility of one multi-MW integrated floating-wind turbine in the Atlantic Ocean conditions

FLOATGEN

Industry-led European initiative with partial public support

IDEOL
Design: Floater, Umbilical Configuration & Moorings Pre-Lay Method & Hook-Up

Bouygues TP
Floater Construction

ECN
Interface with Environment

ideol CENTRALE NANTES BOUYGUES Universität Stuttgart zabala Fraunhofer RSK

Floatgen Installation

- 2-years testing program connected to the grid : 2018-2019
- R&D on monitoring and fatigue life survey : mooring, cables…

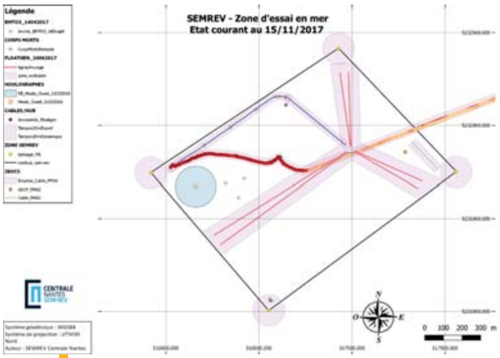

To do List

ML Hook-Up

Umb Hook-Up

Instrumentation

SHAKE THE FUTURE.

SHAKE THE FUTURE.

R&D P1 : Marine environment and resources

SHAKE THE FUTURE.

R&D on floating wind turbines @ LHEEA Lab.

Environmental Monitoring Plan

Applied on Electrical Cables & Connections & Protections, Site & Demonstrators and Onshore Buildings…

Compulsory or Complementary Environmental Survey

Including Physical, Biological & Human Environment

- **Marine life, Birds,**
- **Marine Growth**
- **Corrosion and Abrasion**
- **Anodes, Paints : water**
- **Bathymetry, sediments**
- **Power cables impacts**
- **Marine operations, O&M**
- **Marine traffic (risk an.)**

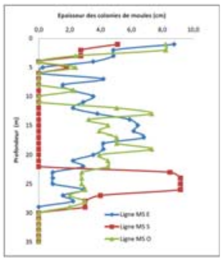

Marine growth :

— Additionnal Mass
— Hydrodynamic Coeffi (drag/inert.)
— Development dissymmetry
— Species Identification
— Spatio-temporal Evolution

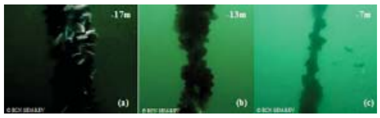

SHAKE THE FUTURE.

Supporting R&D

Collaborative projects with MRE industry

P1 : Marine environment and resources
- Environmental Monitoring : SEA-MON, MOSAIC
- Marine growth : ABIOP, LEHERO
- Soil mechanics : EOGP
- Environmental impacts : SPECIES

P2 : MRE Technologies (FOWT, WEC)
- Floating wind demonstration (FLOATGEN)
- FOWT components and Performances (FORESEA)

P3 : Energy Conversion, Transport and Storage
- Subsea connection units : HUB
- Export and Dynamic Cables : EMODI, OMDYN

P4 : Security, Safety, Marine operation
- Health Monitoring : MHM-EMR
- Marine operation and O&M : HUB installation

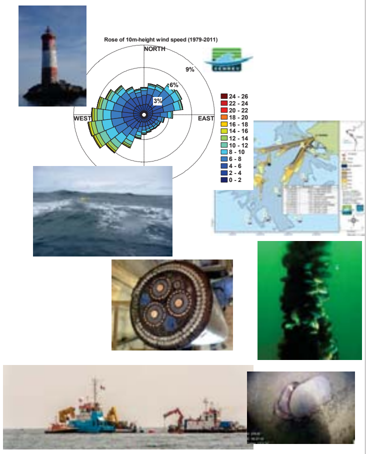

SHAKE THE FUTURE.

SHAKE THE FUTURE.

R&D P2 : MRE Technologies

Demonstration and Access to Market

FORESEA, MARINETII projects

FORESEA under Interreg NWE program

- Supporting LCT developers to access NW Europe's test facilities
- SME / LCT : New Techno, PTO, Mooring, Umbilicals/connectors,
- Test sites benchmarking, Technologies vs market
- From 02/2016 to 12/2019
- Co-Funding of testing cost up to 60%

IHES / IBOCS

MARINET 2 under H2020 Program

- Supporting MRE developers to access Europe's test facilities
- Funding : 100% of the test site cost (directly to the test site)

MARINERG-I / ESFRI : French national Research Infrastructure

- Ifremer + Centrale Nantes MRE testing facilities

SHAKE THE FUTURE.

SHAKE THE FUTURE.

R&D P4 : Security, Safety, Marine operation

SHAKE THE FUTURE.

R&D P3 : Energy Conversion, Transport and Storage

Floatgen

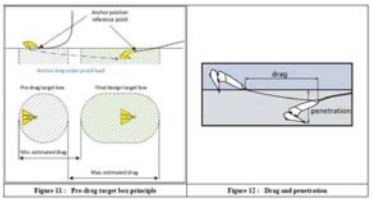

Pre-Lay Methodology

> Anchors Positioning & Pre-stretching

> Deployment

> Recovery

> Tensioning

> Abandonment

Video

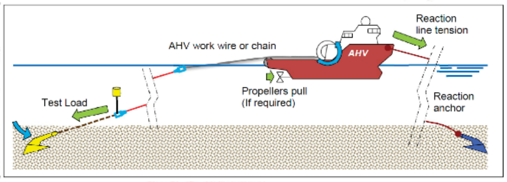

Figure 24 : Reaction line recovery

Power Cables monitoring : from cores to armors

OMDYN project

Dynamic cables: from cores to armors

- Mechanical charcateristics of cable components
- Loads, motions and deformations
- Influence of marine growth
- Default diagnostic
- Cables stabilization on sea bed

Numerical, Bench test, Model Tests

- Numerical modeling of the global configuration and cross section
- Experimental analysis of thermo-mechanical fatigue
- Forced and free dynamic response

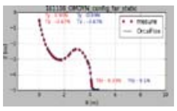

In-situ monitoring

- Monitoring throughout the cable life cycle

With : Un Nantes / GeM, IREENA, MMS, IFSTTAR, Ifremer, CEA Tech, RTE, DCNS, EDF, EOLFI, Nexans, Ideol, …

Modelling of marine operations

→Operations improvement

→Embarked Real-time Calculation

FRYDOM project

> Multibody dynamics
> Cable dynamics
> Unsteady / transient responses
> Waves and wind loads
> Water entry/impact
> Controllers (crane, turbine, winch)
> Dynamic positioning

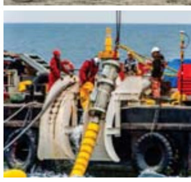

SHAKE THE FUTURE.

CENTRALE NANTES SEM-REV - LHEEA

- General overview of the challenges
- Targeting the cost reduction of MRE
- From TRL 1 to TRL 8
- Attractive Research Platform for MRE
- Open to host other concepts or projects

SHAKE THE FUTURE.

CENTRALE NANTES SEM-REV - LHEEA

ideol CENTRALE NANTES FLOATGEN

www.semrev.fr

SEVENTH FRAMEWORK PROGRAMME

Thank You

CENTRALE NANTES PAYS DE LA LOIRE Loire Atlantique cnrs

Progress in EERA JP Wind towards stronger collaboration and impact

SINTEF-DTU partnership for offshore wind energy

Peter Hauge Madsen
Director, DTU Wind Energy & Coordinator of EERA JP WIND
Deepwind conference 2018
Trondheim

DTU Wind Energy
Department of Wind Energy

Different modes of scale & consolidation

Companies merge

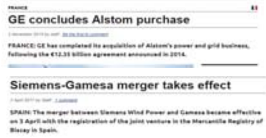
FRANCE
GE concludes Alstom purchase
FRANCE: GE has completed its acquisition of Alstom's power and grid business, following the €12.35 billion agreement announced in 2014.
Siemens-Gamesa merger takes effect
SPAIN: The merger between Siemens Wind Power and Gamesa became effective on 3 April with the registration of the joint venture in the Mercantile Registry of Biscay in Spain.

Public Research organisations collaborate

Why collaborate (more)?

EERA JP WIND - a vehicle for collaboration

- EERA is an organisation under the EU SET-Plan
- EERA JP WIND 1 of 17 Joint Programmes
- 50 member organisations
- Building trust & knowledge exchange
- Major EU projects setup through EERA JP WIND collaboration
- IRPWIND project supporting JP WIND coordination and research

MEGATRENDS

- MATURATION, INDUSTRIALISATION AND GLOBALISATION
- SUBSIDY-FREE WIND POWER AND TECHNOLOGY NEUTRAL TENDERS
- DIGITALISATION
- ENERGY SYSTEMS INTEGRATION

MEGAVIND

Summary - 8 years of learning

- 8 years of coordination growing from 13 to 50+ participants
- General value and impact from
  - Strategy and policy
  - Platform for coordination
  - Data and facility sharing
  - Knowledge sharing
  - Mobility and community building
- Challenges
  - Alignment of national programmes
  - Leveraging "own resources" in joint activities
  - Wide involvement in industry cooperation
  - Managing expectations

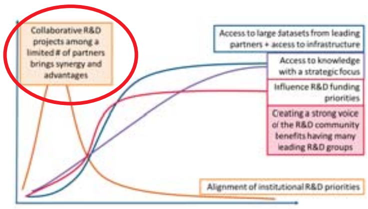

Working together in Europe

- In width and setting the EU Strategy ▶ EERA European Energy Research Alliance
- In depth and working with industry ▶
  - Individually
  - Ad-hoc
  - Strategic partnerships

Strategic areas of collaboration

- Offshore wind energy


Offshore grid development

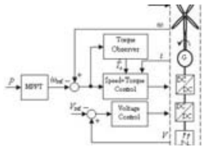

Wind farm control


Wind turbine sub-structures

Why DTU and SINTEF?

Key elements in the partnership

- Focus on key offshore wind challenges
- Partnership for building strength and value
- Commitment to cooperate and coordinate
- Joint roadmap for research
- Transparency and openness within partnership
- Flexible funding approach
- Non-exclusivity and open for collaboration with others

Complementary competence profiles

DTU

A leader in wind energy research including wind turbine loads and control, aerodynamics, and resource assessment

Operating three wind turbine test sites in Denmark and turbine technology labs

PhD and MSc education

Total staff of about 5900 (incl. approx. 1200 PhD students)

SINTEF

Strong competence on offshore wind technology, including substructures, O&M, materials, grid connection and control

Relevant laboratories include ocean basin and smart grids

Strong collaboration with NTNU for PhD and MSc education

Total staff of about 2000

Targeting industry R&D needs

Perspective

- Serving offshore wind industry needs
- A step towards European R&I integration
  - Institutional alignment
  - Public-private collaboration
- Wider knowledge and service portfolio
  - From research to demonstration
  - From education to testing
  - From lab to full scale

Challenges

- Culture
  - From national to international outlook
  - From personal to institutional collaboration
- Administrative issues
  - Aligning national funding
  - Legal
  - Cost and overhead

International collaboration is the new norm

Let us pave the way


SINTEF
EERA DEEPWIND 2018
CLOSING REMARKS
John Olav Giæver Tande, Director NOWITECH
Chief Scientist / Research Manager, SINTEF Energy Research
John.tande@sintef.no
EERA DeepWind, Trondheim, Jan 19, 2018

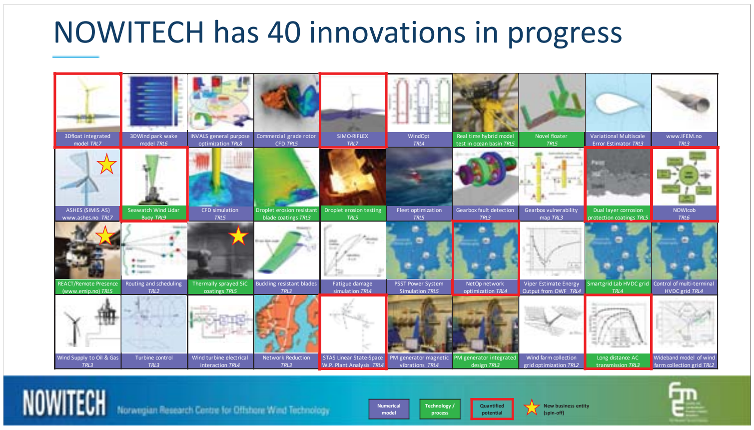
NOWITECH has 40 innovations in progress
NOWITECH Norwegian Research Centre for Offshore Wind Technology

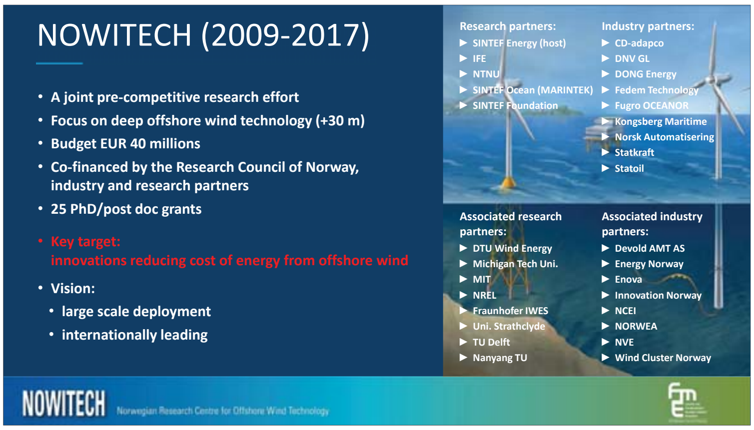
NOWITECH (2009-2017)
• A joint pre-competitive research effort
• Focus on deep offshore wind technology (+30 m)
• Budget EUR 40 millions
• Co-financed by the Research Council of Norway, industry and research partners
• 25 PhD/post doc grants
• Key target: innovations reducing cost of energy from offshore wind
• Vision:
• large scale deployment
• internationally leading
Research partners:
SINTEF Energy (host)
IFE
NTNU
SINTEF Ocean (MARINTEK)
SINTEF Foundation
Industry partners:
CD-adapco
DNV GL
DONG Energy
Fedem Technology
Fugro OCEANOR
Kongsberg Maritime
Norsk Automatisering
Statkraft
Statoil
Associated research partners:
DTU Wind Energy
Michigan Tech Uni.
MIT
NREL
Fraunhofer IWES
Uni. Strathclyde
TU Delft
Nanyang TU
Associated industry partners:
Devold AMT AS
Energy Norway
Enova
Innovation Norway
NCEI
NORWEA
NVE
Wind Cluster Norway
NOWITECH Norwegian Research Centre for Offshore Wind Technology


Potential value of innovations
NPV: > 5000 MEUR*
IMPELLO
* Result from analysis carried out by Impello Management AS for a subset of innovations by NOWITECH. NPV is calculated as socio-economic value of applying the innovations to a share of new offshore wind farms expected in Europe until 2030.
NOWITECH Norwegian Research Centre for Offshore Wind Technology


Offshore wind LCOE
Offshore wind has cost reduction opportunities in multiple areas including scale effects
Turbines & plant
Substructures
Transmission
O&M
Larger turbines and wind farms
Increased reliability
Scale effects and industrialisation
Standardised and optimised offshore foundation design and design criteria
Industrialised manufacturing
eBoP optimisation of substation and transmission capex
Innovative transmission solutions
Improved grid access
Low OPEX drivetrains
Turbine and component quality
Condition monitoring, diagnostics, preventive maintenance
Source: Siemens, MHI-Vestas, MAKE
NOWITECH focus
O&M
Wind turbine
Sub-structure
Grid
LPC distribution of offshore wind farm (example)
MAKE
4 September 2014

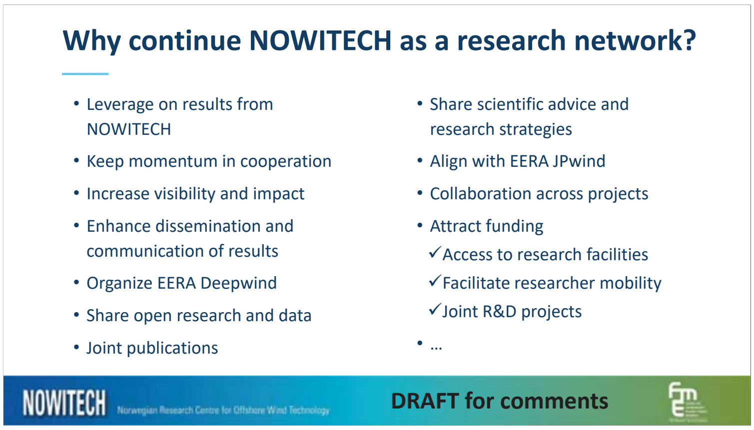
Why continue NOWITECH as a research network?
• Leverage on results from NOWITECH
• Keep momentum in cooperation
• Increase visibility and impact
• Enhance dissemination and communication of results
• Organize EERA Deepwind
• Share open research and data
• Joint publications
• Share scientific advice and research strategies
• Align with EERA JPwind
• Collaboration across projects
• Attract funding
✓Access to research facilities
✓Facilitate researcher mobility
✓Joint R&D projects
• …
NOWITECH Norwegian Research Centre for Offshore Wind Technology
DRAFT for comments

NOWITECH research network

- Research network sharing open results
- Focus on deep offshore wind technology (+30 m)
- Budget in-kind by the individual partners, possibly with additions from the Research Council of Norway and industry
- Key target:
  increasing the economic attractiveness of offshore wind through generation of new knowledge, models, processes and technology
- Vision:
  - large scale deployment
  - internationally leading

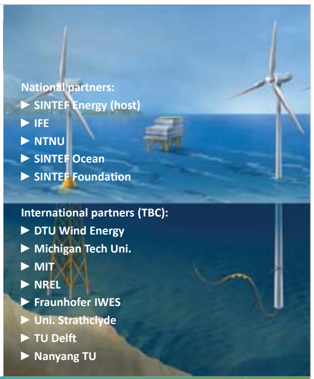

NOWITECH Norwegian Research Centre for Offshore Wind Technology

DRAFT for comments

Summing up EERA Deepwind 2018

- Excellent presentations
- Vibrant positive atmosphere
- Global participation with delegates from all over Europe, but also from USA, Japan, Korea and China
- Good mix of academia and industry
- Gender balance can be better ☺
- Thank you to hotel staff, conference assisting staff from NTNU and SINTEF, session chairs, speakers and audience
- See you at EERA Deepwind 2019!

10

NOWITECH research network

- National network with international participation
- Non-exclusive
- Volunteer basis
- National meetings 4-6 times per year, physical or by skype
- International meeting 1-2 times per year, aligned with EERA Deepwind and other events, possibly also outside Norway
- Lean structure (management board + general assembly)
- Participation by invitation
- Commitment by LoI
- ...

NOWITECH Norwegian Research Centre for Offshore Wind Technology

DRAFT for comments

SINTEF

Technology for a better society

Suggested research priorities

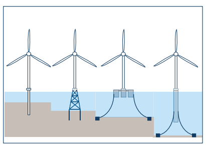

- Support structures
- Marine operations
- Materials

- Grid connection
- System integration
- Energy storage

- Asset management
- Wind farm control
- Digitalization

NOWITECH Norwegian Research Centre for Offshore Wind Technology

DRAFT for comments

Poster session

Session A

1. *Load estimation and O&M costs of Multi Rotor Array turbine for the south Baltic Sea*, M. Karczewski, Lodz University of Technology
2. *Dynamic Responses Analysis for Initial Design of a 12 MW Floating Offshore Wind Turbine with a Semi-Submersible Platform*, J.Kim, University of Ulsan, Korea

Session B

3. *SiC MOSFETs for Offshore Wind Applications,* S. Tiwari, NTNU/SINTEF Ocean

Session C

4. *Extreme met-ocean conditions in a Norwegian fjord,* Z. Midjiyawa, Meteorologisk instiutt
5. *Modelling of non-neutral wind profiles - current recommendations vs. coastal wind climate measurements*, P. Domagalski, Lodz University of Technology
6. *Uncertainty estimations for offshore wind resource assessment and power verification,* D. Foussekis, Centre for Renewable Energy Sources

Session D

7. *Using a Langevin model for the simulation of environmental conditions in an offshore wind farm,* H.Seyr, M.Muskulus, NTNU

Session E

8. *Design optimization with genetic algorithms: How does steel mass increase if offshore wind monopiles are designed for a longer service life?* L. Ziegler, Rambøll Wind
9. *Experimental Study on Slamming Load by Simplified Substructure*, A. Krogstad, NTNU
10. *Effect of hydrodynamic load modelling on the response of floating wind turbines and its mooring system in small water depths*, Kun Xu, NTNU
11. *Supply chains for floating offshore wind substructures - a TLP example,* H.Hartmann, University Rostock
12. *Critical Review of Floating Support Structures for Offshore Wind Farm Deployment*, M Leimeister, REMS, Cranfield University
13. *Asessment of the state-of-the-art ULS design procedure for offshore wind turbine sub-structures*, C. Hübler, Leibniz Univ Hannover
14. *Offshore Floating Platforms: Analysis of a Solution for Motion Mitigation*, A.Rodriguez Marijuan, Saitec Offshore Technologies
15. *State-of-the-art model for the LIFES50+ OO-Star Wind Floater Semi 10MW floating wind turbine*, A. Pegalajar-Jurado, DTU
16. *Validation of a CFD model for the LIFES50+ OO-Star Wind Floater Semi 10MW and investigation of viscous flow effects,* H. Sarlak, DTU
17. *Designing FOWT mooring system in shallow water depth*, V. Arnal, LHEEA, Centrale Nantes
18. *Construction Possibilities for Serial Production of Monolithic Concrete Spar Buoy Platforms,* C. Molins, UPC-Barcelona Tech
19. *Extreme response estimation of offshore wind turbines with an extended contour-line method, J-T.Horn, NTNU*
20. *Fabrication and Installation of OO-Star Wind Floater, T.Landbø, Dr.techn.Olav Olsen*

Session F

21. *Experimental validation of analytical wake and downstream turbine performance modelling*, F. Polster, Technical University of Berlin
22. *Reduce Order Model for the prediction of the aerodynamic lift around the NACA0015 airfoil, M.S. Siddiqui, NTNU*
23. *Fast divergence-conforming reduced orders models for flow, E. Fonn, SINTEF Digital*

Session G

24. *Sensitivity analysis of the dynamic response of a floating wind turbine*, R. Siavashi, University of Bergen
25. *Parameter Estimation of Breaking Wave Load Model using Monte Carlo Simulation*, S. Wang, DTU Wind Energy
26. *Emulation of ReaTHM testing*, L. Eliassen, SINTEF Ocean
27. *Multiple degrees of freedom real-time actuation of aerodynamic loads in model testing of floating wind turbines using cable-driven parallel robots*, V. Chabaud, NTNU/SINTEF Ocean
28. *A 6DoF hydrodynamic model for real time implementation in hybrid testing*, I. Bayati, Politecnico di Milano
29. *Kalman Estimation of Position and Velocity for ReaTHM Testing Applications,* E.Bachmann Mehammer, Imperial College London/SINTEF Energi
30. *Numerical modelling and validation of a semisubmersible floating offshore wind turbine under wind and wave misalignment*, S. OH, ClassNK

Session H

31. *Impact on wind turbine loads from different down regulation control strategies,* C. Galinos, DTU

Load Estimation and O&M costs of Multi Rotor Array Turbine for the South Baltic Sea

NTNU – Trondheim
Norwegian University of Science and Technology

Maciej Karczewski[1*], Piotr Domagalski[1], Michal Lipian[1], Lars Roar Saetran[2]
[1] *Institute of Turbomachinery, Lodz University of Technology, Lodz, Poland, *Email: maciej.karczewski@p.lodz.pl*
[2] *Department of Energy and Process Engineering, Norwegian University of Science and Engineering, 7491 Trondheim, Norway.*

Fig .1. Polish off-shore wind

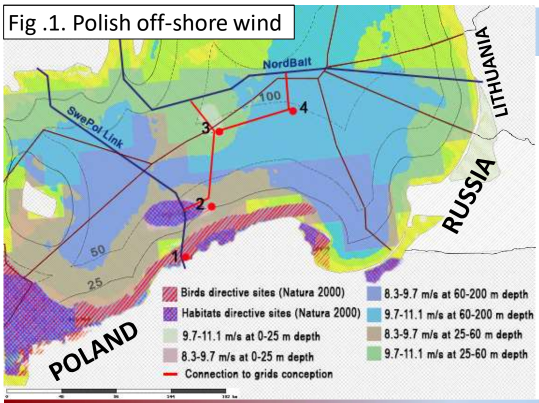

Introduction

- Poland experiences energy shortage at northern parts of the country;
- Polish RES bill significantly limited operations for on-shore wind;
- Gov't plans to support 2-3 shallow off-shore farm locations, but no sight for overall cost reduction and instigation of local heavy industry;
- **AIM1: explore deep off-shore wind locations such as our idea of location 4 to show costs can be reduced.**
- **AIM2: propose floating off-shore wind turbine design in the form of Multi Rotor Array (MRA) to mitigate cost and technology problems. AIM3: revitalise Polish shipyard industry around our own MRA concept.**

Methodology

- Evaluated benchmark Vestas V100 2 MW turbine for costs at all 4 loco by using NREL design cost and scaling model[1];
- Designed a layout of 7 rotor MRA and scaled the baseline NREL 5 MW single rotor turbine[2] down to a 0.714 MW;
- Analysed hourly metocean data for the 50-year period;
- Preapred a FAST add-on tool in Matlab and verified structural integrity of MRA rotors using aero-servo-elastic solver FAST ver 8.0 against approved load cases[3];
- Measured performance of the proposed MRA and compared it to baseline NREL 5 MW turbine.

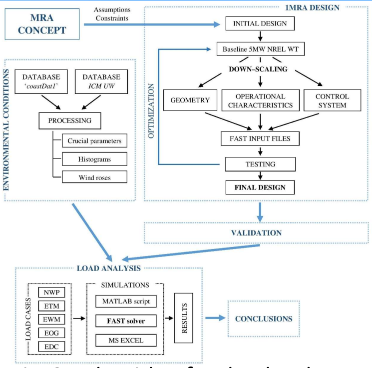

Fig. 2. Algorithm for the development and evalution of MRA

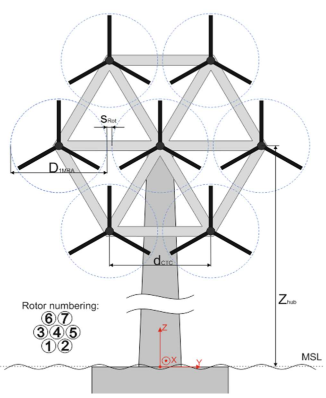

Numerical model

- RNA of the baseline turbine was Froude scaled to derive mass of our 1MRA rotor[1];
- Steady-state validation of the scaled rotor model made;
- Average/extreme sea state from coastDat1 DB for location 4:
  - Mean wind speed V_{ave50}=10.1m/s, extreme V_{max50}=36.7m/s,
  - Mean signific.wave height H_{ave45}=1.2m, wave period T_{ave45}=5.19s, extreme H_{max45}=9.9m, T_{Hmax45}=12.3s.
- Power law wind shear exponent=0.14 adjusting induction to MRA

INPUT PARAMETER	FACTOR
Blade and hub radius	κ_L
Blade, hub, nacelle mass	$\kappa_L{}^3$
Hub, nacelle, generator moment of inertia	$\kappa_L{}^5$
Nacelle CM location in (X), (Y) and (Z)	κ_L
Mass ratio (mass per unit length)	$\kappa_L{}^2$
Blade flapwise/edgewise'stiffness ratios	$\kappa_L{}^3$

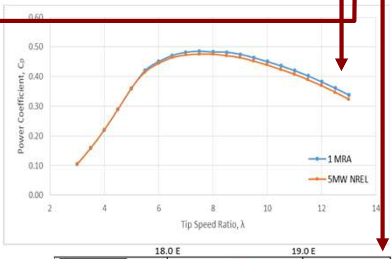

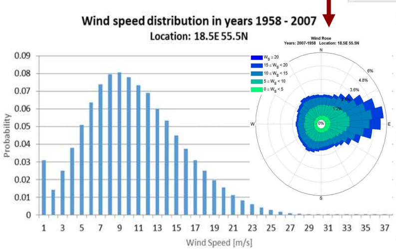

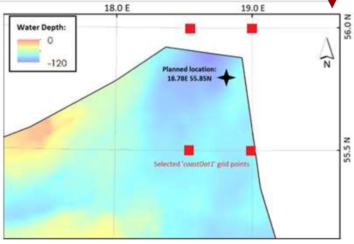

Initial results

Power **reference** vs. **MRA**

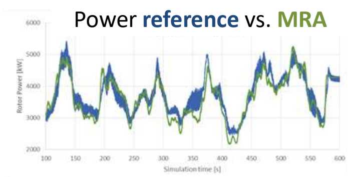

Bl_DefOoP **reference** vs. **MRA**

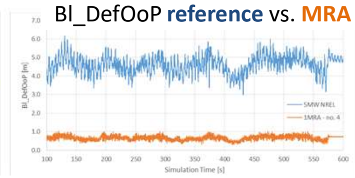

Normal Turbulence Model (NTM load) I_{15}=0.16 and a=3

reference

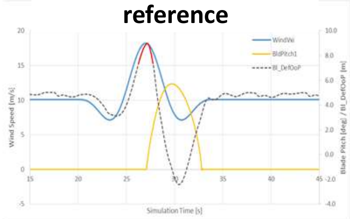

MRA

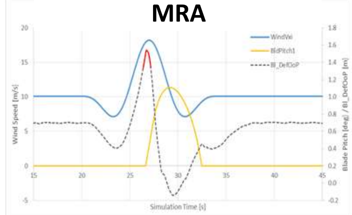

Extreme Operating Gust (EOG load) V_{hub}=10.1 m/s

Model	Bl_DefOoP 1MRA [m]	Bl_DefOoP 1MRA NC%	Bl_DefOoP NREL [m]	Bl_DefOoP NREL NC%	Bl_RootMx [kNm] 1MRA	Bl_RootMx [kNm] NREL	Bl_RootMx [kNm] %	Bl_RootMy [kNm] 1MRA	Bl_RootMy [kNm] NREL	Bl_RootMy [kNm] %
$NWP_{8.0}$	0.45	*23.4*	3.36	*31.9*	37.95	4277	*0.89*	290.8	6065	*4.79*
$NWP_{11.4}$	0.81	*42.2*	5.31	*50.5*	75.15	4956	*1.52*	530.5	9772	*5.43*
$NWP_{18.0}$	0.29	*15.1*	1.97	*18.7*	71.49	4929	*1.45*	248.7	5195	*4.79*
NTM	1.04	*54.2*	6.17	*58.7*	182.3	5376	*3.39*	702.7	11370	*6.18*
EWM	1.04	*54.2*	6.10	*58.0*	512.1	11190	*4.58*	503.5	10590	*4.75*
EOG	**1.54**	*80.2*	**8.97**	*85.3*	153.6	5056	*3.04*	1028	16190	*6.35*

References

[1] Fingersh L., Hand M., Laxson A., *Wind Turbine Design Cost and Scaling Model*, Technical Report NREL/TP-500-40566, 12/2006.
[2] Jonkman J., Butterfield S., Musial W., Scott G., *Definition of a 5-MW Reference Wind Turbine for Offshore System Development*, Technical Report. NREL/TP-500-38060, 02/2009.
[3] Germanischer Lloyd WindEnergie (GL), *Guidelines for the Certification of Offshore Wind Turbines*, 2005.

Summary & conclusions

- Deep off-shore wind in Polish territorial waters: abundant and economically sound
- Around 7% overall COE reduction of location 4 as compared to loco 1
- 62% RNA mass reduction when moving from the 5 MW to MRA
- EOG load led to breaching the safety margin by 10.2% and 15.3% of allowable blade tip clearance for 1MRA and NREL designs respectively
- Proposed MRA rotor withstands other loads by substantial margins

Dynamic Responses Analysis for Initial Design of a 12 MW Floating Offshore Wind Turbine with Semi-Submersible Platform

Junbae Kim*, Pham Thanh Dam, Byoungcheon Seo, Hyunkyoung Shin†
School of Naval Architecture and Ocean Engineering, University of Ulsan, Korea

Introduction

- Why do we need 12 MW Floating Offshore Wind turbine (FOWT)?
  - Able to use in Deep Water : the stable and strong wind flows.
  - Improve energy production capacity and reduce construction costs.
  - Solution for noise and insufficient space.
- The purpose with the design of a 12 MW UOU(University of Ulsan) FOWT.
  - Desing of FOWTs must consider both aerodynamics and hydrodynamics.
  - The floating platform has the lowest natural frequencies.
  - Initial dimensional design of tower to avoid buckling and resonances.
  - Solution for unstable coupling between platform motion and pitch controller
- Dynamic responses analysis for initial design of a 12 MW UOU FOWT using fully coupled analysis was performed to determine the suitability.

Design of 12 MW Floating Offshore Wind Turbine

- The initial design of 12 MW UOU FOWT was performed based on a 5 MW NREL wind turbine for offshore model, using geometric laws of similarity.

12MW FOWT Design Process & Properties

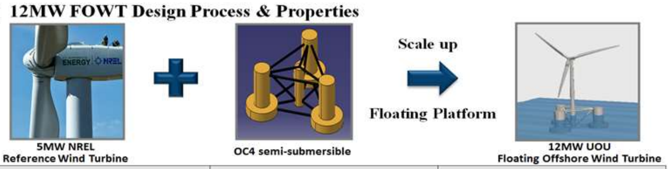

	5 MW	12 MW
Rating	5 MW	12 MW
Control	Variable Speed, Collective Pitch	Variable Speed, Collective Pitch
Drivetrain	High Speed, Multiple-Stage Gearbox	Low Speed, Direct Drive(gearless)
Rotor, Hub Diameter	126 m, 3 m	195.2 m, 4.64 m
Hub Height	90 m	124.6 m
Cut-In, Rated, Cut-Out Wind Speed	3 m/s, 11.4 m/s, 25 m/s	3 m/s, 11.2 m/s, 25 m/s
Cut-In, Rated Rotor Speed	6.9 rpm, 12.1 rpm	3.03 rpm, 8.25 rpm
Overhang, Shaft Tilt, Pre-cone	5 m, 5°, 2.5°	7.78 m, 5°, 3°
Rotor Mass	110,000 kg	297,660 kg
Nacelle Mass	240,000 kg	400,000 kg (*Target*)
Tower Mass (for offshore)	249,718 kg	781,964 kg

Geometric Scale Ratio

- $P = C_p * \frac{1}{2}\rho A V^3$
- $\lambda_g = \sqrt{\frac{12MW}{5MW}} = \sqrt{\frac{A_{12}}{A_5}} = \sqrt{\frac{P_{12}}{P_5}} = 1.549$

- P : Rotor power (kW)
- C_p : Max. power coefficient of rotor
- ρ : Air density. (1.225 kg/m³)
- A : Rotor swept area (m²)
- V : Wind Speed (m/s)
- λ_g : Geometric scale ratio

Scale-up Blade & Tower properties (Beam deflection)

- 61.5 (m) 5MW glass blade : 17.7 ton
- 95.28 (m) 12MW carbon (spar cap) blade : 42.7 ton

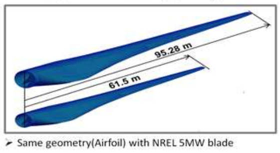

➢ Same geometry(Airfoil) with NREL 5MW blade

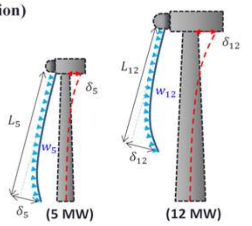

Hub height

- Rotor radius + Extreme wave height (half) with 50-year occurrence × S.F. of 1.8
  : 97.6 + 30.0 / 2 × 1.8 = 124.6 m

Scale-up Platform properties

- Ratio of W_{12}(1480ton) to W_5(600ton)
- OC4 semi-submersible "displaced volume" 13,917m³ (5MW) → 34,336m³ (12MW)

$$\frac{\rho g V_{12MW}}{\rho g V_{5MW}} = \frac{Weight\ of\ wind\ turbine_{12MW}}{Weight\ of\ wind\ turbine_{5MW}}$$

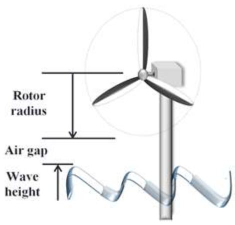

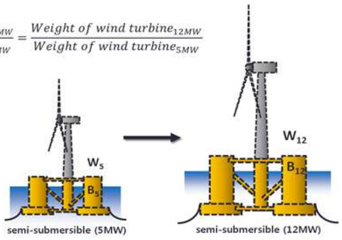

Tower Buckling Analysis

Critical load (P_{cr}) from Euler equation

- $P_{cr} = \frac{\pi^2 EI}{l_e^2} = \frac{\pi^2 EI}{(Kl)^2}$
- $\sigma_{cr} = \frac{P_{cr}}{A}$

Effective load (P_{eff}) of tower axial weight

- $P_{eff} = \frac{33}{140} * W_{Tower} + W_{Head}$
- Equivalent weight of tower
- W_{Head} : Lumped mass of Rotor & Nacelle

Analysis Results (ABAQUS)

σ_{cr} (N)	P_{cr} (N)	P_{eff} (N)	δ (m)
1.586.E+08	7.963.E+07	8.649.E+06	1.001

➢ $P_{cr} < P_{eff}$: the tower is stable

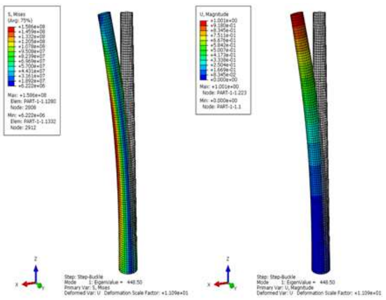

Tower Resonance Analysis

- A tower design is proposed to avoid the 3P resonance problem due to the direct expansion of the 5 MW wind turbine support.

Tower Redesign

- Frequency is inversely proportional to length → Reduced the tower length

	Tower length	Tower-base diameter	Tower-base thickness	Tower-top diameter	Tower-top thickness	Tower weight
Before	110.88 m	9.634 m	0.040 m	5.736 m	0.028 m	781,964 kg
After	104.23 m	9.634 m	0.040 m	5.736 m	0.028 m	735,066 kg

12 MW Tower Natural Frequencies (ABAQUS)

Mode	FAST (MBC3)	ABAQUS
1st Tower Fore-Aft	0.3195	0.3310
1st Tower Side-to-Side	0.3327	0.3310
2nd Tower Fore-Aft	2.7888	2.6997
2nd Tower Side-to-Side	2.8823	2.7103

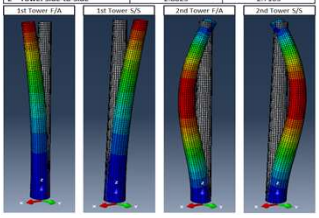

12MW Campbell diagram

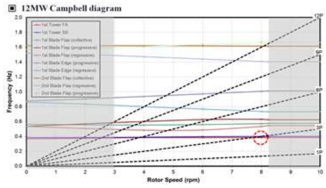

12MW Campbell diagram (Tower Redesign)

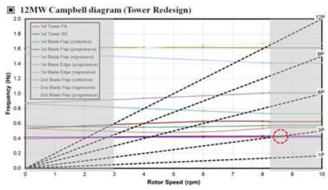

Control system of 12MW FOWT

- In the case of a FOWT, the negative damping problem occurs when applying conventional pitch control system of land-base wind turbine.
- The negative damping has the reducing rated power and increasing fatigue load.
- 12 MW FOWT was modified, the PI controller to avoid negative damping problem and the response speed of the blade pitch controller to be lower than the response speed of the platform.

Negative damping of Floating Offshore Wind Turbine (In Region-III)

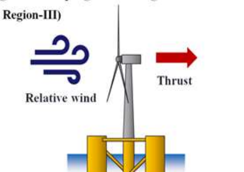

- Tilt out of wind
  - Relative wind speed decrease → Thrust increase
- Tilt into wind
  - Relative wind speed increase → Thrust decrease

Change the gains of PI controller, K_P and K_I

: Adjusting the response speed of the blade pitch controller to be lower than the response speed of the platform

- Natural Frequency of Platform pitch : 0.21 rad/s
- Natural Frequency of PI Contoller : 0.6 rad/s → 0.2 rad/s

Gain-scheduling law (Land based)

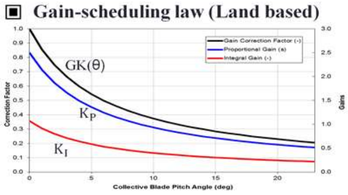

Gain-scheduling law (Offshore)

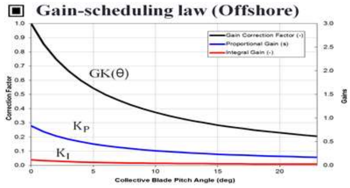

Numerical simulation

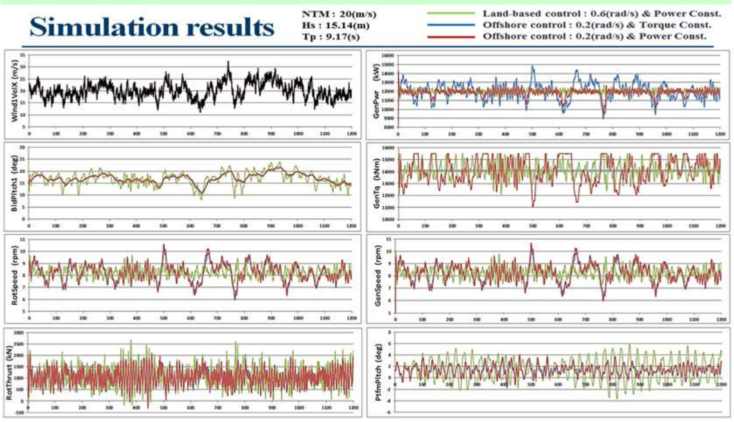

Conclusion

- Initial design of a 12 MW UOU FOWT using fully coupled analysis was performed to determine the suitability.
- Dimensions of tower was approved by buckling analysis.
- 3P Resonance avoided through the redesign of the tower.
- Negative damping was solved through the response speed control of the blade-pitch controller.

ACKNOWLEDGEMENT
This work was supported by the Korea Institute of Energy Technology Evaluation and Planning(KETEP) and the Ministry of Trade, Industry & Energy(MOTIE) of the Republic of Korea(No. 20154030200970 & 20163010024620).

울산대학교 UNIVERSITY OF ULSAN

E-mail
* Author : uou99@mail.ulsan.ac.kr
† Corresponding author : hkshin@ulsan.ac.kr

산업통상자원부 MINISTRY OF TRADE, INDUSTRY & ENERGY MOTIE

KETEP 한국에너지기술평가원 KOREA INSTITUTE OF ENERGY TECHNOLOGY EVALUATION AND PLANNING

NTNU
Norwegian University of Science and Technology

SiC MOSFETs for Offshore Wind Applications

S. Tiwari, T. M. Undeland, and O.-M. Midtgård

Norwegian University of Science and Technology, 7491, Trondheim, Norway

Summary- **This paper investigates the switching performance of half-bridge SiC MOSFET and Si IGBT modules. Both the modules have same packaging and voltage rating.**

Turn-on and turn-off switching energy losses are measured using a standard double pulse methodology. The conduction losses from the datasheet and the switching energy losses obtained from the laboratory measurements are used as a look up table input when simulating the detailed inverter losses in a three-phase grid-side inverter in an offshore wind application.

Simulated inverter loss is verified analytically. The total inverter loss is plotted for different switching frequencies in order to illustrate the performance improvement that SiC MOSFETs can bring over Si IGBTs for a grid-side inverter from the efficiency point of view.

The overall analysis gives an insight into how SiC MOSFET outperforms Si IGBT over all switching frequency ranges with the advantages becoming more pronounced at higher frequencies.

Introduction-

The superior material properties of silicon carbide (SiC) can be translated to switching devices with higher operating temperatures, higher breakdown voltages, lower conduction and switching losses, and higher power density, and thereby fulfil the demand of converters for offshore wind applications. In particular, these converters will be compact, efficient, and thermally stable, and thus can be easily mounted in the nacelle of wind turbine.

Material properties	Si	SiC	Results
Bandgap (eV)	1.1	3.2 (=2.9 × Si)	Higher operating temperature
Breakdown electric field (MV/cm)	0.25	3 (=12 × Si)	Higher blocking voltage and lower losses
Thermal conductivity (W/(cm.K)	1.5	4.9 (=3.2 × Si)	Increased power density

Laboratory setup and measurement results-

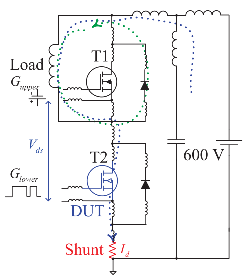

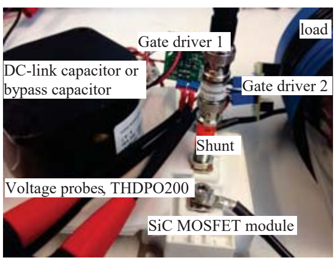

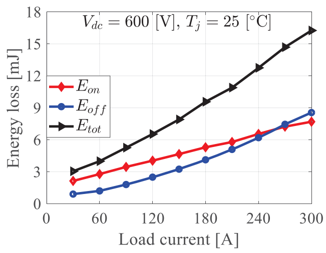

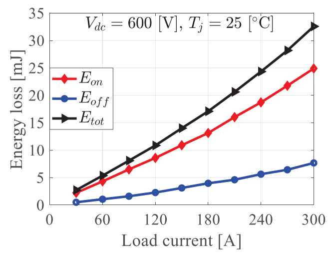

- **Key electrical parameters of SiC MOSFET versus Si IGBT module**

Parameters	CAS300M12BM2 (Wolfspeed)			SKM400GB125D (Semikron)		
	25 (°C)	125 (°C)	difference (%)	25 (°C)	125 (°C)	difference (%)
R_{ds}/R_{ce} (mΩ)	5	7.8	+ 36	6.3	7.6	+ 17
V_{CEO} (V)	Absent	Absent	Absent	1.4	1.7	+ 17
R_d (mΩ), diode	2.25	4.35	+ 48	2.7	3	+ 10
V_{F0} (V), diode	0.925	0.83	- 11	1.4	1.1	- 27

Simulation of inverter loss-

- Conduction loss from datasheet and switching loss obtained from the laboratory measurements are used as a look up table input for simulating detailed inverter loss.

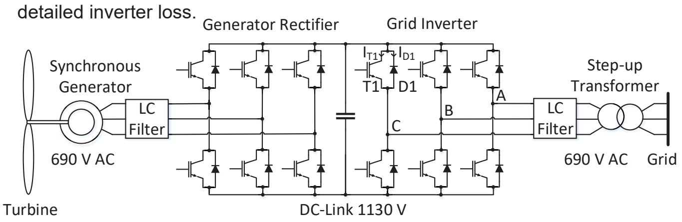

Simulation results-

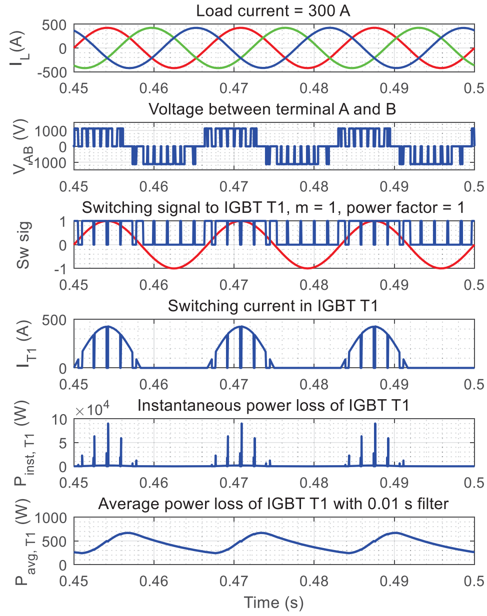

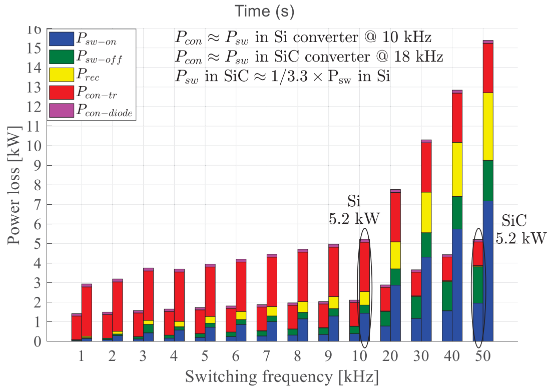

- $P_{rec}+P_{sw\text{-}on}$ is about 69 % of total inverter loss at 25 °C for inverter with Si IGBTs at 50 kHz. Thus, Si IGBT is not a viable solution at high switching frequency.
- For the same output power, the inverter switching frequency with SiC MOSFETs can be increased by 5 times and still have the same total power loss.

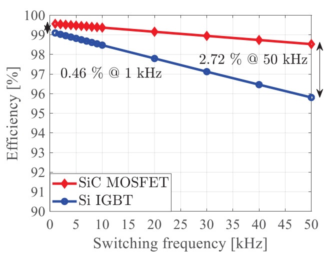

SINTEF
The Research Council of Norway
norwegian electric systems
ELTEK
Statkraft
VACON
SIEMENS
EFD INDUCTION

Analysis of wind shear in Sulafjorden

Midjiyawa Zakari[1], Konstantinos Christakos[1,3], Trond Kvamsdal[2], Birgitte R. Furevik[1]

[1] Norwegian Meteorological Institute

[2] Department of Mathematical Sciences, Norwegian University of Science and Technology

[3] Geophysical Institute, University of Bergen

Introduction

The E39 is a 1100 km highway route that connects Kristiansand to Trondheim (Figure 1). The E39 connects some of the largest Norwegian cities such as Kristiansand, Stavanger, Bergen, Ålesund, Molde and Trondheim.

The purpose of Ferjefri E39 project is to design a ferry-free highway route. Analysis of wind conditions and wind flow characteristics are essential for bridge design. The present study investigates monthly variability of the wind shear in Sulafjorden (Figure 1), which is one of the Norwegian fjord that E39 crosses. The analysis is based on one year of wind measurements, but the results are illustrated for one month chosen per season.

Figure 1. E39 highway route (Source: vegvesen.no)

Theory and Results

The wind profile power law equations is :

$$\frac{u}{u_r} = \left(\frac{z}{z_r}\right)^{\alpha}$$

where U and U_r are the wind speeds (m/s) at height z and z_r (m) respectively. The wind shear or power law exponent (α) is a dimensionless coefficient that describes the wind shear and is widely used for wind energy applications [2]. The α exponent is depending on atmospheric stability [3], [4]. For neutral conditions, α is approximately 0.14 onshore. For offshore conditions, it is suggested that α equals to 0.11 is a good approximation [5].

For this study, wind measurements at heights 44.5 m and 92.5 m (period: 01.2017-12.2017) from the met mast at Kvitneset (Figure 2) has been used. The met mast is located at the northwest fjord entrance. Southwest of the met mast, there are mountains with heights of 627 m and 570 m.

Figure 3 illustrates the wind shear exponent as a function of wind direction at 92.5 m for a reference height of 44.5 m for one month per season in 2017. The different color indicates the different wind speed levels.

Figure 4 shows the wind shear exponent as a function of wind speed at 92.5 m for a reference height of 44.5 m for one month per season in 2017. The black color indicates wind directions from 150 to 200 degrees and the blue color wind directions from 250 to 300 degrees.

Location of Measurements

Figure 2. Location of met mast (orange pointer) in Sulafjorden (Source: Kartverket)

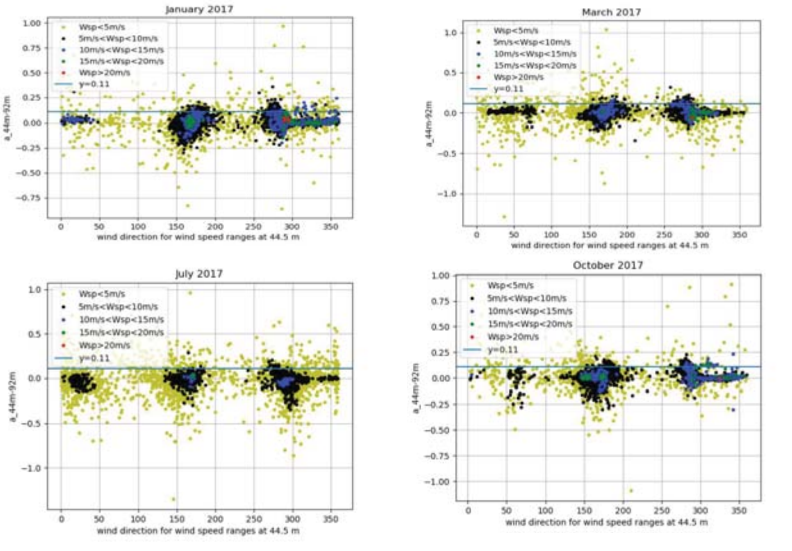

Figure 3. Wind shear exponent as function of wind direction for January 2017 (Top left), March 2017 (Top right), July 2017 (Bottom left) and October (Bottom right) in Sulafjorden

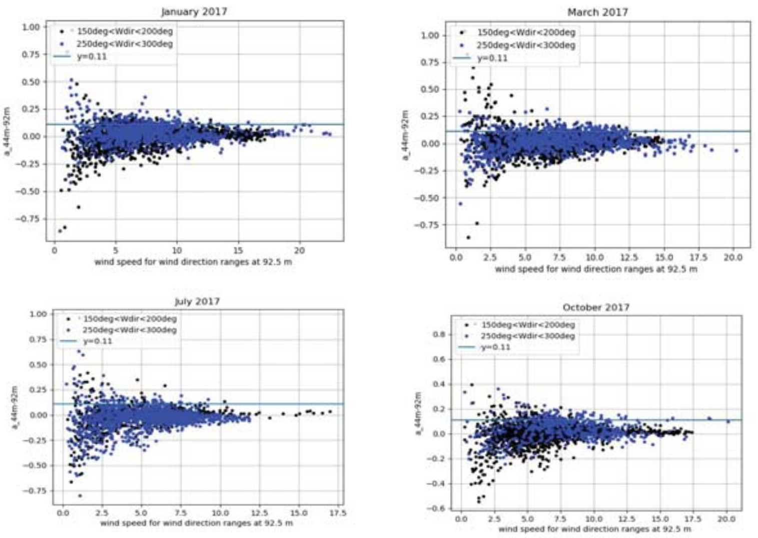

Figure 4. Wind shear exponent as function of wind speed for January 2017 (Top left), March 2017 (Top right), July 2017 (Bottom left) and October (Bottom right) in Sulafjorden for 150 to 200 and 250 to 300 degree in wind direction

Conclusions

The results for Sulafjorden show:

- The strongest winds were mainly observed from southeast and northwest.
- For moderate to high wind speed, the wind shear coefficient tends to decrease to values lower than 0.11 (suggested for offshore conditions).
- For low wind conditions, high absolute values of wind shear coefficient are observed.
- The month of June shows the highest value of wind shear coefficient. The maximum value is 2.51 while the minimum value 0.09 in November.
- The monthly rms value of wind shear fluctuates between 0.09 in November to 0.29 in June, which shows the limitation of using the value of 0.14 onshore and 0.11 ofshore for design purposes.

Acknowledgments

This study is a part of the Ferjefri E39 [1], subproject Fjord Crossing financed by the Norwegian Public Roads Administration (NPRA).

Statens vegvesen
Norwegian Public Roads Administration

References

1. https://www.vegvesen.no/Vegprosjekter/ferjefriE39
2. Christakos K. Characterization of the coastal marine atmospheric boundary layer (MABL) for wind energy applications, Master Thesis, University of Bergen, 2013, URI: http://hdl.handle.net/1956/7186.
3. J.S. Touma. Dependence of the wind profile power law on stability for various locations. Air Pollution Control Association, 27:863–866, 1977.
4. J. Counihan. Adiabatic atmospheric boundary layers: A review and analysis of data from the period 1880-1972. Atmospheric Environment, 79:871–905, 1975.
5. S.A. Hsu, E.A. Meindl, and D.B. Gilhousen. Determining the power-law wind profile exponent under near-neutral stability conditions at sea. Appl. Meteor., 79: 757–765, 1994.

Modelling of non-neutral wind profiles - current recommendations vs. coastal wind climate measurements

Piotr Domagalski[1], Maciej Karczewski[1], Lars Morten Bardal[2], Lars Roar Sætran[2]
[1]Iinstitute of Turbomachinery, Lodz University of Technology, Lodz, Poland
[2]Department of Energy and Process Engineering, Norwegian University of Science and Technology, Trondheim, Norway
E-mail: piotr.domagalski@p.lodz.pl
NTNU – Trondheim
Norwegian University of Science and Technology

Introduction

- Wind velocity at the hub height is a parameter of paramount importance for wind engineering.
- Wind velocity is very often extrapolated from other heights (measured or modeled) - an „old" question: what is the vertical wind profile?
- Logarithmic and power laws are valid only in neutral conditions.
- For non-neutral conditions – Monin Obukhov similarity theory (MOST) is a recommended practice [1,2].

Problem/Objective

- **How do MOST based vertical wind profile models perform?**
- **The test** – knowing the $v_{z=10m}$, humidity, pressure and temperature gradient extrapolate the velocity to $v_{z=100m}$ and compare it with measured velocity.
- **The place** – mid-Norway coast, the Frøya island.

Models tested

Stability corrected logarythmic model:

$$u(z) = \frac{u_*}{\kappa}\left(ln\frac{z}{z_0} - \Psi(\varsigma)\right)$$

$z/L \geq 0$: $\Psi(\varsigma) = -4.8(z/L)$

$z/L < 0$: $\begin{cases}\Psi(\varsigma) = 2\ln(1+x) + \ln(1+x^2) - 2arctan(x)\\ x = [1 - 19.3(z/L)]^{0.25}\end{cases}$

Panofsky&Dutton model:

$$\alpha(\bar{z}/L) = \frac{\Phi(\bar{z}/L)}{ln(\bar{z}/z_0) - \Psi(\bar{z}/L)}$$

$\bar{z}/L \approx 0$: $\Phi(\bar{z}/L) = 1; \Psi(\bar{z}/L) = 0$

$\bar{z}/L > 0$: $\Phi(\bar{z}/L) = 1 + 4.7(\bar{z}/L);\ \Psi(\bar{z}/L) = -4.7(\bar{z}/L)$

$\bar{z}/L < 0$: $\begin{cases}\Phi(\bar{z}/L) = [1 - 15(\bar{z}/L)]^{-0.25}\\ \Psi(\bar{z}/L) = -ln\left[\frac{(\zeta_0^2+1)(\zeta_0+1)^2}{(\zeta^2+1)(\zeta+1)^2}\right] - 2[arctan(\zeta) - arctan(\zeta_0)]\\ \zeta = [1 - 15(\bar{z}/L)]^{0.25};\quad \zeta_0 = [1 - 15(z_0/L)]^{0.25}\end{cases}$

Peña boundary layer height corrected model:

$$u(z) = \frac{u_*}{\kappa}\left[ln\left(\frac{z}{z_0}\right) - \Psi(\varsigma)\left(1 - \frac{z}{2z_{sl}}\right)\right] \quad z_{sl} = 0.1 \cdot 0.25\frac{u_*}{f_c} \quad u_* = \sqrt{\frac{\kappa^2}{\left(\ln\frac{z}{z_0}\right)^2}} \cdot u_{z=10m}$$

Smedman&Högström model:

$$\alpha = c_0 + c_1 log(z_0) + c_2[log(z_0)]^2$$

Stability class	c_0	c_1	c_2
Very Unstable/Unstable	0.18	0.13	0.03
Neutral	0.3	0.17	
Weakly Stable	0.52	0.2	
Stable	0.8	0.25	
Very Stable	1.03	0.31	

Site, equipment & data description

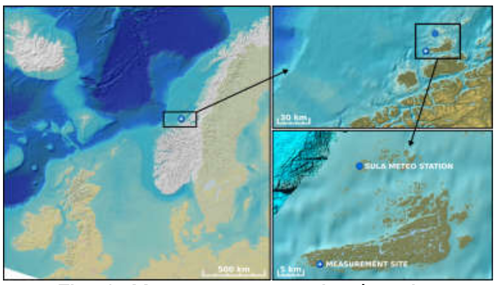

Fig. 1. Measurement station location

Fig. 2. Met mast

- 100 m high Met-mast.
- Velocity (Gill Wind Observer IID) & temperature measurements at: 10, 16, 25, 40, 70 and 100 m.
- Pressure & humidity from nearby Sula meteostation.
- Data acquisition time: Nov 2009-Dec 2012.
- Approx. 160000 of 10 min samples for each height.

Atmospheric stability

For atmospheric stability calculations we used the bulk Richardson number as a basis for Obukhov length calculation:

$$Ri = \frac{g}{\overline{\theta_v}}\frac{\Delta\overline{\theta_v}z_m}{(\Delta u)^2}ln\left(\frac{z_1}{z_2}\right) \qquad L = \begin{cases}\frac{z_m}{Ri}, & Ri < 0\\ \frac{z_m}{Ri}(1 - 5Ri) & 0 \leq Ri \leq 0\end{cases}$$

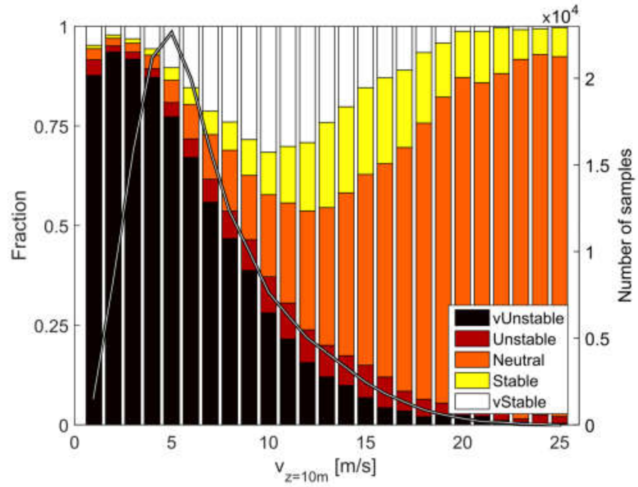

Fig. 3. Atmospheric stability distribution.

Results

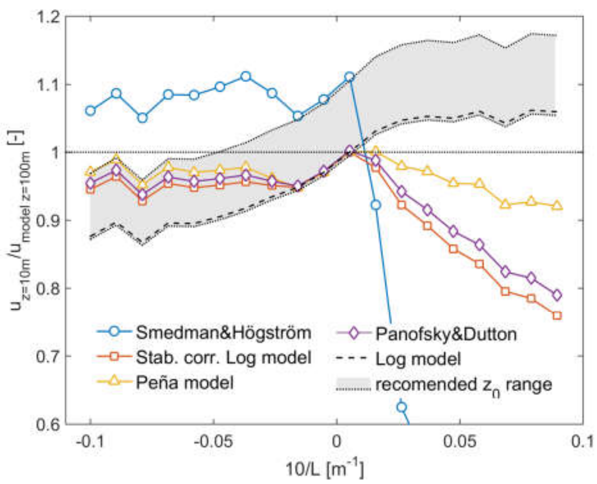

Fig. 4. Wind speed ratio between the measured and predicted wind velocity at z_2=100m against atmospheric stability.

Conclusions

- 5 % underestimation of predicted wind velocity is observed during unstable conditions.
- The deviation grows dramatically up to 20 % (!) in stable atmosphere.
- Given the frequency/number of non-neutral observations that can result in serious error in wind prediction and finally in wind resources estimation.
- Although the problem of is not new, a lot of space for improvement is visible and desired.

References

[1] DNV, G. (2014). DNV-RP-C205: Environmental conditions and environmental loads. DNV GL, Oslo, Norway.
[2] Fisher, et al., (1998). COST-710–final report: harmonisation of the pre-processing of meteorological data for atmospheric dispersion models.

Uncertainty estimations for offshore wind resource assessment and power verification

KAΠE CRES
CENTRE FOR RENEWABLE ENERGY SOURCES AND SAVING
FloatMast Ltd.

D. Foussekis, F. Mouzakis, A. Peppas, T. Papatheodorou
C.R.E.S., 19th km Marathon Avenue, GR-190 09, Pikermi, Greece dfousek@cres.gr - mouzakis@cres.gr
FLOATMAST Ltd, 156A Burnt Oak Broadway, Edgware, Middlesex, HA8 0AX, UK peppas@floatmast.com - papatheodorou@floatmast.com

Scope

- Compare various offshore measurement configurations based on the relevant introduced uncertainty.
- Calculate all the uncertainty components defined in IEC 61400-12-1:2017 for real case scenarios.

Methodology

- Define virtual Power Curve verification cases, based on a NREL 5MW offshore wind turbine, combining its power curve with synthetic data from real onshore campaigns. For each uncertainty component, apply the default recommended values in [1] (or typical ones from similar onshore test campaigns). Statistical uncertainties and the power measurement uncertainties are all assumed common for all five cases
- Introduce 2 additional uncertainties due to : i) data availability issues and ii) structure motion. Based on published data [3],[4],[5],[6] assume wind speed uncertainty of 1.0% for a campaign with 80% data availability, 1.4% for a floating moving structure and 0.7% for a significantly more stable floating TLP platform.

Case	Method	Comments
A	Fixed permanent <u>full rotor height</u> meteorological mast (ie: 150m)	+ High accuracy & TI measurements (cup/sonic) + High data availability + Rotor equivalent wind speed - Very high installation cost - Significant flow disturbance
B	Fixed permanent <u>hub height</u> meteorological mast (ie: 90m) with RSD	+ High accuracy & TI measurements (cup/sonic) + High data availability + Rotor equivalent wind speed + RSD continuously verified against cups - High installation cost - Flow disturbance
C	Fixed permanent <u>below hub height</u> meteorological mast (ie: 40m) with RSD	+ High accuracy & TI measurements (cup/sonic) + High data availability + Rotor equivalent wind speed + RSD continuously verified against cups - High installation cost
D	RSD on floating vessel (i.e. floating LIDAR)	+ Low installation cost + Rotor equivalent wind speed + No flow disturbance - Lower data availability - Motion affected TI measurements - Strong effects from structure movements
E	Temporary TLP meteorological mast (ie: 40m) with RSD (i.e.: FloatMast)	+ Good accuracy & TI measurements (cup/sonic) + High data availability + Rotor equivalent wind speed + RSD continuously verified against cups + Low installation cost - Limited effects from structure movements

Only A, B and C are explicitly defined in [1]

Table 1: The 5 examined configurations

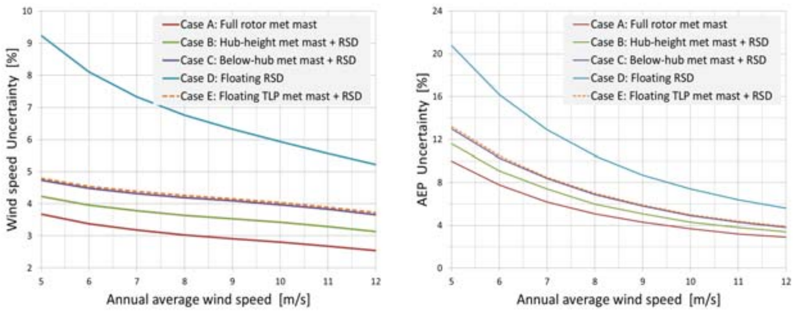

Wind speed (left) and AEP (right) resulting uncertainties

FloatMast TLP Platform tugging at Test Site

Conclusions

When strict compliance to IEC 61400-12-1:20017 is unachievable (deep waters, floating wind farms) or requires high financial costs, the proposed methodology introduces two offshore configurations and compares the resulting uncertainties.

References

1. IEC 61400-12-1:2017 *Wind energy generation systems - Part 12-1: Power performance measurements of electricity producing wind turbines*
2. J. Jonkman et al: *Definition of a 5-MW Reference Wind Turbine for Offshore System Development*, Technical Report NREL/TP-500-38060, February 2009.
3. J.O. Hellevang, J. Reuder: *Effect of wave motion on wind lidar measurements - Comparison testing with controlled motion applied"*, CMR publication, *DeepWind 2013 Conference, Norway*
4. Tony Rogers, Katy Briggs, Gordon Randall, Holly Hughes*: Remote Sensing on Moving Offshore Platforms, DNV publication, EWEA 2011*
5. *Assessment of the Verification for Fugro SEAWATCH floating lidar at Ijmuiden,* Technical Note No.: GLGH-4257 13 10378-R-0003, Rev. B
6. Daniel W. Jaynes: *Investigating the Efficacy of Floating LIDAR Motion Compensation Algorithms for Offshore Wind Resource Assessment Applications", GL-GH publication, EWEA 2011.*

Using a Langevin model for the simulation of environmental conditions in an offshore wind farm

Helene Seyr and Michael Muskulus

Department of Civil and Environmental Engineering, Norwegian University of Science and Technology, NTNU, 7491 Trondheim, Norway

Introduction

- The **optimization** of operations and maintenance (**O&M**) is a focus of current research.
- Many simulation models/optimizations rely on **artificially generated weather** time series to test different strategies.
- We present a **novel approach** to modeling both the significant wave height and wind speed based on measurements from the site.
- We use a stochastic process called **Langevin process**. First, equations are fitted to the available data, which are then used to generate the artificial weather.

Data

- ECMWF: re-analysis, 6 hour resolution, Dogger Bank WF, 37 years
- Fino 1: measurements, 30min/10min means, Alpha Ventus, 6 years

Langevin Process

- Deterministic contribution
$$F = D^{(1)}$$
- Stochastic contribution
$$G = \sqrt{D^{(2)}}\Gamma_t$$
- The stochastic contribution makes it easy to include uncertainty.

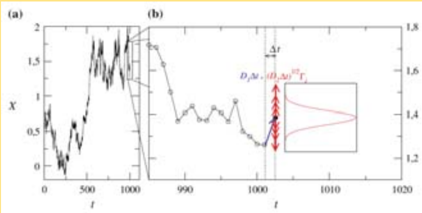

Fig: Example of a Langevin process, from Reinke et al.

Fig: This example shows the drift and diffusion function for the simulation of the wave heights for a selected winter month used in the Fino 1 simulation.

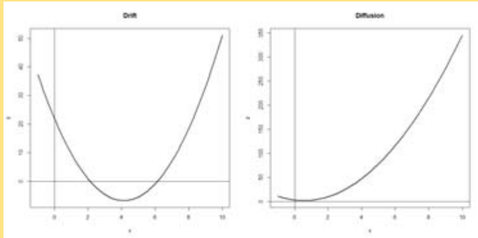

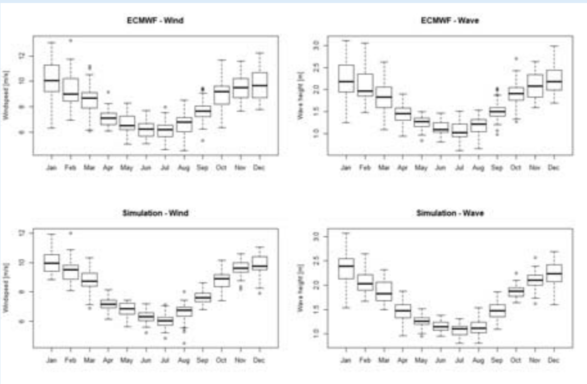

Fig: The monthly means of significant wave height and wind speed, both for the original data and the simulation based on it. The model was fitted to the re-analysis data from the ECMWF.

Fig: The distribution of wave heights and wind speeds over 6 years. Shown is the data, simulation and simulation without the seasonal effect.

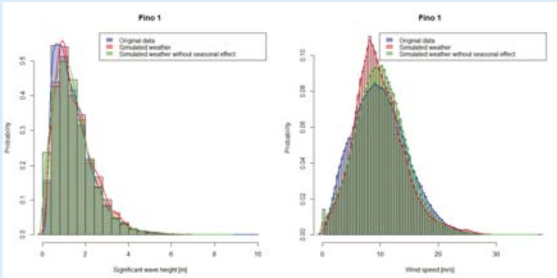

Wave height	Mean	SD
Data	1.44	0.93
Simulation	1.51	0.92
Simulation without seasonal effect	1.44	0.93

Wind speed	Mean	SD
Data	9.99	4.66
Simulation	9.83	4.38
Simulation without seasonal effect	10.03	4.34

Table: Statistics of the Fino 1 data and the simulations that are based on the data. For the simulation without seasonal effect, one system of equations was fitted for the whole year. In the seasonal simulation, each month was estimated separately.

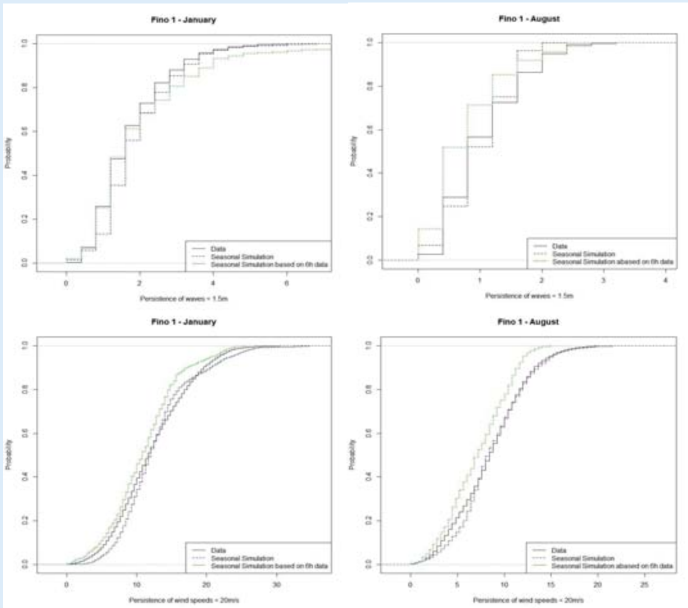

Fig: Persistence of wave heights under 1.5m and wind speeds under 20m/s for two different month for the Fino simulation.

Fig: The distribution of wave heights during a winter month and a summer month. Shown is the data and simulation based on the re-analysis data.

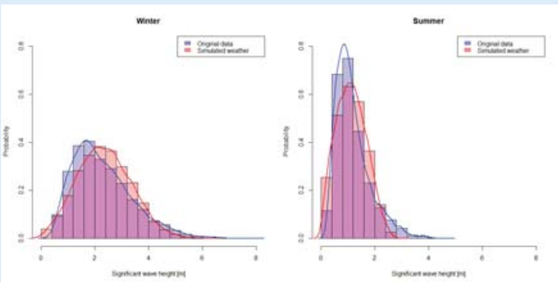

Conclusions and Future work

- The analysis shows that the Langevin process is an adequate alternative to other weather simulation models.
- The properties of the waves (distribution and persistence) are represented very well.
- Higher sampling frequency in the data improves the model.
- Multidimensional Langevin process might capture the correlation between wave heights and wind speeds is another topic for further research.

Selected References

- Czechowski Z and Telesca L. (2013) *Physica A: Statistical Mechanics and its Applications* 392
- Friedrich R, Peinke J, Sahimi M and Tabar M R R. (2011) *Physics Reports* 506
- Reinke N, Fuchs A, Medjroubi W, Lind P G, Wächter M and Peinke J. (2015) *The Langevin Approach: A Simple Stochastic Method for Complex Phenomena*
- Rinn P, P L, M W and J P. (2016) *Journal of Open Research Software* 4
- Seyr H and Muskulus M. (2016) *Journal of Physics: Conference Series* 753

Helene Seyr
Department of Civil and Environmental Engineering
helene.seyr@ntnu.no
+47 40086761

NTNU
Norwegian University of Science and Technology

AWESOME
PHD'S IN WIND POWER O&M

This project has received funding from the European Union's Horizon 2020 research and innovation programme under the Marie Skłodowska-Curie grant agreement No 642108.
Data from Fino 1 was provided by BMWi and PTJ.

Optimization of monopiles with genetic algorithms

Lisa Ziegler[1,2], Matthieu Rhomberg[1,2,3], Michael Muskulus[2]

[1] Ramboll, Hamburg, Germany
[2] Norwegian University of Science and Technology, Trondheim, Norway
[3] Delft University of Technology, Delft, Netherlands

Importance sampling to reduce number of load cases

- ✓ 120 load cases instead of 1700 (93% reduction)
- ✓ Target lifetime of optimization met with only 1-7% difference
- ✓ Fast and accurate method for use in computer-aided optimization

Reduction of load cases with importance sampling

- A cumulative distribution function (CDF) is set up for fatigue damages caused by every load case
- 120 load cases are sampled from the CDF
- Aero-hydro-elastic simulations are performed for these load cases with ROSAP and LACflex
- Fatigue damages are estimated with importance sampling and a correction factor f_k

$$D_{est} = \frac{1}{n}\sum_{i=1}^{n} \frac{D_i^{LC}}{g_i}$$

$$D_{corr} = f_k \cdot D_{est}$$

$$f_k = \mu_k + n \cdot \sigma_k$$

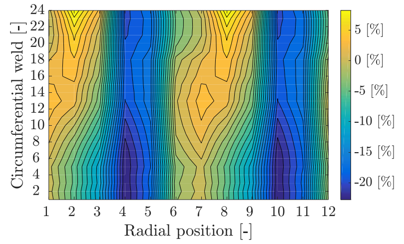

Genetic algorithm

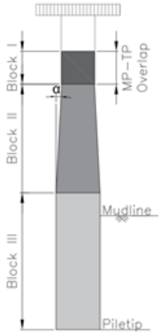

- Minimize monopile mass
- 5 design variables
- Constraints: fatigue damage, weldability, resonance, buckling
- Aero-hydro-elastic load simulations in the time domain with 120 load cases and importance sampling
- Optimization for different design lifetimes: 25, 50, 75, 100 years (DFF=1)

Case study
8 MW turbine
DLC 1.2 + 6.4
1700 load cases

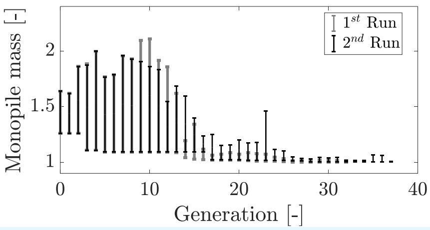

How does steel mass increase if **monopiles** are designed for a **longer lifetime**?

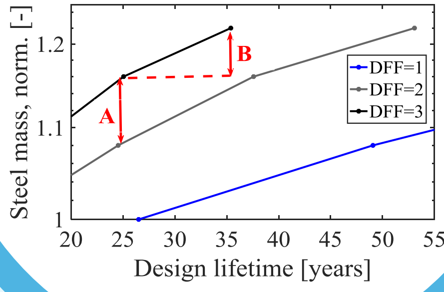

Motivation

Knowledge about the scaling of steel mass of monopiles is needed to decide for which service life an offshore wind farm should be planned. It is impossible to perform computer-aided optimization with aero-hydro-elastic simulations of several thousand of load cases.

Research objective

Develop a smart method to reduce the number of require load simulations during the design optimization while keeping the complexity of load and structural analysis at industrial standard.

Contact
lisa.ziegler@ramboll.com
+49 15144006445

Acknowledgements: Results of this work have been obtained by Matthieu Rhomberg during his master thesis in cooperation with Ramboll, NTNU and TU Delft. Input from several experts from Ramboll is greatly acknowledged. This project has received funding from the European Union's Horizon 2020 research and innovation programme under the Marie Sklodowska-Curie grant agreement No 642108.

Cone penetration data classification by Bayesian inversion with a Hidden Markov model

Ask S. Krogstad[1], **Ivan Depina**[2], **Henning Omre**[1]

[1]Department of Mathematical Sciences, Norwegian University of Science and Technology, Trondheim, Norway
[2]Department of Rock and Geotechnical Engineering, SINTEF Building and Infrastructure, Trondheim, Norway

Introduction

The Cone Penetration Test (CPT) is an in-situ test that is frequently applied to estimate subsurface stratigraphy, soil parameters, and parameters for a direct geotechnical design [4]. Soil classification from CPT data is commonly based on classification charts with predefined soil classes [6] and [7]. These are often considered no more than as indicative. We investigate the application of the Hidden Markov Model (HMM) to the CPT classification problem.

Model

Notation
Consider a CPT profile with measurements along the grid $\mathcal{L}_{\mathcal{Z}} = \{1, ..., Z\}$ with z increasing with depth. A vector of CPT measurements is denoted $\mathbf{d} : \{\mathbf{d}_z; z = 1, ..., Z\}$. The actual soil class profile at the location is denoted $\boldsymbol{\kappa} : \{\kappa_z; z = 1, ..., Z\}$, where κ_z belongs to a set of different soil classes, $\kappa_z \in \Omega_\kappa : \{1, ..., K\}$. Note that soil classes can be arbitrarily defined to describe different geological features.

Model definition
We want to calculate the probability of any profile of soil classes given the CPT measurements, $p(\boldsymbol{\kappa}|\boldsymbol{d})$. In the Bayesian setting, this probability is denoted as posterior because it incorporates the measurements with the additional or prior knowledge. The posterior probability is defined according to the Bayes law as follows $p(\boldsymbol{\kappa}|\boldsymbol{d}) = \frac{p(\boldsymbol{d}|\boldsymbol{\kappa})p(\boldsymbol{\kappa})}{p(\boldsymbol{d})}$, where $p(\boldsymbol{\kappa})$ is the prior model, $p(\boldsymbol{d}|\boldsymbol{\kappa})$, is the likelihood model, and $p(\boldsymbol{d})$ is an normalizing constant. With these two distributions the full posterior is fully defined. The evaluation of the normalizing constant, $p(\boldsymbol{d})$, is usually unfeasible and most often avoided.

Likelihood model
The likelihood model, $p(\boldsymbol{d}|\boldsymbol{\kappa})$, provides a statistical model that relates CPT measurements to soil classes. The likelihood model is based on two assumptions, conditional independence between the CPT data vector at each step, $\boldsymbol{d}_z$, given $\boldsymbol{\kappa}$ and single site dependence between $\boldsymbol{d}_z$ and κ_z. These two assumptions lead to the following relation:

$$p(\boldsymbol{d}|\boldsymbol{\kappa}) = \prod_{z=1}^{Z} p(\boldsymbol{d}_z|\boldsymbol{\kappa}) = \prod_{z=1}^{Z} p(\boldsymbol{d}_z|\kappa_z). \tag{1}$$

A Gaussian bivariate likelihood model is selected to model the aforementioned relations. The Gaussian bivariate model requires the assessment of mean parameters and covariance matrices for all classes. These parameters can be estimated by the using the CPT data, $\mathbf{d}$ and the actual soil class profile $\boldsymbol{\kappa}$ vector available from calibration boreholes.

Prior model
As the prior for $\boldsymbol{\kappa}$ a first order Markov chain is selected. Denote the probability of transitioning from any soil class κ_{z-1} to any soil class κ_z as $p(\kappa_z|\kappa_{z-1})$. The $(K \times K)$ matrix $\boldsymbol{P}$, with K being the number of separate soil classes, outline the probability for all possible transitions. The Markov chain prior is assumed to homogenous. The prior probability of any soil class vector, $\boldsymbol{\kappa}$, is given by the following expression

$$p(\boldsymbol{\kappa}) = p(\kappa_1) \prod_{z=2}^{Z} p(\kappa_z|\kappa_{z-1}), \tag{2}$$

An estimator $\hat{P}$ of the transition matrix P is estimated from observed transformations in known soil profiles. This estimator can be estimated in a strict way, only allowing transitions that are observed, or in a lenient way, allowing transitions from any formation to any deeper laying formation

Posterior model
Our choices for likelihood and prior models result in a posterior model that is a Hidden Markov Model (HMM) [5]. In an HMM, the states or the soil classes of the Markov chain are hidden, but at each step the hidden soil class has a corresponding observation. The structure of the dependencies in the HMM is visualized in Figure 1.

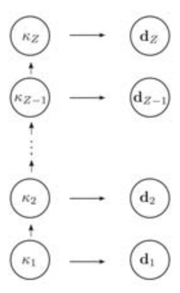

Figure 1: Illustration of the posterior model

We derive the following expression for the posterior model on a first order Markov chain form.

$$p(\boldsymbol{\kappa}|\boldsymbol{d}) = p(\kappa_1|\boldsymbol{d}) \prod_{z=2}^{Z} p(\kappa_z|\kappa_{z-1}, \boldsymbol{d}). \tag{3}$$

Note that this posterior Markov chain does not have a stationary transition matrix. Note also that the Gaussian bivariate distributions, defining the likelihood model, are not updated.

Posterior model inference
The recursive Forward-Backward algorithm e.g. [1] is used to calculate the posterior distribution $p(\boldsymbol{\kappa}|\boldsymbol{d})$ without explicitly calculating the constant $p(\mathbf{d})$. The Forward-Backward algorithm calculates $p(\kappa_z|\kappa_{z-1}, \boldsymbol{d})$ for all combinations of κ_z and κ_{z-1}, and for all values of z thereby fully defining the posterior model $p(\boldsymbol{\kappa}|\boldsymbol{d})$. From this we can find estimators such as the maximum a posteriori prediction, (MAP), and the marginal maximum a posteriori prediction (MMAP). As well as simulate soil class profiles.

To compute the MAP predictor the implementation of the Viterbi algorithm, e.g. [2] is needed. This recursive algorithm exploits the Markov property of the posterior model to find the most probable soil class vector. The predictions are compared to the true profiles or if these are not available some other reliable independent prediction. Also a a simple Naive Bayesian (NB) predictor is used as base for comparisons. This NB predictor suits this purpose as it does not take spatial correlation into account.

Case study

Geological information
The implemented model is applied to the classification of CPT profiles at the Sheringham Shoal Offshore Wind Farm (SSOWF). The geology at the location is described by six formations e.g., [3], these are in order of increasing depth, Holocene sand (HS), the Botney Cut formation (BCT), the Bolders Bank formation (BDK), the Egmond Ground formation (EG), the Swarte Bank formation (SBK) and the Cretaceous chalk (CK) layers beneath.

Extensive soil investigations was conducted at the SSOWF site, a series of CPT soundings and boreholes in the proximity of some of these sites. We will use one CPT profile and one of the bore hole profiles. Given that the borehole is very close to the CPT profile, it assumed that the borehole soil stratigraphy can be used as the actual soil class profile.This information is necessary both to estimate the prior and the likelihood distributions.

Results

The profiles are coloured with red colours corresponding to clay domintated formations and blue corresponding to sand dominated formations. Deeper colours represent deeper formations. As no measurements are taken when chalk is hit the last formation, CK, is not present in the profiles.

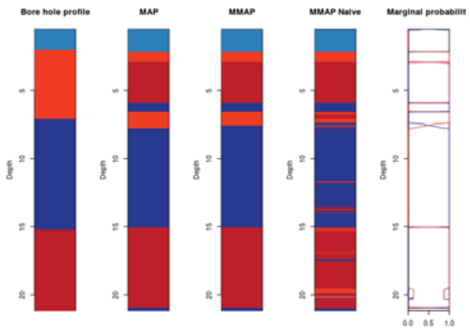

Figure 2: Training CPT profile, non-strict transition matrix: actual soil class profile, model predictions (MAP, MMAP and NB) and marginal probabilities.

The first set of profiles are calculated with a lenient prior matrix while the second set of results are calculated with a strict prior matrix. It is clear that a stricter prior makes sure the ordering stays closer to the observed profiles. With the less strict prior matrix the model tends to mistake formations that are dominated by the same soil characteristics for each other.

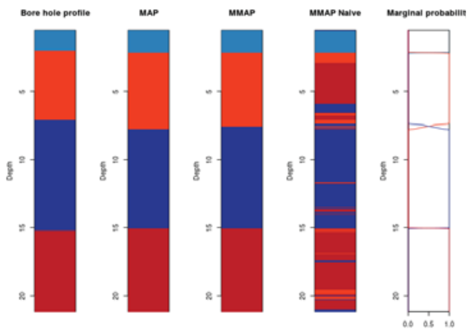

Figure 3: Training CPT profile, strict transition matrix: actual soil class profile, model predictions (MAP, MMAP and NB) and marginal probabilities.

Conclusions

This study examined the application of the Hidden Markov Model to the soil classification based on CPT measurements. The model is composed of a Markov chain that models spatial ordering of soil classes along a CPT profile and a Gaussian likelihood model that links CPT measurements with different soil classes. The Bayesian formulation of the model is considered as advantageous for the considered problem as it allows the model to integrate additional sources of information, commonly available in a CPT-based soil classification. Additional advantages, when compared to the CPT classification based on classification charts, include arbitrary definitions of soil classes supported by the Gaussian likelihood model. The probabilistic framework of the model allows it to account from some of the uncertainties in the classification process. The Bayesian setting of the model provides a framework for a more consistent treatment of additional sources of information in the CPT-based soil classification.
The model achieved good performance when applied to the classification of CPT profiles from the Sheringham Shoal Offshore Wind Farm. However, additional and more extensive tests are necessary to further validate the model performance. Further extensions of the model are planned to adapt the soil class definitions to data clusters instead of geological formations and to consider Bayesian updating of the relations between soil classes and CPT measurements.

References

[1] L. E. Baum, T. Petrie, G. Soules, and N. Weiss. A maximization technique occuring in the statistical analysis of probabilistic functions of Markov chains. *Annals of Mathematical Statistics*, 1970.

[2] G. D. Forney. The Viterbi algorithm. *Proceedings of IEEE*, 1973.

[3] Thi Minh Hue Le, Gudmund Reidar Eiksund, Pål Johannes Strøm, and Morten Saue. Geological and geotechnical characterisation for offshore wind turbine foundations: A case study of the sheringham shoal wind farm. *Engineering Geology*, 2014.

[4] T Lunne, PK Robertson, and JJM Powell. Cone penetration testing. *Geotechnical Practice*, 1997.

[5] I.L. MacDonald and W. Zucchini. *Hidden Markov and Other Models for Discrete- valued Time Series.* Chapman & Hall/CRC Monographs on Statistics & Applied Probability. Taylor & Francis, 1997.

[6] PK Robertson. Soil classification using the cone penetration test. *Canadian Geotechnical Journal*, 1990.

[7] Kaare Senneset and N Janbu. Shear strength parameters obtained from static cone penetration tests. In *Strength Testing of Marine Sediments: Laboratory and In-situ Measurements*. ASTM International, 1985.

Effect of hydrodynamic load modelling on the response of floating wind turbines and its mooring system in small water depths

Kun Xu[1] Zhen Gao[1,2] Torgeir Moan[1,2]

1 Department of marine technology, NTNU, Trondheim, Norway

2 Centre for Antonomous Marine Operations and Systems (AMOS), NTNU, Trondheim, Norway

Abstract

The focus of this paper is on the environmental loads and responses of mooring systems for a semi-submersible at water depth of **50 m, 100 m and 200 m**. Preliminary design has been carried out to determine mooring line properties, mooring system configurations and document the static performances. A fully coupled time domain dynamic analysis for extreme environmental conditions was performed using Simo-Riflex-AeroDyn. Four different load models were applied in order to check the influence of different load components including the effect of wind, current and second order wave forces by means of Newman's approximation and a full QTF method.

Challenges

- Mooring design for moderate water depths is relatively easy to achieve, but it is challenging for **shallow water**. Mooring line tension increases in a **nonlinear** manner when the offset is large and it is more significant in shallow water.
- The highly **non-Gaussian** responses in shallow water indicates possible extreme mooring line tension and floater motion especially.

Methodology

Newman's approximation is good if the frequency difference is small, which is normally the case for horizontal motions for floating structure especially in deep water. Newman's approximation becomes uncertain when it comes to shallow water. In this paper, Newman's approximation will be considered in horizontal motions while full QTF method will include contributions from all six degrees of freedom.

Load models

1, 2, 3: Newman's approximation vs full QTF

3, 4: Influence from wind force

	Wave		Wind	Current
	first-order	second-order		
1	Yes	No	No	Yes
2	Yes	Newman	No	Yes
3	Yes	Full QTF	No	Yes
4	Yes	Full QTF	Yes	Yes

Load cases

The wind and wave conditions correspond to 50-year return period and current condition refers to 10-year return period.

	ULS-1	ULS-2
U_w (m/s)	41.86	38.37
H_s (m)	13.4	15.6
T_p (s)	13.1	14.5
U_c (m/s)	1.05	1.05

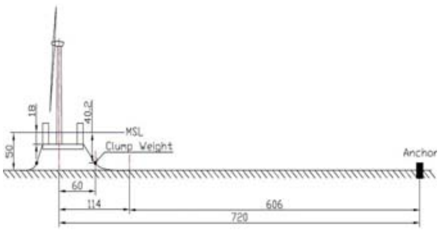

Mooring system in 50 m

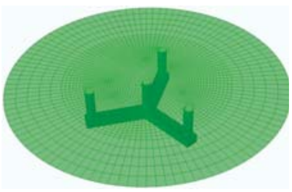

HydroD model

Fully coupled dynamic analysis

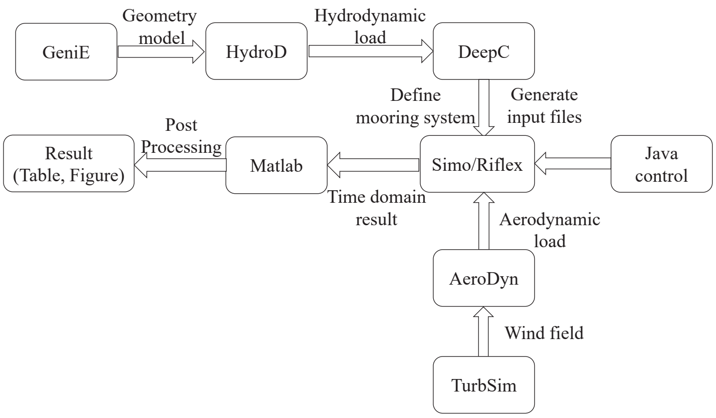

Flowchart of the analysis process and software used.

Results and discussions

Mooring line tension increases nearly **linearly** when the offset is small, then it increases in a **nonlinear** manner for all three water depths. The phenomenon becomes more significant when water depth decreases.

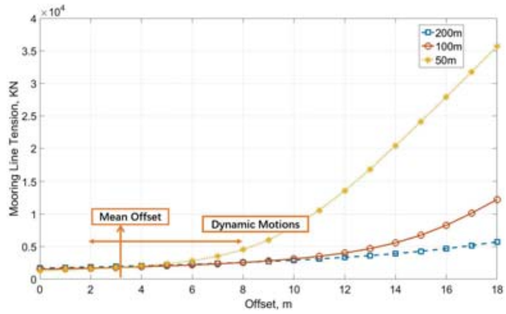

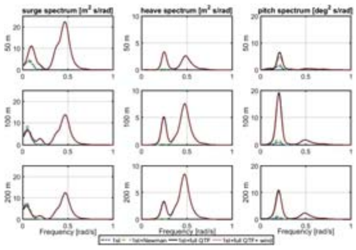

Floater motion spectrum in ULS-1 condition

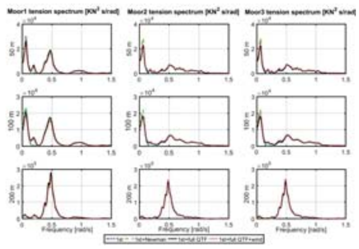

Mooring line tension spectrum in ULS-1 condition

Non-Gaussian response

$$M = \mu + k * \sigma$$

M: Maximum response

μ: mean response

k: coefficient

σ: standard deviation

	ULS-1-0			ULS-2-60		
	Mooring line 1		Surge	Mooring line 3		Surge
	k	*Kurtosis*	*Kurtosis*	*k*	*Kurtosis*	*Kurtosis*
50 m	4.3	3.4	3.5	**14.7**	**49**	**3.7**
100 m	4.4	3.5	3.2	**10.8**	**19**	**3.2**
200 m	5.7	5.4	3.1	**6.0**	**6.1**	**2.9**

- Non-Gaussian nature of mooring line tension is influenced by the nonlinearity of the mooring system.
- Wave parameters e.g. significant wave height and wave peak period also affect the Gaussian nature of the response.
- Kurtosis are close to 3 for all cases in surge motion – Gaussian process.
- Least loaded mooring line tension almost follows Gaussian process in less severe environmental condition.
- Kurtosis and k value increase with decreasing water depths and more extreme sea states – highly non-Gaussian process.

Conclusions

- During mooring system design phase, two factors that can influence mooring line tension significantly were mainly considered: geometrical effect and increased stiffness for large offset.
- As water depth decreases, the contribution from difference frequency part becomes increasingly more significant . Therefore in order to capture the low-frequency response accurately, a full QTF method is recommended while Newman's approximation will underestimate the response.
- The highly non-Gaussian responses in high sea states indicates possible extreme mooring line tension and floater motion, which makes it quite challenging to design mooring system for extreme environmental conditions especially in shallow water.

Acknowledgement

The first author is financially supported by Chinese Scholarship Council (CSC).

Reference

1. Gao Z. and Moan T. "Fatigue damage induced by non-Gaussian bimodal wave loading in mooring lines", Applied Ocean Research, vol 29, p45-54, 2007
2. Gao Z. and Moan T. "Accuracy of narrow band approximation of stationary wide band Gaussian processes for extreme value and fatigue analysis", in Proceedings of the 10th international conference on structural safety and reliability, Japan, 2009

Universität Rostock

Traditio et Innovatio

LWET STIFTUNGSLEHRSTUHL WINDENERGIETECHNIK

GICON®

Supply chains for floating offshore wind substructures – a TLP example

Frank Adam[1], Daniel Walia, Hauke Hartmann, Uwe Ritschel, Jochen Großmann

[1]Endowed Chair of Wind Energy Technology, MSF, Albert-Einstein-Str. 2, 18051 Rostock

FLOATING OFFSHORE WIND

On November 4th 2016 the Paris Agreement on Climate Change came into force. To achieve the goals of this agreement CO_2 emission-free energy production is a key element. Offshore wind power will be a major player in this field. Hereby floating offshore wind solutions can provide an economically viable as well as ecologically friendly power source in water depths of 50m and deeper. From 2011 onwards, the University of Rostock has been involved in a floating offshore wind research project together with the company GICON. The GICON-TLP, a TLP substructure fabricated out of pre-stressed concrete elements, has been developed and tested over several years to reach a development stage as an economic and ecological solution. Tests of the final design in operation conditions have been done successfully at the ECN in Nantes within the course of MaRINET2.
Another characteristic of this TLP is the high level of modularity to maximize the flexibility within the supply chain and with suppliers.

SUPPLY CHAIN OPTIMIZATION

- High modularity of the substructure → The TLP consists only of five main components:
  → Bottom and top nodes, transition piece, buoyancy bodies and pipes

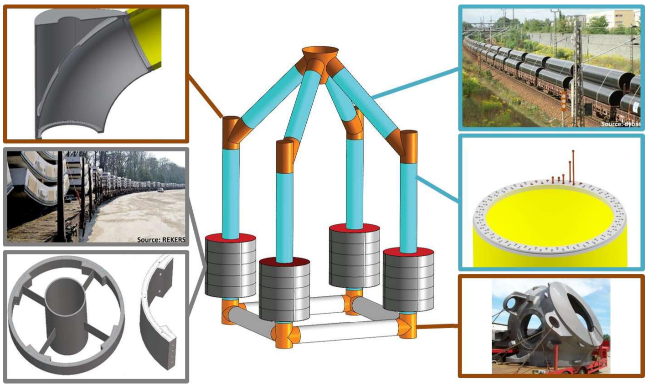

All components can be produced at multiple locations and thus by different suppliers. This leads to cost saving potentials based on the possibility to have a choice of suppliers. Additionally the production capacities of multiple suppliers can be used simultaneously. Since smaller and lighter components will be transporter during most of the transport process, logistical boundary conditions can be considered.

POSSIBLE SUPPLY CHAINS IN EUROPE

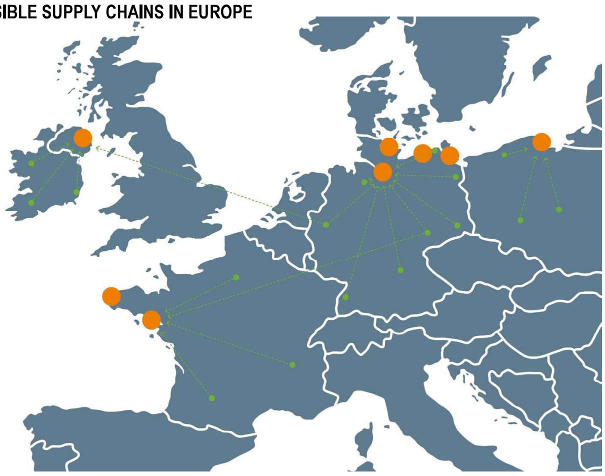

OPTIMIZATION THROUGH DEVELOPMENT

2nd Generation GICON-TLP

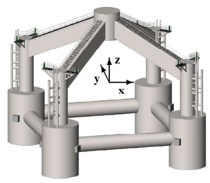

3rd Generation GICON-TLP

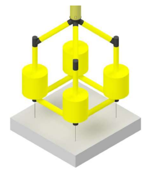

Throughout the development process, some changes have been made with regard to the optimization of the supply chain and manufacturability of the GICON-TLP. To reduce the costs of the structure, the material has been changed from steel to steel reinforced ultra-high performance concrete. Additionally the level of modularity of the structure has been increased by replacing the diagonal beams by pipes of the same type as used for the vertical and horizontal connections. This leads to lower costs for the yard as well as a reduced fabrication and installation time.

	SOF2 -2.3MW	SOF3 -6.0MW – Steel	SOF3 -6.0MW – concrete
Dimensions [m]	28x33x33	51x45x45	51x45x45
Mass [t]	800	1,800	3,400
Single heaviest component	Buoyancy Body 130t	Buoyancy Body 310t	Vertical Pipe 80t
Material	Steel	Steel	Steel-concrete
Material cost TLP [€/t]	2,500	2,500	450
Assembling time	4 months	Min. 4 month	4 weeks
Largest single component	10 m long 9 m diameter	14m long 14m diameter	28 m 3 m diameter

FINAL ASSEMBLY

- The final assembly can be done at a port close to the wind farm.
- All components will be delivered to the assembly side and assembled in four weeks.

Assembling of GICON-TLP Substructure

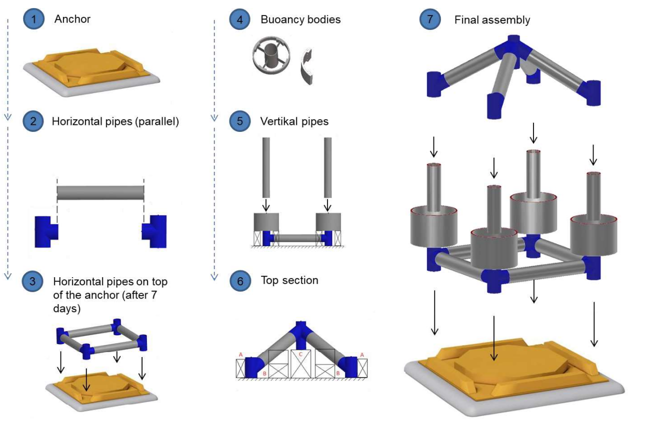

ACKNOWLEDGMENT

We like to express our sincere gratitude to the German Federal State of Mecklenburg-Vorpommern for the financial support provided to the GICON – Großmann Ingenieur Consult GmbH (Project number: V-630-1-260-2012/103).

STIFTUNGSLEHRSTUHL WINDENERGIETECHNIK, **Universität Rostock**, Albert-Einstein-Straße 2 | 18051 Rostock, Germany
GICON – GROßMANN INGENIEUR CONSULT GMBH, Tiergartenstraße 48 | 01219 Dresden, Germany

EUROPÄISCHE UNION
Europäischer Fonds für Regionale Entwicklung

Critical Review of Floating Support Structures for Offshore Wind Farm Deployment

Mareike Leimeister[1,2], Athanasios Kolios[1], Maurizio Collu[1]

[1] Cranfield University, Energy and Power, United Kingdom
[2] Fraunhofer Institute for Wind Energy Systems IWES, Germany

Abstract

Current situation: - numerous deep water sites with promising wind potential → floating structures possible, bottom-fixed systems not;
- large diversity in floater concepts → fast achievement of high technology readiness levels (TRLs) inhibited.

Thus, different floating support structures are assessed with respect to their suitability for offshore wind farm deployment. Based on a survey, a multi-criteria decision analysis (MCDA) is conducted, using the technique for order preference by similarity to ideal solution (TOPSIS). With the individual scores of ten floater categories, considering the weighting of ten specified criteria, suitable concepts are identified and potential hybrid designs, combining advantages of different solutions, are suggested.

Methodology

Set of alternatives

I.	spar - standard	common spar floater type
II.	spar - advanced	improved spar (horizontal transport, short draft, vacillation fins, delta configuration)
III.	semi-sub - standard	common semi-sub floater type
IV.	semi-sub - advanced	improved semi-sub (braceless, active ballast, wave-cancelling, inclined columns)
V.	barge floater	common barge floater type
VI.	TLP - standard	common TLP floater type
VII.	TLP - advanced	improved TLP (redundant mooring lines, gravity anchors)
VIII.	hybrid floater	mixed spar, semi-sub, TLP floater types
IX.	multi-turbine floater	floater supporting more than one wind turbine
X.	mixed-energy floater	floater for wind & wave/tidal/current/ photovoltaic utilisation

Set of criteria

1.	(-)	LCOE	rate of return, power density, mooring footprint, dimensions, turbine spacing
2.	(+)	volume production	ease to manufacture, fabrication time, onshore fabrication, modular structure
3.	(+)	ease of handling	weight, assembly, transport, installation, decommissioning, equipment, dimensions
4.	(+)	durability	redundancy, corrosion resistance, fatigue resistance, aging
5.	(+)	flexibility	site, water depth, soil, environment
6.	(+)	certification	time & ease to achieve, TRL
7.	(+)	performance	deflections, displacements, nacelle acceleration, dynamic response
8.	(-)	maintenance	frequency, redundancy, costs, downtime
9.	(+)	time-efficiency	assembly, transport, installation, maintenance, decommissioning
10.	(-)	mooring requirements	number & length of lines, need of flexible cables (motions), anchor system costs

Results

Survey: - scores (1: least applicable - 5: most applicable) assigned for each criterion to each alternative;
- weights (1: not important - 5: important) represent importance of each criterion with respect to offshore wind farm deployment.

Analysis using TOPSIS: - scores yield a decision matrix, which is - after normalisation - multiplied with the weight vector;
- final ranking of alternatives based on their closeness/distance to the positive/negative ideal solution (table 1);
- comparison of TRL wrt to potential to scale up to mass production for multi-MW wind farm deployment (figure 1).

Table 1: Weights, scores, ranks

	Weight		Score	Rank
1.	**4.26**	I.	0.651	2
2.	3.43	**II.**	**0.763**	**1**
3.	2.91	III.	0.532	5
4.	3.24	IV.	0.600	3
5.	2.33	V.	0.549	4
6.	3.40	VI.	0.319	10
7.	3.38	VII.	0.335	9
8.	3.59	VIII.	0.425	7
9.	3.02	IX.	0.436	6
10.	3.10	X.	0.390	8

Figure 1: TRLs wrt potential to scale up to mass production for multi-MW wind farm deployment

TRL	Description (based on Horizon 2020 https://ec.europa.eu/)
(0	idea for an unproven concept)
1	basic principles observed
2	technology concept formulated
3	experimental proof of concept
4	validation in lab
5	validation in relevant environment
6	demonstration in relevant environment
7	demonstration in operational environment
8	system complete and qualified
9	proven in operational environment

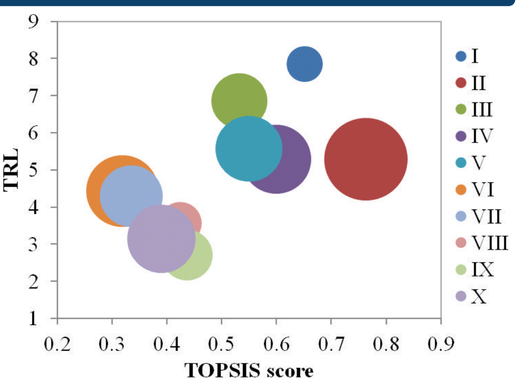

* the bubble size represents the standard deviation of the TRL

Conclusions

- Assessment of ten floating wind turbine support structures wrt ten criteria focusing on wind farm deployment;
- MCDA based on survey results and TOPSIS method;
- Costs are still most important and advanced spars have the highest potential to develop for multi-MW wind farm deployment.

EERA DeepWind'18
Trondheim
17 - 19 January 2018

REMS RENEWABLE ENERGY MARINE STRUCTURES EPSRC Engineering and Physical Sciences Research Council Fraunhofer IWES

INSTITUT FÜR STATIK UND DYNAMIK

Leibniz Universität Hannover

Assessment of the state-of-the-art ULS design procedure for offshore wind turbine sub-structures

Hübler, C. | Gebhardt, C. G. | Rolfes, R.
Institute of Structural Analysis, Leibniz Universität Hannover
c.huebler@isd.uni-hannover.de

Abstract

Sub-structures of offshore wind turbines are designed according to several design load cases (DLCs). These DLCs are given in the current standards, and are supposed, on the one hand, to cover accurately all significant load conditions to guarantee reliability. On the other hand, they should include only necessary conditions. **Here, for ULS conditions, the question whether the current design practice is, firstly, sufficient, and secondly, sensible concerning the computing time by only including necessary DLCs is addressed.** Probabilistic simulation data of five years of normal operation is used to extrapolate 20-year ULS loads (comparable to a probabilistic version of DLC 1.1 for sub-structures). These ULS values are compared to several deterministic DLCs required by current standards (e.g. DLC 6.1). Results show that probabilistic, extrapolated ULS values can exceed standard DLC-loads. Hence, the current design practice might not always be conservative. Especially, the benefit of an additional DLC for wave peak periods close to the eigenfrequency of the sub-structure is indicated.

Simulation setup

For all time domain simulations, the FASTv8 code is used. A soil model applying soil-structure interaction matrices enhances the FASTv8 code [1]. The NREL 5MW reference turbine with the OC3 monopile is investigated.
For the probabilistic approach, statistical distributions for environmental conditions were derived using the FINO3 data (North Sea) [2]. For the DLC-based approach, extreme values are derived here using the same data.
For the ULS analysis several limit states, including the plastic limit state and the buckling limit state for the monopole, are used to calculate utilization factors (UFs). Additionally, ULS proofs for the foundation piles are performed according to GEO2. Aging effects etc. are not taken into account.

ULS calculation

DLC-based approach

The DLC-based approach is uses extreme environmental conditions, e.g. the 50 year storm. Hence, extreme values are derived using 4-week maxima that are directly extracted from the data. Fig. 1 illustrates this process for DLC 6.1. 4-week maxima are extracted for the wind speed, but for the turbulence intensity only the corresponding values are used. These values are not the maxima, as the highest turbulence does not coincide with extreme wind speeds. Statistical distributions are fitted to the 4-week maxima (or there corresponding values) using a maximum likelihood estimation (MLE). Having determined a statistical distribution, the values corresponding to a recurrence period of 50 years can be determined (see Fig. 1).

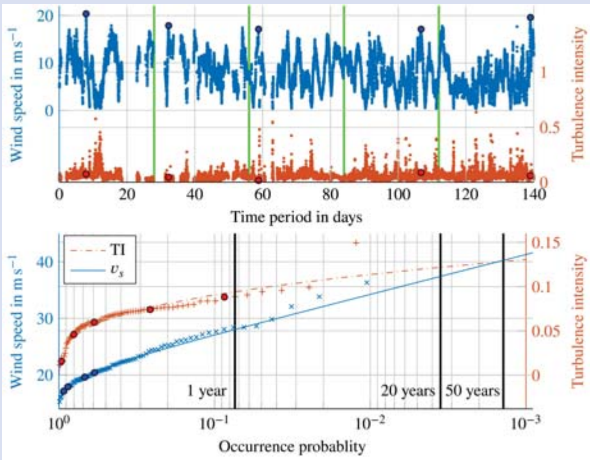

Fig. 1: Top: Wind speed and TI data of 24 weeks. 4 week periods and selected peaks are marked
Bottom: Extrapolation of 50-year wind speeds and the corresponding turbulence

Probabilistic approach

A possible addition to the deterministic DLC-based approach that takes scattering conditions into account is a probabilistic or Monte Carlo simulation approach. Environmental conditions are sampled according to their depending distributions to enable a simulation of 5 years of realistic lifetime (~250000 samples) including unfavourable, but realistic parameter combinations. An extrapolation to 20 years of operation is possible by fitting distributions to the extracted peaks (maxima of all simulations). For the fit, an MLE and only the highest utilisation factors (tail fitting) are used.

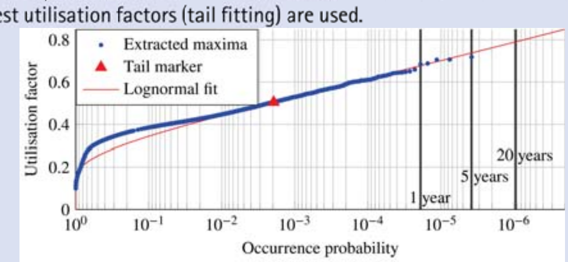

Fig. 2: UFs of all probabilistic simulations (5 years): lognormal tail fit for 20-year extrapolation

Results

In Fig. 3, the DLC-based approach is compared to the probabilistic one. For the DLCs, mean and maximum values (error bars) of 100 DLC simulations are shown. For the probabilistic approach, 1-year, 5-year, and 20-year values are displayed. The 5-year value is the maximum UF of all simulations, while 1 and 20-year values are based on bootstrap samples (and an extrapolation for the 20-year value). The probabilistic approach leads to the highest ULS loads. As these loads exceed the ULS values of the DLC-based approach for the 5-year value, this fact is independent of the extrapolation technique. Most of the extreme UFs occur at wave periods of around 4s being close to the resonance frequency of the monopile. Hence, the probabilistic approach reveals the fact that wave resonance might be a problem for monopiles with larger diameters. Wave resonance is not covered sufficiently by the DLC-based approach, as deterministic wave periods are assumed.

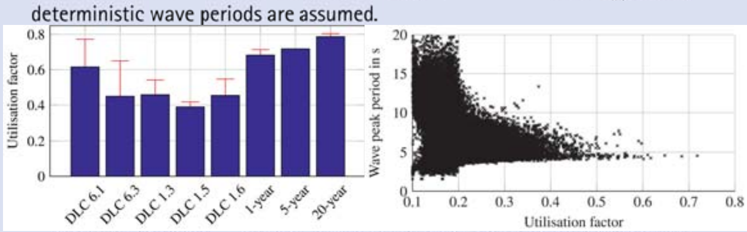

Fig. 3: Left: Comparison of UFs; Right: Investigation of high UFs for the probabilistic approach

Conclusion and Outlook

Results show that - independent of the load extrapolation technique - probabilistic, extrapolated ULS values can exceed the deterministic 50-year ULS loads of the standard DLCs. Therefore, for sub-structures, the current DLCs (excluding fault cases etc.) might not be always conservative. The extrapolation of loads in power production can lead to higher loads, if a probabilistic approach is applied.
In the long term, a reconsideration of DLCs might be valuable. Some load cases can perhaps be removed; others, like a DLC for wave resonance problems, might be missing. Still, due to the limitation of this work to simplified models (FASTv8), sub-structures, no fault cases etc. an exclusion of DLCs based on this work would be premature.

References

[1] Häfele J, Hübler C, Gebhardt CG, Rolfes R. An improved two-step soil-structure interaction modeling method for dynamical analyses of offshore wind turbines. Applied Ocean Research 2016; 55: 141-150.
[2] Hübler C, Gebhardt CG, Rolfes R. Development of a comprehensive database of scattering environmental conditions for offshore wind turbines. Wind Energy Science 2017; 2: 491-505.

OFFSHORE FLOATING PLATFORMS

EXPERIMENTAL ANALYSIS OF A SOLUTION FOR MOTION MITIGATION: THE HEAVE PLATES IN **SATH**

Author: Alberto Rodríguez Marijuán
MSc Civil & Bridge Engineer - Saitec Offshore Technologies, S.L.U.
albertorodriguez@saitec.es

1 Abstract

This study covers an experimental analysis of the pressure levels recorded on the heave plates of a new concept of floating platform —SATH, developed by Saitec Offshore Technologies— during some wave tank tests performed in the facilities of IHCantabria, in Santander (Spain).

These 1:35-scale tests (modelled following Froude's similitude) simulated a 2-MW-turbine prototype, under sets of linear monochromatic waves aligned with the platform's bow-to-stern axis, as in a pure heading sea, in deep water.

The motion of floating platforms, in contrast to that of a fixed structure, tends to have an important contribution in the accelerations of the fluid around it, causing instantaneous pressure increments in the structure. With this study, the author wanted to investigate whether the magnitude of the pressure is related with simple motion indicators, such as the acceleration vector normal to the heave plates in the steady-state oscillation, for structures in which the motion of the heave plates is not negligible compared to the wave amplitude.

2 SATH

The experimental data was gathered from tank tests on a scale model of SATH (Swinging Around Twin Hull), which is a new concept of floating platform for wind turbines developed and owned by Saitec Offshore Technologies.

SATH technology incorporates several characteristic features worth pointing out. First, the whole structure is made of prestressed concrete, improving fatigue life and minimizing corrosion, usual in offshore steel structures. As for the geometry, the two identical hulls provide the needed buoyancy and stability, while the heave plates around the structure improve damping and hydrodynamic performance in general.

The heave plates are the core of the study presented here. Since they are rigidly attached to the main body of the platform, they accelerate the fluid when the platform oscillates in pitch, roll or heave.

Fig 1. Render of a SATH platform equipped with a wind turbine.

3 Objectives

Time series of tank tests were used to identify the averaged peak pressure level, both in every face of the plate and as a net pressure defined as the absolute difference between the two.

The main objectives of this study were:

- Identify the magnitude of the pressure and how it changes with the characteristics of the incident wave: wave height H and period T, helping in a subsequent structural analysis of the structure.
- Compare the variation in the magnitude of the net pressure with simpler general motion indicators, such as the normal acceleration to the face of the plate, defined in terms of the measured pitch, heave and surge motions.

4 Method and data acquisition

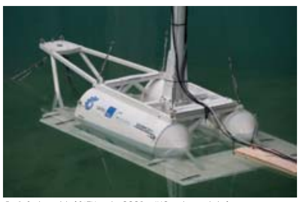

Fig 2. Scale model of SATH, in the CCOB in IHCantabria, right before a wave test.

The experimental tests included 25 series of monochromatic waves of diferent wave heights and amplitudes, in a deep water environment, which were used in the data collection for this study.

Data acquisition: two custom-made submersible pressure transducers —Honeywell 40PC series—, with a pressure rZange of 0-15 psi were used to measure the dynamic pressure (meaning all pressure components not included in the static pressure as measured before the test begins). Sampling frequency on these transducers was 50 Hz.

For motion tracking, a Qualisys system was used, with a set of 4 infrared cameras and a sampling frequency of 100 Hz.

In every time series, the transient part was disregarded and the peaks identified in the stationary signal.

Fig 3. Qualisys Oqus 3+ (L) and Honeywell 40PC (R), from catalogue

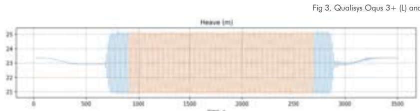

Fig 4. Heave motion time series. Sample of signal taken from Qualisys, with the selected stationary part to be used in the analysis.

The time series of the acceleration at the center of the bow heave plate was computed by combining those in heave, pitch and surge (as in the equation that follows —rigid body mechanics—). The peaks identified in these series were then compared to the magnitude of the pressure for the corresponding regular wave (H, T) that caused them.

In the following equation, a_{pl} is the plate acceleration, and is computed from the linear acceleration in surge ($\ddot{\eta}_1$) and heave ($\ddot{\eta}_3$). The angular acceleration in pitch ($\ddot{\eta}_5$) also causes an acceleration on the plate proportional to the lever arm r.

$$a_{pl} = \ddot{\eta}_1 \sin(\eta_5) + \ddot{\eta}_3 \cos(\eta_5) - \ddot{\eta}_5 r$$

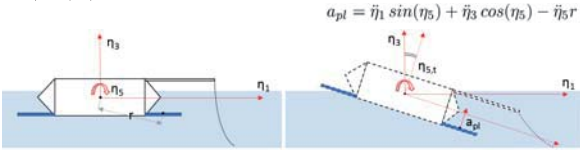

Fig 5. Coordinate system for the rigid body motion in pitch.

5 Results

Fig 6. Identification of significant peaks in the pressure difference time series.

The pressure field was recorded in the transistors on the center of the top and bottom faces of the bow heave plate. The data analyzed was the *significant pressure difference*, which will cause a net force on the structural components (see pressure peaks identification, Fig 6).

When the pressure magnitudes (and the difference —or net— pressure) on the faces of the plates were graphed against the ratio of incident wave period T_w to the natural period in heave T_n, some clear trends could be identified (see images in Fig 7).

In general terms, hydrodynamic pressures (especially the pressure difference that causes a net force on the plate) and normal plate accelerations were greater in magnitude waves close to the natural period in heave, which is coherent since global motions are amplified at these resonant periods.

In addition to that, although larger waves obviously cause higher pressure variations, the net pressure acting on the plate was not that much affected by it (Fig 7, bottom-right corner).

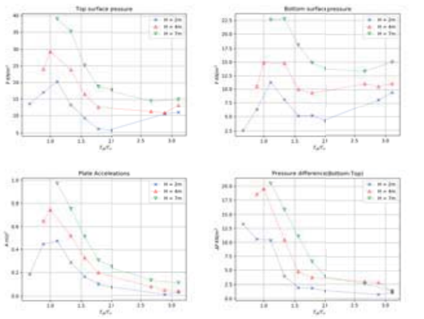

Fig 7. Pressure magnitude and plate accelerations for 3 different wave heights and by incident wave to natural heave period.

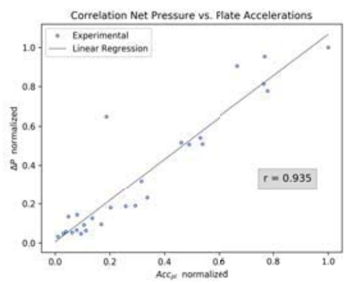

Fig 8. Correlation graph for the normalized pressure and plate's normal acceleration.

It was noticed that the evolution of the plate pressures had a similar shape to that of the normal accelerations. This can be graphically shown, too, with the correlation between the average peak magnitudes of these two variables, as in Fig 8.

The *Pearson's r coefficient* for the normalized pressure difference and the plate's normal acceleration turned out to be **r > 0.93**, indicating an important correlation between these two magnitudes.

This is coherent with the idea that a normal acceleration in the heave plate will tend to drag (accelerate) fluid with it (added mass phenomenon), causing a net force on it.

6 Conclusions

- Regular wave tests were performed on a scale model of the SATH platform, recording the values of the pressures on the heave plates at the top and bottom, in order to compute the net force acting on them.
- Pressure on the top and bottom surfaces of the plate increases at periods closer to the heave resonant period, where motions are slightly amplified too.
- The pressure difference shows a strong correlation with the normal acceleration of the heave plates, which is coherent with the fluid added mass being accelerated to move with them.
- Currently, some numerical analyses (including the use of potential theory software -Sesam-) is being carried out in order to compare these experimental results with those obtainable numerically.
- Some future work on this matter might include analysis on irregular wave trains as well as variation in the pressure distribution in addition to the magnitude.

7 Acknowledgments

The work presented here was originally performed as part of a Master's Thesis for **KTH Royal Institute of Technology** (Stockholm). Great thanks to the main supervisor, Prof. Karoumi, for his help and advice during the research.

I wish to thank as well the **IHCantabria** and their staff, who worked hard to successfully perform the tests in their facilities and who kindly agreed to share the raw data for further analyses, such as this one.

8 References

- J.M.J. Journée and W.W. Massie. Offshore Hydromechanics. First Edition. Delft: Delft University of Technology, 2001.
- S.K. Chakrabarty. Handbook of Offshore Engineering Vol. 1 and Vol. 2. Plainfield, Illinois, USA: Elsevier. Offshore Structures Analysis, Inc., 2005.
- A. K. Chopra. Dynamics of structures: theory and applications to earthquake engineering (4th ed.) Hoboken, NJ: Pearson, 2017.
- J. Jonkman. Dynamics Modelling and Loads Analysis of an Offshore Floating Wind Turbine. Technical Report NREL/TP-500-41958. National Renewable Energy Laboratory, 2007.

9 Contact info

About the author:

Alberto Rodríguez Marijuán

albertorodriguez@saitec.es

linkedin.com/in/albertorodriguezmarijuan

About **Saitec Offshore Technologies**:

www.saitec-offshore.com

@saitecoffshore

linkedin.com/company/saitec-offshore-technologies/

State-of-the-art model for the LIFES50+ OO-Star Wind Floater Semi 10MW floating wind turbine

Antonio Pegalajar-Jurado (ampj@dtu.dk), Michael Borg and Henrik Bredmose
DTU Wind Energy, Nils Koppels Allé, Building 403, DK-2800 Kgs. Lyngby, Denmark

Jonas G. Straume, Trond Landbø and Håkon S. Andersen
Dr.techn. Olav Olsen AS, Vollsveien 17A, 1366 Lysaker, Norway

Wei Yu, Kolja Müller and Frank Lemmer
Stuttgart Wind Energy, University of Stuttgart, Allmandring 5B, 70569 Stuttgart, Germany

Introduction

A FAST [1] model of the DTU 10MW Reference Wind Turbine [2] mounted on the LIFES50+ OO-Star Wind Floater Semi 10MW platform [3] has been developed from a FAST model of the onshore turbine [4]. The changes entail controller, tower structural properties, platform hydrodynamics and mooring system. The basic DTU Wind Energy controller was tuned to avoid the negative damping problem. The flexible tower was extended down to the still water level to capture some of the platform flexibility. Hydrodynamics were precomputed in WAMIT, while viscous drag effects are captured in HydroDyn by the Morison drag term. The platform was defined in HydroDyn to approximate the main drag loads on the structure, keeping in mind that only circular members can be modelled. The mooring system was implemented in MoorDyn. A set of simulations was carried out to assess the system natural frequencies, the response to regular waves, the controller behavior and the global system response to stochastic wind and waves. Further details on the modelling approaches, the simulation results and the model availability can be found in [5].

Modelling of the tower

To capture some of the floater flexibility, the portion of floating platform between SWL and tower interface was modelled as part of the tower, and the inertia properties of the platform were modified accordingly. This approach reduced the tower coupled natural frequency from 0.786 Hz to 0.75 Hz. However, the tower natural frequency obtained with a fully flexible numerical model was 0.59 Hz. This difference highlights the effect of the flexible substructure on the dynamics of the system.

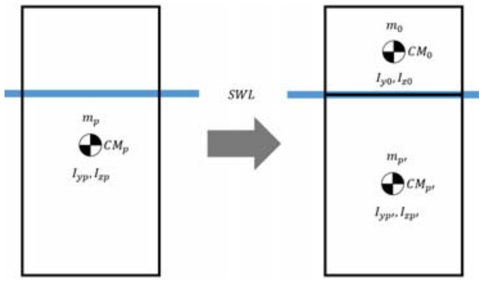

Modelling of the viscous drag

Given the complexity of the floating platform, the viscous drag loads on the physical structure (left) were modelled in HydroDyn with a series of cylindrical members and heave plates (right). This ensures that the global drag loads in surge, heave and pitch are well captured.

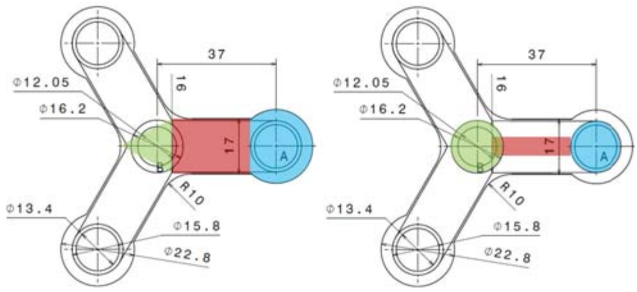

The object of study

DTU 10MW Reference Wind Turbine + OO-Star Wind Floater Semi 10MW

Response to stochastic wind and waves

The system's response to small irregular waves and near-rated turbulent wind is shown here. The platform responses are excited by wind (surge, pitch) and waves (heave, nacelle). The tower natural frequency is also excited. The controller can be seen in action around 5200 s, when the rotor exceeds the rated speed and the blades are pitched to return the wind turbine to below-rated conditions.

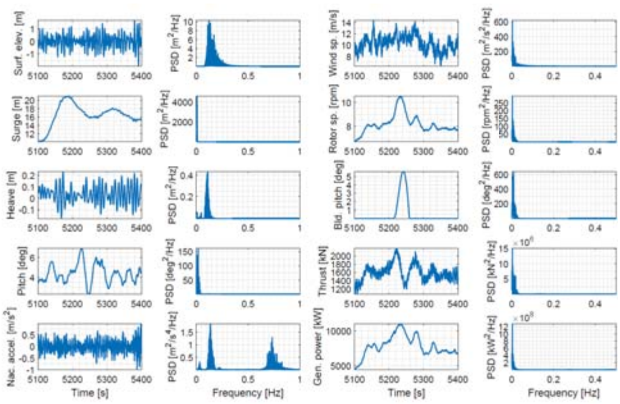

Literature cited

[1] Jonkman J, Jonkman B. NWTC Information Portal (FAST v8). https://nwtc.nrel.gov/FAST8

[2] Bak et al., 2013. "Description of the DTU 10MW reference wind turbine," DTU Wind Energy.

[3] Yu et al., 2017. "LIFES50+ D4.2: Public definition of the two LIFES50+ 10MW floater concepts," University of Stuttgart.

[4] Borg et al., 2015. "LIFES50+ D1.2: Wind turbine models for the design," Technical University of Denmark.

[5] Pegalajar-Jurado et al., 2017. "State-of-the-art model for the LIFES50+ OO-Star Wind Floater Semi 10MW floating wind turbine", *Journal of Physics: Conference Series.* Unpublished.

Acknowledgments

This work is part of the project LIFES50+. The research leading to these results has received funding from the European Union Horizon2020 programme under the agreement H2020-LCE-2014-1-640741.

DTU Wind Energy
Department of Wind Energy

ACFD model for the LIFES50+ OO-Star Wind Floater Semi 10MW

H Sarlak (hsar@dtu.dk), A. Pegalajar-Jurado, M. Borg and H. Bredmose
DTU Wind Energy, Nils Koppels Allé, Building 403, DK-2800 Kgs. Lyngby, Denmark

Introduction

Development of offshore wind farms at intermediate depths rely on the efficient design of floating platforms. While their motion response in wind and waves is often well predicted by the established aero-hydro-elastic models, the forcing from nonlinear waves, viscous damping effects and green-water events require higher fidelity modelling such as fully coupled computational fluid dynamics (CFD) simulations. In this paper, we present the numerical setup and validation of a two-phase CFD solver for the LIFES50+ OO-Star Wind Floater Semi 10 MW, hereafter called OO-Star floater for brevity. The floater has been selected by the LIFES50+ [1] project for extended numerical modelling and physical model tests.

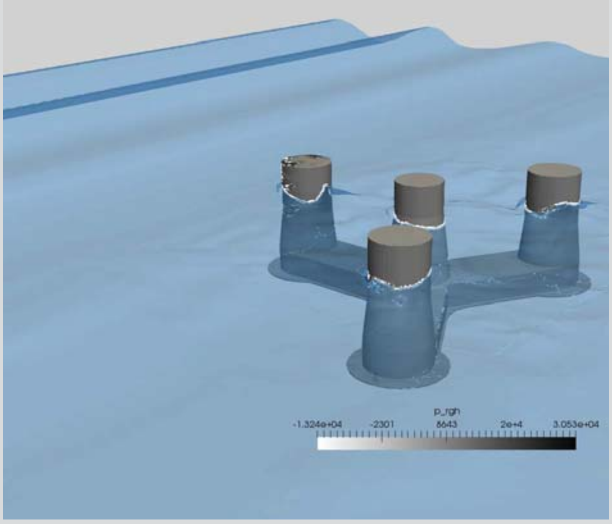

Type	Material	Draft	Freeboard	Displaced volume	Platform mass
		[m]	[m]	[m^3]	[kg]
Semisubmersible	Post-tensioned concrete	22.00	11.0	2.3509E+04	2.1709E+07

Figure 1. A snapshot of the floater subject to linear waves in CFD domain (up), main characteristics of the floater (down)

Numerical set up

The open source toolbox, OpenFOAM [2] is employed and a moving mesh technique is used to account for floating body motions in waves. The grid is generated and refined by importing the geometry and using the unstructured meshing library, snappyHexMesh. For this presentation, first order Stokes waves are generated with the waves2Foam wave generation toolbox [3] and by use of a relaxation zone approach on the far-field. Figure 1 shows a snapshot of the numerical domain and the floater and the corresponding dimensions. .

Results – Wave excitation forces on the fixed floater

Three incident waves of steepness ratios from 0.05 to 0.35 are simulated:

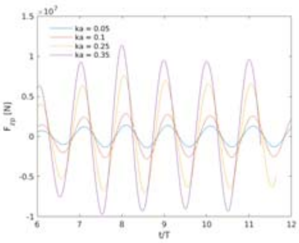

Pressure forces

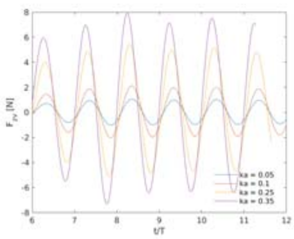

Viscous forces

Results – Floater's hydrodynamic coefficients

Response of the floater to forced surge and heave motions in calm water are analysed to obtain added mass and damping coefficients:

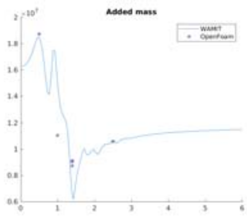

Added mass in surge

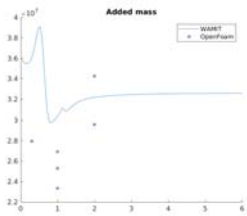

Addedmass in heave

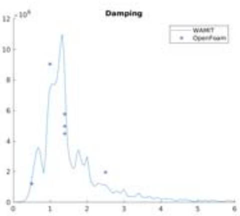

Damping in surge

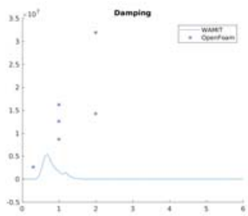

Damping in heave

* CFD _______ Fast computations [1]

References

[1] Pegalajar-Jurado, A; Borg, M.; Bredmose, H., Qualification of innovative floating substructures for 10MW wind turbines and water depths greater than 50m, LIFES50+ Deliverable, project 640741.

[2] H. G. Weller, G. Tabor, H. Jasak, C. Fureby, A tensorial approach to computational continuum mechanics using object-oriented techniques, COMPUTERS IN PHYSICS, VOL. 12, NO. 6, NOV/DEC 1998

[3] Jacobsen, N.G., Fuhrman, D.R. and Fredsøe, J., 2012. A wave generation toolbox for the open-source CFD library: OpenFoam®. International Journal for Numerical Methods in Fluids, 70(9), pp.1073-1088.

Acknowledgments

This work is part of the project LIFES50+. The research leading to these results has received funding from the European Union Horizon2020 programme under the agreement H2020-LCE-2014-1-640741.

DTU Wind Energy
Department of Wind Energy

Designing FWT mooring system in shallow water depth

V. Arnal, T. Soulard, JC. Gilloteaux and C. Berhault
Main Contact: *Vincent Arnal, LHEEA, Centrale Nantes* **Email:** *vincent.arnal@ec-nantes.fr*

STATIONIS

INTRODUCTION

Floating Wind Turbine (FWT) prototypes and pilot farms are located in shallower zones than most of the studies in the literature about moored FWT.

- For water depth > 150m , studies have been successful in defining a conventional catenary mooring system with heavy chains.
- For shallower water depth, solutions like taut or semi-taut configurations using material elasticity of synthetic ropes could be attractive for Marine renewable energy devices [1].

Design and comparisons of conventional catenary mooring chain systems and Taut mooring systems using synthetic fibres are done at 65m.

- Comparisons in terms of **Key Performance Indicators**
- Importance of **mooring modelling hypotheses** for line tensions and floater horizontal motions.

Numerical model

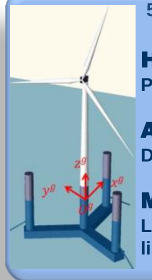

5MW – CSC Semi-submersible [2]
NEMOH + OrcaFlex

Hydrodynamics :
Potential theory + Drag forces

Aerodynamics :
Drag forces on rotor and tower

Moorings :
Lumped-mass model and non-linear load-strain curve

METHODOLOGY

Key Performance Indicators (KPI)

- **CAPEX**
  - Procurement Cost
  - Installation Cost

  k€
- **Operation And Maintenance (OAM)**
  - Preventive maintenance
  - Heavy maintenance
- **Environmental Impact and risk (EI)**
  - Footprint on seabed
  - Touchdown point excursion
- **Station keeping performance**
  - Maximum floater excursion

KPI range : 1 (Low score) to 5 (High score).

Design Methodology

Mooring configurations defined parametrically covering design space

Several Checks for each mooring configuration :
✓Admissible Draft in static position
✓Admissible eigen periods at steady positions
✓Tension criteria according to DNV – OS – J103

Static → Frequency Domain → Time Domain

Reduced number of **Design Load cases (DLC)** with operating and parked wind turbine cases.

	Dir. (°)	Hs (m)	Tp (s)	Uc (m/s)	Uw (m/s)
DLC 1	247.5	11	15	0.7	44
DLC 2	187.5	7	15	0.6	44
DLC 3	247.5	11	15	0.3	11.4
DLC 4	187.5	7	15	0.2	11.4

X 2 depth (EWLR)
w/ and w/o Marine Growth

Table 1 : Limited number of Design Load Cases

Site conditions

Shallow water:
Representative of planned pilot wind farm site around Groix Island on Atlantic French Coast.
Depth : $LAT \sim 62{,}5m$; $HAT \sim 67{,}5m$
Waves conditions :47° 30 N, 3° 30 W from HOMERE [3]
$(H_s, \theta_{wave})_{50years}$ contour calculated with Peak Over Thresold (POT) and fitted Generalized Pareto Distribution (GPD)

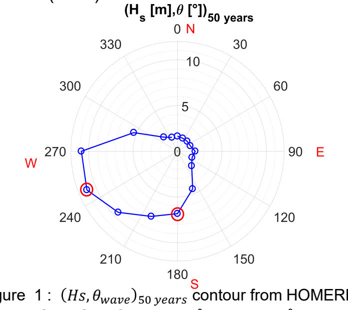

Figure 1 : $(Hs, \theta_{wave})_{50\,years}$ contour from HOMERE with POT + GPD for point 47° 30N and 3° 30 W

KPI Preliminary Evaluation

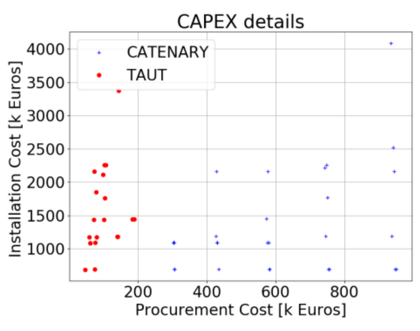

Figure 2 : Installation cost versus Procurement Cost for Taut and catenary mooring configurations.

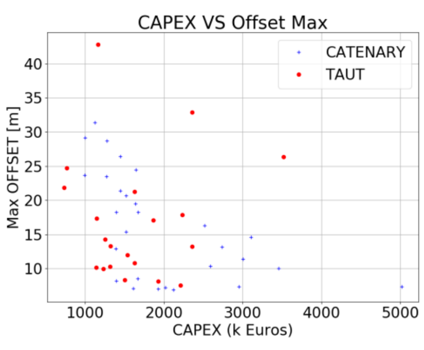

Figure 3 : CAPEX versus station keeping performance

Taut mooring configurations

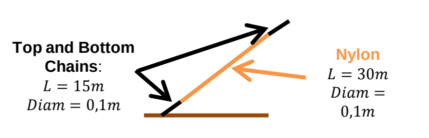

Catenary mooring chains

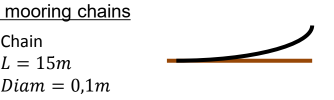

CONCLUSIONS

The main outcomes can be summarized by:

a) Different wave directions could significantly change loads in the mooring lines

b) A synthetic methodology with Key Performance Indicators has been defined

c) When taking into account not only CAPEX but also Environmental impact and Station keeping performance, Taut mooring configurarions appear efficients.

d) Actual uncertainties on Marine Growth properties on site lead to a certain level of risk and unadapted mooring system.

REFERENCES

[1] Ridge, I. M. L., S. J. Banfield, and J. Mackay. "Nylon fibre rope moorings for wave energy converters." *OCEANS 2010*. IEEE, 2010

[2] Luan, C., Gao, Z., & Moan, T. (2016, June). Design and analysis of a braceless steel 5-mw semi-submersible wind turbine. In *ASME 2016 35th International Conference on Ocean, Offshore and Arctic Engineering*

[3] Boudière, E., Maisondieu, C., Ardhuin, F., Accensi, M., Pineau-Guillou, L., & Lepesqueur, J. (2013). A suitable metocean hindcast database for the design of Marine energy converters. *International Journal of Marine Energy*, 3.

Acknowledgment

Y. Perignon from LHEEA is gratefully acknowledged for guidances and scripts for wave data analysis.
The STATIONIS project has been partly funded by BPIFrance, region Pays de la Loire, Vaucluse department, la Metropole Aix-Marseille Provence, la region PACA laureate of 19th call for project FUI

CONSTRUCTION POSSIBILITIES FOR MONOLITHIC CONCRETE SPAR BUOY SERIAL PRODUCTION

CLIMENT MOLINS, ADRIÁN YAGÜE, PAU TRUBAT

CONSTRUCTION

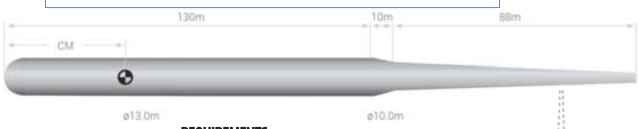

REQUIREMENTS

- Watertight structure of excellent quality
- Durable under harsh offshore conditions
- Cost-efficient construction
- Post-tensioning equipment
- Minimal handling of finished structure
- Smooth transition construction-transport

CONCRETE PLACEMENT SCHEMES:

Concrete poured **radially** — Concrete poured from **above** — Concrete poured **axially**

Through valves at different heights on the inner or outer forms panels — Ideal way of filling forms — Difficult and time consuming

GENERAL RECOMMENDATIONS

- Ensure continuous supply of concrete
- Use steel standard form panels
- Back-up equipment and quick response plan in the event of failure
- High-rate placement systems (>100 m³/h) like boom pumps, tremies, conveyor belts
- Maximize reuse of forms
- Enable repetition of operative cycle to maintain smooth workflow
- Evalue the risk of joints appearing during all construction stages
- Enhance productivity and minimize delivery time

HORIZONTAL

Coastal facilities like dry-dock . Launching of structure into the sea also possible using sliding/skidding system.

- ✓ Cluster all construction works on land
- ✗ Unfavorable concreting direction for slipforming

SPECIFIC RECOMMENDATIONS

- Around-the-clock pouring of concrete
- Use self-propelled formwork systems that slide on temporary service tracks and with the ability to retract-collapse
- Prioritize use of commercial products from the tunnel industry
- Use vibrating form panels
- Mechanize form erecting, stripping, cleaning and treating
- Use inner concreting train(s)
- Use self-propelled devices for removal of inner forms
- On-site steel welding workshop for form panel fabrication and repair and rebar welding.

VERTICAL

- ✗ Unpractical handling
- ✓ Vertical slipforming

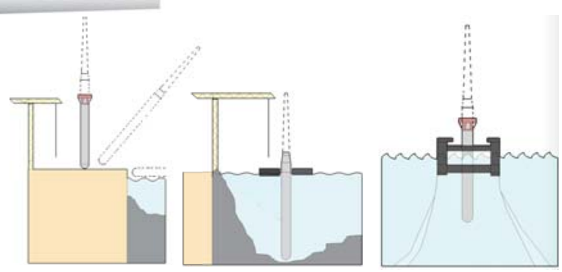

ON-LAND

- ✗ Unpractical handling
- ✗ Incompatible transport

SHELTERED WATERS

- ✗ Large water depth required
- ✗ Only feasible at very specific locations (fjords)

OFFSHORE FACTORY

- ✓ Minimum transport
- ✗ Logistic difficulties
- ✗ Extremely expensive

Production directly at sea is an ambitious solution (design & construction of remote concrete plant, transport of raw materials, unstable working conditions). The idea becomes somewhat more viable by recycling and adapting an obsolete O&G platform due to be de-commissioned. It would allow an interesting space for collaboration between Wind and O&G industries and increase the residual value of old platforms.

SEGMENTAL

CENTRIFUGE

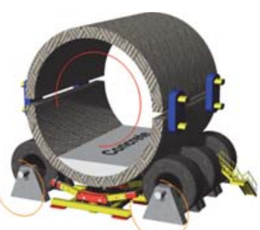

Compactation by centrifugation is a technique typically limited to ϕ 1-2m, arguably applicable to a ϕ13 m of the tower. Plus, spinning the 200-m long structure, if at all possible, results in unprecedented up-scaling in terms of equipment and energy and presents unreasonable execution risk (many spinning devices perfectly synchronized). Centrifuging discrete segments is the only realistic option but results in a non-monolithic structure.

Tolerating a certain number of joints may result in a cheaper construction process. The cost reduction in construction by allowing joints in a segment approach will need to be compared to the costs of high-quality sealing of these joints, the increased maintenance costs and the impact on the life-time of the structure.

- ✓ High quality of centrifuge concrete
- ✓ High-production speed
- ✓ No need of inner core
- ✗ Non-monolithic
- ✗ High energy requirements to spin
- ✗ Increase of maintenance due to the presence of joints.

SEGMENTS JOINED IN FRESH

ASSEMBLY-LINE

Several identical "casting stations" operate in staggered cycles with a fixed lag time t_{lag} (e.g. 15 min between the start of two consecutive stations) and produce identical rings. It takes each station a time $t_{production}$ to complete a ring. Once a given ring has been completed its transported to the assembly line where it 'waits' in place during $t_{waiting} = t_{lag}$ before the next ring produced at the consecutive station is ready to be connected.

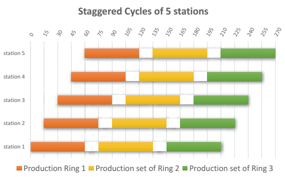

A Gantt Diagram is shown corresponding to the 3 first cycles of 5 identical stations with $t_{lag} =$ 15 min and $t_{production} = 60$ min. After 270 min the total number of rings produced is $5 \times 3 = 15$ rings. When Station No. 5 completes its first ring (min. 120) Station No. 1 is close to completing it's second ring. (min 135). From that point on stations can connect rings for as long as required. As soon as a station has finished producing a ring it will re-start its operative cycle to fabricate another ring

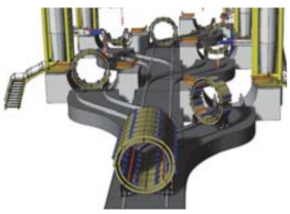

As long as $t_{waiting} \ll t_{setting\ concrete}$ joints between rings will not form. To ensure bonding, extra concrete can be pumped radially at the interphase of a completed ring while waiting for the next ring to be connected. Train-like bogies and rail tracks allow swift transport of freshly filled molds.

- ✓ High-production speed
- ✗ Risk of cold-joints occurring
- ✗ Very time-sensitive
- ✗ High execution risk

INCREMENTAL LAUNCHING

Based on adaptation of pipe-jacking techniques. Instead of using hydraulic jacks to push prefab concrete segments into the soil, a circular arrangement of jacks will 'launch' previously filled molds into a reception lane. A new set of forms are then interlocked with the previous, filled with fresh concrete and launched again. All concreting operations are located at a fixed location

Hydraulic jacks retracted to make room for cranes to assemble a new set of forms

Hydraulic jacks in pushing position 'extrude' the cross-section

Forms must interlock so action force of jacks can be transmitted throughout the system.

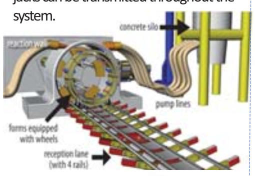

Forms are equipped with 4 sets of wheels matching rails on reception lane.

- ✓ High-production speed
- ✓ Use experience from pipe jacking
- ✗ High-jacking forces on form panels
- ✗ Loads exerted on panels lead to buckling and early replacement of forms

CONTINOUS

CONCRETE CROWN

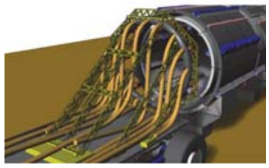

Comparable to slipforming in the sense that concrete is introduced axially, perpendicular to the cross-section of the tower into previously erected forms. The fundamental difference is how concrete is placed, linked to the fact that the device moves horizontally instead of vertically.

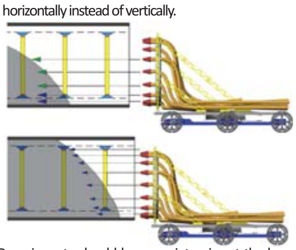

Pumping rate should be more intensive at the lower part to create a concrete slope within forms so concrete placed at higher levels has a base to fall on. Slope angle must be such that freshly pumped concrete does not slide off. Pumplines must be extendable and can rest on reinforcement bars not yet reached by concrete. New forms must be in place before the previous are completely filled whilst pouring never stops. The device slides backwards as construction progresses.

- ✓ Create value through new technology
- ✓ Highly automated
- ✗ Uncertain outcome
- ✗ Unproven and requires research
- ✗ Horizontal placement is difficult and slow

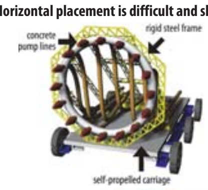

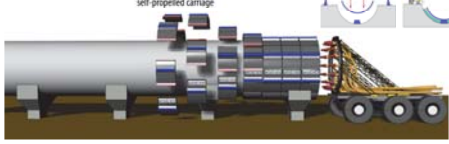

ARCH-TRAVELLERS

Highly-specialized travelers that move on rails parallel to the structure on both sides, they lower forms in place with a pulley system and then release them. A carriage supporting concreting equipment then follows while the Arch travelers are fed new forms and move on to the next section to erect. Different carriages should slide on separate rails to avoid interference between equipment

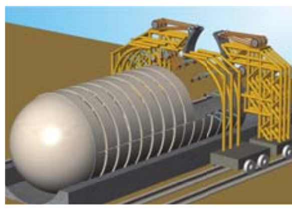

- ✓ Quick delivery
- ✓ Optimized form-handling
- ✗ Large up-front costs to design and build traveler

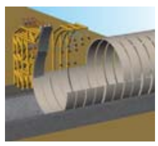

GIANT RE-USABLE MOLD

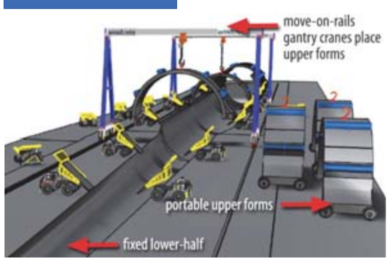

The giant re-usable mold, in which the bottom half is fixed and spans the entire length of the structure while the top half are a series of removable arch-forms. This method allows simultaneous pouring of the whole structure with directly discharging dumpster trucks and other high-throughput placement systems.

- ✓ High throughput
- ✓ Technological simplicity
- ✓ Low execution risk
- ✗ Large up-front costs to manufacture massive mold
- ✗ Permanency of facilities

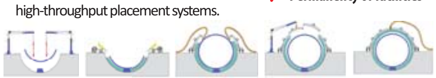

Contact

C. Molins, A. Yagüe
UNIVERSITAT POLITÈCNICA DE CATALUNYA, UPC-BarcelonaTech
Email: climent.molins@upc.edu , adrian.yague@windcrete.com
Website: http://www.windcrete.com/

References

- A. Campos, C. Molins, X. Gironella, and P. Trubat, "Spar concrete monolithic design for offshore wind turbines," Proc. Inst. Civ. Eng. - Marit. Eng., vol. 169, no. 2, pp. 49–63, Jun. 2016.
- P. Trubat, A. Campos, D. Alarcón, and C. Molins, "WINDCRETE CONCEPT SCALABILITY : FROM 2MW TO COMMERCIAL STAGE," in Proceedings of Offshore Wind Energy 2017.
- C. Molins, A. Campos, F. Sandner, and D. Matha, "Monolithic concrete off-shore floating structure for wind turbines," in EWEA 2014 Scientific Proceedings, 2014, pp. 107–111.

Extreme Response Estimation of Offshore Wind Turbines with an Extended Contour-line Method

Jan-Tore Horn[(a)], Steven R. Winterstein [(b)]
[(a)]Centre for Autonomous Marine Operations and Systems (NTNU AMOS), Trondheim, Norway,
[(b)] Probability-Based Engineering, Menlo Park, CA.
Email: jan-tore.horn@ntnu.no

NTNU AMOS
Centre for Autonomous Marine Operations and Systems

Introduction

A method for long term extreme value analysis of a system with multiple sub-populations of dynamic response characteristics is presented. Offshore wind turbines have, simply formulated, two dynamic response models; one for operating turbine, and one for an idle or parked turbine. Depending on the response of interest, both sub-populations may be important to consider in FLS and ULS design. The present work investigates whether such an approach is feasible on a large monopile-mounted offshore wind turbine for extreme response analysis. The long-term extreme values are to be found with environmental contours for parked and operational turbine, and verified with an extreme value distribution based on a full long-term analysis (FLTA). The work is inspired by [1].

Basic Concept

For each operational sub-population, the extreme response functions are evaluated separately, and later combined into a total extreme response. Let X_{1h} denote the 1-hour extreme response of a given parameter, and $F_{X_{1h}}$ is its cumulative distribution and $G_{X_{1h}}$ is the complementary CDF (CCDF). The total response CCDF is simply found by a weighted sum of the contributing populations:

$$G_{X_{1h}}(x) = \sum_i p_i \cdot G^{(i)}_{X_{1h}}(x) \tag{1}$$

where p_i is the probability of sub-population i. The CDF conditioned on response sub-population i can be evaluated accurately with an FLTA, or with a contour-line approach [2]. The objective is to extended the latter for use with offshore wind turbines, which is done with an alternative approach in [3].

Models

The environmental parameters to be considered are the wind speed V, significant wave height H_S and peak period T_P. Turbulence intensity is set to 10% and the JONSWAP wave spectrum with long-crested formulation aligned with the wind is used. Sub-populations defining the dynamic response models in a consistent manner are shown in Fig. 1 with probabilities of occurrence. It is assumed that $p_3 \cdot F_3 \approx 0$ due to small p_3, and that $p_4 \cdot F_4 \approx p_4$ due to small response. Hence, only sub-populations 1 and 2 will be evaluated here. The total availability is set to 90% in accordance with [4].

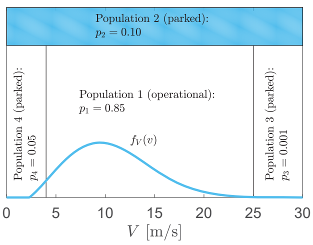

Figure 1: Sub-populations

The numerical model is an FEM model in USFOS/vpOne of the 10MW DTU reference wind turbine mounted on a monopile in 30 meters water depth at Dogger Bank in the central North Sea. The nacelle/tower-top acceleration is the investigated response parameter in this case, as it is prone to low fore-aft damping when the turbine is parked. First fore-aft natural period is 4.4 seconds.

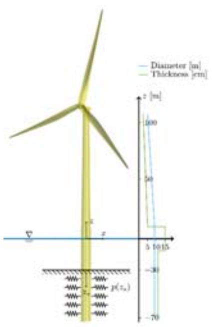

Figure 2: Model

Procedure

For sub-population i, the CDF of the maximum response in a 1-hour sea state using a full long-term analysis is found by numerical integration as:

$$F^{(i)}_{X_{1h}}(x) = \iiint F^{(i)}_{X_{1h}|V,H_S,T_P}(x|v,h,t) f^{(i)}_{V,H_S,T_P}(v,h,t)\, dv\, dh\, dt$$

where $F^{(i)}_{X_{1h}|V,H_S,T_P}$ is the short-term CDF of the maximum response in population i and $f^{(i)}_{V,H_S,T_P}$ is the environmental joint distribution conditioned on population i. The triple integral is evaluated numerically using 90 independent 10-minute simulations for each environmental combination. The maximum from these short term simulations are assumed Gumbel distributed, which is raised to the power of six for estimate of the 1-hour maximum response CDF. The environmental contour method assume that the long term extreme response with T years return period can be estimated using a sea-state on the T-year contour line:

$$F_{X_{1h}}(x_T) \approx F_{X_{1h}|V,H_S,T_P}(x_\alpha | v_T, h_T, t_T)$$

at some fractile α, typically between 0.7 and 0.9. To estimate the 50-year combined response using the extended contour-line approach, the procedure is as follows:

1. Estimate extreme response x_T in each sub-population for two return periods, say $T = 50$ and $T = 500$. Use the standard contour-line method, assuming only this population is acting. Typical points on contour-lines are shown in Fig. 3 and 4.
2. Estimate $G_{X_{1h}}(x) = 1 - F_{X_{1h}}(x)$ for each sub-population using the obtained responses, using e.g. a linear fit in Gumbel paper.
3. Find the total $G(x)$ using Eq. (1).

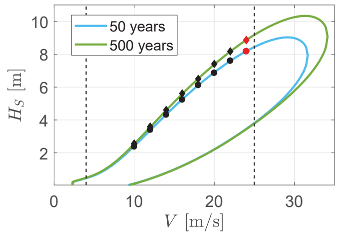

Figure 3: Contours for wind speed and significant wave height used for sub-population 1, expected T_P given H_S is used. Dashed lines indicate sub-population limits. Sea-states used in red.

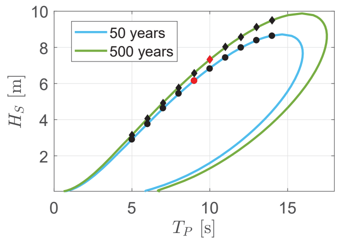

Figure 4: Contours for significant wave height and peak period used for sub-population 2, expected V given H_S is used. Sea-states used in red.

Results and discussion

In Fig. 5, a characteristic nacelle acceleration as function of wind speed is illustrated. Due to low aerodynamic damping, the response in the parked population is in general larger. From the FLTA, exact exceedance probability functions $G(x)$ are plotted in Fig. 6, with the corresponding contour-line estimates. Relatively high fractiles of 0.96-0.99 are used for the contour method estimates to account for variations in environmental parameters not present in the 2D contours. The best linear fits $G^C(x)$ are shown in Fig. 6, and the combined response in Fig. 7.

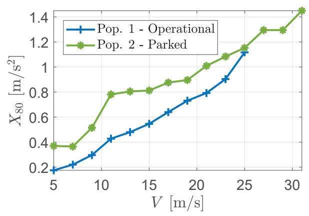

Figure 5: 80% fractile response given wind speed bin

Results show that a reasonable estimate for the combined response from several operational sub-populations can be obtained using an extended contour-line method. However, calibration of response fractiles and possible extension to 3D contour is recommended and will be elaborated on in the paper to follow.

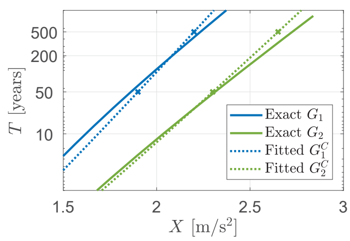

Figure 6: Results from each sub-population

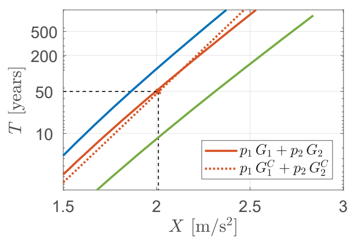

Figure 7: Combined CCDFs and total response estimate

References

[1] Steven R. Winterstein. Environmental Contours : Including the Effects of Directionality and other sub-populations. Technical Report August, Menlo Park, CA, 2017.

[2] S Haver and S R Winterstein. Environmental contour lines: A method for estimating long term extremes by a short term analysis. *Transactions - Society of Naval Architects and Marine Engineers*, 116:116–127, 2009.

[3] Qinyuan Li, Zhen Gao, and Torgeir Moan. Modified environmental contour method for predicting long-term extreme responses of bottom-fixed offshore wind turbines. *Marine Structures*, 48:15–32, 2016.

[4] DNV GL. Loads and site conditions for wind turbines. Technical Report November, 2016.

Acknowledgements

This work has been carried out at the Centre for Autonomous Marine Operations and Systems (NTNU AMOS). The Norwegian Research Council is acknowledged as the main sponsor of NTNU AMOS. This work was supported by the Research Council of Norway through the Centres of Excellence funding scheme, Project number 223254 - NTNU AMOS.

Floating Offshore Wind

Fabrication and Installation of OO-Star Wind Floater

Simen Kleven Rasmussen, Dr.techn.Olav Olsen AS
Håkon Andersen, Dr.techn.Olav Olsen AS
Trond Landbø, Dr.techn.Olav Olsen AS

Objective and scope

The key objectives of the poster, for the **OO-Star Wind Floater**, is to describe:

- A viable and understandable execution model for floating offshore wind
- A way to reduce cost of energy
- A method with acceptable technical and commercial risk
- A model with feasible extention to future larger wind turbines
- A supply chain for floating offshore wind as an understandable long term total business model

The objective of this presentation is to describe a cost effective floating wind turbine, the **OO-Star Wind Floater**, and a viable and understandable execution model for floating offshore wind at a competitive cost of energy, and with an acceptable technical and commercial risk. It is particularly important to show an execution model which is feasible for future large wind turbines. This will help developers and large contractors to understand how a supply chain for floating offshore wind can be developed as a part of an understandable long term total business model.

Introduction

The execution model is based on a robust and cost effective floating solution, the **10 MW OO-Star Wind Floater** semi-submersible designed by **Dr.techn.Olav Olsen AS** during the first Phase of the LIFES50+ project (grant agreement No 640741) funded by the European Commission (EC). The **OO-Star Wind Floater** is very robust with regard to the following parameters:

- Wind turbine size and weight
- Environmental conditions
- Water depths available during assembly, tow, installation and operation
- Design life and durability
- Accidental scenarios
- Local industry, availability

Fabrication and Installation features:

- Fabrication onshore
- Assembly at quayside while resting on seabed
- Lifting of RNA by onshore crane
- No relative motion between crane and floater during lift and mounting
- No need for complicated ballasting operations during lifting
- Completed and tested inshore
- Towed fully assembled to the offshore site
- Connected to pre-installed mooring and power cable

Ambition

Floating wind has some significant advantages over bottom fixed. One is to extend the application of offshore wind turbines to water depths beyond bottom fixed. 70-80 percent of the worlds wind resources are in areas suitable for floating wind turbines. Enabling the use of floating sub-structures will allow for new markets to emerge in locations that does not have shallow water depths.

Competing with bottom fixed wind turbines can only be done through cost reduction, and previous studies point to manufacturing cost as the most influencing design dependent parameter on the LCOE [1].

Floating offshore wind can be standardized beyond bottom fixed offshore wind due to less dependency on water depths and soil conditions. This will in the long term help to reduce fabrication cost for floating wind and make it competitive with respect to bottom fixed solutions. Considering the large energy potential related to floating offshore wind, and the fact that many countries and areas do not have suitable shallow water sites for bottom fixed developments, the future demand for floating offshore wind is expected to be high.

Another advantage for floating solutions, like the **OO-Star Wind Floater**, is the ability to do all assembly and testing at quayside before towing to offshore site. Elimination of offshore heavy lift operations is a great benefit and can not be achieved for bottom fixed wind turbines without large additional investments to solve stability issues during temporary phases. These arguments will only be stronger in the future with larger wind turbines and no existing installation tools capable of offshore installations. Most likely there will be a split in the market between bottom fixed and floating wind with larger turbines used for floating wind than for bottom fixed. We already have a similar split between land based wind and offshore wind, where land based wind turbines are smaller than offshore turbines due to transport and handling limitations.

Conclusion

The division of construction into stages and parallel production lines allows for an industrialized fabrication process, easy to control and standardize. In addition, the construction of the different units are overlapping - for a better utilization of the resources and improved execution time. This is an efficient system for fabrication of a large number of units, where cost of establishing the construction yard is compensated with the total saving on cost and time.

Floating wind will outperform bottom fixed solutions for larger turbines (15-20 MW). EWEA acknowledge that a 20 MW turbine is possible with existing materials [2].

OO-Star Wind Floater - benefits:

- Favourable motion characteristics - robust and durable substructure - minimum maintenance cost - long design life/reuse
- Modular construction
- Shallow minimum draft, full assembly and testing at quayside
- Limited use of heavy lift equipment, no offshore lifts
- Step change in tower and RNA handling

Process benefits:

- Division of the pontoon in parts reduces the number of skidding lines needed to maintain the production schedule, by localizing part of the construction outside the assembly line
- Construction in stages allow for an industrialized fabrication process, easy to control and standardize
- Skidding system avoids the use of large, specialized and expensive cranes
- Construction of the units is overlapped, for a better utilization of the resources and improved execution time

Acknowledgements

The research leading to these results has received funding from the European Union Horizon2020 programme under the agreement H2020-LCE-2014-1-640741.

General overview

Below is a typical layout for a construction site, aiming to deliver 25 complete wind turbines each year. Based on parallel operations, and dedicated construction stations.

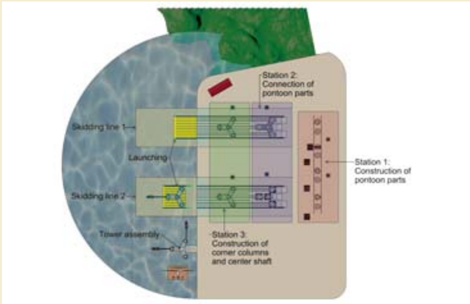

- **Station 1:** Pre-fabrication of pontoon parts (one month)
- **Station 2:** Connection and completion of pontoon parts, including post-tensioning (one month)
- **Station 3:** Slip forming of corner column and center shaft, and installation of structural steel (TP) and mechanical outfitting (one month)
- **Station 4:** Controlled launch to sea from slipway cradle or shiplift
- **Finalization:** Assembly of tower and RNA, completion and testing (two weeks)

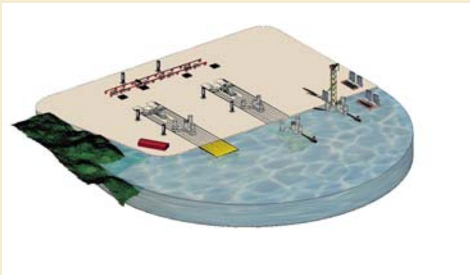

Pontoon Fabrication and Assembly

Station 1: the pontoon will be pre-fabricated, as four (4) independent pieces. Construction will be in parallel with other operations. The parts will be transported to skidding lines on multiwheelers. Skidding lines are accessible for multiwheelers from below ground access. Typical construction time is one month for four pieces.

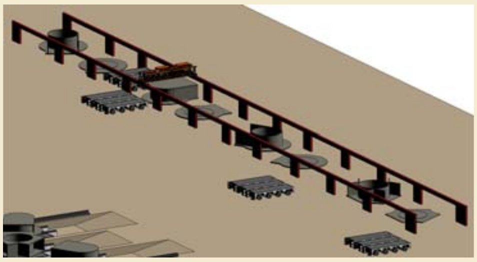

Station 2: The pontoon parts are accurately placed with a separation between the parts. The pre-fabricated pontoon parts will have protruding rebars, and splicing rebars will fill the gap between the parts. The concrete joint surface will be cleaned and prepared for proper bonding to the fresh concrete which will be cast in-situ to fill the gaps.

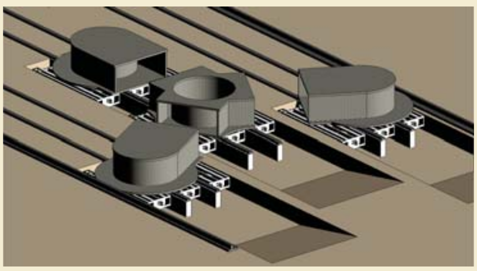

Prior to cast prestressing ducts in the existing pieces will also be properly connected and prepared for the post-tensioning process. The cables will be tensioned and grouted when the concrete in the pontoon joints has reached sufficient compressive strength, typically 1-2 weeks after casting. The tendons in the base slab will be tensioned when pontoon walls are cast. The top slab tendons will be tensioned after slip forming of the first part of the central shaft and corner columns.

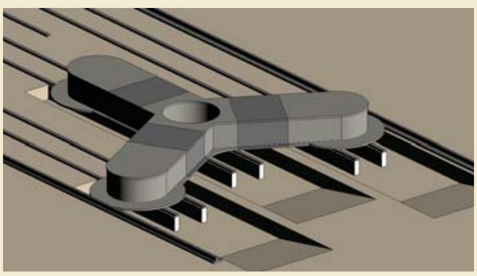

Estimated time for completing the star pontoon at Station 2, including enough curing time before skidding, is typically 1 month.

Station 3: Corner columns and central shaft

Key features of Station 3:

- Last fabrication station
- Slip forming of corner columns and central shaft
- Adjustable formwork adapting to the changing geometry
- Parallel fabrication for each corner cell and center shaft
- Post-tensioning possible without the use of dead-end anchors

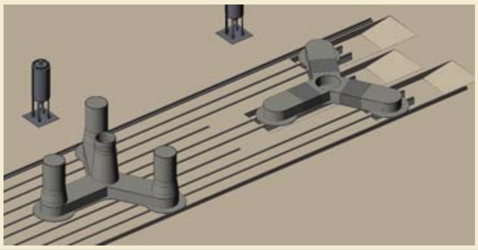

Launching

The following procedure is planned for launching:

- Assembly lines with continuity onto slipway cradle (or shiplift)
- Transfer to the cradle by skidding system used for Station 2 and Station 3
- Cradle has a trapezoidal shape with top surface always horizontal, supporting the concrete substructure
- Decent performed through a set of steel cables pulled by jacks
- The cradle is lowered along the inclined plane until the concrete substructure disconnect from the cradle and a tug boat intervenes

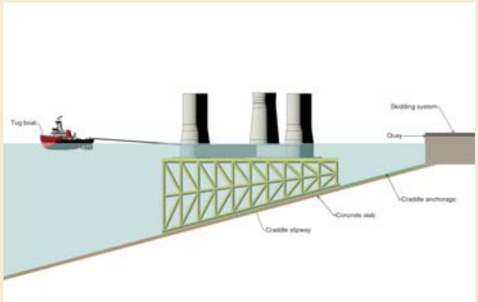

Tower and RNA operations

Two possible ways of installing tower and RNA is proposed:

1. Assembly of tower and RNA is crucial for a robust and cost effective execution model. Our concept eliminates offshore heavy lifts, and use of floating crane vessels in general. An efficient and purpose built pier will facilitate the assembly operations. The seabed outside the pier will be leveled and the substructure will be grounded in exact position relative to the pier. Land based crane solutions may be used for the assembly operations.
2. For future large floating wind turbines the tower and RNA may be assembled onto a long steel cradle, resting on multiwheelers. The cradle, with completely assembled turbine, can be moved and skidded into a support frame with a pivot point close to the quayside.

The substructure is towed into position, and grounded (by ballasting) onto supports to eliminate the typical challenge of relative motion between substructure and lifting arrangement.

A set of climbing beams makes it possible to tilt the support frame with the cradle, with tower and nacelle secured and fixed, to a vertical position. When tower and RNA is positioned over the substructure, the cradle can slide inside the support frame, and the tower and RNA can be landed onto the central shaft. The complete floating WTG is then ready for testing and subsequent tow to site and installation into pre-installed mooring system.

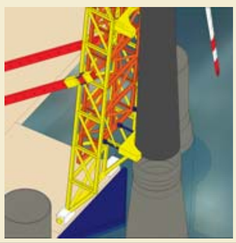

There is no need for specialized vessels with long reach cranes. This makes the method very robust wrt. future large WTGs.

The "telescopic ladder" system described is based on a patent owned by **Dr.techn.Olav Olsen AS**. The method will require that turbine manufacturers modify their design and allow for horizontal assembly. Until this is in place the land-crane method will be used.

References

[1] LIFES50+ Deliverable D7.6
[2] UpWind - Design limits and solutions for very large wind turbines [EWEA]

Experimental validation of analytical wake and downstream turbine performance modelling

F. Polster[1], J. Bartl[2], F. Mühle[3], P. U. Thamsen[1], L. Sætran[2]

[1] Technical University of Berlin (TUB), Berlin, Germany
[2] Norwegian University of Science and Technology (NTNU), Trondheim, Norway
[3] Norwegian University of Life Sciences (NMBU), Ås, Norway

*contact: felix.polster@t-online.de

NTNU

MOTIVATION

- Wake effects in wind farms can cause significant power losses (up to 20%)
- Wind farm layout and control optimization can be applied to reduce losses
- Accurate, simple and fast tools to predict the wake flow are needed
- Comparison of wake models and small-scale turbine wind tunnel measurements to determine the most accurate wake model

EXPERIMENTAL SETUP

- Wind tunnel measurements at NTNU wind tunnel with a test section of 1.8m (height) x 2.7m (width) x 12.0m (length)

- Experiment 1: **Wake measurements**
  - Wake measurements behind small scale turbine (D=0.45m) at
    - Ambient turbulence intensities $I_a = 0.23\%, 10\%$
    - Upstream turbine pitch angles $\beta = 0°, 2°, 5°$
- Experiment 2: **Performance measurements**
  - Performance measurements of a two aligned small-scale turbines (D=0.90m)

Figure1 : Two alinged turbines in the NTNU wind tunnel

MODELLING METHODS

- Applied wake models:
  - Jensen
  - Frandsen
  - Ishihara
  - Bastankah & Porte Agel
  - Jensen-Gaussian Wake model (JGWM) [3]
- Adjustment of JGWM: Combination with Crespo and Hernandez turbulence model
- Application of wind tunnel blockage effect correction [2]
- Blade Element Momentum method with guaranteed convergence for performance modelling

RESULTS

Wake Modelling

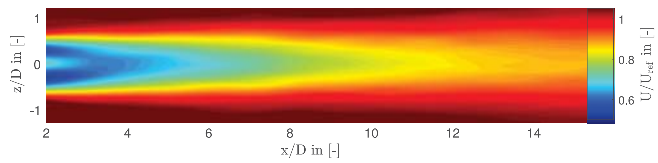

Figure 2: Wake measurement result at $I_a = 10\%$ and $\beta = 0°$ from $x/D = 2 - 15$

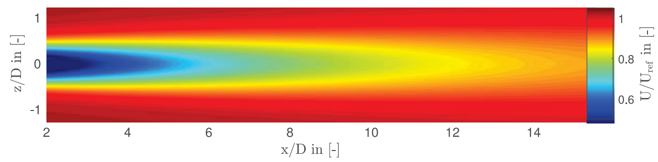

Figure 3: Adjusted Jensen-Gaussian Wake Model simulation result

- The adjusted JGWM shows the most accurate wake flow prediction at all test cases

Performance Modelling

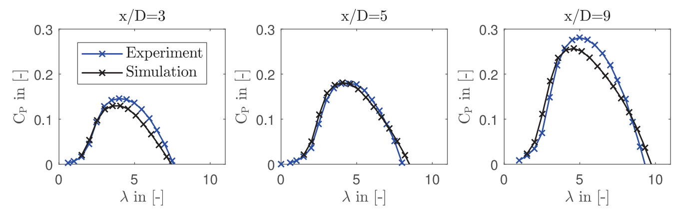

Figure 4: Downstream turbine power measurement and modelling comparison

- Average prediction error at design tip speed ratio amounts 6,8%

CONCLUSIONS

- An improvement of the Jensen-Gaussian Wake Model was proposed
- The adjusted Wake Model was found to give the most accurate wake flow prediction at all test cases
- Wake Model application on downstream turbine performance modelling resulted in a reasonable performance prediction

REFERENCES

[1] S Ning. *A simple solution method for the blade element momentum equations with guaranteed convergence*. Wind Energy, 17(9):1327–1345, 2014.
[2] Jaeha Ryi, Wook Rhee, Ui Chang Hwang, and Jong-Soo Choi. *Blockage effect correction for a scaled wind turbine rotor by using wind tunnel test data*. Renewable Energy, 79:227–235, 2015.
[3] Xiaoxia Gao, Hongxing Yang, and Lin Lu. *Optimization of wind turbine layout position in a wind farm using a newly-developed two-dimensional wake model*. Applied Energy, 174:192–200, 2016.
[4] A Crespo, J Hernandez, et al. *Turbulence characteristics in wind-turbine wakes*. Journal of wind engineering and industrial aerodynamics, 61(1):71–85, 1996.

Reduced Order Modeling of lift characteristics of NACA0015 using van der Pol equation

M. Salman Siddiqui[1], Adil Rasheed[2], Trond Kvamsdal[1,2]

[1]NTNU, Dept. of Mathematical Sciences, NO 7491 Trondheim. [2]SINTEF ICT, Dept. of Applied Mathematics, NO 7465 Trondheim.

INTRODUCTION

The ability to accurately predict vortex shedding around wind turbine blades is paramount, particularly at high Reynolds number. We employed RANS approach with the use of three turbulence models (Spalart-Allmaras, k-ϵ and k-ω Shear Stress Transport model) to investigate the vortex shedding pattern on a NACA0015 airfoil. Spectral analysis is performed over the time history of aerodynamic coefficients to identify the dominant frequencies along with their even and odd harmonics. A reduced-order model based on van der Pol equation is proposed for the aerodynamic lift calculation. The model is also tested in a predictive setting, and the results are compared against the full order model solution.

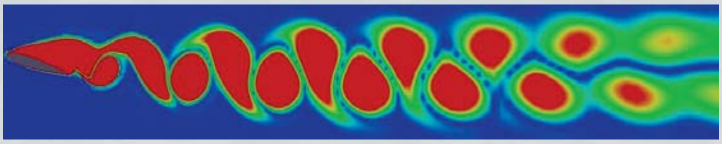

Fig: Von karman vortex street

METHODOLOGY

A multiblock approach has been adapted to allow more control over the generation of computational mesh. Quality orthogonal cells are clustered due to the presence of sharp gradients arising from the rapid changes in the flow physics on the surface and the wake region of the airfoil.

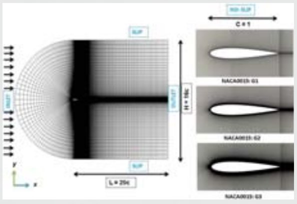

Fig: Mesh domain

No transverse flow distribution is observed, which is considered a prime reason for similar flow pattern in the third spatial dimension. Over the entire span of angle of attack, three-dimensional results consistently matched well with the two-dimensional predictions.

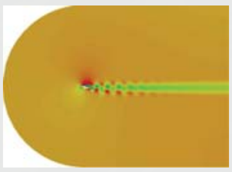

Fig: 2D simulation

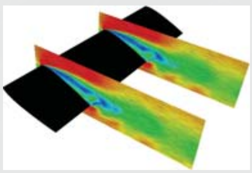

Fig: 3D simulation

RESULTS AND DISCUSSION

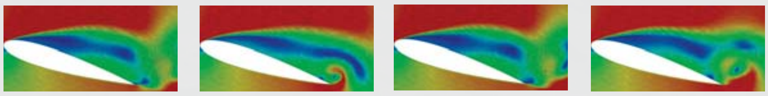

(a) (b) (c) (d)

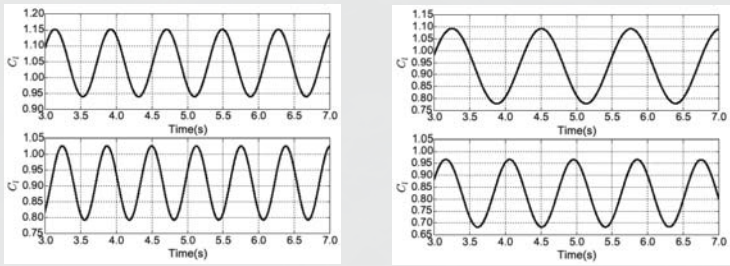

k-ω SST turbulence model

k-ϵ turbulence model

Fig: Lift coefficient oscillations

Van der Pol ROM model

Based on the high fidelity solution and spectral decomposition of the time history of coefficients a ROM is developed to model lift.

$$\ddot{C}_l + \varpi^2 C_l = \upsilon \dot{C}_l - \Gamma C_l \dot{C}_l - \varrho C_l^2 \dot{C}_l$$

Spectral analysis

Spectral analysis is performed on the time series of the aerodynamic list coefficient to extract the dominant frequencies. A strong quadratic and cubic couplings is observed in the frequency harmonics. The magnitude of the fundamental frequency at aoa 17 is 0.9 and 1.5 for k-ϵ and k-ω SST models respectively. The second harmonic is exhibited at the quadratic frequency of 1.8 and 3.0 ($f_s + f_s = 2\ f_s$), whereas cubic coupling of the frequency is seen at 3 f_s . Both models have shown distinct magnitudes and peaks for the fundamental frequency and its quadratic and cubic couplings.

.

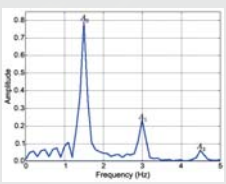

Fig: Frequency spectrum k-ω SST turbulence model

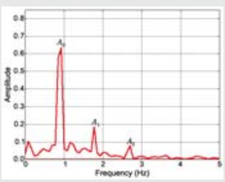

Fig: Frequency spectrum k-ϵ turbulence model

Fig : Frequency plots

Rom in predictive settings

The obtained result from ROM is compared with FOM. The proposed ROM model is further analyzed in a predictive setting to access its validity. Lift is computed at aoa = 16, using both high-fidelity simulation models and ROM approach.

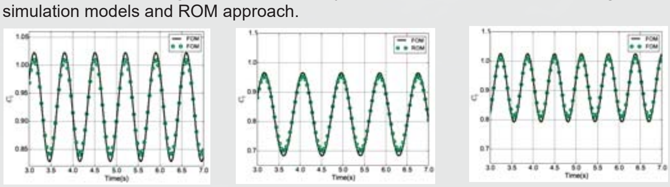

Aoa = 15 Aoa = 17 Aoa = 16

Fig : ROM vs FOM

CONCLUSION

- Flow separation and vortex shedding pattern of NACA0015 is investigated at high Reynolds number over different angles of attack.
- Spalart-Allmaras, k- ϵ, k-ω Shear Stress Transport model turbulence models are investigated in two and three-dimensional spatial setting.
- Spectral analysis results show the even and odd frequencies harmonics in the temporal coefficients.
- A reduced-order model (ROM) of lift based on van der Pol equation is proposed.
- ROM model is tested in a predictive setting, and the results are compared against the full order model solution.

The authors acknowledge the financial support from the Norwegian Research Council and the industrial partners of the FSI-WT-project (216465/E20) and NOWITECH-project (Grant No.:193823/S60)

Contact: muhammad. siddiqui@math.ntnu.no

Fast divergence-conforming reduced order models for flow

E. Fonn, H. v. Brummelen, T. Kvamsdal, A. Rasheed, M. S. Siddiqui
SINTEF Digital
eivind.fonn@sintef.no — +47 41 44 98 89

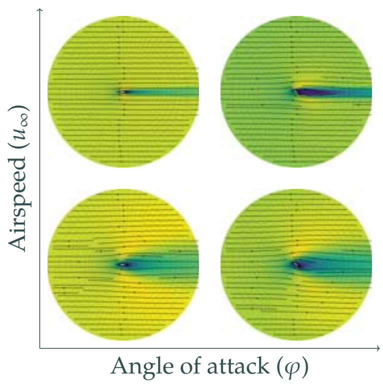

Problem: Repetitive solutions of parametrized flow problems (see left) can be quite demanding, each solution involving up to 10^6–10^9 degrees of freedom and hours or days of computational time.

Answer: Reduced Order Modelling (ROM) offers solutions with lower accuracy but dramatic speedups. When tied to a divergence-conforming high-fidelity method, the gains can be even greater.

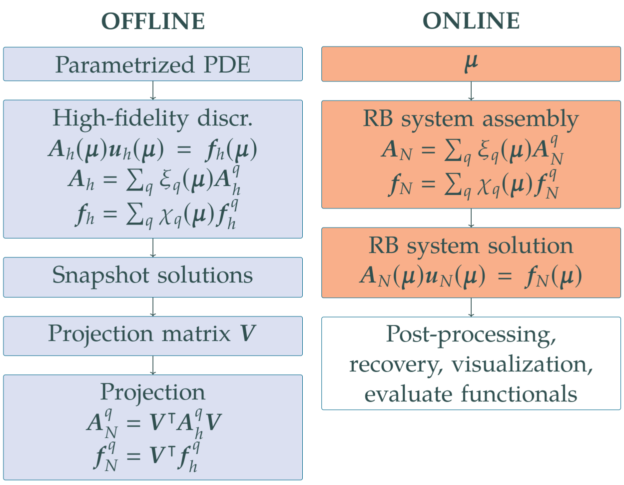

Problem specifics

High fidelity simulations of *stationary Navier-Stokes* were performed of flow around a NACA0015 airfoil with chord length of 1 m. The inflow velocity u_∞ varied from 1 to 20 m/s, and the angle of attack φ varied from −35 to 35°. The viscosity was fixed at 1/6. Snapshots were evaluated at the 15 × 15 Gauss points on the parameter domain, and reduced models created with $N = 10, 20, \ldots, 50$ degrees of freedom.

First four velocity modes

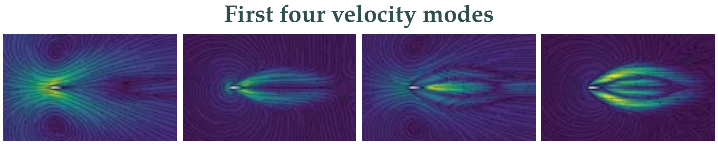

First four supremizer modes

First four pressure modes

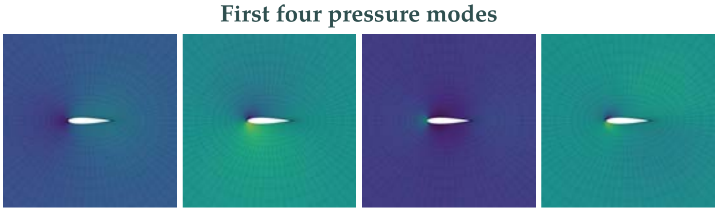

Energy spectrum of snapshots

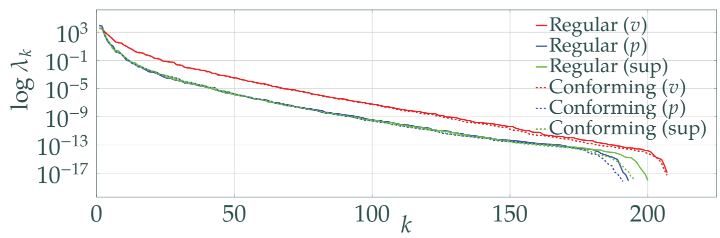

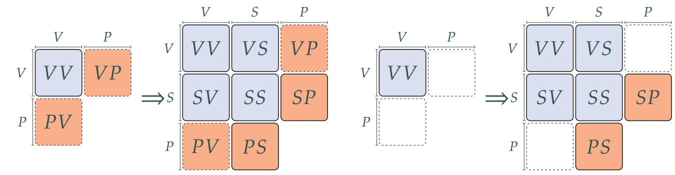

The system matrix (size $2N$) will usually have a rank-deficient velocity-pressure block (VP, indicated with dashed lines). Enriching the velocity space with so-called *supremizers* ensures a full-rank system matrix with size $3N$. A divergence-conforming method will produce a fully divergence-free basis, so the VP-block vanishes, giving a block-triangular system, solvable as two size-N systems instead of one size-$3N$ system.

Error as a function of speed

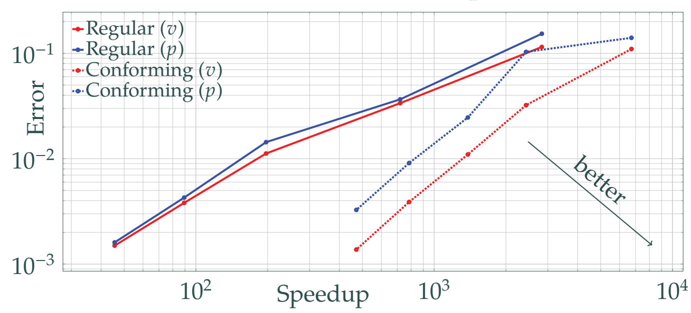

Actual error as a function of expected error

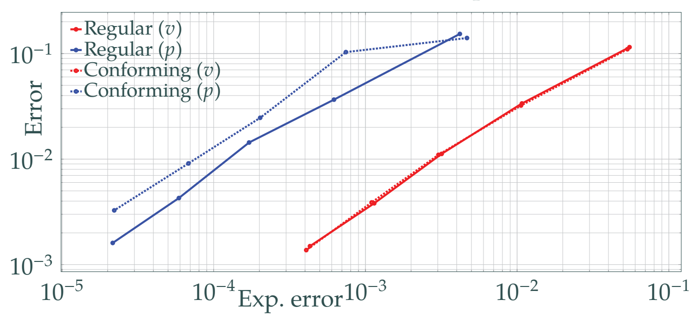

Mean solver time usage

	Hi-Fi	$N = 10$	$N = 20$	$N = 30$	$N = 40$	$N = 50$
Regular	104 s	29 ms	126 ms	503 ms	1.02 s	2.51 s
Conforming	165 s	21 ms	54 ms	104 ms	183 ms	284 ms

Discussion

- ROMs are able to deliver results within two to three orders of magnitude at dramatic speedups.
- Divergence-conforming ROMs can deliver higher speeds, up to one order of magnitude faster in the present examples, by exploiting specific properties of the velocity bases.

Sensitivity analysis of the dynamic response of a floating wind turbine

Rouzbeh Siavashi, Mostafa Bakhoday Paskyabi, Finn Gunnar Nielsen and Joachim Reuder
Geophysical Institute, University of Bergen

Introduction

The dynamic response of HYWIND Demo due to the combined action of wind and waves is numerically simulated by the computational tool SIMA (Simulation of Marine Operations). The numerical model has previously been compared to full scale measurements by Skaare et al. [1]. To better understand the sensitivity of the responses to the various environmental parameters, a sensitivity study is performed. In this preliminary study, the sensitivity of various motion parameters are investigated as function of the wave conditions, wind speed, turbulence intensity, wind shear as well as the spatial resolution of the numerical wind field. A more comprehensive study is under way.

Objective

This study was conducted by performing sensitivity studies to identify the relative importance of each environmental parameter to the total structural responses of HYWIND Demo based on study made by Skaare et al. [1].

Methods

- The environmental conditions studied by Skaare et al. [1] are used as base cases. Both below rated and above rated wind speeds are considered. Firstly, results were checked to be consistent with the results in Skaare et al. Then, the environmental characteristics are varied around the values corresponding to the base cases while the length of simulations were 30min.
- Environmental parameters such as wave peak period and significant wave height, the exponent (α) in wind shear profile power law, the spatial resolution of the numerical wind field and turbulence intensity of wind were changed. To perform sensitivity study of a parameter, only that parameter was changed while other environmental parameters remained unchanged.
- For each parameter, responses of the structure such as electrical generator output, platform pitch motion at nacelle level and blade out-of-plane tip motion were recorded.
- Mean and standard deviation of each response were compared to understand the importance of each parameter.

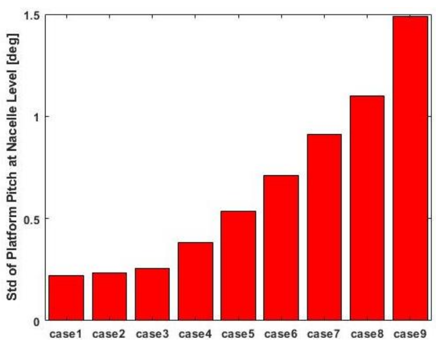

Figure 1. Sensitivity of changing H_s and T_p in below the rated wind speed (wave characteristics vary from case 1 where H_s=0.75m and T_p=6.5s to case 9 where H_s =12.25m and T_p=15.5s)

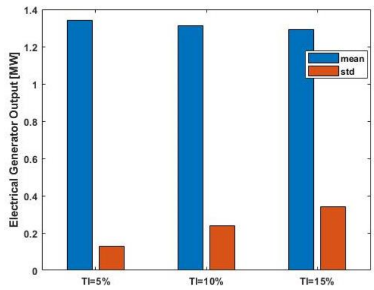

Figure 2. Sensitivity of changing turbulence intensity in below the rated wind speed (turbulence intensity varies from 5% to 15%)

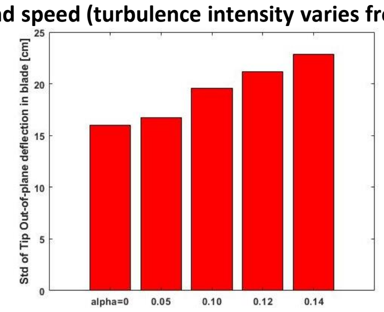

Figure 3. Sensitivity of changing alpha while TI=1% in above the rated wind speed (alpha varies from 0 to 0.14)

Results

- Higher H_s and T_p generated higher standard deviation in evaluated responses. For instance, while mean platform pitch at nacelle level is almost the same equal to 1.55 degrees in all cases, Figure 1. shows that standard deviation of platform pitch at nacelle level in case 9 where H_s=0.75m and T_p=6.5s is 1.49 degrees compared to 0.22 degree for case 1 where H_s=12.25 and T_p=15.5s.
- Higher turbulence intensity produced higher standard deviation in evaluated responses. For example, it is shown in Figure 2. that by increasing the turbulence intensity from 5% to 15%, the standard deviation of electrical generation output increases from 0.1275 to 0.341 MW, while the mean electrical generation output slightly decreases from 1.339 to 1.291 MW.
- Varying α in wind shear profile power law and the spatial resolution of the numerical wind field had no significant effect on the responses.

Conclusions

- The wave characteristics and turbulence intensity had significant influence on the dynamic behaviour of HYWIND Demo. However, within the range of parameters considered in this study, the wind shear exponent, alpha, and the spatial resolution of the numerical wind field did not show to have any significant impact on the dynamics. However, more detailed analysis is planned to investigate the impact of the wind field parameters on the dynamic response.
- High turbulence intensity of wind could be an important player that variation of alpha has no significant effect on the responses. For instance, when turbulence intensity reduced from 11 % to 1% in above the rated wind speed base case, Figure 3. shows that the standard deviation of blade out-of-plane tip motion increased from 15.98 to 22.85 cm when α increases from 0 to 0.14.

References

[1] B. Skaare, F. G. Nielsen, T. D. Hanson, R. Yttervik, O. Havmøller and A. Rekdal, "Analysis of measurements and simulations from the Hywind Demo floating wind turbine," Wind Energy, no. 18, p. 1105–1122, 2015.

Parameter Estimation of a Breaking Wave Slamming Load Model using Monte Carlo Simulation

Shaofeng Wang[1], Torben Juul Larsen[1], Ove Tobias Gudmestad[2]
[1] DTU Wind Energy, Frederiksborgvej 399, 4000 Roskilde, Denmark
[2] University of Stavanger, Kjell Arholmsgate 41, 4036 Stavanger, Norway

Introduction

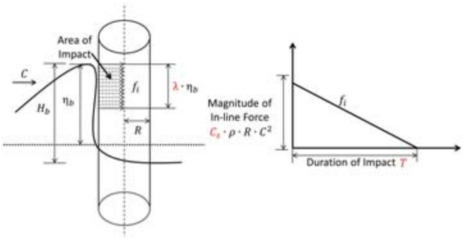

Fig 1. Breaking wave induced slamming load

- Offshore wind turbines (OWTs) are installed in intermediate and shallow water with occurrence of breaking waves.
- OWTs subjected to the breaking wave, especially plunging breakers, are excited by an impulsive impact force referred to as the slamming load influencing the design loads significantly.
- Engineering model of the slamming load with significant parameter variabilities [1, 2]:

$$F(t) = \lambda \cdot \eta_b \cdot C_s \cdot \rho \cdot R \cdot C^2 \cdot (1 - \frac{t}{T})$$

- Objective: Estimate the governing parameters: Slamming Coefficient C_s, Curling Factor λ and Impact Duration T by a combination of large-scale experimental data and numerical simulations performed with the Monte Carlo method.
- Methodology : Estimate the parameters from 5000 random MC combinations of the three parameters by comparing simulated response in HAWC2 against the measured response from a large-scale experiment.
- Monte Carlo Simulations: 5000 simulations with an independent, uniform distributed input parameters of C_s $(0.5\pi - 2.5\pi)$, λ $(0.3 - 0.5)$ and T $(0.02 - 0.26)$.

Large-Scale Experiment

- Experiment setting: regular wave (H 1.3m, T 4s, D 1.5m), sloped wave tank.

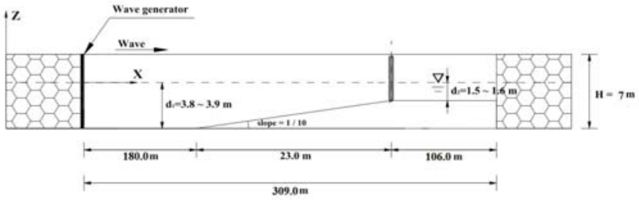

Fig 2. Experimental set up in GWK [3]

- Experiment data: wave elevation at pile, measured force at pile top and bottom. Repeated wave packets include nonbreaking wave and breaking wave.

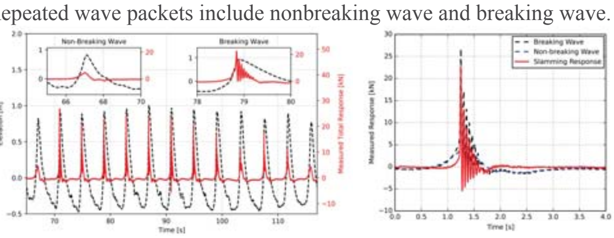

Fig 4. Measured wave elevation and total response force (left). Decomposition of slamming load response from total force measurement for a breaking wave (right)

Numerical Simulation

- OceanWave3D: fully nonlinear potential flow solver at DTU Mechanical. The wave surface elevation and wave particle kinematics are obtained.

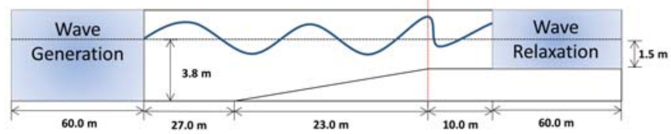

Fig 3. Numerical set up in OceanWave3D

- HAWC2: Aero-Elastic-Hydro Code at DTU Wind Energy. The quasi-static force is calculated using Morison equation associated with wave kinematics from OceanWave3D. The responses simulated from 5000 Monte Carlo simulations are quantified against experimental responses using RMSE.

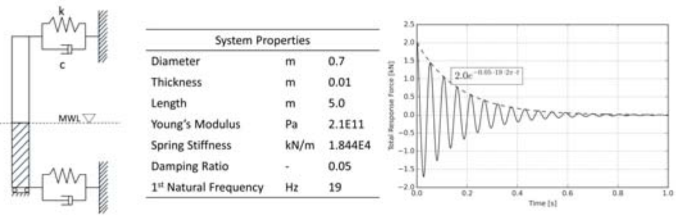

System Properties		
Diameter	m	0.7
Thickness	m	0.01
Length	m	5.0
Young's Modulus	Pa	2.1E11
Spring Stiffness	kN/m	1.844E4
Damping Ratio	-	0.05
1st Natural Frequency	Hz	19

Fig 5. Verified pile model set up in HAWC2 with first NF around 19Hz

Results

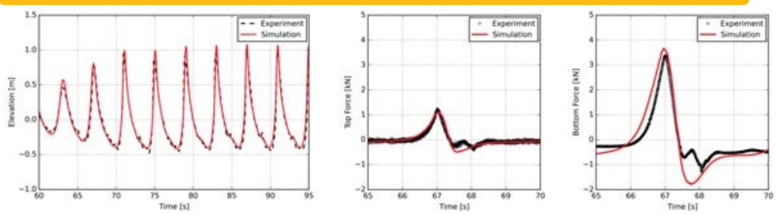

Fig 6. Wave surface elevations simulated in OceanWave3D agree well with experimental data. Response force for a non-breaking wave are simulated in HAWC2 with the wave kinematics from OceanWave3D showing good agreement with measurements

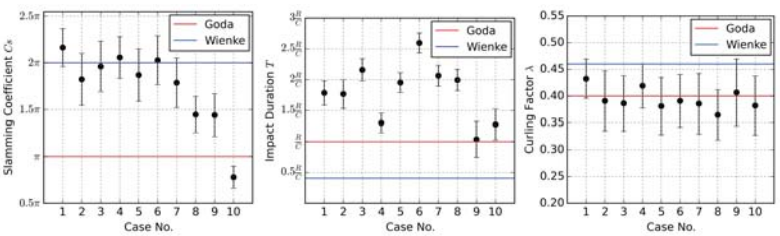

Fig 7. Estimated parameters for all breaking wave packets in the experiment

Parameter	Slamming Coefficient C_s	Impact Duration T	Curling Factor λ
Mean	1.89π	$1.95\,R/C$	0.39
Standard deviation	0.21π	$0.35\,R/C$	0.02
Goda	π	R/C	0.40
Wienke-Oumeraci	2π	$13\,R/32C$	0.46

Table 1. Statistics of the estimated parameters (case 1-8)

Conclusions

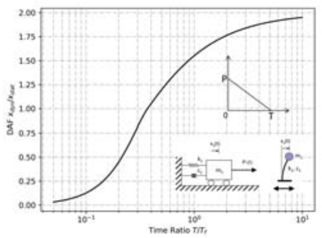

Fig 8. DAF is dependent on time ratio

- OceanWave3D reproduces highly nonlinear wave elevation with good agreement.
- The Morison's equation is able to calculate steep non-breaking wave force with wave kinematics from OceanWave3D.
- The slamming coefficient C_s and curling factor λ are close to values in Winek-Oumeraci model.
- Slamming load impact duration T is significantly larger than the values found by the Goda and Wienke-Oumeraci model, which decides the dynamic amplification for OWTs.
- For OWTs located in areas where breaking waves are present, a flexible structure is recommended to eliminate its dynamic amplifications.

References

[1] Goda Y, Haranaka S, Kitahata M. Study of impulsive breaking wave forces on piles. Report Port and Harbour Technical Research Institute. 1966 Apr;6(5):1-30.
[2] Wienke J, Oumeraci H. Breaking wave impact force on a vertical and inclined slender pile: theoretical and large-scale model investigations. Coastal Engineering. 2005 May 31;52(5):435-62.
[3] Irschik K, Sparboom U, Oumeraci H. Breaking wave characteristics for the loading of a slender pile. InProc. 28th Int. Conf. Coastal Eng., ICCE 2003 (Vol. 2002, pp. 1341-1352).

Acknowledgement

This study is a part of the project DeRisk (Grant Number 4106-00038B), which is funded by Innovation Fund Denmark. Further funding is provided by Statoil and the participating partners. All funding is gratefully acknowledged.

Emulation of ReaTHM® testing

Lene Eliassen[1], Valentin Chabaud[1,2], Maxime Thys[1]
[1]SINTEF Ocean, [2]NTNU

Model scale testing of offshore wind turbines is challenging due to the incompatibility between Froude and Reynold scaling. Real-Time Hybrid Model (ReaTHM®) testing is an experimental method where numerical simulations are combined in real-time with model testing. Using this method alleviates the scaling issue since the aerodynamic loads are simulated and applied on the physical model by use of six winches and lines connected to the tower top. These loads are calculated by FAST, and include the elasticity, aerodynamics and control system. Prior to the test in the Ocean Basin, the ReaTHM® tests are emulated by simulating the physical part of the experiments. This is an important step in the design of the experiments, used to verify the complete hybrid testing loop, to ensure the quality of the tests to be performed.

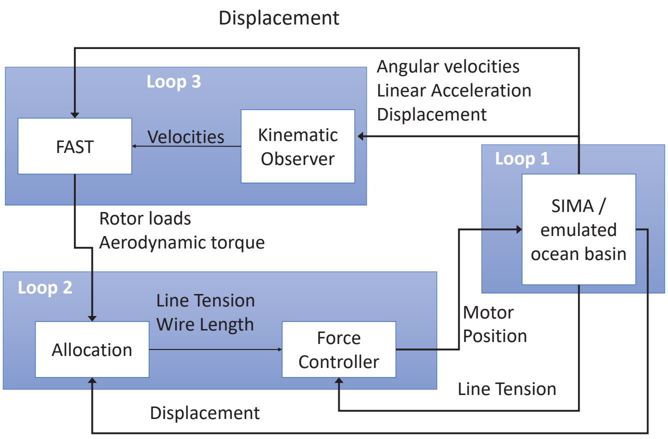

Figure 1: A schematic overview of the emulated hybrid system.

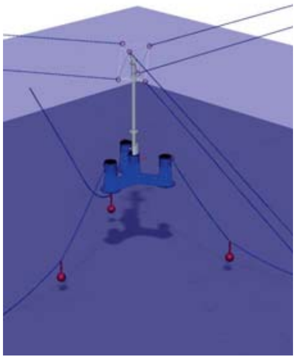

Figure 2: The OO-Star Wind Floater modelled in SIMA

DTU 10 MW RWT main properties [2]		
Rated power	10	MW
Rotor diameter	178.3	m
Hub height	119	m
Rated wind speed	11.4	m/s
Nacelle mass	446 036	kg
Rotor mass	227 962	m
Blade prebend	3.3	m

Method

An overview of the emulated hybrid system is shown in Figure 1. Loop 1 is the emulated physical experiments performed in SIMA, Loop 3 computes the aerodynamical loads based on the measured platform motions and Loop 2 is allocating the aerodynamic loads to the six different winches (see Figure 2).

From Loop 1 the displacements and velocities of the tower top are sent to Loop 3. The displacements and velocities are calculated in SIMA[4]. A Simo model is made of the OO-Star Wind Floater in SIMA. Simo is a time domain simulation program for study of motions and station-keeping of multibody system developed at SINTEF Ocean [3].

The FAST module in Loop 3 estimates the rotor loads. The FAST module contains a dll of the FAST program (v8, with AeroDyn v14) developed at NREL, which is an aero-hydro-servo-elastic software [5]. Only the first flapwise mode is included in the aeroelastic calculation in FAST, the remaining elastic modes are stiff. The weight of the rotor is included in both the Simo model and in the FAST calculation, thus, the rotor loads transferred from the FAST module in Loop 3 does therefore not contain the gravitational and inertial loads.

The rotor loads are transferred from the FAST module in Loop 3 to the Allocation module in Loop 2. The Allocation module transfers the rotor loads to commanded line tension. The Force Controller module takes the line tensions as input and controls the winches to obtain the desired tension, which is sent to the SIMA module in Loop 1.

Floating Offshore Wind Turbine Model

Hybrid testing of a semi-submersible floating wind turbine was conducted in the wave basin at SINTEF Ocean in fall 2017 as a part of the EU project Lifes50+[6]. The wind turbine tested was the OO-Star Wind Floater, which is developed by Dr Tech Olav Olsen and is a semi-sub platform for floating wind turbines [1]. The platform consists of a star shaped pontoon, which connects the central column to three outer columns. The mooring system is a catenary system with three mooring lines. The rotor used is from the DTU 10 MW reference wind turbine[2].

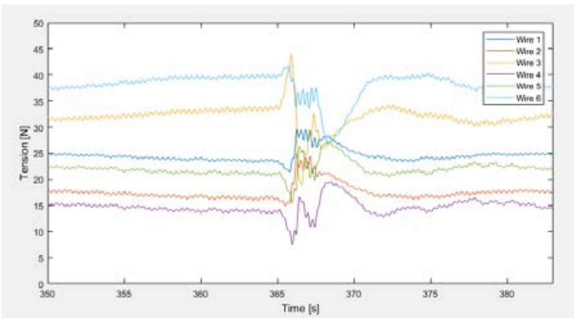

Figure 4: The commanded line tensions in the 6 wires for the ECD test

Acknowledgement

Also, we are grateful to Dr. techn. Olav Olsen AS for the permission and contribution to set up the public 10MW semi-submersible design based on their concept of the OO-Star Wind Floater (www.olavolsen.no).

Discussion

The emulated testing prior to the hybrid tests in the ocean basin is valuable both for increased quality of the tests and for the safety. It is possible to investigate the tension in the wires prior to the tests and establish that they are within the maximum and minimum levels. The tests giving the highest tension loads were the extreme wind tests; extreme operating gusts (EOG) and extreme coherent gust with direction change (ECD). The tension in the wind lines for the emulated ECD test is shown in Figure 4.

The effect of flexible blades compared to stiff blades was also investigated. In the left graph of Figure 5, the blade tip deflection of a stiff blade (no elasticity), a flexible blade (only the first flapwise mode of the blade included) and the full-flexible blade (first and second flapwise mode and the first edgewise mode are activated). The difference between the fully flexible blade and the flexible blade is small, however the difference is large for a stiff blade, around 8 m. This has an effect on the global response of the platform, which is illustrated in the right graph of Figure 5. Here the spectra of the platform pitch is shown for one turbulent wind case, and one can see that the platform pitch response is dependent on the elasticity of the blade. The flexible blade was chosen for the hybrid tests as this provided an increase in accuracy, but kept the computational time to a low level. It is important to limit the computational efforts since the hybrid tests are real-time and downscaled.

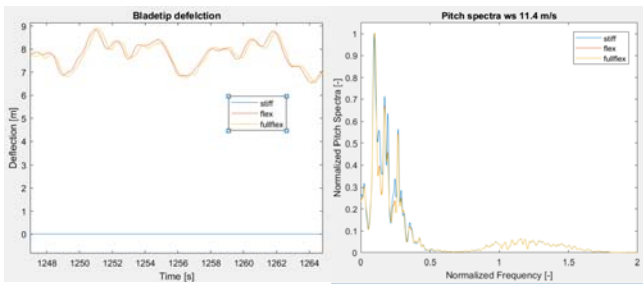

Figure 5: The blade tip deflection and the platform pitch spectra for the OO-Star wind floater. The frequencies are normalized with the wave frequency and the spectra value with the maximum value.

Referanser
[1] O. Olsen, "OO-Star Wind Floater," [Online]. http://www.olavolsen.no/nb/node/149.
[2] Bak C., Zahle F., Bitsche R., Kim Z., Yde A., Henriksen L. C., Natarajan A., Hansen M. H., Description of the DTU 10 MW Reference Wind Turbine, DTU Wind Energy Report-I-0092, July 2013
[3] Simo – Simulation of Marine Operations [Online] https://www.sintef.no/globalassets/project/oilandgas/pdf/simo.pdf
[4] Sima - SINTEF [Online]. https://www.sintef.no/programvare/sima/
[5] FAST v8|NWTC Information Portal [Online] https://nwtc.nrel.gov/FAST8
[6] Thys M., Eliassen L., Chabaud V. B. Real-Time Hybrid Model Testing of semisubmersible 10 MW floating wind turbine. To be published in Proc. Of 37th OMAE conf. 2018

The research leading to these results has received funding from the European Union Horizon2020 programme under the agreement H2020-LCE-2014-1-640741

Multiple-degree-of-freedom actuation of rotor loads in model testing of floating wind turbines using cable-driven parallel robots

Valentin Chabaud, NTNU/SINTEF Ocean (valentin.chabaud@ntnu.no)

Lene Eliassen, SINTEF Ocean   Maxime Thys, SINTEF Ocean   Thomas Sauder, NTNU AMOS/SINTEF Ocean

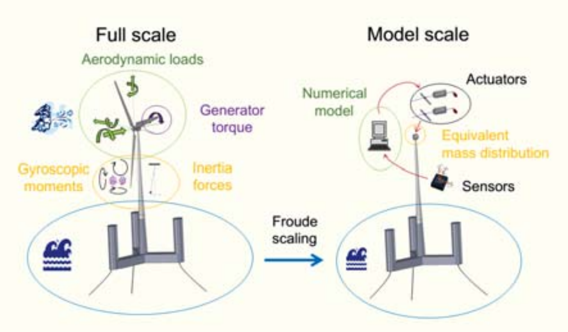

ReaTHM® testing circumvents limitations of hydrodynamic laboratories, and in particular inherent issues of physical wind/wave testing of floating wind turbines. The rotor and wind field are numerical and interact in real tim with the scale model subjected to physical hydrodynamic loads, by means of sensors and actuators.

Actuator requirements:

- Force-based (actuate loads, not motions)
- Multiple-degree-of-freedom (thrust, pitch and yaw moments, gen. torque, hor. shear force)
- Large workspace (follow the structure anywhere it moves)
- High accuracy and bandwidth (up to 3p frequency)

Cable-driven parallel robots (set of motor-winch-cable 1DOF actuators)

Lines should be kept in tension → One more line than actuated load components →

1 From where and in which direction should they pull on the structure?

2 How to allocate tensions from rotor loads, and how to control pretension?

$$\textit{Line tension setpoint vector} = f(\textit{motor locations, line attachment point locations on structure, motions, loads to actuate, pretension})$$

NOWITECH setup

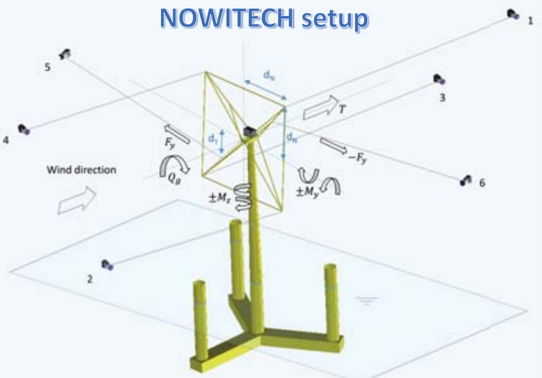

Line nr	Function
1	Thrust force/2 + Pitch moment/2d_N + Pretension
2	Pitch moment/2d_N – Yaw moment/2d_N + Pretension
3	Thrust force/2 – Yaw moment/2d_N + Pretension
4	Pretension
5	Generator torque/2d_T + Shear force/2
6	Generator torque/2d_T – Shear force/2

Similarity with physical rotor: *Intuitive*

1 Design

VS

LIFES50+ setup

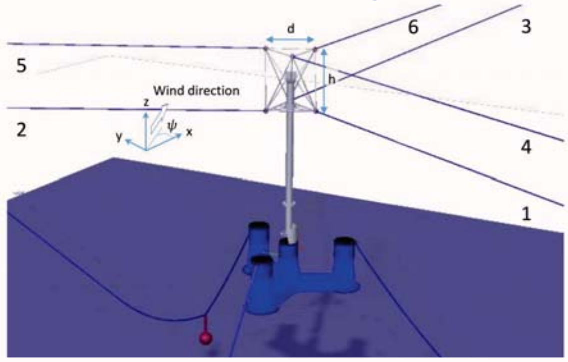

Rotational symmetry: *Flexible*

- Each line contributes to each load component depending on the wind direction ψ
- Pretension is added to all lines

Coefficient line nr i	Load component
$cos\left(\psi+\frac{2i\pi}{3}\right)/3$	Thrust force
$-sin\left(\psi+\frac{2i\pi}{3}\right)/3$	Shear force
$(-1)^{\left\lfloor\frac{i+2}{3}\right\rfloor}\frac{2}{3h}sin\left(\psi+\frac{2i\pi}{3}\right)$	Generator torque
$(-1)^{\left\lfloor\frac{i+2}{3}\right\rfloor}\frac{2}{3h}cos\left(\psi+\frac{2i\pi}{3}\right)$	Pitch moment
$(-1)^{\left\lfloor\frac{i+2}{3}\right\rfloor}\frac{1}{\sqrt{3}d}$	Yaw moment

2 Allocation strategy

Minimize Euclidean norm of line tension setpoint vector: stay close to reference
Convenient

VS

Specify tension on one particular line
Intuitive

VS

Minimize higher-order norm of line tension setpoint vector: stay away from slack and peaks
Performant

Power spectral densities of Euclidean and infinte norms of commanded tension vector at near-cutout condition (25 m/s), from LIFES50+ model tests

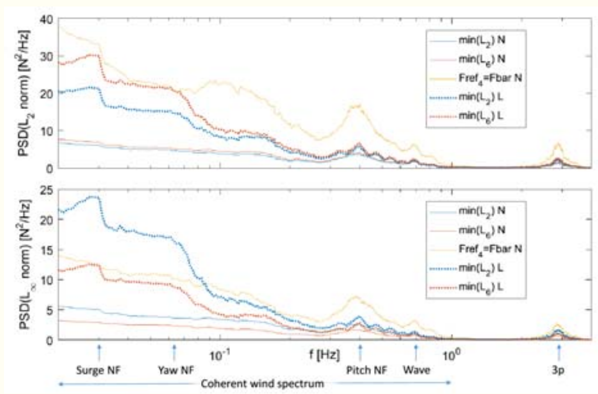

Results

1 Line tensions need to adjust for changes in model orientation more with the LIFES50+ setup than with the NOWITECH one
→ Higher line tensions, as a drawback among the many avantages of the LIFES50+ setup

2
- The intuitive strategy (setting line 4 to reference tension in NOWITECH setup) gives physical meaning to the cost of much higher tensions
- Using higher-order norm as minimization objective is significantly more effective in keeping tensions further away from slack and excessively high values than using the Euclidean norm. The tensions still stay close to reference when using higher-order norms. → It should be used
- The choice of the norm to minimize is less important for the NOWITECH setup

NOWITECH · NTNU · LIFES50+ · SINTEF OCEAN

The research leading to these results has received funding from the European Union Horizon2020 programme under the agreement H2020-LCE-2014-1-640741

KPN Hybrid
This work has been funded by the Research council of Norway, contract no. 193823

References

[1] Valentin Chabaud, *Real-Time Hybrid Model Testing of Floating Wind Turbines*, Phd thesis, NTNU, 2016
[2] Gosselin et al.., *On the determination of the force distribution in overconstrained cable-driven parallel robots*. Meccanica, 46(1):3-15, 2011
[3] Thys et al., *Real-Time Hybrid Model Testing of a semisubmersible 10 MW floating windTurbine*, to be published in Proc. Of 37th OMAE conf., 2018

A 6DoF hydrodynamic model for real time implementation in hybrid testing

L. Delbene, I. Bayati*, A. Facchinetti, A. Fontanella & M. Belloli

Dipartimento di Meccanica, Politecnico di Milano
Via La Masa 1, 20156, Milano, Italy.
**ilmasandrea.bayati@polimi.it*

Abstract

This work deals with the numerical approach and technical implementation of the 6-DoF hydrodynamic model, which is combined with the Politecnico di Milano HexaFloat robot (Fig.1,2), adopted for wind tunnel Hybrid/HIL tests floating offshore wind turbines.

The wind tunnel hybrid testing methodology, along with its ocean-basin counterpart [1], is currently being considered as a valuable upgrade in the model scale experiments, for its capability to reduce the effect of the typical scaling issues of such systems.

The work reports an overview of the setup and the testing methodology, presenting briefly the main challenges about the deployment on the real-time hardware and summarizing the key solving choices. A set of results related to code-to-code comparison between the optimized HIL numerical model and the reference FAST [2] computations are included, confirming the correctness of the approach.

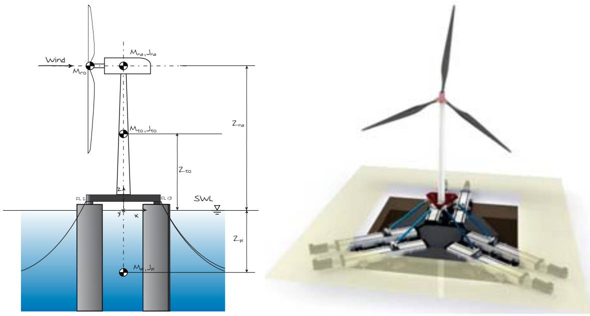

Figure 1: SWE Triple Spar concept (left) [3], whose FAST model is taken as reference, and Politecnico di Milano 6-DoF Hybrid/HIL wind tunnel setup (right), [5].

Figure 2: Hexafloat robot [5] (left) and fully controlled 1/75 aero-elastic scale model of the 10 MW DTU reference wind turbine (right), [6], [7].

1 Numerical model

Equations of motions:

$$[M_s + A_\infty]\,\underline{\ddot{x}} + [R_s]\,\underline{\dot{x}} + [K_s]\,\underline{x} = \underline{F}_{hydro} + \underline{F}_{aero} \tag{1}$$

aerodynamic forces $\underline{F}_{aero}$ measured by dynamometric balance $\underline{F}_{bal}$ placed at the tower's base combined with a correction $\underline{F}_{corr}$ due to inertial and gravitational contributions of the scale model (no Froude scaling):

$$\underline{F}_{aero} = \underline{F}_{bal} + \underline{F}_{corr} \tag{2}$$

$$\underline{F}_{corr} = [M_t]\underline{\ddot{x}} + [K_t]\underline{x} \tag{3}$$

$$\underline{F}_{hydro} = \underline{F}_{rad} + \underline{F}_{diff} + \underline{F}_{visc} + \underline{F}_{moor} \tag{4}$$

Platform radiation, diffraction and viscous forces ($\underline{F}_{rad}$, $\underline{F}_{diff}$ and $\underline{F}_{visc}$) are implemented as in [4] (extended to 6 DoF). Mooring line forces $\underline{F}_{moor}$ are included through a lumped-mass model, as in [8], where the internal nodes' contributions are: tensile load $\underline{T}$, damping $\underline{C}$, weight $\underline{W}$, contact with seabed $\underline{B}$ and viscous drag forces $\underline{D}$, depending on the nodes' position $\underline{r}$ and/or velocities $\underline{\dot{r}}$.

$$[M(\underline{r})]\,\underline{\ddot{r}} = \underline{F}_{moor}(\underline{r},\underline{\dot{r}}) = \underline{T}_{i+1/2}(\underline{r}) - \underline{T}_{i-1/2}(\underline{r}) + \underline{C}_{i+1/2}(\underline{\dot{r}},\underline{r}) - \underline{C}_{i-1/2}(\underline{\dot{r}},\underline{r}) + \underline{W}_i + \underline{B}_i(\underline{\dot{r}},\underline{r}) + \underline{D}_{p_i}(\underline{\dot{r}}) + \underline{D}_{q_i} \tag{5}$$

The mass matrix $[M]$ includes also the hydrodynamic added masses of each node $[a_i]$:

$$[M(\underline{r})] = [m] + [a(\underline{r})] \tag{6}$$

2 Modelling optimization

Simplification of the model, without loosing physical consistency, is required due to real-time constraints. As an example, the importance of each contribution of Eq.5 is evaluated for combined decay tests.

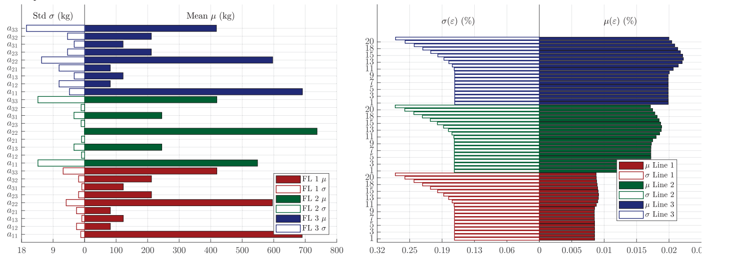

Figure 3: Added mass $[a_i]$ contribution (Eq.6) for the node # 20 for the combined decay tests $\underline{x} = \{x, y, z, \varphi, \vartheta, \psi\}^T = \{20\,m, 20\,m, 10\,m, 15°, 15°, 15°\}^T$ (left) and strain ϵ contribution for the internal nodes (#2-20) in the same decay tests (right).

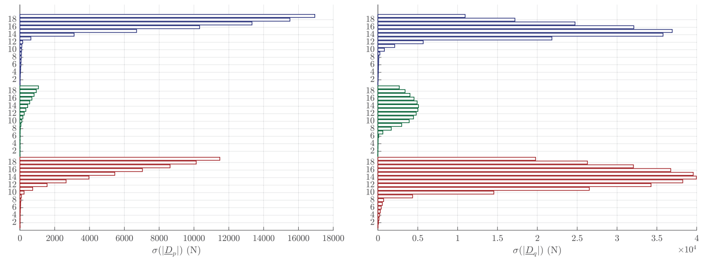

Figure 4: Viscous transverse D_p (left) and tangential D_q (right) damping contribution for the internal nodes (#2-20) in the combined decay tests $\underline{x} = \{x, y, z, \varphi, \vartheta, \psi\}^T = \{20\,m, 20\,m, 10\,m, 15°, 15°, 15°\}^T$.

	1	2	3	4	5	6	7	8	9	10	11	12	13	14	15	16	17	18	19	20	21
M	$\underline{\triangle}$	–	–	–	–	–	–	–	–	–	–	–	–	–	–	–	–	–	–	–	$\triangle$
$\underline{T}$	$\underline{\triangle}$	–	–	–	–	–	–	–	–	–	–	–	–	–	–	–	–	–	–	–	$\triangle$
$\underline{C}$	$\underline{\triangle}$	–	–	–	–	–	–	–	–	–	–	–	–	–	–	–	–	–	–	–	$\triangle$
$\underline{D}_p$	$\underline{\triangle}$	✗	✗	✗	✗	✗	✗	✗	✗	✓	✓	✓	✓	✓	✓	✓	✓	✓	✓	✓	$\triangle$
$\underline{D}_q$	$\underline{\triangle}$	✗	✗	✗	✗	✗	✗	✗	✗	✓	✓	✓	✓	✓	✓	✓	✓	✓	✓	✓	$\triangle$
$\underline{B}$	$\underline{\triangle}$	–	–	–	–	✓	✓	✓	✓	✓	✓	✓	✓	✓	✗	✗	✗	✗	✗	✗	$\triangle$

Table 1: Summary of the inclusion in the model of the various mooring line's force contributions from the internal nodes, from anchor ($\underline{\triangle}$) to fairlead ($\triangle$): constant nodes (–), potentially constant (–), varying (✓) and neglected (✗). Nodes (–) are kept variable due to numerical (integration) issues.

	f (Hz)	f (Hz)	p	p	q	q
	HIL	**FAST**	**HIL**	**FAST**	**HIL**	**FAST**
Surge	0.0052	0.0050	0.24	0.28	0.039	0.033
Sway	0.0049	0.0049	0.26	0.30	0.034	0.028
Heave	0.0628	0.0628	0.31	0.31	0.015	0.015
Roll	0.0360	0.0361	0.38	0.32	-0.059	-0.018
Pitch	0.0380	0.0380	0.35	0.29	-0.037	0.001
Yaw	0.0134	0.0134	0.10	0.10	0.014	0.017

Table 2: Summary of the comparison between the real-time HIL model and the reference FAST model, including the natural frequencies f, the linear and quadratic damping parameters p and q.

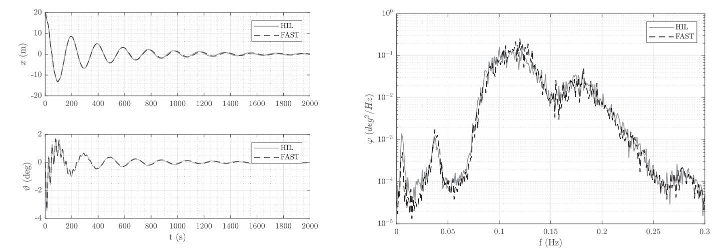

Figure 5: Surge x and pitch ϑ decay comparison (left) and pitch ϑ PSD comparison for irregular sea, $H_s = 2.2m$ and $T_p = 8s$ (right).

3 Conclusions

In Fig.5 the free decay and irregular sea results results are reported to compare the HIL model to the reference FAST one, for a subset of selected DoF, that are those envisaging the most significant amplitudes. The HIL model shows an almost overlapped behaviour. The same conclusions can be drawn looking at Tab.2, which reports the corresponding natural frequencies, linear and quadratic damping p and q, respectively defined as intercepts and slope of the graph $\frac{\Phi_n - \Phi_{n+1}}{1/2(\Phi_n + \Phi_{n+1})}$ Vs $\frac{1}{2}(\Phi_n + \Phi_{n+1})$, being Φ_n and $+\Phi_{n+1}$ the peaks of two consequent cycles of the DoF.

Tab.2 confirms the correctness of the procedure reported, where very close values between HIL and FAST can be seen. This confirms that the sensitivity analysis, supporting the definition of the simplified real-time model, can be considered satisfactory.

References

[1] Bachynski, Erin Elizabeth; Thys, Maxime; Sauder, Thomas Michel; Chabaud, Valentin Bruno; Sther, Lars Ove. (2016) *"Real-time hybrid model testing of a braceless semi-submersible wind turbine. Part II: Experimental results.* ASME 2016 35th International Conference on Ocean, Offshore and Arctic Engineering - Volume 6: Ocean Space Utilization; Ocean Renewable Energy.

[2] Jonkman J., Buhl Jr. M., *"FAST users guide"*, NREL TechRep, August 2005.

[3] Lemmer F, Amann F, Raach S et al., *"Definition of the SWE- TripleSpar Floating Platform for the DTU 10MW Reference Wind Turbine"*, Technical report, University of Stuttgart, 2016.

[4] Bayati, I., Belloli, M., Facchinetti, A. *"Wind tunnel 2-DOF hybrid/HIL tests on the OC5 floating offshore wind turbine* (2017) Proceedings of the International Conference on Offshore Mechanics and Arctic Engineering - OMAE, 10,

[5] Bayati, I., Belloli, M., Ferrari, D., Fossati, F., Giberti, H. *"Design of a 6-DoF robotic platform for wind tunnel tests of floating wind turbines* (2014) Energy Procedia, 53 (C), pp. 313-323.

[6] Bayati, I., Belloli, M., Bernini, L., Zasso, A. *"Aerodynamic design methodology for wind tunnel tests of wind turbine rotors* (2017) Journal of Wind Engineering and Industrial Aerodynamics, 167, pp. 217-227.

[7] Bayati I, Belloli M, Bernini L et al., *"Scale model technology for floating offshore wind turbines"*, IET Renewable Power Generation, 2017.

[8] Matthew Hall, Andrew Goupee, *"Validation of a lumped-mass mooring line model with DeepCwind semi submersible model test data"*, Technical report, University of Maine, 2015

Kalman estimation of position and velocity for ReaTHM testing applications

Eirill Bachmann Mehammer[1,5], Martin Føre[2], Thomas Sauder[2,4], Valentin Chabaud[3] and Thomas Parisini[1]
[1]Dept. Of Electrical and Electronic Engineering, Imperial College London, SW7 2AZ, UK
[2] SINTEF Ocean, P.O. Box 4762 Torgard, NO-7465 Trondheim, Norway
[3]Dept. of Marine Technology, NTNU, NO-7491 Trondheim, Norway
[4]Centre for Autonomous Marine Operations and Systems (NTNU AMOS), Marine Technology Centre, NO-7491 Trondheim, Norway
[5]Present address: SINTEF Energy Research, P.O. Box 4761 Torgarden, NO-7465 Trondheim, Norway

Introduction

•Model testing can reduce the costs of offshore wind turbines (OWTs).

•Real-time hybrid model (ReaTHM) testing provides solution to challenges related to such tests.

•The system is divided into physical and numerical substructure.

•State estimator is designed to estimate and filter the positions and velocities of the physical substructure.

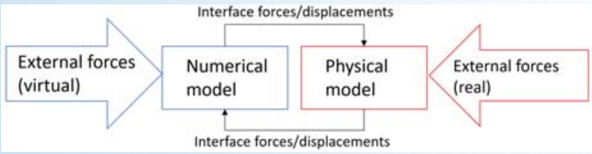

Numerical Model

Two different versions of the system are designed for tests using virtual and physical data:

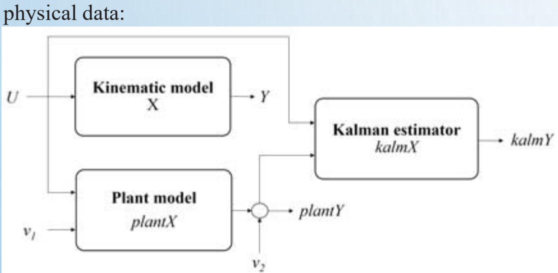

Virtual data

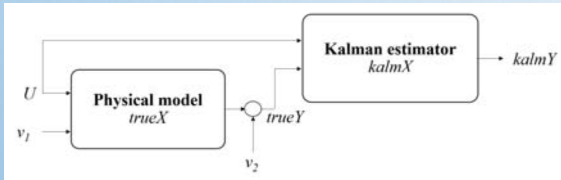

Physical data

Kinematic model

• Can represent the motion of any floating structure in 6-DOF.
•Plant model intended to simulate the physical system is implemented using the same state-space matrices.
•State vector consists of the variables to be estimated.
•Output vector consists of the variables which can be measured.
•System matrices are defined according to Fossen [1].
• Simplified model for tests with SIMA: linear and time-invariant.

Estimator design

•Kalman estimator chosen since it provides optimal estimates, minimizing the estimation error in the statistical sense.
•Both steady-state and time-varying versions are designed, implemented in MATLAB and tested.

References

[1] Fossen T I 2011 *Handbook of Marine Craft Hydrodynamics and Motion Control* (Chichester, UK: John Wiley & Sons, Ltd.)
[2] Vilsen S A, Sauder T and Sørensen A J 2017 *Dyn. Coupl. Struct.* **4** 79-92

Sensitivity analyses using virtual data

Sensitivity analyses addressing the robustness towards different types of disturbances are performed to identify the limits of the estimator. Time-varying Kalman estimator used for signal loss, otherwise steady-state version is used.

Measurement noise (SNR=10dB)

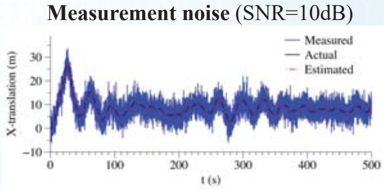

Uncertainties in *R* (x10)

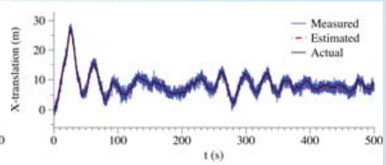

Signal loss (10 time steps, 4 instants)

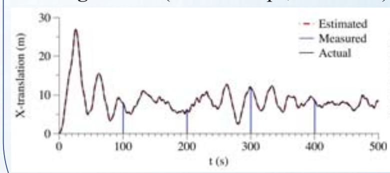

Time delays (1 time step)

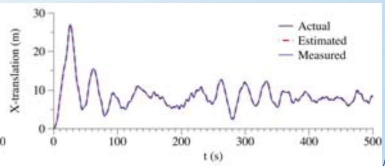

The estimator is robust towards noise, uncertainties, time delays and signal loss.

Validation of estimator using physical data

Both versions of the Kalman estimator are further tested against the laboratory experiments by Vilsen et al. [2]. Knowledge about delays and inaccuracies in the sensors used is taken into account.

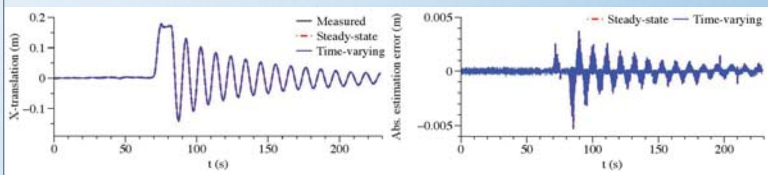

Comparison of steady-state and time-varying Kalman estimates with physical data

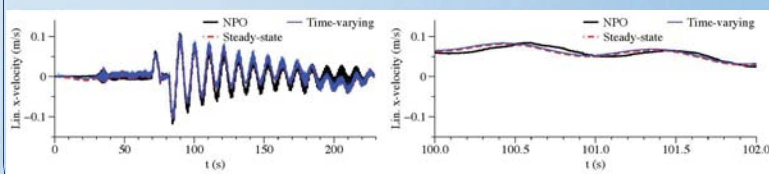

Comparison of steady-state and time-varying Kalman estimates with NPO

Good results are obtained for both versions of the Kalman estimator.

Conclusions

- The generic kinematic model developed can recreate the SIMA simulated motions with reasonable accuracy.
- A Kalman estimator providing smooth and accurate position and velocity estimates in 6-DOF is designed, implemented and tested.
- The estimator is proven to be robust towards different types of disturbances.
- The estimator is able to estimate the states with a good accuracy, when compared with physical measurements.
- An improvement from the previously implemented estimators is demonstrated.

Numerical modelling and validation of a semisubmersible floating offshore wind turbine under wind and wave misalignment

Sho Oh[1], Toshiya Iwashita[1], Hideyuki Suzuki[2]
1) ClassNK, 2) University of Tokyo

1. Introduction

Coupled aero-hydro-servo-elastic simulation tools play important role in the design of offshore floating wind turbines. For rational design of the system, accuracy of the numerical tool is important in predicting the system responses. While the load cases where the wind and wave are aligned are sometimes the largest contributor to the design, evaluation of the load cases where the wind and wave are in misaligned condition are also required in the design codes. In this study, first a series of water tank test is performed for a 1/50 scale semisubmersible floater and results for irregular wave tests with aligned and misaligned wind were analyzed. Then, an in-house numerical tool, NK-UTWind is used to model the full scale system, and results for aligned and misaligned cases are validated.

2. Water tank test

The water tank test were conducted using a 1/50 scale semisubmersible floater with 2MW wind turbine at Ocean Engineering Basin of National Maritime Research Institute, Japan, in July 2011. To simplify the effect from the moorings, tout mooring was chosen for the system.

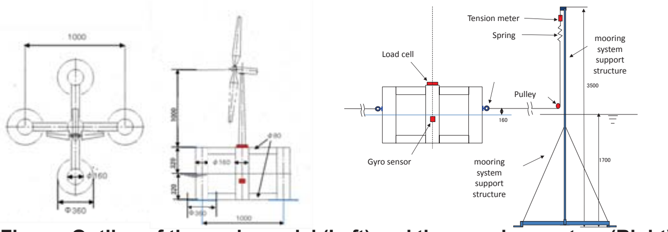

Figure. Outline of the scale model (Left) and the mooring system (Right)

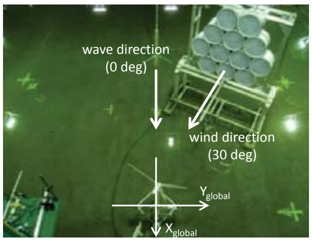

Figure. Picture of main shaft measurement

Results for irregular waves with the wind turbines in steady rotation are used for the validation. The wave conditions, wind conditions and wind turbine rotational conditions are the same for the two cases, except the direction of the wind and the nacelle yaw are set in 30 degree misalignment to the wave direction for the misaligned case.

Table. Test conditions for the validation

Wave condition	Wind condition	RPM	Duration	Blade pitch
JONSWAP, $\gamma = 3.3$ Hs=6 m, Ts=13.01s	U=13.05m/s, Iu=5.9%	22.0	6120 sec	2.4 deg

3. Numerical modelling

NK-UTWind is an in-house code of coupled analysis for floating offshore wind turbine developed by ClassNK and University of Tokyo. The code solves the equation of motion for wind turbine support structure modelled with FEM beams. The hydrodynamics for the platform is evaluated with Morison equation, and the forces from the wind turbine calculated with FAST are passed to NK-UTWind as tower top loads. The mooring lines are modeled using linear spring in this study.

The added mass coefficient Cm and the drag coefficient Cd in Morison equation as well as the Rayleigh damping term were calibrated using the free decay tests. Most of the calibrated coefficients were in the range of theoretical values for cylinders. Rayleigh damping was obtained as 2.5% from the results of linear damping coefficients.

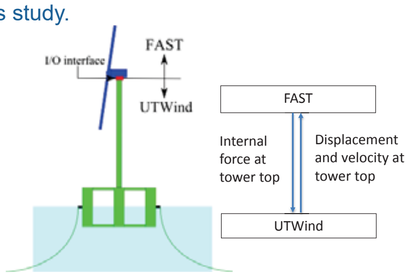

Figure. Outline of the coupling of NK-UTWind and FAST

Table. Calibrated added mass and drag coefficients

	Centre Column (X, Y)	Centre Column (Z)	Side Column (X, Y)	Side Column (Z)	Horizontal Brace (X, Y)
C_m	0.9	1.0	0.75	0.57	0.9
C_D	1.0	5.0	1.0	6.0	1.0

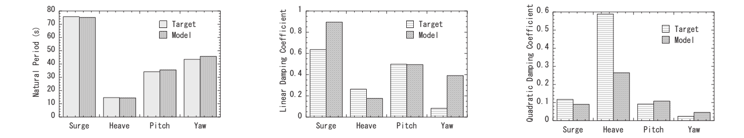

Figure. Comparison of calculated and measured natural period (left), linear damping coefficient (middle) and quadratic damping coefficient (right)

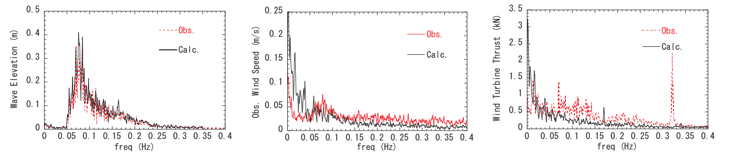

Figure. Comparison of calculated and measured amplitude spectra of wave (left), wind (middle), and wind turbine thrust force (left)

4. Results

Comparison of the calculated and measured floater motions for aligned and misaligned wind and wave conditions are shown in the figures below. Measured motions in surge, heave, and pitch are similar for the aligned and misaligned cases, while sway and roll motion were dominated by components in the natural frequency for the aligned case, while the wave frequencies are also excited for the misaligned case. Calculations agreed well with the measurement for the roll motion, while several peaks were not captured by the calculation for the sway motion.

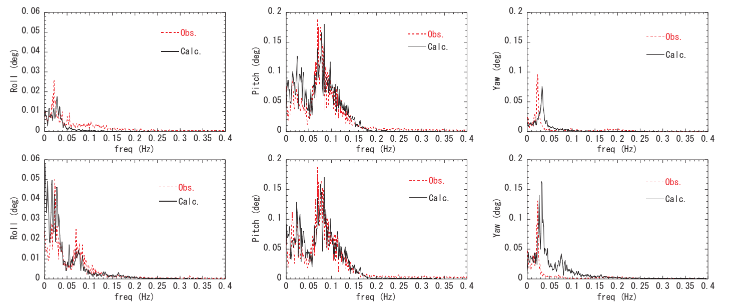

Figure. Amplitude spectra of the floater rotational motion for the aligned case (Upper Row) and the misaligned case (Lower Row)

The characteristics of frequency distribution of measured tower-base My were similar for both aligned and misaligned cases. Measured tower-base Mx showed that while the roll natural frequency component was dominant in the aligned case, the wave frequencies are also excited in misaligned case

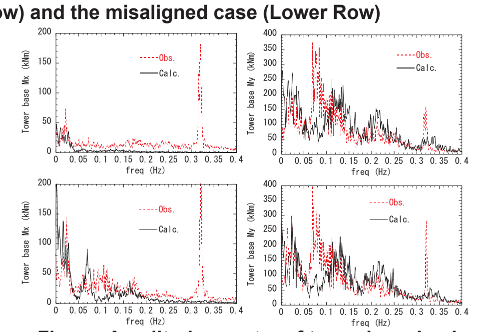

Figure. Amplitude spectra of tower base loads for the aligned case (Upper Row) and the misaligned case (Lower Row)

5. Conclusion

Measured surge, heave, and pitch motions and tower-base Fx and My loads are similar for the aligned and misaligned cases, and were well reproduced by the calculation. Measured sway and roll motion and tower-base Fy and Mx loads were dominated by components in natural frequency for the aligned case, while the components in wave frequencies increases for the misaligned case. Calculation agreed with the measurement for roll motion, while other responses needed further investigation.

Impact on wind turbine loads from different down regulation control strategies

Christos Galinos, Torben J. Larsen and Mahmood Mirzaei
Technical University of Denmark, Department of Wind Energy, Loads and Control, DTU Risø Campus, Fredriksborgvej 399, 4000 Roskilde

Abstract

Three characteristic derating strategies on the upstream wind Turbine are studied and the load impact to the downstream one is assessed. These are defined as minimum/maximum rotor speeds (minRS, maxRS) and minimum thrust (minT) modes. Derating factors of 20% and 40% on available power are applied together with 4 and 7 diameters WT interspace. The study is based on aeroelastic simulations of a 2MW generic WT model including wake effects. The results show that below rated wind speed (8m/s) the downstream WT blade flap fatigue loads are minimized when the upfront WT is derated with the minRS strategy. The maxRS mode returns always the highest loads. When the WTS are aligned with the wind direction (full wake situation) the load levels for minRS and mint strategies are almost equal. Above rated wind speed (16m/s) the tendency is the same as at 8m/s. Finally, the fore-aft fatigue loads on the tower base and the main bearing yaw moment follow the same trends as the blade for both below and above rated wind speed.

Objective

Power down regulation can be done in different ways by adjusting the rotor speed and blade pitch angle on the individual turbines, which affect the fatigue loads on the turbine components. Until know the main focus was on power optimization [4, 5] and there has been limited documentation on the load variations as a result of different down-regulation strategies on wind turbines under wakes.

Main objective: Load impact for three characteristic derating strategies on the upstream WT to the downstream one

Method

- High fidelity aeroelastic simulations
  - HAWC2 - Including the Dynamic Wake Meander model (DWM) [1, 2, 3]
  - Generic 2MW Wind Turbine (WT)
  - Two WTs in wind farm configuration
  - Upfront WT-2 is down-regulated, downstream WT-1 normal operation
- Wind farm derating control strategies
  - minimum/maximum rotor speeds (minRS, maxRS)
  - Minimum thrust (minT)
- Cases
  - Down regulation by 20% and 40% on available power
  - WT interspaces of 4 and 7 Diameters (D)
  - Ambient wind speed and direction: 8m/s, 16m/s and ±15 degrees

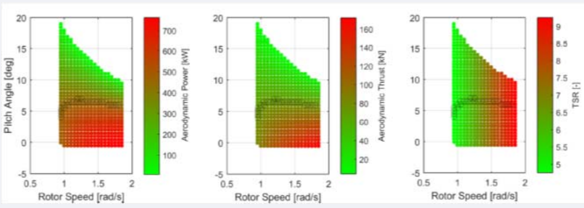

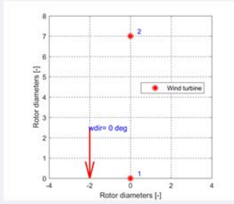

Key parameters of the WT aeroelastic model

Parameter	Value
Rotor Orientation	Clockwise rotation - Upwind
Control	Variable speed and collective pitch
Controller	DTU controller
Number of blades	3
Rotor diameter	80 m
Rated electrical power	2 MW
Cut-in wind speed	3 m/s
Cut-out wind speed	25 m/s
Hub-height	69 m
Rotor pre-cone angle	2 deg
Shaft tilt angle	6 deg

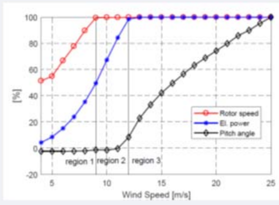

Results

- Equivalent fatigue loads on downstream WT-1

Blade root flapwise BM

Tower base fore-aft BM

Main bearing yaw moment

Wind Speed 8m/s

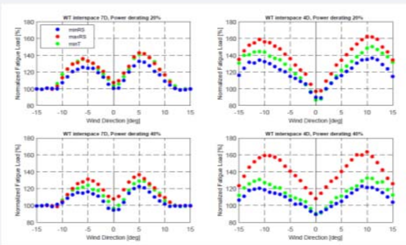

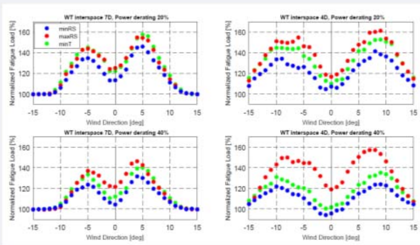

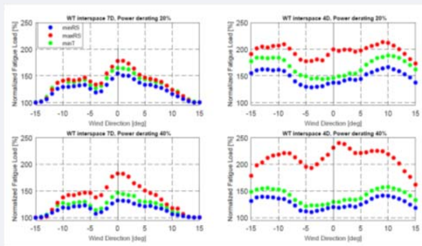

Wind Speed 16m/s

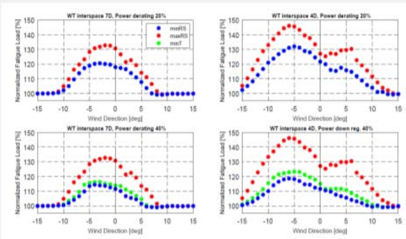

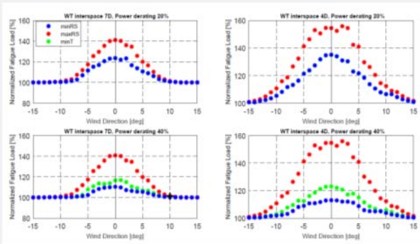

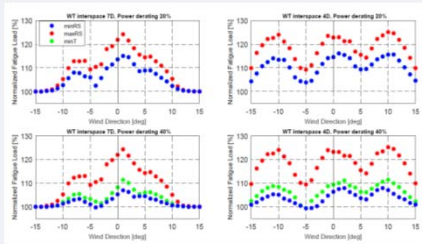

Conclusions

- Below rated wind speed (8m/s) the downstream WT blade flap loads are minimized when the upfront WT is derated with the minRS strategy
- The maxRS mode returns always the highest loads variations
- The load levels for minRS and minT strategies are almost equal when the WTS are aligned with the wind direction (full wake situation)
- Above rated wind speed (16m/s) the tendency is the same as at 8m/s
- Tower base fore-aft fatigue loads and main bearing yaw moment follow the same trend as the blade for both below and above rated wind speed.

References

1. Larsen, T. J., Madsen, H. A., Larsen, G. C., & Hansen, K. S. (2013). Validation of the dynamic wake meander model for loads and power production in the Egmond aan Zee wind farm. Wind Energy, 16(4), 605–624.
2. Larsen, T. J., Larsen, G. C., Madsen, H. A., & Petersen, S. M. (2015). Wake effects above rated wind speed. An overlooked contributor to high loads in wind farms. Scientific Proceedings. Ewea Annual Conference and Exhibition 2015, 95–99.
3. Madsen, H. A., Larsen, G. C., Larsen, T. J., Troldborg, N., & Mikkelsen, R. F. (2010). Calibration and Validation of the Dynamic Wake Meandering Model for Implementation in an Aeroelastic Code. Journal of Solar Energy Engineering, 132(4).
4. Mirzaei, M., Göçmen Bozkurt, T., Giebel, G., Sørensen, P. E., & Poulsen, N. K. (2015). Turbine Control Strategies for Wind Farm Power Optimization. Proceedings of 2015 American Control Conference, 2015-, 1709–1714.
5. Mirzaei, M., Soltani, M., Poulsen, N. K., & Niemann, H. H. (2014). Model based active power control of a wind turbine. Proceedings of the American Control Conference, 5037–5042

Acknowledgments: **This work is part of the CONCERT project (CONtrol and unCERTainties in real-time power curves of offshore wind power plants), which is funded by ForskEL Programme under contract 12396.**

Technology for a better society

www.sintef.no